U N I V E R S I T Y OF S T R A T H C L Y D E

FACULTY OF ENGINEERING

The Influence of Limb Alignment on the Gait of Above-Knee Amputees

By

Yang Lang

Thesis submitted for the Degree of Doctor of Philosophy in Bioengineering

Bioengineering Unit

October, 1988

To

my beloved wife

XIAOLING

ACKNOWLEDGEMENT

I would like to first thank Professor John P. Paul for giving me the opportunity to undertake the work described in this thesis, for his realistic support and being there when he was most needed throughout my stay in the Bioengineering Unit.

I am extremely grateful to Mr. S. E. Solomonidis, my supervisor, for his guidance, constructive criticism, invaluable advice and encouragement given to me throughout this project.

I would also like to express my appreciation to the assistance given to me by the staff of the Bioengineering Unit and the National Centre, in particular, Mr. W. D. Spence (prosthetist), Mrs. S. Nicol (computer advisor), Mr. R. Donaldson (prosthetic technician) and Mrs. Mary Bennett (nurse). Assistence offered by Mr. J. Martin and Mr. J. Gibson (prosthetists) from the Belvidere Limb Fitting Centre is highly appreciated.The patients are also acknowledged with thanks for their kind participation of the gait test.

The financial support of the Overseas Research Student Award and John Anderson Studentship of the university is greatly appreciated.

I am deeply indebted to my beloved wife Xiaoling for not only typing most of the thesis but also for her understanding, perseverance and trust in me. Many thanks also to the members of my family for their understanding and support.

Professor Yupeng Wu is also acknowledged with thanks for his recommendation to study in the Bioengineering Unit, University of Strathclyde.

ABSTRACT

Alignment of the above-knee prostheses is one of the important factors affecting the success of patient/prosthesis matching. It has been found that the prosthetist and the patient can accept a number of alignments which produce different intersegmental loads and it has been suggested that it is possible to obtain an 'optimal' alignment satisfying certain criteria. In order to enhance the efficiency of the alignment procedure, it is necessary to understand how alignment affects the amputee's gait and the patient compensations for changes in the alignment.

Biomechanical gait tests on above-knee amputees were conducted in which the alignment of the prosthesis was changed systematically. The Strathclyde television-computer system was used to record the kinematic data of the amputee, and the ground reactions were measured by two Kistler forceplates. An 8-segment biomechanical model of the above-knee amputee was developed and implemented by a suit of FORTRAN computer programs to analyze and present 3-D kinematic and kinetic data obtained. The effects of alignment changes on the above-knee amputees' gait were studied in terms of the temporal-distance parameters, angular displacements of the lower limbs and the trunk, ground reactions and intersegmental moments.

It was found that the angular displacement at the hip joint on the prosthetic side showed compensatory actions of the amputee for the alignment changes. The ground reaction force was sensitive to alignment changes, and in particular, the changes in the characteristics of the fore-aft ground force could be related to the alignment changes. The antero-posterior intersegmental moments about the prosthetic ankle and knee joints were evidently influenced by alignment.

List of Contents

ACKNOWLEDGEMENT·····T-2

ABSTRACT·····T-3

CHAPTER 1 INTRODUCTION AND AIMS·····1

CHAPTER 2 LITERATURE REVIEW ON GAIT ANALYSIS

§ 2.1 Introduction ·····5

§ 2.2 What is Gait Analysis·····5

§ 2.3 Mass Properties of the Body Segments·····9

§ 2.4 Motion Measurement Techniques ·····11

§ 2.5 Ground Reaction Measurement Techniques ·····21

§ 2.6 Gait Patterns of the Normal ·····24

CHAPTER 3 PROSTHETICS OF THE LOWER LIMBS

§ 3.1 Introduction ·····36

§ 3.2 Amputation Surgery ·····36

§ 3.3 Lower Limb Prosthetic Systems·····39

§ 3.4 Prosthetic Methods·····48

§ 3.5 Alignment of Lower Limb Prostheses ·····50

§ 3.6 Prosthetic Gait Analysis ·····56

CHAPTER 4 EXPERIMENTAL ASPECTS OF THE WORK

§ 4.1 The prostheses, Their Inertia Properties
and Alignments·····62

§ 4.2 The Strathclyde Biomechanics Laboratory ·····70

§ 4.3 On the Accuracy of the Kinematic Data·····73

§ 4.4 Approaches to Biomechanical Gait Testing ·····83

CHAPTER 5 THEORETICAL ASPECTS OF THE WORK

§ 5.1 Introduction·····89

§ 5.2 Biomechanical Model of the Above-Knee Amputee ·····96

§ 5.3 Kinematic Analysis of the Model·····105

§ 5.4 Kinetic Analysis of the Model·····112

CHAPTER 6 RESULTS AND DISCUSSION

§ 6.1 Patient Profiles·····117

§ 6.2 Alignment Measurement Results·····118

§ 6.3 Temporal-Distance Parameters·····122

§ 6.4 Angular Displacements of the Trunk·····123

§ 6.5 Angular Displacements of the Lower Limbs·····127

§ 6.6 Ground Reaction Forces·····132

§ 6.7 The Ankle Joint Moments·····143

§ 6.8 The Knee Joint Moments·····148

§ 6.9 The Hip Joint Moments·····153

Chapter 7 CONCLUSIONS AND RECOMMENDATIONS·

§ 7.1 Conclusions·····157

§ 7.2 Recommendations for Future Work·····159

APPENDIX·····161

BIBLIOGRAPHY·····220

KEY ABBREVIATIONS AND NOTATIONS

ACS	Alignment Change Sequence.
AJC	Ankle Joint Centre.
AK	Above-Knee.
A/P	Anterior/Posterior.
ASIS	Anterior Superior Iliac Spine.
BK	Below-Knee.
CNORM	Configuration of the prosthesis in NORMal alignment.
CFACS	Configuration of the prosthesis in Foot Alignment Change Sequence.
CFSACS	Configuration of the prosthesis in Foot & Socket Alignment Change Sequence.
CG	Centre of Gravity.
CP	Centre of pressure of the ground–foot reaction.
CSACS	Configuration of the prosthesis in Socket Alignment Change Sequence.
DNORM	Dynamic Configuration of the prosthesis in NORMal alignment.
DFACS	Dynamic Configuration of the prosthesis in Foot Alignment Change Sequence.
DFSACS	Dynamic Configuration of the prosthesis in Foot & Socket Alignment Change Sequence.
DSACS	Dynamic Configuration of the prosthesis in Socket Alignment Change Sequence.
FACS	Foot Alignment Change Sequence: dorsi flexion → normal → plantar flexion.
FSACS	Foot & Socket Alignment Change Sequence which results in the antero-posterior shift of the knee joint centre: posterior → normal → anterior shift.
HS	Heel Strike.
HJC	Hip Joint Centre.
KJC	Knee Joint Centre.
KSI	Knee Stability Index: orthogonal distance of the knee joint centre to the line connecting the hip joint centre and the ankle joint centre.
LHS	Left Heel Strike.
LTO	Left Toe Off.
M/L	Medial/Lateral.

RHS	Right Heel Strike.
RTO	Right Toe Off.
SACH	Solid-Ankle-Cushioning-Heel.
SAL	Socket Axes Locator.
S.D	Standard Deviation.
TCP_e	Time at which the centre of pressure of the ground–foot reactions enters the toe area, i.e. the end of the transient period of the progression of the centre of pressure.
TCP_s	Time at which the centre of pressure of the ground–foot reactions leaves the heel area, i.e. the start of the transient period of the progression of the centre of pressure.
TO	Toe Off.
Φ_{FACS}	A/P angular changes of the prosthetic ankle in the FACS: (–6°, –3°, 0°, 3°, 6°) with plantar flexion positive.
Φ_{FSACS}	A/P angular changes of the prosthetic ankle in the FSACS: (6°, 3°, 0°, –3°, –6°) with plantar flexion positive.
Φ_{NORMAL}	static A/P orientation angle of the prosthetic foot with respect to the ground frame of reference.
$\Phi(t)_{NORMAL}$	dynamic A/P orientation angle of the prosthetic foot with respect to the ground frame of reference.
Ψ_{FSACS}	A/P angular changes of the socket in the FSACS: (–6°, –3°, 0°, 3°, 6°) with flexion positive.
Ψ_{SACS}	A/P angular changes of the socket in the SACS: (–6°, –3°, 0°, 3°, 6°) with flexion positive.
Ψ_{NORMAL}	static A/P orientation angle of the socket with respect to the ground frame of reference.
$\Psi(t)_{NORMAL}$	Dynamic A/P orientation angle of the socket with respect to the ground frame of reference.
θ_{NORMAL}	static A/P orientation angle of the prosthetic shank with respect to the ground frame of reference.
$\theta(t)_{NORMAL}$	dynamic A/P orientation angle of the prosthetic shank with respect to the ground frame of reference.

CHAPTER 1

INTRODUCTION AND AIMS

Successful rehabilitation of amputees requires that the prostheses fitted to them fulfill the needs of each individual amputee with respect to three most important criteria: comfort, function and appearance during use. It is known that cosmesis is also most important although not relevant to this study. In order to satisfy the requirements, the socket must be fitted accurately and comfortably around the stump so as to form an effective connection to the prosthesis, and the various prosthetic components should be correctly chosen, assembled and aligned to provide maximum restoration of function and minimum gait deviation.

The alignment of the prosthesis, defined as the relative position and orientation of the prosthetic components, affects all three criteria. Improper alignment would result in undesirable and ineffective pressure distribution at the socket/stump interface, giving rise to discomfort, pain and even tissue break down. Incorrect alignment could also influence the function of the prosthesis. For example, an excessive knee set back would make knee flexion at the time of push off difficult. Finally, apart from the direct influence of the alignment on the standing appearance of the amputee, the amputee would change his/her normal manner of walking in an attempt to compensate for any problems in the comfort and function of the prosthesis, resulting in greater gait deviations.

In current prosthetic practice, the final alignment of the prosthesis is arrived at by combining the prosthetist's skill and experience with the patient's comments. During the phase of dynamic alignment, the prosthetist observes the walking amputee from all angles, listens to his/her comments and makes adjustments, based on subjective judgement, aiming to satisfy the patient and to achieve minimum gait deviation. This final alignment, which ideally should be optimum and unique, is commonly referred to as the "optimal alignment".

However, the present subjective techniques of assessing the amputee's gait are stated to be inadequate (Saleh, 1985). Visual observation is neither reliable nor sensitive enough to detect minute gait deviations and the amputee's comments are not always helpful particularly in the case of geriatric patients. Therefore, modern gait analysis techniques have been adopted in an attempt to increase efficiency in obtaining prosthetic alignment. Several papers (eg. Pearson *et al*, 1973; Winarski & Pearson, 1987) reported the effects of alignment changes on the socket/stump pressure distribution. Due to technical difficulties, only the normal pressures at selected sites were monitored. These investigations more or less concentrated on the aspect of comfort and the whole picture of the gait pattern was missed. Some other investigators (eg. Hannah & Morrison, 1984; Mizrahi *et al*, 1986) refer to the symmetry of the gait between the prosthetic and unaffected limbs. These researchers believe that correct alignment should reduce the asymmetry in the movement of the lower limbs. This concept is questionable since, as Winter & Sienko (1988) pointed out, the function of an amputee with major structure asymmetry in the neuromuscular skeletal system cannot be optimal when the gait is symmetrical. Instead, the amputee is probably seeking a new asymmetrical optimum within the constraints of his/her residual system and prosthesis. Therefore, there is a need to study the amputee's gait represented by variables such as joint moments and power. However, few detailed reports dealing with this subject (Bresler *et al*, 1957; Cappozzo, 1976; Lewallen *et al*, 1985; Winter & Sienko, 1988) have appeared in the literature, and only three (Zahedi *et al*, 1985; Saleh, 1985; Morimoto, 1987) reported studies, two of them on below knee amputees, relating the joint moments to alignment.

Since the 1970s, investigations into the alignment of lower limb prostheses have been carried out at the Bioengineering Unit, University of Strathclyde. Solomonidis (1975 & 1980) developed a method of defining the alignment parameters and a technique for measuring the parameters, making it possible to

compare the different alignments quantitatively. During an evaluation programme of the current modular limbs (Solomonidis, 1975 & 1980), the alignment of the BK and AK prostheses was one of the factors studied. It was found that the prosthetist aligning any one amputee with several limbs could come to a different final alignment for each limb, thus throwing the idea of a unique alignment for each amputee into doubt. Zahedi *et al* (1986) conducted an extensive study on the alignment of BK and AK prostheses and the results confirmed that an amputee could tolerate several alignments. In another report (Zahedi *et al* , 1985), they presented the effects of alignment on the amputee's gait and suggested that it was possible to select biomechanically the most suitable alignment from the range of acceptable alignments for any one amputee. However, it was recognized that the biomechanical aspects of the process were not fully established.

This study was therefore undertaken in order to gain a better understanding of the biomechanics of AK amputee locomotion and the effects that alignment changes have on his gait. Specifically, answers to the following questions were sought: How does a variation in any particular alignment parameter (eg. socket flexion or knee set back) influence the gait of the amputee? Does a certain change in alignment parameters have consistent influence on a gait parameter? Can any particular gait variable be controlled by a certain alignment parameter? Does the amputee compensate for changes in the alignment? What methods does he use for compensation? Which gait variables are most sensitive to alignment changes? Is the effect consistent and easy to measure? Is the alignment configuration arrived at by current subjective method the "optimum" from a biomechanical point of view?

In order to answer the above questions, it was decided to carry out a study by systematically changing the alignment of above knee prostheses and analyzing the resulting gait of the amputee in terms of the gait variables such as temporal-distance parameters, angular displacement of the body segments, ground reaction forces and joint moments. Different alignments were compared biomechanically, and the amputee's compensation for the alignment changes was studied.

In order to obtain a general guide for the behaviour of the various gait parameters during locomotion,.it was decided to test extensively a normal subject. Such a test also allows for the verification of the computer program as there is considerable amount of data available in the literature on normal gait.

This study has some limitations. Firstly, due to the nature of the study in which an amputee is required to perform many test walks, only the group of amputees classified as "active" participated in the project. Secondly, because it was necessary at this stage to examine as many gait variables as possible so as to establish the most sensitive and important parameters for future work, it was decided to limit the number of amputees to 4. Furthermore, it was decided to restrict the alignment changes in the antero-posterior plane.

The thesis commences with a literature review on the methodology of gait analysis and the gait patterns of normal people, followed by a outline of lower limb prosthetics and a review of the current state of prosthetic gait analysis. Chapter 4 is given to the description of the experiment design. The biomechanical model of the above knee amputee and its gait analysis is presented in Chapter 5. Chapter 6 presents the results of the study and the discussion. Finally, Chapter 7 states the conclusions reached by this work and suggestions for future work.

CHAPTER 2

LITERATURE REVIEW ON GAIT ANALYSIS

§2.1 Introduction

An up to date summary of published studies in gait analysis which are relevant to the work presented in this thesis is given in this chapter.

The review starts with a look at the various models and methods used in gait analysis. With access to this information, it becomes possible to discuss later in some detail certain important aspects of gait analysis on the one hand, and to locate where we are in the sea of references on the other hand. After that, several sections concern the recording techniques used in gait analysis which also form a basis for the selection of a recording system suitable for this project. The gait pattern of the normal, which has served as basis for describing, comparing and evaluating how a handicapped person compensates for defects during walking, is presented in the final section.

§2.2 What Is Gait Analysis ?

Walking from one place to another on two legs seems to be a simple act, but it actually is a very complicated phenomenon. In producing only one step, one must continuously support oneself against the action of gravity, employ muscle action which involves energy transformation to produce or prevent relative rotations at almost every major joint in the body, and co-ordinate all the actions, by means of a sophisticated control system, according to the changing conditions in the external and internal forces and motions. Therefore, an adequate description of walking requires a multi-disciplinary approach involving anatomy, physiology, and mechanics.

According to Cappozzo (1984) the quantitative description of all mechanical aspects of walking is commonly referred to as gait analysis.

Like any scientific discipline, the first step towards gait analysis is to create an

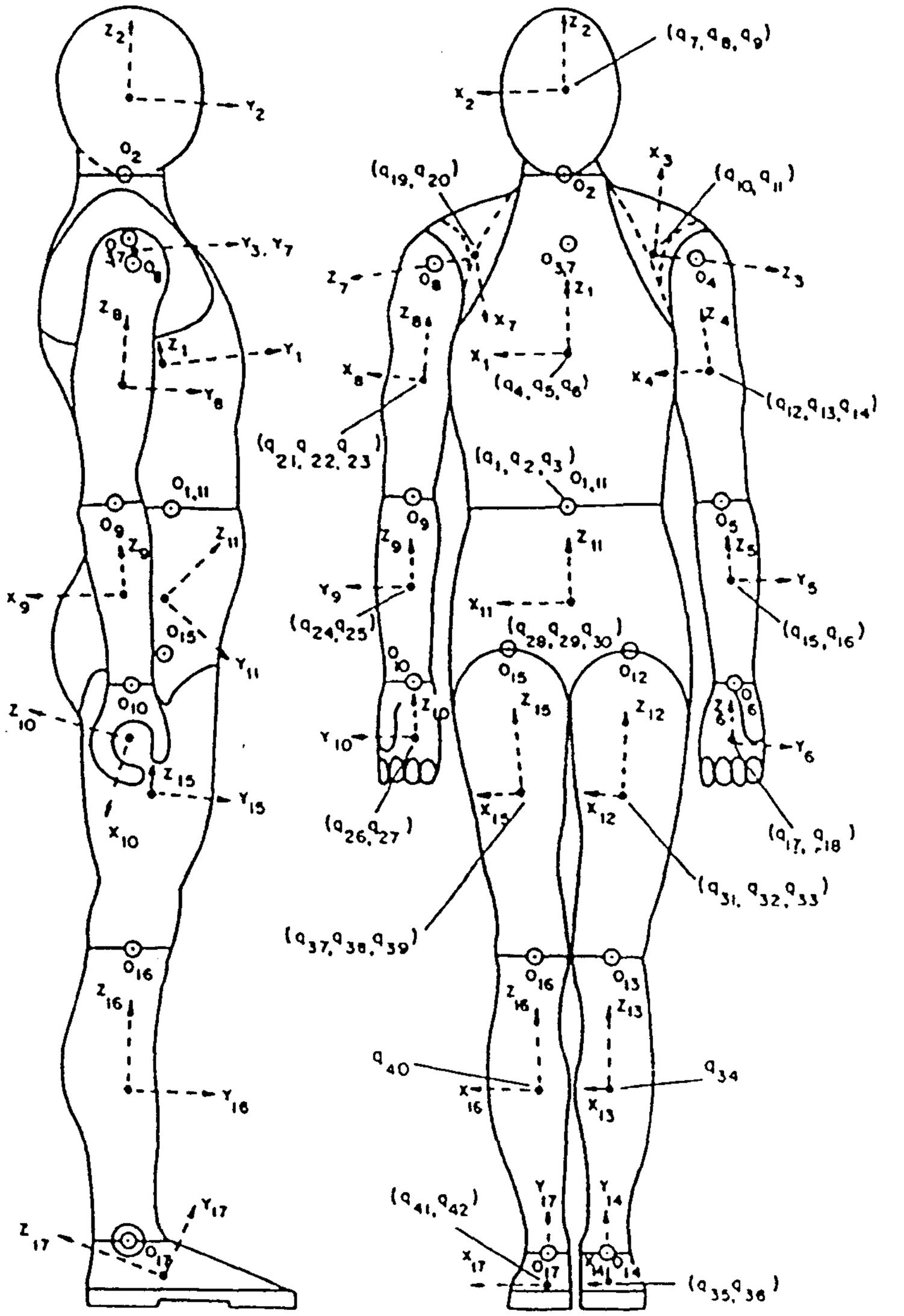

Fig.2.1 A 17-segment biomechanical model of the human body.
(from Hatze, 1984)

adequate model for the human body which achieves the practical combination of simplicity and accuracy. A fundamental assumption in the biomechanical model of the human body, that has been universally accepted, is that the human body consists of rigid segments connected by joints. The number of segments and the number of degrees of freedom of the joints vary with the purpose of the model, and no direct relationship exists between these two numbers. Hatze (1984) suggested that a model consisting of 13 segments was regarded as adequate for gait analysis although he in fact presented a 17 segmental model as shown in Fig. 2.1. As far as the number of degrees of freedom of a joint is concerned, there are in general six independent parameters: three translations and three rotations. Joint translations, however, are of small magnitude and can not be accurately measured using the experimental techniques available in the gait analysis laboratory, therefore only three rotational components of movement are dealt with in gait analysis.

The first problem posed by gait analysis is the movement of the segments in terms of kinematic variables such as linear and angular displacement, velocity and acceleration. At this stage no considerations are taken of the forces that cause the movement. This kinematic analysis of gait concerns not only the lower limbs but also the upper limbs and torso,and not only the motion range of the segments, but also the phase relationship between these motions (Braune & Fischer, 1895; Murray *et al*,1964; Lamoreux, 1971; Eberhart *et al*, 1954; Cappozzo, 1982). Careful inspection of the kinematic variables can give trained observers some insight into the basic mechanisms of movement and direction for diagnosis, training and therapy.

In order to describe movement, a spatial reference system must be introduced which can be either relative or absolute. The spatial system established in anatomical literature is the means by which the position of one segment relative to another is defined using terms such as flexion, proximal and anterior, while the one used in biomechanics is absolute and describes the motion of a segment relative to the ground or any inertia system of reference. The relative system is effective in describing biological function and the absolute system is convenient for mathematical formulation. Since the relative motions are caused by the muscular activity and the muscles are grouped according to their relative function, the kinematic data must be

capable of interpretation in terms of the anatomical directions, that is, using the anatomical relative system.

The kinematic data can be obtained by several techniques which fall into two categories: direct and imaging techniques. In direct measurement the instrument such as a goniometer or an accelerometer is directly attached to a subject so that the movement of the segment can be registered, while in imaging technique, television or cinematography for instance, a number of markers fixed onto the subject can be identified by the imaging devices that either coincide or permit the subsequent determination of the anatomical landmarks of the segments.

The raw data obtained from experimental instruments are contaminated with random errors which must be removed before further processing is undertaken, particularly when differentiation is involved. Fourier analysis of normal walking (Winter *et al* 1974) has shown that over 99% of the signal power was contained in the lower seven harmonics (below 6Hz). Basically, two kinds of techniques are used to remove noise: smoothing and filtering. In smoothing the raw data, a number of coefficients in a trial function, a polynomial of a certain order or a sum of sinusoidal functions for instance, are determined by minimizing the mean square error, and further mathematical operations are performed on the smoothed functions. Digital filtering of a signal, based on the analysis of the frequency spectra of both signal and noise, aims at the selective rejection, or attenuation of certain frequencies. It appears that the Butterworth filter which follows a numerical method of differentiation is most appropriate (Pezzack *et al*, 1977; Cappozzo, 1983).

A further problem posed by gait analysis is that concerning forces, ie, kinetics. It is here that a major focus of the gait analysis is made because it is these forces that cause the observed movement. The forces acting on the human body during walking may be classified into two categories: external and internal. External forces come from gravity inertia and ground reaction forces, and internal forces from muscle activity, ligaments and bone-on-bone forces.

The ground reaction force is distributed over an area of the foot and can be measured by various methods (Elftman, 1934; Hertzberg, 1955; Nicol and Henning, 1976; Chodera & Lord, 1978; Cavanagh *et al*, 1981; Gerber, 1982). The reaction

also can be represented as a 3-dimensional vector acting on a point called the centre of pressure. The force vector and centre of pressure can be measured by a dynamometric platform which forms part of the walkpath on which the locomotion act is performed (Elftman, 1939; Cunningham & Brown, 1952; Laura, 1954, 1957; Kistler, 1977).

The gravitational forces acting at each body segments together with the segmental moment of inertia can be determined by means of a prediction technique from anthropometric measurements (Harless 1860, Braune and Fischer, 1889 & 1892; Dempster, 1955; Drillis & Contini, 1966; Clauser *et al*, 1969; Chandler *et al*, 1975; Hanavan, 1964; Jensen, 1978; Hatze, 1980).

There have so far not been any non-invasive techniques available to measure directly the internal forces. As a result, analytical procedures have to be employed which use classical mechanics and modelling approaches (Elftman, 1939; Bresler and Frankel, 1950; Paul, 1967; Morrison, 1967; Cappozzo, 1982). The segment under investigation is separated from its adjacent parts of the body by an imaginary surface, and all physical connections of the segment with the others are represented by the intersegmental forces and moments which are assumed to maintain both body parts in the same dynamic state as they had before separation. The equations of rigid body mechanics are applied to the segment and the intersegmental forces and moments can thus be calculated.

It should be emphasized that intersegmental loads are not the muscle forces nor the bone-on-bone forces but their nett effects. The inter-segmental moments are balanced by the moments generated by muscle contraction and ligament constraints. If the effects of the ligaments are much smaller than those of the muscles, as in normal walking, the intersegmental moments can be approximated as a measure of muscle function. That is why the inter-segmental moments are often referred to as muscle moments and are valuable in understanding musculoskeletal functions.

If the bone-on-bone forces are considered, another two fundamental pieces of information are required: (1) the geometry of the muscle and its attachment to the bone which determine the muscle force lever to the joint centre; (2) muscle activity relative to the phase of the motion of the body segments during motion. The first piece of information can be obtained from cadaver studies and the second from

electromyography (EMG). Having defined the muscle groups involved in the period of the gait cycle, the bone-on-bone forces are calculated (Paul, 1967; Morrison, 1967; Cappozzo, 1982). These forces are valuable in the study of endo-prosthetics problems.

Investigation into energy expenditure is another reason for carrying out gait analysis. In the process of walking, energy is converted from metabolic to mechanical energy and some energy is dissipated during the process. Therefore the study of energy expenditure has been pursued at two levels, that is, metabolic and mechanical. Metabolic energy cannot be measured directly, but can be calculated indirectly from the amount of oxygen required or carbon dioxide given off (Ralston, 1960; McDonal, 1961; Zarrugh *et al* ,1974; Passmore and Durnin, 1955). Mechanical energy and work can be computed from the kinematic and kinetic data already mentioned above (Elftman, 1939; Bresler and Berry, 1951; Ralston and Lukin, 1969; Cavagna *et al*, 1963; Robertson &Winter, 1980; Aleshinsky, 1986). By comparing the metabolic energy expenditure and mechanical work done by muscles, an overall muscle efficiency can be assessed.

Gait analysis has been pursued for a long time and has shown significant promise in associating normal and abnormal gait patterns with underlying musculoskeletal pathology. However, since walking is extremely complex, our knowledge about it is still far from complete.

§2.3 Mass Properties of the Body Segment

It is a fundamental requirement in the study of biomechanics of human locomotion to determine the physical properties of the body segments under consideration, especially when kinetic analysis is performed. These body properties are the mass of the segment, the location of the mass centre (the CG) and mass moment of inertia.

The estimation of these segment parameters falls into two principal categories: prediction through regression equations and geometric approximations.

§2.3.1 Regression technique

The regression equations have been determined through the statistical analysis

Table 2.1 Regression Equations for Predicting Segmental Weight in Kilograms

Head	*Head Circ*	*Weight (kg)*		*Constant*	*R*	*SE Est*
	0.148			−3.716	814	0.20
	0.104	+0.015		−2.189	.875	0.17
Trunk	*Weight (kg)*	*Trunk Length*	*Chest Circ*			
	0.551			−2.837	.966	1.33
	0.494	+0.347		−19.186	.979	1.11
	0.349	+0.423	+0.229	−35.460	.986	0.92
Upper Arm	*Weight (kg)*	*Arm Circ(ax)*	*Acrom-Rad Lth*			
	0.030			−0.238	.879	0.14
	0.019	+0.060		−1.280	.931	0.12
	0.007	+0.092	+0.050	−3.101	.961	0.09
Forearm	*Wrist Circ*	*Forearm Circ*				
	0.119			−0.913	.827	0.09
	0.081	+0.052		−1.650	.920	0.06
Hand	*Wrist Circ*	*Wrist Br/Bone*	*Hand Brdth*			
	0.051			−0.418	.863	0.03
	0.038	+0.080		−0.660	.917	0.03
	0.029	+0.075	+0.031	−0.746	.942	0.02
Thigh	*Weight (kg)*	*Upper Thigh C*	*Iliac Cr Fat**			
	0.120			−1.123	.893	0.54
	0.074	+0.138		−4.641	.933	0.45
	0.074	+0.123	+0.027	−4.216	.944	0.43
Calf	*Calf Circ*	*Tibiale Ht*	*Ankle Circ*			
	0.135			−1.318	.933	0.14
	0.141	+0.042		−3.421	.971	0.09
	0.111	+0.047	+0.074	−4.208	.979	0.08
Foot	*Weight (kg)*	*Ankle Circ*	*Foot Length*			
	0.009			+0.369	.810	0.06
	0.005	+0.033		−0.030	.882	0.05
	0.003	+0.048	+0.027	−0.869	.907	0.04

* Iliac Cr Fat (mm) = 0.78 Skinfold. Iliac Crest (mm) − 0.27; weight is kg; and all other dimensions are in cm.

(from Miller & Nelson, 1973)

Table 2.2 Body segment parameters

(from Goh, 1982)

Body segment	C1	C2	C3
Foot	0.0152 (0.00)	0.5000 (0.00)	0.4750 (0.00)
Shank	0.0453 (0.00)	0.4030 (0.03)	0.2890 (0.01)
Shank & Foot	0.0632 (0.01)	0.4673 (0.05)	0.3467 (0.06)
Thigh	0.1027 (0.01)	0.4169 (0.03)	0.2912 (0.04)

of data obtained from a sample population of subjects of either cadaver or living subjects. They often consist of only one anthropometric item of data for each mass property, thus the mass properties are usually quoted as the coefficients in the regression equations, that is,

$$C_1 = \frac{\text{segment mass}}{\text{whole body mass}}$$

$$C_2 = \frac{\text{distance from proximal joint centre to the mass centre of the segment}}{\text{total length of the segment}}$$

$$C_3 = \frac{\text{radius of gyration of the segment inertia moment}}{\text{total length of the segment}}$$

Harless (1860) and Braune & Fischer (1892) worked on cadavers and investigated the body segment mass and the locations of the CG. Dempster (1955) carried out one of the most extensive studies based on 8 cadavers and determined all three mass properties. Drillis & Contini (1966) and Contini (1972) investigated the segment mass properties of living normal subjects and patients with hemiplegia and amputations. They also compiled the data obtained by previous investigators and provided weighted average coefficients. Clauser *et al* (1969) derived the stepwise regression equations from 14 cadavers as shown in Table 2.1. It is believed that the inclusion of two or more anthropometric variables in the regression equations improves the accuracy of the prediction. Goh (1982) presented a set of body parameters by averaging the previous data obtained by various investigators, as shown in Table 2.2. In this thesis, data derived by Clauser *et al* and Goh were used.

§2.3.2 Geometric approximation

This method simplifies the irregular shapes of the different segments as standard geometric forms, such as ellipsoid, sphere and truncated circular cone, which permit simple mathematical description. Hanavan (1964) perhaps was one of the earliest to employ such a technique. Jensen (1978) estimated the body segment properties using the photogrammetric method. Hatze (1980) derived an very complicated and accurate model which needed 107 anthropometric measurements and could reach 2% accuracy.

§2.4 Motion Measurement Techniques

Data collection for the kinematic analysis of human motion plays a very important role in biomechanical analysis and therefore great efforts have been made to improved the quality of data obtained. Presented in this section is a review of the motion measurement techniques which are classified into two parts: imaging and direct measurement techniques.

§2.4.1 Imaging measurement techniques

In this category two techniques are included: photographic and optoelectric methods. Only the displacement data can be obtained by these techniques and considerable calculations are required to obtain other kinematic variables meaningful to gait analysis. Combined with ground reaction data, a comprehensive gait analysis can be conducted.

§2.4.1.1 Photographic techniques

The photographic techniques of recording human locomotion have been well developed and extensively used since the late nineteenth century. There are basically two kinds of photographic recording methods:

(1) chronophotography, i.e., recording the entire movement on a single photographic plate;

(2) cinematography, i.e., recording each instant of movement in time on separate frames.

Chronophotography

This method was first introduced in France by Marey (1873). The subject was dressed in black with bright reflective strips to define the limbs and buttons to mark the joint axes. The movement of the subject was photographed by a camera viewing from the side of the walkway. The camera had an open lens with a rotary shutter placed before it. A series of images of strips and buttons was thus produced on a single plate, forming a 'stick diagram'.

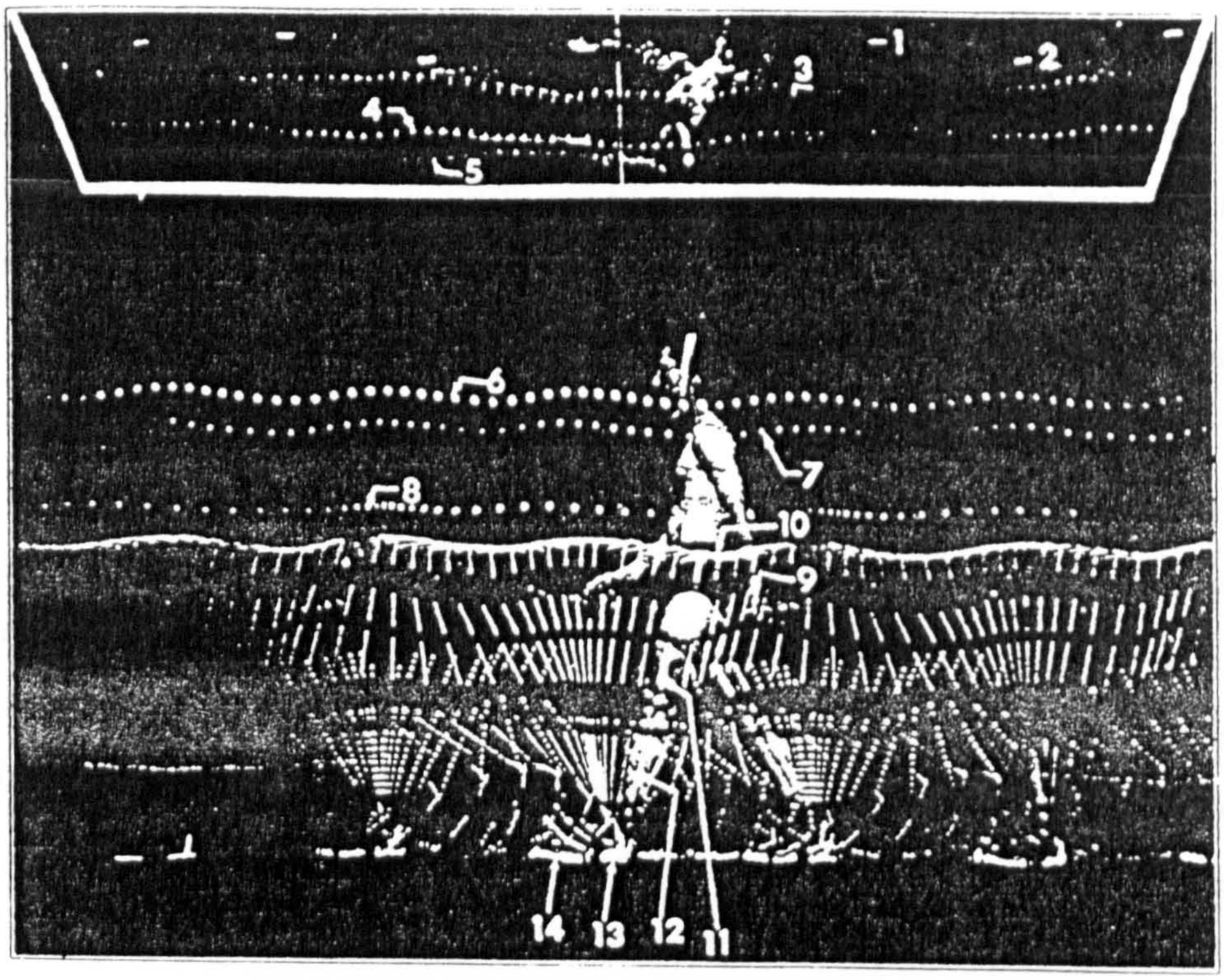

Fig.2.2 A typical photograph of a walking man obtained by chronophotography.
(from Murray et al, 1964)

Braune and Fischer (1895) used four cameras for three-dimension measurement. In order to enhance the contrast, the passive strips were replaced with "Geissler" tubes which flashed at a frequency of 26 Hz. Parallax errors were corrected using a reference grid positioned in the object field. Velocities and accelerations were calculated from displacement data and the resultant force acting at the centres of the segment joints were derived. Because of their pioneering work they earned the title of 'the fathers of the modern biomechanics'.

Eberhart and Inman (1947) combined the chronophotography with a forceplate to study human walking. A flash lamp, synchronized to the rotary shutter, fired once during the event for synchronization of all recording equipment.

As an alternative to the rotary shutter, a stroboscope was introduced by Murray (1964) which fired 20 times per second. A mirror was mounted at an angle of 25 degrees over the walkpath such that the transverse movement could be recorded on the same photographic plate, see Fig. 2.2.

Cappozzo (1981) used 4 cameras to study the 3-D movements of the head and the upper body. Yellow light emitting diodes (LED) were used as body markers which flashed from 30 to 60 times per second. The laboratory was illuminated with green light to enhance contrast. An accuracy of 2.5mm for the 'X' and 'Z' co-ordinates and 8mm for the 'Y' co-ordinates was claimed for the stereo-scopic field of (2.2m ×1.9m × 0.3m).

Chronophotography is one of the most economical and simple technique to measure movement in human locomotion studies. It has the advantage of providing all the information on a single photographic plate and gives rapid assessment if a polaroid camera is used. With an electric strobe of high flash frequency, it is possible to record high speed movement. This method is particularly suitable for recording the motions in the plane parallel to the line of progression.

However, several disadvantages are inherent in the chronophotographic method. One of these is the problem of image overlapping when movement overlaps or when a point is more or less stationary. The strobe flash light in a dimmed room is very distracting, even dangerous, to a subject and may alter his/her gait pattern.

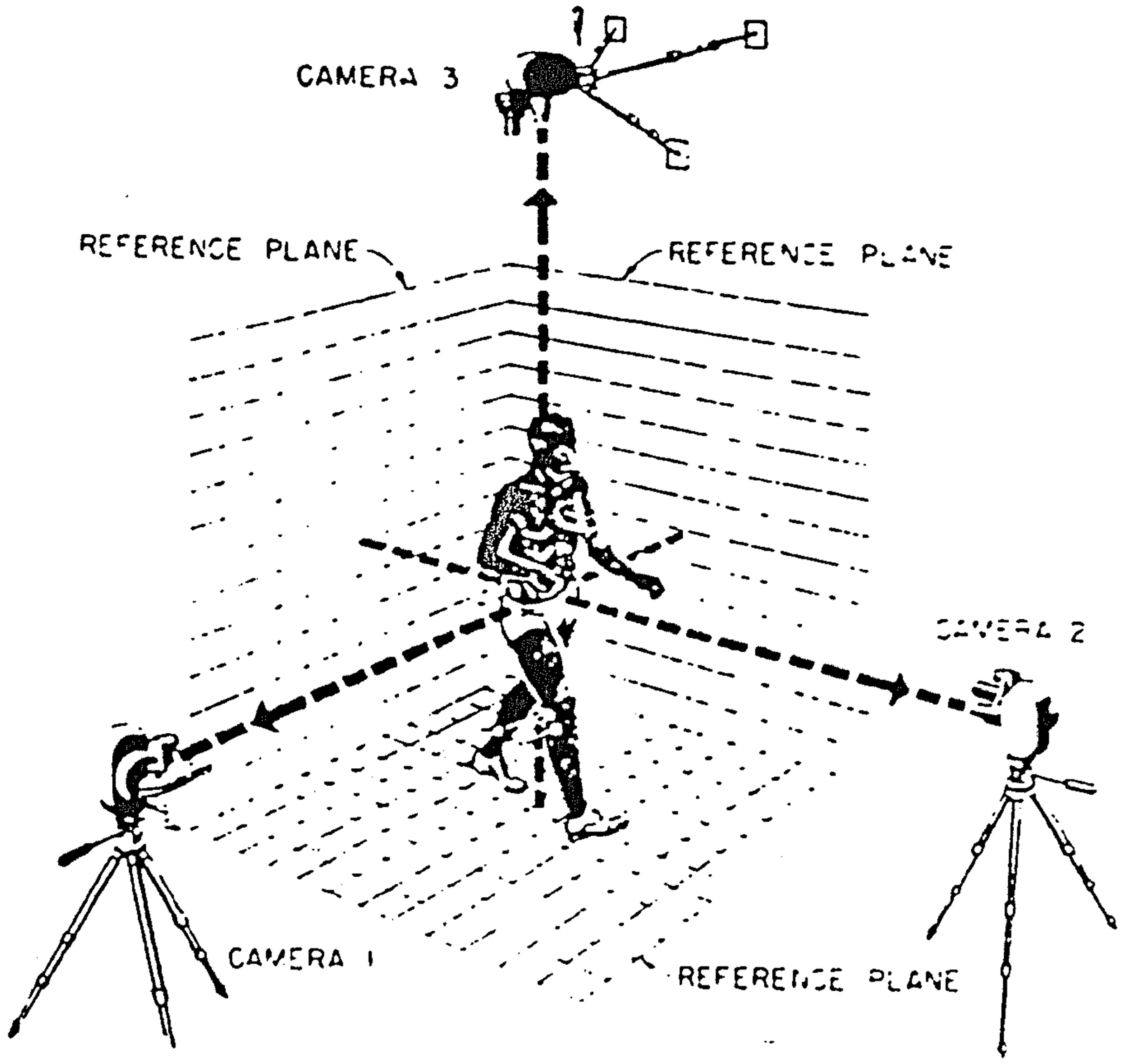

Fig.2.3 Arrangement for recording pin-study data using cinematography.
(from Klopsreg & Wilson, "Human limbs and Their Substitutes", 1954)

Cinematography

Muybridge (1883) first introduced this method to human locomotion studies and Dercum (1888) presented the displacement-time curves of the normal and pathological gait recorded by Muybridge.

Elftman (1939) used one camera with its lens axis perpendicular to the progression plane together with a forceplate to study human gait. The camera operated at the rate of 93 exposures per second. Since only one camera was used, his study was limited to two dimensions.

Eberhart and Inman (1947) described two cine camera systems for three dimensional gait analysis. The first employed 35mm cameras which viewed a straight walkway from above, in front and to the right of the subject at a distance of 25ft, as shown in Fig.2.3. The three cameras were synchronized by a clock system seen simultaneously by all three cameras. The second system involved a glass walkpath with an inclined mirror underneath and two cine cameras. One of the cameras was situated normal to the sagittal plane, taking the lateral view as well as the view from the mirror, while the other camera took the frontal view. The frame rates in both systems were 48 per second. No data about the accuracy were provided.

Paul (1967) presented a system using two 16mm cinecameras viewing the subject laterally and from the front. The cameras operated at 50 frames per second. The film was re-exposed to superimpose a grid board of 5 inch squares as a reference such that the accuracy of the data was improved to within 1mm for lower-limb studies. A flash bulb fired once during the test to synchronize the camera with the forceplate and EMG records. In order to study the whole body kinematics during walking, Ishai (1975) extended this system to include an additional side camera, so that the movement of both the right and the left side could be recorded simultaneously.

Cinematography provides a non-contact, comprehensive, stable, high resolution and permanent visual record of the events. It avoids some of the limitations associated with chronophotography such as image overlap and high marker/background contrast. However, this technique is relatively expensive and

considerable delay is inevitable because the film must be firstly processed.

§2.4.1.2 Optoelectric techniques Optoelectric imaging techniques used in human locomotion studies were developed in the 1960s and 1970s. At the present time there are basically three kinds of optoelectric imaging systems used in locomotion studies. They are

(1) Television/computer system,

(2) the SELSPOT system

(3) the CODA system.

Television/computer system

Although several television/computer systems have been developed independently, they share the same basic principles. The spatial co-ordinates of markers are dérived from the position in the television camera scan of the video signal produced by the markers. This is done by digitizing either the complete video signal or the co-ordinates when a marker is detected in the video signal. In the latter case, two digital counters are used to register the ordinate line number from the start of each field and the time lapse period from the start of each scan line respectively. When a marker is amplitude detected in the video signal the states of these two counters are sampled, giving a marker's (X,Y) position in the TV raster.

Furnee (1967) was perhaps the first to introduce TV/computer system to human movement studies. Miniature electric light bulbs were used as body markers and their positions were determined by two digital counters.This system was later improved by including buffer memories and synchronous rotary shutters which reduced image streaking. However, only 5 markers could be detected and only one television camera was used in the system, thus restricting the studies to two dimensions.

Winter (1972) described a TV/computer system which was originally designed by Dinn (1970). A standard vidicon camera was mounted onto a movable trolley which ran parallel to a 7m walkway at a distance of 4m from the subjects. The leg was marked by seven hemispherical reflective markers. In order to define the

15a

Fig.2.4 Computer print-out of one converted TV field.
(from Winter et al, 1972)

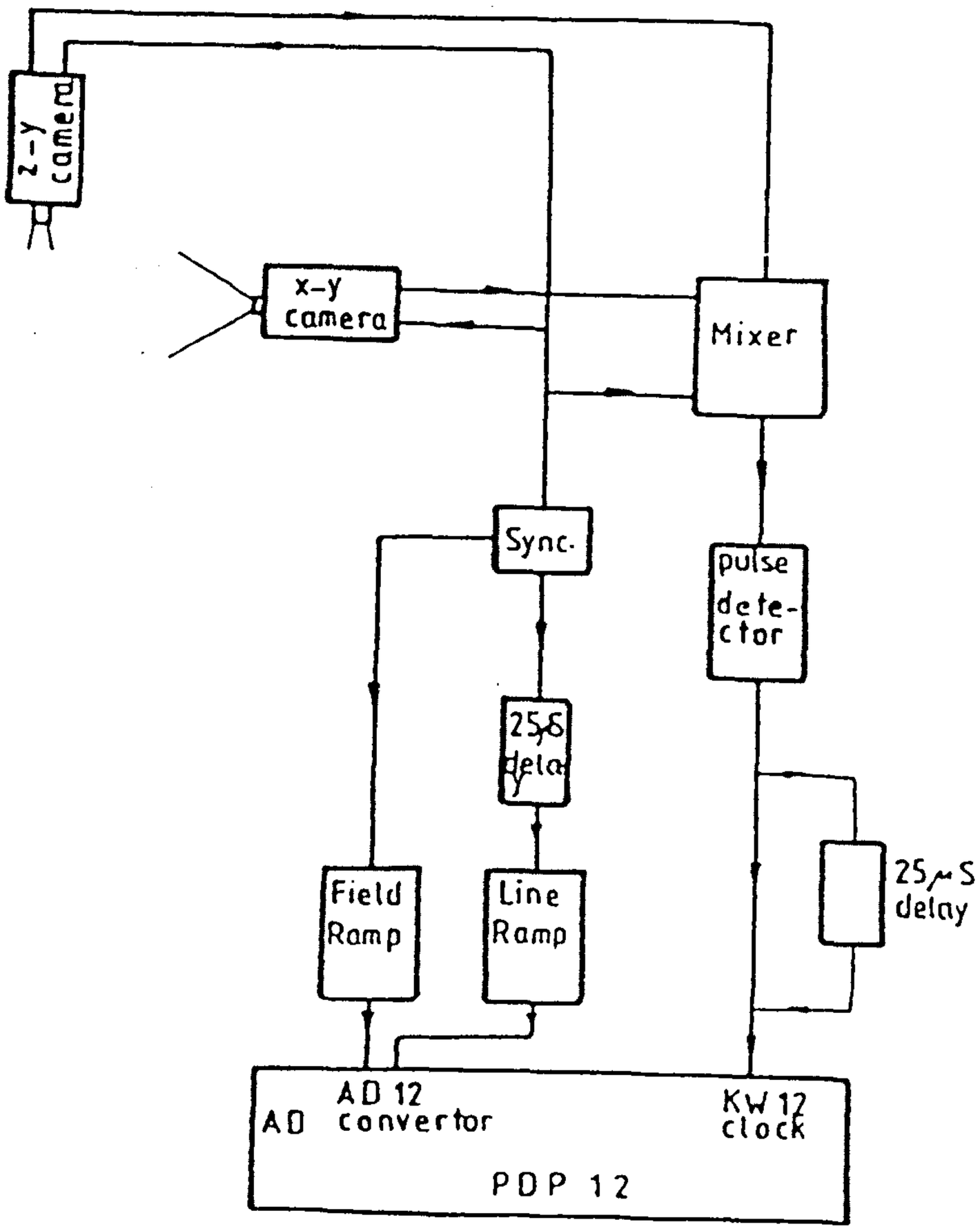

Fig.2.5 block diagram of 3-D TV-computer system.
(from Jarrett, 1976)

absolute marker co-ordinates, several large spatial markers were positioned at equi-spaced intervals along the walkpath behind the subjects. The video signal was first recorded by a video recorder and then re-played through the computer interface. A typical line printer output of a converted field matrix is shown in Fig. 2.4. Only 2-dimensional analysis can be performed using this system. This system converts the whole television image so that a computer with large memory is required.

Jarrett (1976) developed a 3-D TV/computer system in Strathclyde University which had a potential use of up to six television cameras, see Fig.2.5. Instead of recording the whole TV field in computer memory as Dinn did, Jarrett recorded only the (X,Y) co-ordinates of the pinlights brighter than the background. The contents of digital counters were sampled at a rate of 50Hz, stored in the buffer memory and transferred to a PDP12 minicomputer during the line blanking period. Up to 6 horizontal co-ordinates could be digitized and stored in a single scan line. It was reported that this system had a resolution of 0.1% and 0.3% for the horizontal and vertical data, respectively. However only a two-camera system was installed at that time. Andrews (1981) introduced several improvements to the system and, as a result, the third camera was installed and the system can be used in a daylight.

Jarrett (1980) re-designed the system for a PDP11 computer and it is now commercially available under the name 'VICON' (Oxford Medical Systems Ltd, 1980).

The calibration of the VICON system and its performances was assessed by Whittle (1982). A stationary marker was sampled for 20 frames and the frame-to-frame variance was found to be 2mm or less. The accuracy for relative measurement was assessed by comparing the measured distance between two markers with that calculated. It was found that the deviation was 2.6mm. Long-term stability was assessed through a 6 hour study and it was found that after 1.5 hours the standard deviation did not change significantly, although there was drift in the absolute co-ordinate of about 1mm per hour. The overall accuracy of the VICON system was assessed to be 4-5mm of standard deviation at a camera-to-subject distance of 4m.

The most promising advantage of the television-computer system is its ability to automatically manipulate raw data. However, compared with photographic

16a

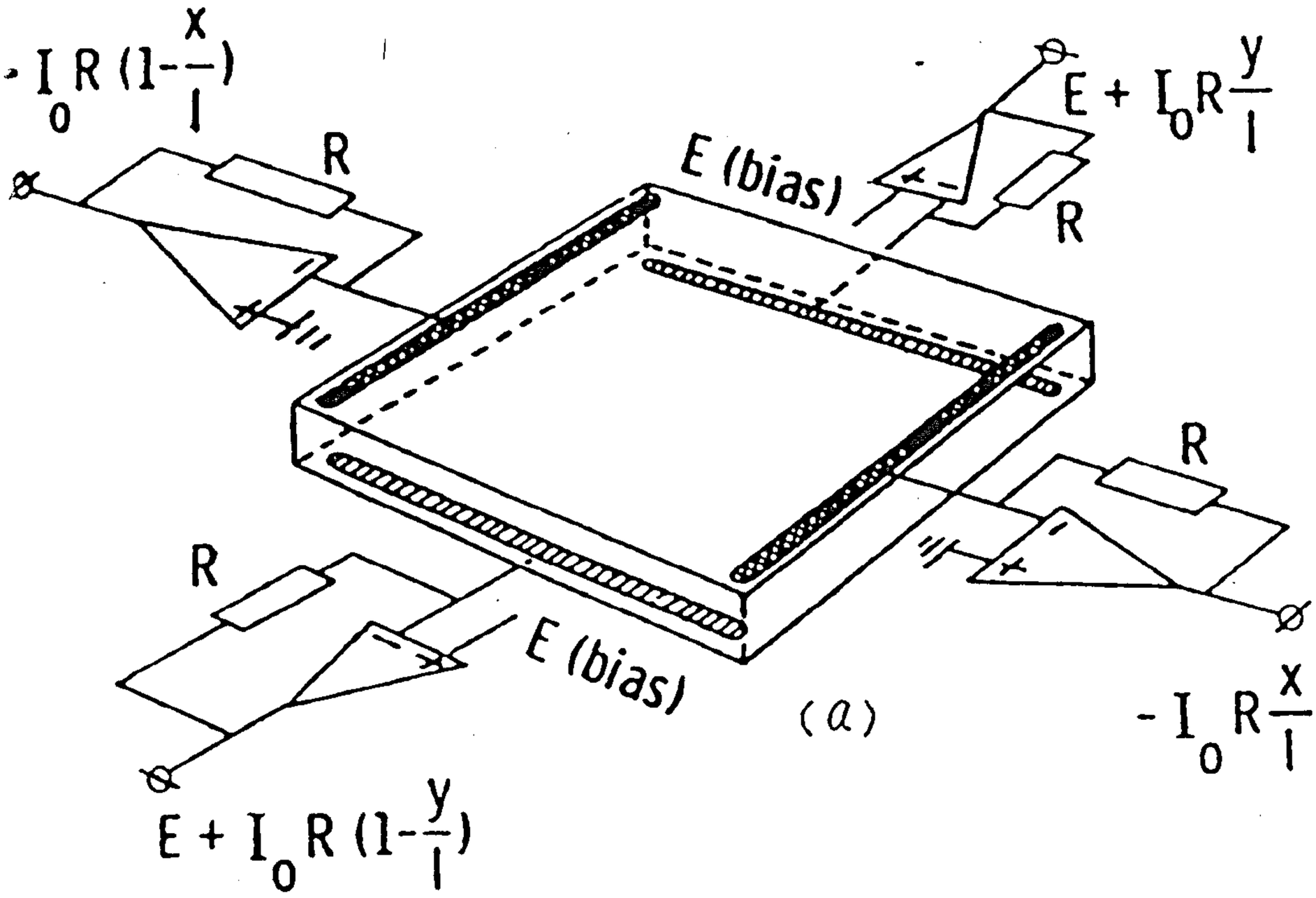

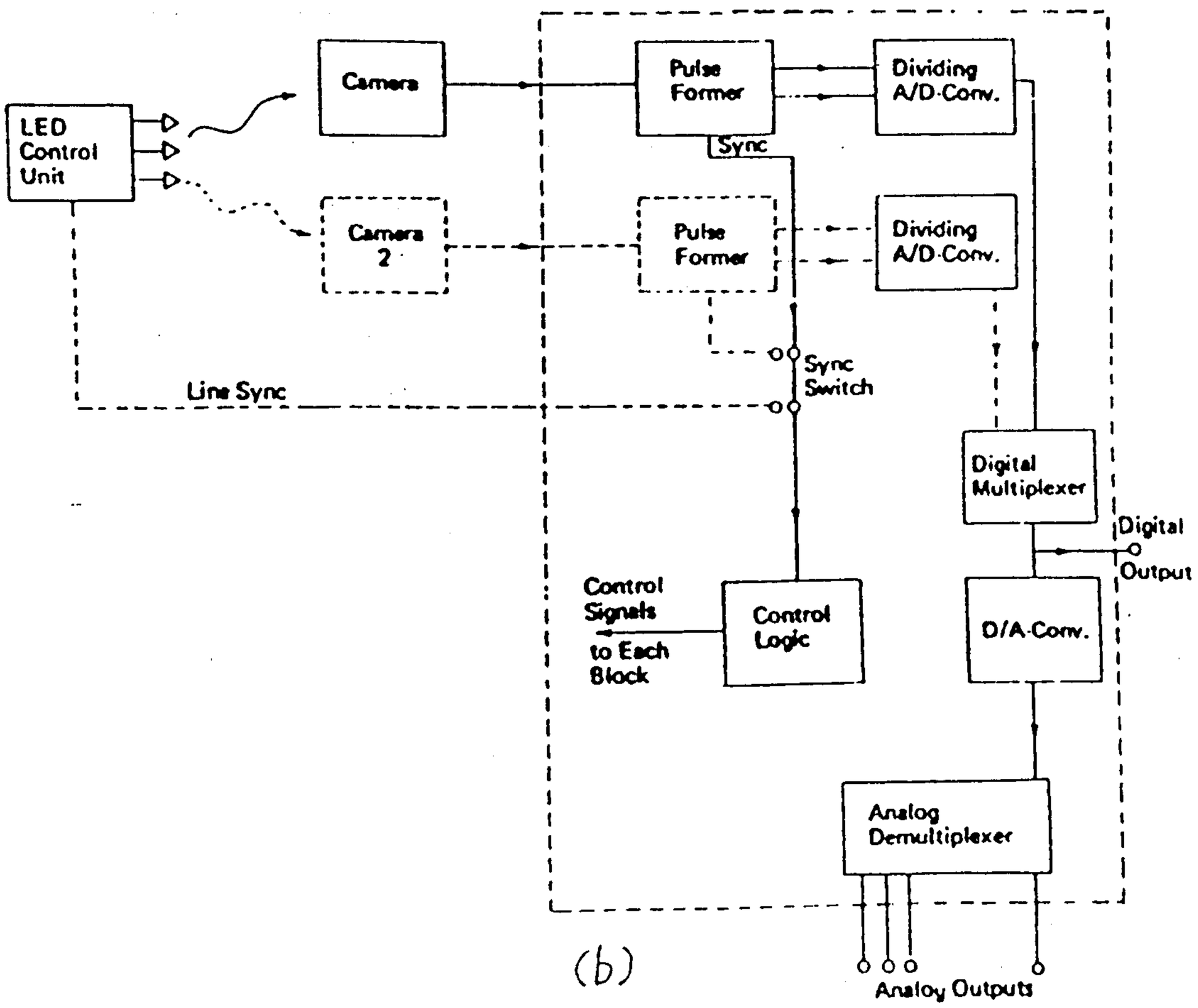

Fig.2.6 The SELSPOT system. (a) Dual-axis, Duo-lateral position sensitive photodiode. (b) block diagram of the SELSPOT system.

techniques, television system suffers from several disadvantages: (1) The interlace scan reduces resolution in the vertical direction; (2) Horizontal and vertical axes have different scales; (3) Installation of the system is very expensive.

The SELSPOT system

SELSPOT is an acronym for 'selective light spot recognition'. This system was originally designed by Lindholm (1974) based on a continuous light spot position sensor developed by Wallmark (1957) and marketed by Selcom (1975) under the name of 'SELSPOT'. The position sensor is basically a large area silicon photo-diode which gives an electric output signal proportional to the two dimensional average position of a light spot on the sensor surface. The markers used in the system are specially developed multichip, high power, infrared LED's. An optical filter matched to these LED's is fitted over the sensor lens to suppress background illumination. By means of a timing-multiplexing technique, the LED's give short bursts of intense infrared light in turn from each LED so that there is no problem with co-ordinates marker identification, making the system potentially viable for clinical use. Up to 30 markers can be sampled at a frequency of 322Hz.

The resolution of the system is largely dependent on the light intensity to noise ratio in the analogue processing circuitry. Woltring and Marsolais (1980) found that the signal to noise ratio decreased when the LED's moved further away from the camera. They obtained a resolution of better than 0.1% for a field width of 3m at an object distance of 6m.

Paul and Nicol (1981) conducted a test to assess the usability of SELSPOT in biomechanical data acquisition. It was found that 'stray' reflection error due to the high light power of the LED's used was very substantial and that the peripheral image was unstable. Moreover, it was difficult to attach the LED'S to some anatomical landmarks. They concluded that the use of the SELSPOT system for routine biomechanical measurement was quite difficult.

Perhaps due to the difficulties involved, not many references were found in which the SELSPOT was used to acquire motion data. Stokes (1984) reported experiments using the SELSPOT system for obtaining the 3-D kinematics of the

17a

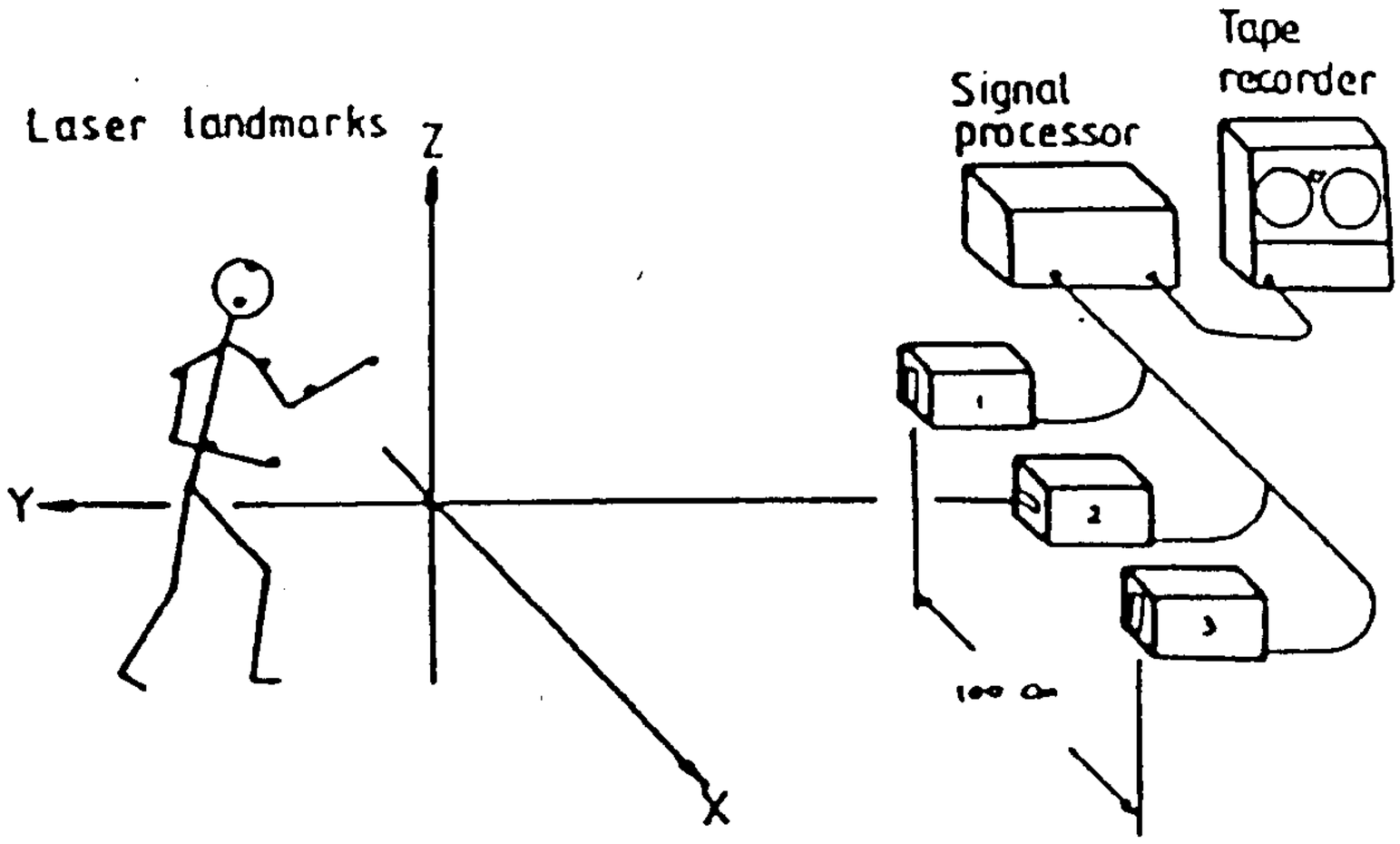

(a)

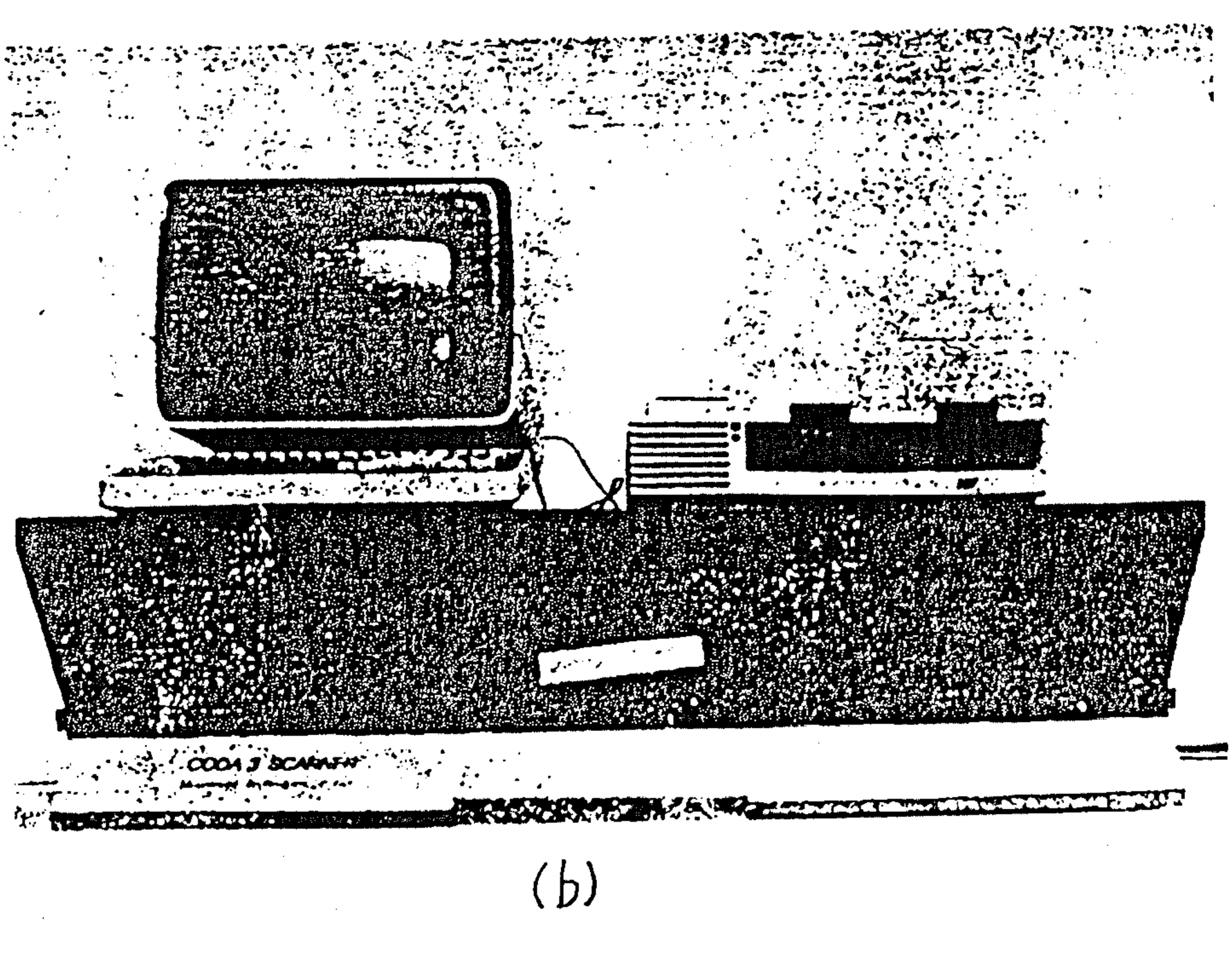

(b)

Fig.2.7 The CODA system. (a) Schematic representation of the system arrangement (from Mitchlson,1975) (b) Main components of CODA-3 (from Towle, 1986).

pelvis and thorax during locomotion. The accuracy of the system was tested statically and dynamically. It was found that the static overall accuracy was about 5mm, dynamic translation resolution 4mm and dynamic angular resolution 2 degrees.

The CODA-3 system

The CODA system, a Cartesian Optoelectronic Dynamic Anthropometer system, has several versions. It was first proposed by Mitchelson (1971) named CODA-1, and later re-designed and marketed under the name of CODA-3. This system uses passive prism markers made from glass and mirror in the shape of a pyramid, each being identified uniquely by a colour filter. The scan unit, the main part of CODA-3, consists of three mirrors, two placed horizontally and one vertically, which produce three fan shaped beams of white light which sweep cross the field of view. The prisms reflect brief pulses of light back along the emitting path, these then being detected by photo-detectors in the scanner unit. The position of a marker is derived from the phase measurement between mirror rotation and the returning pulse, and it is available in both analogue and digital forms. The system can detect 12 markers simultaneously at a maximum frequency of 300Hz. The vertical and transverse resolution of this system is specified as better than 1:8000, and the resolution along the longitudinal axis is specified as better than 1:1600 when the scanner-object distance is 5 metres. The system was used successfully by Towle (1986) to measure the knee joint kinematics during walking.

§2.4.2 Direct measurement techniques

Only two direct measurement techniques are reviewed in this section: Goniometry and Accelerometry. In these techniques the measuring element is directly attached to a subject so that the movement of the underlying element can be monitored. Since a relative system of reference is used in these techniques, no information about where a segment actually is can be obtained, which is one of the major drawbacks associated with these methods.

§2.4.2.1 Goniometry A protractor goniometer used in orthopaedic

18a

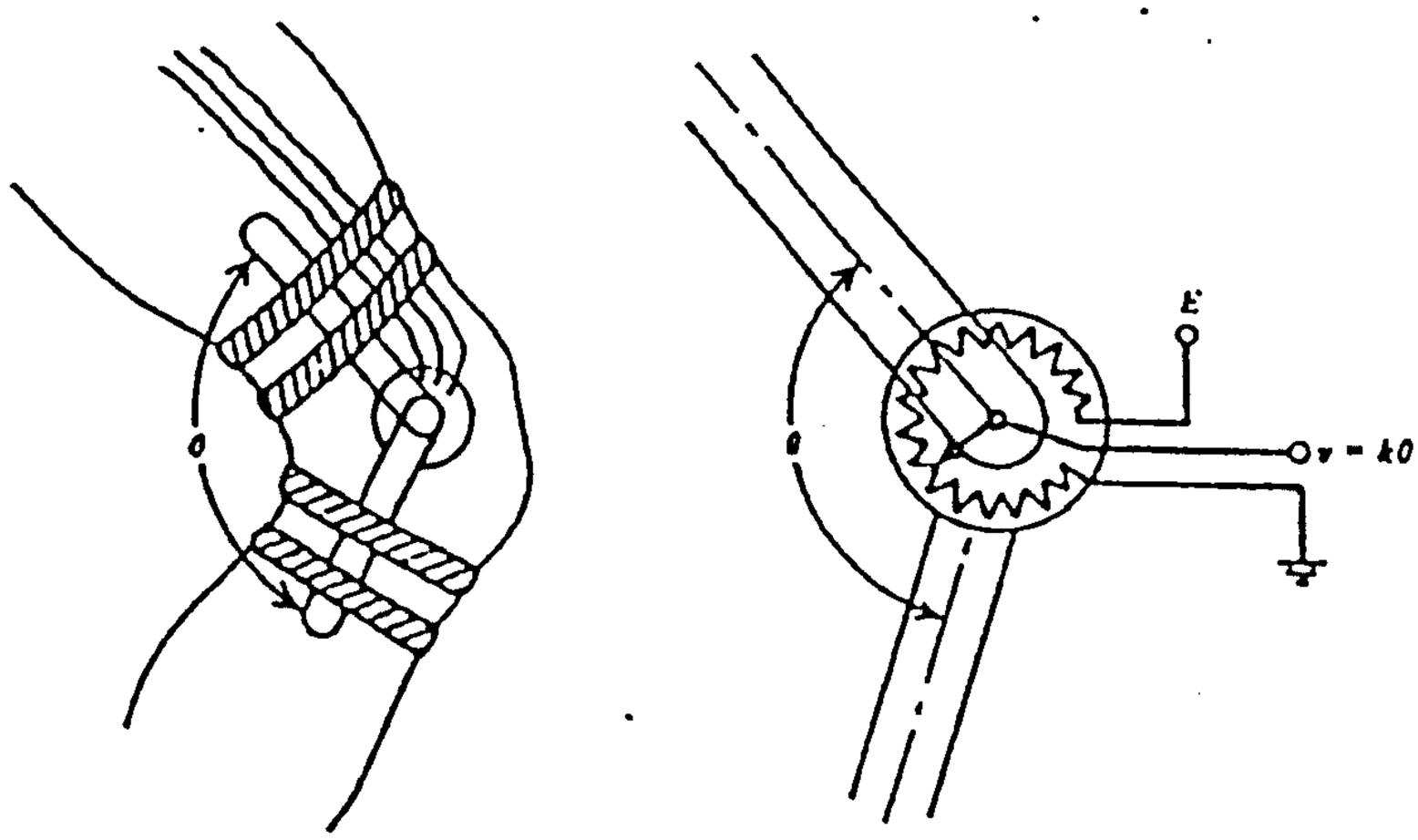

Fig.2.8 A simple planar electrogoniometer.
(from Winter, 1980)

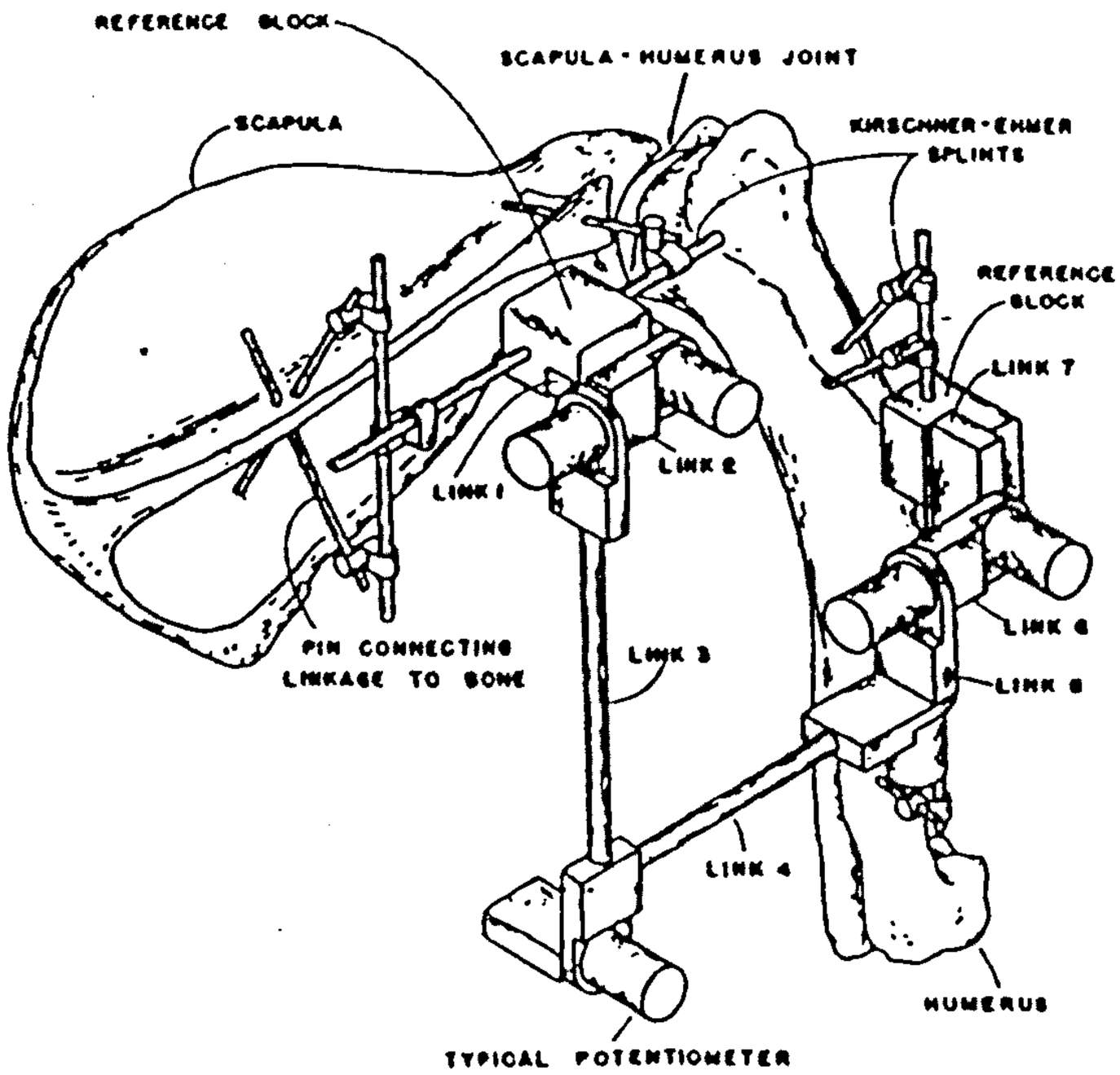

Fig.2.9 An electrogoniometer system with 6 degrees of freedom. (from Kinzel et al, 1972)

examinations is the simplest form of goniometer but it is not particularly useful in comprehensive gait analysis as only passive movement can be measured with it it. Therefore two other kinds of goniometer, that is, electronic and polaroid goniometers, will be discussed here.

Electrogoniometer

A simple electrogoniometer consist of an electrical potentiometer fixed to an arm with its spindle fixed to another arm. When used for measuring, the axis of the potentiometer is aligned to the joint axis and the arms are firmly fixed to the adjacent segments, as shown in Fig.2.8. Because of its single-axis feature, this device is commonly used only when very accurate measurement is not required.

Johnson and Smidt (1969) reported a triaxial electrogoniometer.used for measuring hip joint movement. The goniometer consisted of three potentiometers, each of which was aligned to be in one of the three primary planes. The proximal arm of the goniometer was fixed firmly to a pelvic belt while the distal arm was placed through a hole in the metal collar attached to the suprapaella cuff. In practice, considerable effort was required in adjusting the axes of the potentiometer to be coincident with the anatomical axes of the hip joint.

Errors due to misalignment of the goniometer were assessed by Chao *et al* (1970). The electrogoniometer assembly, the hip joint and the femur constituted a closed 7-link spatial mechanism and the motion of the linkage was theoretically solved, by the analytical method of 4×4 matrix originated by Denavit and Hartenberg (1955), with 3 input motion being defined from potentiometers attached to the goniometer linkage. As the femur was one of the segments in the 7-linkage, the theoretical angles of the femur were thus obtained and compared with the data from the goniometer. It was found that less than 5 degrees of error at any point in the walking cycle for a normal subject existed.

Kinzel *et al* (1972) described a goniometer system which was capable of measuring movement with six degree of freedom, that is, three rotations and three translations, see Fig.2.9. Based on a relative kinematic analysis of two rigid bodies, the movement of rigid body-1 relative to rigid body-2 was represented as a rotation about and a translation along the so-called screw axis fixed in body-2. A 7-bar

Fig.2.10 A flexible electrogoniometer in use.
(from Nicol, 1987)

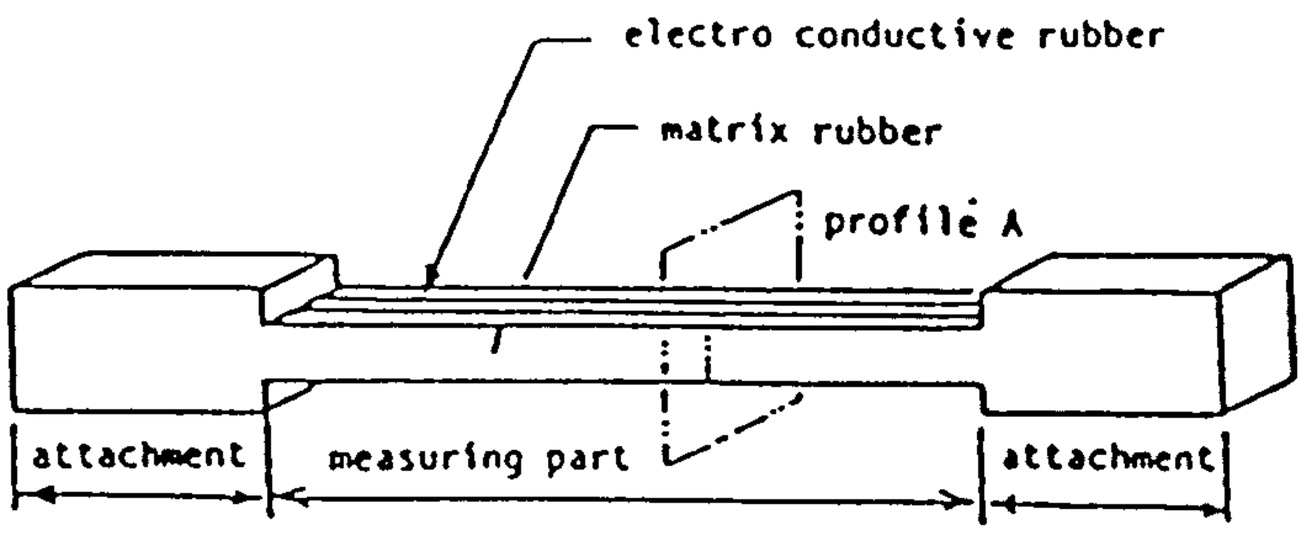

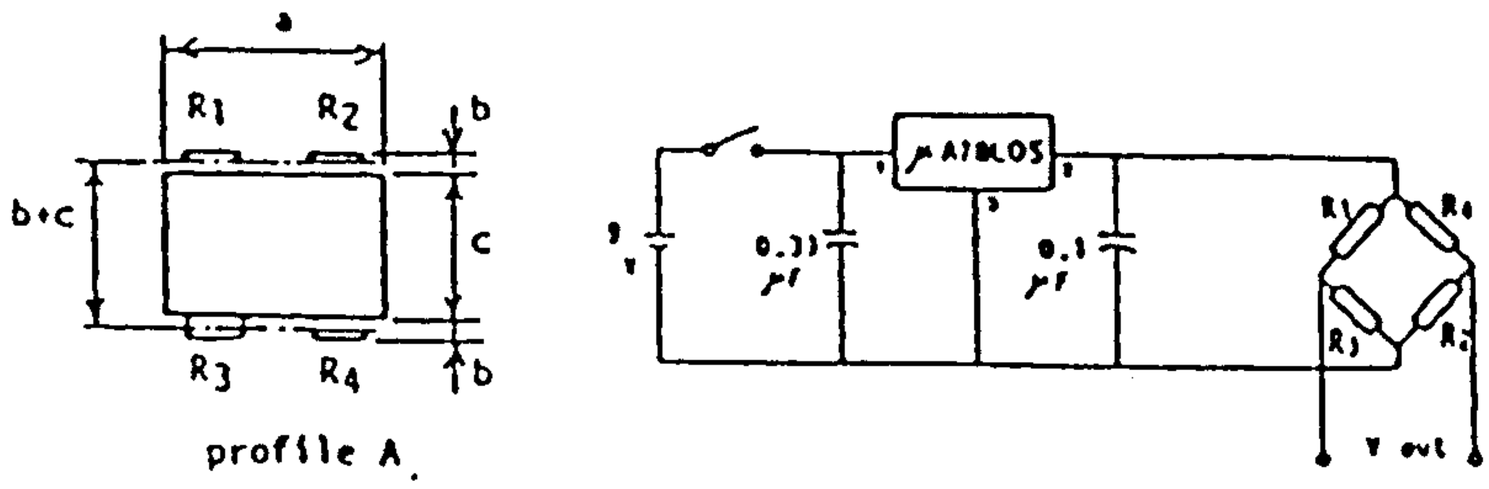

Fig.2.11 Schematic representation of a flexible electrogoniometer. (from Morimoto et al, 1987)

linkage with 6 revolute and cylindrical joint was constructed and precision potentiometers were used to monitor the six variable angles of the linkage. The two end members of the linkage were fastened rigidly to the two segments under consideration. The system was applied to a dog's shoulder. No data about the accuracy of the system were given. This system is attractive in that much more extensive information about the motion permitted by a given joint can be obtained than possible from conventional goniometers, but the absence of one-to-one correspondence between any of the potentiometer angles and the angle usually associated with the joint motion makes its usefulness limited.

Nicol (1987) reported a flexible type of electrogoniometer which consisted of a narrow steel foil fitted with a long strain gauge, as shown in Fig.2.10. This device has a resolution of 0.02 degree and a very good linear relationship between the electrical output and the angles subtended between one encapsulated end and the other. A similar device was described by Morimoto (1987). Four parallel thin beams made of electro-conductive rubber are attached at each end to an elastic rubber and they form a Wheatstone bridge circuit, see Fig.2.11. The total amount of elongation of each beam changes in proportion to the angle between both ends. The unique feature of these two devices is that the measurement of the angle is independent of the bend curve.

Polaroid goniometer

Polaroid goniometers were developed independently by Reed & Reynold (1969) and Grieve (1969) almost at the same time. Mitchelson (1975) also reported a similar polaroid goniometer, see Fig.2.12.

The polaroid goniometer consists of one optical projector, a polaroid screen and as many polaroid receivers attached to the body segments as required. The receivers consist of a polaroid filter to which is attached a photocell that provide a linear current changing with intensity of illumination. The polaroid screen is inserted into the light path of the illuminator and rotates at an uniform angular velocity ω, causing the plane of polarization of the projected beam to rotate. The transmitted intensity of illumination of the polaroid receivers was thus sinusoidal with the same

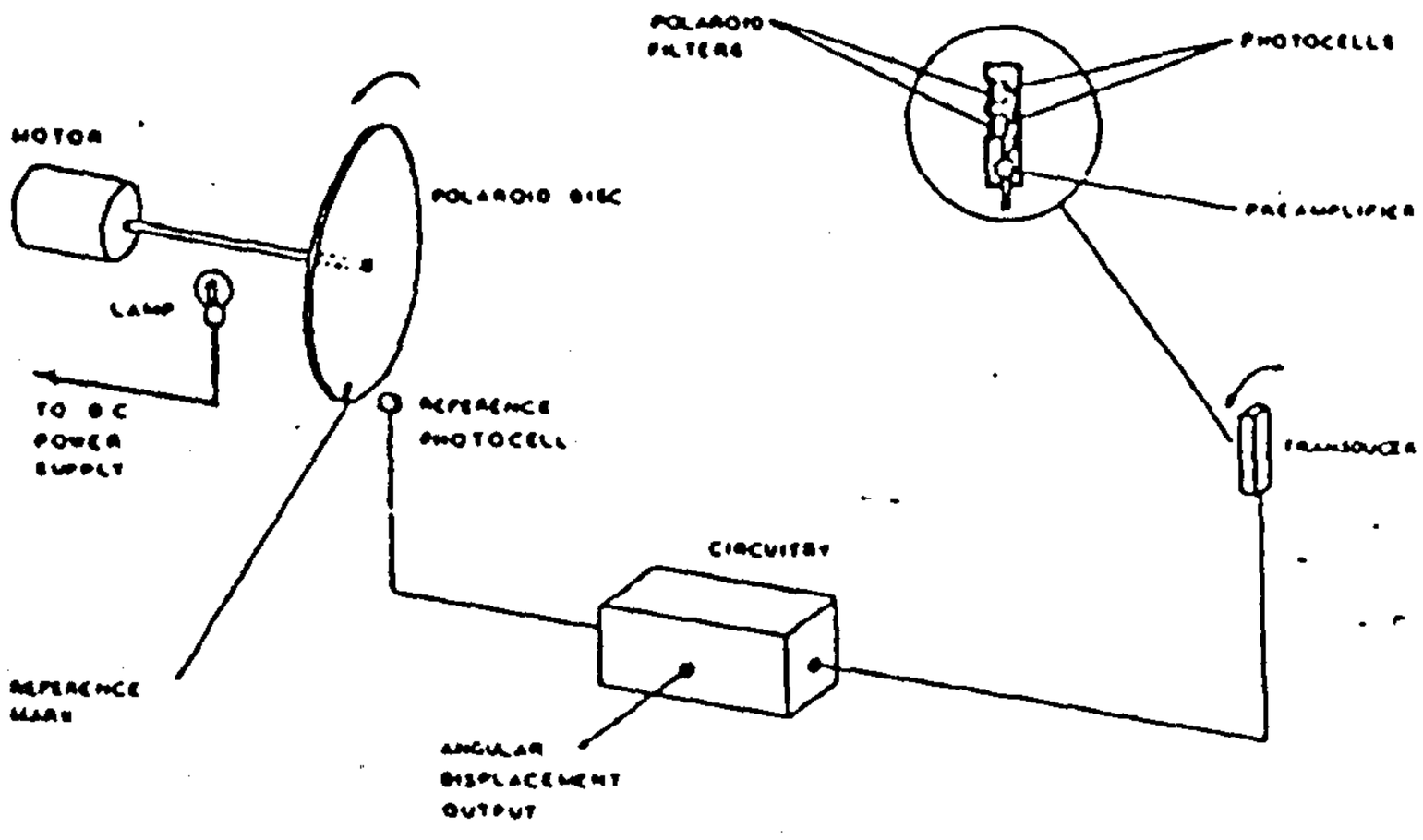

Fig.2.12 Schematic diagram of the polaroid goniometer. (from Mitchelson, 1975)

frequency as that of the polaroid screen but with different phases. An electronic circuit is designed to give pulses when either the plane of polarization of the projector beam is vertical or the currents from the solar cells reach zero. The angle of the receiver to the vertical is measured by timing the interval τ between the output pulses of the screen and the receivers and comparing this with the period of rotation of the screen T, that is $360\tau/T$ degrees. As the absolute angles of any two receivers are known, the relative angles between them can be obtained by simple subtraction. There were no data on the accuracy of the system.

The advantage of the polaroid goniometer over the conventional electrogoniometer would be that it is not necessary to align it to the joint centre. Additionally, as no exoskeleton is fixed to the segments, it is likely less encumbrance during walking.

In summary, the most prominent advantage of goniometry is that a large amount of angular displacement data can be obtained instantaneously without tedious data reduction procedures. Moreover, it is fairly cheap and relatively easy to operate.

However, goniometry suffers some disadvantages. First of all, the accuracy of the system is limited by the accuracy with which the exoskeleton follows the movement of the internal structure. Secondly, attachment of the exoskeleton will inevitably cause some encumbrance to the subject.

§2.4.2.2 Accelerometry An accelerometer usually consists of a mass, a sensor and a kind of "spring" system. As the device undergoes acceleration, the inertial force due to the mass will cause the spring to deflect, and the sensor will detect the deformation and transform it into an electrical signal.

Liberson (1936) was perhaps the first to use accelerometers in human locomotion studies. He used a piezo-electric accelerometer which had a mass, a quartz crystal and a spring system.

Ryker and Bartholomew (1951) described a 3-accelerometer system capable of measuring both linear and angular components. By arranging two linear accelerometers in the same plane, as shown in Fig.2.13, the angular acceleration can

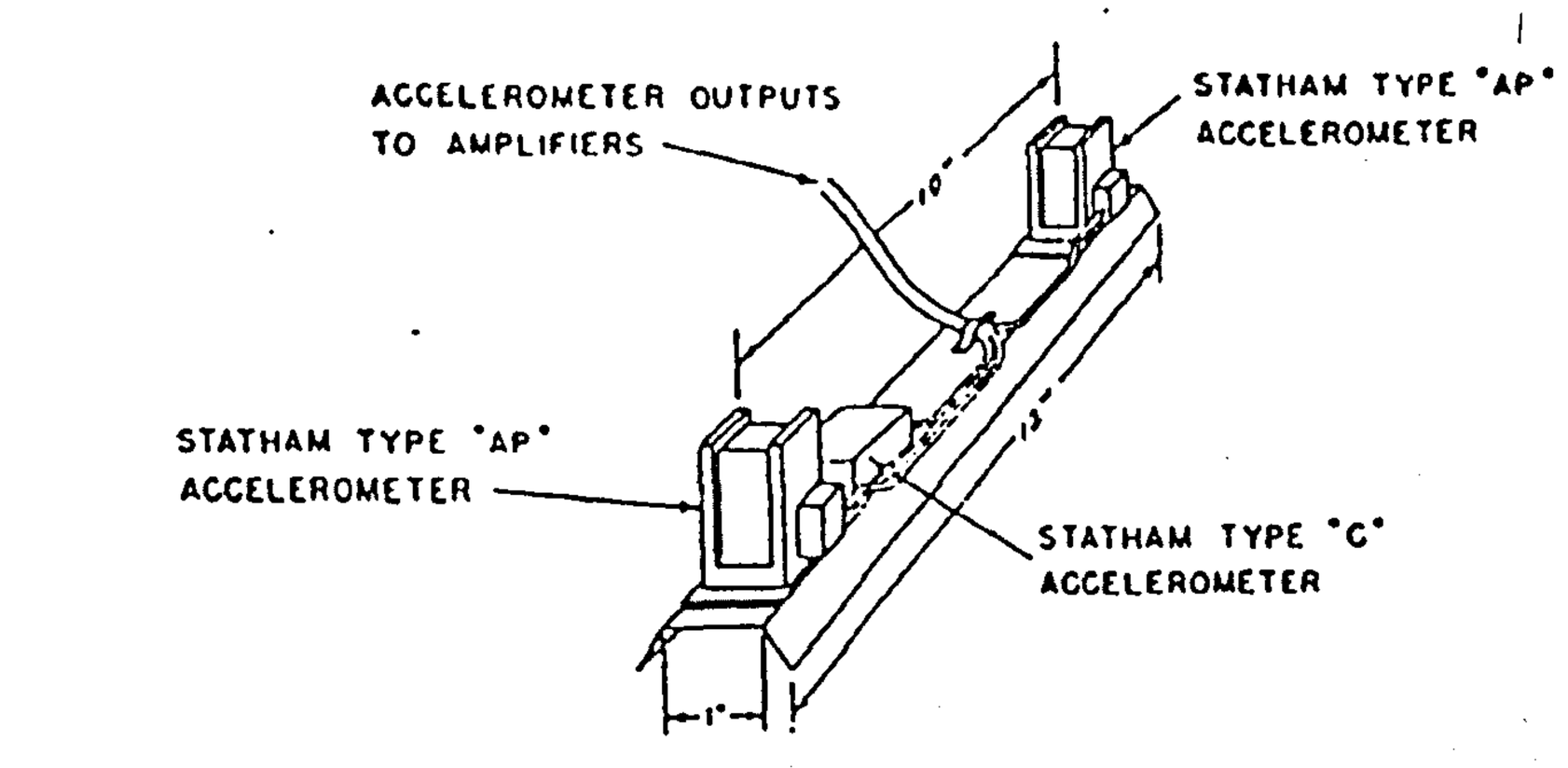

(a) ACCELEROMETER MOUNTING ASSEMBLY

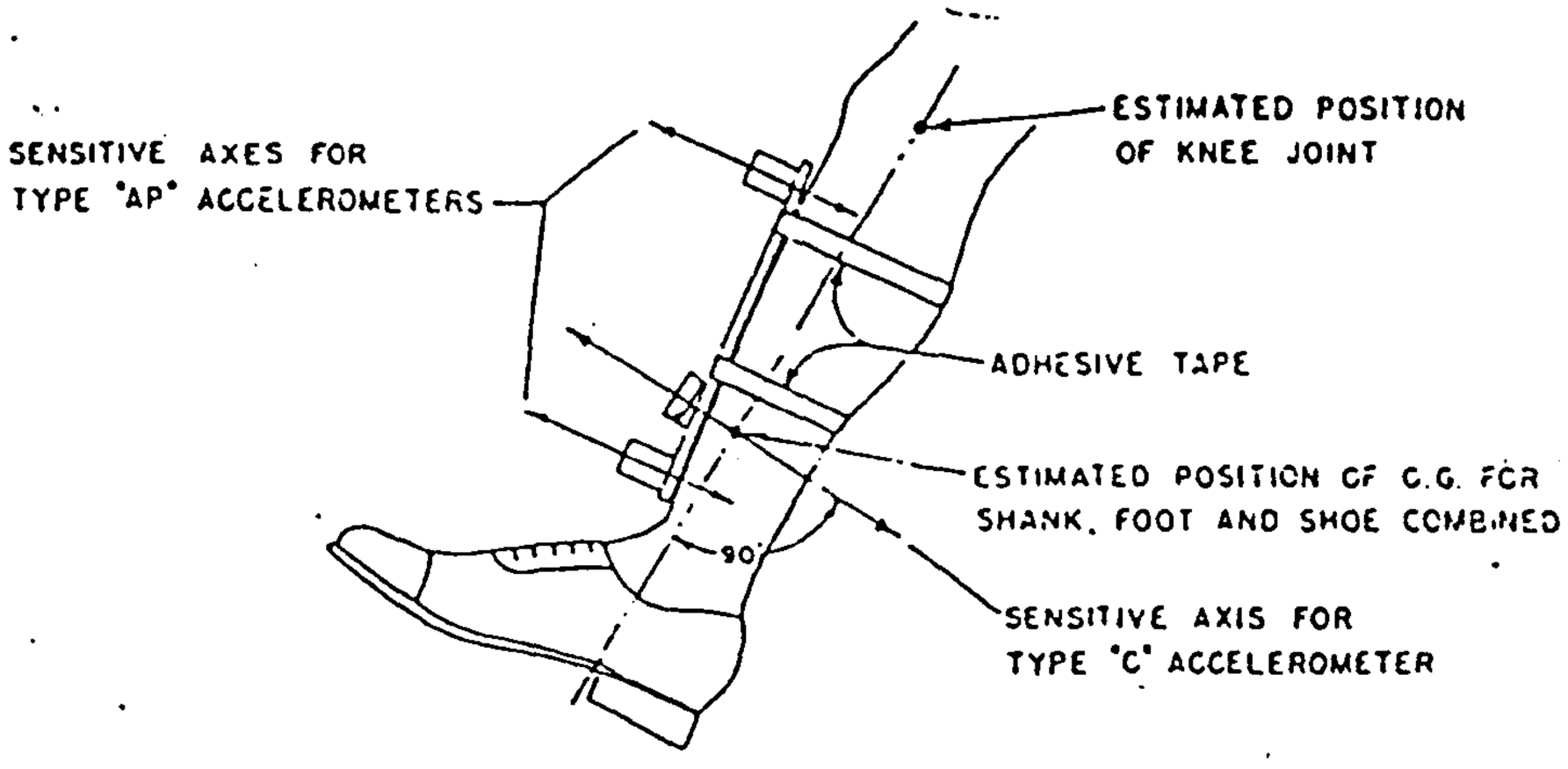

(b) ACCELEROMETER MOUNTING ASSEMBLY ON SHANK

Fig.2.13 Arrangement of the 3-accelerometer system.
(from Ryker & Bartholomew, 1951)

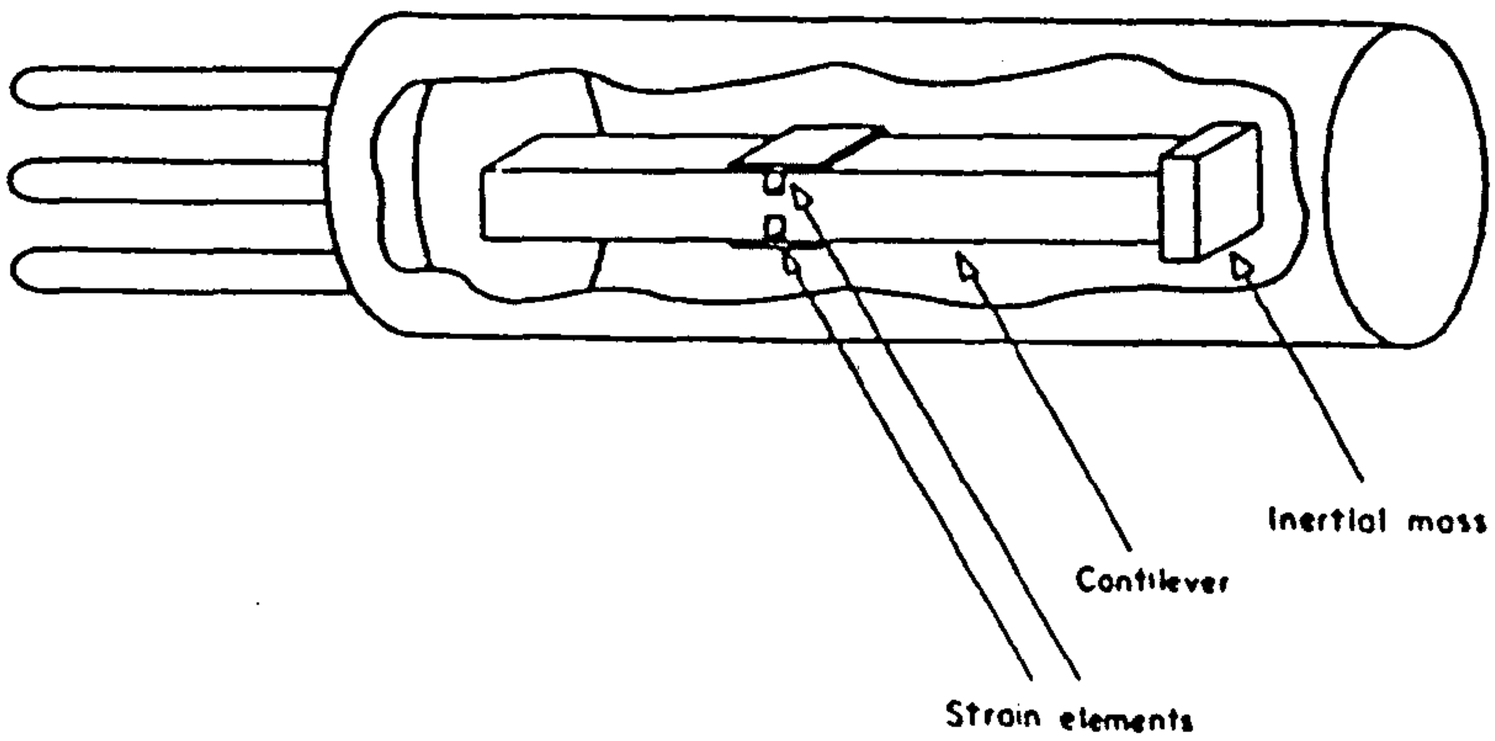

Fig.2.14 Strain-gauged cantilever type accelerometer.
(from Morris, 1973)

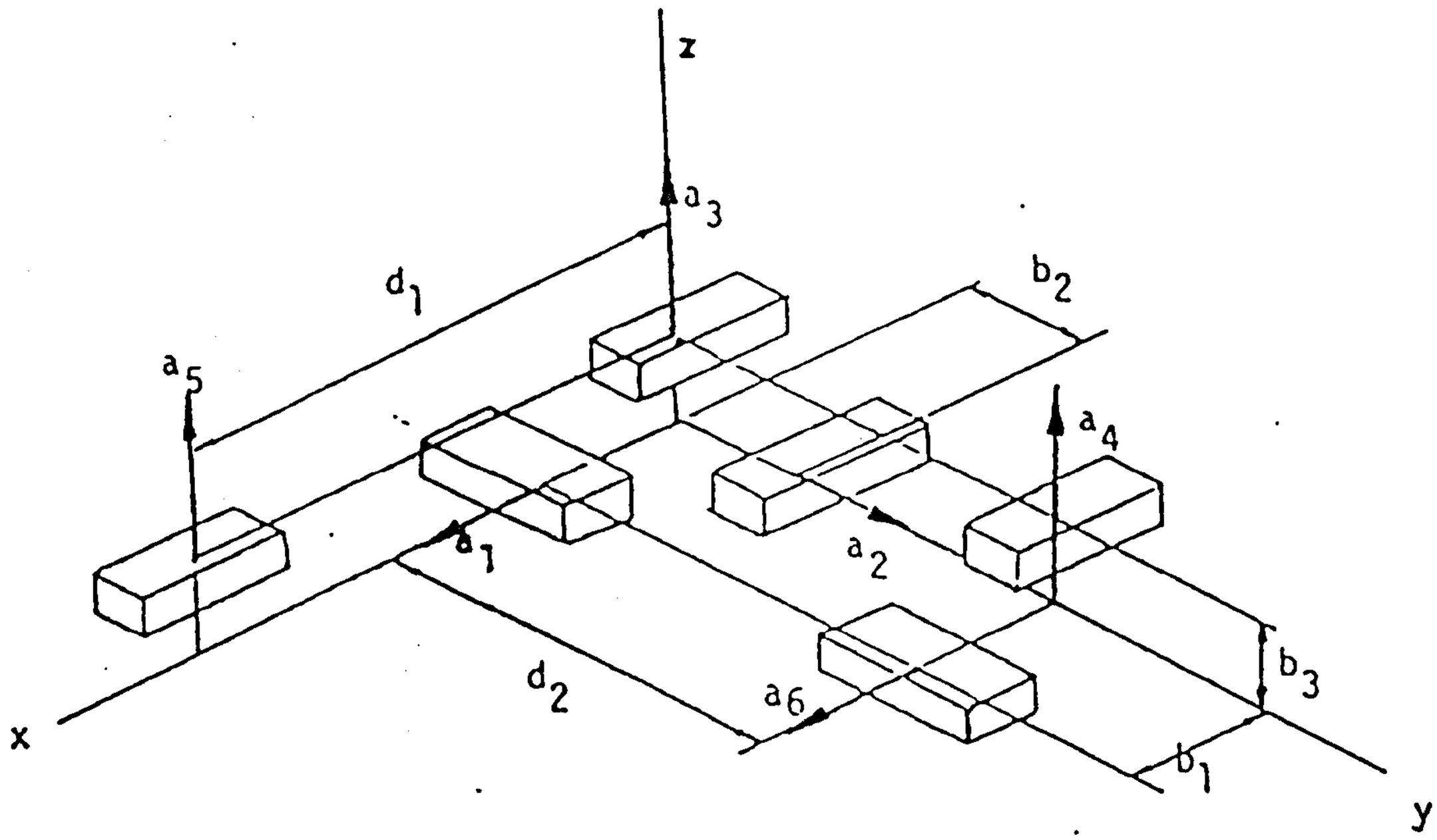

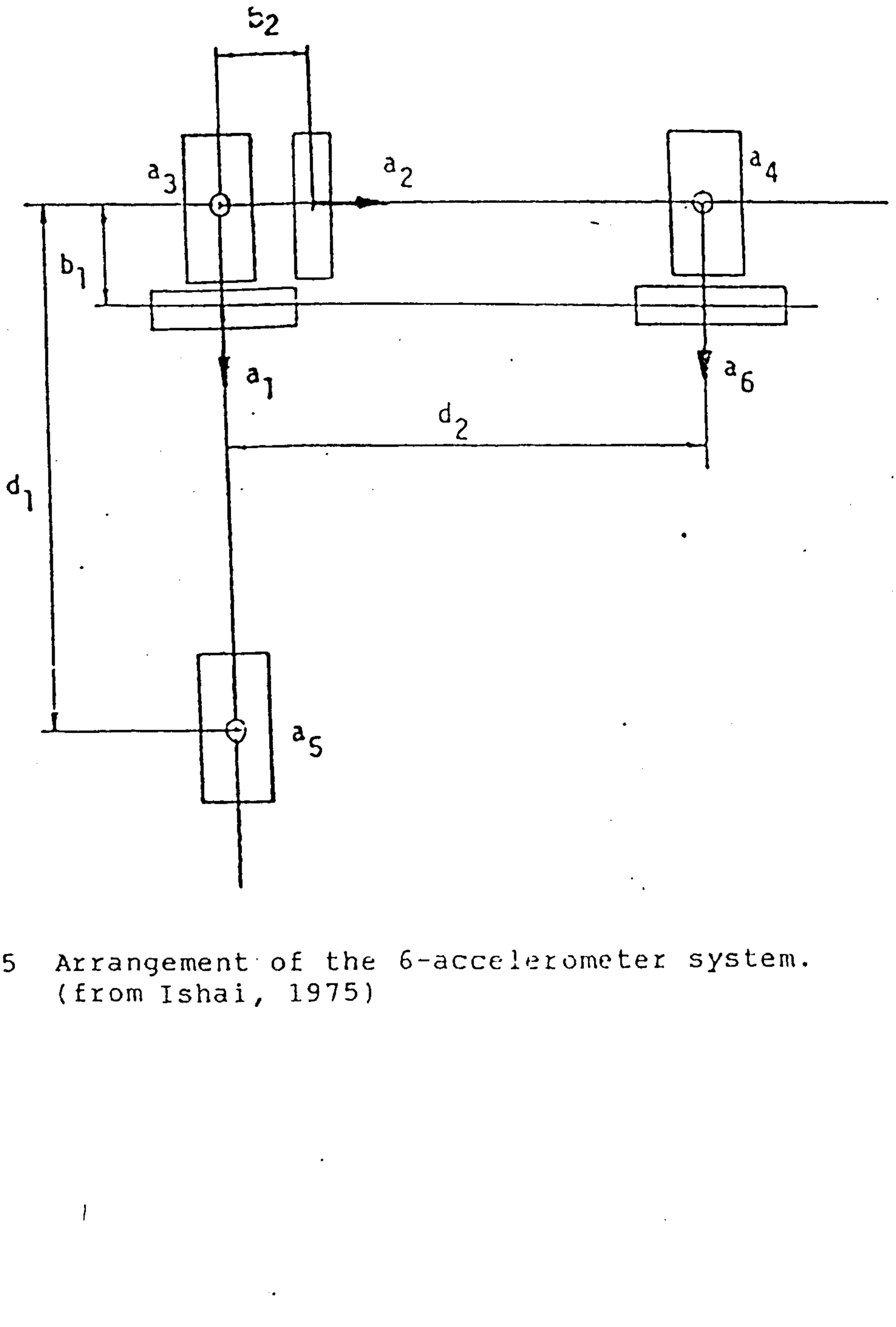

Fig.2.15 Arrangement of the 6-accelerometer system.
(from Ishai, 1975)

be obtained. The third accelerometer is positioned normal to the long axis of the shank at the estimated centre of mass.

Morris (1973) developed a mathematical model for a six-accelerometer system capable of determining the absolute acceleration vector of a point. The mathematical operations included solving for the angular velocity vector followed by calculation of the direction cosine matrix. In applying this new approach to the kinematics of the shank, Morris assumed the absence of transverse rotation of the shank and used a five-accelerometer system. A strain gauged cantilever type accelerometer, as shown in Fig.2.14, was used but the arrangement of the accelerometers on the platform was not specified.

Adopting a similar mathematical model, Ishai (1975) designed a six-accelerometer system taking into account the transverse rotation. The arrangement of the accelerometers is shown in Fig.2.15.

Padgaonker *et al* (1975) described a system using nine accelerometers to minimize error due to cross sensitivity. However, the physical size and weight of the system created considerable inertial effects which might alter the subject's gait. Furthermore, attaching the system to the subject presented difficulties.

The accelerometer has the obvious advantage of providing acceleration data directly without the tedious reduction procedure and potentially erroneous differentiation. However, the method of attachment, especially on soft tissue, the instrument noise and system inertial effect can cause serious problems in the reliability and accuracy of the data obtained.

§2.5 Ground Reaction Measurement Techniques

Gravity and friction enable the muscles to generate ground reaction forces that accelerate and decelerate the human body. These forces are distributed over an area of the foot and can be represented by a three dimensional vector acting on a point called the centre of pressure (the CP). Accordingly, two types of load measurement equipment have been developed, that is, forceplates for measuring the resultant ground reaction forces and devices for recording the pressure distribution.

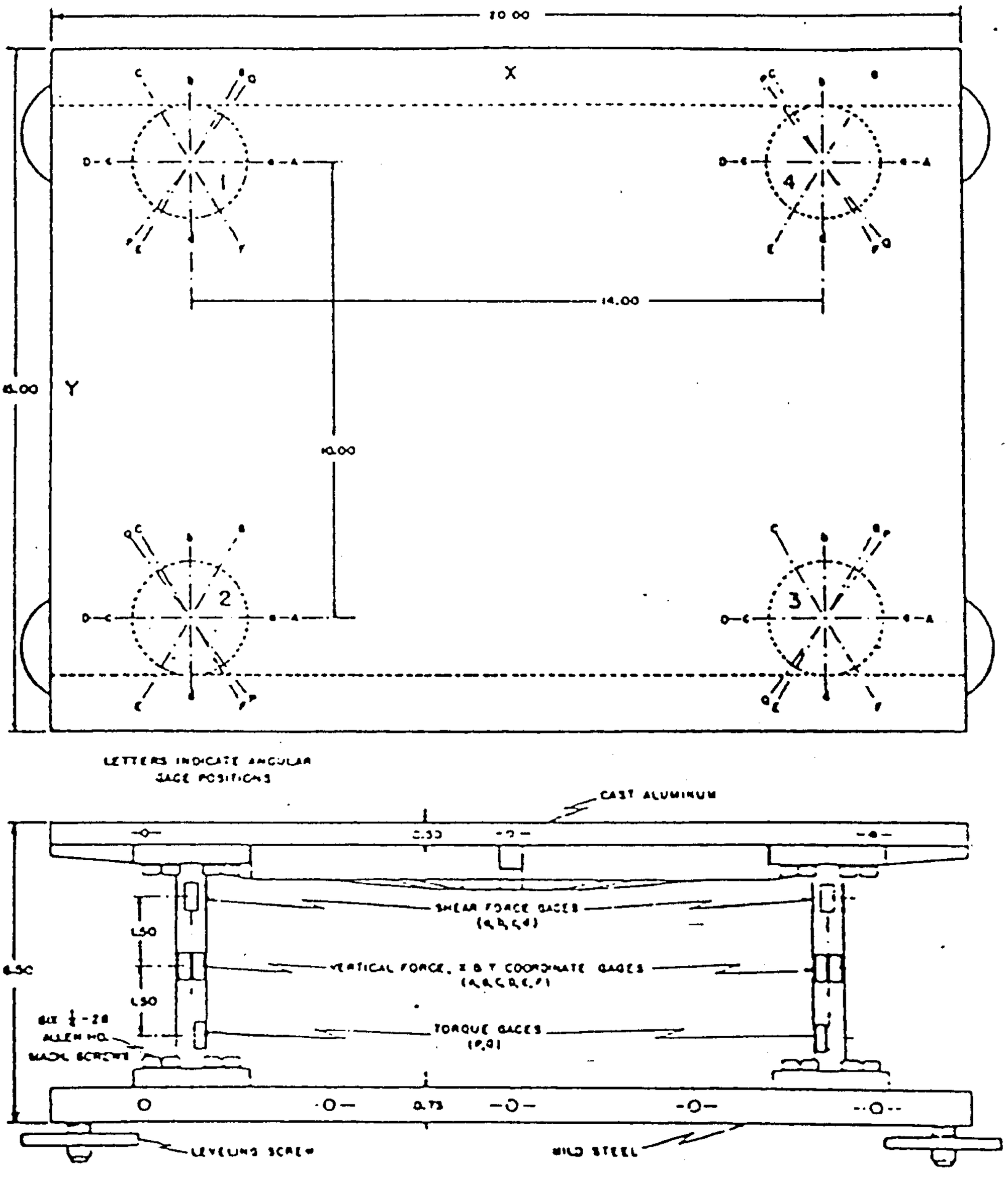

Fig.2.16 Forceplate using strain gauges.
(from Cunningham & Brown, 1952)

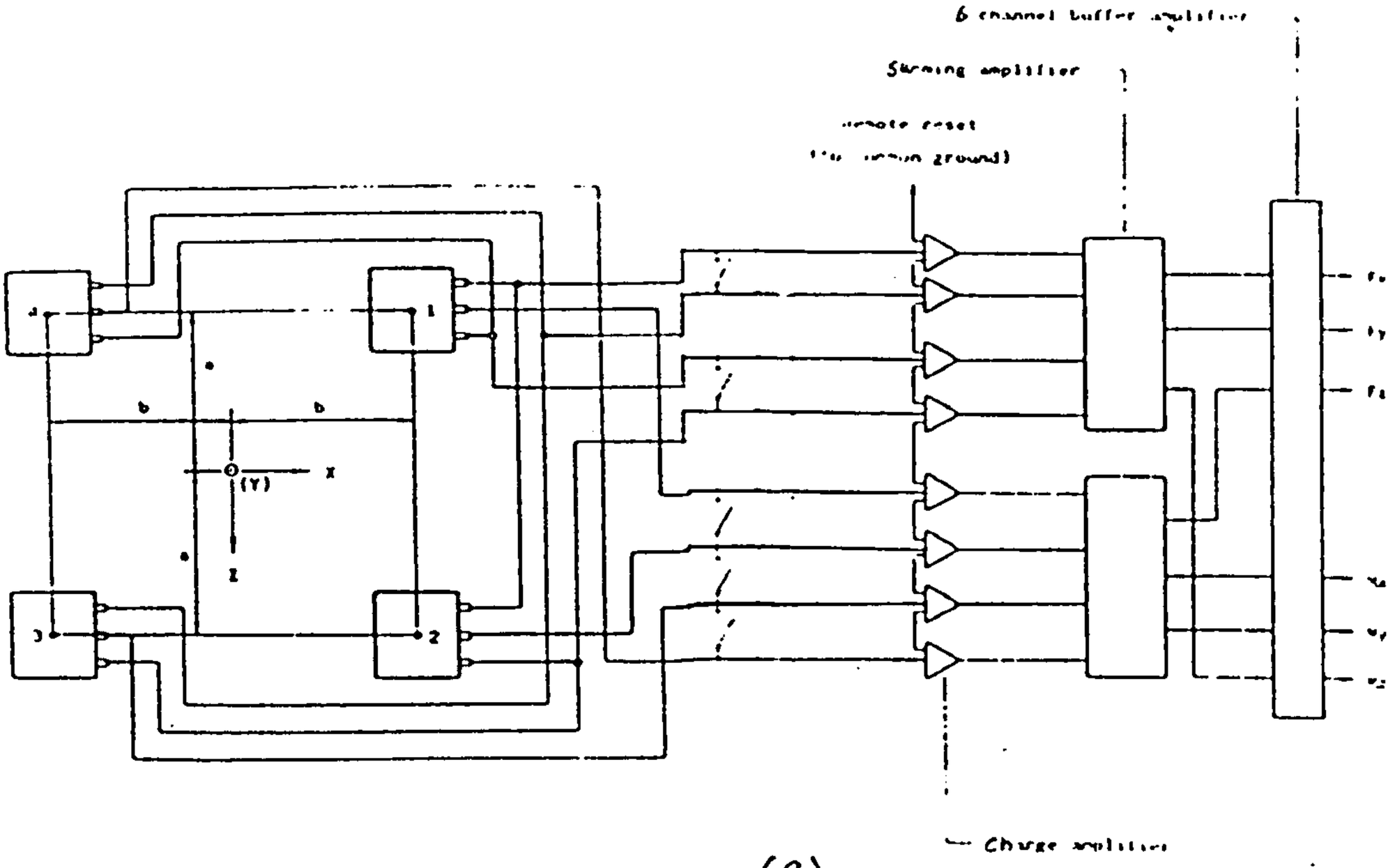

(a)

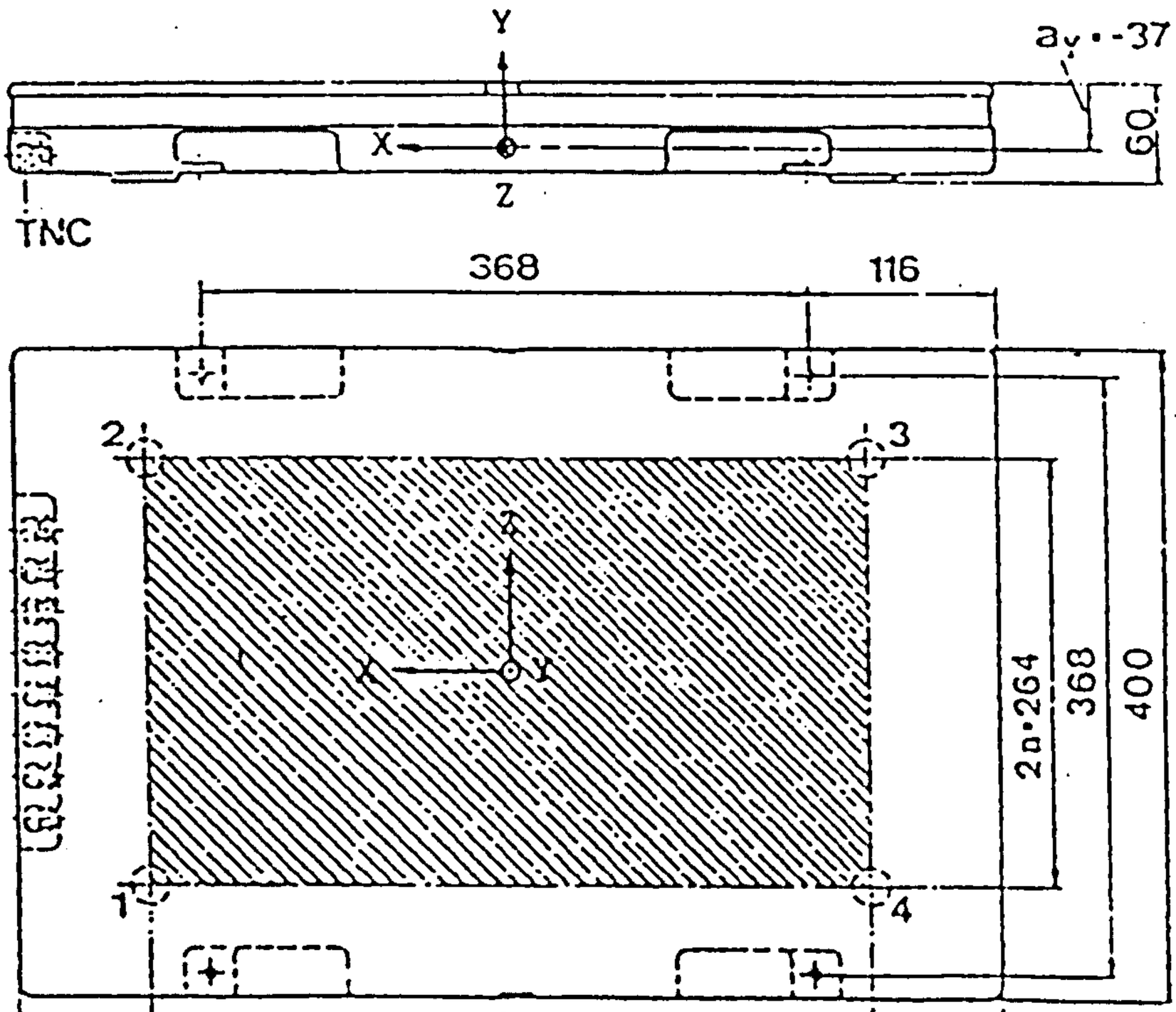

(b)

Fig.2.17 Kistler's forceplate (type 9261A).
(a) Block diagram of the forceplate.
(b) Physical dimension of the forceplate.
(from Goh, 1982)

§2.5.1 The forceplates

Elftman (1939) developed one of the earliest forceplates which operated on a strictly mechanical basis. Stiff springs were used as force sensors. A plate mounted on the springs deflected as forces were applied to it and a level system was used to enlarge the deflection which in turn was recorded on a rotating drum. Although such a mechanical recording system was not capable of accurate response to rapid changes in forces and would not be used now, Elftman's early work did introduce the concept of a forceplate and stimulated further development.

All modern forceplates use transducers to record load actions in terms of electrical signals, such as strain gauges, piezo-electric, and so on.

Cunningham and Brown (1952) reported on a forceplate using strain gauges as force transducers. The two ends of each four specially machined tubular columns were rigidly connected to two rectangular platforms at the corners.Six sets of strain gauges attached to each column sensed three orthogonal forces, the torque about the vertical axis and the location of the resultant force. An natural frequency of 105Hz for shear and 140Hz for vertical forces was cited.

A major difficulty in designing a forceplate using strain gauges lies in the contra-requirements of having high sensitivity and at the same time, high natural frequency. It is difficulty therefore to have a strain gauged forceplate with a natural frequency higher than 150Hz. On the other hand, a piezo-electric sensor is very rigid so that it can be used to make a forceplate having a very high resonant frequency.

The first forceplate using piezo-electric transducers was developed by Lauru (1957). This forceplate consisted of two rigid equilateral triangular platforms with three piezo-electric transducers fitted between them, one on each corner of the platform for measuring the vertical force. The horizontal force was measured by two other piezo-electric transducers at an apex of the lower platform and along one side.

Kistler (1977) marketed a forceplate also using piezo-electric sensors, see Fig. 2.17. A cast aluminum rectangular plate is supported on a platform below it at each corner by a stack of three quartz transducers, corresponding to vertical, fore-aft and lateral forces respectively. By electrically summing and coupling the appropriate components of the transducers, three orthogonal forces and three orthogonal

23a

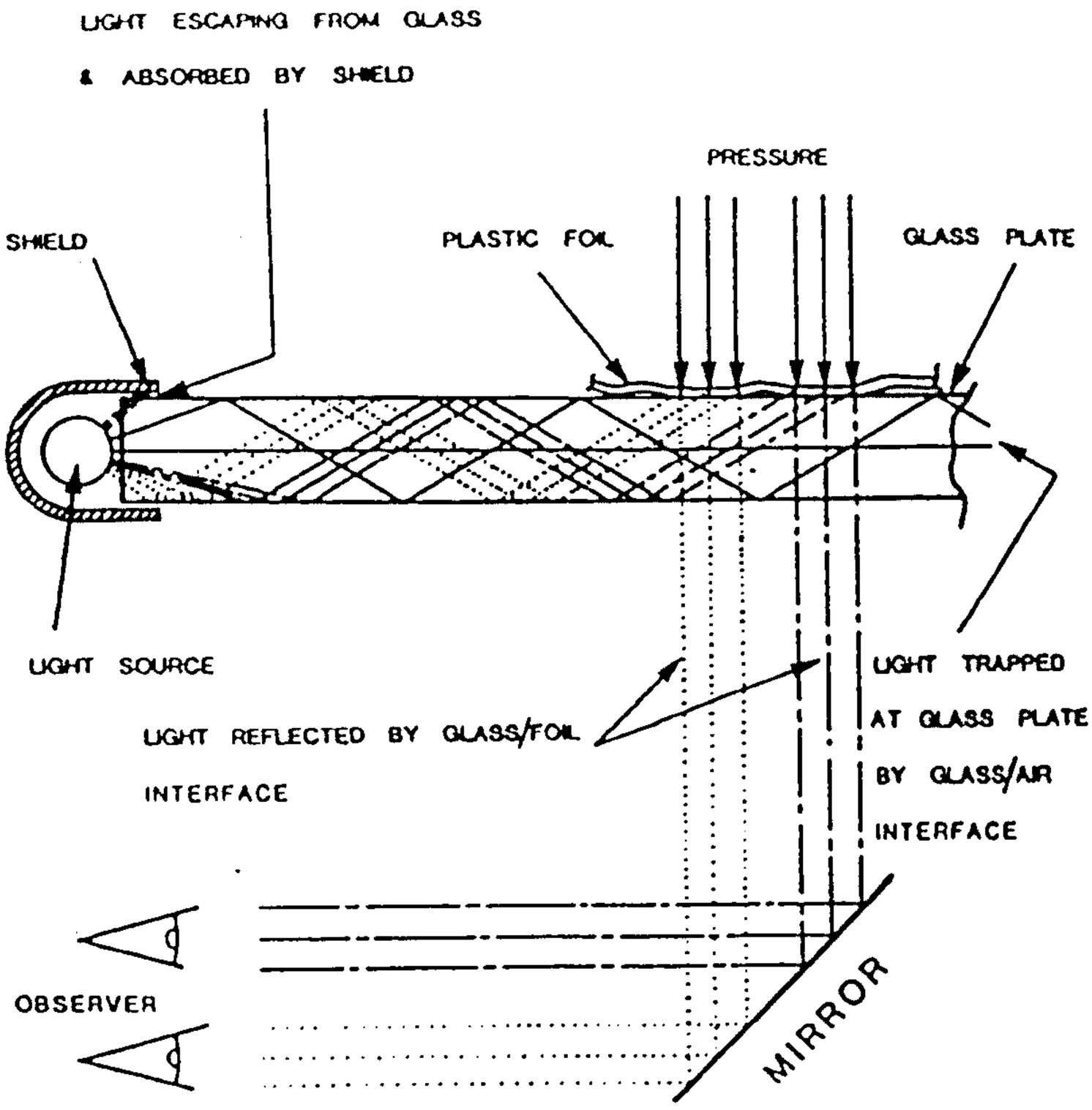

Fig.2.18 Schematic diagram of the Padobarograph. (from Chodera & Lord, 1978)

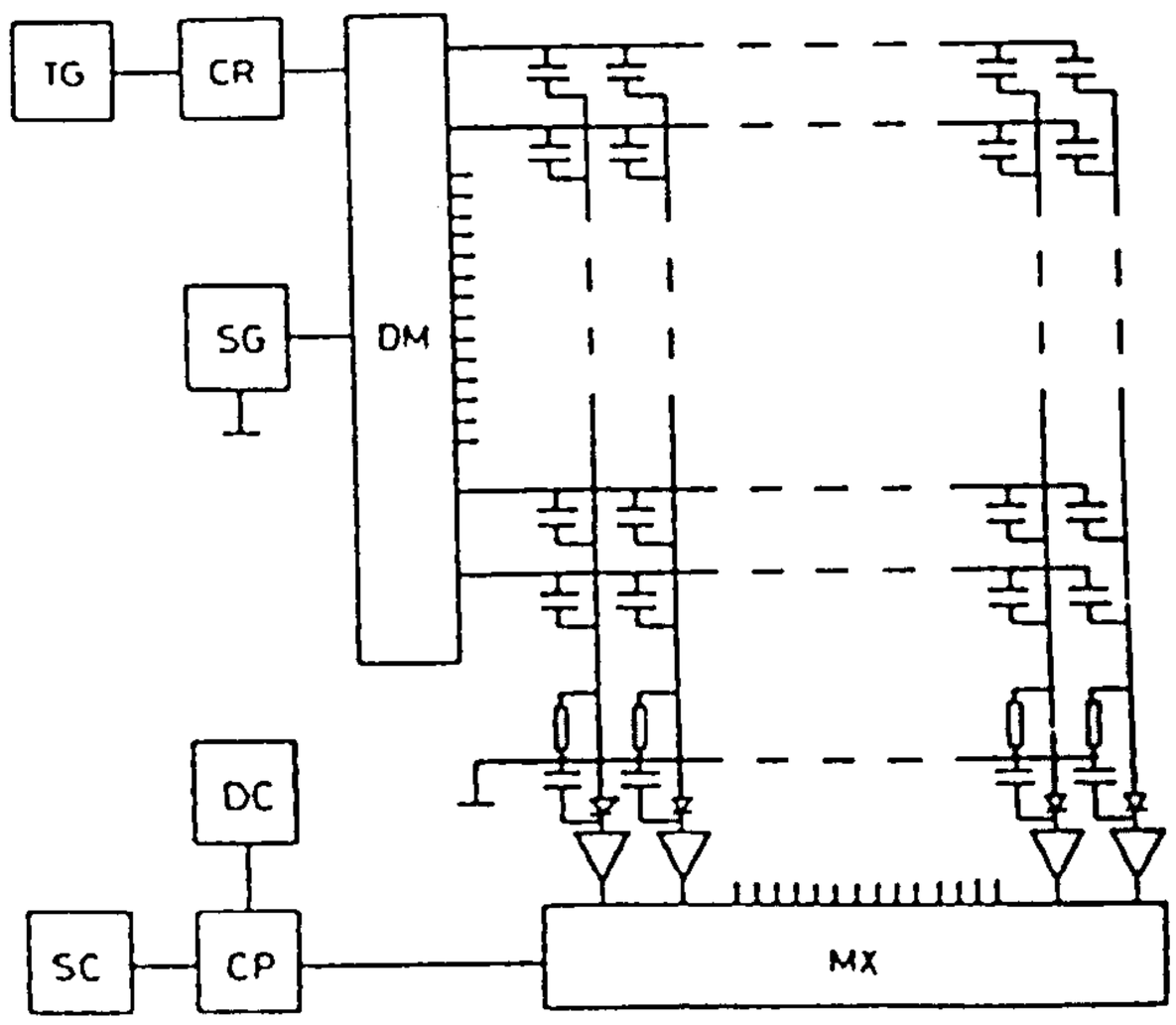

Fig.2.19 Block diagram of the measuring system of Nicol's mat. (from Nicol & Henning, 1976)

moments were produced. The minimum natural frequency claimed by the manufacturer is 200Hz and the maximum "cross-talk" is less than 3%. This system has been widely used in biomechanical research because of its excellent dynamic response characteristics.

§2.5.2 Pressure distribution measurement

Elftman (1934) reviewed early techniques of measurement of foot pressure distribution. He described a system called 'barograph' which consisted of a rubber mat placed over a plate of glass floodlit from beneath. Foot pressure on the mat caused projections on the lower surface of the mat flattened against the glass plate so that the foot print appeared as a matrix of black on a light background.

Chodera & Lord (1978) described a device comprising a flat optically-clear plate illuminated along two opposing narrow edges, see Fig.2.18. The light introduced into the plate was conducted across by a series of internal reflections at the plate/air interface. A plastic foil was placed on the plate and when the subject stood on the plate, the foil contacted the glass under pressure. The conditions for internal reflection were destroyed, and light escaped from the plate to illuminate the under-surface of the sheet, producing a black and white intensity modulated footprint or "pedobarogram". A video camera was used to pick up the direct pedobarogram for display or further analysis.

Nicol and Henning(1976) described a transducer capable of measuring pressure distribution. The transducer consisted of a flexible mat covered with 256 capacitor plates on each side, the capacity of the transducer being recorded via multiplexers. The upper condenser plates were jointed in rows, the lower ones in columns, see Fig. 2.19. An alternating current was intermittently connected to the row by means of a switch ("demultiplexer") and a "multiplexer" was successively connected to all the columns with a measuring resistor while the demultiplexer was in a constant position. Thus each measuring capacitor was an element of a voltage divider. The voltage appearing on the resistor depended on the acting forces. The accuracy of the system was claimed to be good, but no quantitative data were given.

Gerber (1982) described a complete system for measuring pressure

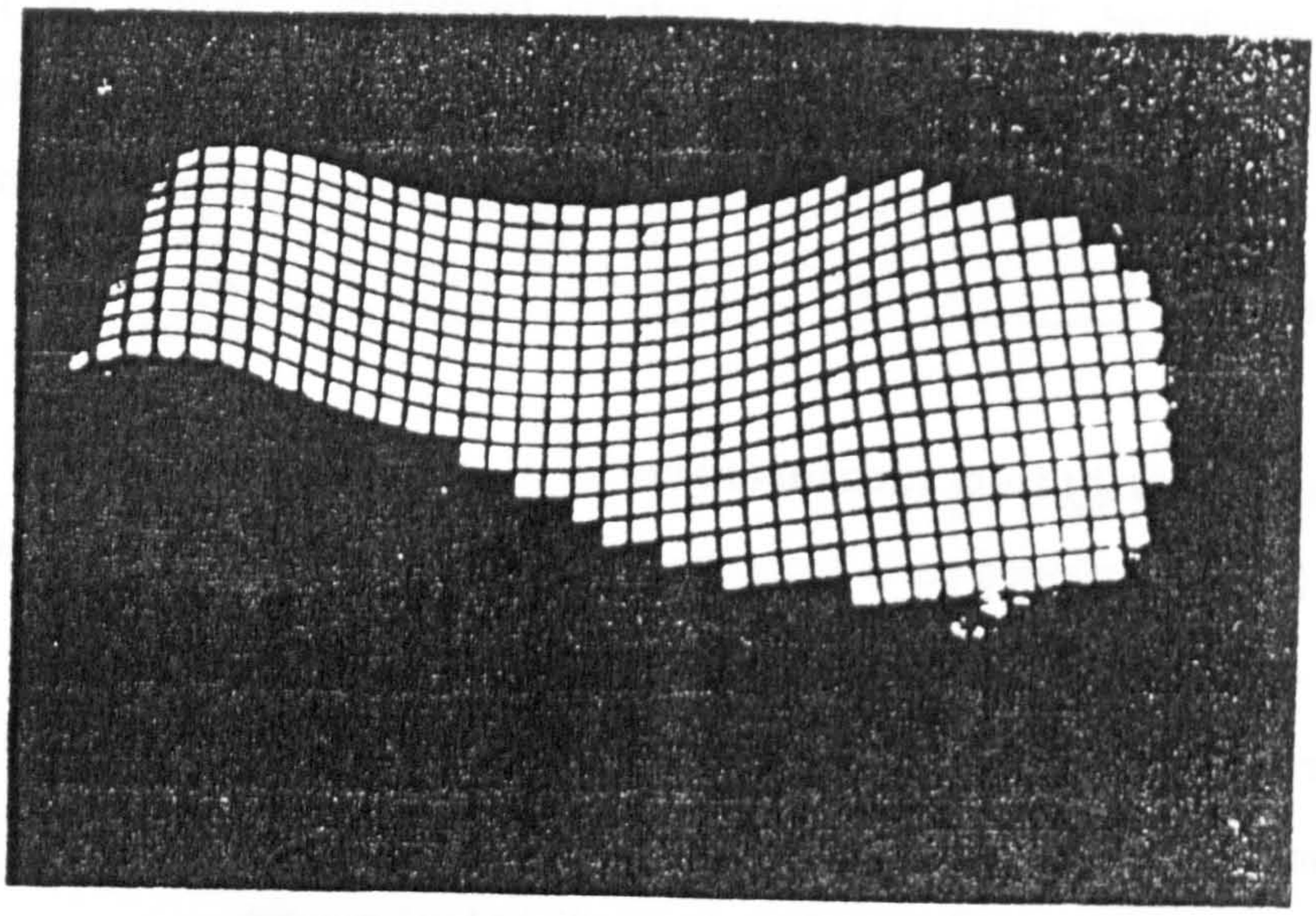

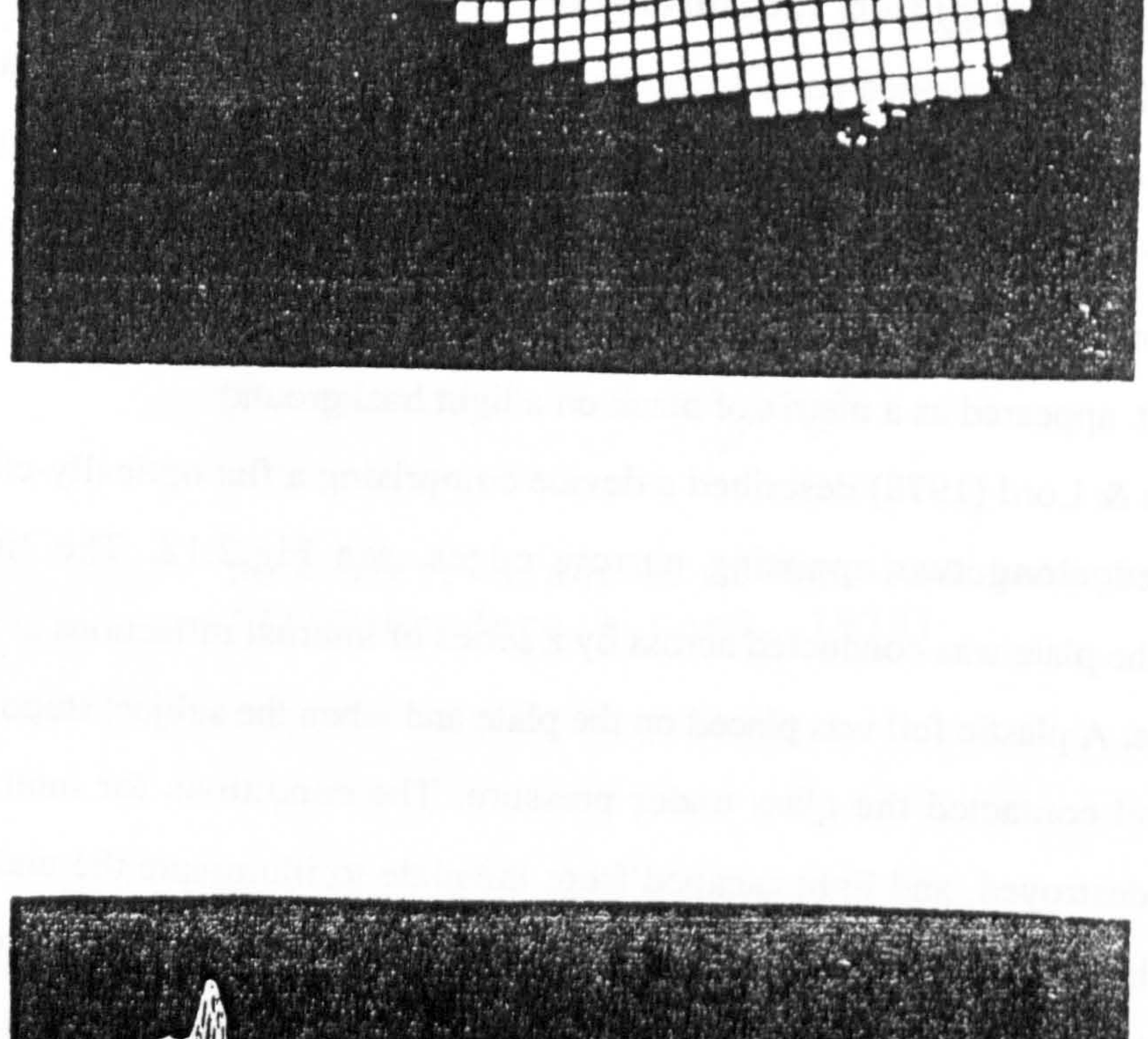

Fig.2.20 The pressure-sentive shoe insole. (a) The protocol type of the insole. (b) Typical pressure distribution on the foot during walking.
(from Cavanagh et al, 1981)

distribution using Nicol's mat. The mat was sampled in series with a frequency of 100Hz and the analog output was connected to an A/D converter and then transferred to a PDP11 mini-computer. The resolution of the system was 10mm by 10mm square. This system has the potential to measure fast walking and running because of its high sampling rate and high resolution.

Cavanagh's group (1981) reported a "pressure-sensitive shoe insole" which consisted of an array of 499 high precision piezo-electric transducers embedded in silicone rubber, as shown in Fig. 2.20. Together with the insole, electric circuits and a computer interface were developed capable of handling approximately 100,000 8-bit words of data generated per second by the array. Compared with Nicol's mat, this system seems to have a higher frequency response which is necessary for accurate measurement.

§2.6 Gait Patterns of the Normal

The investigation of the normal gait mechanism has been pursued for quite some time and a basic understanding of it has been achieved. In this section a review of the normal gait is categorized into four basic groups: temporal-distance parameters, kinematics, kinetics and energy expenditure. It is, by no means, inclusive of every investigator's work, but an attempt is made to include all the important gait variables.

§2.6.1 Temporal-distance parameters

The typical temporal-distance parameters are depicted in Fig. 2.21. These parameters are not only the basic gait characteristics themselves but also essential in interpreting other gait variables.

The brothers Weber (1936) were perhaps the first to study the temporal-distance factors for human walking, but no data were available for this author to discuss.

Murray *et al* (1964) systematically investigated the temporal-distance parameters and their relations to age and body built. A total of 60 subjects in 5 age groups (between 20 to 65 years) was included and each age group consisted of four

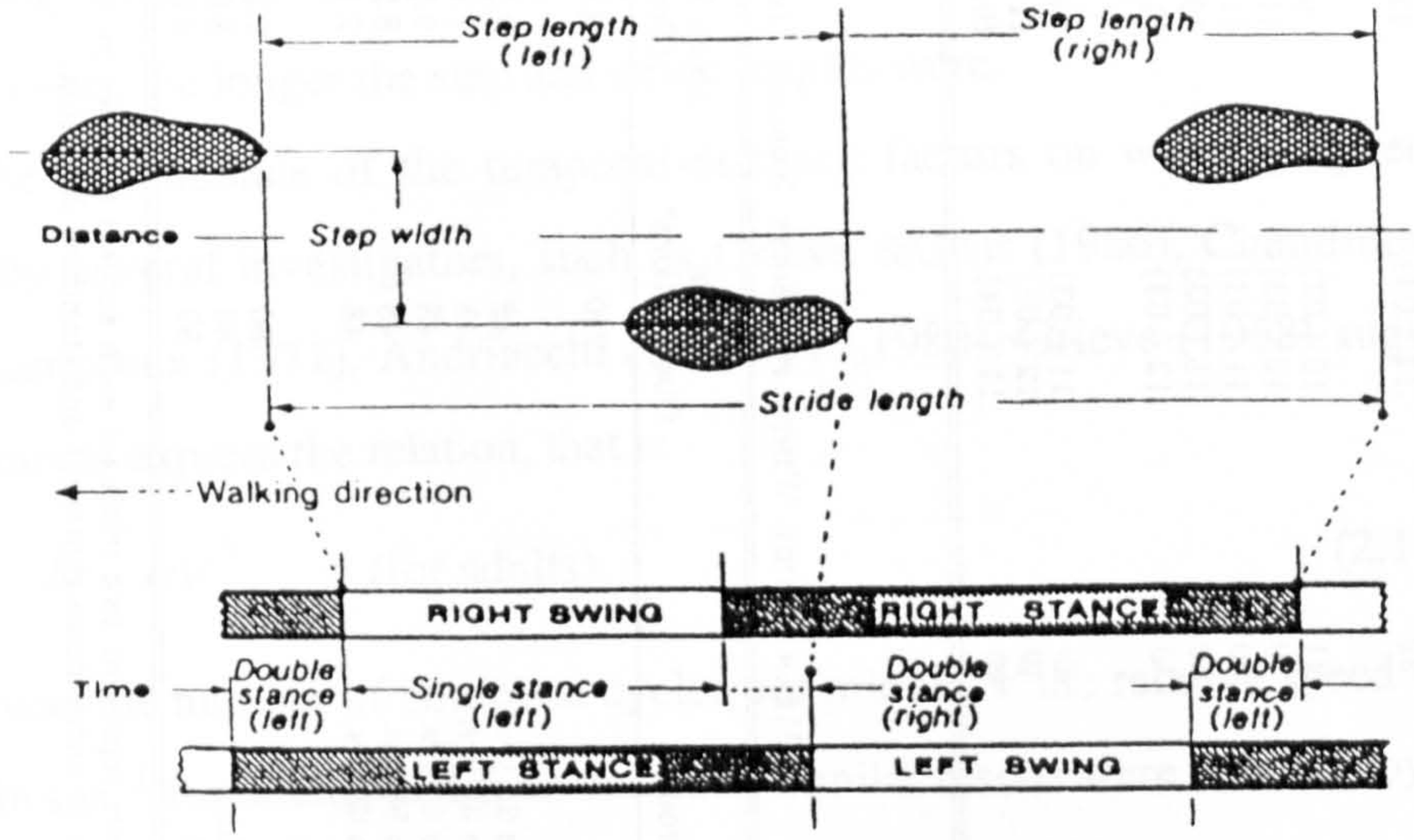

Fig.2.21 Typical temporal distance parameters used in gait analysis. (from Chao, 1985)

THE MEAN DURATIONS OF STANCE, SWING, AND DOUBLE-LIMB SUPPORT FOR SIXTY NORMAL MEN

Groups	No. of Observations*	Duration of Stance (Both Limbs) Seconds†	Duration of Stance (Both Limbs) Per cent of Walking Cycle	Duration of Swing (Both Limbs) Seconds†	Duration of Swing (Both Limbs) Per cent of Walking Cycle	Duration of Double-Limb Support (First and Second Periods) Seconds†	Duration of Double-Limb Support (First and Second Periods) Per cent of Walking Cycle
Total	240	.63 (.07)	61	.40 (.04)	39	.11 (.03)	11
Age							
20 to 25 yrs.	48	.63 (.07)	60	.42 (.04)	41	.10 (.03)	9
30 to 35 yrs.	48	.67 (.08)	61	.42 (.04)	39	.12 (.03)	11
40 to 45 yrs.	48	.59 (.05)	61	.38 (.03)	39	.11 (.03)	11
50 to 55 yrs.	48	.62 (.07)	60	.40 (.04)	40	.11 (.03)	10
60 to 65 yrs.	48	.64 (.08)	61	.40 (.04)	39	.12 (.03)	11
Height							
Tall	80	.61 (.07)	60	.40 (.04)	39	.11 (.03)	10
Medium	80	.65 (.07)	61	.41 (.04)	39	.12 (.03)	11
Short	80	.63 (.07)	61	.40 (.03)	40	.11 (.04)	10

* These numbers represent two trials for each subject and two measurements for each trial.
† The numbers in parentheses represent one standard deviation.

MEAN STEP AND STRIDE LENGTH FOR SIXTY NORMAL MEN

Group	No. of Observations*	Left to Right Step Length (*Centimeters*)†	Right to Left Step Length (*Centimeters*)†	Left Stride Length (*Centimeters*)†
Total	120	78.4 (5.9)	78.1 (6.3)	156.5 (11.4)
Age				
20 to 25 yrs.	24	79.5 (6.8)	79.3 (6.0)	158.8 (12.4)
30 to 35 yrs.	24	78.7 (5.5)	78.2 (6.5)	156.9 (11.2)
40 to 45 yrs.	24	77.7 (5.1)	78.2 (6.7)	155.9 (10.8)
50 to 55 yrs.	24	79.5 (6.4)	78.4 (5.9)	157.9 (11.6)
60 to 65 yrs.	24	76.4 (4.9)	76.6 (6.0)	153.0 (10.0)
Height				
Tall	40	81.1 (6.1)	81.4 (6.8)	162.5 (12.0)
Medium	40	78.1 (5.5)	78.1 (5.9)	156.2 (10.6)
Short	40	75.9 (4.9)	74.9 (4.0)	150.8 (7.9)

* These numbers represent two trials for each subject.
† The numbers in parentheses represent one standard deviation.

MEAN STRIDE WIDTH FOR SIXTY NORMAL MEN

Group	No. of Observations*	Mean Stride Width (*Centimeters*)†
Total	240	8.0 (3.5)
Age		
20 to 25 yrs.	48	7.2 (2.9)
30 to 35 yrs.	48	7.9 (3.3)
40 to 45 yrs.	48	9.6 (3.2)
50 to 55 yrs.	48	8.2 (3.8)
60 to 65 yrs.	48	7.1 (3.6)
Height		
Tall	80	7.2 (3.5)
Medium	80	8.6 (3.7)
Short	80	8.2 (3.0)

* These numbers represent two trials for each subject and two measurements for each trial.
† The numbers in parentheses represent one standard deviation.

Fig.2.22 Temporal distance parameters of 60 normal subjects. (from Murray et al, 1964)

tall, four short and four medium height subjects. The mean values of the parameters obtained are shown in Fig. 2.22. It was found that no systematic relationship existed between the parameters and age, but the oldest subjects took shorter steps and strides and demonstrated a greater toe out than younger subjects. The step and stride length were the only parameters found to be related systematically to height, that is, the taller the subject was, the longer the step and stride lengths were.

The dependence of the temporal-distance factors on walking speed was reported by several investigators, such as Grieve &Gear (1966), Chantinier *et al* (1970), Lamoreux (1971), Andriacchi *et al* (1977,1980). Grieve (1968) suggested an equations to express the relation, that is

$$N = \alpha V^{b} \qquad \text{(for adults)} \qquad (2.1)$$

where N was the number of complete cycles per minute, V the relative speed (speed /stature) in sec^{-1} for adults, and α an constant. Similar results were obtained by other researchers.

Molen (1973) reported on the temporal-distance parameters for the different sexes. A total of 309 males and 224 females were observed. It was found that in the range of velocity of between 40 to 100 m/min, the ratio of step length to step frequency of the male was significantly larger than that of the female.

§2.6.2 Kinematic analysis

Linear displacements of the body segments during walking were investigated by several researchers. Inman *et al* (1981) presented the linear displacements of the leg and the pelvis. Since the mass centre of the whole body is near the centre of the pelvis and the leg is jointed to the rest of the body at the pelvis, the movement of the pelvis received much attention. Fig. 2.23 shows the typical linear displacement of the pelvis at different walking speeds.It was found that as the walking speed increased, the progressional oscillation and the medio-lateral swing of the pelvis decreased in amplitude while the vertical movement increased. The displacements of the head, shoulder and pelvis were investigated by Braune &Fischer(1895), Lamoreux (1971) and Cappozzo (1981). The data were depicted in three anatomical planes rather than in the forms of displacement-time curves, as shown in Fig.2.24. It was found that the

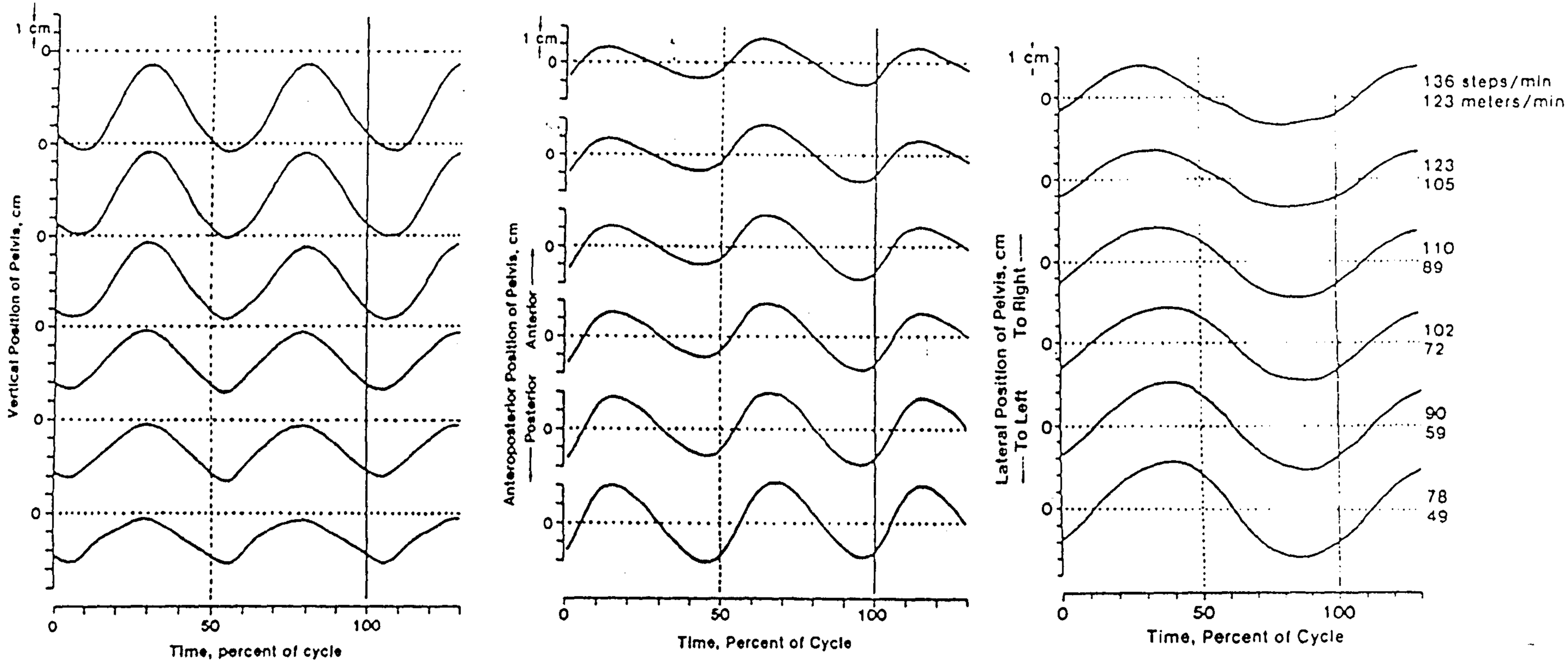

Fig.2.23 Linear movement of the pelvis related to walking speed. (from Inman et al, 1981)

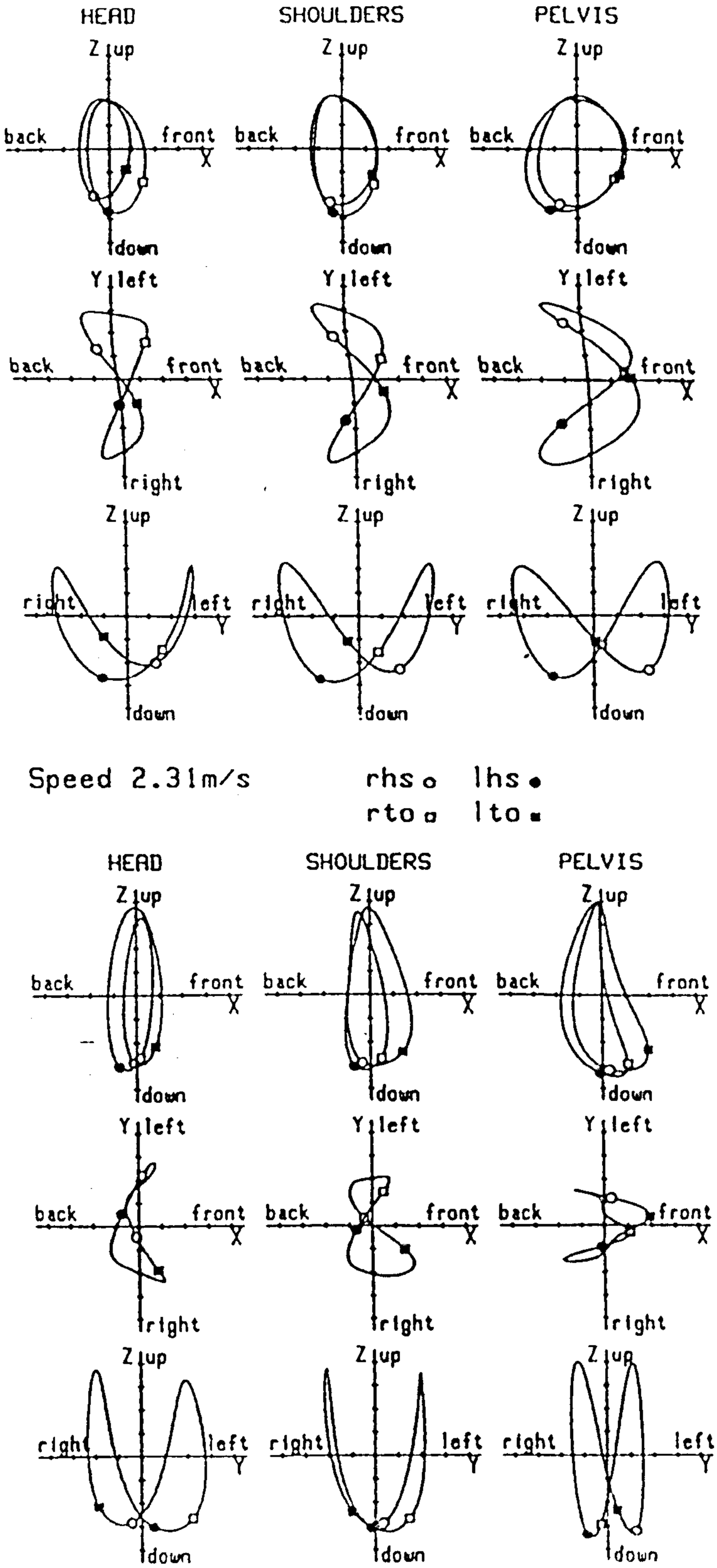

Fig.2.24 "Lissajous" figures of the head, shoulder and pelvis related to walking speed.
(from Cappozzo, 1981)

excursion of the pelvis in the sagittal plane, with respect to an observer moving at mean speed, was larger than those of the shoulder and head by approximately 20mm. In the coronal plane, the contrary applies.

Harmonic analysis of the kinematic data is believed to be capable of extracting more characteristic information about walking from the basic time-domain data. Cappozzo (1981) performed harmonic analysis on the 3-D linear displacements of the pelvis, shoulder and head. He introduced a concept of "intrinsic" and "extrinsic" harmonics according to the perfect symmetry of the upper body movement. It was found that in a normal population the intrinsic harmonic coefficients were highly repeatable while the extrinsic harmonic coefficients were mostly of a random nature.

Angular movement of the body segments were extensively studied. Inman *et al* (1981) published the results of an early project carried out at University of California, as shown in Fig. 2.25. It was observed that the reason for the rapid flexion of the hip and the knee at the beginning of the swing phase was to secure toe clearance and the knee flexion immediately after heel strike was to absorb the shock of the body weight. The patterns of axial rotation, which had been neglected before then, were also investigated. It was found that the joints of the foot absorbed the axial rotation when the foot was in contact with the floor. The pelvis rotation in the coronal plane was found to be an important factor in maintaining a smooth gait.

Murray (1964) conducted an investigation into the normal gait related to age and height and she obtained similar mean values for all the gait variables to those arrived at by Inman *et al*. The results showed that the angular movements of pelvis, hip, knee and ankle in the sagittal plane did not vary systematically with height and age. The hip joint was found to approach its anatomically possible motion limits. Transverse rotations of the pelvis and thorax were also studied, as shown in Fig. 2.26. It was observed that the pattern of rotation once again did not vary with age and height systematically. It was noted that the pattern of pelvis rotation was out of phase to that of the thorax, suggesting a damping effect in order to reduce the overall rotation of the body and also to give a smooth walking pattern.

Lamoreux (1971) investigated the effect of walking speed on the angular velocity and acceleration. Some results are shown in Fig.2.27. It was observed that

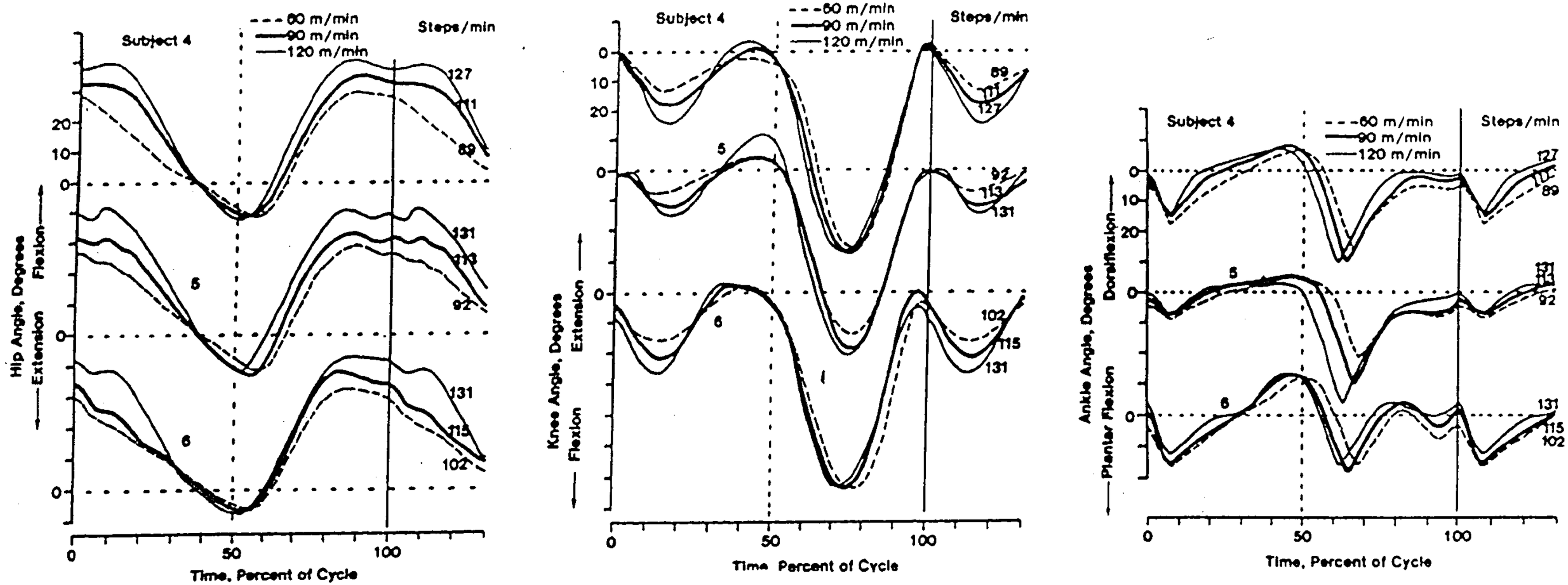

Fig.2.25 Relative angular movement of the lower-limbs related to walking speed.

(from Inman et al, 1981)

26b

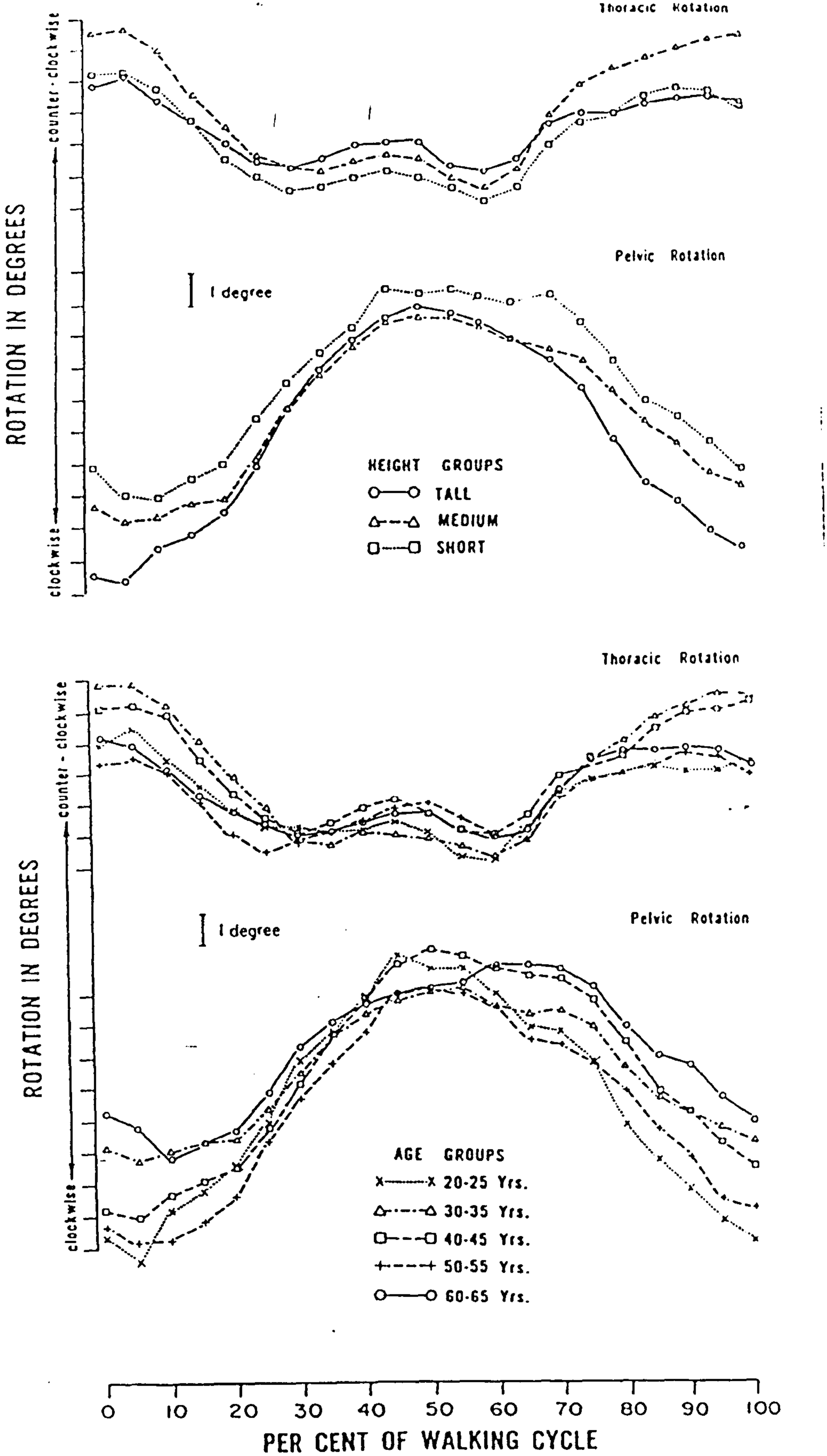

Fig.2.26 Transverse otations of the thorax and pelvis related to age and height.
(from Murray et al, 1964)

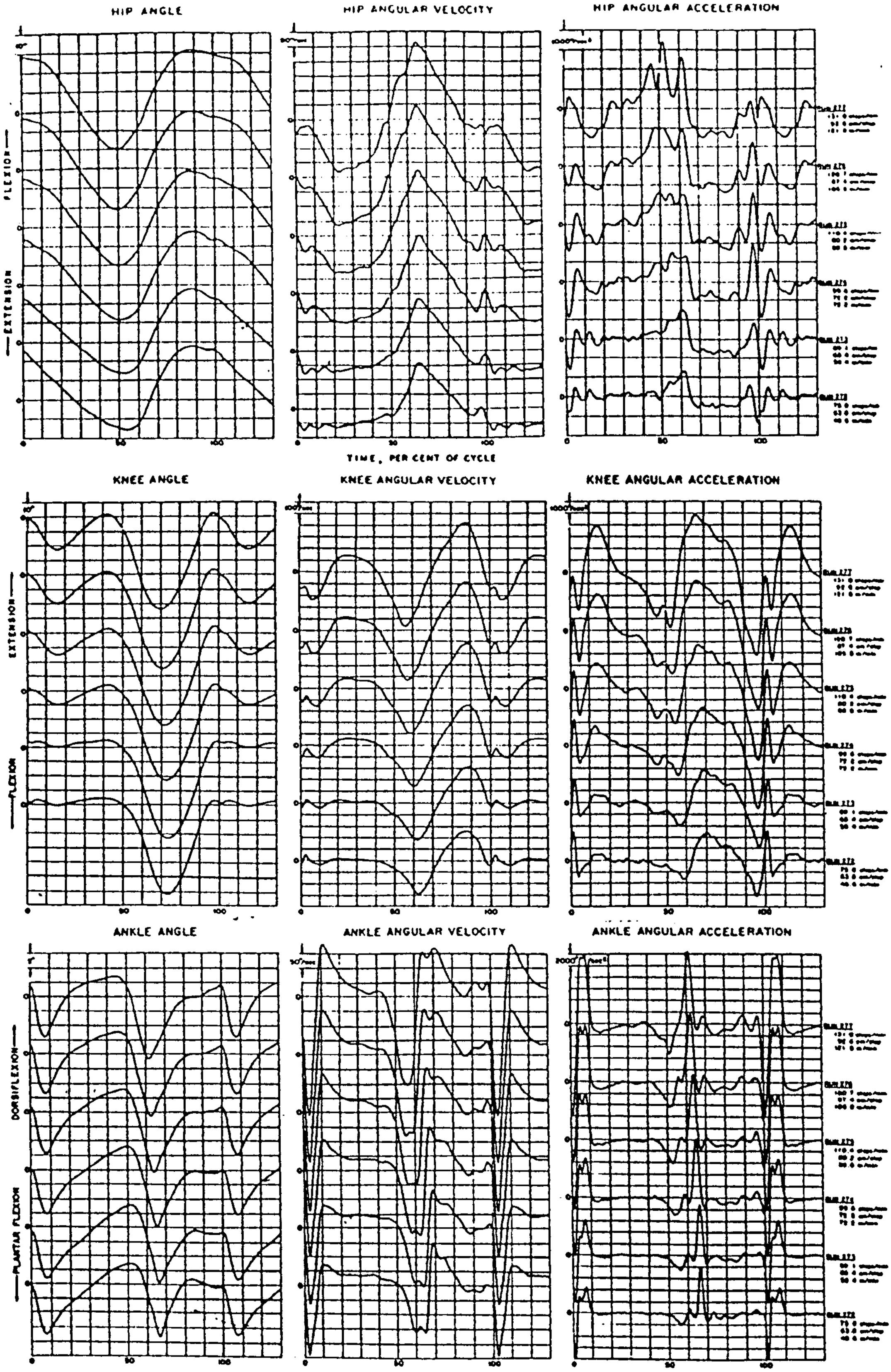

Fig.2.27 Angular displacement, velocity and acceleration of the lower limbs. (from Lamoreux, 1971)

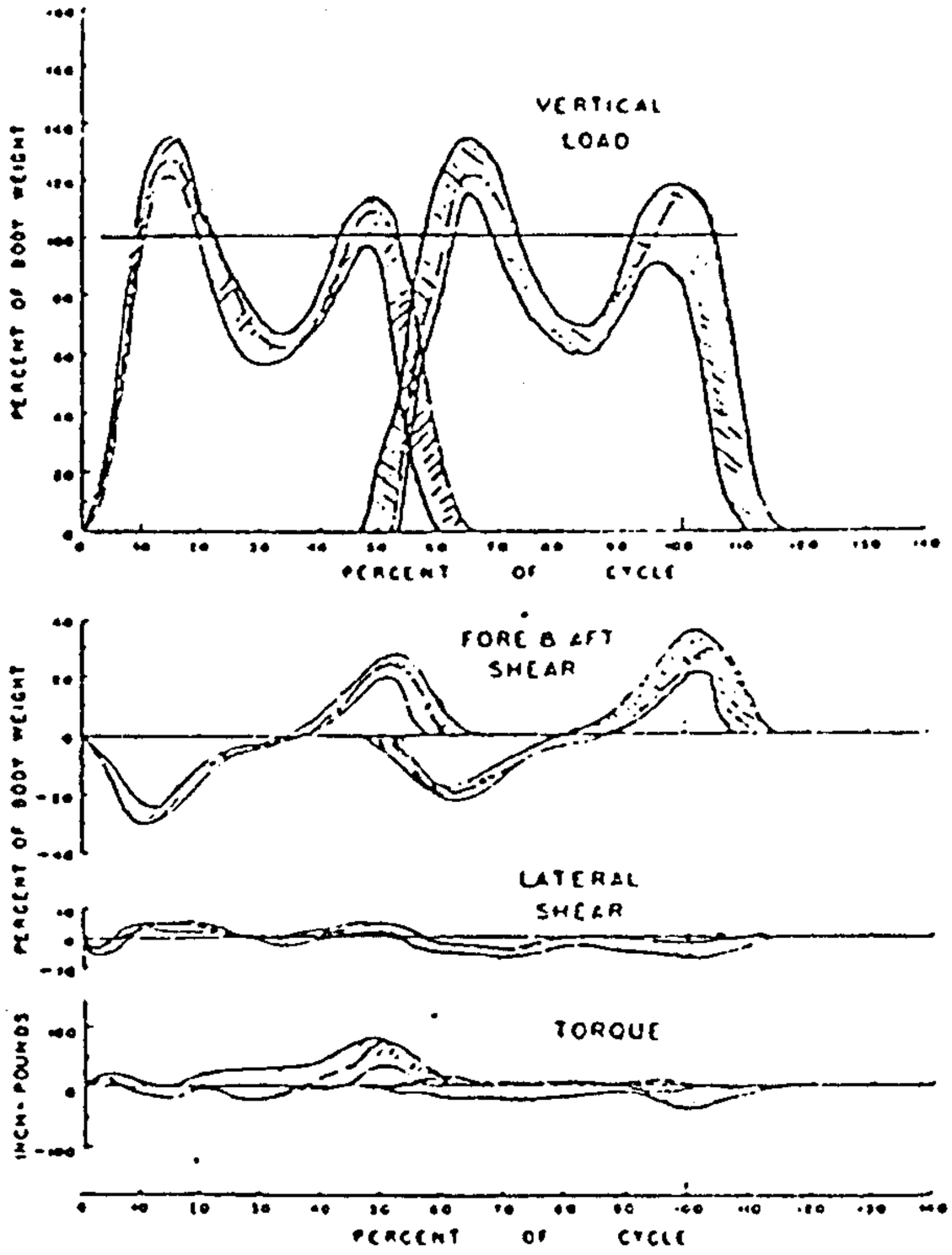

FLOOR REACTIONS ON THE FOOT
ONE NORMAL SUBJECT WALKING LEVEL SIX TIMES

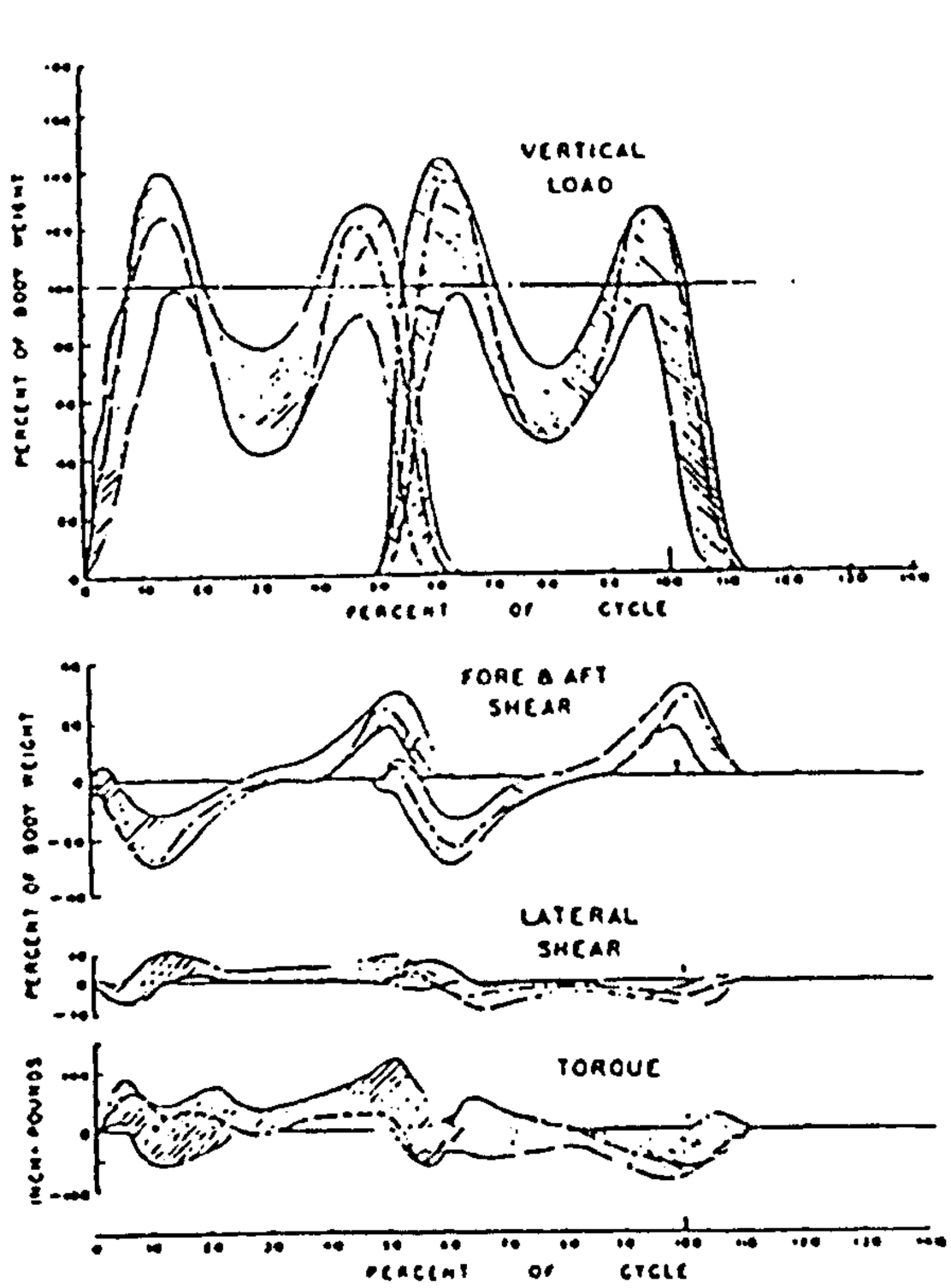

FLOOR REACTIONS ON THE FOOT
TEN NORMAL SUBJECTS WALKING LEVEL

Fig.2.28 Ground reaction forces. (a) One subject walked six times; (b) Data from ten subjects. (from Cunningham 1950)

all variables had their own individual patterns which changed with speed. As the speed was increased, higher amplitudes and additional high-frequency components were obtained.

Symmetry of the events between the left and right legs is believed to be a characteristic of normal gait. Hannah *et al* (1984) investigated the kinematic symmetry of the lower limbs using bilateral electrogoniometry. The angular displacement of the hip and knee joints were examined in both the time and frequency domains, and the symmetry was evaluated by a correlation coefficient

$$\gamma = \frac{\Sigma(X \cdot Y) - (\Sigma X \cdot \Sigma Y)/N}{N \cdot \sqrt{\{[N \cdot \Sigma X^2 - (\Sigma X)^2][N \cdot \Sigma Y^2 - (\Sigma Y)^2]\}}} \qquad (2.1)$$

where X and Y were the amplitudes of frequency spectra of kinematic data for corresponding joint motion pairs. It was observed that the greatest symmetry appeared in the knee and hip sagittal plane motion (γ=0.99), slightly less symmetry (γ=0.93) in hip rotation and the lowest symmetry (γ=0.8) in the rest of the motion components.

§2.6.3 Kinetics

Although the forceplate has existed since the early 19th century, it was not until 1950 when Cunningham and Brown designed the first electronic forceplate that satisfactory ground reaction forces were obtained. Fig.2.28 shows envelopes of ground reactions of one subject and of 10 subjects. It is obvious that considerable variations presented in all force components. They suggested that the intra-subject variation was caused by cadence variations while the inter-subject variation was due to the height and weight of the subject. They pointed out that these curves could not be compared on an absolute basis until those factors were evaluated and eliminated.

Andriacchi *et al* (1977) characterized the waveform of ground reaction forces with 9 amplitude parameters (see Fig.2.29) and investigated the relationship between ground action and speed. It was found that the Z1, Z2, Z3, Y2, Y3, and X1 varied linearly with velocity, see Fig.2.29.

Chao *et al* (1983) used 18 parameters to characterize the pattern of ground

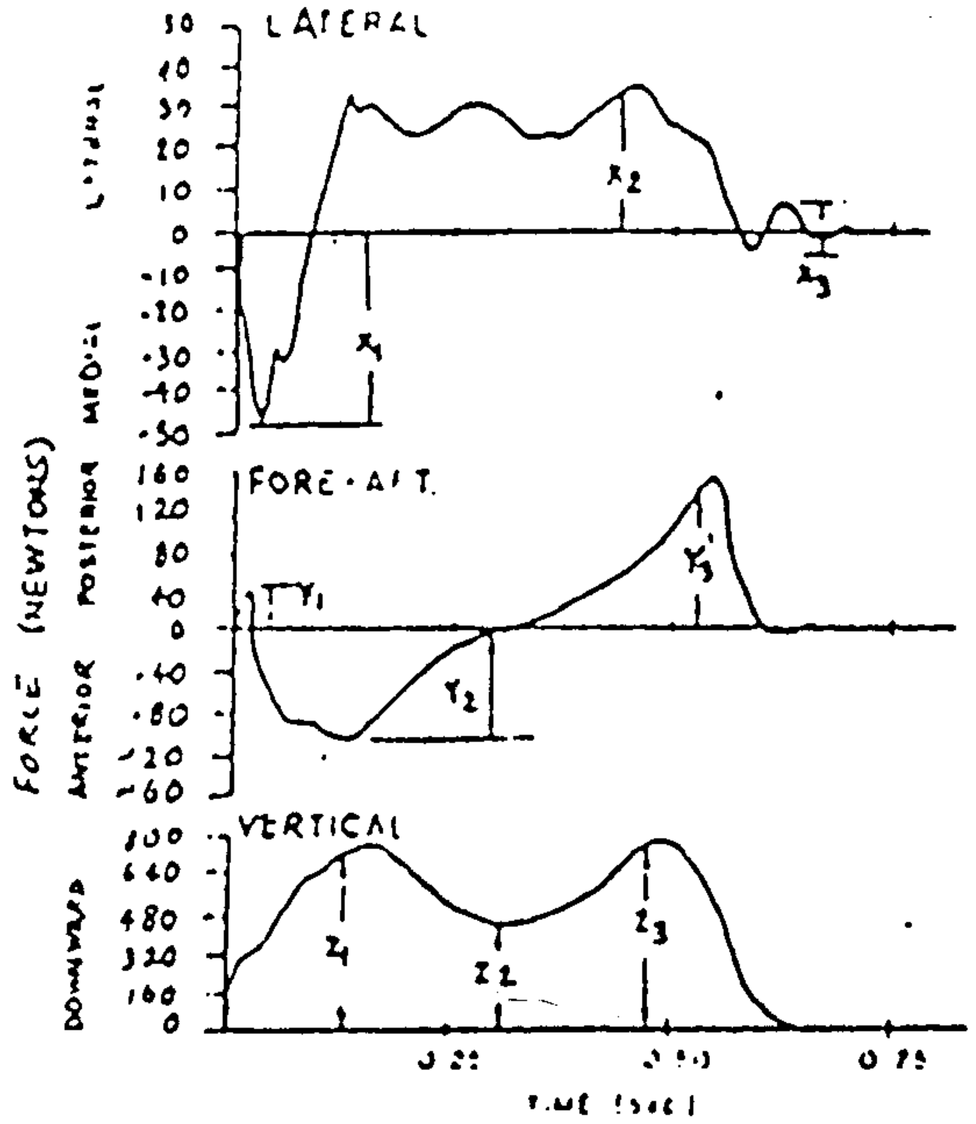

An illustration of the waveforms depicting the three components of foot ground reaction force.

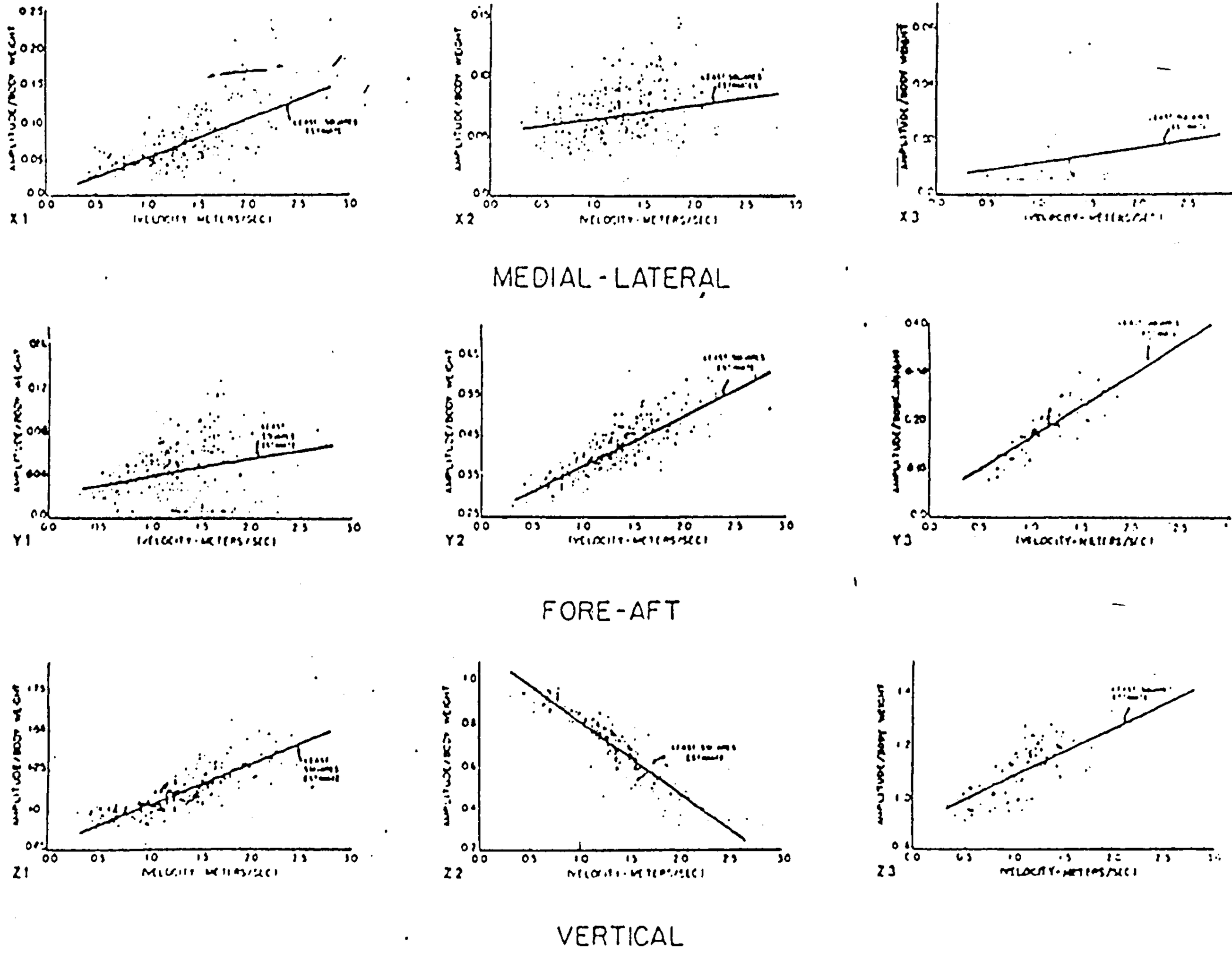

Fig.2.29 Ground reaction forces related to walking speed. (from Andriacchi et al, 1977)

Table 3. Temporal distance factors in the normal population groups I (ages 32–85) and II (ages 19–32). The values for the me and standard deviation are presented. (Refer to Fig. 1 for definitions)

Parameter	Men (n = 53)			Women (n = 57)		
	I (n = 32)	II (n = 21)	Total	I (n = 37)	II (n = 20)	Total
Cadence (stride min^{-1})	52 ± 5	50 ± 8	51 ± 6	56 ± 5	51 ± 5	54 ± 5
Stride Length/LEL*	1.56 ± 0.15	1.48 ± 0.17	1.53 ± 0.16	1.40 ± 0.14	1.39 ± 0.17	1.40 ± 0.1
Speed (m min^{-1})*	76.1 ± 12.5	71.9 ± 18.3	74.4 ± 15.1	69.4 ± 11.0	63.9 ± 11.1	67.5 ± 11.
Step length, right (cm)*	73 ± 8	69 ± 9	71 ± 8	61 ± 8	60 ± 7	61 ±
Step length ratio (small/large)	†	1.0 ± 0	†	†	1.0 ± 0	†
Step length/LEL, right	0.78 ± 0.07	0.73 ± 0.08	0.76 ± 0.08	0.70 ± 0.07	0.69 ± 0.08	0.70 ± 0.0
Right stance (% G.C.)	59 ± 2	60 ± 2	59 ± 2	60 ± 2	59 ± 2	59 ± 2
Left stance (% G.C.)	†	60 ± 3	†	†	59 ± 3	†
Single stance, right (% G.C.)	41 ± 2	40 ± 2	41 ± 2	40 ± 2	41 ± 2	41 ± 2
Double stance, right (% G.C.)	8.8 ± 1.9	10.2 ± 2.6	9.4 ± 2.3	10.0 ± 5.5	8.9 ± 2.0	9.6 ± 4.6
Double stance ratio (small/large)	†	0.8 ± 0.1	†	†	0.9 ± 0.1	†

"% G.C. = Percent of Gait Cycle
*Significantly corrected with 10 or more parameters ($p < 0.01$).
†The stride characteristics were assumed symmetric in this group.

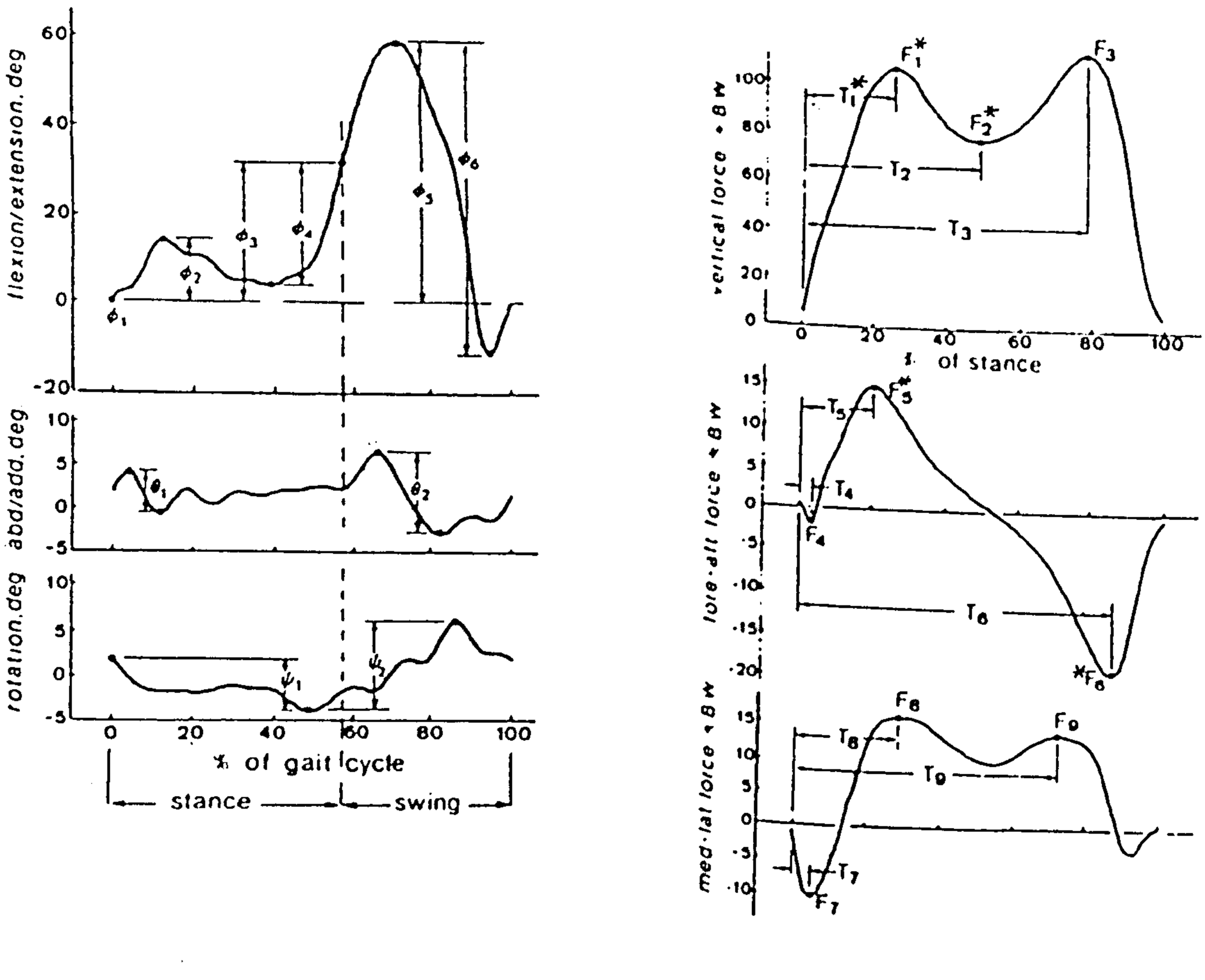

Fig.2.30 Parametric analysis of the ground reactions and temporal distance factors. (from Chao et al, 1993)

reaction forces of normal subjects, referred to in Fig.2.30. A total of 62 normal subjects walking at their natural speeds was studied. It was found that the relative variations were smaller for the force components with higher magnitudes (F1, F2, F3, F5 and F6) and corresponding time of occurrence, suggesting that the main features contained in ground reaction force patterns appeared consistent. The temporal/distance parameters were also studied, and a linear correlation matrix analysis was conducted on 41 parameters. It was found that 8 parameters, marked by an asterisk, had significant correlation with ten or more of the remaining parameters. It was interesting to note that no joint motion parameters appeared in the list of the 8 parameters, tending to suggest that kinematic data could be redundant in the study of normal gait of adults.

Fourier analysis on the ground reaction forces was performed by several researchers (Alexander and Jayes, 1980; Jacob *et al*, 1972; Chao, 1975). Chao (1982) conducted such an analysis on 26 normal subjects and 10 patients with knee joint diseases. Three definitions of period, that is, the stance phase, stride period and that proposed by Alexander and Jayes (1980), were compared and it was found that the stance phase was the best period for reconstructing the force patterns. The key Fourier coefficients were found to be the first two to four terms plus the constant term. Alexander and Jayes (1980) reported that the Fourier coefficients were different with respect to the walking speed and in different subjects walking at the same speed.

The intersegmental moments and forces, which are essential to a complete understanding of the gait mechanism, have received most attention. Bresler and Frankel (1950) were perhaps the first to perform a 3-D analysis of the leg by calculating the intersegmental loads on the lower limb joints. Kinematic data were obtained by cinematography, ground reaction by forceplate and segmental physical properties by using Braune and Fischer's coefficients. A total of 4 normal male subjects was used and only the left leg was measured. The results are shown in Fig.2.31. It was found that the medio-lateral forces were small but important in providing lateral stability in walking and contributed to a large share of the lateral hip moment. The fore-aft component has an approximately full sine wave during stance phase. The vertical force has a typical double-peak shape, due to upward and

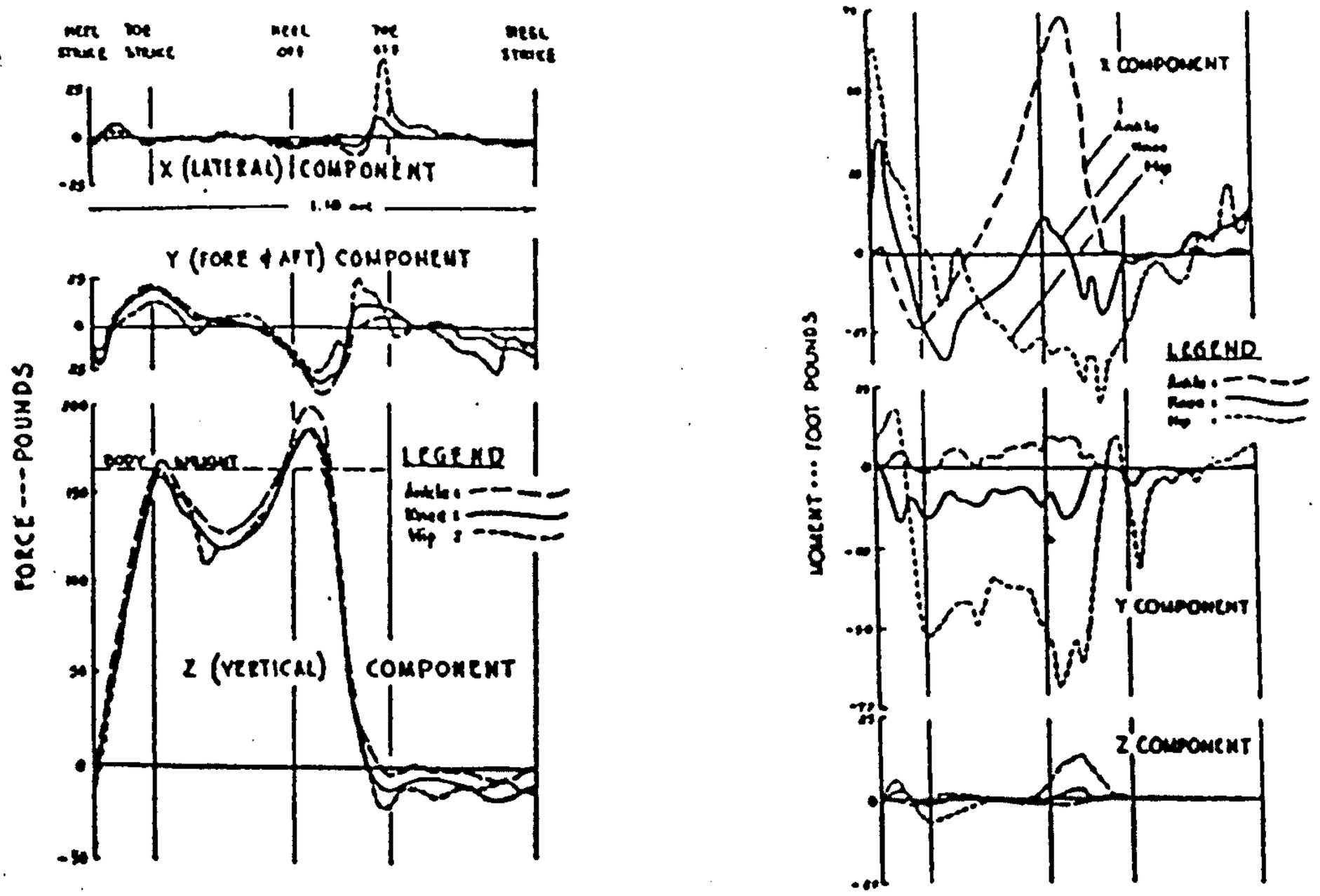

Fig.2.31 Intersegmental loads. (from Bresler & Frankel, 1950)

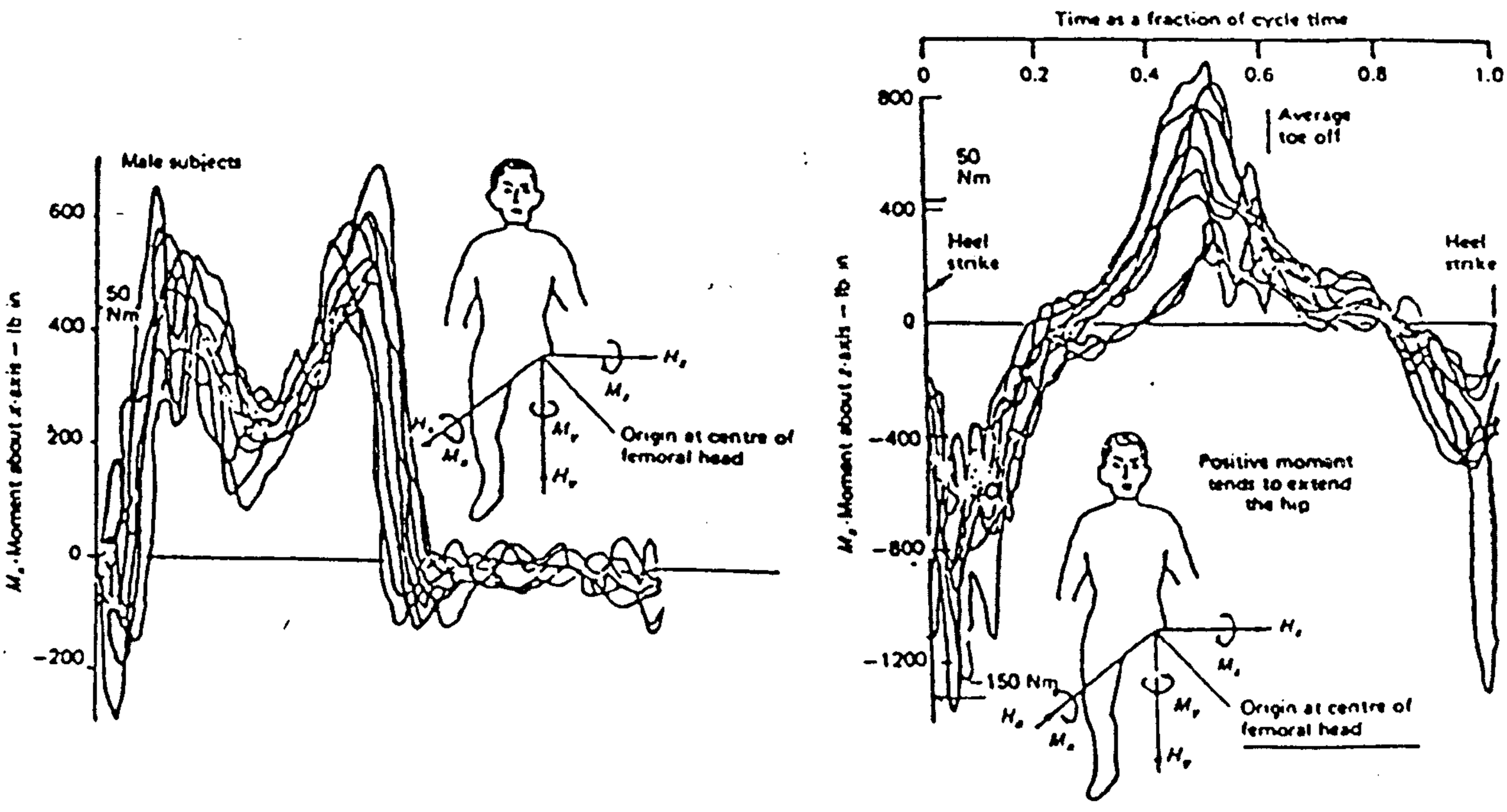

Fig.2.32 Hip moments of ten normal subjects. (from Paul, 1971)

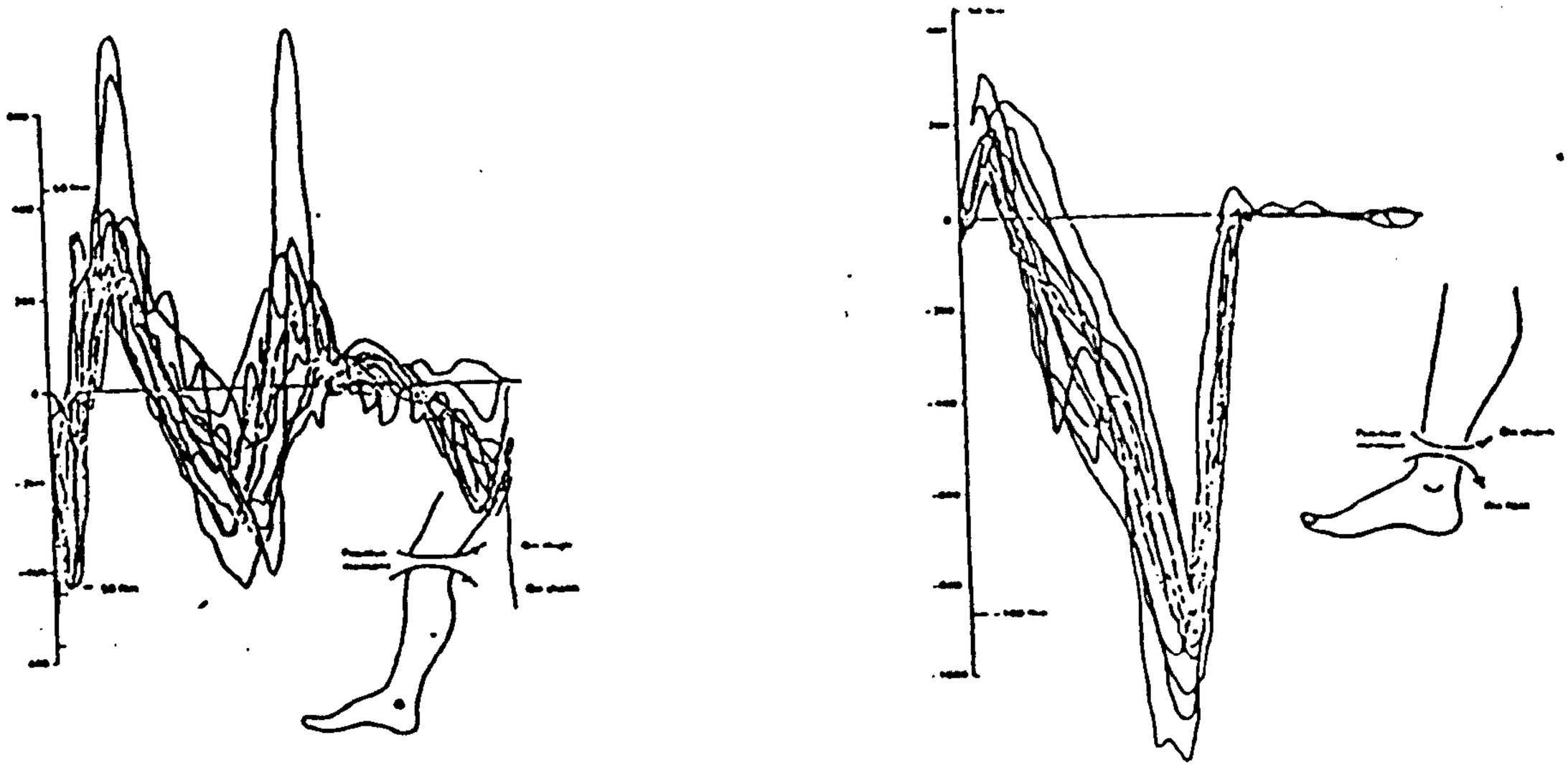

Fig.2.33 Summary curves of the knee and ankle moments.
(a) Knee moments; (b) Ankle moments.
(from Paul, 1971)

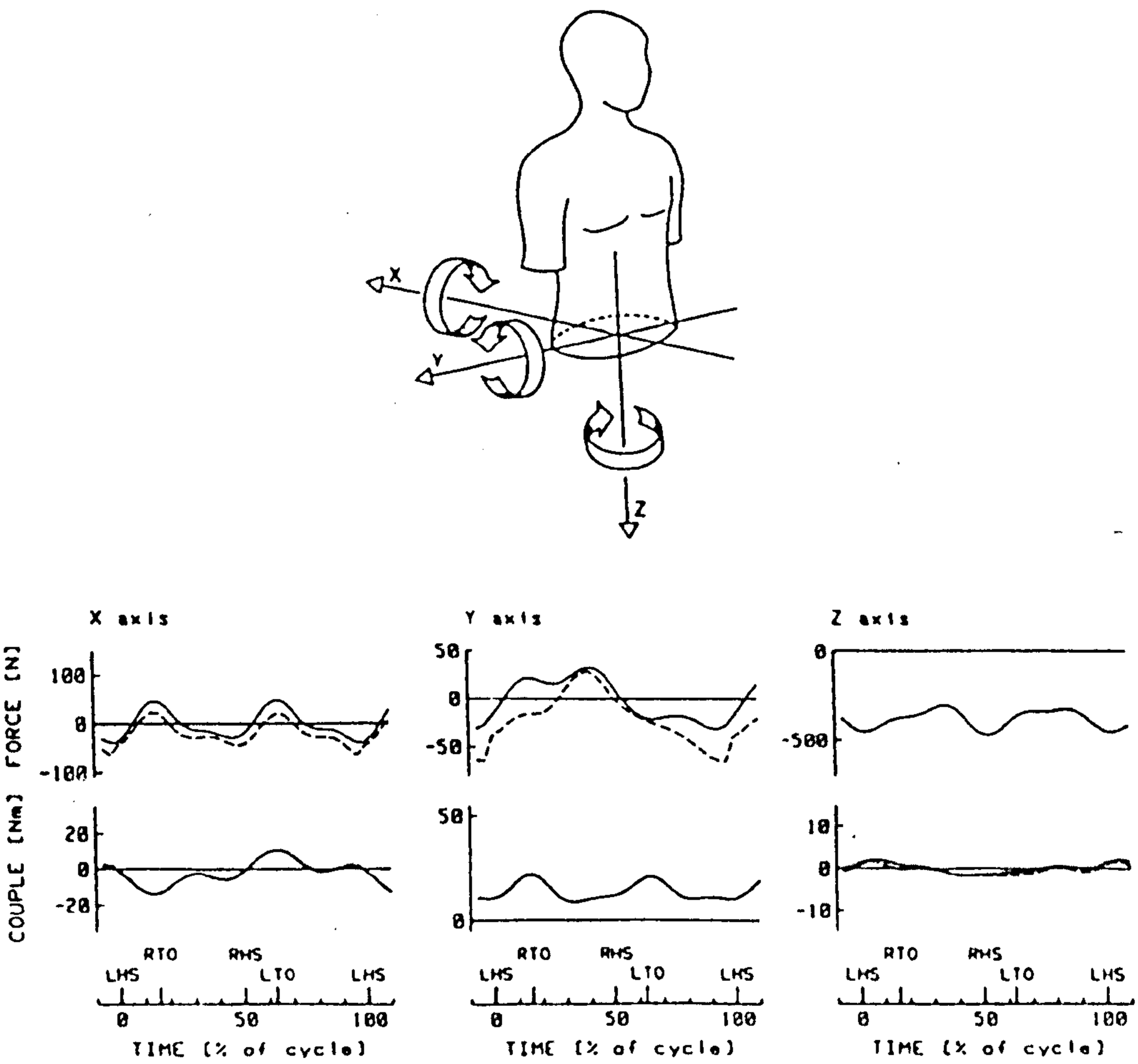

Fig.2.34 Intersegmental loads at the L4.
(from Cappozzo, 1983)

downward acceleration of the body. The difference between the hip, knee and ankle joint forces indicates the effect of gravity and inertia at these joints. The ankle moment at the sagittal plane has small plantar flexion moment just after the heel strike and a large dorsi flexion at the time of push off. The authors suggested that the magnitude and the timing of the plantar flexion moment at the ankle would be sensitive to pathological gait. The knee sagittal moment presented a clear "double-locking" pattern, permitting the subject to move forward with a minimum raising of his centre of gravity, and therefore with less expenditure of work. The initial positive moment in the sagittal plane at the hip indicated that the forward rotation of the torso is retarded, while the change to negative moment indicated the renewal of forward torso rotation.

The lateral moment reflects the requirement of bipedal walking on the joint of the leg.

The torque about the long axis of the leg was believed to be associated largely with the twist of the body and the leg as well.

The significance of inertia and the gravitational effect on the fore-aft moments was studied. It appears that the effect was very small for the knee and ankle moments, and relatively small on the hip moment throughout most of the stance phase.

Large differences in the force and moment values were found among subjects.

Paul (1967) and Morrison (1967) performed a similar analysis to that of Bresler and Frankel, but went on further to calculate the bone-on-bone forces by grouping muscles across the hip and knee joints. A total of 18 runs was conducted on three female and ten male subjects. Summary curves for the lower-limb joint moments were presented by Paul (1971), as shown in Fig. 2.32 and Fig. 2.33. It was found that the pattern of the curves compared fairly well with that of Bresler and Frankel's. The large difference in the magnitude of the data was suggested to be due to the difference in the walking speed and the subject's body weight.

Cappozzo (1983) investigated the intersegmental loads between the upper and lower body at L4 level. Twenty walking cycles of five normal male adults were analysed. Fig.2.34 demonstrates the results obtained. It was found that the principle

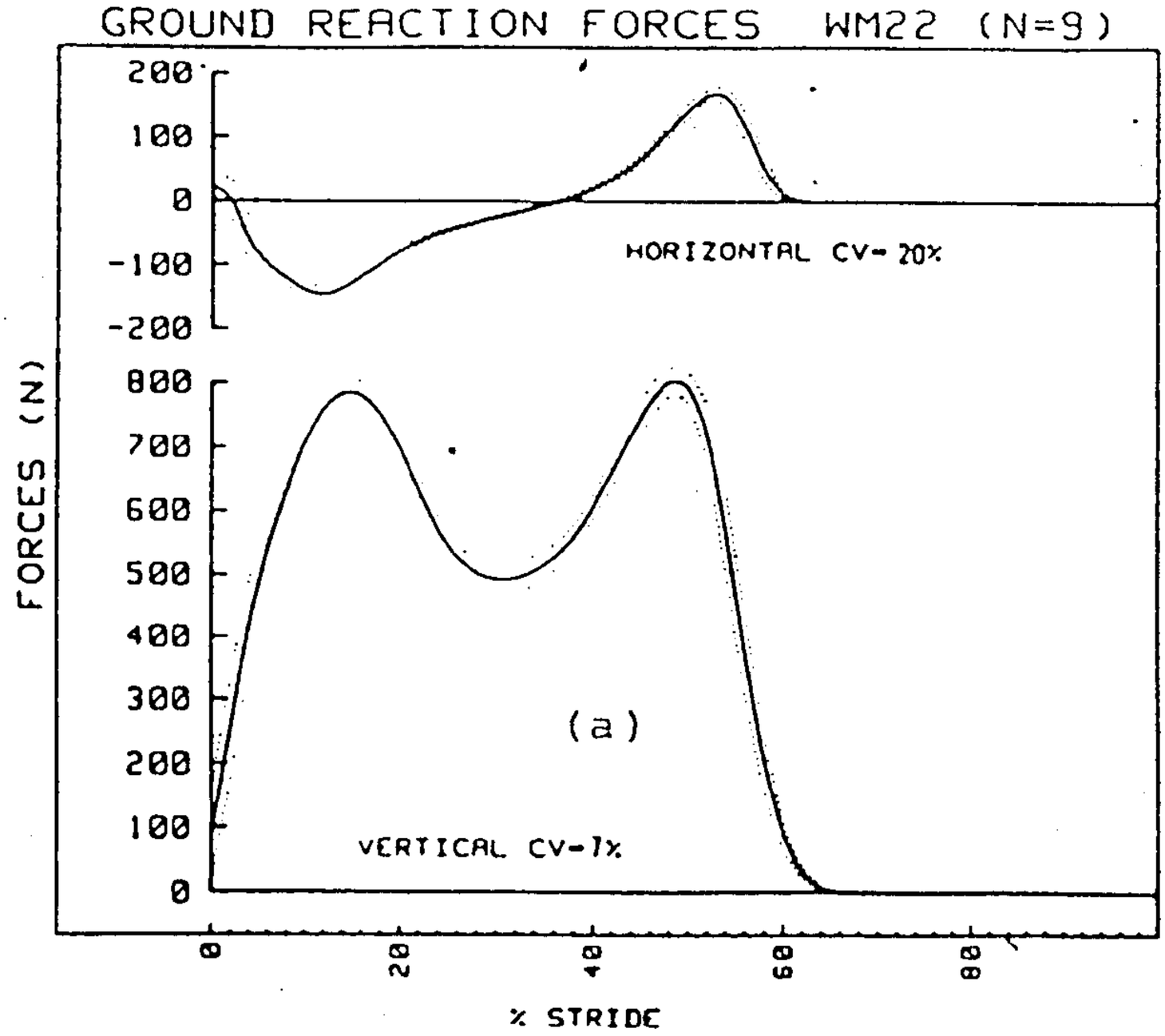

Average horizontal and vertical ground reaction force curves for same nine trials.

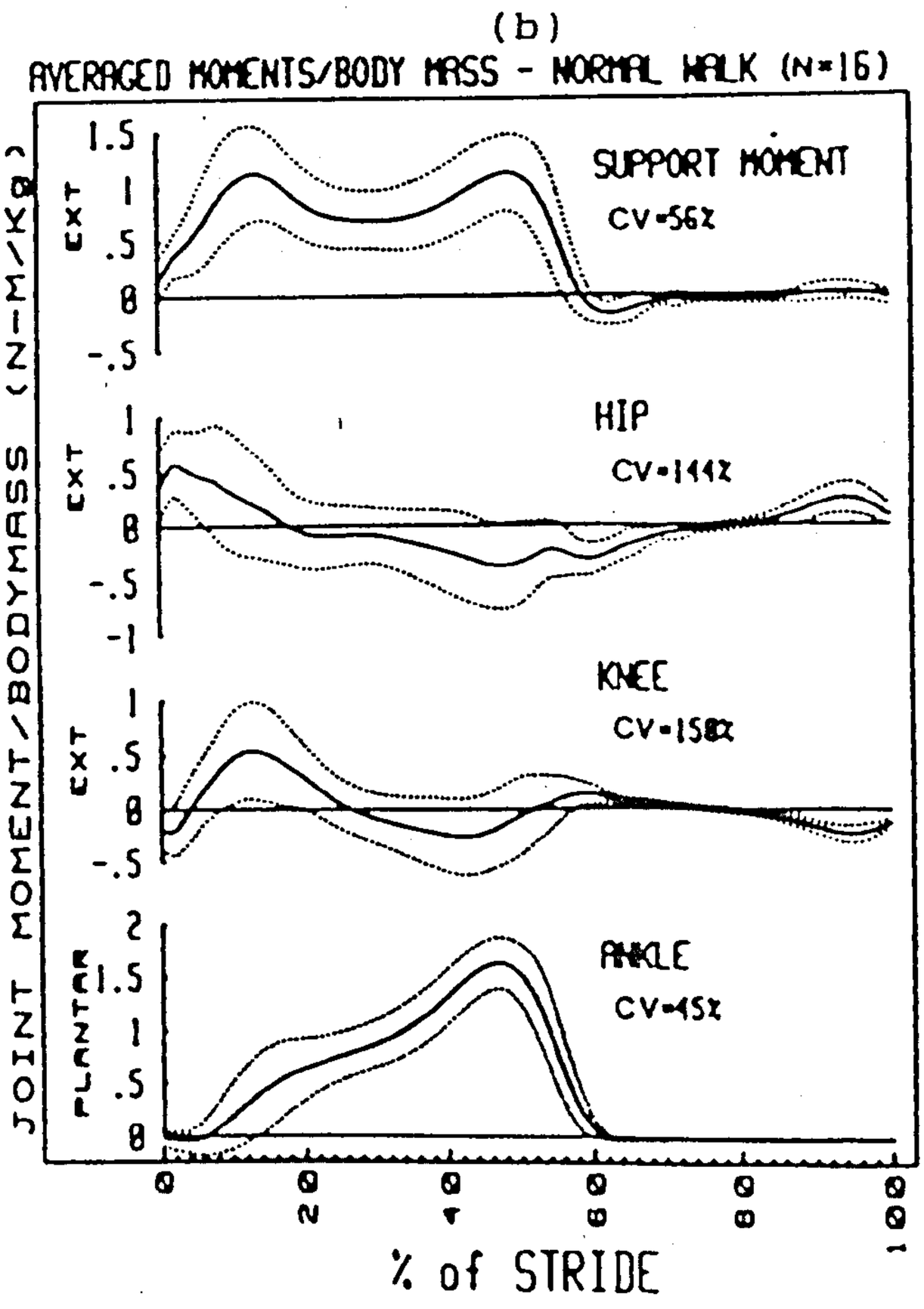

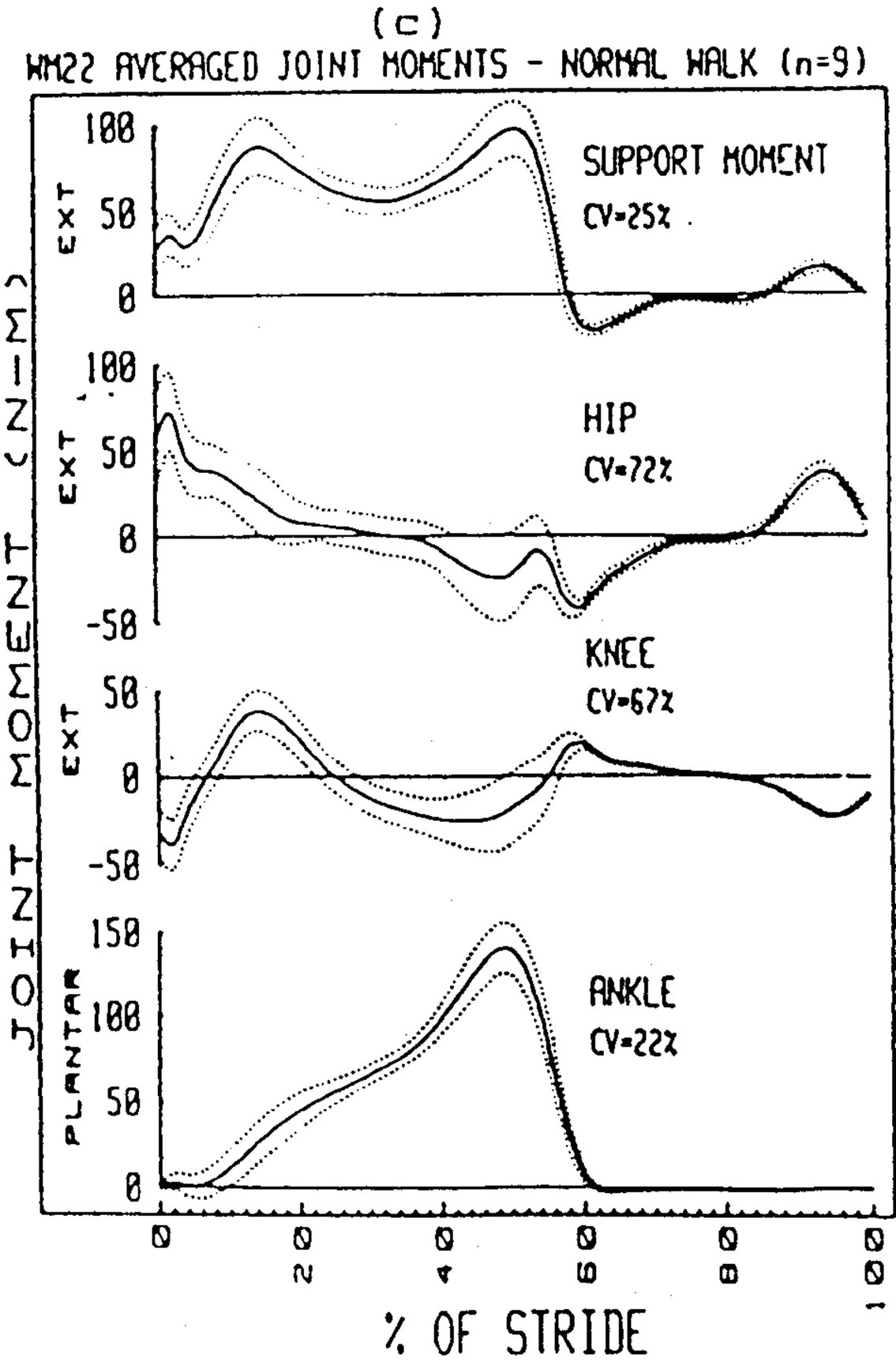

Fig.2.35 Variations of the inter-segmental moments. (a) Ground reactions. (b) inter-subject variations; (c) intra-subject variations. (from Winter, 1984)

ABDUCTION - ADDUCTION MOMENT PATTERNS (EXTERNAL)

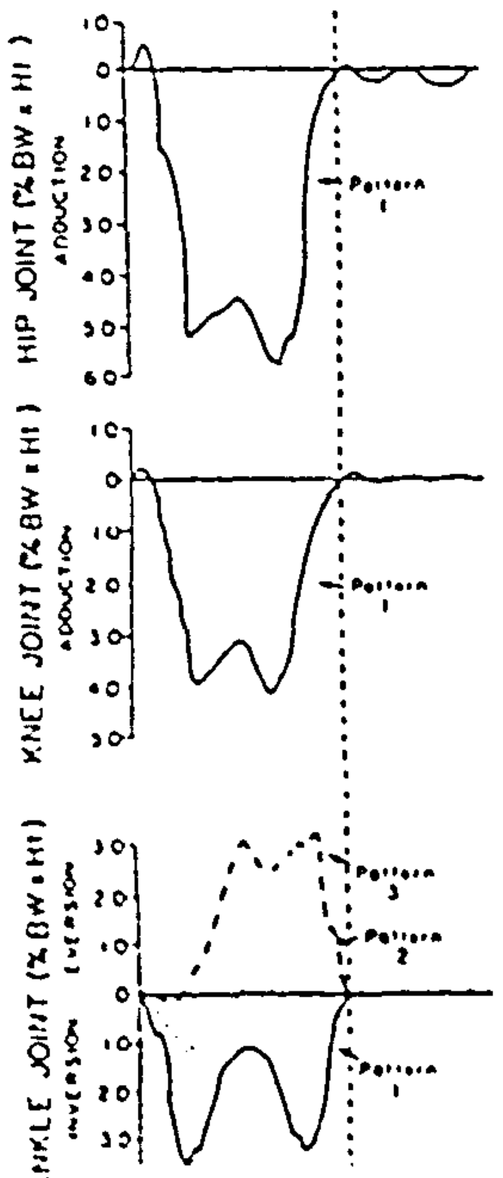

PATTERN FREQUENCY
PERCENT TOTAL OBSERVATIONS

Speed	Pattern No	All Subjects	Male	Female
Slow	1	100	100	100
	Other	0	1	0
Normal	1	99	98	100
	Other	1	2	2
Fast	1	100	98	100
	Other	1	2	0
Slow	1	99	98	100
	Other	1	2	0
Normal	1	99	98	100
	Other	1	2	0
Fast	1	100	100	100
	2	·	·	·
	3	·	·	·
	Other	0	0	0
Slow	2	73	64	81
	3	15	18	4
	Other	11	18	15
Normal	2	66	56	73
	3	24	24	24
	Other	9	16	3
Fast	2	63	60	65
	3	23	21	25
	Other	10	17	10

INTERNAL - EXTERNAL ROTATIONAL MOMENT PATTERNS (EXTERNAL)

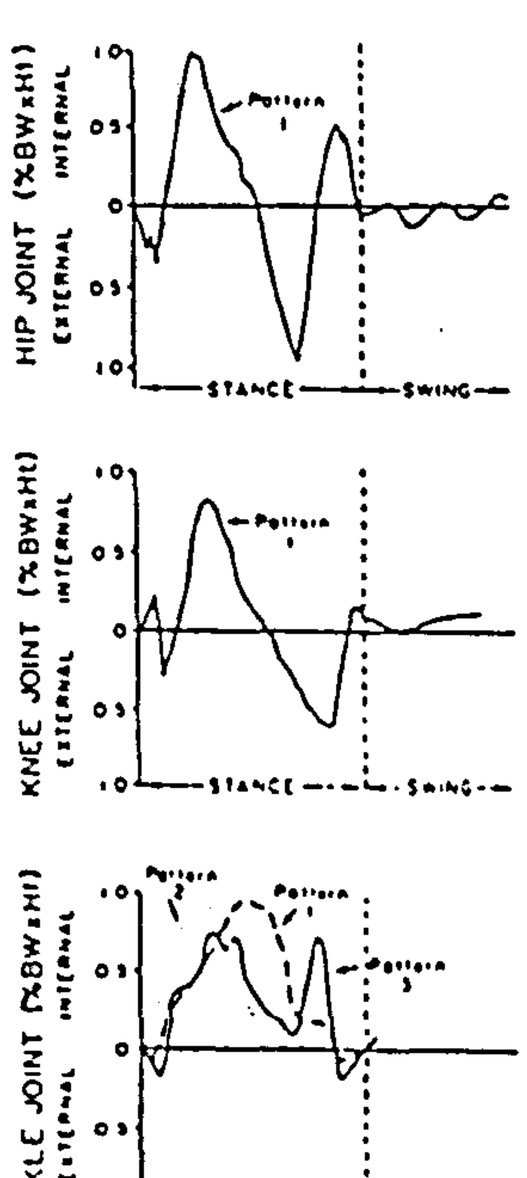

PATTERN FREQUENCY
PERCENT TOTAL OBSERVATIONS

Speed	Pattern No	All Subjects	Male	Female
Slow	1	99	100	98
	Other	1	0	2
Normal	1	99	98	100
	Other	1	2	0
Fast	1	99	98	100
	Other	1	2	0
Slow	1	99	98	100
	Other	1	2	0
Normal	1	98	96	100
	Other	2	4	0
Fast	1	99	100	99
	Other	1	0	1
Slow	1	55	62	49
	2	25	16	34
	3	14	16	11
	Other	6	6	6
Normal	1	40	40	40
	2	29	22	35
	3	18	24	13
	Other	13	14	12
Fast	1	33	38	29
	2	36	25	47
	3	16	22	11
	Other	15	16	13

FLEXION - EXTENSION MOMENT PATTERNS (EXTERNAL)

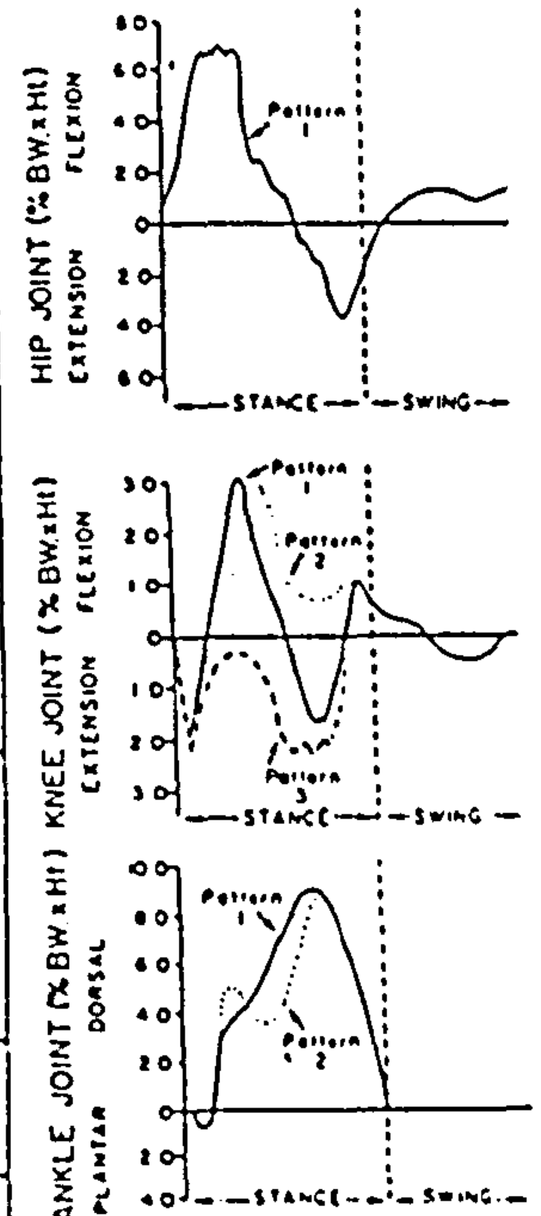

PATTERN FREQUENCY
PERCENT TOTAL OBSERVATIONS

Speed	Pattern	All Subject	Male	Female
Slow	1	99	98	100
	Other	1	2	0
Normal	1	99	98	100
		1	2	2
Fast	1	100	100	100
	Other	1	0	0
Slow	1	60	62	58
	2	13	12	13
	3	27	26	29
	Other	0	0	0
Normal	1	79	84	75
	2	5	6	5
	3	16	10	20
	Other	0	0	0
Fast	1	86	81	91
	2	9	11	7
	3	5	8	2
	Other	0	0	0
Slow	1	90	88	92
	2	10	12	8
	Other	0	0	0
Normal	1	77	70	84
	2	23	30	16
	Other	0	0	0
Fast	1	51	49	53
	2	49	51	47
	Other	0	0	0

Fig. 2.36 Variations of the joint moments for normal subjects.
(from Andriacchi & Strickland, 1985)

component of the muscular moment was the extension moment and the less important one was that about the antero-posterior axis. From the intersegmental loads, various factors that contributed to the loads were also analysed and their relative importance assessed.

Winter (1984) analysed the intra-subject and inter-subject variability on both kinematic and kinetic data, see Fig.2.35. He introduced a support moment concept, being the algebraic sum of the moments at the hip, knee and ankle joints, to characterize the total limb moment pattern. He also introduced a coefficient of variation to quantify the variations:

$$CV = \sqrt{\frac{1}{N}\sum_{i=1}^{i=N}\sigma_i^{\,2}} \Bigg/ \frac{1}{N}\sum_{i=1}^{i=N}|M_i| \qquad (2.3)$$

It was found that intra-subject variability of joint moment patterns over the stride was high at the knee and the hip, but low at the ankle and in the support moment. A similar pattern was also presented in inter-subject variability. Although the concept of the support moment does not have sound mechanical grounds, it has, according to Winter, served well as an indicator of leg stability during walking. A covariance analysis was conducted and the results showed high correlation between these joint moments, pointing to a compensating mechanism by the biarticulated muscles across these joints.

Andriacchi and Strickland(1985) reported variations in the joint moment patterns of the normal subjects during level walking, see Fig.2.36. Twenty-nine subjects (15 females and 14 males) were tested. It was found that the variabilities of the joint moment patterns decreased from the ankle joint to hip joint. It is interesting to note that walking speed had an influence on the occurrence frequency of the patterns, indicating that different walking strategies were adapted at different walking speed.

§2.6.4 Energy expenditure

Investigations into energy expenditure during walking have been conducted

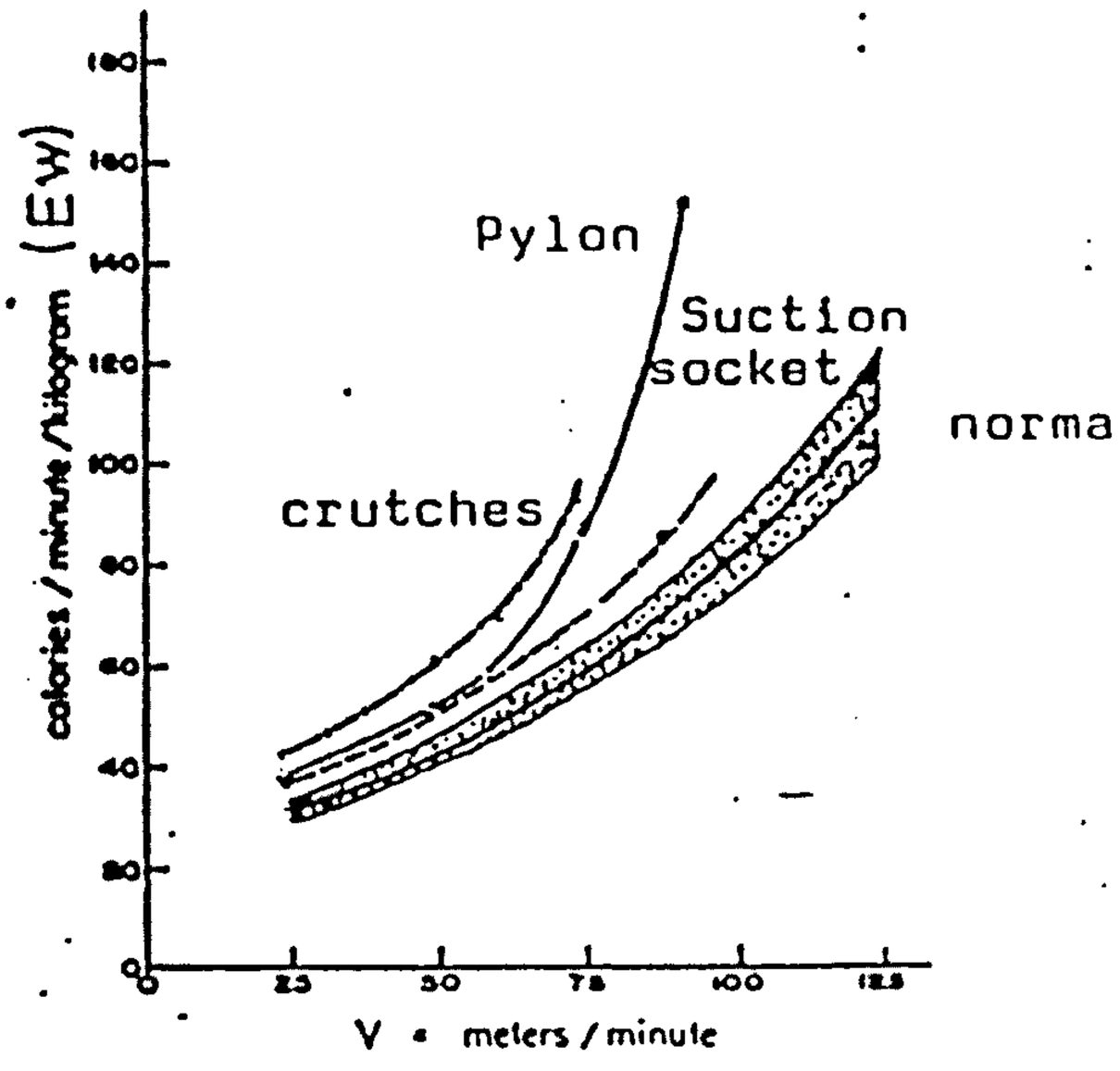

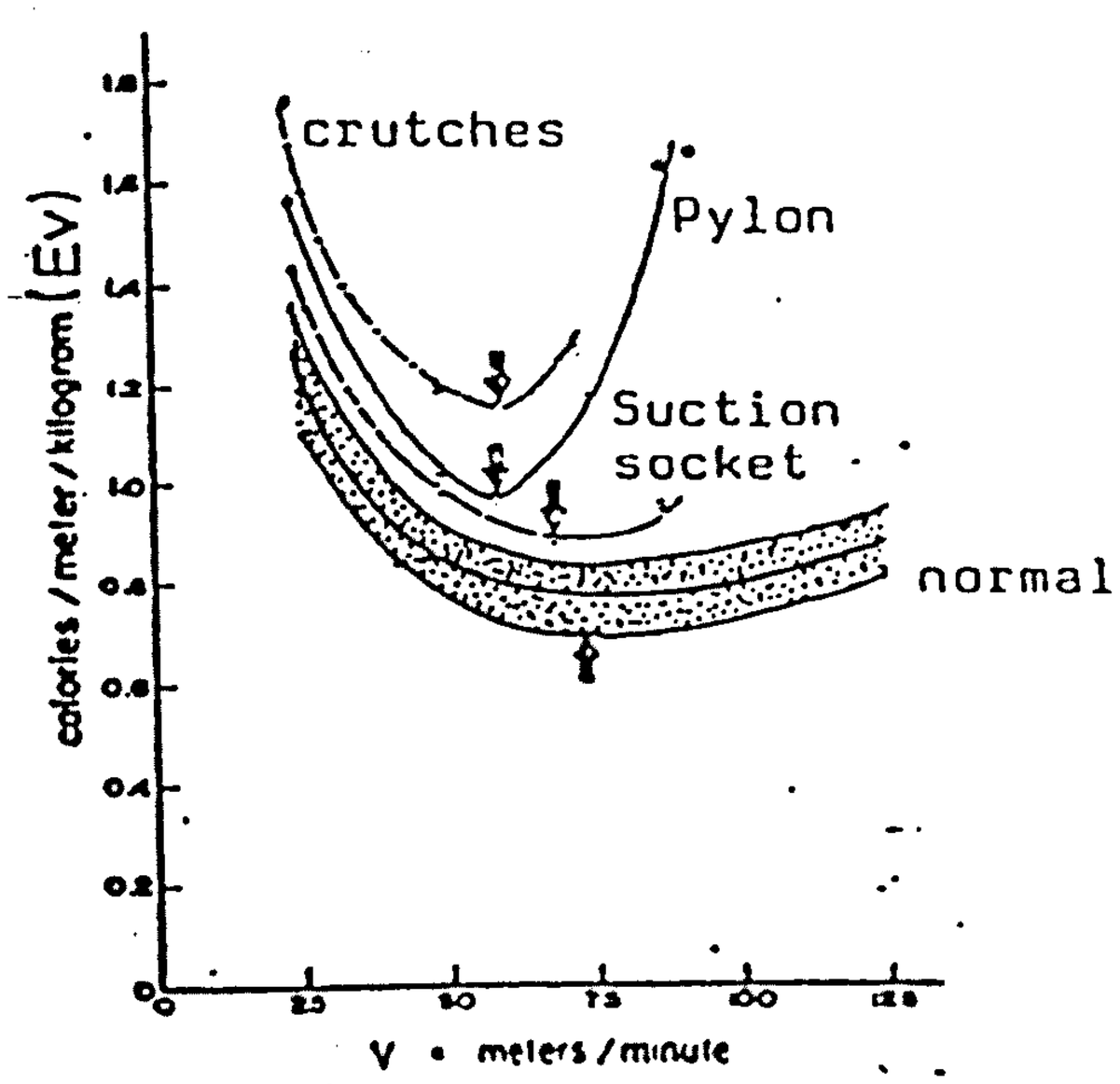

Fig.2.37 Averaged energy expenditure
during walking
(from Bard & Ralston, 1959)

since the 1920s and follow two different methodologies. One is, from the physiology point of view, to consider the total energy cost in walking by relating it to the metabolic energy consumed by the body, and this is often referred to as the "metabolic rate method". The other is, from the mechanical point of view, to consider the mechanical energy level of the body due to its kinematic state and the mechanical work done by the forces involved in walking. This method is often called the "mechanical energy method".

§2.6.4.1 Metabolic energy expenditure Since there is no direct method available to measure the metabolic energy expended by the body during activities, several kinds of indirect techniques have to be used. Garton (1979) presented a literature survey which included measurement techniques, the control of experimental protocol and the up-to-date equipment available. The literature survey shows that among the parameters available to estimate the metabolic energy expenditure, those involving respiratory function or heart rate appear to correlate with energy expenditure. He pointed out that the analysis of expired gas, from which can be deduced the rate of oxygen uptake by the body, was the most reliable method and was least affected by extraneous and uncontrollable influences. However, in order to achieve consistent and meaningful results, a stringent control of the experimental protocol is required, especially when small variations are to be resolved for an energy cost benefit analysis, such as would be expected when relatively minor changes in locomotion aids are being explored. Other problems associated with this method are the cumbersome facial attachments and the need for long experimental duration in order to obtain "good" average values over the sampling period.

In correlating energy expenditure to the walking speed, a parabolic relationship was found by many investigators (Passmore & Durnia, 1955; Ralston, 1958; Cotes & Meade, 1960; Robert, 1960; Molen & Rozendal, 1970). Based on data obtained on a number of subjects (57 males, 29 females), Zarrugh *et al* (1974) combine the parabolic equations obtained by the early investigators by using weighted averages of the constants and yielded the grand equation:

32a

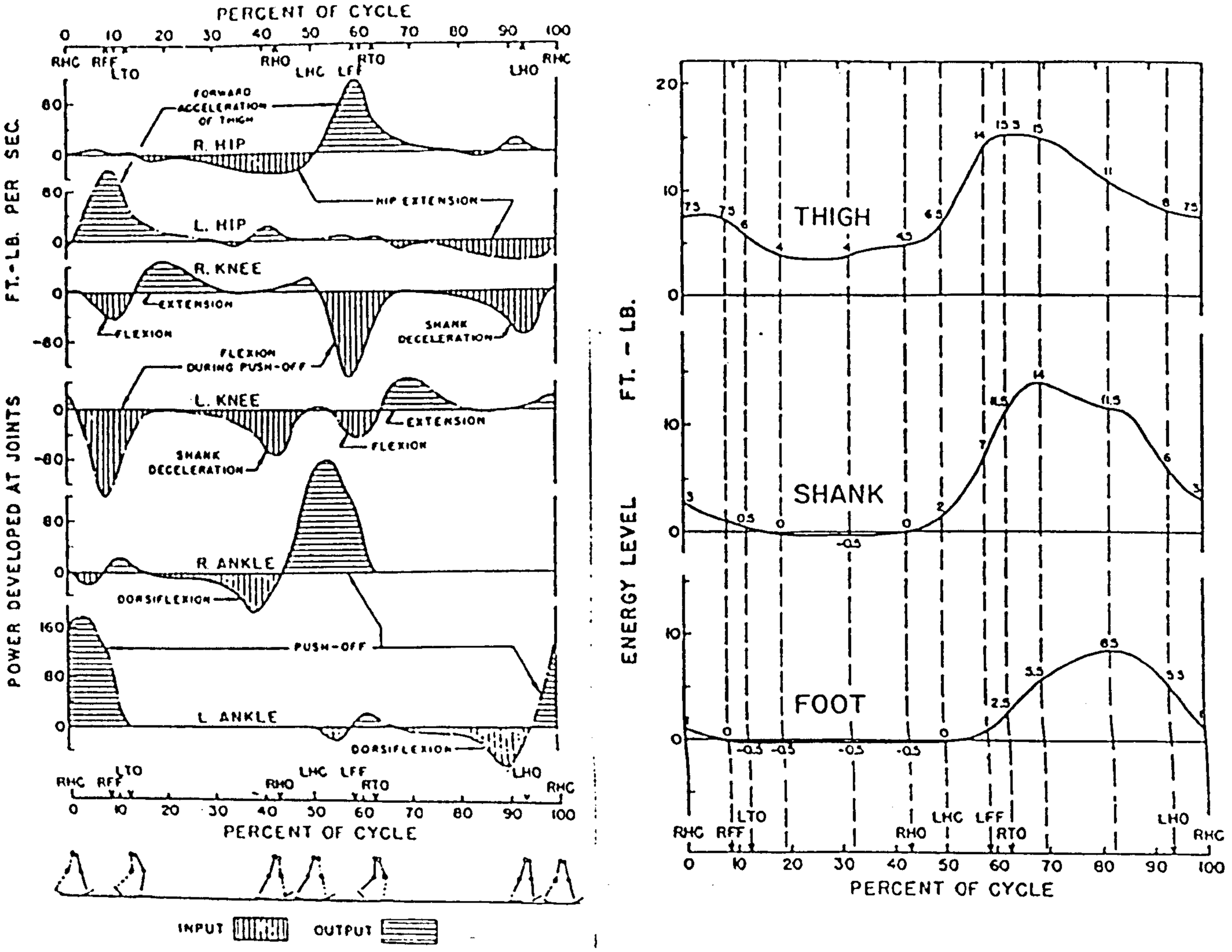

Fig.2.38 Average mechanical energy and power during walking. (from Bresler & Berry, 1951)

$$E_w = 32.0+0.0050V^2 \tag{2.2}$$

where E_W is the energy expenditure in cal/min/kg, V the walking speed in m/min. Dividing the equation by V results in a hyperbolic expression which give rise to a walking speed $V' = 80\ (m/min)$ at which the least energy is consumed.Ralston (1958) found that the normal walking speed was very close to 80 m/min and this finding was confirmed by Corcoran & Brengelmann (1970). It is therefore accepted that the 'conservation of energy' law applies to normal level walking.

§2.6.4.2 Mechanical energy expenditure (MEE) A number of investigations into the mechanical energy expenditure during walking have been performed since the pioneer work of Fenn (1930), and generally can be classified according to the following two methods of analysis:

(1) Energy expenditure for mechanical movement determined by the product of joint moment and joint angular velocity, that is, by joint power. Both kinematic and kinetic information are required in this method.

(2) Energy expenditure is determined from changes in the mechanical energy level of the body limbs. Since the energy level of the body segments can be obtained merely from the kinematic data and body physical parameters, this method does not require information on the external force.

Elftman (1939) investigated MEE using the first method. The ground reaction forces were measured by a forceplate and the kinematic data obtained from the cinematographic records. The analysis was performed only in the sagittal plane and the energy level and power were calculated. He noted that when the rate of energy change of a segment is positive, ie, its energy level is increasing, energy must flow into the segment from work done by forces acting at the segment's joints or by muscle moments.

Bresler and Berry (1951) conducted a 3-D analysis on the MEE using the first method. Four normal male subjects were tested. The mechanical power was determined by the product of the joint moment and the joint angular velocity and the mechanical work done by graphically integrating the power-time curve. Fig.2.38 shows the average energy levels and the average power of the leg, respectively. It

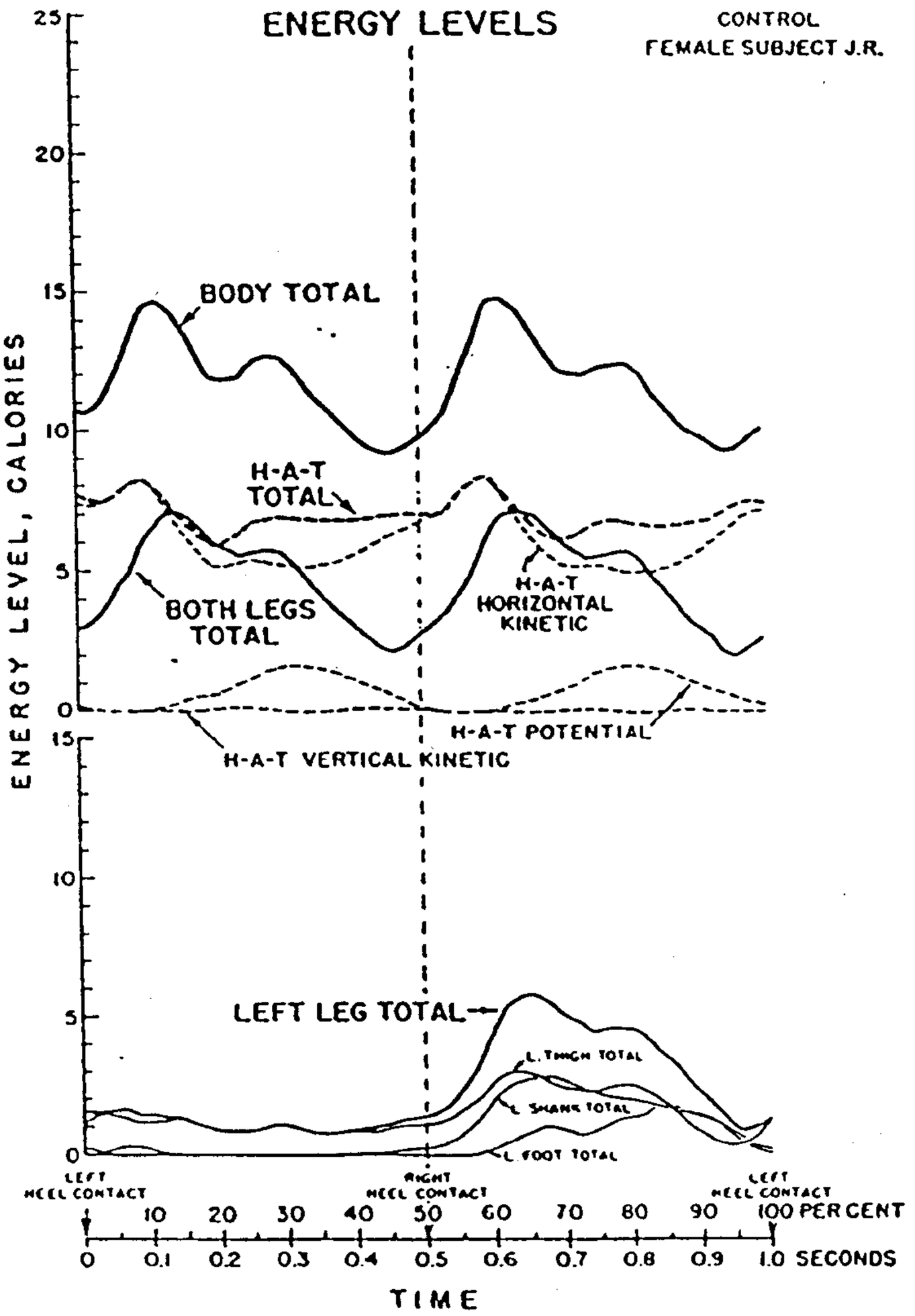

Female, 19, 159 cm, 53·7 kg. Walking speed 73·2 m/min. Energy levels of body segments and of whole body, as labelled.

Fig.2.39 Energy level of body segments and of whole body. (from Ralston & Lukin, 1969)

Description of movement	Type of contraction	Directions of segmental ang. velocities	Muscle function	Amount, type and direction of power
Both segments rotating in opposite directions (a) joint angle decreasing	Concentric	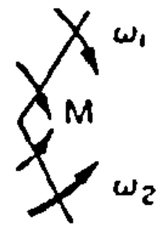	Mechanical energy generation	$M\omega_1$ generated to segment 1. $M\omega_2$ generated to segment 2.
(b) joint angle increasing	Eccentric	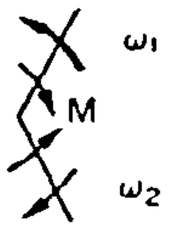	Mechanical energy absorption	$M\omega_1$ absorbed from segment 1. $M\omega_2$ absorbed from segment 2.
Both segments rotating in same direction (a) joint angle decreasing (e.g. $\omega_1 > \omega_2$)	Concentric	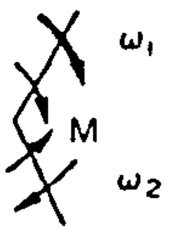	Mechanical energy generation and transfer	$M(\omega_1 - \omega_2)$ generated to segment 1. $M\omega_2$ transferred to segment 1 from 2.
(b) joint angle increasing (e.g. $\omega_2 > \omega_1$)	Eccentric	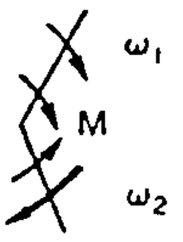	Mechanical energy absorption and transfer	$M(\omega_2 - \omega_1)$ absorbed from segment 2. $M\omega_1$ transferred to segment 1 from 2.
(c) joint angle constant ($\omega_1 = \omega_2$)	Isometric (dynamic)	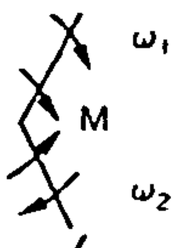	Mechanical energy transfer	$M\omega_2$ transferred from segment 2 to 1.
One segment fixed (e.g. segment 1.) (a) joint angle decreasing ($\omega_1 = 0, \omega_2 > 0$)	Concentric	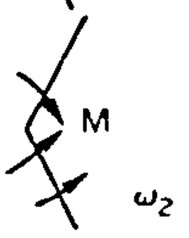	Mechanical energy generation	$M\omega_2$ generated to segment 2.
(b) joint angle increasing ($\omega_1 = 0, \omega_2 > 0$)	Eccentric	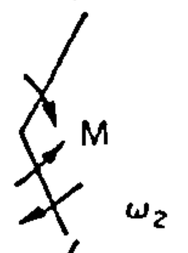	Mechanical energy absorption	$M\omega_2$ absorbed from segment 2.
(c) joint angle constant ($\omega_1 = \omega_2 = 0$)	Isometric (static)	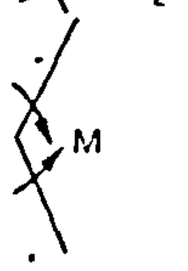	No mechanical energy function	Zero.

Fig.2.40 Possible work functions of a muscle connecting two segments.
(from Robertson & Winter, 1980)

was found that the ankle and the hip joints had energy outputs considerably greater than energy inputs and provided most of the energy required for level walking, while the knee joint, having an output less than the input, acted as an energy absorber during walking.

Cavagna *et al* (1963) computed the external work required in walking from 3-D accelerometer records of the trunk. The external work was defined by them as the energy change of the centre of mass of the body. Based on this definition, they only utilized forceplate data to analyze the energy of the centre of mass of the body, i.e, velocities and displacements were obtained by single and double integration of the ground reaction forces respectively. This analysis does not take into account the reciprocal movements of the limbs and would thus underestimate the total energy of the body. Winter (1979) showed in his study that it would be lowered by 16.2 percent.

Ralston and Lukin (1969) reported research in which both the mechanical energy level and metabolic energy expenditure were measured simultaneously, see Fig.2.39. It was observed that the HAT (the head, arms & trunk) tended to act as a conservation system in that there appeared to be an interchange of potential and kinetic energy.

Robertson & Winter (1980) presented a detailed analysis of the mechanical energy generation, absorption and transfer amongst segments during walking. It was shown that the joint force power, defined as the product of the joint force and the joint velocity, indicated the rate of flow of energy into or out of the segment. However, for the joint moment power, defined as the product of the joint moment and the joint angular velocity, it not only merely indicated a transfer of energy through the muscles but also the generation or absorption of mechanical energy. Fig.2.40. shows all possible work functions that can occur between two segments connected by an active muscle. An experiment was performed on two male subjects and a comparison was made between the total power and the total rate of change of energy of the segment. The results indicated that the work-energy principle holds in their study.

Zarrugh (1981) investigated the influence of walking speed on the mechanical

34a

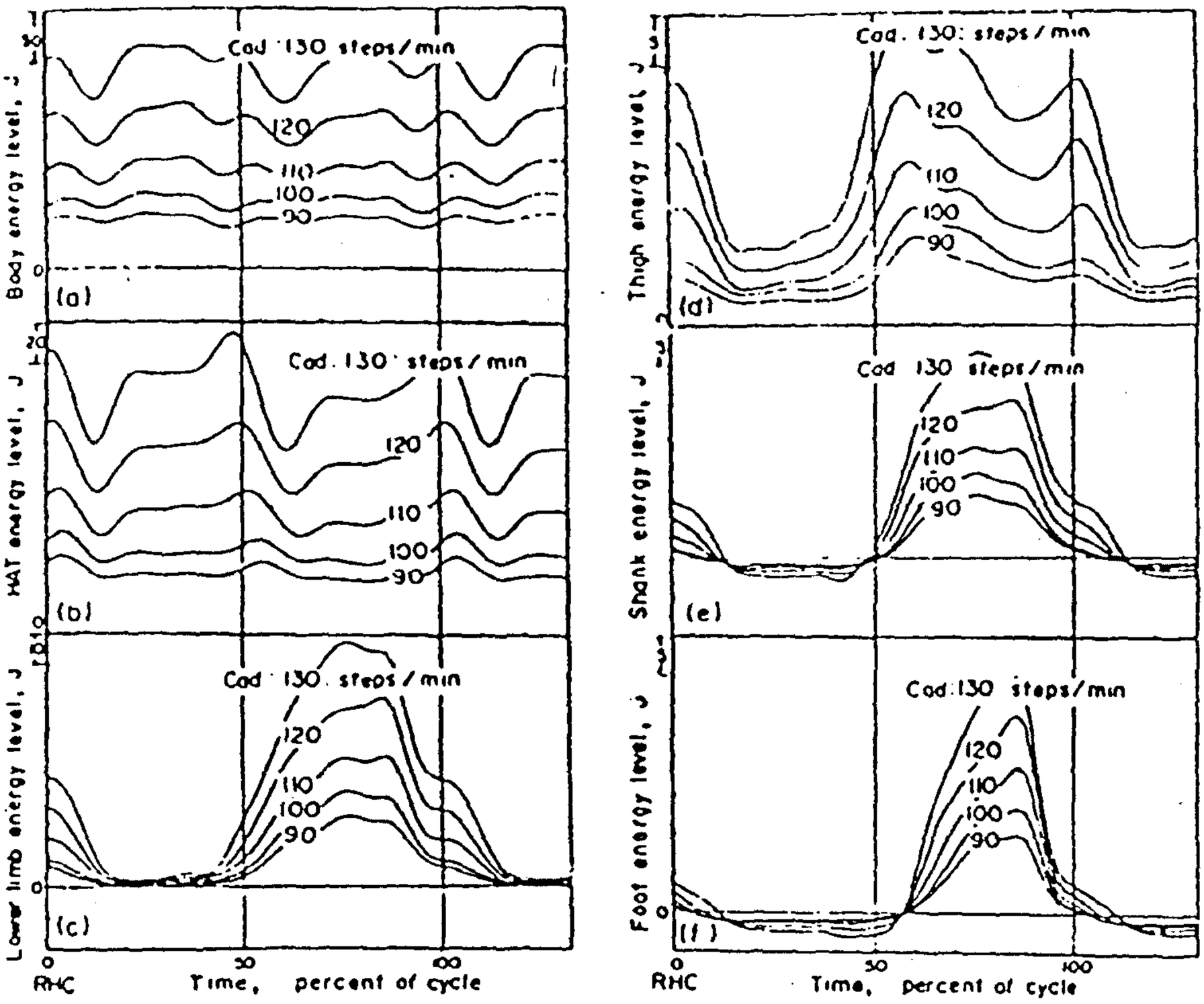

Instantaneous energy levels of the body and its divisions in free walking. For this subject, the walking speed in m sec can be obtained by dividing the cadence squared in (steps/min)^2 by 8000, e.g. (110 steps/min)^2/8000 = 1.51 m/sec.

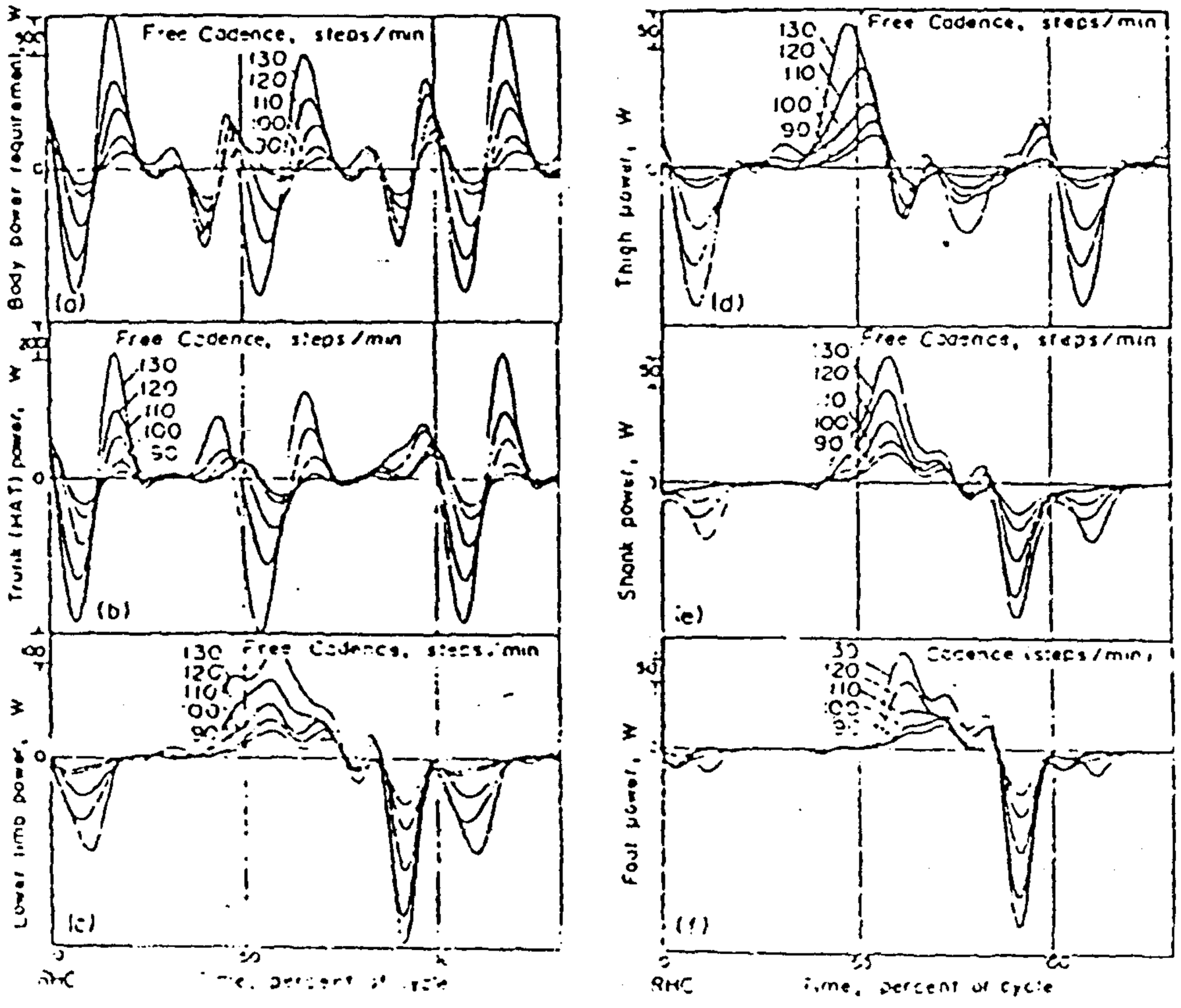

Fig.2.41 Mechanical energy and power related to walking speed. (from Zarrugh, 1981)

energy and power, see Fig.2.41. It was observed that all the variables increased with the speed.

Several algorithms have been proposed in an attempt to assess the *MEE* from changes in the segmental energy levels. If the potential energy, the translation and angular kinetic energies of a segment are denoted as *PE, TKE, RKE* respectively, the total instantaneous energy of the segment will be

$$E_S = PK + TKE + RKE \tag{2.3}$$

Norman *et al* (1976) proposed a method, termed pseudowork, to assess the MEE as

$$TPW = \sum^{N} \sum^{M} (| \Delta PE | + | \Delta TKE | + | \Delta RKE |) \tag{2.4}$$

where *TPW* was Total body Pseudo Work, M the total number of segments, N the total number of frames during a walking cycle. This method does not allow for either energy transfer between segments or exchange of energy forms within a segment, and thus greatly overestimates the *MEE*.

Winter (1979) developed a procedure to estimate energy transfer and exchange. If there were no exchange of energy forms within a segment, the MEE of the segment would be

$$W_S = \sum^{N} (| \Delta PE | + | \Delta TKE | + | \Delta RKE |) \tag{2.5}$$

and the amount of energy exchanged will be

$$W_S - \sum^{N} | \Delta E_S | \tag{2.6}$$

Similarly, if there was no inter-segmental energy transfer, the MEE of the whole body would be

$$W_b = \sum^{M} \sum^{N} | \Delta E_S | \tag{2.7}$$

and inter-segmental energy transfer may be estimated by

$$W_b - \sum^{N} | \Delta E_b | \tag{2.8}$$

where

$$\Delta E_b = \sum^{M} \Delta E_S \tag{2.9}$$

Aleshinsky (1986) presented a rigorous analysis of the mechanical energy expenditure (MEE) problem. The principle concept in his analysis is that whether the work done by a muscle is positive or negative the muscle always demands metabolic energy. The MEE of the muscle therefore does not equal the conventional mechanical work, as defined in mechanics:

$$W = \int \boldsymbol{F} \cdot \boldsymbol{V} dt = \int P dt \tag{2.10}$$

but

$$W = \int | \boldsymbol{F} \cdot \boldsymbol{V} | dt = \int | P | dt \tag{2.11}$$

where $\boldsymbol{F}$ is muscle force, $\boldsymbol{V}$ the velocity of the application point of the muscle force and P the power of the muscle force. Based on some basic and reasonable assumptions, he formulated the *MEE*, analyzed the different methods used for MEE determination and clarified the possibilities for minimizing energy expenditure.

CHAPTER 3
PROSTHETICS OF THE LOWER LIMB

§ 3.1 Introduction

Such a progress has been made in amputee rehabilitation over the last half century, including new surgical techniques, better understanding of the biomechanical principles involved in normal and abnormal human locomotion, and improved design of artificial limbs using new materials, components and techniques, that it is beyond the scope of this thesis to elaborate on all the improvements. Only a general review on the lower-limb prosthetics relevant to the work described in this thesis is presented in this chapter.

§ 3.2 Amputation Surgery

The loss of part of the body can be a profound shocking experience for any human being since it is irretrievable. Therefore, amputation surgery should be treated seriously and performed carefully. Confronting the surgeons are three questions: (1) is amputation the correct treatment? (2) At what level should the amputation be done? (3) What are the objects of the operation itself? In order to achieve a satisfactory solution to these questions, all the following factors require careful consideration: pathological, anatomical, surgical, prosthetic and personal (*viz* sex, age and occupation). Each of these factor will play some part in the decision making and each will have different emphasis in the light of the clinical situation.

Generally, the amputation surgery has two purposes: ablation and reconstruction. The operation must remove all the tissues necessary to eliminate the pathological state and to provide primary or second wound healing. The reconstruction must create the optimum motor and sensory stump for prosthetic substitution and restraining function. Amputation therefore should be regarded as the beginning of a rehabilitation process rather than the end of the story.

Only a brief account of the aspects relevant to amputation surgery is presented

in this section.

§3.2.1 Development of the amputation surgical techniques

The development of amputation surgery follows closely the evolution of medical surgery itself, especially orthopaedic surgery. Readers who are interested in a comprehensive history of amputation surgery are recommended to refer to Garrison (1963) or Slocum (1949) .

For many centuries (22 A.D-1500 A.D), bleeding during the operation was controlled by crushing the stump or dipping it in boiling oil. Ligatures, which had once been used by Hippocrates, were re-introduced by Ambroise Pare in 1629 and resulted in an increase in the rate of survival. Towards the early 19th century, amputation was the commonest of all surgical procedures thanks to the further improvement in techniques such as the use of the tourniquet by Morel (1674), appropriate handling of soft tissues and secondary wound closure.

Two events of immense surgical importance were the discovery and use of chloroform as an anaesthetic (Samisen, 1847) and carbolic acid as an antiseptic agent (Lord Lister, 1860s), marking the beginning of modern surgery. From that time onwards it has not been necessary to remove a limb in seconds and surgeons could focus their attention on improving methods of stump shaping.

§3.2.2 Indications for amputation

Vascular disease is by far the most common cause of amputation in North America and Europe. Statistical surveys on amputation (Glattly 1964; Kay and Newman 1975; DHSS 1976,1978) have shown that over 70 percent of amputees fall into this group and moreover that an increasing trend in the percentage of amputations has been observed in the USA and U.K. It was also noted that nearly all (more than 97 percent) of amputees in this group were over 50 years old. This disease appears to be associated directly with standards of living and long life expectancy. Obesity and some fatty diets probably contribute to the disease.

As far as the level of amputation is concerned, the operation should give viable tissues likely to survive the operation, and at the same time maximize the functional

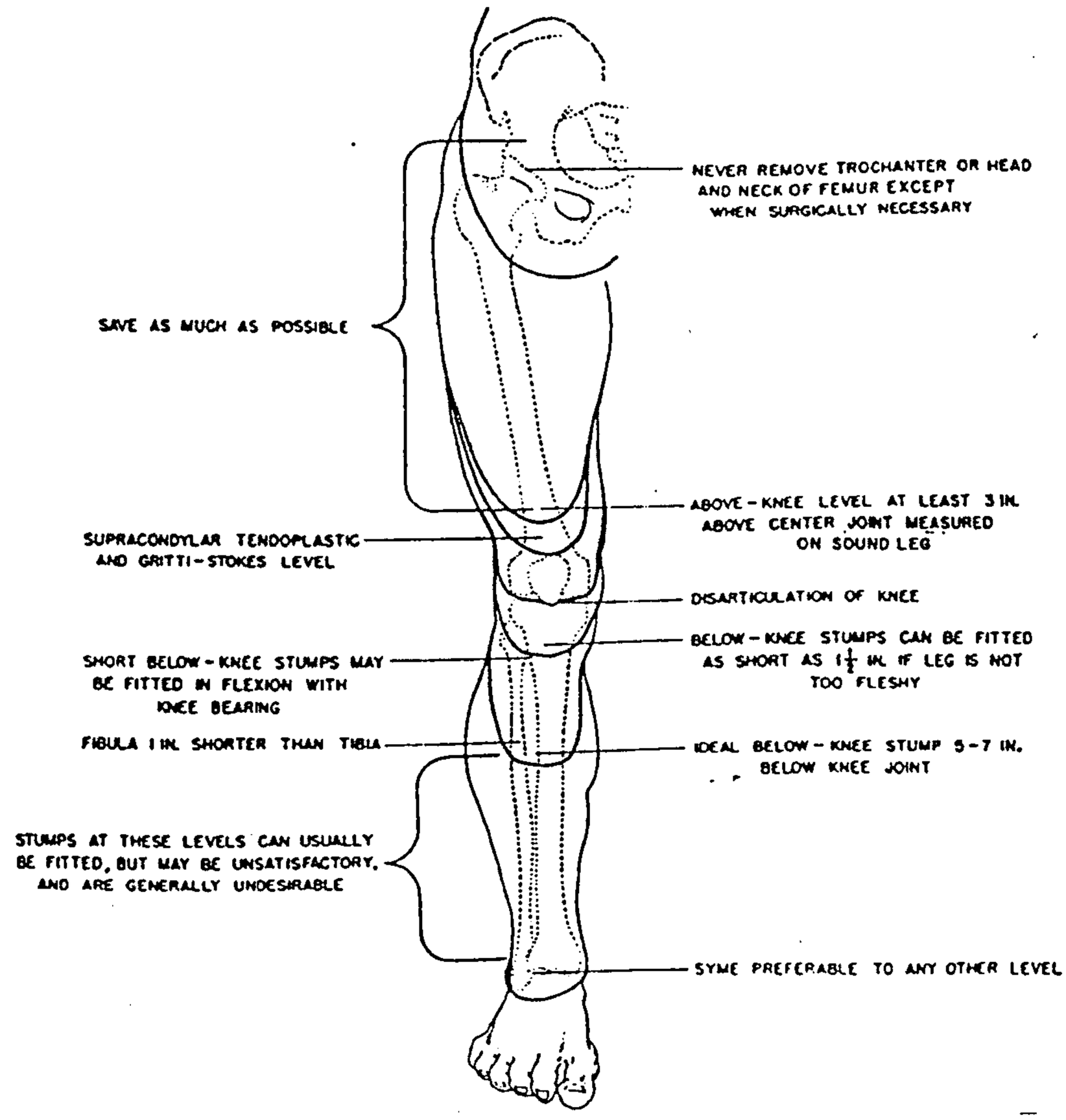

Fig.3.1 Major sites of amputation in the lower-limb extremity.
(from Alldredge & Murphy in Wilson, 1968)

results. Saving the knee joint in lower limb amputation is always desirable.

Trauma or injury, generally as a result of industrial or road traffic accidents, rates second (about 10 percent) of the causes that leads to amputation. It naturally affects all age groups. The surgeon usually pursues a two-stage operation, that is, firstly saving as much tissue as possible and then, at a later date, performing a more definitive amputation procedure.

Tumour, usually sarcoma of the bone or soft tissues, is an indication for amputation in the younger age group, although rarely. In order to safeguard prognosis, amputation must be performed at rather a high level, usually with a joint intervening between the disease site and the amputation level.

Other indications for amputation include chronic infection, paralysis, deformity and limb discrepancy, and congenital limb deficiency. Fortunately, these are rare, less than 2 percent altogether.

Amputation, of course, is by no means the only solution to these problems, indeed it is usually the last course of action. Recent progress in reconstructive surgery make amputation very rare for patients with severe injury. Tumour may be treated with deep radiotherapy and chemotherapy, or can be excised and an orthopedic implant or transplant inserted in place.

§3.2.3 Levels and limiting factors in lower limb amputation

The levels of lower-limb amputation vary considerably (see Fig.3.1), each of them has its particular points of importance in treatment and governed by different limiting factors. With the advancement of prosthetic systems and fitting techniques, prosthetic considerations have become less important and the surgical consideration are the primary determinants of the level of lower-limb amputation. The principle is to conserve joints and preserve as much limb length as possible.

Hindquarter amputation and hip disarticulation are mainly determined by pathology. The indication for these amputations are nearly always tumour. Obviously, a gross functional limitation is imposed on the patient.

Above-knee amputation should leave a stump as long as possible, subject to pathology and to the need for an adequate space for the functional knee mechanism of

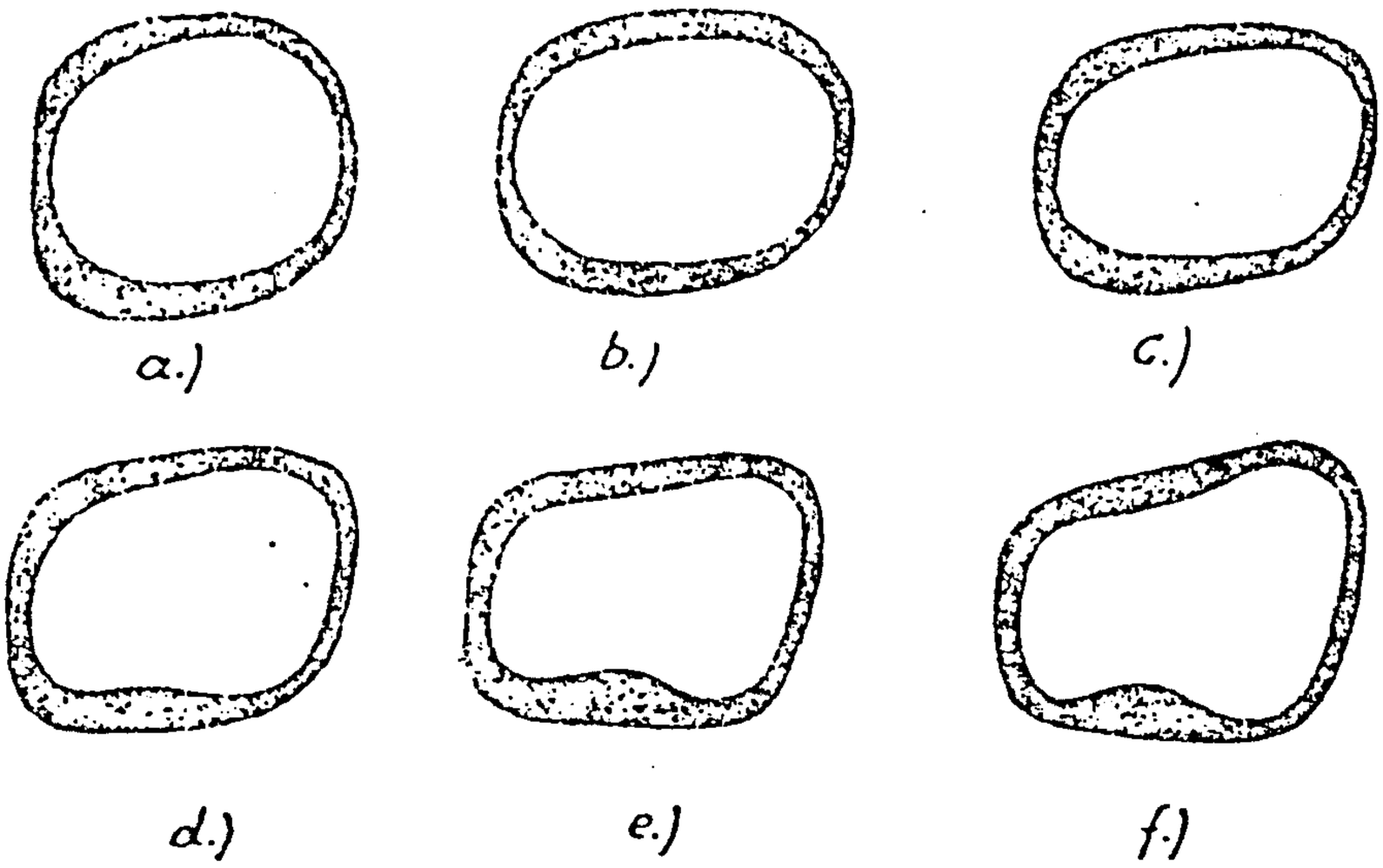

(a) for a stump without bony support;
(b) for a big flabby stump;
(c) for a stump without muscle relief;
(d) for a stump with "average" muscle development;
(e) for a muscular stump;
(f) for an athletic stump.

Fig.3.2 Different shapes of the socket brim for AK prosthese.
(from Kuhn, 1956)

a prosthesis. It is said that an ideal level is 10~15cm above the knee centre.The Gritti-Stokes amputation is not recommended as end bearing tends to be unacceptable to the patient and furthermore fails to provide adequate space for a knee mechanism.

The through-knee amputation or knee disarticulation has been proved to be an excellent procedure. It is easy to perform and relatively bloodless, and the resulting stump bears weight very well. In the past, cosmesis used to be a problem but this has been largely overcome.

There is a common limiting factor in above-knee and through-knee amputation, that is, the presence of hip flexion deformity.

The below-knee amputation is the most preferred in most cases since it preserve the knee joint. With the advent of new surgical techniques, its viability has steadily increased even in vascular disease. The main limiting factor is knee-flexion deformity.

The Syme's amputation resulfs in a stump which can accept the full body weight. However, the prostheses fitted has cosmetic disadvantages.

The partial foot amputation is performed in many ways at various levels, but only a few give good functional results.

§ 3.3 Lower-Limb Prosthetic systems

§3.3.1 Above-knee sockets

There are four major interrelated considerations in prosthetic socket design: support, control, suspension and alignment.

Support in a socket is provided through the distribution of pressure on residual limb tissues in relation to those tissues which are pressure sensitive or pressure tolerant. The distribution of pressure must based on socket contouring that distributes limb contact pressures as evenly as possible on pressure tolerant areas.

During swing phase, full stump-to-socket contact is necessary to provide control over the prosthesis that is lifted off the walking ground. The total-contact socket best fulfills these requirements.

Suspension can be provided in any one or in a combination of basic types:

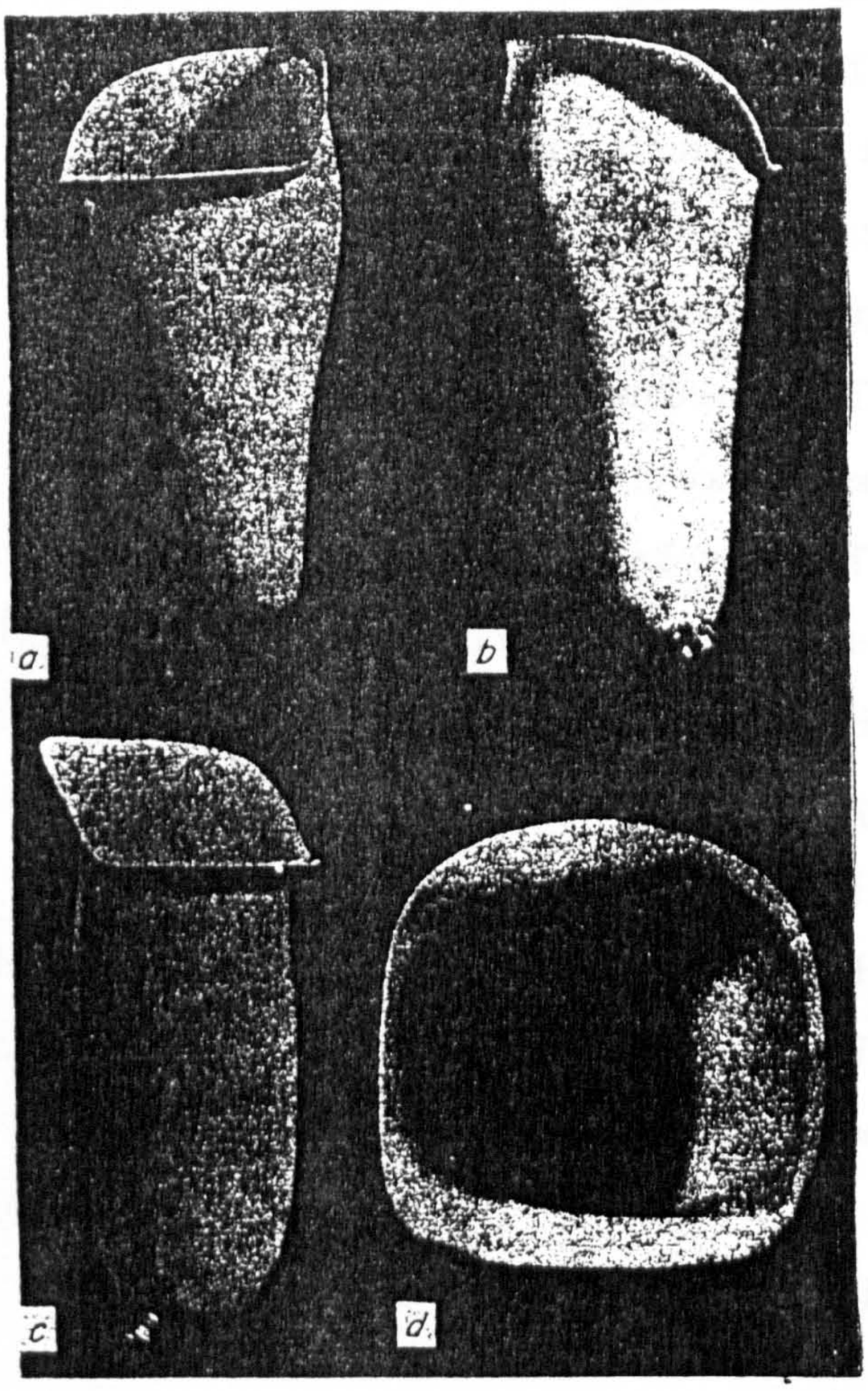

The Above-Knee socket. *a* posterior view; *b* anterior view; *c* medial view; *d* viewed from above.

Fig.3.3 The total-contact gluteal-ischial bearing quadrilateral socket. (from Lyquist in Murdoch, 1969)

mechanical joint with corset, suspension belt, suction socket and socket contouring.

Alignment refers to the angular and linear position of the socket in relation to the knee and foot. The angular alignment of the socket is particularly important in that the socket must be in that position in which the amputee can gain best control with the remaining musculature. The linear alignment must be adjusted to position the socket over the prosthetic knee to achieve proper balance and/or to obtain the maximum function from the prosthetic components.

There have been many different shapes of socket brim designed for the above-knee socket. They vary from circular or oval to triangular or quadrilateral. Kuhn (1956) distinguished and list six different shapes of brim, as shown in Fig.3.2. They range from the total absence of muscle relieving contours to that for an athlete's muscular stump.

The most popular socket used nowadays is the total contact gluteal-ischial bearing quadrilateral socket. The origin of this socket is attributed to Striede of Austria. Eberhart *et al* (1949) introduced this design into the U.S.A., and extensive studies were conducted to produce the biomechanical rationale for the shape of this socket design at University of California.

Fig.3.3 shows the quadrilateral socket. The inner contour of the socket is significantly different from that of the relaxed amputee's thigh and it is this difference, deliberately modified, that achieves a certain type of pressure distribution. On the socket's inner surface, there are concave areas (reliefs) for reducing pressure on relatively firm tissues, such as the tendons, contracting muscles and bony prominences, and convex areas (bulges) for pressing on soft, pressure-tolerating areas of the stump so that these areas will take higher pressure and thereby their appropriate share of the load. Extending from the posterior wall of the socket is a widely flared area to provide support through the ischial tuberosity and gluteal muscles. The anterior wall is 5 to 7.5cm higher than the posterior wall, maintaining the ischial tuberosity in its proper place on the ischial seat of the socket and providing more area over which to distribute the force required. The lateral wall is adducted and relatively flat to evenly distribute the large forces during mid-stance. The lateral wall is also high and curved in over the greater trochanter to provide increased lateral stability. This socket has another

QUADRILATERAL

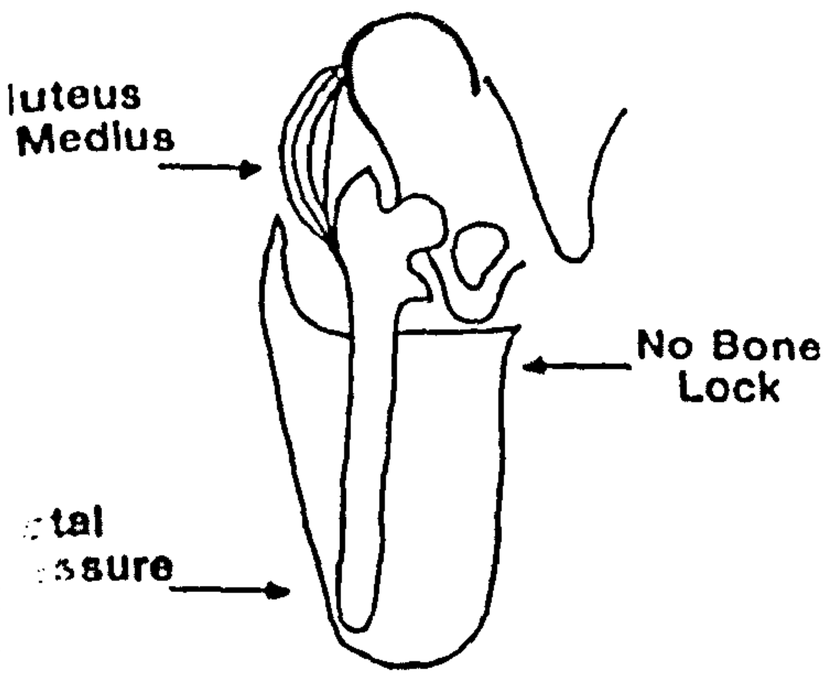

No bone block and no real force system to vent femoral or ischial drift. Ischial tuberosity acts a fulcrum. Pelvis can rotate as well as the femur duct.

CAT-CAM

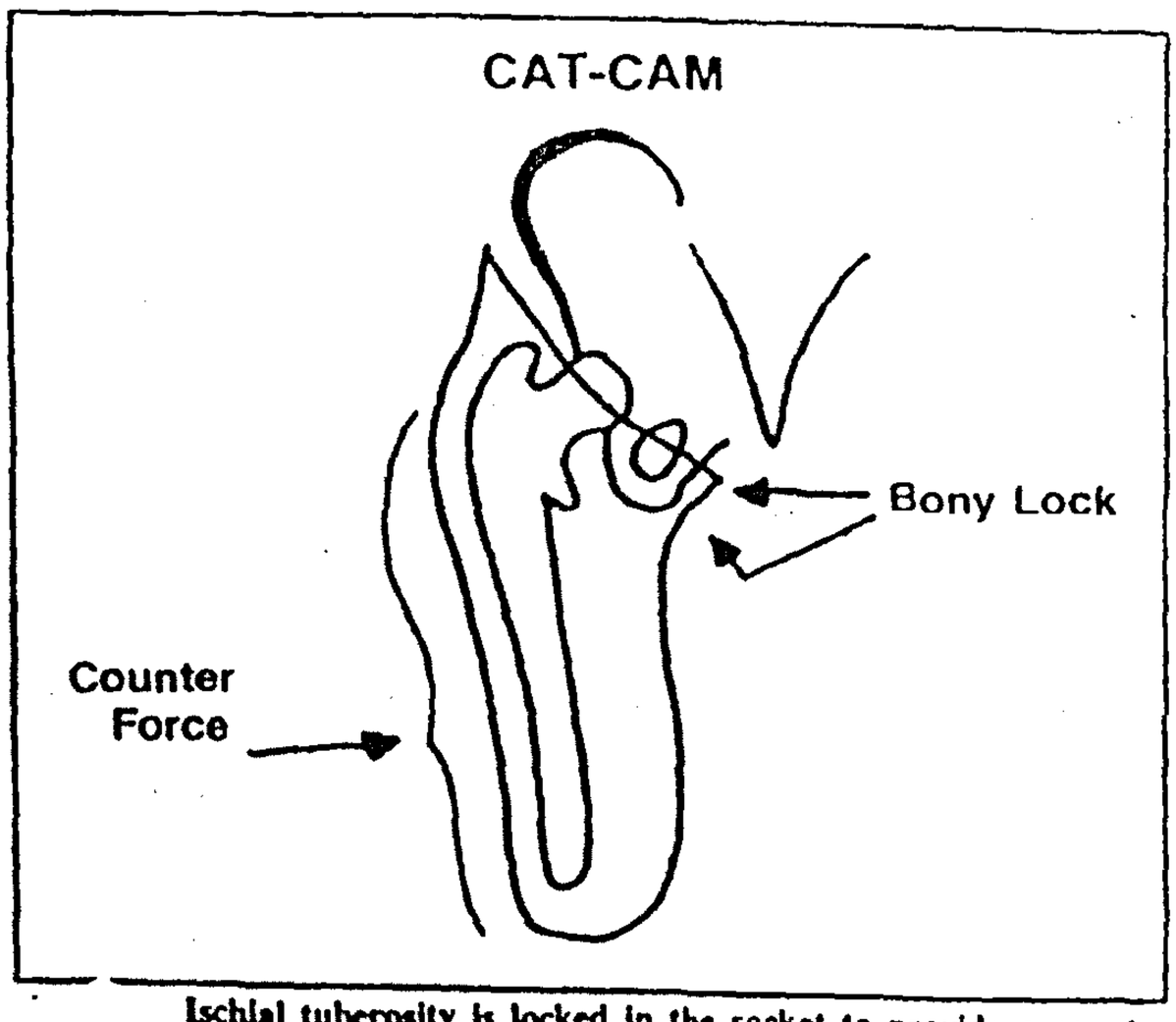

Ischial tuberosity is locked in the socket to provide a counter force against femoral shift.

CAT-CAM vs QUAD

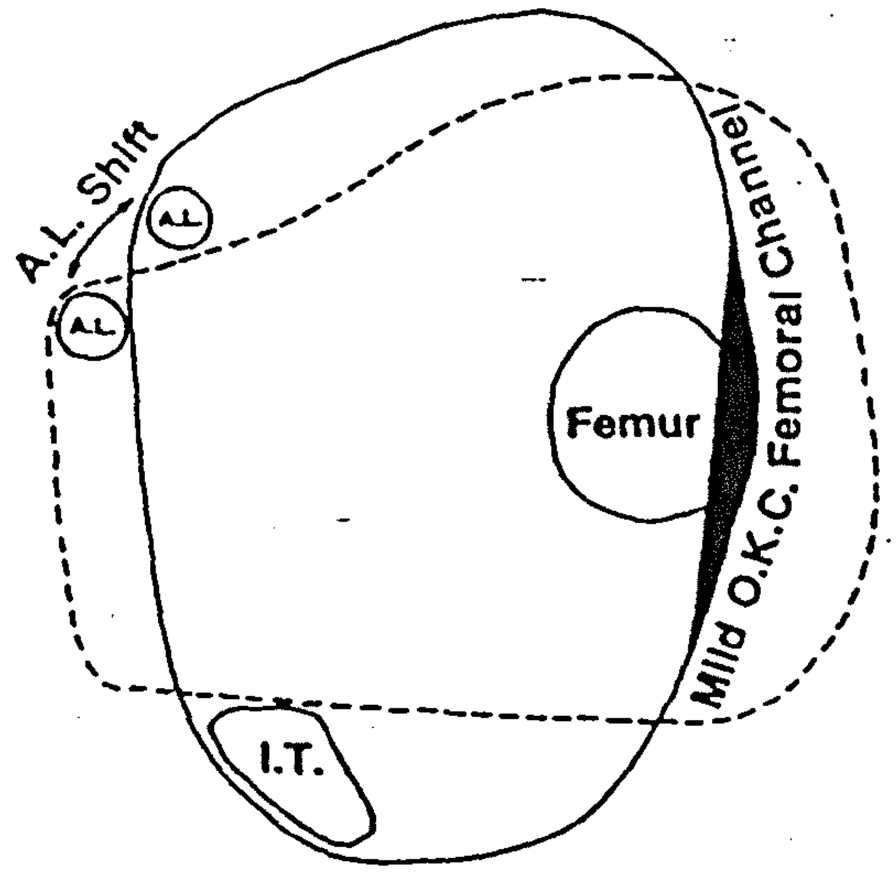

Comparison of CAT-CAM and quadrilateral sockets in a transverse view. Since the femur and ischial tuberosity are fixed in position, the adductor longus tendon has to shift a small amount. Note mild O.K.C. (Oklahoma City) channel about the femur.

Fig.3.4 Comparison between the CAT-CAM socket and the quadrilateral socket.
(from Sabolich, 1985)

advantage that provides good rotational stability without restricting muscle function.

Although the quadrilateral socket is most frequently seen in amputees, the above-knee socket is undergoing dramatic evolutionary changes at the present time. The reports of Lehneis (1985), Long (1985) and Sabolich (1985) are most significant in this regard. They point out that with the change in amputee population, overwhelmingly geriatric, the limiting factors associated with the quadrilateral socket have become more apparent. The quadrilateral design impinges directly onto the neurovascular bundle in the area of the scarpa's triangle and the patient's seat area bears directly onto an anatomical area which is usually atrophied to the point of being uncomfortable. Furthermore, no bone block and no real force system exist in the quadrilateral socket to prevent femoral or ischial shift in the frontal plane. The ischial tuberosity acts as a fulcrum, the pelvis can rotate and the femur can abduct, resulting in inadequate stabilization in the frontal plane and the gluteus medius gait most AK amputees demonstrate. The normal shape-normal alignment (NSNA) by Long (1985) and the contoured adducted trochanteric- controlled alignment method (CAT-CAM) by Sabolich attempt to overcome the above disadvantages and share the same rationale, see Fig.3.4. The ischial tuberosity and part of the inferior ramus of the ischium rest inside the socket proper and bear laterally directed forces which work in conjunction with medially directed forces borne by the femur to keep the femur adducted and the ischium stable. The M/L dimension of the socket is narrowed and the lateral wall of the socket is shaped to give support over a wide area, in addition supporting the femur in adduction. Approximately 900 CAT-CAM prostheses and many NSNA prostheses over a period of 11 years have been fitted to the patients, and the results have been proven by the patients' acceptance.

§3.3.2 Above-knee suspension system

Three different types of suspensions are used in AK prosthesis: suction, Silesian belt, and hip joint and pelvic band. Suction suspension can also be combined with the other two methods.

Suction suspension maintains the prosthesis by negative air pressure in the socket during swing phase. This is accomplished by an air expulsion valve at the distal

end of the socket and a very well-contoured socket that fits around the patient's leg directly against the skin to form a seal. Donning the suction socket requires a certain amount of effort and skill from the patient. He must pull himself into the socket by applying a sockinette, through the valve hole at the distal end, around the stump and pulling the stump down into the socket. Therefore, suction sockets are contraindicated for patients suffering from heart disease, those experiencing significant stump volume fluctuations, balance problems, upper limb disabilities or other physical problems that will not allow the exertion required to don the prosthesis.

The Silesian belt consists of a flexible belt usually made of cloth or leather. The belt is attached at a pivot at the lateral aspect of the socket at the approximate location of the trochanter and extends around the back over the iliac crest to the anterior middle line where it terminates in a D ring. The belt is attached to the anterior of the socket by a strap that extends from 2.5cm anterior to the ischial level through the D ring and down to a buckle, which is attached 2.5cm distal to the ischial level of the prosthesis on the anterior wall of the socket. The Silesian belt can provide a very comfortable, positive suspension. It is lightweight and is not affected by the factors that affect suction suspension. The disadvantages of the Silesian belt are that it is more cumbersome and less cosmetically appealing than the suction suspension and does not provide the same degree of control of movement as does a hip joint and pelvic band suspension.

The hip joint and pelvic band provides positive suspension and control to an AK prosthesis. The hip joint is placed anteriorly and proximally to the greater trochanter to approximate the location of the anatomical hip joint centre and the metal extension from the proximal hip joint is used for attachment of the pelvic band. The pelvic band, being located between the greater trochanter and the iliac crest and extending from the anterior superior iliac spine, is attached to a wide cloth or leather waist belt that wraps around the patient's waist and buckles anteriorly. This kind of suspension is indicated for patients who have poor ability to control their prostheses. Geriatric patients are the most common user of this suspension system.

§3.3.3 Prosthetic knee units

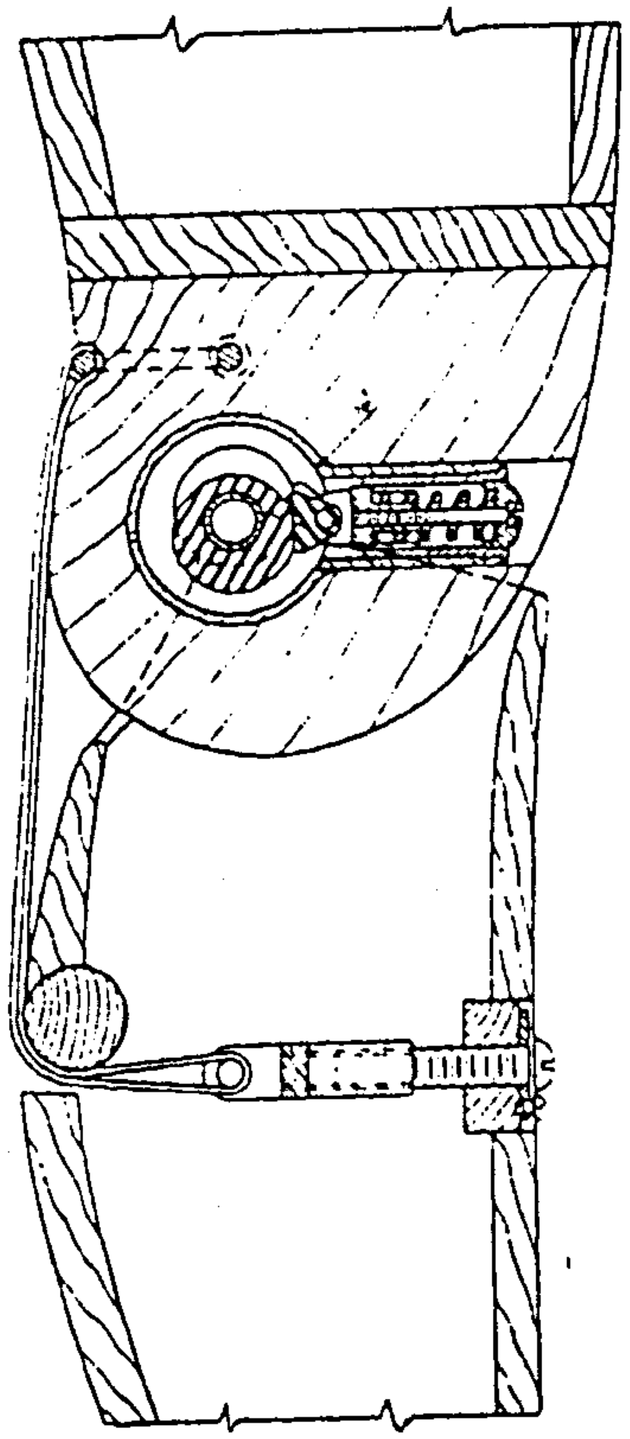

Fig.3.5 University of California variable-friction knee. (from Wagner & Catranis in Wilson, 1968)

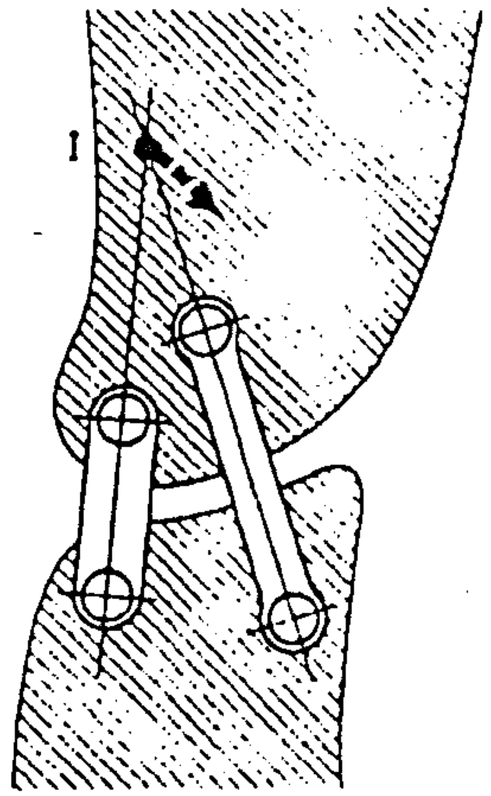

Fig.3.6 Four-bar multicentric knee mechanism. (from Radcliffe in Murdoch, 1969)

There are a wide variety of prosthetic knee mechanisms, ranging from the simple single-axis knee to those with increasingly complex components that control characteristics of flexion/extension of the knee in various ways. Their major differences are related to the methods employed to provide stance phase stability and allow smooth and natural flexion during swing phase, especially when patients are walking at different cadences. Readers are recommended to refer to Radcliffe (1970) and Judge (1980) for extensive review of various knee mechanisms. Only a brief description of seven knee mechanisms is presented in this section.

(A) Constant friction knee (Fig. 3.7) The constant friction knee consists of a hinge type mechanism that swings in both flexion and extension. The friction on the knee bolt is obtained by using a rubber pad round the knee bolt, and the amount of friction can be adjusted to the patient's normal cadence. This knee is commonly used in children. Its simplicity, durability, relatively low cost and good cosmesis make it a popular prescription. The major disadvantage of this knee unit is that the friction can be set for only one cadence, making change of walking speed difficult.

(2) Manual locking knee This knee unit consists of a constant friction knee hinge with a positive lock, usually a pin automatically engaged by a spring mechanism that drops through the knee, locking the knee mechanism in extension. The lock can be reset to the unlock position if the patient wishes to walk with a free knee. This knee unit is generally used for patients who are weak, unstable, and for whom a fall down would be serious.

(3) Variable friction knee (Fig.3.5) The resistance to knee flexion of the variable friction knee unit increases as the knee flexes from the fully extended position. Variable friction was provided by a number of staggered pads. The advantage of this knee unit is that it allows cadence response. However, this unit tends to wear quickly and to lose adjustment and become noisy.

(4) Weight-activated friction knee The unit functions as a constant friction knee during swing phase but when weight is applied through the knee, a housing with a high coefficient of friction presses against the knee mechanism and prevents it from flexing. The amount of weight required before the knee "freezes" can be adjusted to

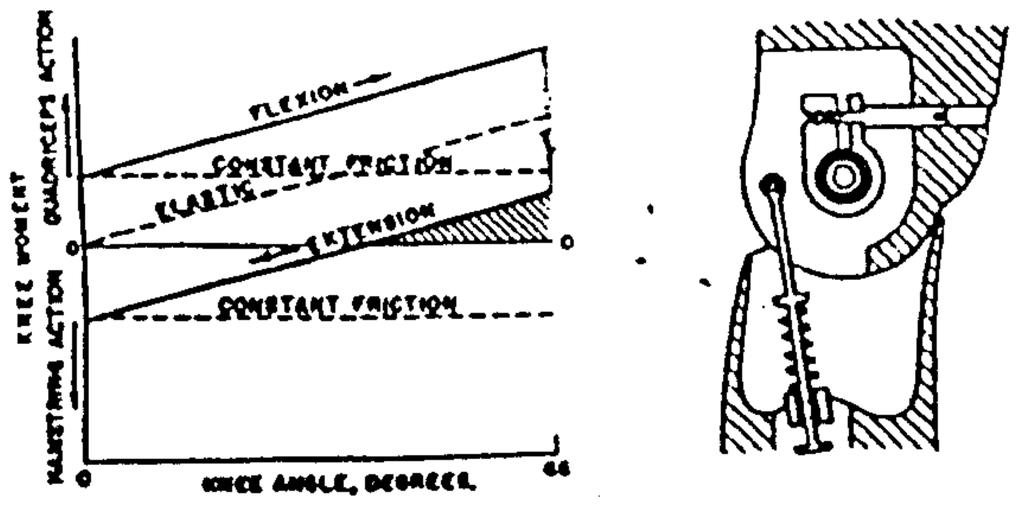

Fig.3.7 Mechanical swing control: constant friction plus a linear elastic extension bias. (from Radcliffe in Murdoch, 1969)

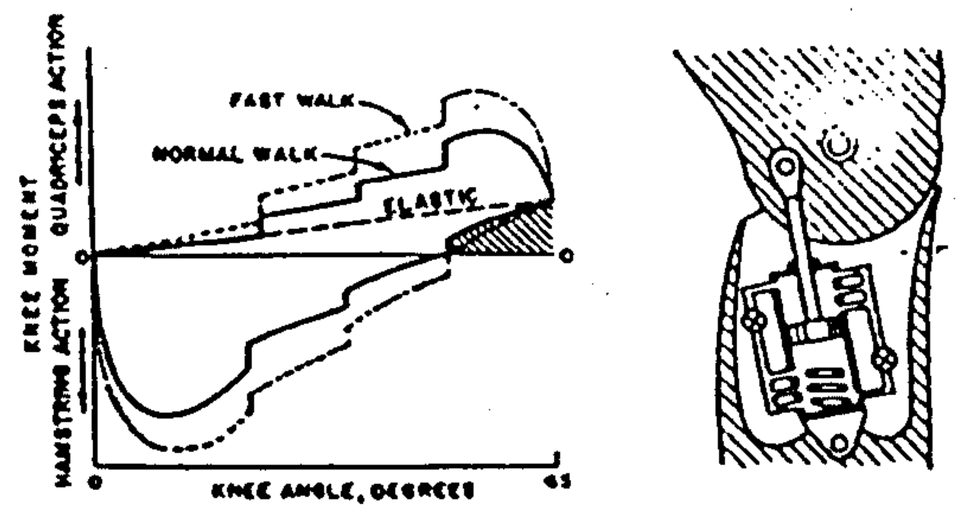

Fig.3.8 Hydraulic swing control with linear elastic extension bias. (from Radcliffe in Murdoch, 1969)

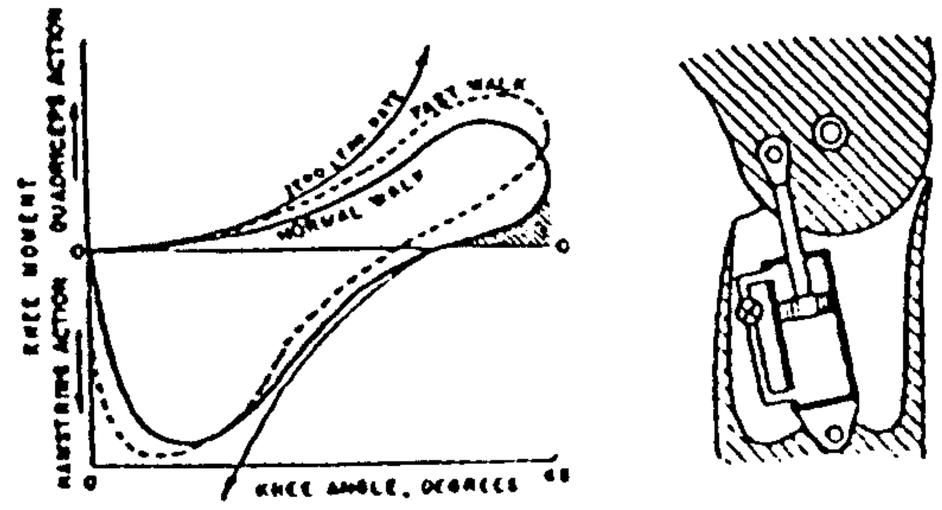

Fig.3.9 Pneumatic swing control. (from Radcliffe in Murdoch, 1969)

meet the patient's requirements. This knee unit is used in most geriatric amputees and contraindicated for younger, more active patients.

(5) Polycentric knee (Fig.3.6) The polycentric knee unit usually consists of a four-bar linkage that has the ability to change the instantaneous centre of rotation between the prosthetic thigh and shank. The advantage of this knee unit is that it can provide different stability characteristics during the gait cycle and an increased range of knee flexion. The disadvantage of it is the increased weight. This unit is generally used for patients with knee disarticulation or short stump or weak hip extensors.

(6) Hydraulic swing control The working principle of the hydraulic swing control unit is depicted in Fig. 3.8. As the knee flexes the piston is pushed down the oil-filled cylinder, forcing the oil out through one or more by-pass channels and back through a check valve into the cylinder above the piston. The resistance to the knee flexion increases as the channels are covered successively by the piston. At knee extension, the oil flow reverses. Adjustment screws allow the prosthetist to vary the cross-sectional area of the by-pass channels, thus increasing or decreasing resistance to flexion and extension. Present design of this knee mechanism allows excellent cadence response and it is very durable and easily adjusted. Adult males are the greatest user of the hydraulic knee, and adult females also use these units to a lesser degree.

(7) Pneumatic swing control (Fig.3.9) The pneumatic control knee mechanism physically resembles the hydraulic system and also provides cadence response. The pneumatic knee differs the hydraulic knee in that it uses air, which is compressible and acts like a spring, as working medium. The resistance to knee flexion can be adjusted by a screw that lowers a needle valve into the port at the top of the cylinder and the resistance to knee extension by another screw that regulates the distance the needle valve can float out of the port during knee extension. The pneumatic swing control unit is generally lighter and smaller than the hydraulic one and easy to maintain. This knee unit is indicated for the type of patient who could used a hydraulic unit. It is preferred when both cadence response and light weight are required.

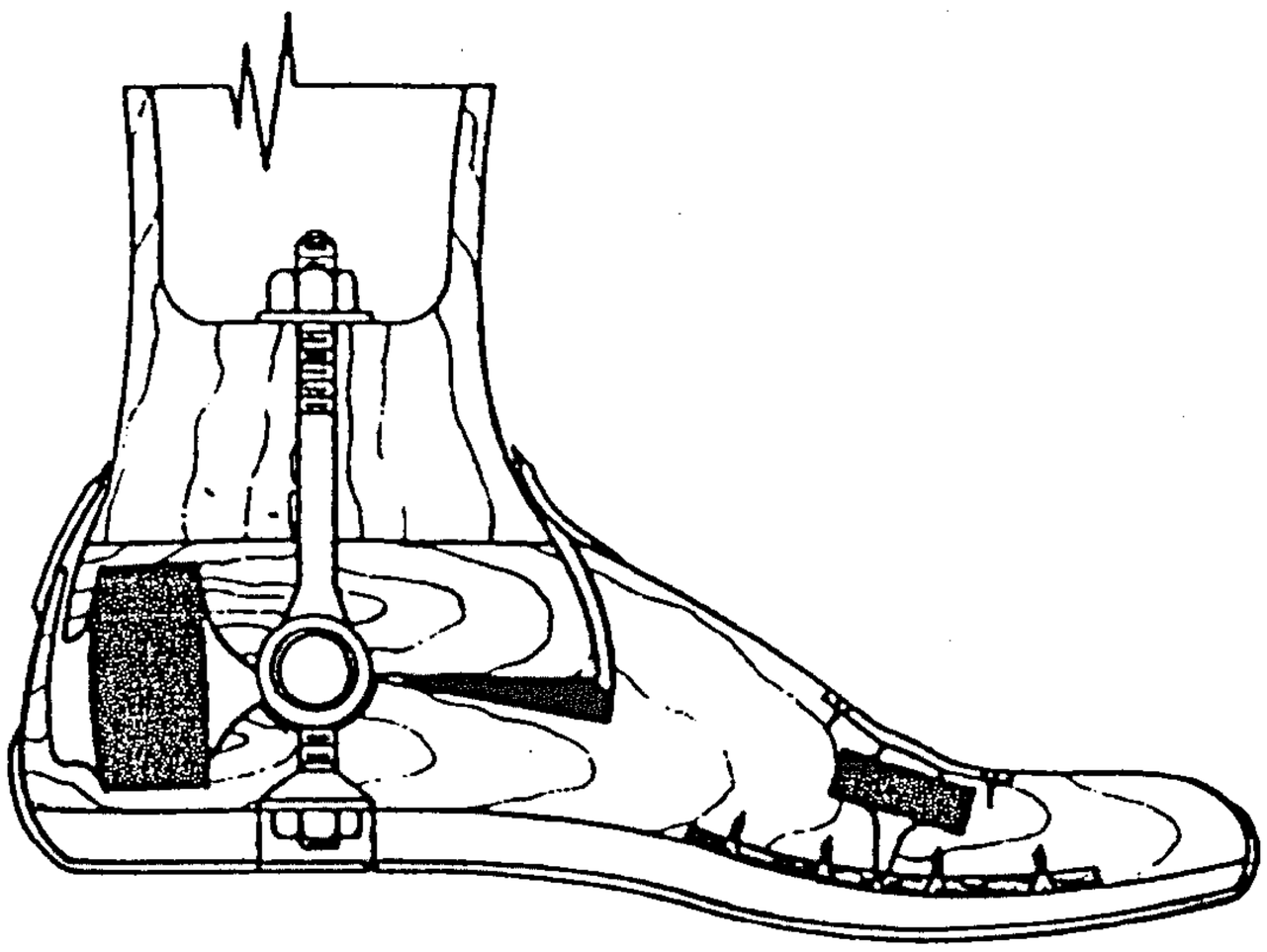

Fig.3.10 Conventional uniaxial ankle/foot assembly.
(from Candie in Murdoch, 1969)

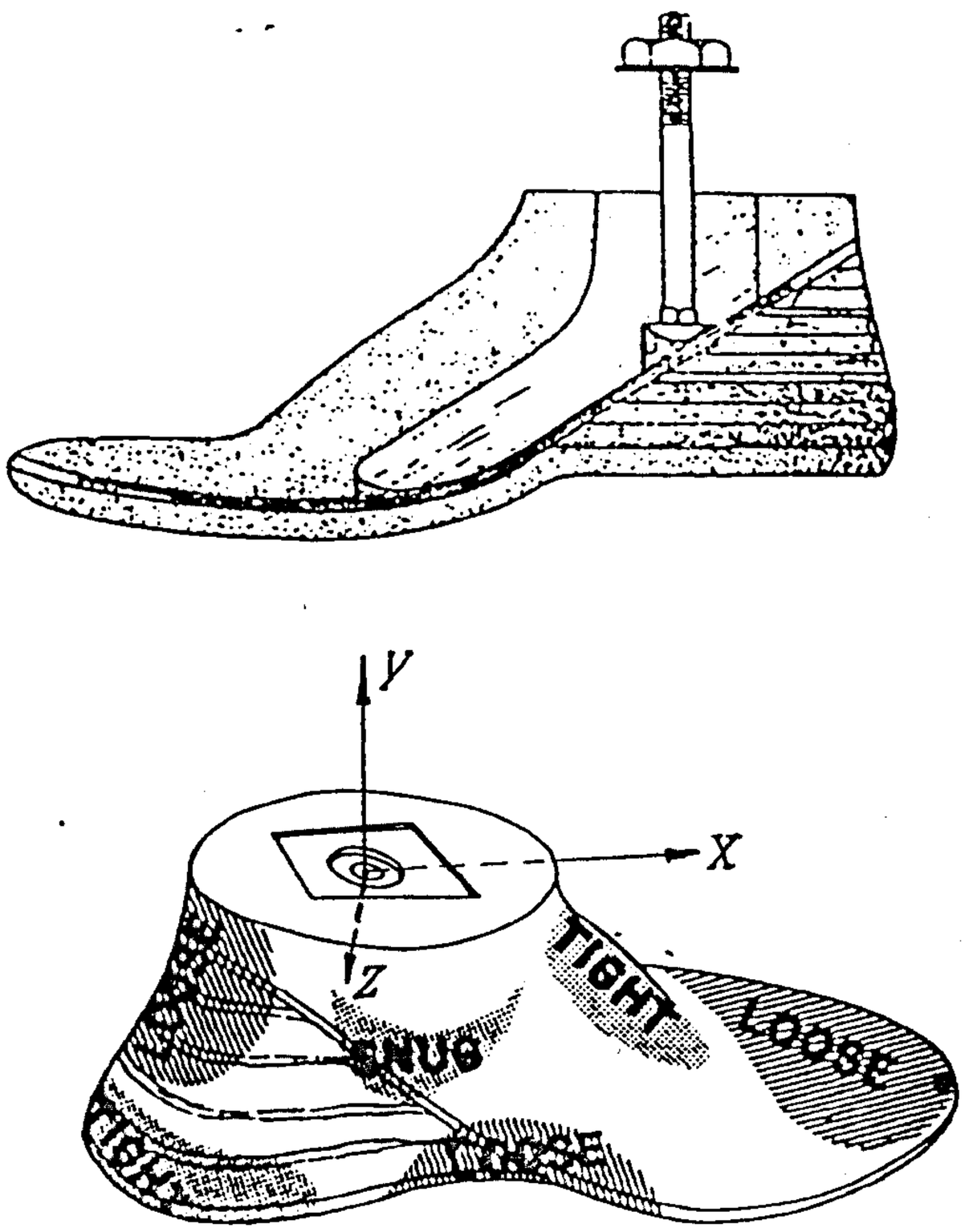

Fig.3.11 The Solid Ankle Cushion Heel (SACH) foot.
(from Condie in Murdoch, 1969)

§ 3.3.4 Prosthetic ankle/foot assembly

Although a large number of prosthetic feet have been designed, they all provide a similar function. During the stance phase, the foot serves as a weight bearing platform, absorbing the impact of knee strike, and then plantar flexes to allow the forefoot to contact the floor smoothly and rapidly, giving the patient a solid base of support. When the patient rolls forward over the fore-foot, the foot and shoe bend in a natural way to allow the patient to roll smoothly.

Only three kinds of prosthetic foot will be briefly discussed.

(1) Uniaxial foot (Fig.3.10) A metal hinge is used in the uniaxial foot to provide dorsiflexion and plantar flexion. Behind this metal ankle joint is a rubber plantar flexion bumper insert which can be adjusted to allow a quick plantar flexion of the foot at heel strike. Anterior to the ankle hinge is a flat rubber dorsiflexing stop that prevent the foot from excessive dorsiflexion and forces the heel rise after mid-stance phase. This uniaxial foot can allow maximum stability of the knee joint by adjusting the plantar flexion of the ankle joint. An obvious disadvantage of this foot is its lack of medio-lateral and axial rotation. Other limitations of this foot include the moving parts of the ankle mechanism which cause noise and wear. Although the foot itself is fairly durable, the rubber bumpers require replacement at intervals of about a year or more (Vitali *et al*,1978).

(2) SACH foot (Fig. 3.11) The design principle of the solid ankle cushioning heel (SACH) feet is to approximate joint motion by the compression of rubber around a solid hard core called the "keel". A wedge of cushioning material is built into the wooden heel shaped at the ball of the foot, which being normally available in three different degrees of compressibility. Extending from the wooden keel is a toe-spring to reinforce the simulated rubber toe piece and also to assist in providing the retaining and restoring motion required during late stance phase and toe-off.

The durability, light weight and excellent cosmesis of the SACH foot make it the most popular of all the prosthetic feet. The SACH foot has no actual moving parts and requires little or no maintenance. Presently, the majority of above knee prostheses are fitted with the SACH foot in the U.S.A. However, the SACH foot is

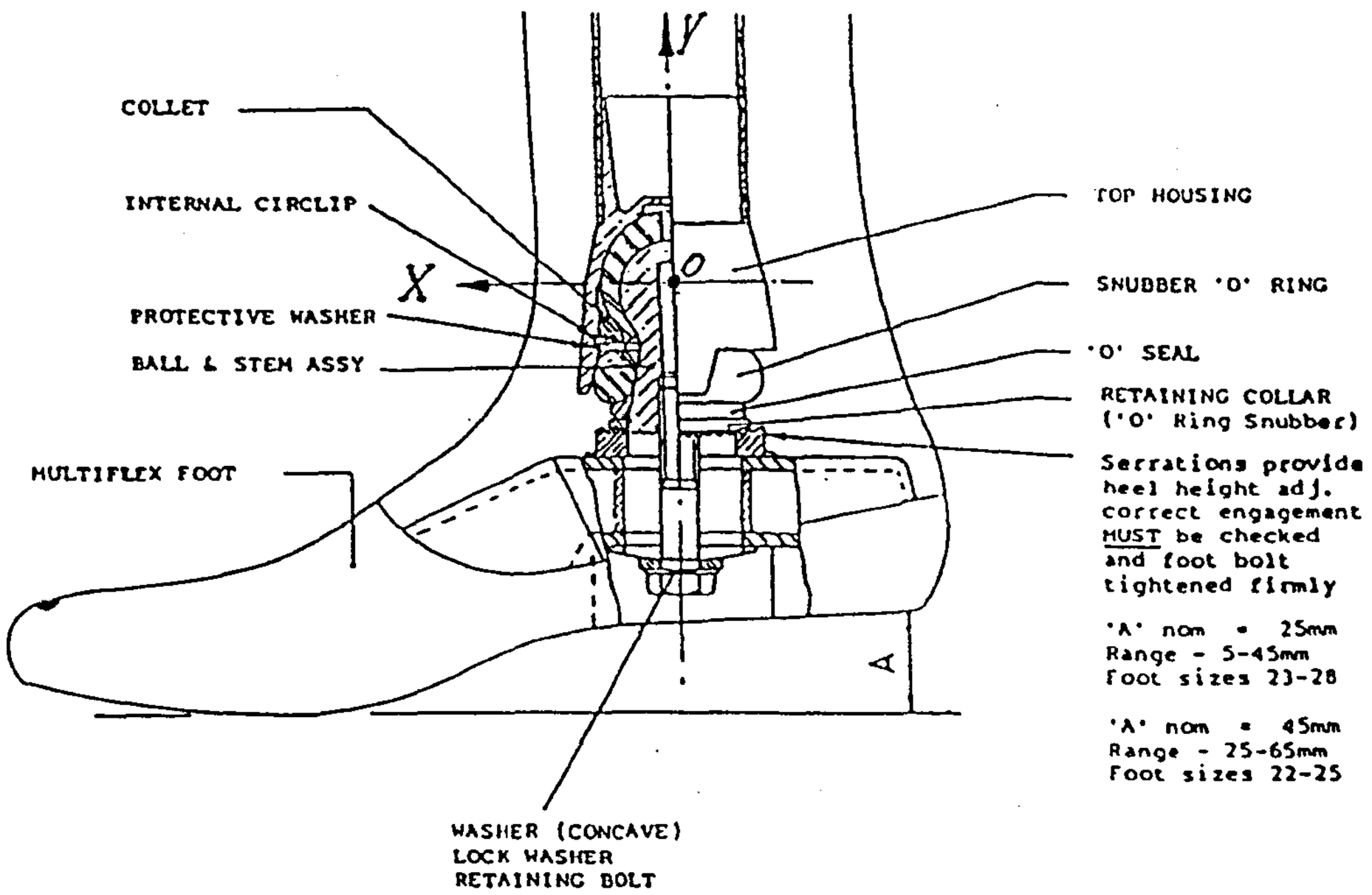

Fig.3.12 The multiflex ankle/foot assembly.
(from Blatchford & Sons Ltd, 1985)

contraindicated for the patients who require very rapid plantar flexion of the foot at heel strike.

(3) Multiaxial foot The Multiflex Foot/ankle Assembly shown in Fig. 3.12. is one example of multiaxial foot. A solid rubber ball and stem assembly is housed in the collet on the shank and connected to the foot by a bolt, acting as the ankle joint. The serrations at the interface of the foot and stem provide heel height adjustment. The advantage of the multiaxial foot is its ability to absorb medio-lateral force and rotational torques. The disadvantage of this foot is the regular replacement of the rubber ball.

§3.3.5 Below-knee prosthetic systems

The PTB socket, introduced in 1959 (Radcliffe and Foort, 1961), is currently widely prescribed. It is designed such that a substantial amount of weight is borne on the patella tendon and the medial flare of the tibial condyle, without excessive movement of the prosthesis relative to the skeletal structures. A good socket fit should make the compression of soft tissue consistent with the pressure tolerant areas and pressure sensitive areas of the below knee stump (see Fig. 3.13). Most of the sockets are used with a soft insert which has the same shape as that of the socket and is made of a soft synthetic material.

Since the introduction of the PTB prosthesis a wide range of its variants have appeared. The variants are of two kinds: (1) socket designs to improve the distal pressure and weight bearing control or to improve the environment around the residual limb and (2) mechanism for improvement in suspension and knee stabilization. These variants however do not affect the fundamental principles of PTB fitting, especially the total-contact.

§3.3.6 Modular assembly prostheses

The concept of the modular assembly prosthesis (MAP) came from the recognition that prostheses were expensive and time-consuming to fabricate on a tailor-made basis. Furthermore, it was found that adjustment of the prostheses may become necessary from time to time, requiring alignment devices to be incorporated permanently in the prostheses. An ideal modular assembly prosthesis therefore is

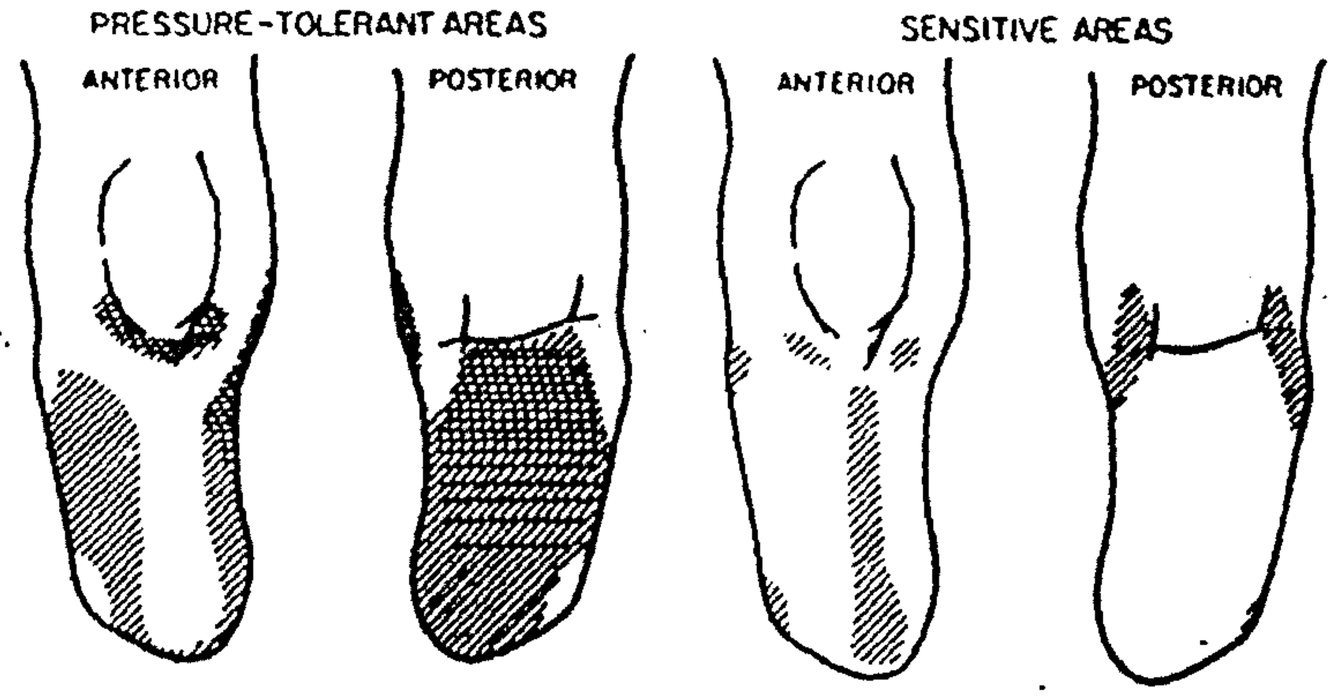

Fig.3.13 Pressure-sensitive and pressure-tolerant areas of the BK stumps. (from Barclay in Murdoch, 1969)

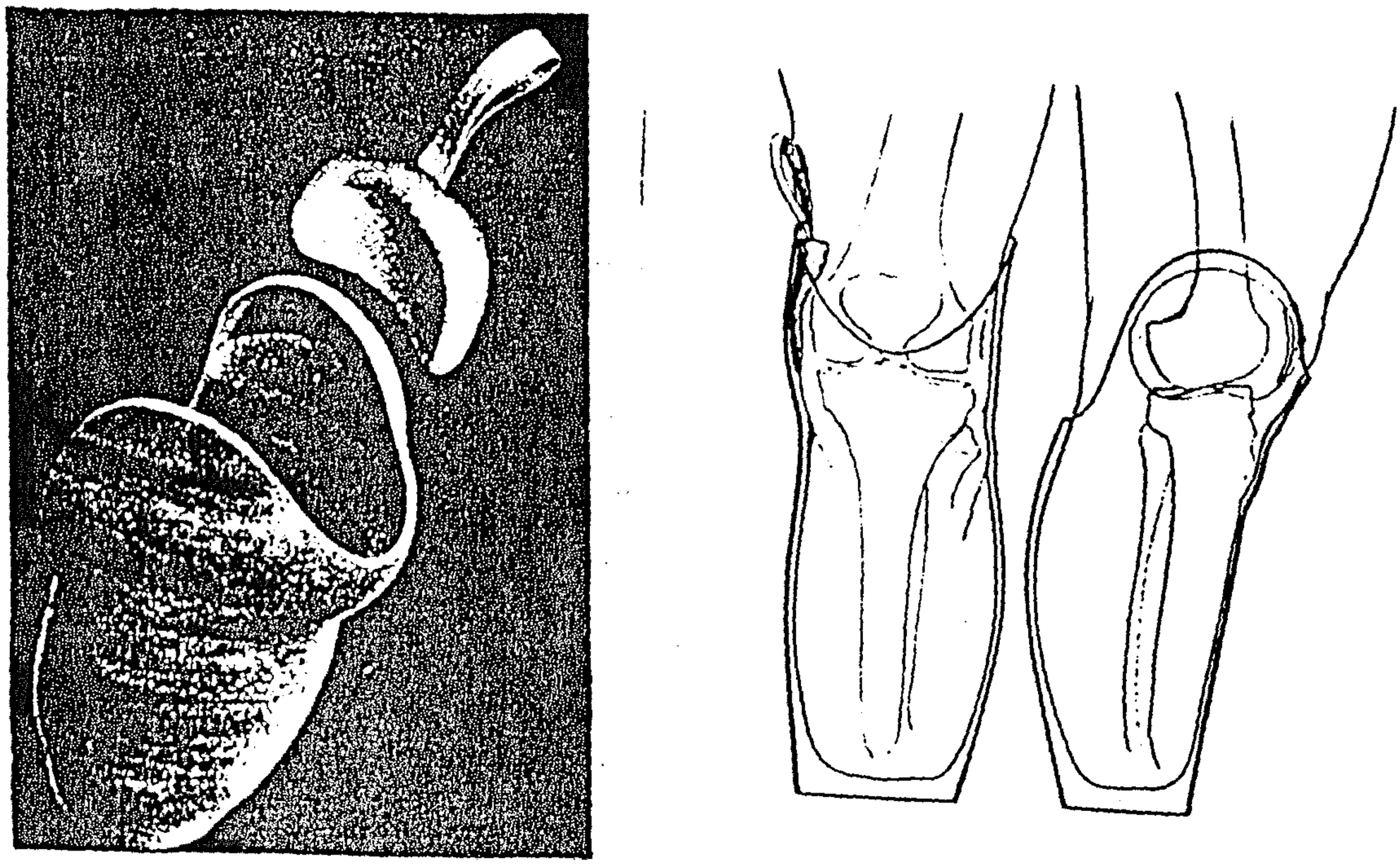

Fig.3.14 The PTB socket with supracondylar suspension using medial wedge. (from Fillauer, 1968)

visualized as having the following advantages:

(1) the provision of a good practical prosthesis for a wide spectrum of patients, giving good fit, function and cosmesis.

(2) the prosthesis can be constructed quickly, largely from pre-manufactured standard parts.

(3) prosthesis alignments can be made easily.

(4) if required, changes in prescription can be made easily.

(5) the amount of skilled handicraft works required is minimized.

There are a number of MAPs commercially available. The structures of most MAPs comprise a central tube to which adapters are mounted at the ends to attach the socket, alignment devices or prosthetic joints. The tubes are cut to the required length to give the correct height of joints and socket. The total limb is enclosed in a soft cosmetic cover. Of the components, only the socket and cosmic finishing are custom made to the individual amputee's requirement.

An evaluation programme was conducted at the University of Strathclyde, Bioengineering Unit (Solomonidis, 1975 and 1980), which dealt with comparative studies of available MAPs. The objective of the evaluation were, firstly, to assess the clinical suitability of the MAPs both from the patients' point of view and that of service, and secondly to produce design information relating to the clinical and constructional requirements of the MAPs. Four aspects of the parameters were evaluated:

(1) Objective measurements of the alignment of the MAPs.

(2) Time taken to construct the prosthesis.

(3) Mass properties of the prosthesis.

(4) Subjective impressions of the patients, surgeons, prosthetists and the prosthetist technicians.

In the 1975 report, six BK system were evaluated: Biomechanical Research and Development Unit (BRADU), Blatchford, Otto Bock, Hanger, Veterans Administration (VA) and Winning. A total of 23 patients participated in the evaluation and each of them was supplied with 6 MAPs to wear consecutively for 6 weeks at a

time. It was found that the Hanger, VA and Winning systems were clinically unsuitable, the BRADU was rather complex and the Blatchford and Otto Bock were the most acceptable..

Four AK MAPs were evaluated in the 1980 report: Blatchford, Otto Bock, United State Manufacturing Company (USMC) and Hosmer. On this occasion twenty patients were fitted with each of four prostheses. The evaluation concluded that the Blatchford and Otto Bock were the preferred systems for the limb fitting service in Britain. It was, however, pointed out that both systems still have disadvantages and require further development.

§ 3.4 PROSTHETIC METHODS

The aim of the rehabilitation of an amputee is not only fitting him/her with a prosthesis, but also ensuring that he/she is reinstated in society and can take his/her rightful place with the limits of his/her own disability and state of health. A multi-discipline approach therefore must be adopted to the rehabilitation of the amputee and this is ensured by having an amputee clinical team. The amputee clinical team should consist of a physician, a prosthetist, a physical therapist, a nurse and possibly a social worker and a clinical co-ordinator. Each of them should have an acceptable educational standard and have experience in the area of amputee rehabilitation management in order to tender optimum service to the patient. Only if all members fully contribute their expertise can the ultimate results be achieved.

The patient, being the reason for the clinic's existence, is the most important member of the team and should be the centre of attention of the clinic's activities. It is essential to instill confidence into the patient and encourage him to participate as an active member of the team.

The provision of a prosthesis to an amputee involves several stages and the patient is generally seen by the prosthetist a minimum of five times before the fitting is considered to be completed. Different methods are employed by the prosthetist in each of the visits.

At the first visit, the patient is examined by a physician or a clinical team and the prescription for the prosthesis is written after all the input has been received from

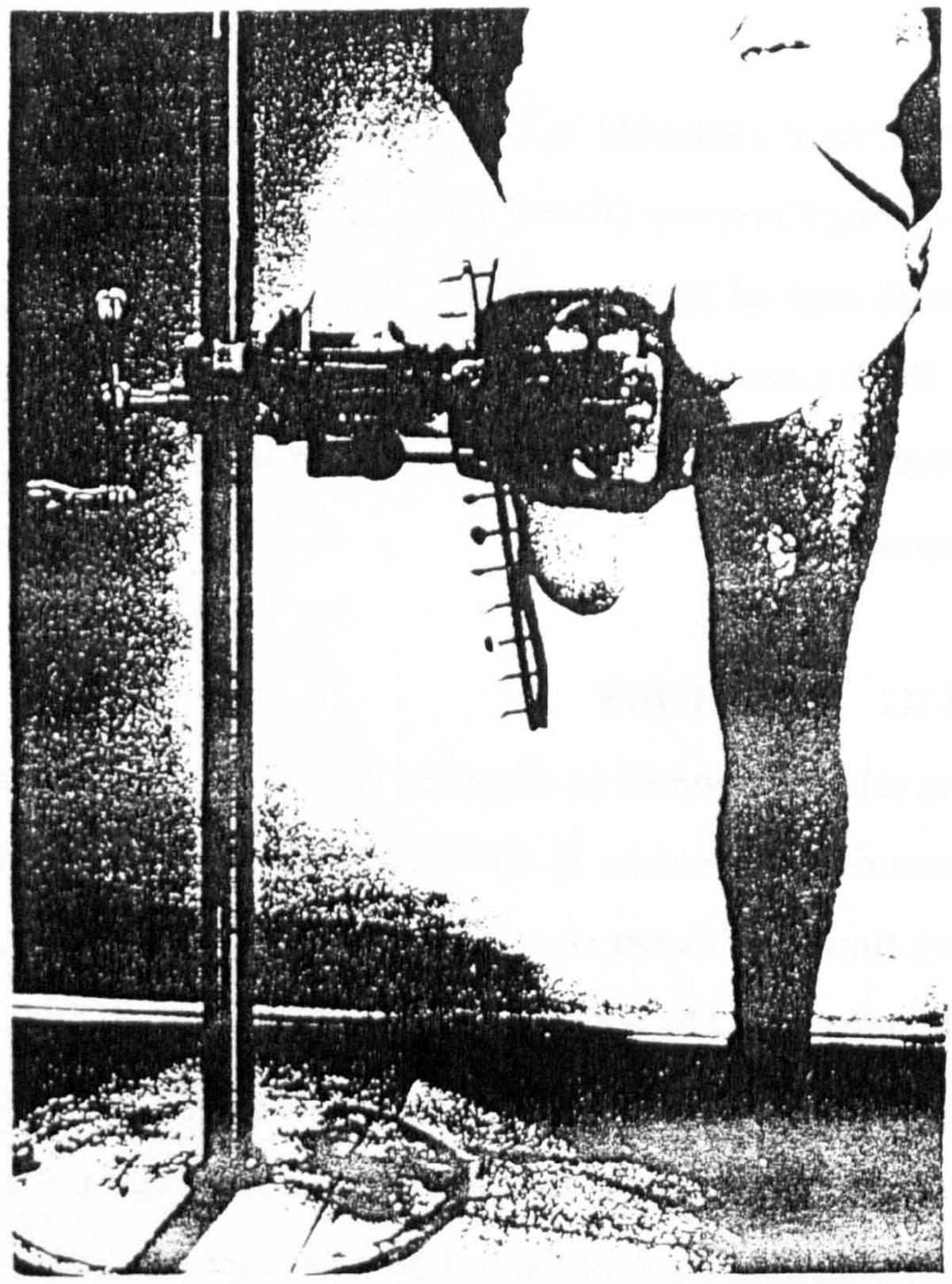

Fig.3.15 Amputee seated in the socket forms with adjustment completed.
(from Lyquist in Murdoch, 1969)

all members of the team. The description contains the status of the amputee with respect to his/her amputation and general medical condition. It also includes a list of components for the prosthesis which will permit the amputee to overcome his/her handicap to the greatest possible degree.

During the second visit the patient receives general examination and casting. In this session, the prosthetist explains many aspects associated with the design, fitting and expectation of the prosthesis, predicts many problems the patient will face and suggest solution as these problems occur. Measurements are then taken of the patient's residual and sound limbs and special forms are used for evaluation and measurement of the patient. The final session of the second visit is to take an accurate mould of the patient's stump. The negative mould is usually taken in a specified position and is intentionally deformed by the prosthetist to clearly define anatomical landmarks.

The negative mould of the patient's stump is filled with plaster to provide a positive mould that is then modified by removing the plaster in the pressure bearing areas and adding plaster to the mould in the pressure-relieving areas. The socket is made over this modified positive mould of the stump from a laminate process in which the most commonly used material is polyester resin in its liquid form.

The CAD-CAM (computer Aided Design-Computer Aided Manufacture) has been under development by several prosthetic centres (Oberg, 1985;). The stump's shape data required by the CAD program is obtained by an opto-electric system. The CAD program generates a 3-D image of the stump, viewing from any angle on the monitor, and allows the prosthetist to modify it at will to satisfy the pressure distribution requirements. The CAM system manufactures a positive mould of the modified stump using a numerical mill and then the socket is made over this mould. This method greatly increases the speed of producing prostheses.

The third appointment is made for a test socket fitting. The purpose of a test socket fitting is to ensure that the socket fits the patient properly before it is attached to an artificial limb. Four areas are especially observed during the test socket fitting: comfort, even distribution of the pressure, suspension and freedom motion for the proximal joint.

After test socket fitting, the definite socket is made and assembled with the rest

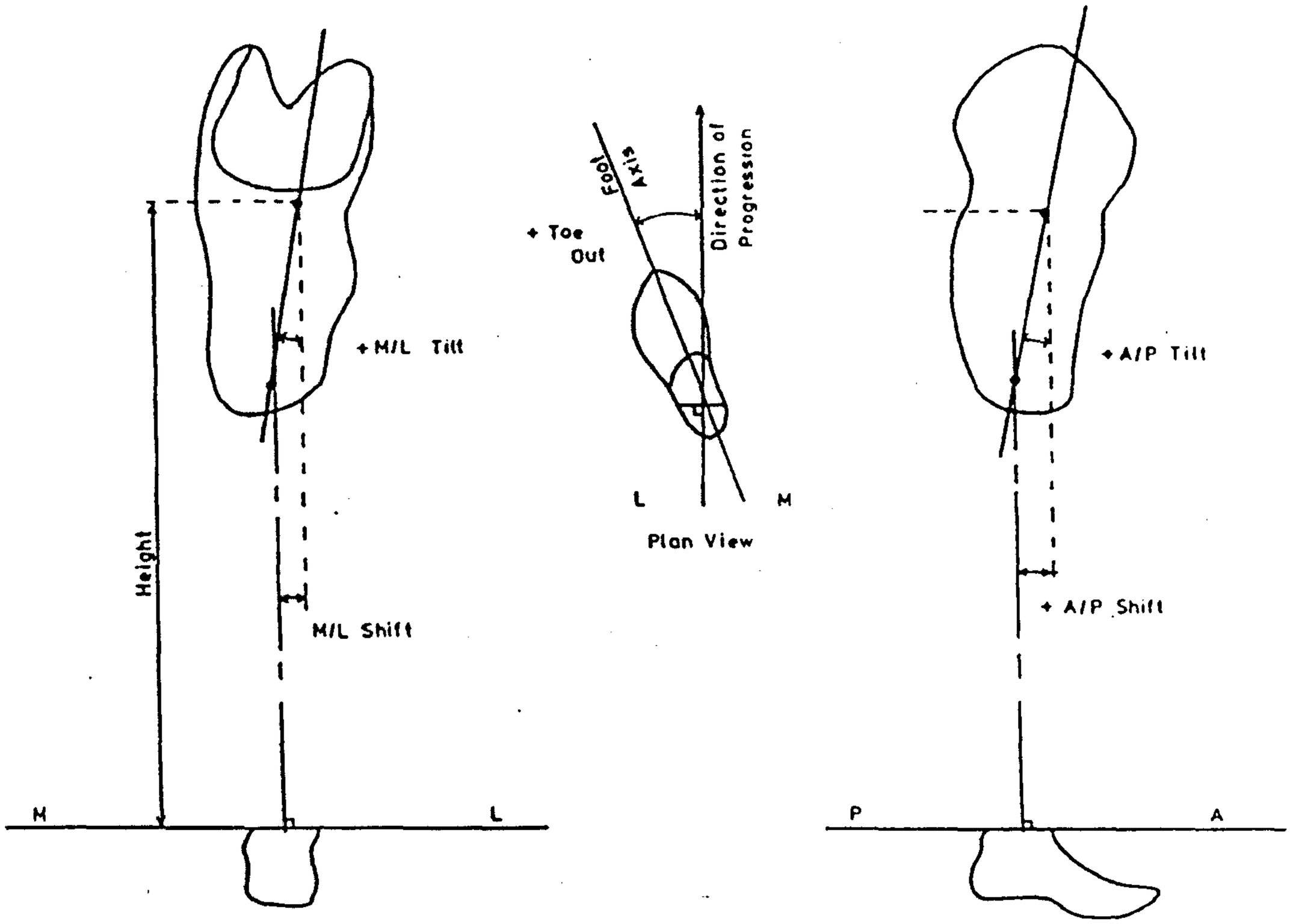

Fig.3.16 Definitions of alignment parameters for below-knee prostheses.

of the prosthetic components. Included in the assemble is an alignment device which allows the prosthetist to change the relative position of the components.

The patient is called in to try the prosthesis for alignment. The whole prosthesis is statically and dynamically aligned to provide maximum comfort, efficient function and cosmesis. Alignment of the prosthesis will be discussed in some detail in section §3.5. Fitting and alignment of the prosthesis are completed when the patient and prosthetist are convinced and satisfied that the prosthesis is functioning as well as possible. The alignment device is then transferred to a transfer rig while keeping the relative position of the components the same. The spaces between the prosthetic components are filled up with foam or wood which are then shape to match the sound limb. Covered with plastic lamination, the prosthesis is ready for delivery.

For a modular assembly prosthesis the alignment device is incorporated in the system and therefore no transferring is required. The accepted alignment is locked by a strong bonding glue and the desired cosmesis is achieved by shaping the foam covering the endo-skeletal structures.

§3.5 Alignment of the Lower-Limb Prostheses

Alignment of a prosthesis is defined as the position and orientation of the prosthetic components, mainly the socket, joints and terminators (such as foot), relative to each other. The aim of alignment is to arrange the components of the prosthesis in such a way that the amputee has optimum physical security, the best possible gait and minimum energy expenditure.

There are three alignment procedure which are performed during the fitting and fabrication of lower-limb prostheses, namely bench, static and dynamic alignment. The bench alignment of a lower-limb prosthesis is the alignment setting of the limb during the assembly process. The prosthesis should be assembled in such a way that minimum adjustment is required when the patient wear it, and there are rules and guidelines which the technician follows to achieve this object.When the leg is first fitted to the patient, the prosthetist makes any necessary adjustment with the patient, first sitting and then standing. During this stage of the fitting process, namely static alignment, the prosthetist checks the fit of the socket, the height of the prosthesis, knee

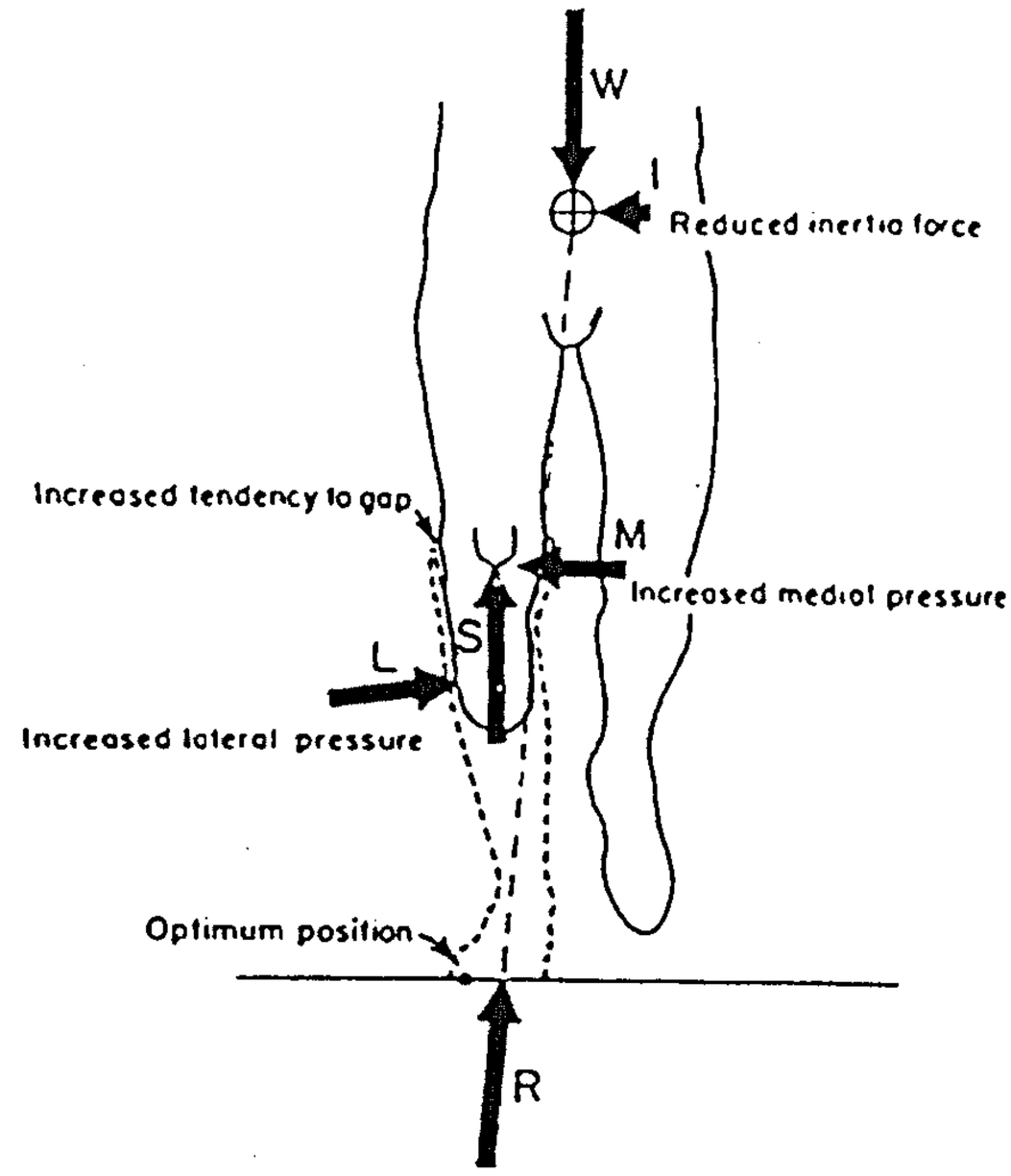

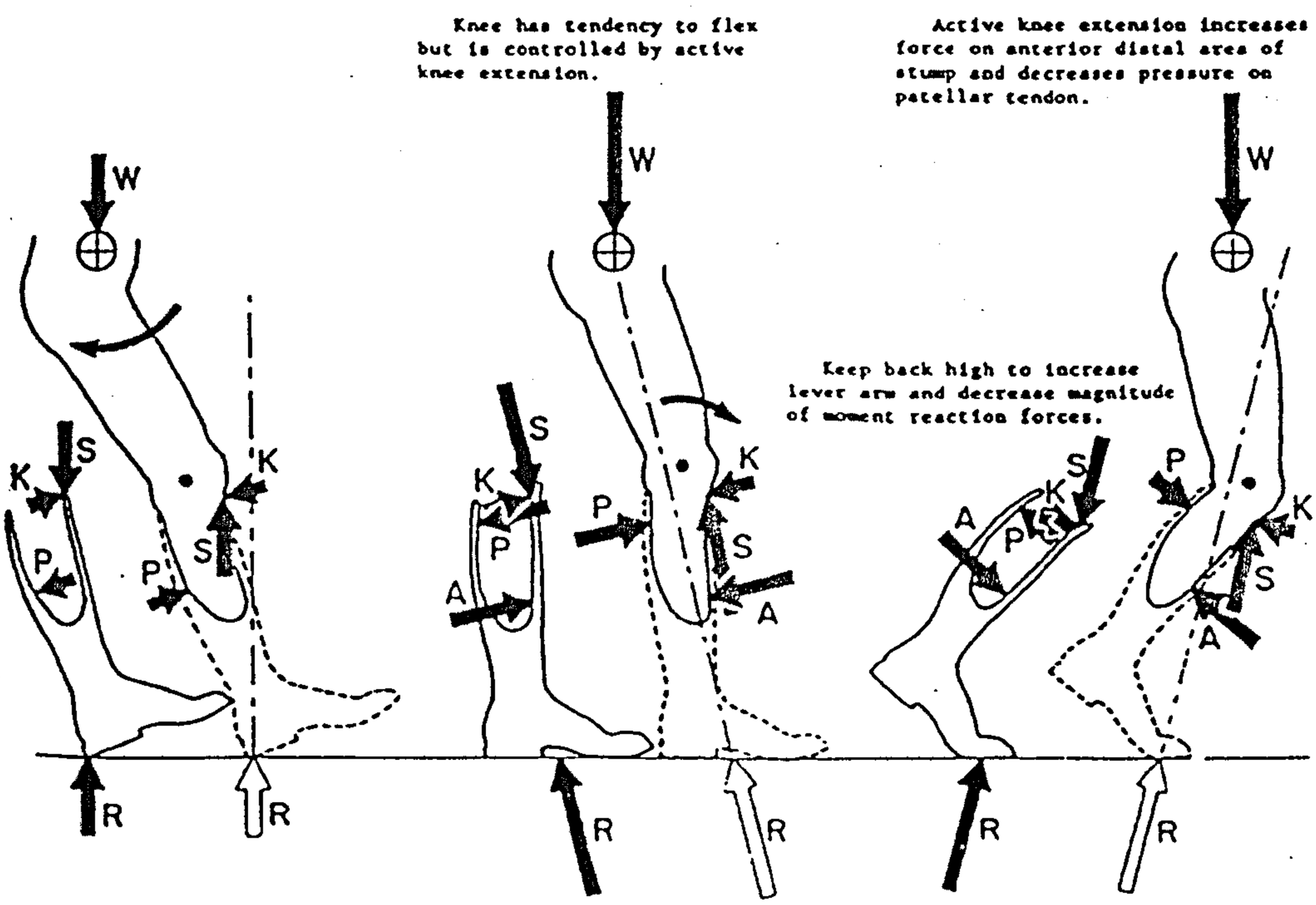

Fig. 3.17
PTB biomechanics.
(from PTB Manual - Radcliffe & Foort, 1967)

stability, toe out/in angle and pressure applied to the stump due to the alignment of the prosthesis. Following static alignment, the patient is asked to walk and the prosthetist aligns the prosthesis dynamically. The prosthetist observes the walking amputee from all angles and listen to his/her comments on the pressure distribution on the stump, and on sensation of security and foot position. The prosthetist makes adjustments aiming to satisfy the patient and to achieve minimum gait deviation and energy consumption.

§3.5.1 Alignment of the BK prostheses

There are six geometric parameters to define the socket position relative to the foot (refer to Fig. 3.16): Height of the prosthesis, socket forward set, socket lateral set, socket flexion, socket lateral tilt and toe-out angle of the foot.

Radcliffe and Foort (1961) illustrated the resultant forces loaded on the PTB prosthesis during walking, see Fig.3.17, and recommended bench alignment settings of the PTB prosthesis. The socket is usually set at 5° flexion and 5° lateral tilt, throwing the majority of the force onto the patellar bar, the anterior and lateral surfaces of the stump. The foot is typically 15mm medial to the knee joint centre so that the trunk side-to-side movement is minimized during the swing phase. The foot is also set 40mm backward to the knee joint centre.

At the static alignment stage the prosthetic height is set to give a level pelvis as the amputee stands evenly on both legs and the toe-out angle to be symmetrical to the contralateral side.

During the dynamic alignment the socket flexion angle is adjusted so that the ball of the foot contacts the ground shortly after heel strike, with the knee flexed at about 20 degrees. The socket lateral tilt is adjusted to give a slight evidence of the lateral socket forces tending to create a varus knee. The medio-lateral position of the foot is adjusted to give a normal walking base and the posterior position of the foot is adjusted so that the flexion moment at the knee is not so great as apparently to cause the amputee difficult in controlling his knee angle at heel strike nor premature knee flexion after mid-stance.

§3.5.2 Alignment of the AK prosthesis

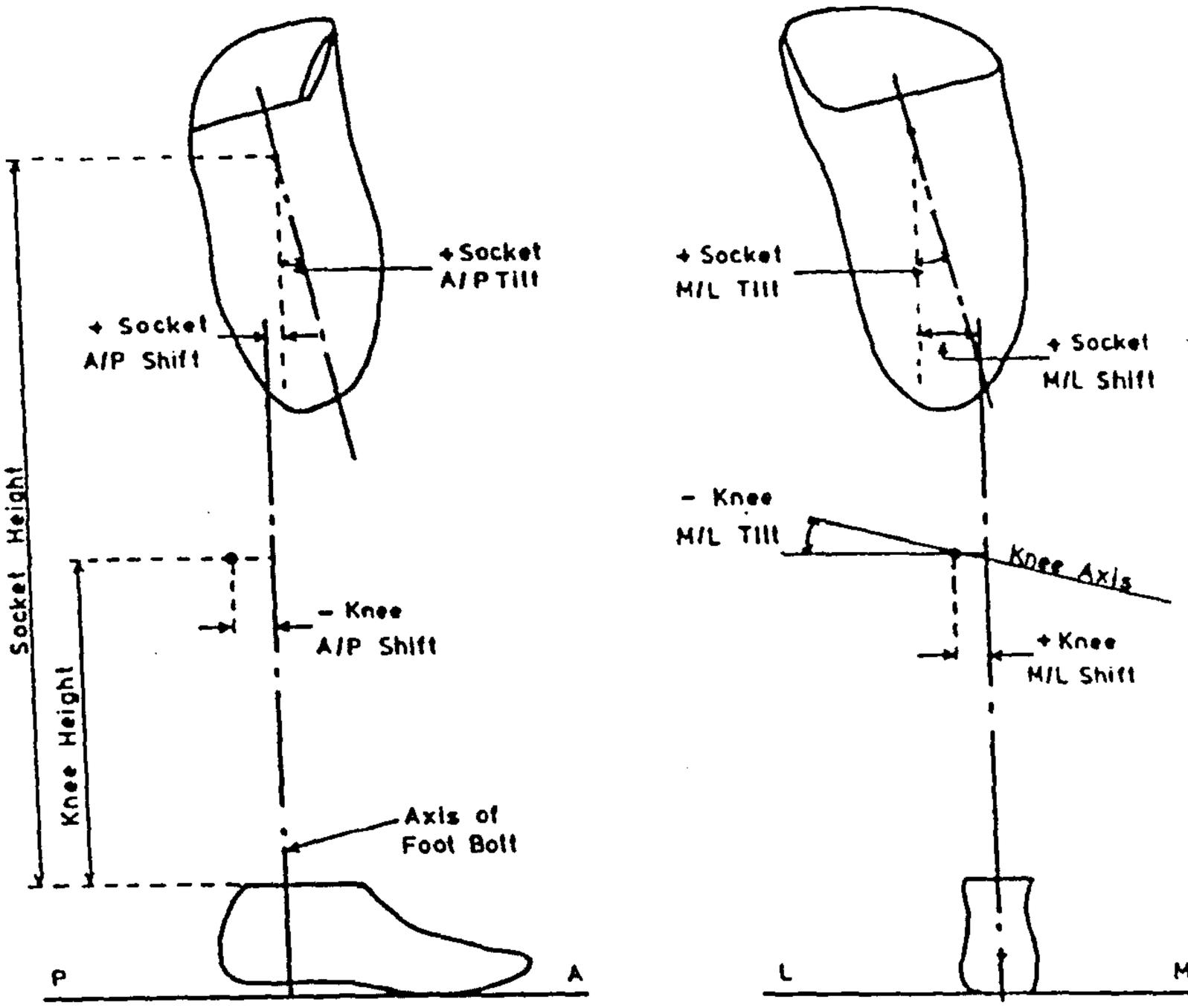

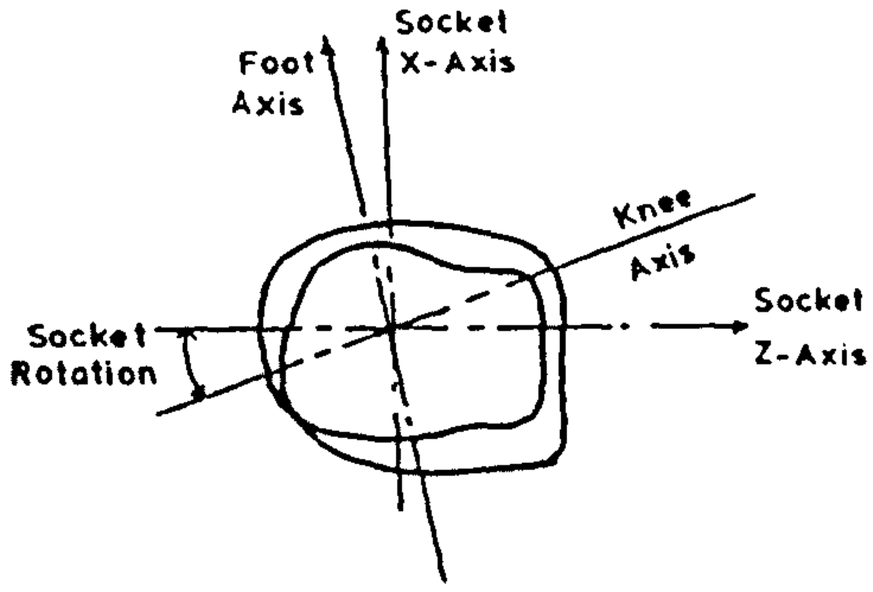

Fig.3.18 Definitions of alignment parameters for above-knee prostheses.

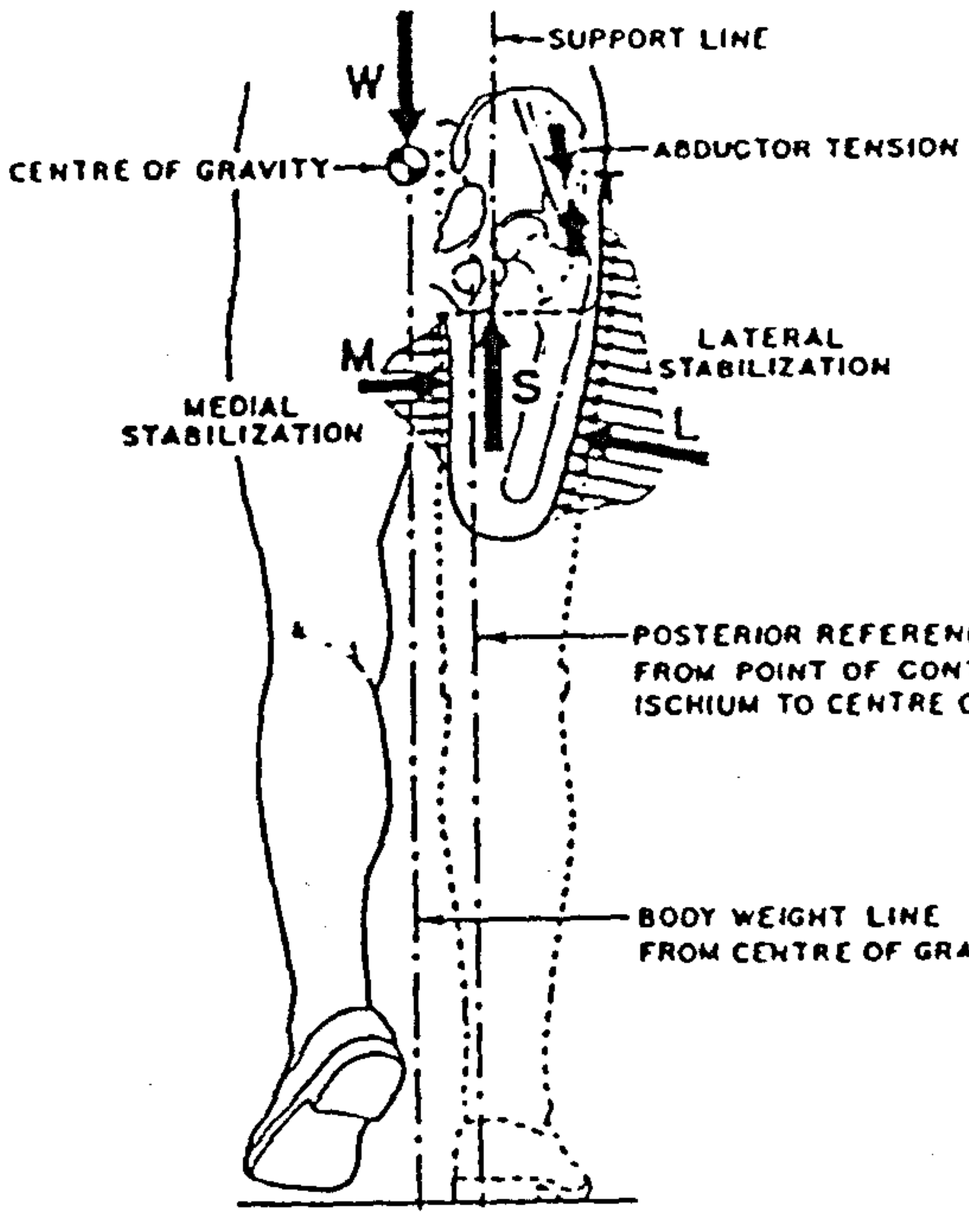

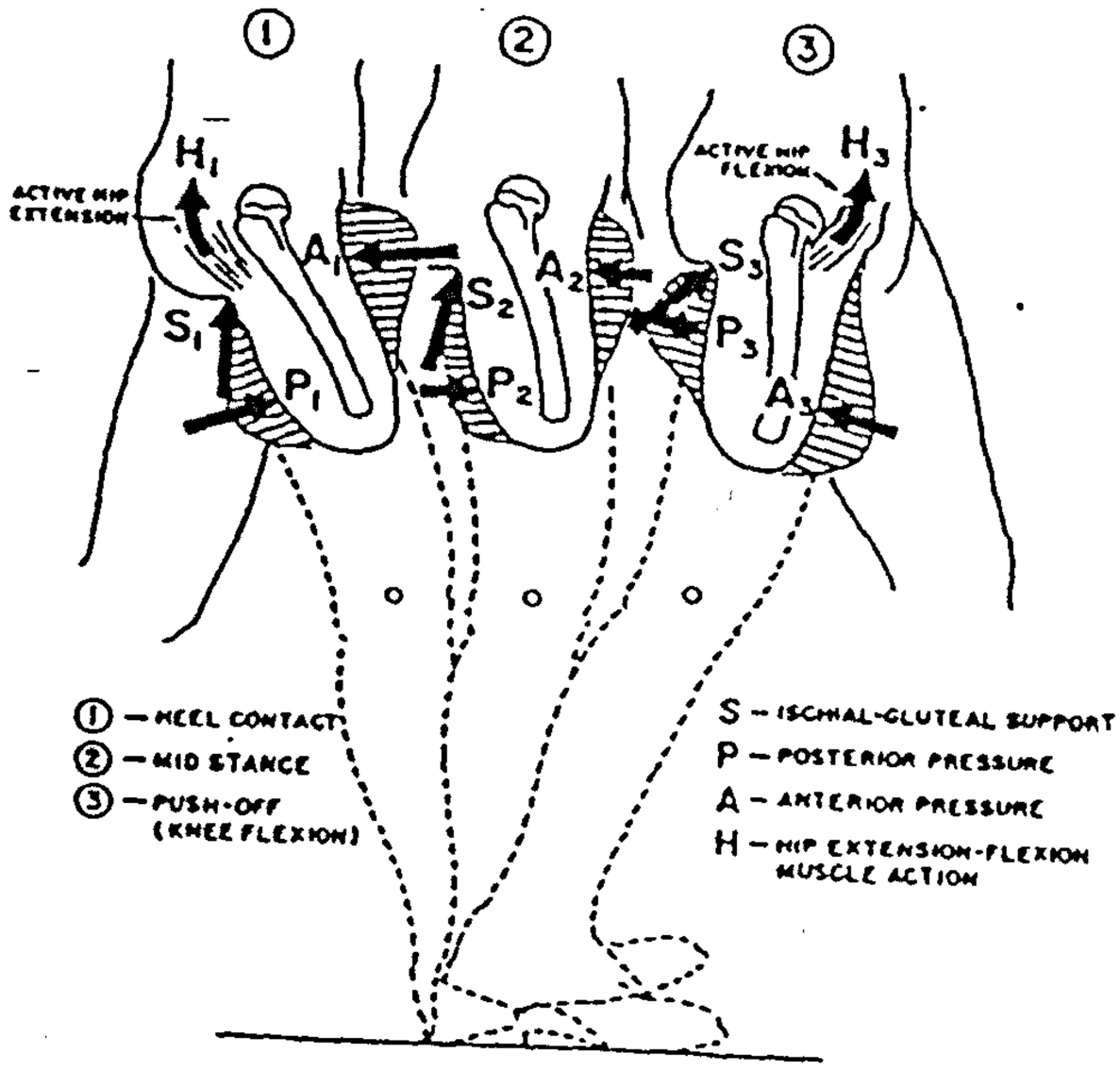

Fig.3.19 Biomechnics of above-knee prostheses.
(from Radcliffe in Murdoch, 1969)

Besides the same six variables relating the socket to the foot in a below knee prosthesis, five more parameters specify the knee position of the AK prosthesis in relation to the foot: knee height, knee set out, knee set back, medio-lateral tilt of the knee axle and knee rotation angle about vertical axis (see Fig.3.18). Only uniaxial knees are considered as they are by for the most commonly found.

A biomechanical analysis of the above-knee prosthesis was also made by Radcliffe (1970) which provided guidelines for aligning the AK prosthesis, see Fig.3.19. The socket is aligned to be slightly in flexion, but it varies with stump length (refer to Fig.3.20). This is to obtain greater advantage from the hip extensor (gluteus maximum and hamstrings), as their performance is improved when slightly extended. In the medio-lateral plane, the socket is adjusted so that the stump in it is in a slightly adductive position, biasing load bearing away from the medial side of the stump and correcting the abducted stump due to the loss of a large portion of the hip adductors during amputation surgery.

The position of the knee axle in the saggital plane is critical to the knee stability and varies also with the condition of the stump. For a longer and thus more powerful stump, it is placed slightly forward to the hip-ankle line and thus a smoother transition from knee extension to flexion is obtained at late stance phase. A shorter and weaker stump necessitates the knee axle being placed slightly posterior to the hip-ankle line to secure stability.

Knee saggital stability is increased when the prosthetic foot is moved forward with respect to the stump (socket).The medio-lateral setting of the foot for amputees with long stumps is set to provide a normal walking base. With short stump, this is often not possible as too high a pressure is caused at the sensitive end of the stump.

As in the case of the BK prosthesis, the toe-out angle of the AK prosthesis is set to give body symmetry.

The best prosthetic length depends on how long the stump is and how much voluntary control the amputee can and will exert over the prosthesis. A rule of thumb is that except for a very long stump, where equal length between the normal and prosthetic sides will be used, a slightly shorter length may be desired as it increases ease of balancing over the prosthesis in stance phase and secures foot clearance during

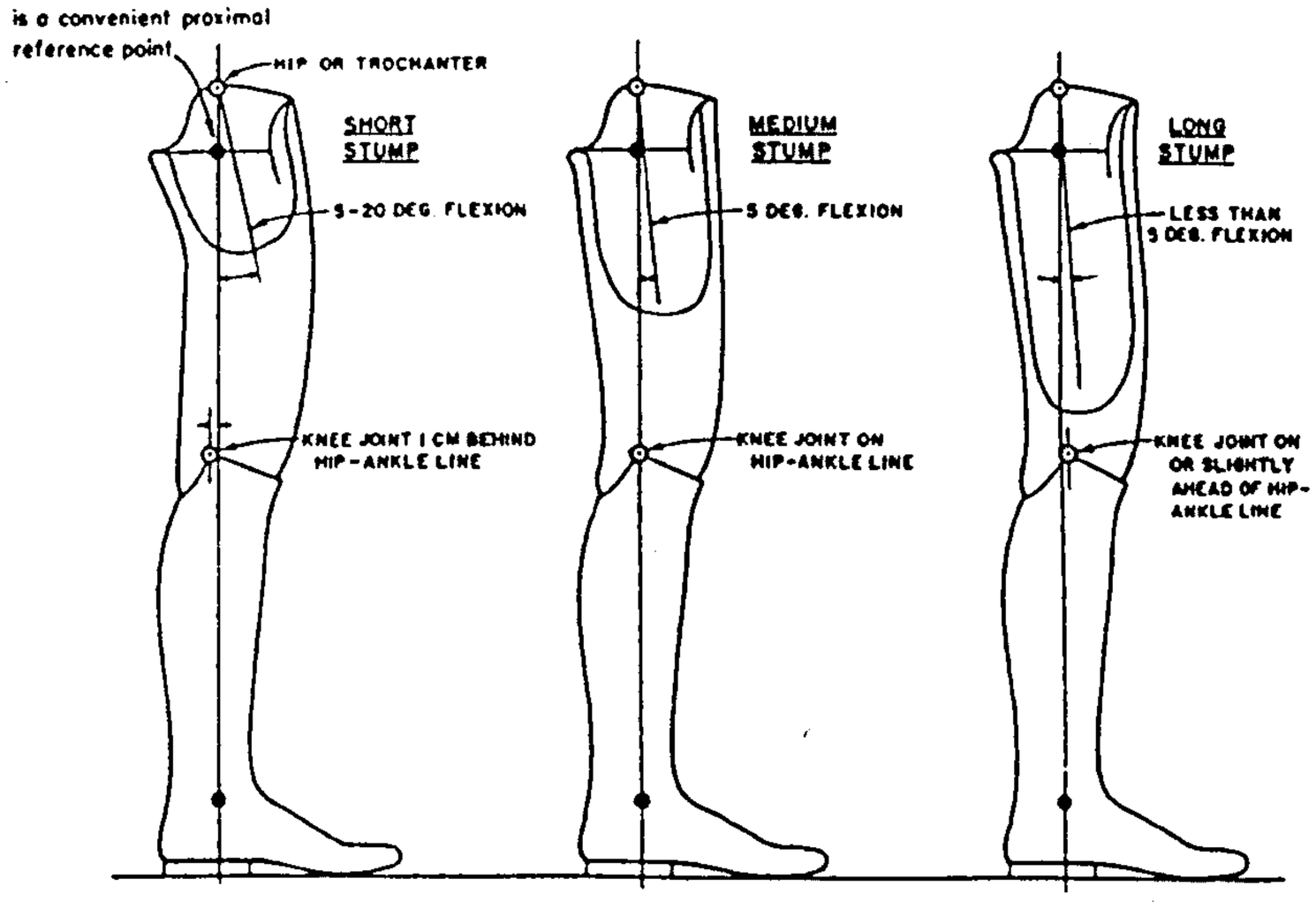

Fig.3.20 Standing alignment of AK prostheses for typical short, medial and long stumps.
(from Radcliffe in Murdoch, 1969)

Table 3.1

Recommended ranges of operation of alignment unit
(from Zahedi et al, 1985)

	Socket					Knee			Foot
	Shifts (mm)		Tilts (deg)		Rot. (deg)	Shifts (mm)		Tilts (deg)	Toe Out/In (deg)
Above-Knee Prostheses									
	AP	ML	AP	ML	In/Ex	AP	ML	ML	
Range (±)	70	70	9	13	11	30	40	5	14
Datum offset	30	10	0	1	4	10	-20	0.5	0
Foort's data	38	38	10	10	10	25	--	--	10
Below-knee Prostheses									
Range (±)	60	60	10	13	--	--	--	--	12
Datum offset	-5	-10	3	-2	--	--	--	--	0
Foort's data	38	38	10	10	--	--	--	--	10

swing phase.

§3.5.3 Research into the alignment of prostheses

The criteria for determining the alignment of prostheses are mainly subjective and good subjective judgement is needed throughout the total process of limb fitting. However, this particular subjective assessment was found to be inadequate on three counts. Firstly, visual observation was found to be unreliable clinically. Secondly, the amputee's response to alignment changes was not always apparent in the appearance of the gait. Finally, the patient's comments were not always helpful. Therefore, some research efforts have been made into methods of objective assessment of alignment.

Pearson *et al* (1973) monitored the interface pressure of a PTB socket. The transducers were located in the patellar tendon, distal anterior tibia, lateral tibia condyle, and medial tibia condyle regions. It was found that socket angles were of greater importance to the patient than linear shifts.

In the evaluation programme reported by Solomonidis (1975 and 1980), alignment of BK and AK prostheses was one aspect studied. It was observed that a wide variation exists in the alignment parameters. It was believed that it might be possible for the prosthetist to achieve an acceptable alignment configuration using only bench alignment procedures without the need for dynamic alignment, but a more extensive study would be necessary before such comments could be made definite.

Zahedi *et al* (1986) reported the results of an extensive series of studies on above and below knee amputees. A total of 10 below-knee and 10 above-knee amputees anticipated in the project, and a total of 183 below-knee and 100 above-knee fittings was studied. A method was also described to measure the alignment parameters. It was observed that an amputee can tolerate several alignments ranging in some parameters by as much as 148mm in shift and 17 degree in tilt, and that the amputee tolerance was related to the degree of control the amputee had over the prosthesis. The prosthetist was found to be unable to repeat a given alignment at will, and different prosthetists produced different ranges on any one patient. Ranges of operation of alignment units for both AK and BK prostheses were recommended, see Table 3.1. In another report (Zahedi *et al*, 1985), the effects of alignment on the

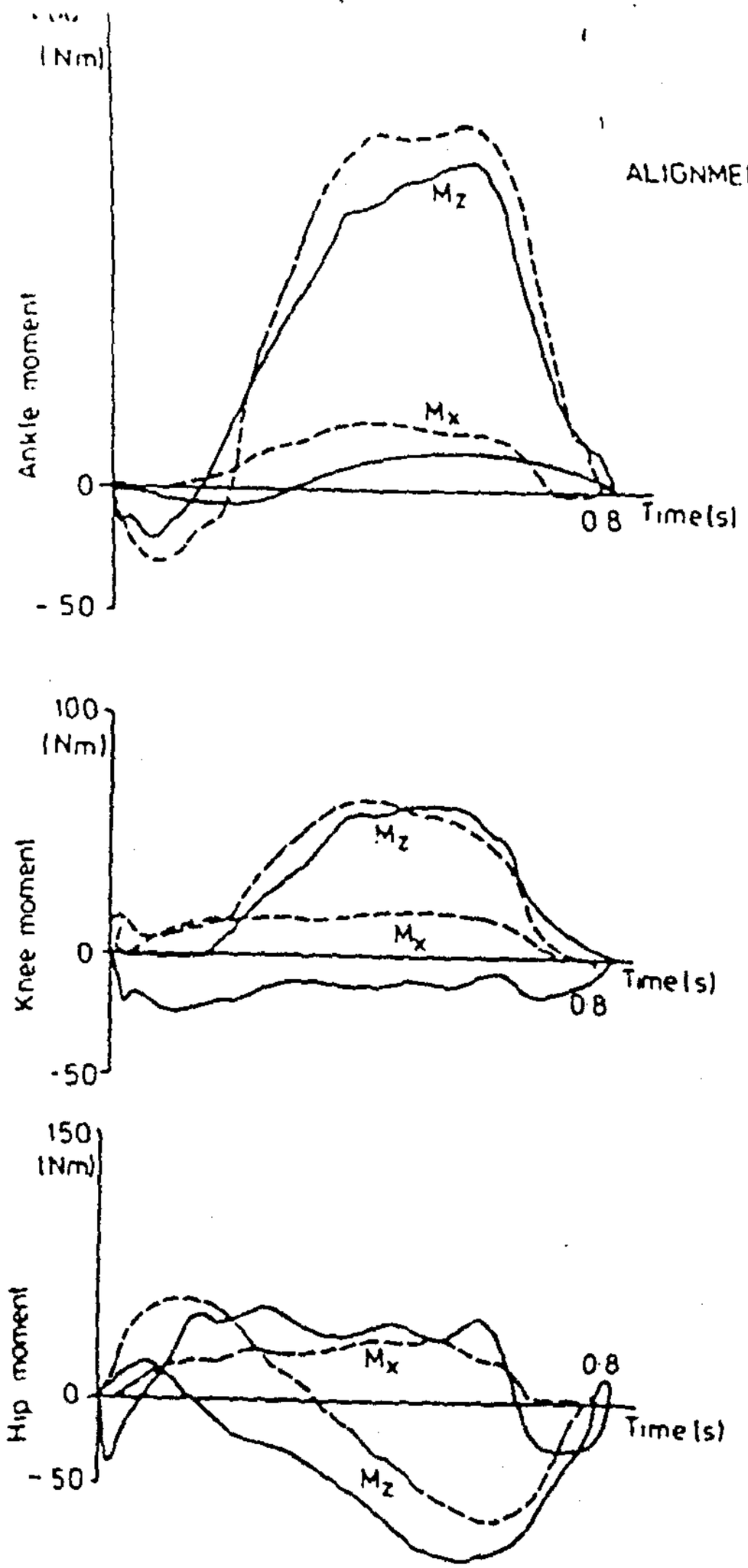

Fig.3.21 Inter-segmental moments of two acceptable alignments. (from Zahedi, 1985)

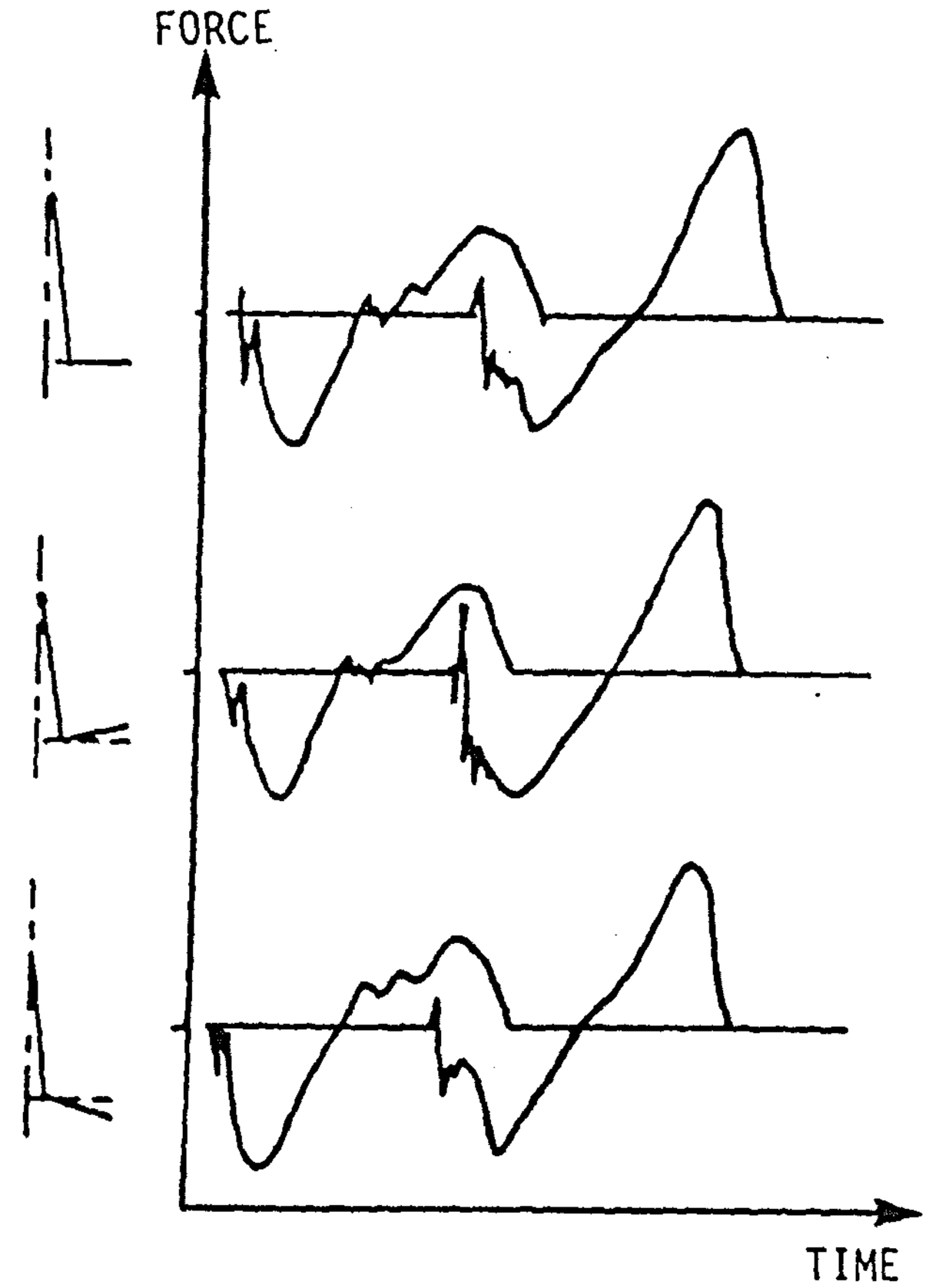

Fig.3.22 Effect of foot flexion on the A/P ground reaction force. (from Mizrahi et al, 1986)

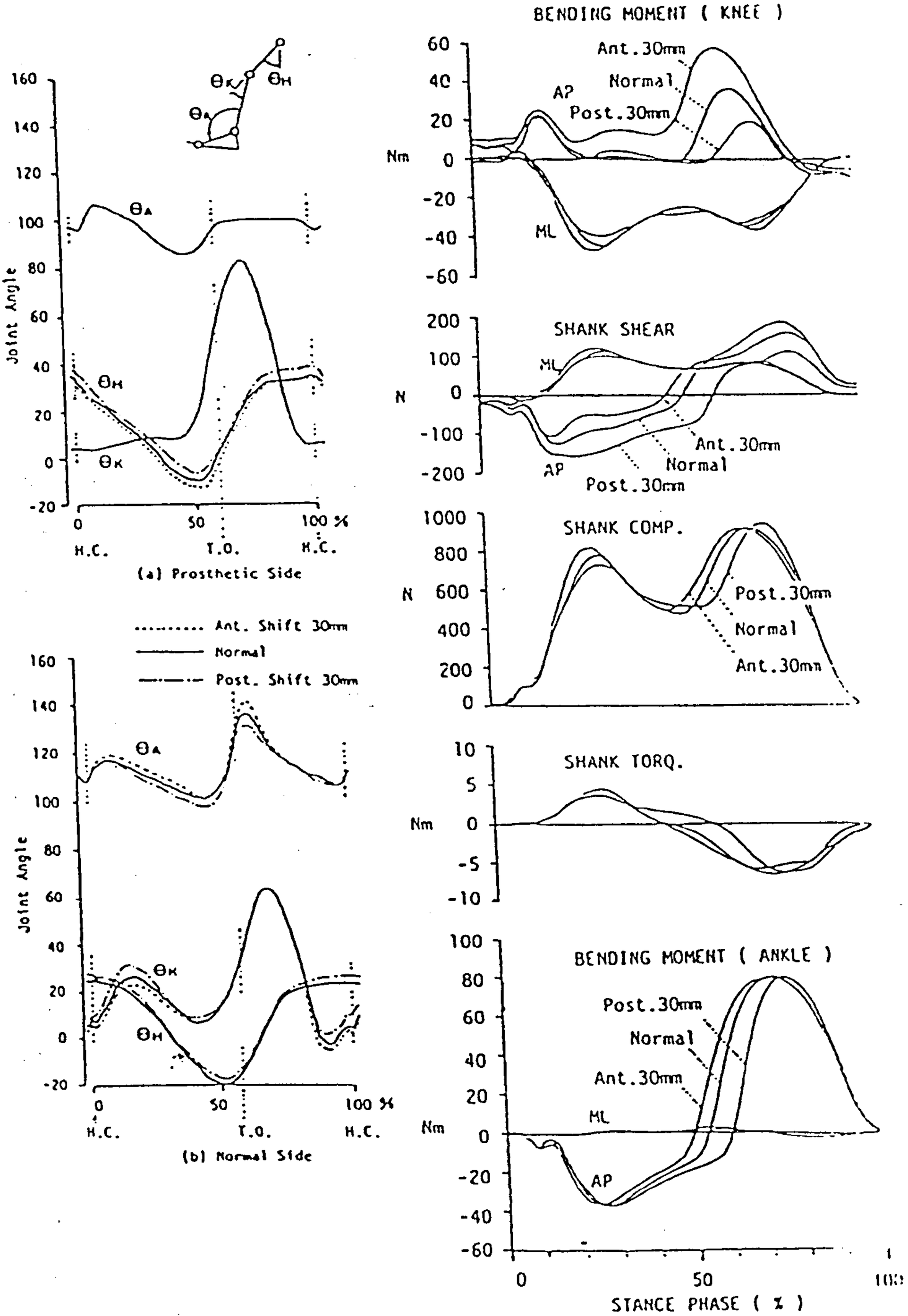

Fig.3.23 Relation between load and alignment of BK prosthese. (from Morimoto, 1987)

amputee's gait were also investigated. It was noted that acquisition of kinematic data alone would not detect small variations in gait were patterns and a more complete evaluation of gait should included temporal-distance parameters, kinematic and kinetic analysis. They demonstrated how two different acceptable alignments contributed to the difference in the loading patterns (refer to Fig.3.21) and also suggested that there was a possibility that the kinetic analysis could help the prosthetist select an optimum alignment among several acceptable alignments. However, the biomechanical aspect was not elaborately investigated.

Hannah *et al* (1984) reported on an alignment study which involved 5 below-knee amputees. Goniometers were attached bilaterally at the hips and knees on all subjects. A symmetry index (see Equ. 2.11) was used to assess the effects of alignment. It was observed that alignment changes to the prosthetic foot disrupted gait to a greater extend than do other alignment changes and asymmetry of hip flexion-extension motions were more sensitive to alignment changes than were other asymmetries.

Mizrahi *et al* (1986) investigated the effects of alignment on the symmetry and ground reaction forces. Four amputees were studied. A television system was used to obtain kinematic data and two Kistler forceplates were used for measuring ground reaction forces. It was found that the perturbations on the ground reaction force indicated a phenomenon of limited instability and could be minimize by adjusting the prosthesis to optimum alignment, see Fig.3.22.

Morimoto *et al*(1987) presented the changes in joint motions and loads of BK amputee wearing a PTB socket and a single-axis foot at different alignments using a pylon load cell and flexible eletrogoniometers, see Fig.3.23. The foot was moved in the AP and ML directions in the horizontal plane, flexed in a dorsal or plantar direction, inverted and everted, toe in and out separately, and tests were conducted on level, ramp and stair ways. It was found that most parameters changed noticeably in proportion to the alignment changes. Foot anterior set resulted in higher knee bending moment, longer duration in positive ankle bending moment and forward shift in shank shear force. Plantar flexion of the foot caused a higher knee bending moment, a longer duration of positive ankle moment, a higher negative shank torque and a shallow

trough in shank compressive force.

Winarski and Pearson (1987) reported a method to quantify the correlation between stump stresses and prosthetic loads for BK amputees with respect to alignment changes. Pressure sensors were placed on the patellar tendon and gastrocnemius to measure the relevant pressures (P_p & P_G) and pylon force transducers were used for shank loads (F_x & M_z). They introduced an influence-factor matrix to model the relation between the stump pressure and shank loads, that is

$$\begin{bmatrix} \sigma_P(\theta, t) \\ \sigma_G(\theta, t) \end{bmatrix} = \begin{bmatrix} W_{11} + \frac{dW_{11}}{d\theta}\theta & W_{12} + \frac{dW_{12}}{d\theta}\theta \\ W_{21} + \frac{dW_{21}}{d\theta}\theta & W_{22} + \frac{dW_{22}}{d\theta}\theta \end{bmatrix} \begin{bmatrix} F_Z(\theta, t) \\ M_X(\theta, t) \end{bmatrix}$$

It was found that the relationship between the socket stresses and shank loads was in agreement with the original qualitative one postulated by Radcliffe, and that this method had promise for future studies.

Another direction in which alignment analysis has been conducted is by means of computer simulation. Ishai *et al* (1983)developed a technique by which the optimum alignment of above-knee prostheses could be reached through the minimization of thigh-axial-torque. The leg kinematic data of amputees were obtained by modifying the normal data published by Lamoreux (1971). This technique was illustrated in three cases and the results proved its feasibility in optimizing prosthetic alignment. However, only the swing phase is considered in the model. This technique requires further verification in clinical practice and stance phase needs to be included.

Van De Veen *et al* (1987) investigated the effects of mass and mass distribution on the maximum stump load and energy level by simulating the dynamic behaviour of above-knee prostheses. Only the swing phase of a locked knee prosthesis and two-dimensional movement were considered. The result show that the required power and the maximum stump force increase with the walking speed and decrease when the total mass of the prosthesis is decreased. The results also show that the

Table 3.2 Temporal-distance parameters for lower-limb amputees

Level	Velocity (m/min)	Cadence (steps/ min)	Stride length (m)	Gait cycle (sec)	Single support (sec.) Prosth.	Sound	Ref
AK	60	87	1.36	1.38	0.43	0.58	19
AK	--	--	--	1.43	0.48	0.60	28
AK	52	84	1.21	1.44	--	--	5
AK	36	72	1.00	1.67	--	--	26
AK	52	87	1.20	1.38	--	--	26
AK	56	85	1.29	1.41	0.49	0.61	14
AK	63	90	1.38	1.32	0.48	0.58	5
Mean	50	83	1.20	1.44	0.47	0.59	123
BK	45	87	1.02	--	--	--	26
BK	71	99	1.44	--	--	--	26
BK	64	96	1.32	--	--	--	22
BK	81	104	1.56	1.15	0.46	0.50	5
Mean	61	94	1.28	1.15	0.46	0.50	79
Normal	90.6	113	1.56	1.06	--	0.41	18

influence of the shoe is almost equal to that of the prosthetic foot.

§3.6 Prosthetic Gait Analysis

Gait analysis is a useful method for evaluating amputees, particularly in monitoring the rate of rehabilitation and the effectiveness of therapy. Prosthetic gait analysis has been pursued by many researchers from different aspects.Presented in this section is a review of gait analysis on below-knee and above-knee amputees. Again it is categorized into four areas: temporal/distance parameters, kinematic assessment, kinetic assessment and energy expenditure.

It will be seen that the variability of data obtained in prosthetic gait analysis is so wide that it makes generalization of the gait pattern for a particular level of amputees very difficult. A number of factors affect the variability of the data, such as the prostheses used, alignment and comfort of the prostheses, skill and co-ordination of the subject, training effect, walking speed, physical and psychological state of the subject, and the environmental conditions of the experiments. As many variables as possible have therefore to be controlled in order to achieve any realistic assessment. This may lead to imposing certain constraints on the selection of patients and the type of prostheses to be worn.

§3.6.1 Temporal/distance parameters

James and Oberg (1973) investigated 34 unilateral AK amputees. Foot switch were used for timing and footprints for distance parameters. Gait analysis was conducted at two different walking speeds, normal and fast. All the patients were fitted with a total contact suction socket and a constant friction knee prosthesis. It was found that walking velocity was reduced significantly (38 percent on the average), because of a shorter step length and a longer gait cycle than normals and that the amputees walked with a greater stride width (31 percent on average) to maintain medio-lateral stability. The stance phase duration of the prosthetic leg was found, on an average, 13 percent shorter, while its swing phase duration was 25 percent longer and its step length 10 percent shorter than that of the intact leg. No difference was observed in two double-support durations, and the change in walking velocity did not appear to affect the

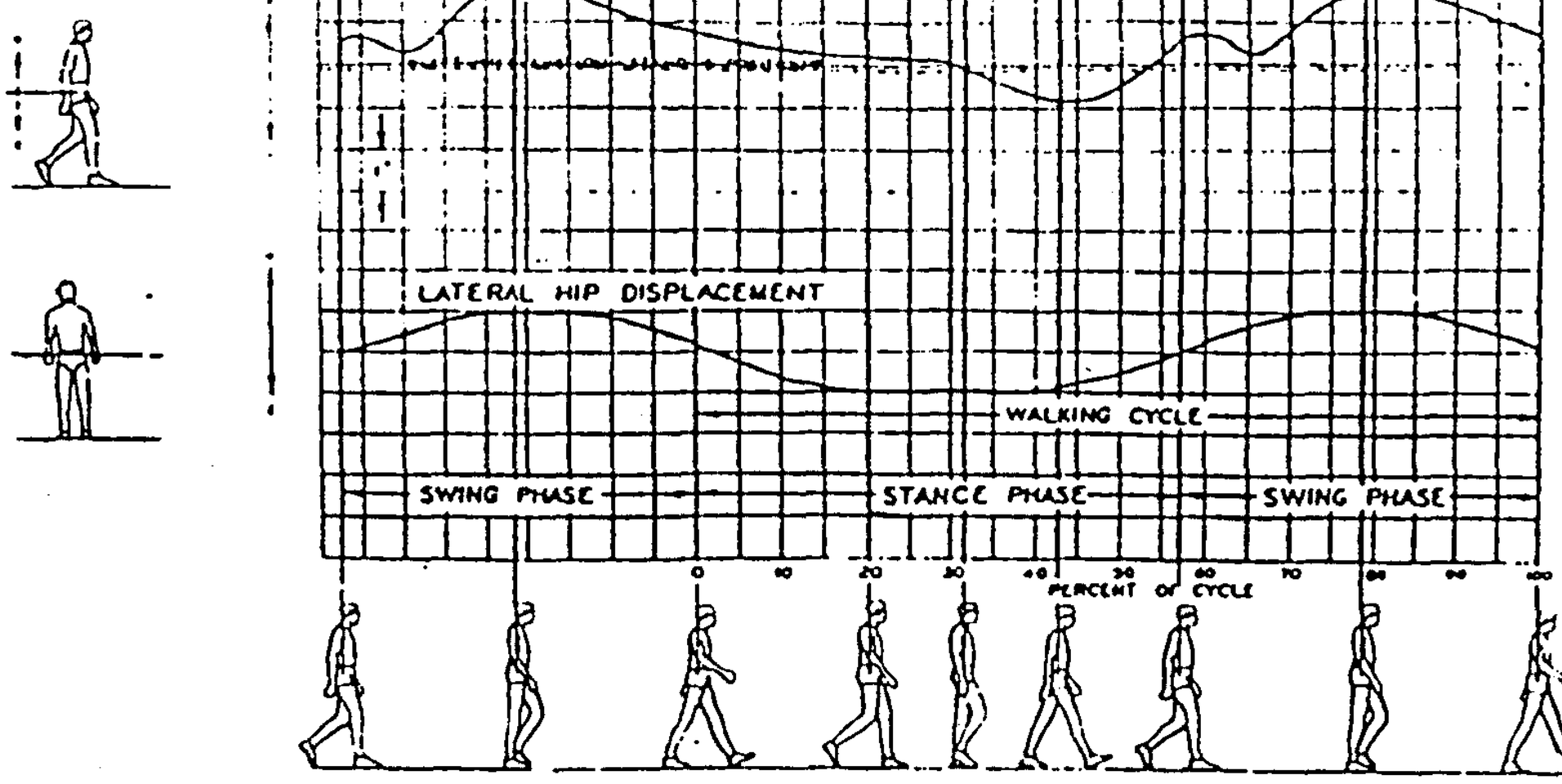

Fig.3.24 Linear movement of the hip of a AK amputee.
(from University of California, 1947)

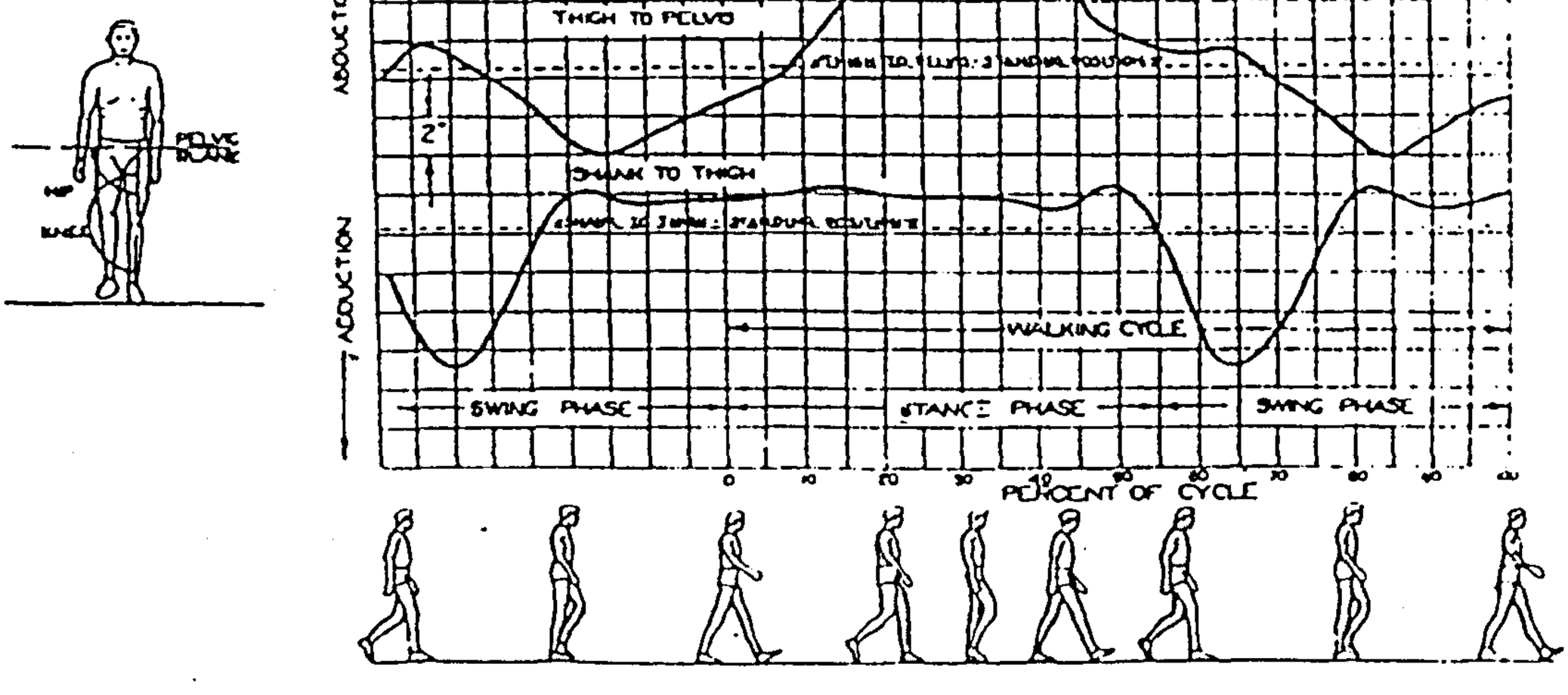

Fig.3.25 Relative rotations of the lower limbs of a AK amputee in the coronal plane.
(from University of California, 1947)

asymmetry observed between the intact and prosthetic legs.

Godfrey *et al* (1975) attempted to establish indications for six different knee units by the use of gait analysis on AK amputees. Seven subjects were studied and the temporal/distance data were compared with those reported by other researchers. The principle finding of the study was that little advantage was gained by using a more complicated knee unit, especially when the patients walked on a flat level surface.

Time parameters of BK amputees were studied by Breakey (1976). He found that the stance phase and single support durations were larger in the sound limb than those in the prosthetic limb.

Murray *et al* (1980) studied gait patterns of AK amputees using the constant friction knee. The results were found similar to those obtained by James and Oberg.

Table 3.2 summarizes the temporal-distance parameters obtained by various investigators for AK and BK amputees. It is obvious that there are significant variations from normal in both BK and AK groups in all the parameters studied.

§3.6.2 Kinematic analysis

The research group at the University of California, Berkeley (UCB,1947) analysed and compared the gait patterns of normals and amputees, see Fig.3.24-3.27. They found that AK amputee tilted the pelvic and iliac crest higher and rotated the pelvis more than normal in order to swing the prosthesis. It was noted that the prosthetic knee remained locked for a greater part of the stance phase, showing a deviation from the two-peak pattern of normal knee flexion. The amputee is unable to dorsiflex and plantar flex, the total angular change of the prosthetic ankle being less than normal. It was also noted that the transverse rotation occurred between the stump and socket, definitely causing discomfort to the patient. Use of ankle rotator was claimed to relieve the patient of much discomfort.

Fishman *et al* (1953) investigated the gait pattern of AK amputees wearing different knee units. Generally, a much smoother and more symmetrical gait was found with the hydraulic knee unit. Bresler *et al* (1957) confirmed that significant differences could be observed in the gait patterns when different knee mechanism were used.

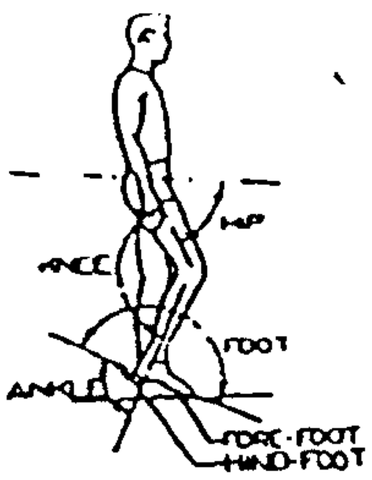

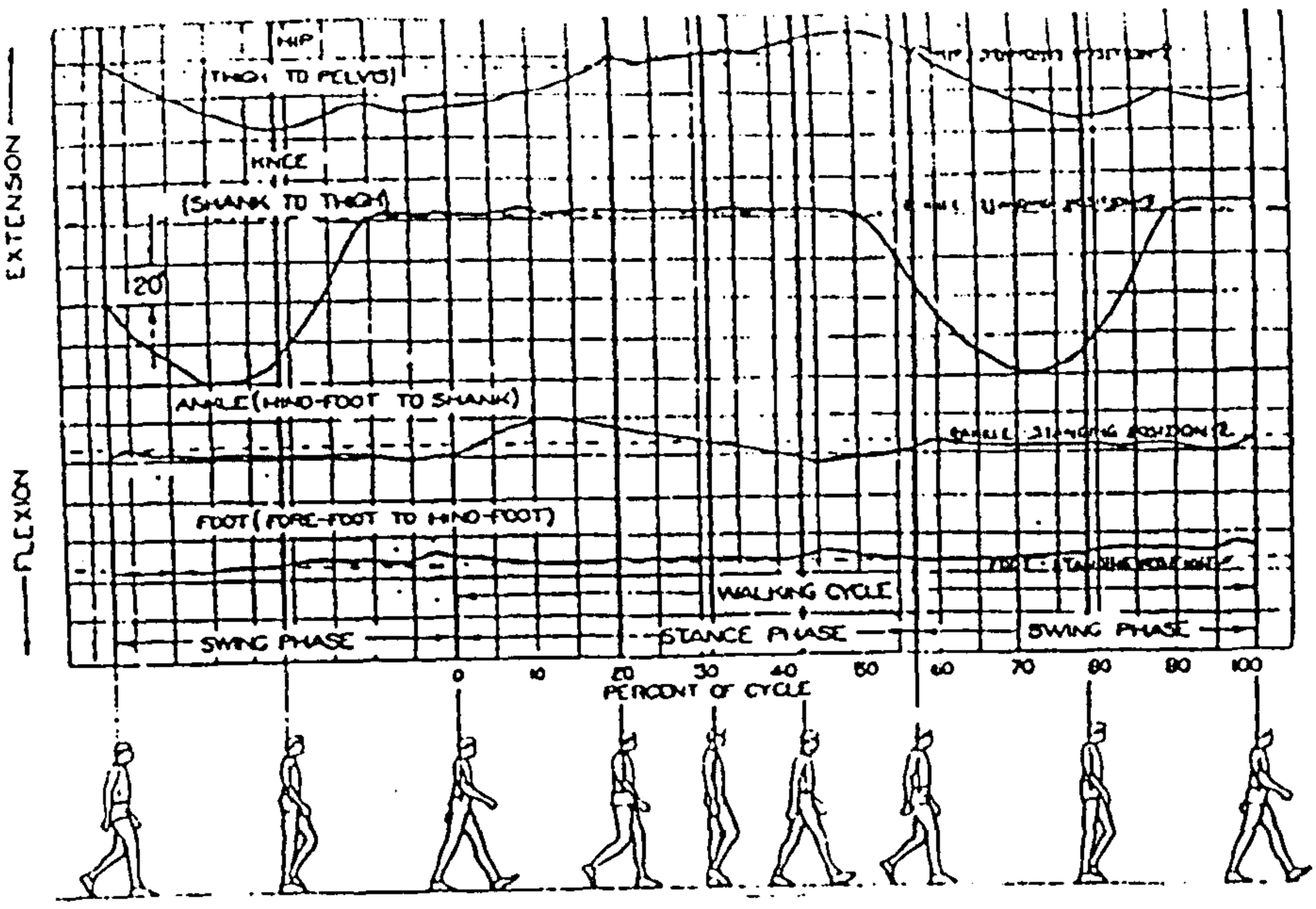

Fig.3.26 Relative rotations of the lower limbs of a AK amputee in the saggital plane.
(from University of California, 1947)

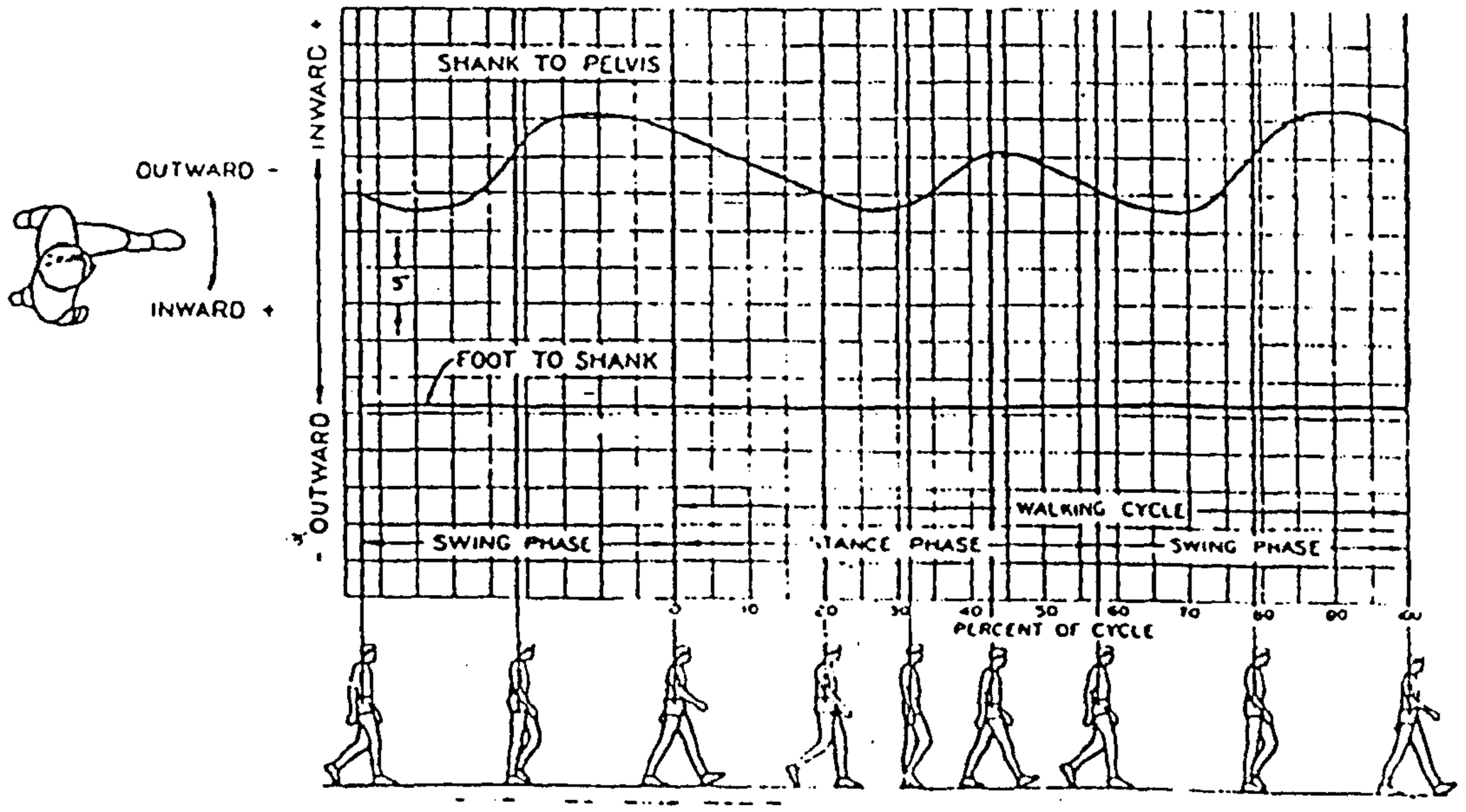

Fig.3.27 Relative rotations of the lower limbs of a AK amputee in the transverse plane.
(from University of California, 1947)

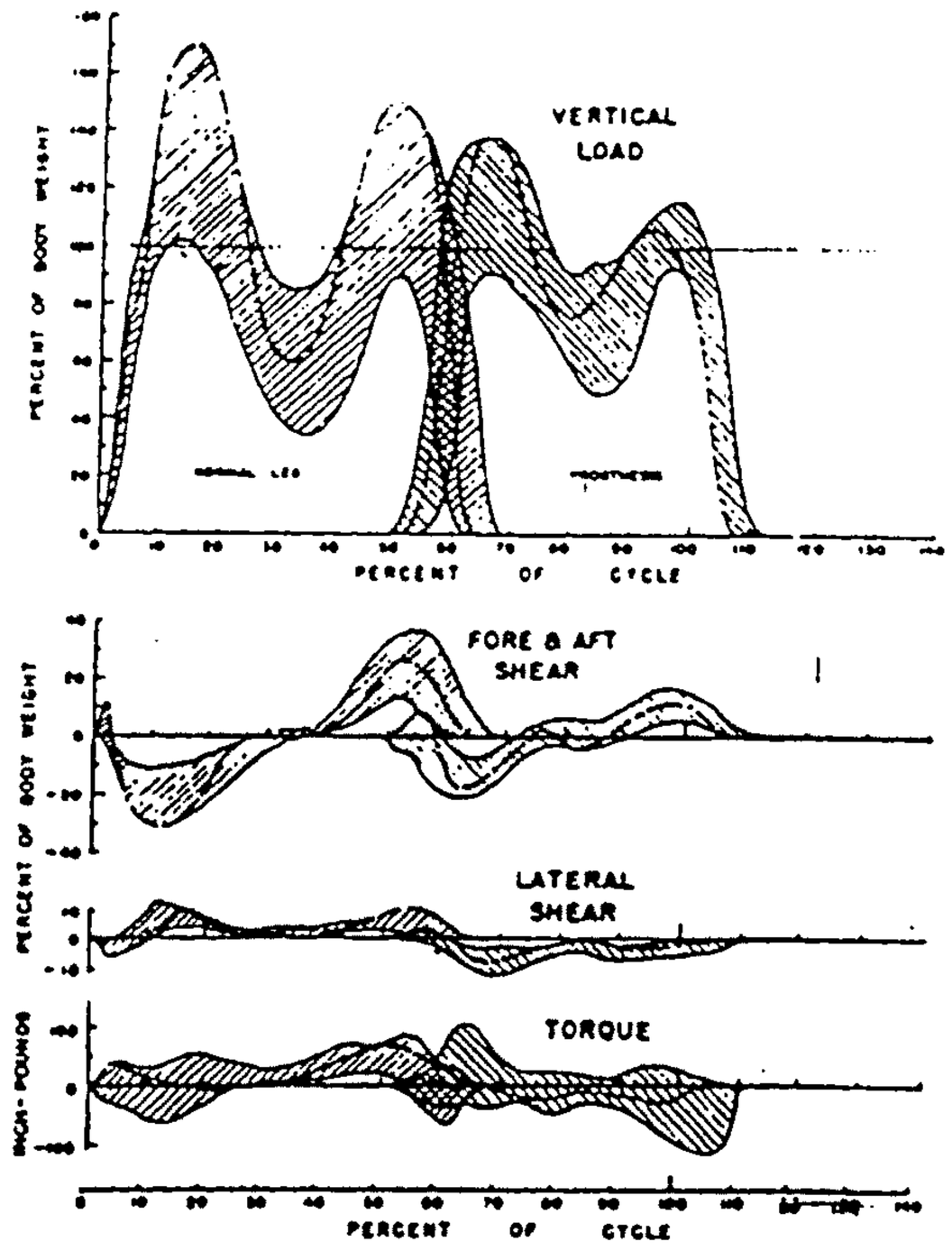

Fig.3.28 Ground reaction forces of seven below-knee amputees.
(from Cunningham, 1950)

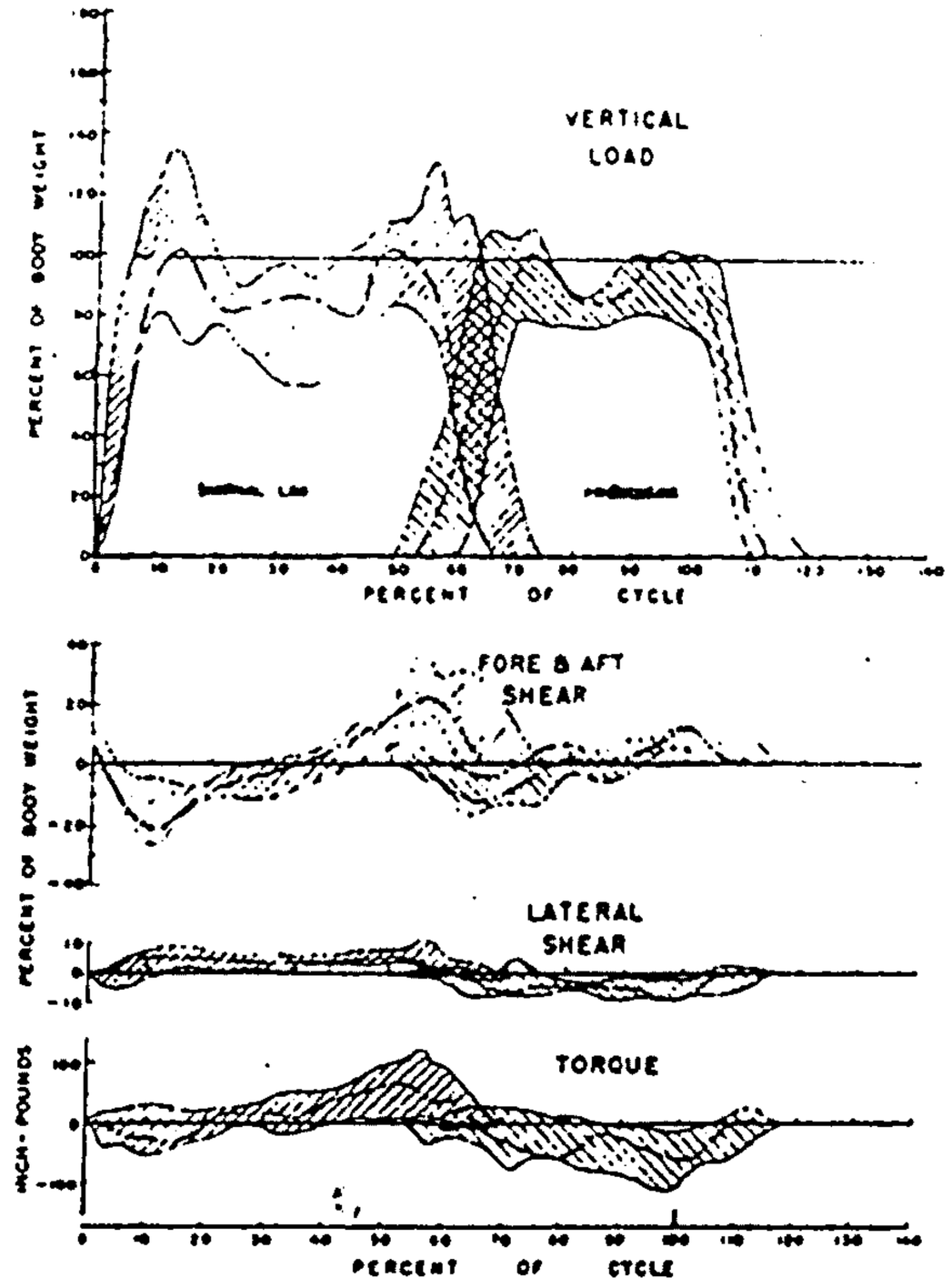

Fig.3.29 Ground reaction forces of eleven AK amputees.
(from Cunningham, 1950)

Murray *et al* (1980) measured the motion of the limbs in AK amputees and the results obtained were similar to those obtained by the UCB.

Upper body angular movements of amputees were investigated by Cappozzo *et al* (1982). It was observed that remarkably large amplitudes were observed in all of the rotations investigated and these variable presented asymmetry. They suggested to incorporate an active mechanism in the prosthetic knee and ankle so that the symmetry of the upper body movement could be improved and energy expenditure reduced.

§3.6.3 Kinetic assessment

The UCB group (1947) conducted a pylon study on the forces and moments on the prosthetic shank. It was found that the forces acting on the prosthetic shank were essentially the same for both above- and below-knee amputees. It was suggested that it was due to the great number of variable involved and also partly to the small number of subject tested.

The effect on the forces of the changes from the standard pelvic belt type to the suction socket type prosthesis was investigated on an AK amputee. The results indicated that the amputee was putting more weight on his prosthesis and presented greater medio lateral stability and more symmetrical gait when he wore the suction socket type prosthesis.

Cunningham (1950) reported on the forceplate studies conducted by the UCB group. A total of seven BK and 11 AK amputees was tested. Large inconsistency was observed in the results of each group, which were caused by many variable such as walking velocity, the ratio of leg length to stride length, body build, weight, comfort during walking, and so on. Fig.3.28 shows the ground reaction forces of seven BK amputees. The vertical forces display the typical two peak pattern and the unaffected leg takes more weight than does the prosthetic leg. This is attributed to the sound leg's take-over of the prosthetic leg's function in producing upward movement of the body to maintain an average elevation. The lack of push-off mechanism in the prosthetic foot explains the much smaller second peak in the vertical force of the prosthetic side. The fore-aft force of the prosthetic side also demonstrated this characteristic.

The ground reactions for 11 AK amputees are shown in Fig.3.29. It was

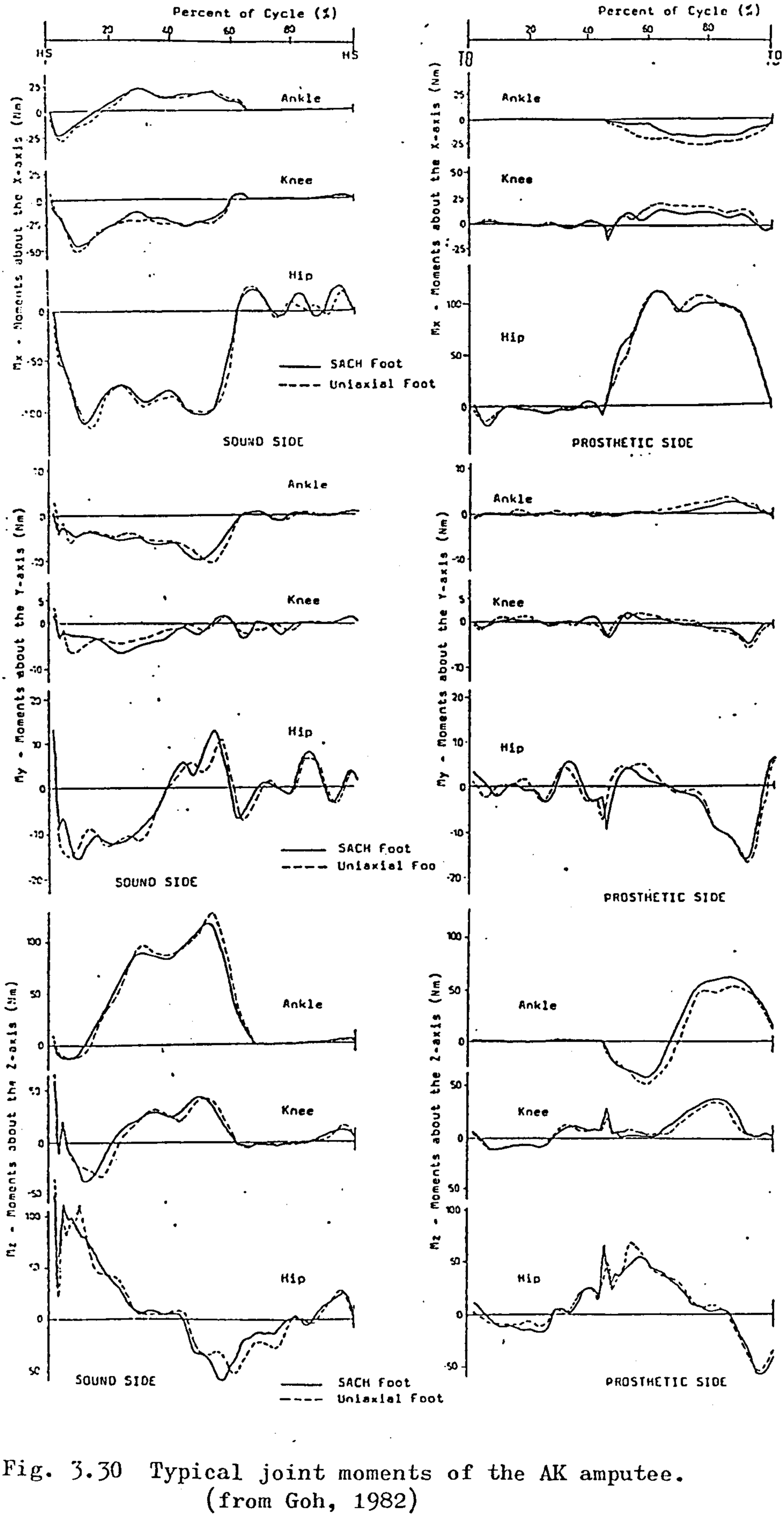

Fig. 3.30 Typical joint moments of the AK amputee.
(from Goh, 1982)

suggested that the middle peak of the vertical force for the unaffected leg was due to the downward reaction to the rising of the hip on the prosthetic side when swing. This middle peak was found to vary greatly from one individual to another and to be closely correlated with the difficulty experienced in the forward swing of the prostheses. It is also immediately apparent that the sound leg carried more weight and produced much more forward propulsion than did the affected leg.

Bresler *et al* (1957) investigated the intersegmental moments of four AK amputees wearing different types of knee mechanisms and walking at different speed. Great variabilities were found in the results which indicated the influences of the knee mechanism as well as walking speed and also demonstrated the need of control over variables that would affect gait patterns in comparative studies.

Cappozzo *et al* (1976) reported a study on two AK amputees wearing a single-axis knee unit without swing control and a SACH foot. A high knee flexion moment, found at the normal leg during early stance, was caused by the prosthesis' inability to control the forward falling of the body, resulting in the normal leg striking the ground at a considerable speed. Furthermore, an extra effort was performed by the normal ankle of the amputee in order to keep the trunk on a suitable trajectory and gain clearance for the swinging prosthesis.

Lawes (1982) investigated the forces acting on the ischial seat of the quadrilateral socket during level walking using a pylon transducer. It was found that approximately 50 to 60 percent of the external vertical load by-passed the hip joint for the two subjects studied. It was estimated that the effect of ischial bearing could reduce the total force at the hip joint by between 25 to 50 percent, and may eventually cause deterioration of the hip joint.

In a project of assessing the Uniaxial and SACH feet, Goh (1982) studied 3-D joint moments of the lower limbs of the AK and BK amputees. Fig. 3.30 shows the results for the AK amputees.Although no conclusive evidence was found as to which prosthetic foot is functionally better for the amputee, the results suggested that the prosthetic foot alignment and/or the stiffness of the dorsiflexion stop was critical for a "smooth roll-over" during push-off.

Zahedi *et al* (1987) investigated the repeatability of kinetic and kinematic

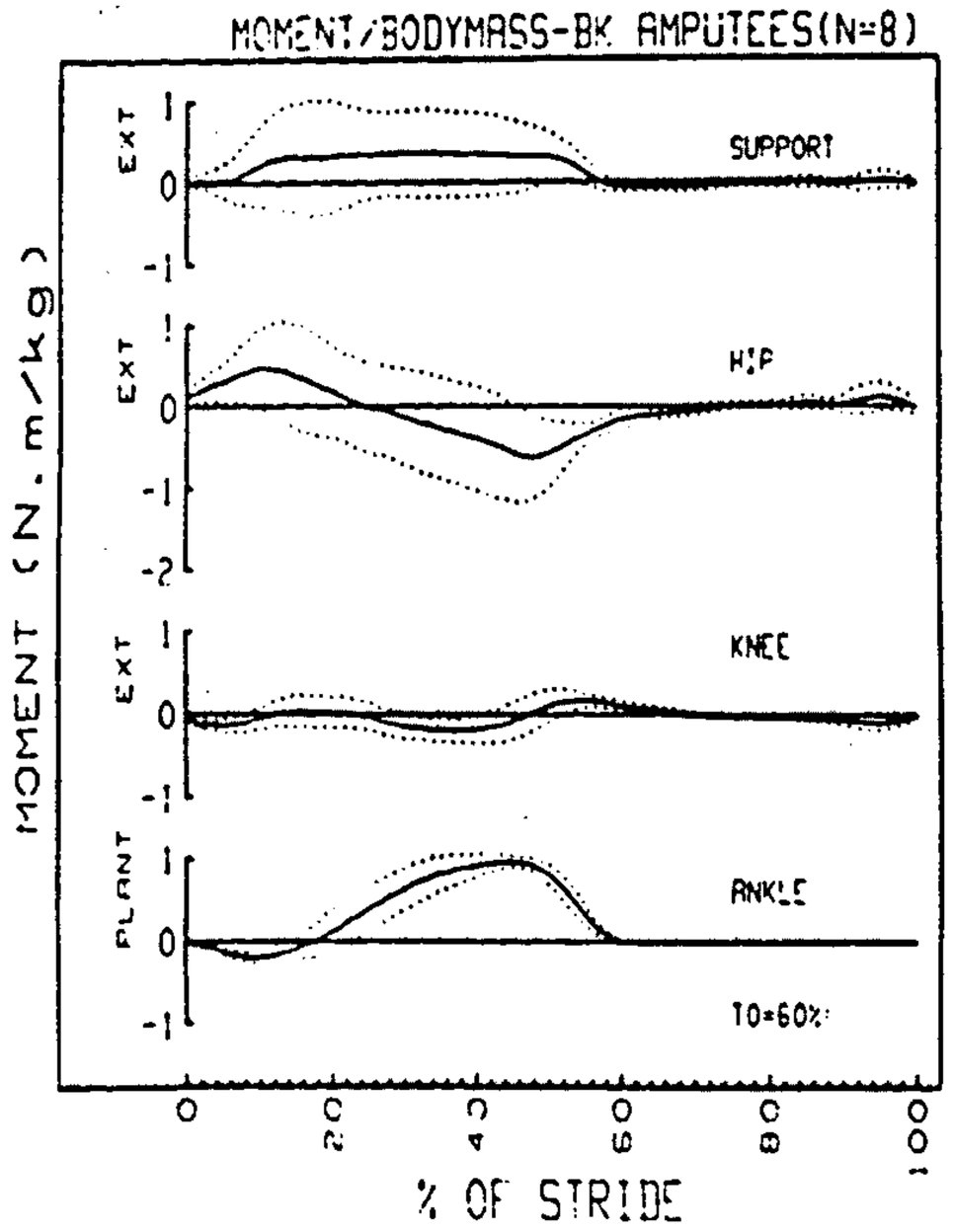

Fig. 3.31 Ensemble averages of joint moments for eight BK amputees.
(from Winter, 1988)

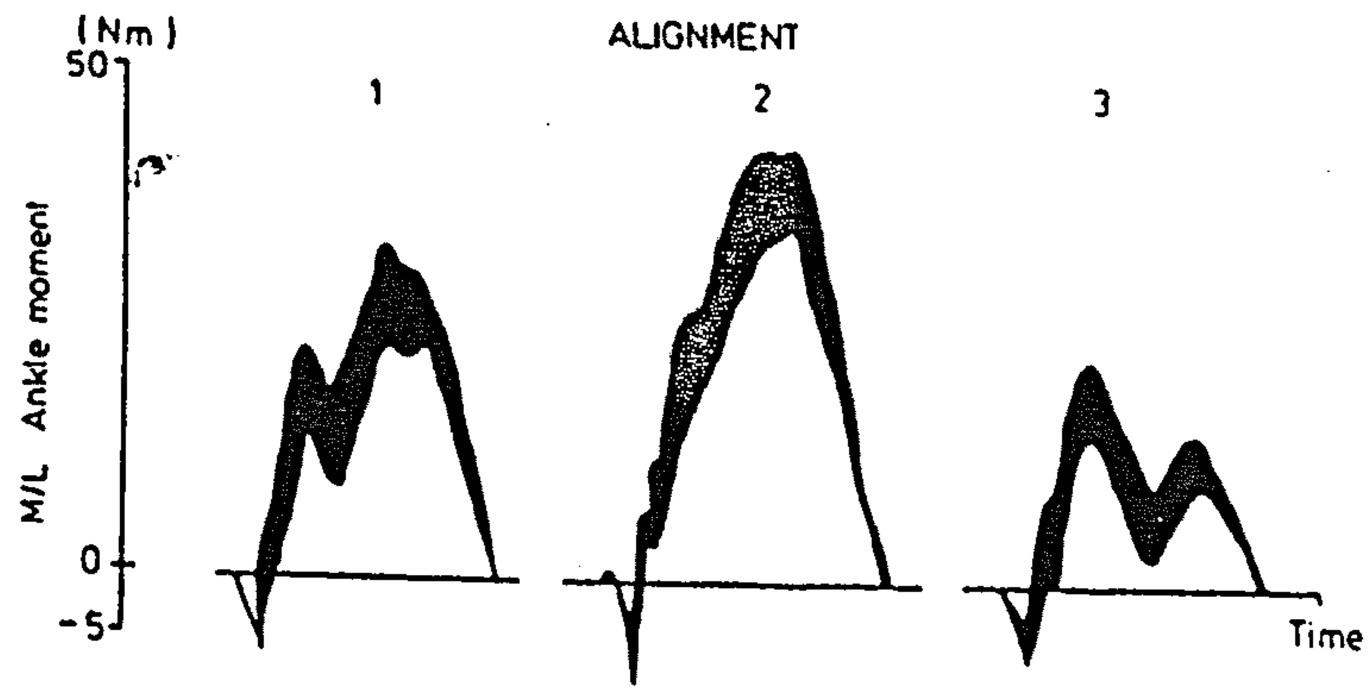

Fig. 3.32 Repeatability envelopes showing the extend of step-to-step variations.
(from Zahedi et al, 1987)

measurements in gait studies of lower-limb amputees. It was found that the degree of step-to-step variation increased for the amputee population compared with normals, and it increased further as the level of amputation became proximal. It was reckoned that the amount of step-to-step variation is dependent on the degree of control during walking.

Winter & Sienko (1988) studied 8 BK(5 SACH, 2 Uniaxial and one Gressinger foot) amputees' gait in terms of joint moments and power and EMG profiles. It was found that the patterns of the prosthetic ankle and knee moments were similar to that of the normal subject, but with lower magnitudes. The hip moment were highly variable, from total flexion moment for 3 SACH trials to excessive extension moment for other two SACH and Uniaxial trials.

§3.6.4 Energy expenditure

Bresler *et al* (1957) discussed the application of energy method to the evaluation of prostheses. He pointed out that the strict controls imposed on the subjects would be unlikely to be fulfilled with amputees, although metabolic energy requirements for walking is one of the most important criterion of the performance of a prostheses. A great number of variables such as alignment, fit, training, environmental conditions were involved in the energy cost and could hardly be eliminated, throwing a great doubt on the validity of using this method to evaluate prosthetic mechanisms.

However, mechanical energy analysis is valuable for an understanding of the various operations in walking and establishing reasonable design criteria. Bresler *et al* (1957) investigated the mechanical energy and power in the leg of AK amputees during level walking. Four subjects using 6 different knee mechanisms and walking at 3 different speeds were analysed. Although the results were not conclusive, the following observations were made.

(1) In general, the net energy from the prosthetic leg is not adequate to provide for its required articulation in space. The energy deficiency (about 15ft-1b) is usually compensated for by the excess of energy provided by the natural leg or body movement.

(2) The greater energy requirement of AK amputees during walking, about 25

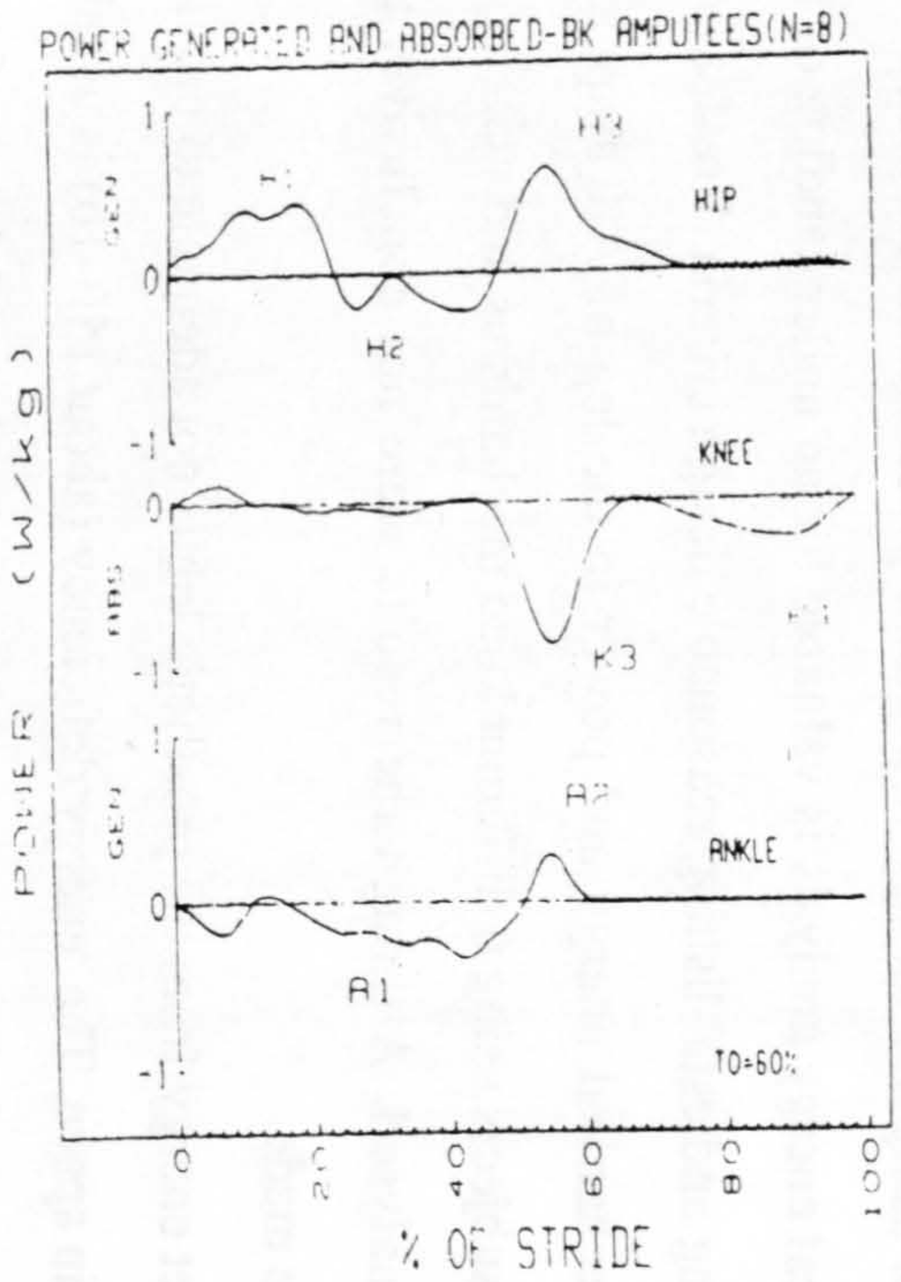

Fig. 3.33 Ensemble averages of mechanical power of eight BK amputees.
(from Winter, 1988)

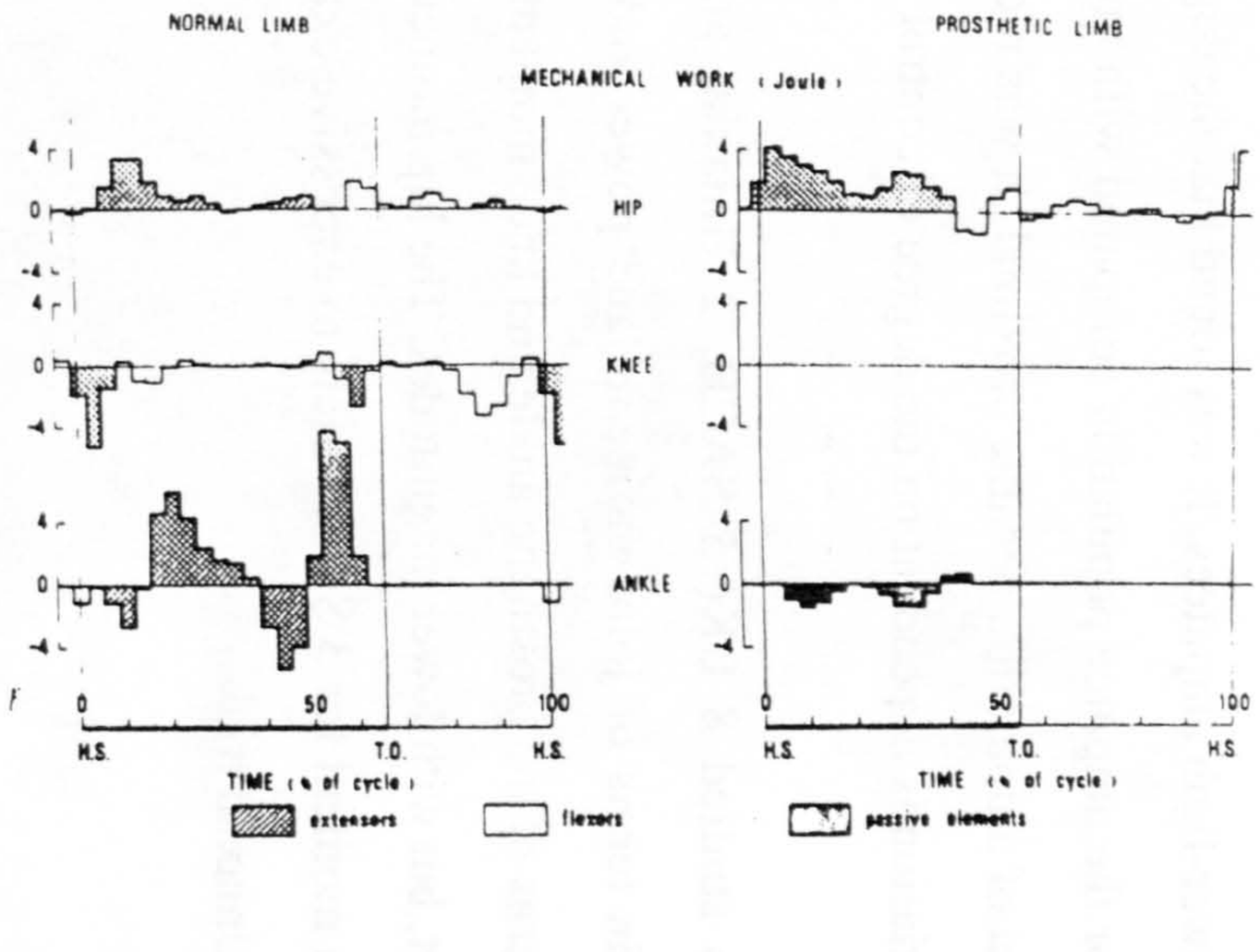

Fig. 3.34 Typical energy variations of the AK amputee.
(from Cappozzo, 1976)

to 50 percent of the total effort more than normals, is largely due to the body movements compensating for the inability of prostheses to replace the function of the normal leg.

(3) Improvements in the functional characteristics of a prosthesis which may reduce the energy requirements are: initial knee stability, minimizing vaulting, push-off compensation, preparation for swing, and swing phase control.

(4) It seems reasonable that with proper design and/or training the amputees could reduce the excessive expenditure of energy.

Fischer and Gullickson (1978) conducted a literature review on the energy requirements of ambulation in health and disability. It was found that a great variability existed in the results, confirming the comment made by Bresler (1951). If averaging the results it is shown that the below-knee amputee walks at 53m/min, expends 63.4(cal/min/kg) or 1.077(cal/m/kg) while the above-knee amputee walks at 49m/min, consumes 59.8 (cal/min/kg) or 1.444(cal/m/kg).

Cappozzo *et al* (1976) and Winter & Sienko (1988) reported the energy studies of the BK and AK amputees respectively, and similar results were obtained to those of Bresler *et al*(1957). It was noticed that energy generation at the prosthetic hip joint was higher than normals, compensating for the loss of major energy generation by the plantar flexion of the foot at push off.

OTTO BOCK LIST OF PARTS

	Item	Material
1.	Socket shell	Polyester or acrylic laminate
2.	Pedilen ring	Rigid P.U. foam
3.	Block	Wood
4.	SACH foot	P.U. foam rubber & wood
5.	Foot adaptor	Steel
6.	Adjustable adaptor	Steel
7.	Shank tube	Aluminium alloy
8.	Adjustment screws	Steel
9.	Extension assist mechanism	Steel/plastic
10.	Friction wedge/extension stop	Nylon
10A.	Screw	Steel
11.	Clamp adaptor	Steel
12.	Knee unit	Steel
13.	Adjustment screws	Steel
14.	Socket attachment block	Plastic/wood
15.	Baseplate adaptor	Steel
16.	Adjustment screws	Steel
17.	Socket head screws	Steel
18.	Wire bow	Spring steel
19.	Pyramids	Steel
20.	Extension assist cover (not shown)	PVC
21.	Cosmetic foam cover	Flexible P.U. foam
22.	Perlon adhesion rim (not shown)	Nylon
23.	Connection plate	Plastic
24.	Cosmetic stocking	Nylon

OTTO BOCK SYSTEM LEG

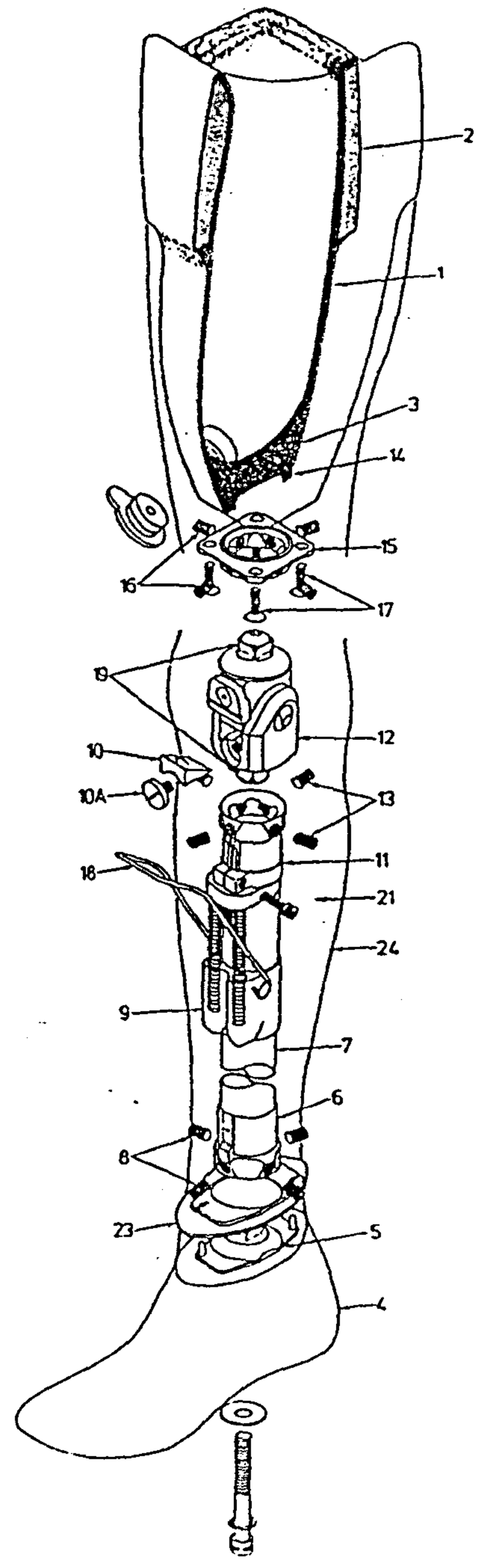

Fig.4.0(a) The Otto Bock above knee prosthesis.
(from Solomonidis, 1980)

CHAPTER 4

EXPERIMENTAL ASPECT OF THE WORK

The experimental aspect of the work presented in this theses is described in this chapter.

Two properties of a prosthesis were measured in the project: mass properties and alignment. The mass properties, i.e. mass, the location of the centre of gravity and the moment of inertia of the prosthetic segments, needs a little description. The measurement of the alignment of the prostheses is described in detail.

The second section of this chapter is given to a brief description of the Strathclyde biomechanics laboratory in which the present gait tests were carried out.

An assessment of the accuracy of the kinematic data obtained through television-computer system and cinematography is presented in §4.3 which served as a basis for selecting a suitable motion recording system for this project.

The biomechanical gait test is reported in §4.4. A body marker system was developed and an experimental protocol is presented.

§4.1 The Prostheses, Their Inertia Properties and Alignment

The prostheses worn by the amputees tested are briefly described. Then many frames of reference and their identifications on the prosthesis were defined and the procedure of alignment measurement described.

§4.1.1 The prostheses

Two different AK prostheses were worn by the amputees tested: the Otto Bock and the Endolite systems.

The Otto Bock system was fitted with a quadrilateral suction socket, a Uniaxial knee and a SACH foot, as shown in Fig. 4.0(a). All components in the

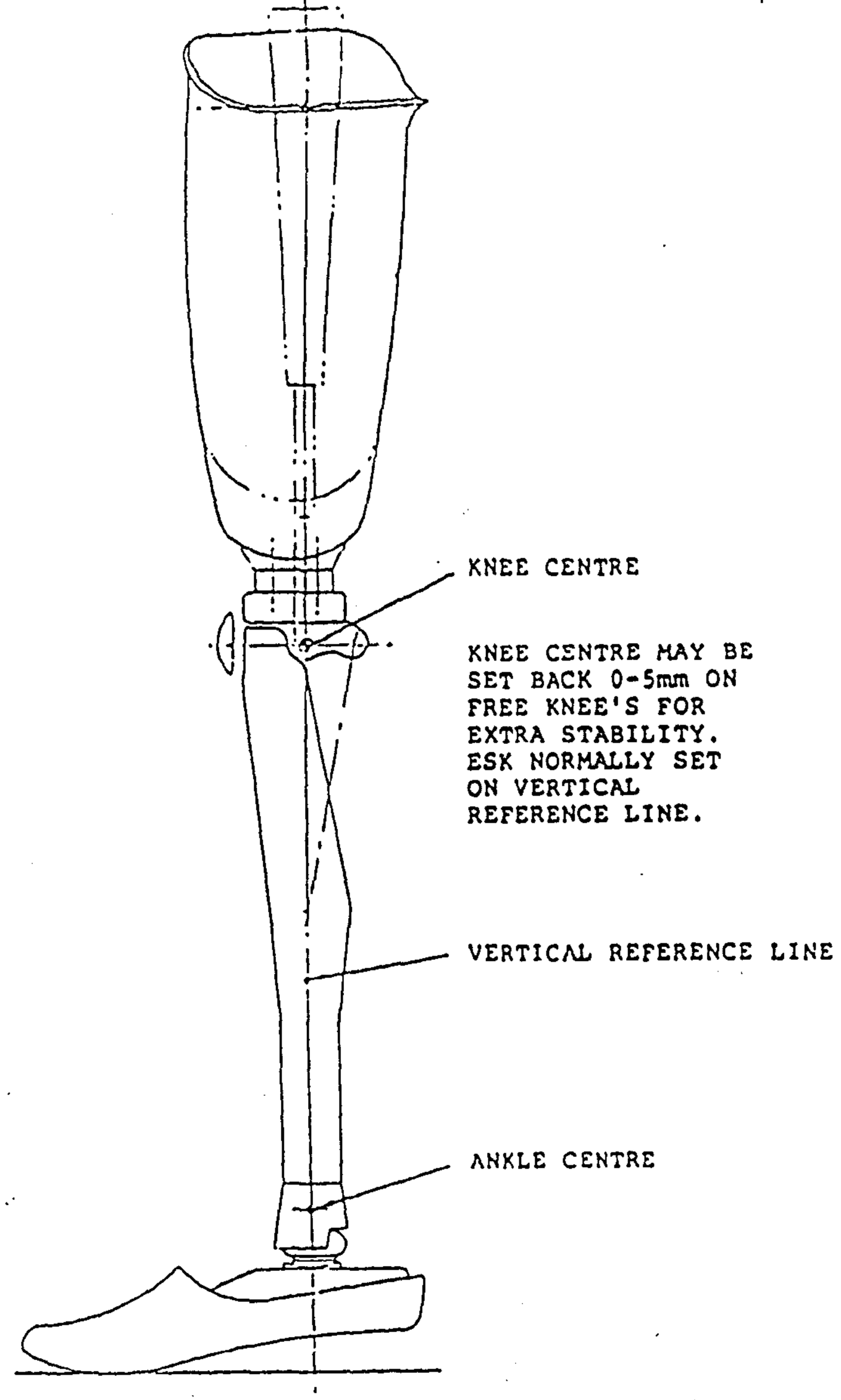

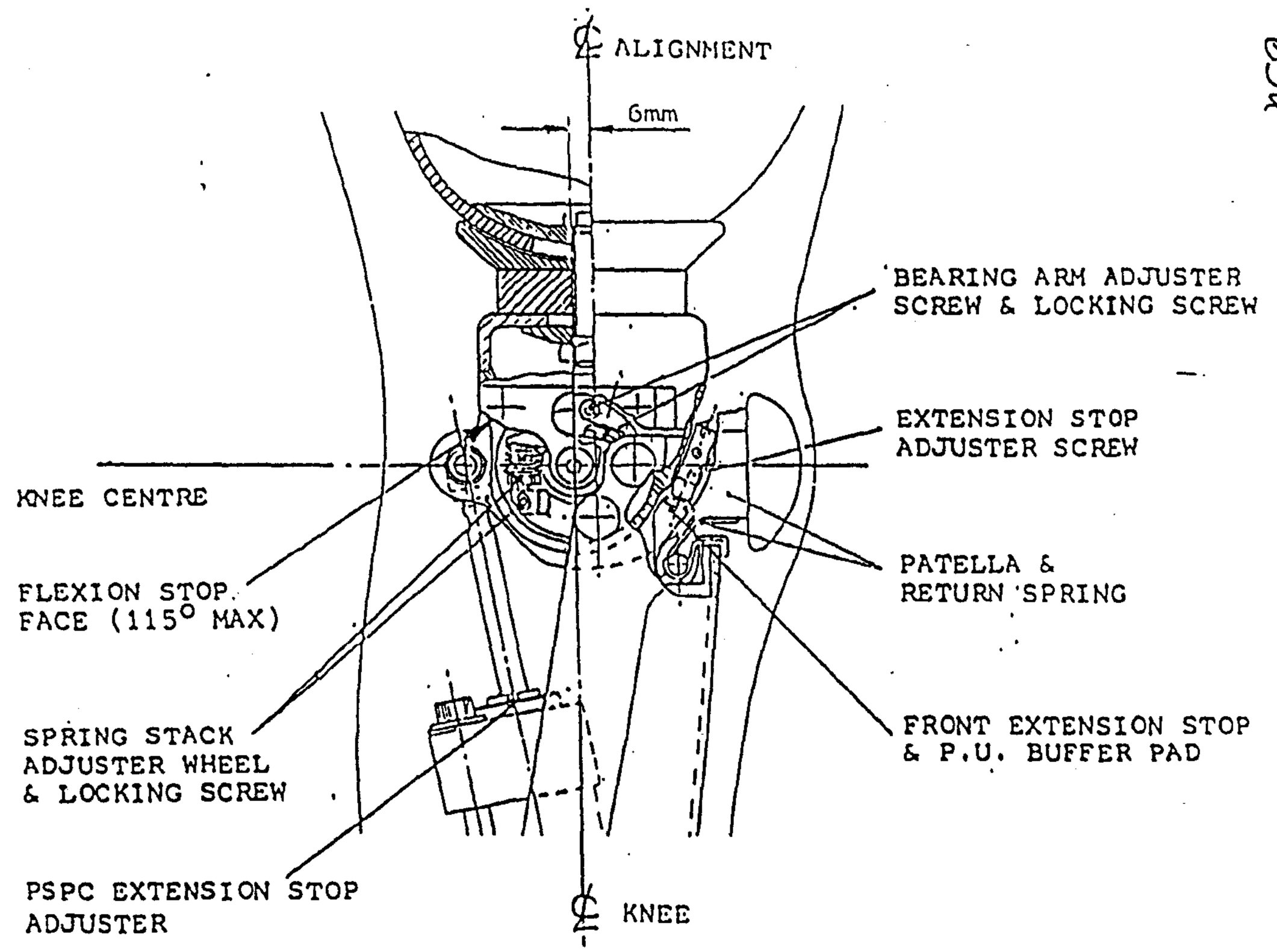

Fig. 4.0(b) The Endolite Above-knee prosthesis. For the detail of the foot, see Fig. 3.12.
(from Blatchford & Son Ltd, 1985)

system can be rotated relative to each other in antero-posterior and medio-lateral planes via the four tilting screws in the adjustment adaptor securing the pyramid. The rotation centre of the socket is approximately at the centre of the pyramid. Internal and external rotation of the foot can be made by loosening the clamp screw on the adaptor distal to the knee unit and rotating the shank tube and the foot.

The Endolite system was fitted with a metal socket, a uniaxial knee unit with pneumatic swing control and a Multiflex ankle/foot assembly, as shown in Fig. 4.0(b) and Fig. 3.12. The foot can be rotated in the A/P plane via the foot serrations. After loosening the nut to the socket plate and the bolt assembly, the socket can be shifted in the transverse plane via the slot in the knee chassis or/and rotated in 3-D via the slot in socket base whose proximal surface is part of a sphere. The rotation centre of the socket is therefore at the origin of the sphere.

§4.1.2 Coordinate system of reference

The Cartesian system was used throughout this thesis. The Committee on Prosthetics Research and Development (CPRD, 1975) recommended an international convention of the system as shown in Fig. 4.1. The positive direction is *X* forward, *Y* upward and *Z* to the right, and the positive rotation is clockwise when viewed along the corresponding axis in the positive direction.

This system was identified in relation to each limb and joint in the prosthesis. The following describes how this was done.

§4.1.2.1 The above-knee socket Two types of above-knee socket were fitted to the amputees tested and different methods were adopted to define the socket frame of reference.

The Quadrilateral socket

The definition of the frame of reference for AK quadrilateral socket is shown in Fig. 4.2. Two planes perpendicular to the long axis of the socket are first defined: one is 25mm proximal to the distal end of the socket and the other 25mm distal to the ischial seat. The *Y* axis is located equidistant from the socket wall in these two

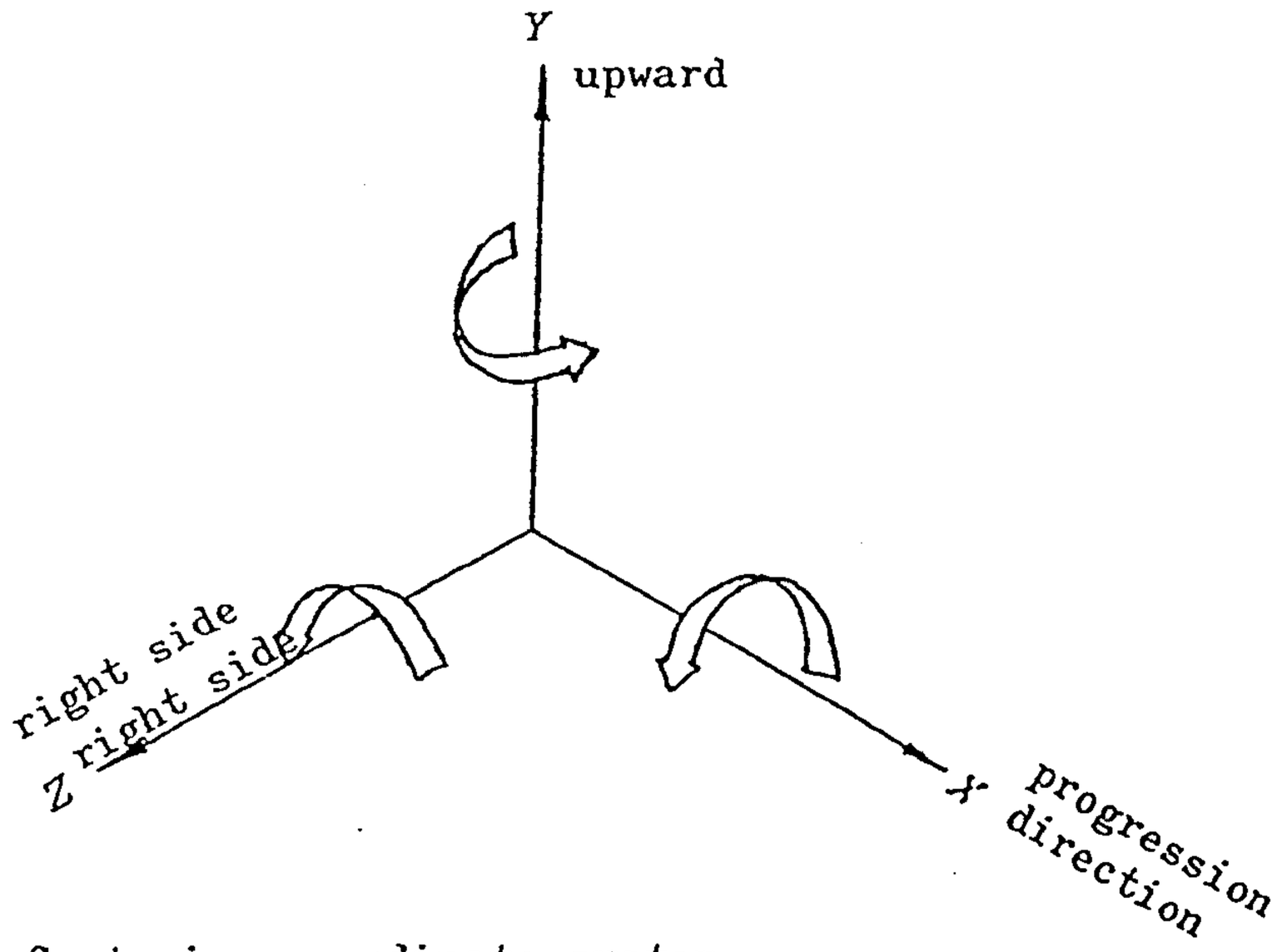

Fig. 4.1 Cartesian coordinate system.
Ground frame of reference.

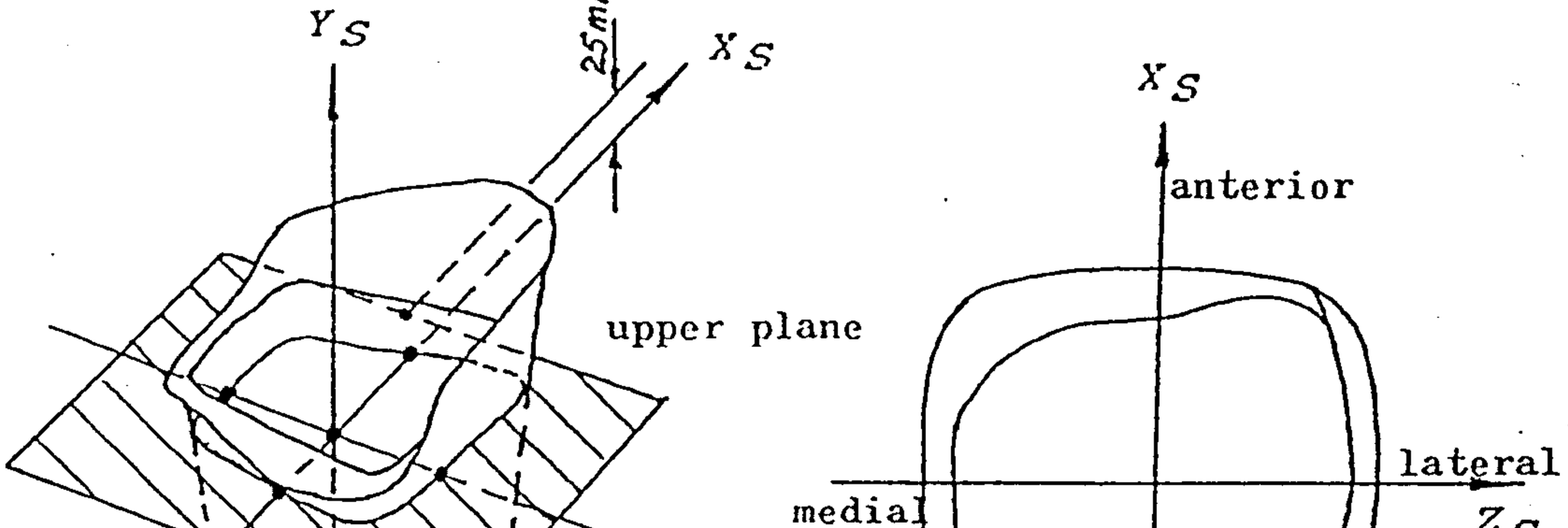

Fig. 4.2 Definitions of the socket frame of reference (right amputee).

planes, and positive is directed upward. The *X* axis is defined to be parallel to the medial brim in the transverse plane and anteriorly directed. The *Z* axis is then identified so as to form a right-hand orthogonal set.

A custom-built socket axes locator (the SAL), developed by Szulc (1983), facilitated the establishment of the socket reference axes. This device consisted of a central bar upon which are mounted two sub-assemblies and each of them comprised 4 spring-actuated pointers that operated like an umbrella. The SAL was positioned in the socket so that the cross formed by four pointers was coincident with the *X* and *Z* axes of the socket system. Four points, two each on the medial and lateral wall of the socket, were marked permanent for later identification.

Other types of sockets

The non-quadrilateral sockets do not have a similar brim contour to the quadrilateral socket to allow the system to be set readily. This means that no unique definition of a socket reference frame can be derived regardless of other factors other than the socket alone. The socket was therefore marked as the prosthesis was mounted on the alignment measuring jig, as described in §4.1.4.2.

§4.1.2.2 Prosthetic knee joint Only the single axis knee joint was considered as it was the only one fitted to the amputees tested. Since the knee joint consists of two segments, *ie*, the shank and the thigh, two sets of axes have to be defined, one for each segment. The *Z* axis of both two segments was common and naturally defined by the pivot or axle of the joint itself, and the origin *O* was at the mid-point between the medial and lateral ends of the pivot. In order to identify the remaining two axes, a plane was defined which was normal to the *Z* axis and contained the centre *O*. The orthogonal projection of the ankle and hip joint to the plane was produced, and the *Y*-axis of the thigh joined *O* to the hip joint projection and the *Y*-axis of the shank passed the ankle joint projection to the center *O*. The *X*-axes of both segments were defined as such that they constituted right-hand orthogonal sets. Fig. 4.3 shows how this was done.

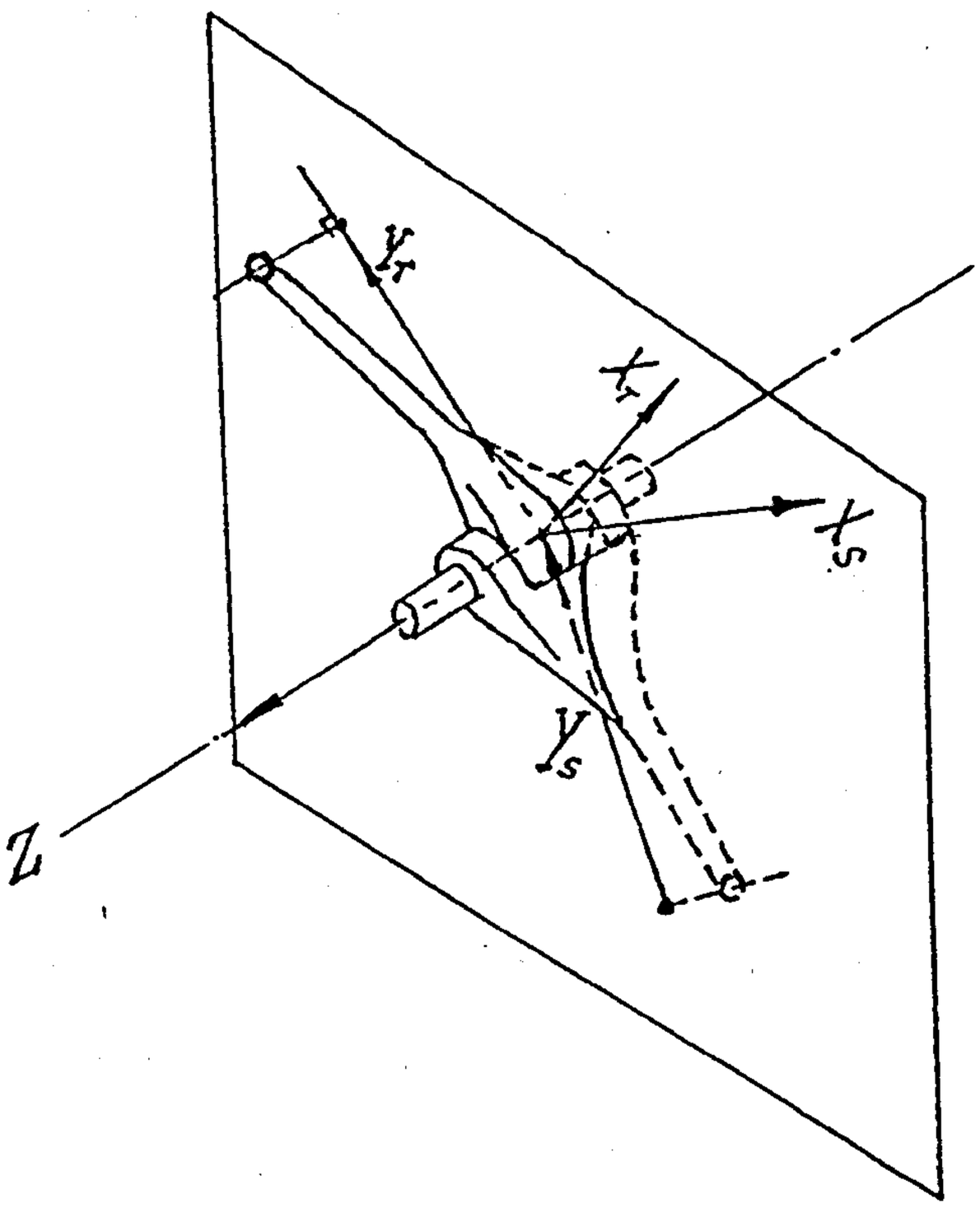

Fig. 4.3 Definition of the knee joint frame of reference.

§4.1.2.3 Prosthetic foot Two kinds of prosthetic foot, the SACH foot and the Multiflex foot, were fitted to the amputees tested and similar reference systems were established on these two types of foot. A plane was identified for each type of the prosthetic foot in which the *X* and the *Z* axes were located and to which the *Y* axis was normal. For the SACH foot this plane was the one at the foot/adaptor interface and for the Multiflex foot the plane passes through the centre of the top housing and parallels to the metal plane on which the dorsi/plantar flexion serrations was mounted, see Fig. 2.11 and Fig.2.12. The origin was at the centre of the bolt holes. The *X* axis passed the midpoint at the toe and the *Z* axis directed to the right regardless of whether the subject was a right or left amputee. A point was marked on the midpoint of the toe for later identification.

§4.1.3 Measurement of inertia properties

In measuring its mass properties, the AK prosthesis was divided into two segments: (1) socket consisting of all components above the knee joint; (2) shank comprising all components below the knee joint including foot wear. Furthermore, the principal moments of inertia about the *X* and *Z* were assumed to be equal, and that about the *Y* axis zero.

The mass of each prosthetic segment was determined by a weighing scale.

The location of the centre of gravity of each prosthetic segment was estimated by balancing the segment lengthwise across a knife edge and expressed as the distance from the knee joint to the centre of gravity.

The compound pendulum method was used to establish the moment of inertia of the prosthetic segment. For a compound pendulum undergoing small-amplitude free oscillation, the equation of motion can be written as

$$I\ \ddot{\theta} = -mgS\theta \qquad (4.1)$$

where *I* is the moment of inertia about the pivot and l the distance from the pivot to

INERTIA PROPERTY OF PROSTHESIS

Name: Affected side: L/R Date: / /198

Shank pendulum test (sec./10 cycles)

	1	2	3	4	5	Mean
Time						

Socket pendulum test (sec/10 cycles)

	1	2	3	4	5	Mean
Time						

Results

Paramter	Shank	socket
Mass (kg)	$m_{PS}=$	$m_{SO}=$
C.G. (m)	$S_{PS}=$	$S_{SO}=$
Izz (kg*m**4)	$I_{PS}=$	$I_{SO}=$

Fig. 4.4 Form for measuring the inertia properties of the prosthesis.

the centre of mass. Since $\ddot{\theta}=-\omega^2\theta$ and $\omega=2\pi f$, the moment of inertia about the pivot can be presented as

$$I = \frac{mgST^2}{4\pi^2}$$

(4.2)

where T is the period of oscillation.

In determining the moment of inertia of the prosthetic segment, the segment was suspended about the knee joint , the duration of 10 cycles of small amplitude free oscillations was measured using a stop watch and recorded. A total of 5 pendulum tests was made for each segment, and the averaged period of oscillation was produced.

Fig. 4.4 shows the form for measuring the mass properties of the prosthesis.

§4.1.4 Measurement of alignment of the prosthesis

§4.1.4.1 Mounting the prosthesis on the jig Procedures and equipment were produced to measure the coordinates of the reference points on the prosthesis with SACH foot, see Zahedi *et al* (1986). A bracket with an accurately machined vertical surface was fitted to a horizontal baseplate on which fixed a perspex plate marked with a grid of 1cm squares. A jig frame of reference was established as shown Fig. 4.5. With the foot off, the prosthesis was mounted on the vertical surface of the bracket, with the foot directed upward, by means of a bolt passing through a vertical plate into the threaded hole at the ankle adaptor. A constant extension moment of 50 N·m was applied to the prosthetic knee joint to prevent the knee from flexing and to improve the repeatability.of the measurement.

However, other types of foot did not have a useful surface for mounting the prosthesis on the measuring jig. Furthermore, it was difficult to apply the same amount of hyperextension moment about the knee joint. Two modifications therefore were made on the measuring jig to overcome these difficulties. A *V*-shaped cramp, capable of holding tubes of different diameters, was fixed on the baseplate and

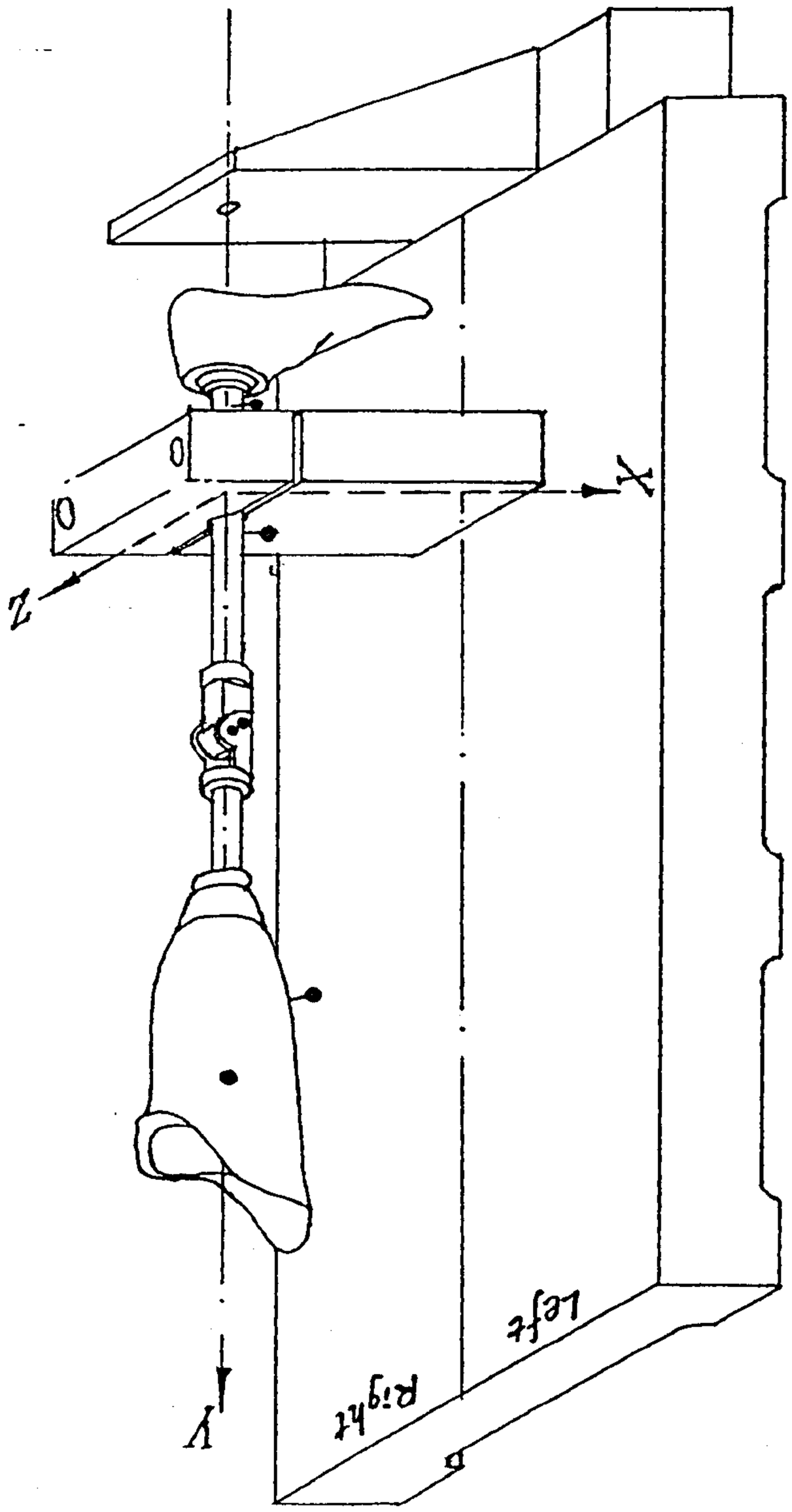

Fig. 4.5 The arrangement of the jig and prosthesis for aligment measurement.

ALIGNMENT OF PROSTHESIS

1. Technique of aligment measurement

a) Dimension of the toucher

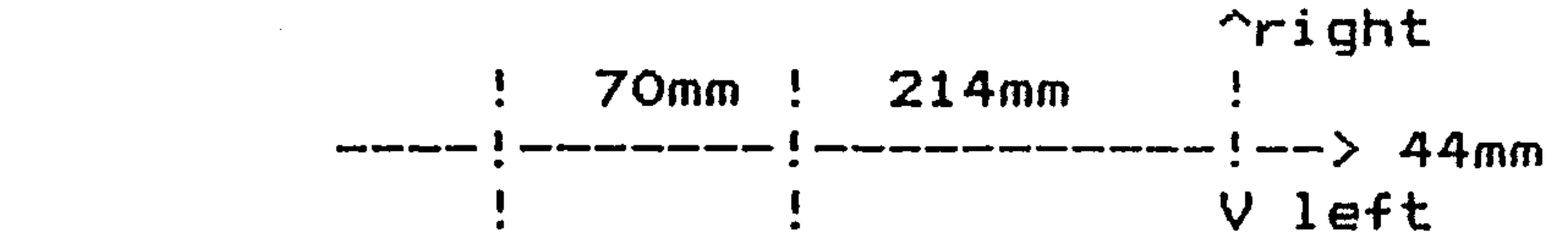

b) Marker 1 and 4 are measured using long-bar with right tip point to the centre of the marker.

2. Results

Name: Affected side: L/R

Date: / /198 Quad. Socket: Y/N

Read (mm)	X	Y	Z
Ankle			0.0
Toetip		*******	
Knee R.			
Knee L.			
S.R.U.			
S.R.L.			
S.L.U.			
S.L.L.			
M1			
M2			
M3			
M4			
M5			
S.R.C			

Fig. 4.6 Form for alignment measurement of the prosthesis.

carefully aligned so that the clamped tube axis coincided with the *Y*-axis of the jig system. The prosthesis with its foot on was mounted on the jig by clamping the shank tube. Another modification was to mount the prosthesis on the jig with its foot directed downward, so the knee joint was stabilized by the weight of the prosthesis itself. Fig. 4.5 also shows a prosthesis on the jig ready for measurement.

§4.1.4.2 Measuring procedures Two different procedures were adapted to measure the alignment of the prostheses with quadrilateral or other types of sockets.

The four reference points inside the quadrilateral socket have been marked with the aid of the SAL, the prosthesis was mounted on the measuring jig with the knee axle parallel to the baseplate. All the marked points on the socket and the foot, two extremes of the knee axle, as well as the body markers on the prosthesis were measured with respect to the jig frame of reference. A form was designed to record the data as shown in Fig. 4.6.

For the prostheses not fitted with the quadrilateral socket, the socket frame of reference had to be established first. The prosthesis was mounted on the jig with the knee axle parallel to the baseplate and the upper and lower 25mm planes were then determined. For the metal socket, the lower plane was set approximately at the level of the distal end of the stump. At the plane of each level, two points were marked, one on each of the medial and lateral wall, as such that the line connecting them was parallel to the baseplate and equidistant to the anterior and posterior wall of the socket. The measurement was then taken in the same way as that with the quadrilateral socket.

§4.1.4.3 Alignment measurement during gait tests The measurement procedures described above is designed to obtain normal alignment parameters and approximately half an hour is required to complete the measurement. This method is obviously unsuitable for the biomechanical gait test in the project since during a patient's single visit, a number of variations from normal alignment are made and the

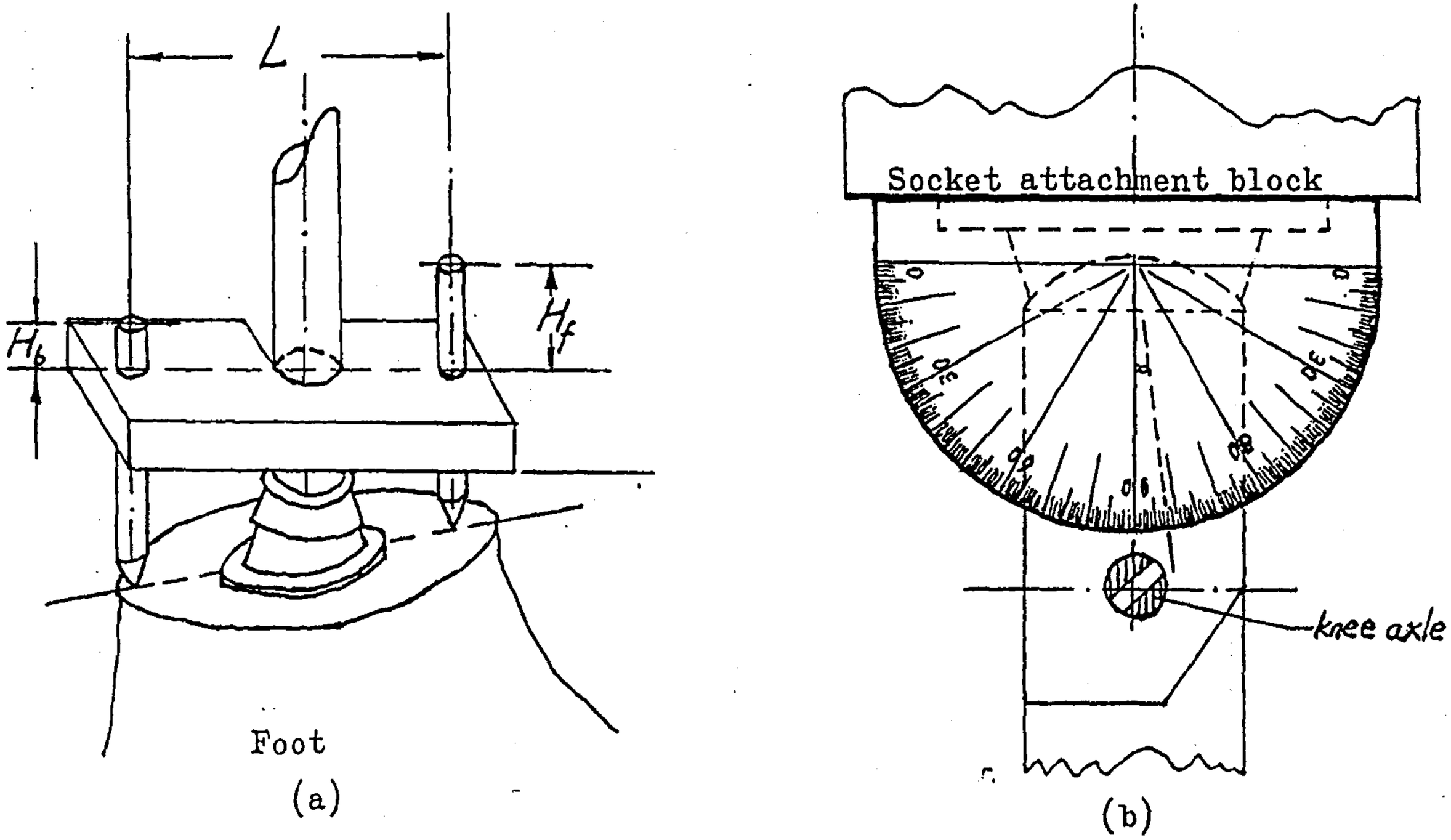

Fig. 4.7 Techniques for measuring the alignment changes during gait test: (a) foot dorsi/plantar flexion angle; (b) socket extension/flexion angle change.

time is not permitted to be spent on time-consuming alignment measurement. Different methods were therefore adopted to measure the variations of particular alignment parameters.

Foot dorsi/plantar flexion angle

The method to measure the foot dorsi/plantar flexion angles is shown in Fig. 4.7(a). A accurately machined perspex plate was fixed on the shank tube with the plate being perpendicular to the shank axis. Two iron bars with equal length passed through the holes on the plate and touched the upper surface of the foot adaptor. By measuring the heights of the two bars above the perspex plate, the foot dorsi/plantar flexion angle could be calculated as

$$\Phi = arc\ tg\ (\frac{H_f - H_b}{L}) \qquad (4.3)$$

where $L=60mm$ was the distance between the two holes.

Changes in the socket extension/flexion angle

The socket extension/flexion angle changes can be represented by the angles between the surface of the socket attachment block and the line marked on the prosthetic knee unit. A protractor goniometer was used to measure the angles, as shown in Fig.4.7(b). The angle at normal alignment was regarded as a reference and other measurements were made relative to this angle. The rotation centre of the socket was also measured at normal alignment measurement session so as to calculate the absolute extension/flexion angles of the socket.

§4.1.5 Alignment parameters

Alignment of a AK prosthesis is specified by a set of parameters (see Fig. 3.18) and their calculations are described as follows.

First, all data obtained through alignment measurement were changed to be with respect to the AJC by subtracting the coordinates of the AJC and then the alignment parameters were determined.

(A) The foot

If the coordinates of the point marked on the toetip (TT) were (TT_x, TT_y, TT_z), the toe-out angle of the foot can be found as

$$TOUT = arc\ tg\ (\frac{TT_Z}{TT_X}) \cdot ILEG \tag{4.4}$$

where

$$ILEG = \begin{cases} 1 & Right\ amputee \\ -1 & Left\ amputee \end{cases} \tag{4.5}$$

(B) The knee joint

The knee joint centre is first determined:

$$[KJC_X, KJC_Y, KJC_Z] = [\frac{RK_X+LK_X}{2}, \frac{RK_Y+LK_Y}{2}, \frac{RK_Z+LK_Z}{2}] \tag{4.6}$$

where RK and LK are right and left ends of the knee axle respectively. Then the alignment parameters for the knee joint can be found

$$\begin{cases} Knee\ medial\ tilt = 57.3^\circ arc\ tg\ (\frac{RK_Y - LK_Y}{RK_Z - LK_Z}) \cdot ILEG \\ Knee\ set\ back = KJC_X \\ Knee\ height = KJC_Y \\ Knee\ set\ out = KJC_Z \cdot ILEG \end{cases} \tag{4.7}$$

(C) The socket

The four points marked on the inner wall of the socket were identified as right upper (RU), right lower (RL), left upper (LU) and left lower (LL) markers. If the coordinates of a point, say the RU, are

$$[RU] = [RU_X, RU_Y, RU_Z] \tag{4.8}$$

the long axis of the socket could be determined by two points:

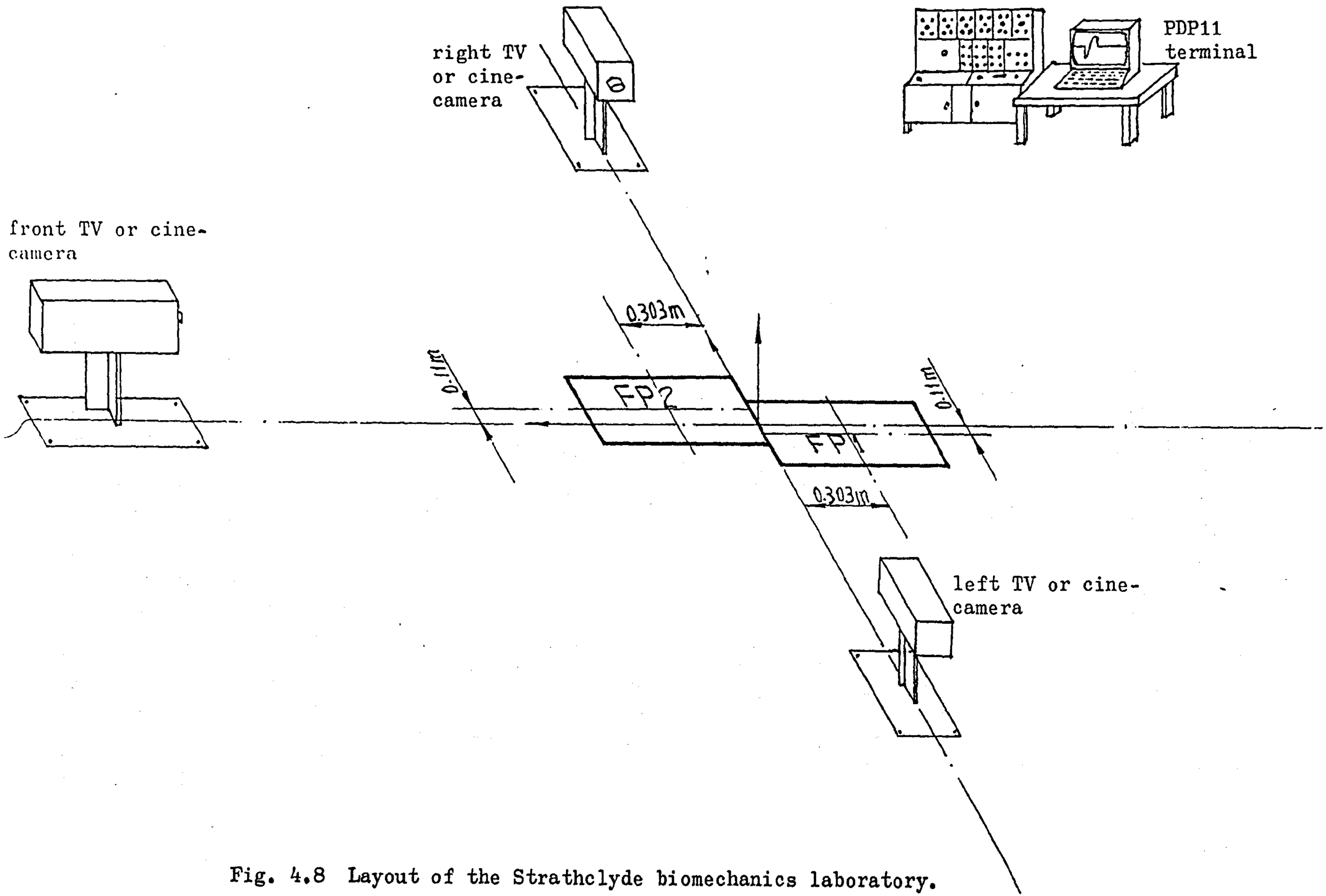

Fig. 4.8 Layout of the Strathclyde biomechanics laboratory.

$$\begin{cases} [SU] = [SU_X, SU_Y, SU_Z] = \dfrac{[RU]+[LU]}{2} \\ [SL] = [SL_X, SL_Y, SL_Z] = \dfrac{[RL]+[LL]}{2} \end{cases} \tag{4.9}$$

According to the definitions of the alignment parameters, we have

$$\begin{cases} \text{Socket int. Rotation} = 57.3^\circ arctg(\dfrac{RU_X\text{-}LU_X}{RU_Z\text{-}LU_Z})\ ILEG \\ \text{Socket adduction} = 57.3^\circ arctg(\dfrac{SU_Z\text{-}SL_Z}{SU_Y\text{-}SL_Y})\ ILEG \\ \text{Socket Flexion} = 57.3^\circ arctg(\dfrac{SL_X\text{-}SU_X}{SU_Y\text{-}SL_Y})\ ILEG \\ \text{Socket forward set} = SU_X \\ \text{Socket Height} = SU_Y \\ \text{Socket set out} = SU_Z \end{cases} \tag{4.10}$$

§ 4.2 The Strathclyde Biomechanics Laboratory

Over the years of investment and development, the Strathclyde biomechanics laboratory has been equipped with two forceplates, two different motion recording systems and a mini-computer with a large amount of application software.

§ 4.2.1 The Forceplate system

The forceplates in the laboratory were produced by Kistler and their brief description is given in §2.5.1.

The two forceplates are mounted in the concrete pit and formed part of the walkpath which is approximately 20m long, as shown in Fig. 4.8. Forceplate No.1 (FP1) is positioned in a reverse order to that of the forceplate No.2 (FP2) due to the wiring difficulties, and the resulting reversions are corrected by the calibration factors.

Interfaces has been produced to store the data in the computer's memory. Connected to the output of the summing amplifiers are the buffer amplifiers which incorporate with variable attenuator to adjust the analog signals within the limiting range of the A/D converters. The digital signals are then written on the disk under the control of program.

The forceplate system can be used alone to acquire ground reactions only or combined with one of the two motion recording systems to form a complete system for acquiring both kinetic and kinematic data.

§ 4.2.2 The cine-matographic system

The cine-matographic system consists of 3 cine-cameras, a digitizer table and a set of overhead floodlights over the forceplates.

The three cameras are trade-named Paillard Bolex H16. Each camera is driven by a synchronous motor and the frame frequency is 50Hz (i.e. 20ms per frame). The shutter speed is set at 1/125th of a second, i.e., the shutter remains open for 8ms of the 20ms duration.

The cameras are aligned and bolted to the ground such that the optical axes of the three cameras intersect just above the origin of the ground frame of reference, as shown in Fig. 4.8. Two sets of lens are fitted on the cameras, that is, 10mm for the left and right cameras and 15mm for the front, resulting a view field of 3×2×2m.

A single filament flash bulb fires when operating the system, sending a pulse to be registered in the computer along with the forceplate data and producing a flash bulb image on the film of each camera. Since sampling frequency of the forceplates and the cine cameras are chosen to be the same, the data from these two systems can be synchronized.

After gait test, the film is re-exposed to superimpose a grid board of 5 inch squares as the reference, so that the error due to lens distortion is minimized.

Having been developed, the film is projected onto a digitizing table (trade name CALCOMP) interfaced with the PDP11/34 computer. The centre of the body markers on the subject and the intersection of the grid are determined by vision and

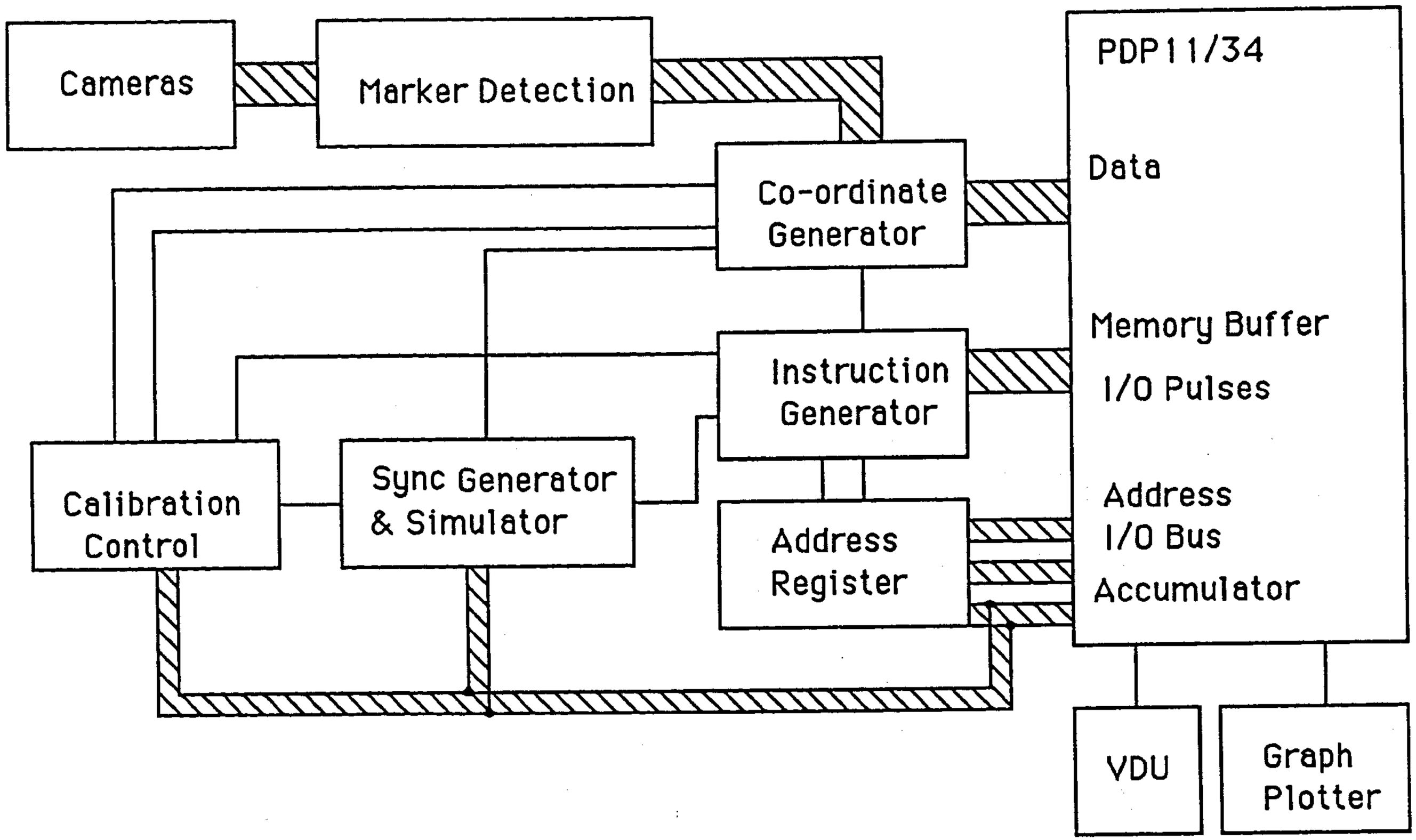

Fig. 4.9 Block diagram of the TV-computer system.

digitized and restored in the computer memory, coming to the end of the stage of acquiring raw data.

§4.2.3 Television-computer system

The Television-computer system installed basically consists of three TV cameras and their video computer interface.

The TV cameras are positioned in the positions of the cine cameras and each of them has a vidicon faceplate with a rotary shutter and a optical filter before it. Arrays of infra-red light emitting diodes positioned around the cameras' lenses are used as light source and pulsed on in synchronism with the opening of the shutters. In operation, infra-red light emitted from the rings of the LEDs strikes the retro-reflective markers and returns to the faceplate, exciting individual units on the faceplate. The camera is operated at 50 Hz (20ms per cycle) with 2ms for recording the information on the units and 18ms for scanning the fields and reset the scanning pointer.

Since the opening of the shutter of the two side cameras are arranged to be out of phase with each other, both sides of the subject can be viewed simultaneously without blinding each other.

The video-computer interface contains the marker detector, co-ordinate generator, instruction generator, address register, and sync generator and simulator. The interaction of these components is shown in Fig. 4.9.

A marker in the video signal is amplitude detected by the marker detector which instruct the co-ordinate generator to generate locations of excited units of the faceplate. An encoded 16 digital words representing the camera number, the co-ordinates of the excited units are transferred, during the line blanking period, to the location in the computer memory defined by the address generator. The sync generator provides the necessary pulses to increment and reset the counters and some other synchronous control operations. Hardware operations are controlled by software interactions which are translated by the instruction generator.

With the system outline above, the co-ordinate information of a marker is acquired in the form of encoded data. Software has been developed to process the data which included averaging, sorting and phase correcting. The averaging program read in the encoded data, sorts out the camera numbers, matches vertical and horizontal values, sets a window around the marker and the mathematically averages all points within the window, thus producing the coordinates of the marker in TV units. Following averaging, the sorting algorithm starts with manually labelling the markers of interest, and then automatically tracks the markers frame by frame and stores the frame numbers, coordinates of the markers and marker numbers. When a marker is missing from the data, the software will provide a linear extrapolated estimation. Some human interventions are required at this stage when a few points 'competing' for a predicted position of a marker or a marker is lost for over 5 frames or so. The final stage of processing the raw data is to correct any phase delay, and a linear intrapolation algorithm is employed. The data are, up to now, ready to be transformed into 3-D coordinates relative to the laboratory frame of reference through an appropriate calibration procedure which is the topic of the next section (§4.3).

§4.3 On the Accuracy of Kinematic Data

Three concepts (accuracy, precision and exactitude) should be carefully distinguished. Let X_t be the true value of a physical quantity which, in practice, cannot be attained and can only be estimated as X_e base upon a particular measuring system. The accuracy of the estimation of the quantity could be expressed as the difference between X_t and X_e, that is,

$$\begin{aligned}\varepsilon = X_e - X_t &= [X_e - E(X_e)] - [E(X_e) - X_t)] \\ &= E_r - E_b \end{aligned} \qquad (4.11)$$

where $E(X_e)$ is the expectation of X_e , The arithmetic mean of the X_e for instance; E_r the random error of the measuring system; E_b the bias of the measuring system. As a rule, the distribution of the random error is normal, that is,

$$E_r = N(0,s).$$

The precision of X_e is indicated by the closeness of X_e to $E(X$ characterized by the standard deviation s. The exactitude of X_e is identified as the bias Eb and represents the closeness of $E(X$ estimation X_e indicates the closeness of X_e to X_t and may be defined as RMS error:

$$RMS = \sqrt{E(\varepsilon^2)} = \sqrt{E\left[(E_r+E_b)^2\right]} = \sqrt{s^2+E_b^2} \tag{4.13}$$

It is difficult to get the accuracy of the system used because there are a lot of variables involved. For the TV-computer system used in the Bioengineering Unit, a number of conditions exists which are capable of limiting the overall accuracy of the system. The most important of these are basic resolution, streaking error, phase error and mal-alignment of the TV cameras. Here, it should be emphasized that by the "TV-computer system" is meant the whole hardware (*ie*.TV cameras, charge amplifiers, computer interface and so on) and also the software (averaging and sorting programs) used.

The objective of this section is to assess the overall accuracy of the TV-computer system so as to obtain some basic information for the selection of the techniques in kinematic measurements. Originally, there were two sets of lens for each of the TV cameras so as to meet the different requirements on the viewfield for the whole body and lower limbs biomechanical analyses, as shown in Table 4.1. It was recognized that the basic resolution of the front camera for whole body analysis might not be adequate enough, a new set of lens designated as set-3 was installed, in an attempt to achieve as accurate results as possible, in which the front camera was mounted on its side to increase its resolution in the vertical direction. The overall accuracy of the three lens sets were assessed.

Table 4.1 The Field Range of the TV/Computer System

camera	f-value (mm)	basic resolution (mm/TV units) horizontal	vertical	field range (m m) (length height)
Lower-limb biomechanics (camera set-1)				
left	25	2.5	5.0	2.57 x 1.33
right	25	2.5	5.0	2.42 x 1.30
front	50	2.3	5.6	2.00 x 1.26
Whole body biomechanics (camera set-2)				
left	16	3.9	8.1	2.28 x 1.67
right	16	3.9	8.3	2.92 x 1.68
front	25	4.5	11.0	3.32 x 2.04
Whole body biomechanics (camera set-3) (front camera mounted on its side)				
left	16	3.9	8.1	2.28 x 1.67
right	16	3.9	8.3	2.92 x 1.68
front	50	5.6	2.3	1.26 x 1.72

Table 4.2 Frame-to-frame Variability

coor.	camera	mean		standard deviation	
		odd	even	odd	even
horiz.	front	494.4	493.5	0.43	0.34
	left	707.6	706.8	0.23	0.16
	right	738.4	738.3	0.22	0.26
verti.	front	204.8	205.3	0.00	0.00
	left	121.5	121.5	0.00	0.00
	right	124.5	124.8	0.00	0.00

Unit: TV units

A limited assessment of the accuracy of the cinematographic system was also conducted.

§4.3.1 Frame-to-frame variability

Frame-to-frame variability is caused by electronic instability in both the cameras and the computer interface. A further error is introduced by the interlace of the TV line scan, reducing the vertical resolution in a single frame and causing discrepancy in the vertical coordinate of a marker between successive frames. The standard deviation of the TV readings therefore may be indication of the precision of the TV system.

In order to investigate the frame-to-frame variability, a stationary marker in the field of view of the TV cameras was recorded for 10 frames and the means and the standard deviations of the horizontal and vertical TV readings were calculated out for odd and even frames respectively. The results are listed in Table 4.2. This was done only for camera set -2.

It was obvious that the vertical coordinates of the TV readings are of (0-1) characteristic, that is, they have the value of either odd or even frames. It was noted that the difference of the vertical coordinates between the odd and even frames was larger than the standard deviation of the horizontal coordinates. This suggested that the basic resolution of the TV cameras is of the greatest important to accuracy. The results showed that an error of approximately ±0.25 vertical and ±1.0 horizontal TV units existed for any camera combinations. This was corresponding to about ±1.5mm (X) and ±2.5mm (Y) errors for lens set-1 and ±2.5mm (X) and ±3.5mm (Y) for lens set -2.

§ 4.3.2 Resolution of the TV-computer system

Resolution of a measuring system is defined as the minimum scale of measurement the system can provides. For the TV-computer system, it is limited vertically by the number of scanning lines, usually 312, and horizontally by the

Table 4.3 Resolution of the Television/computer System

co.	camera	mean	S.D.	min	max	F1	F2	F3
		205.2	0.24	204.8	205.3			
		205.9	0.16	205.8	206.3	1		
		206.0	0.26	205.8	206.3	-1	1	
	Front	206.3	0.00	206.3	206.3	0	0	1
		206.8	0.00	206.8	206.8	1	-1	1
		207.0	0.26	206.8	207.3	0	1	1
		177.8	0.26	177.5	178.0			
		178.0	0.00	178.0	178.0	0		
		178.3	0.28	178.0	178.5	0	0	
	Left	178.7	0.42	178.5	179.5	0	1	1
		179.0	0.16	178.5	179.0	-1	0	1
		179.1	0.16	179.0	179.5	0	-1	1
		180.0	0.10	180.0	180.2			
		180.2	0.27	179.8	180.5	-1		
		180.5	0.10	180.3	180.7	-1	1	
	Right	181.0	0.10	180.8	181.0	-1	1	1
		181.0	0.00	181.0	181.0	0	1	1
		181.4	0.27	181.0	181.7	0	0	1
		697.4	1.05	695.8	698.9			
		697.2	0.57	696.2	697.9	0.40		
		696.0	1.03	693.8	697.0	9.73	9.08	
	Front	695.3	1.05	692.8	696.4	2.55	25.45	20.88
		694.5	1.03	692.4	695.4	2.40	10.03	49.31
		693.4	1.08	691.2	694.4	5.43	14.68	29.51
	Pooled		0.98			-1	1	1
		707.3	0.44	706.7	707.8			
		706.9	0.71	706.0	708.3	2.29		
		706.2	0.51	705.7	706.8	5.40	23.98	
	Left	705.9	0.42	705.0	706.3	2.35	13.50	49.19
		705.3	0.63	704.3	706.0	5.97	12.58	26.25
		704.7	0.69	704.3	705.3	4.99	24.06	34.02
	Pooled		0.58			-1	1	1
		736.3	0.64	735.0	737.0			
		736.9	0.41	736.0	737.5	5.71		
		737.2	0.44	736.5	738.0	3.20	13.81	
	Right	738.2	0.26	738.0	738.5	5.87	73.93	75.09
		738.3	0.45	737.5	739.0	0.53	29.73	55.35
		739.1	0.43	738.0	739.5	8.52	29.66	88.52
	Pooled		0.45			-1	1	1

NB: Critical value of F-test with confidence degree of 0.05 is 4.41.

resolution in camera lens and detection electronics, typically 1:1000. Furthermore, the resolution of the system also relates to the size of the reflective markers used, as illustrated by Winter (1974), since if a marker covers several lines, the vertical position of its centre can be determined to an accuracy better than one line.

A limited investigation was carried out to assess the resolution of the TV-computer system (lens set-3). A marker of the same size as that used in patient tests was attached to the moving part of a vernier caliper with resolution of 0.02mm. The caliper was mounted on the calibration board positioned at the centre of the viewfield with the camera perpendicular to it. The marker moved 10 mm by an increment of 2.00mm and at each increment, 20 frames of data were recorded. This procedure was carried out for each 3 cameras. Than the caliper was mounted on the board vertically and the same procedure was repeated.

The resolution of the TV-computer system was assessed as follows. For the vertical coordinate Y, considering its (0-1) distribution property, a score F_j was first calculated for every ($j=1$), every second ($j=2$) and third ($j=3$) increment, that is,

$$F_j = \begin{cases} 1 & min\{Y_k\} > max\{Y_{k-j}\} \\ 0 & min\{Y_k\} = max\{Y_{k-j}\} \\ -1 & min(Y_k\} < max\{Y_{k-j}\} \end{cases} \qquad (k=1,2,...,6;\ j=1,2,3) \tag{4.14}$$

where $min\{Y_k\}$ means the minimum value of the 20 Y-coordinates for kth increment. The resolution of the Y-coordinate was then defined as the first increment at which all $F_j>0$.

For the horizontal coordinate X, considering its normal distribution characteristics, a different approach was used. For every, every second and every third increment, an analysis of variance was performed and a score F_j was defined as

$$F_j = \begin{cases} 1 & \text{F-test is significant} \\ -1 & \text{F-test is unsignificant} \end{cases} \tag{4.15}$$

The resolution of the X-coordinates was defined as the minimum increment at which all the F_j were positive.

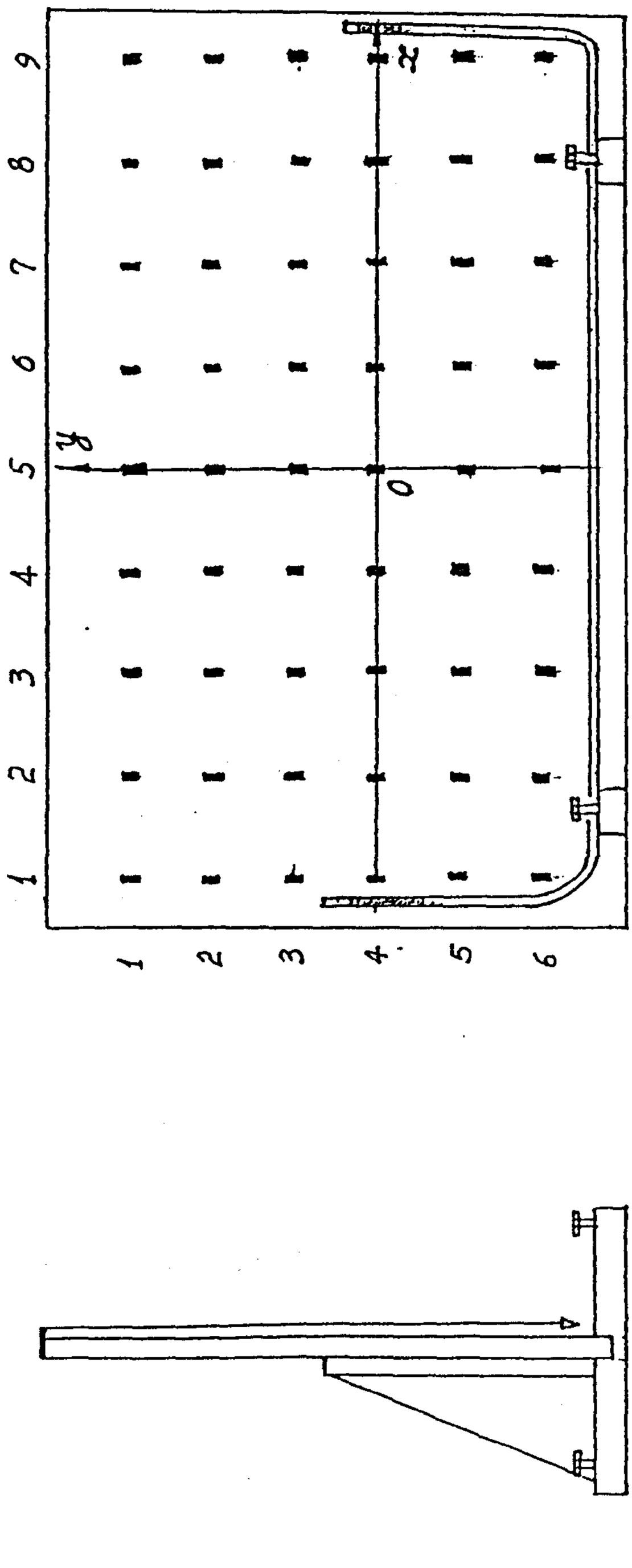

Fig. 4.10 The grid board used for detecting the misalignment of the cameras and calibration.

The results of the resolution of the TV-computer system were shown in Table 4.3. As an estimation, the horizontal resolution is 4mm and the vertical 6mm for lens set-3.

§ 4.3.3 Orientation of the TV cameras

In order to investigate the alignment of the cameras, a planar board with a 6 by 9 marker matrix, which formed a grid of 20cm squares, was constructed as shown in Fig. 4.10. A Cartesian coordinate system was established with its directions of the axes consistent with those of the ground frame of reference and with the origin at the centre of the marker (4,5) which had nearly same the height as the cameras. A water level made of plastic tube and a plumb line were mounted on the board for surveying the orientation of the board. In calibrating the TV system, the board was carefully positioned in the X-Y plane of the ground frame of reference for the side cameras and in the Y-Z plane for the front camera, with its own origin being sited just vertically over the centre of the ground system. This was achieved by adjusting four bolts in the support feet of the board in terms of the water lever and the plumb line. Having warmed up the television system for at least 30 minutes, a short sample of data was recorded and then 50 frames of the data were sorted and was subjected to statistical analysis.

The arithmetic means of the coordinates of the markers were used to calculated the magnification factors which were defined as

$$MAGX(i,j) = \frac{x(i,j)}{[X(i,j)-X(4,5)]} \quad , \qquad MAGY(i,j) = \frac{y(4,5)}{[Y(i,j)-Y(4,5)]} \tag{5.16}$$

where MAG represents the magnification factors, (x,y) the coordinates (in millimeters) of the markers on the grid, (X,Y) the coordinates (in TV units) on the screen and (i,j) the markers at the intersection point of the i-th row and j-th column. Obviously, the magnification factors of the marker (4,5) were undefined. The change patterns of the magnification factors with the position of the markers may reveal some information on the orientations of the TV cameras relative to the ground

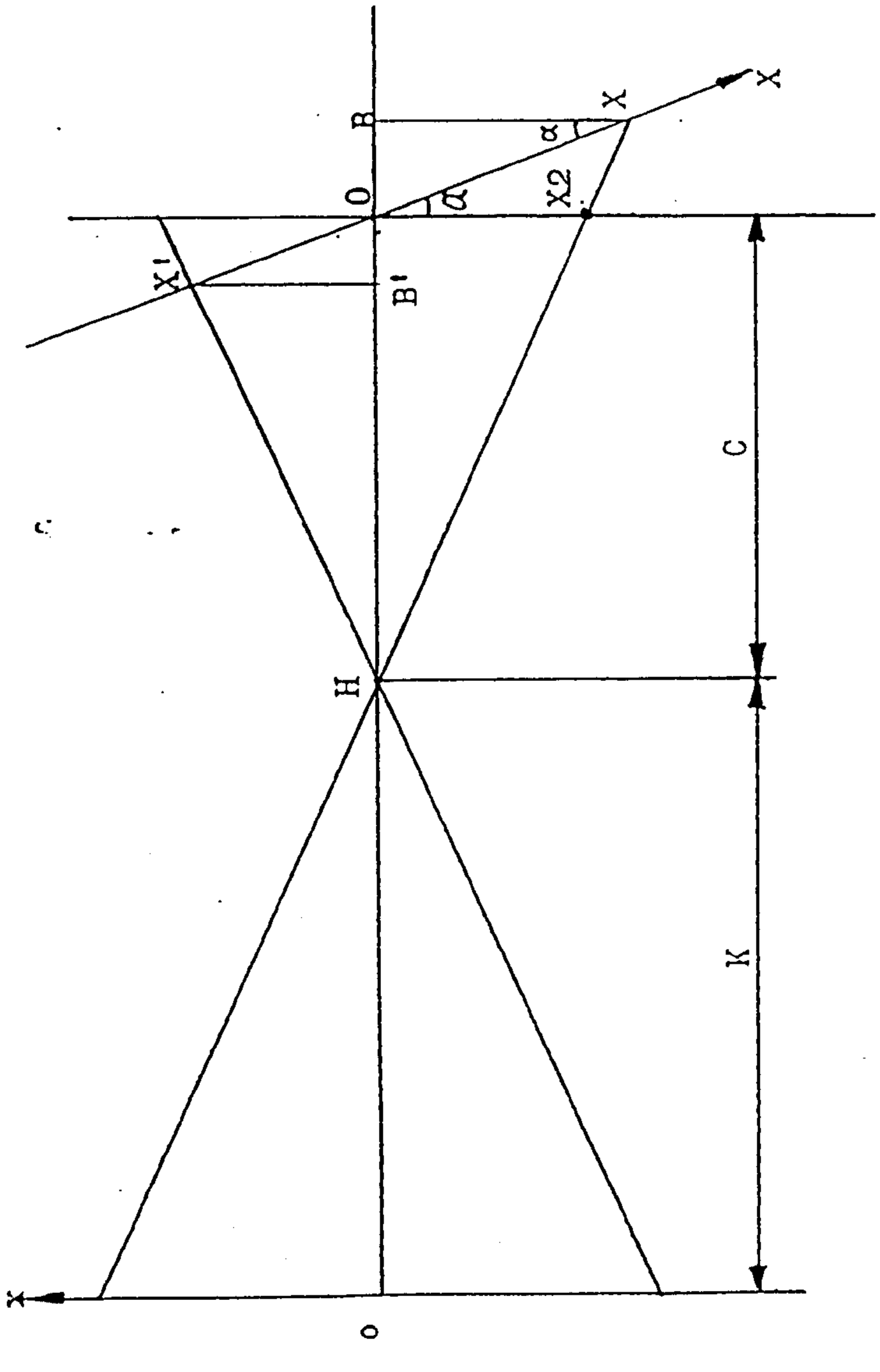

Fig. 4.11 . Misaligment of the television camera. The coordinates system o-x is on the grid board and O-X on the image plane.

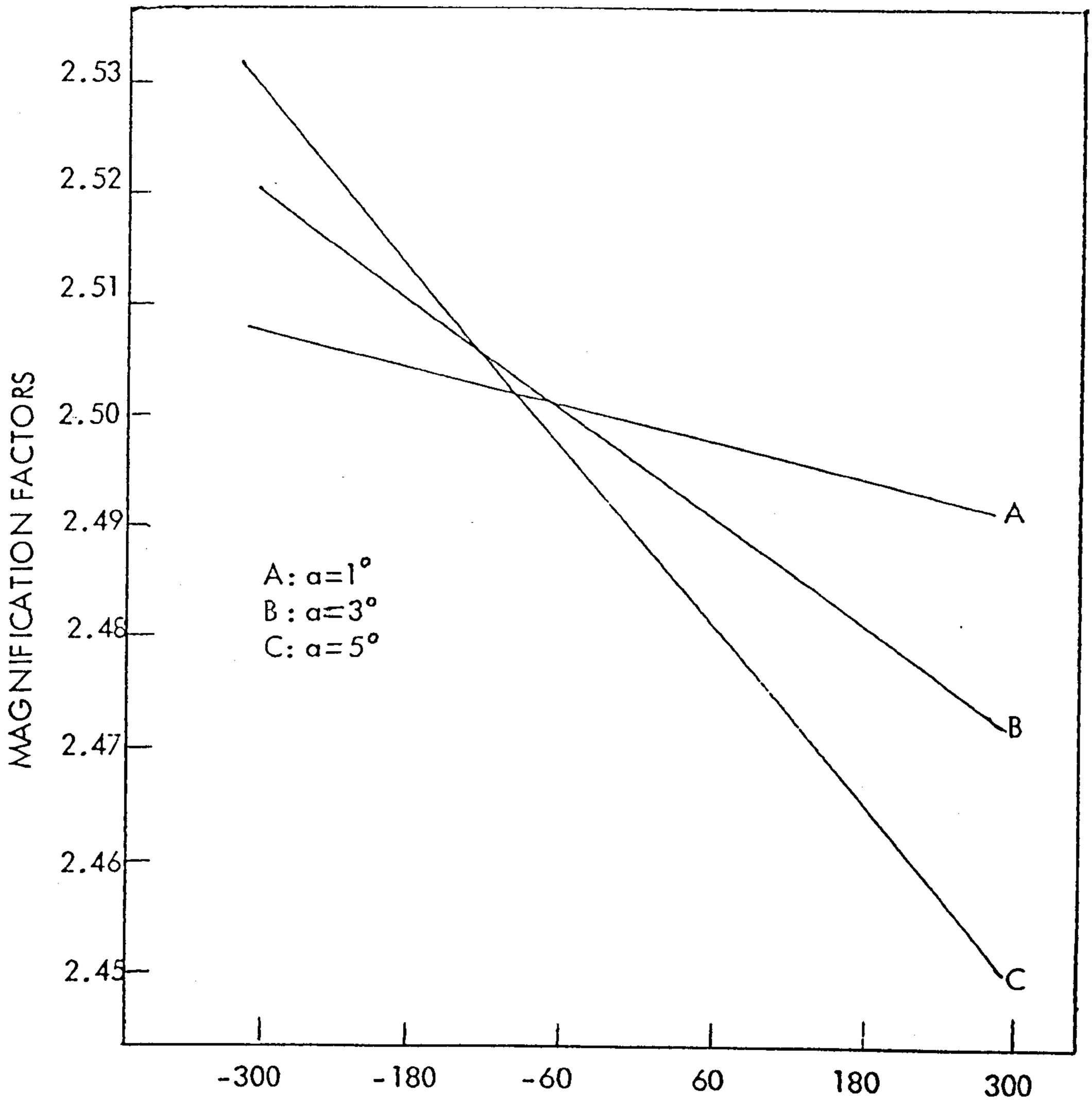

Fig. 4.12 Theoretical relations between the magnification factors and the position of the markers for different mal-alignment angles of the camera.

77d

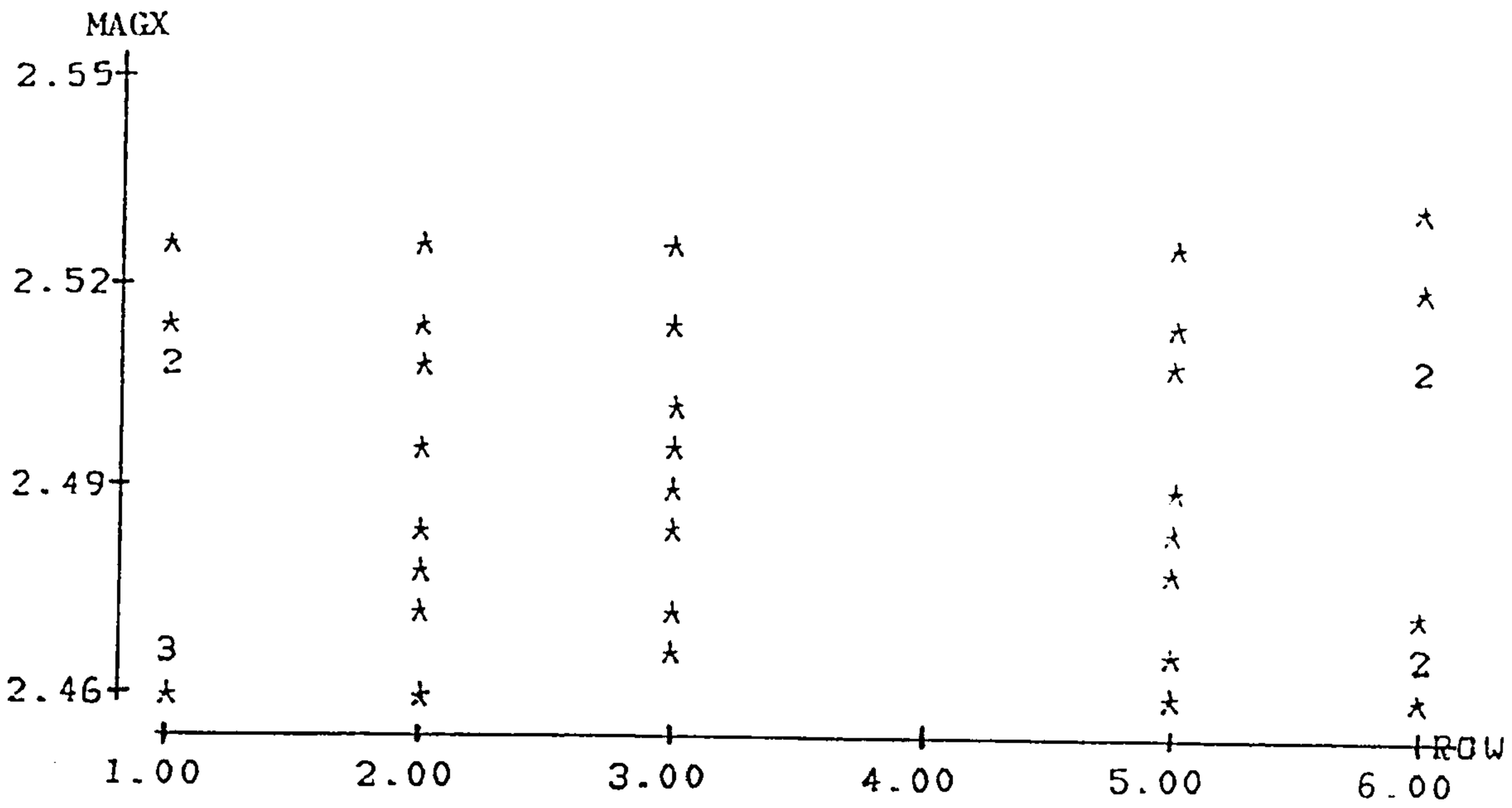

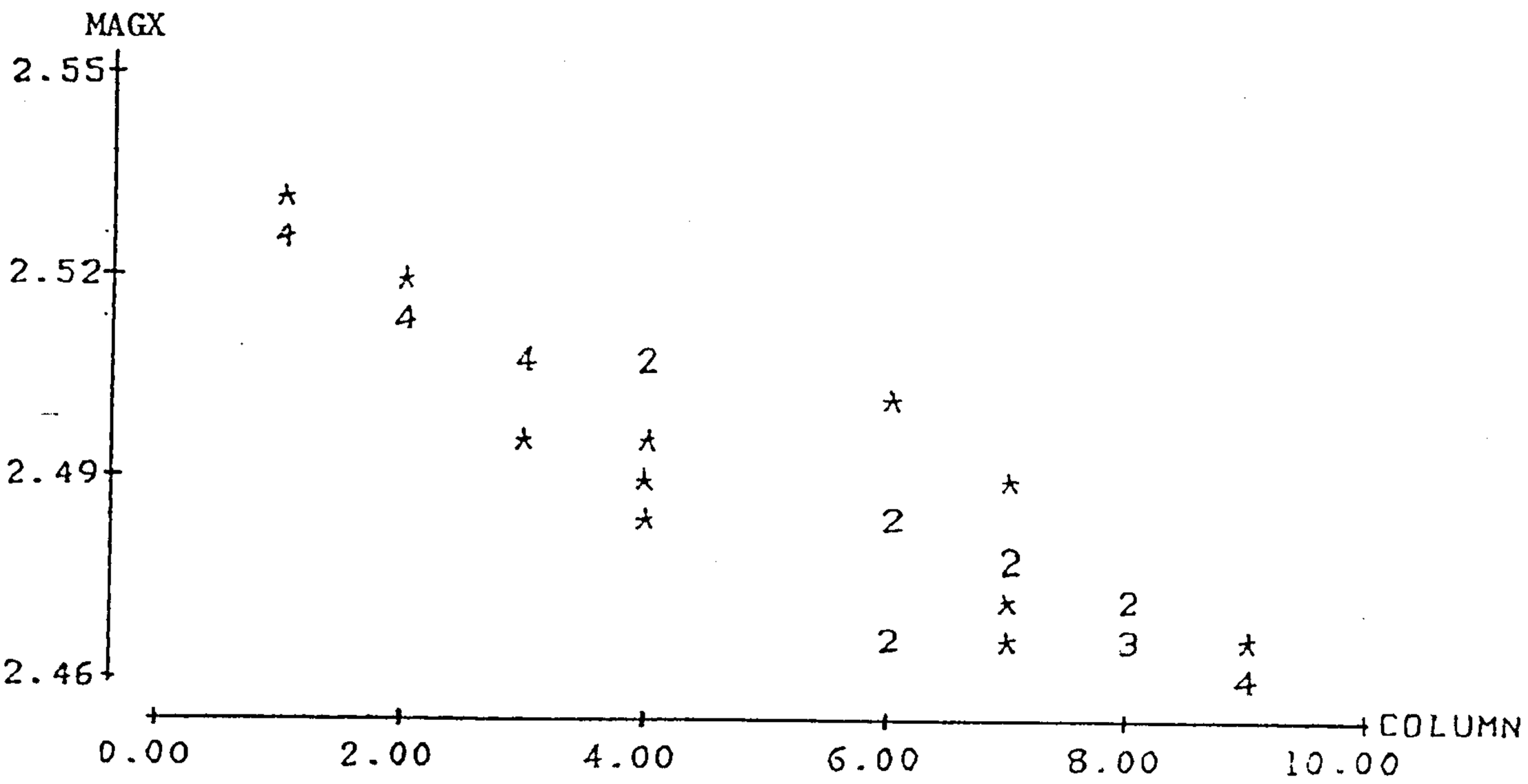

Fig. 4.13(a) Relation between the magnification factors and the positions of the markers (right camera).

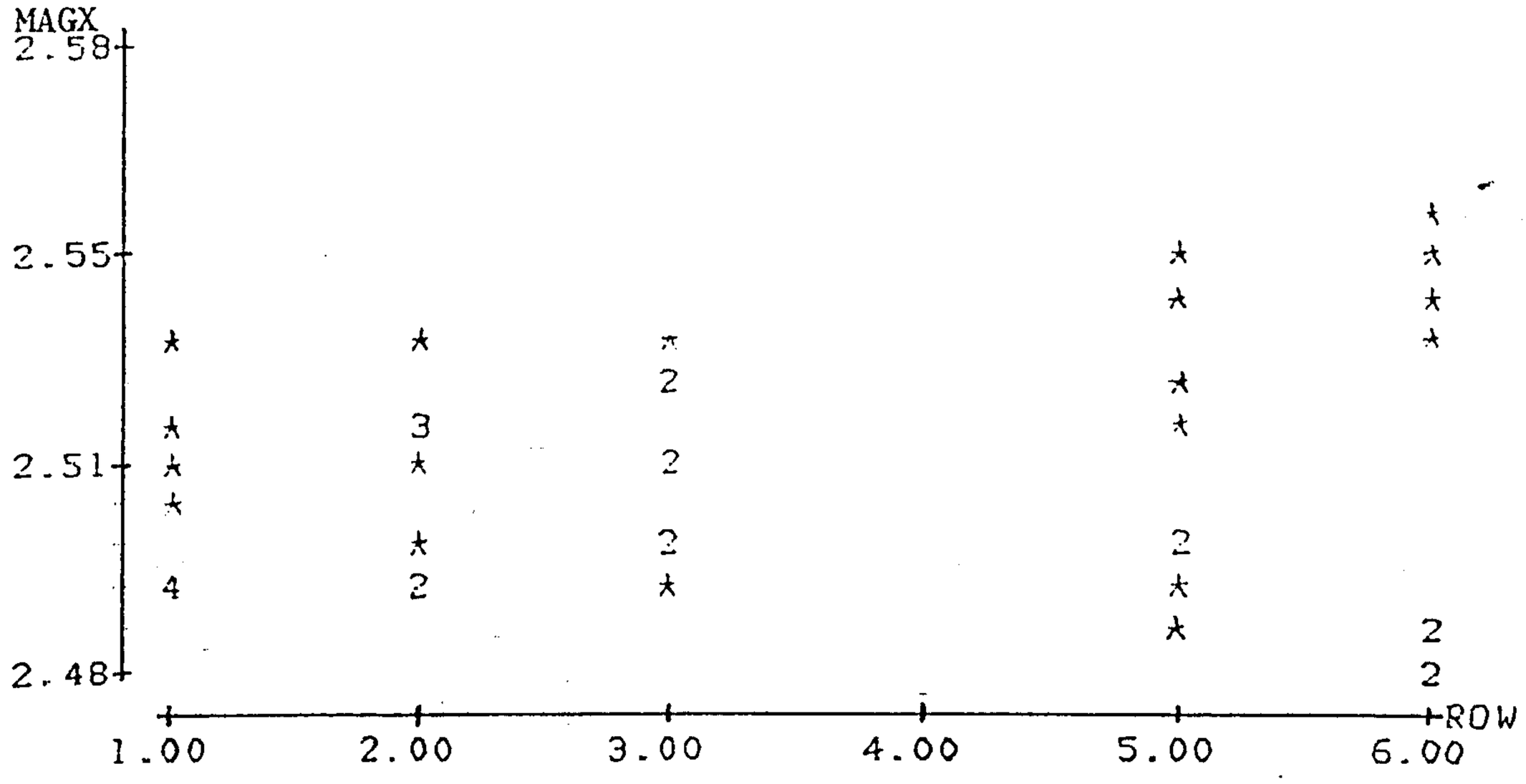

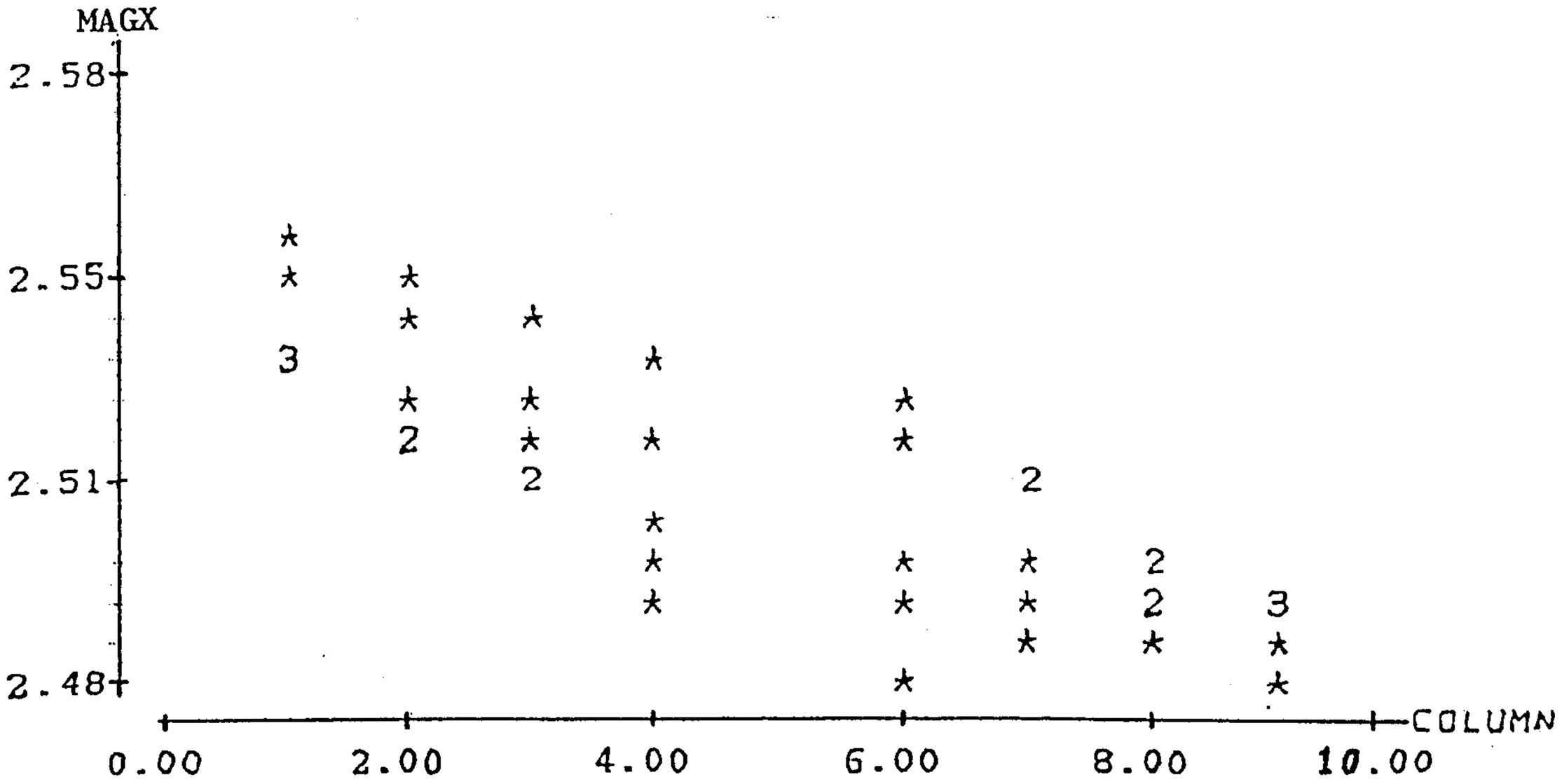

Fig. 4.13(b) Relation between the magnification factors and the positions of the markers (left camera).

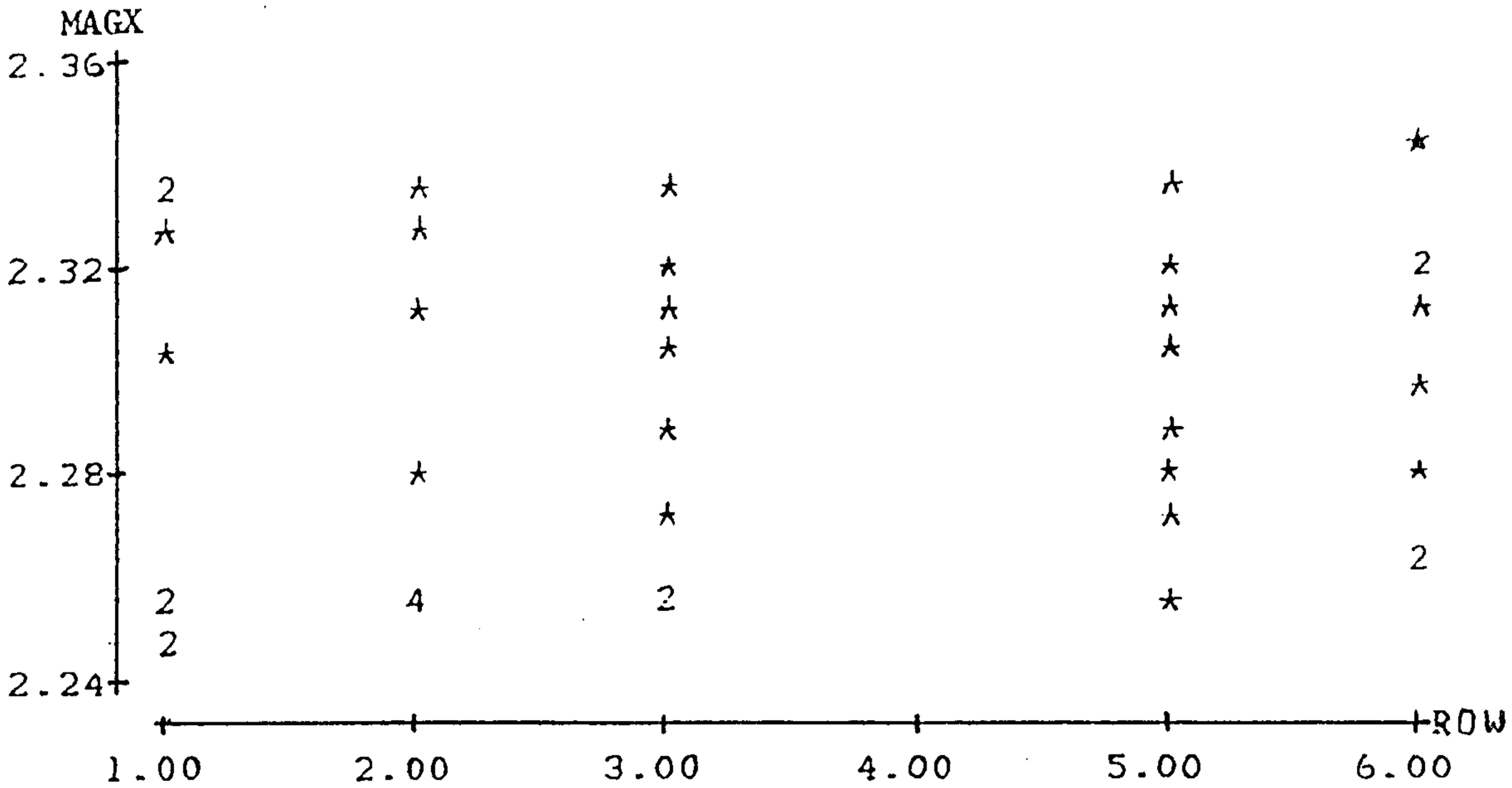

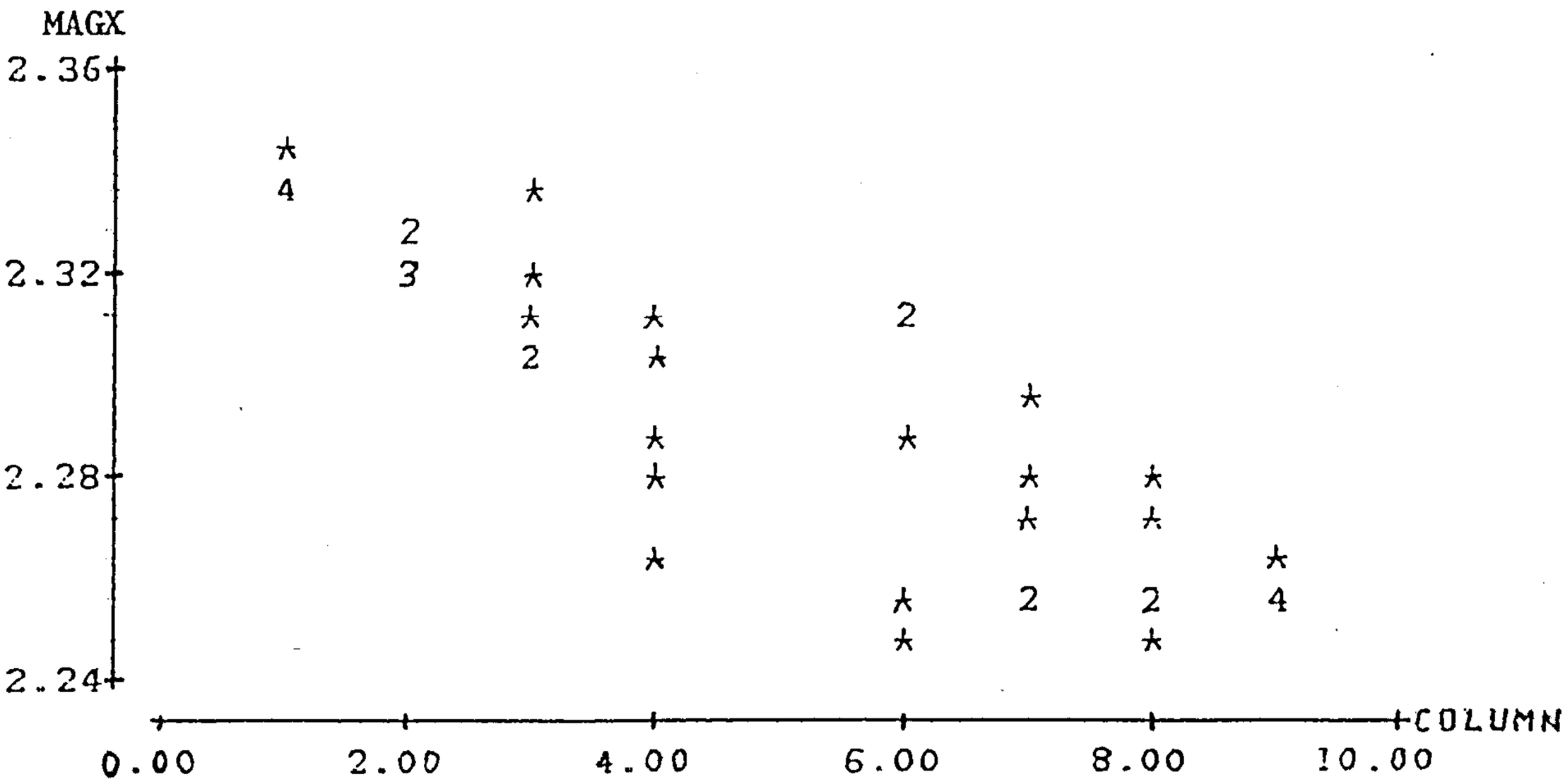

Fig. 4.13(c) Correlation between the magnification factors and the positions of the markers (front camera).

coordinate system, as shown in Fig. 4.11. From Fig. 4.11 we can see that the triangle *H-O-X2* and *H-B-X1* are similar to each other, so that

$$\frac{X}{X2}=\frac{C+X\sin\alpha}{C} \tag{4.17}$$

that is

$$X2=\frac{CX}{C+X\sin\alpha}=\frac{CX\cos\alpha}{C+X\sin\alpha} \tag{4.18}$$

Because

$$x=X2\ \ K/C \tag{4.19}$$

then

$$x=\frac{K\ X\cos\alpha}{C+X\sin\alpha}=\frac{X}{v+uX} \tag{4.20}$$

or

$$MAG=\frac{K\cos\alpha}{C+X\sin\alpha}=\frac{1}{v+uX} \tag{4.21}$$

It was noted that once the cameras were fixed, the v and u were constants.

The theoretical relation between *MAG* and the angle α was plotted in Fig. 4.12 with *K=4000* and *C=1600* which produce similar value of *MAG* to that in practice. The computation showed that mal-alignment of 5° would, as *X=300* which corresponded to about 800mm off the origin of the ground system, result in 0.05 unit error in *MAG* and a 15mm error in the reconstruction of the marker coordinates

The magnification factors obtained from the experiment were plotted against the position of the markers in an attempting to show the correlation between them, see Fig. 4.13a-c. It was found that the *MAGX*s are related almost linearly to the *X* coordinates of the markers, indication that the three cameras were mal-aligned along their vertical axes.

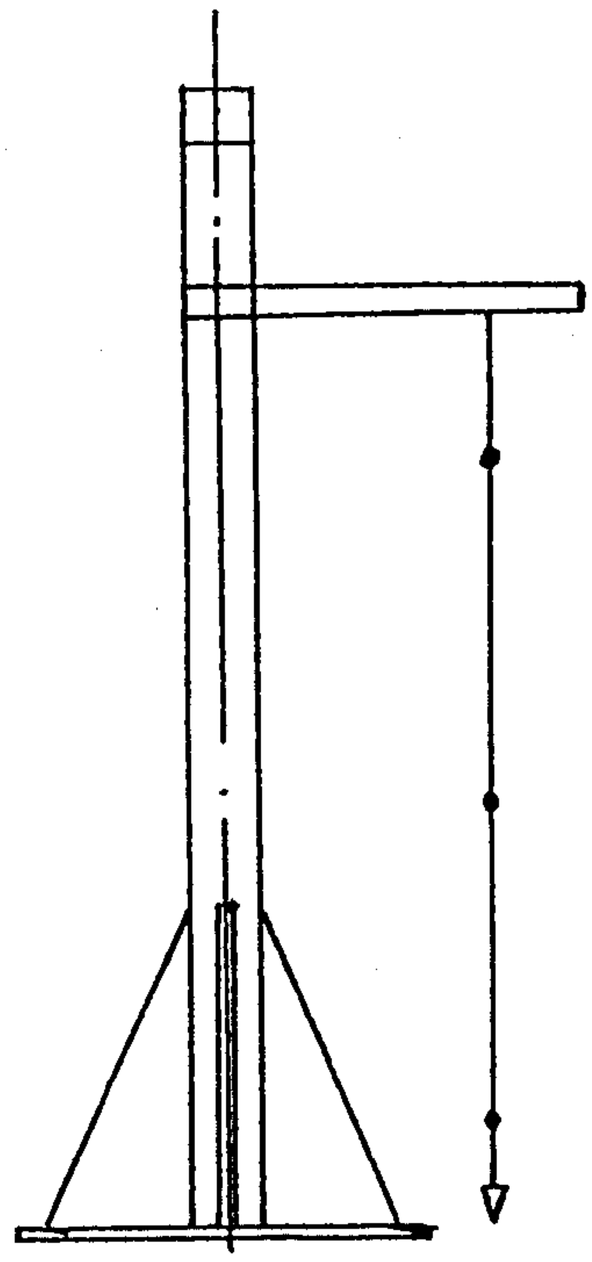

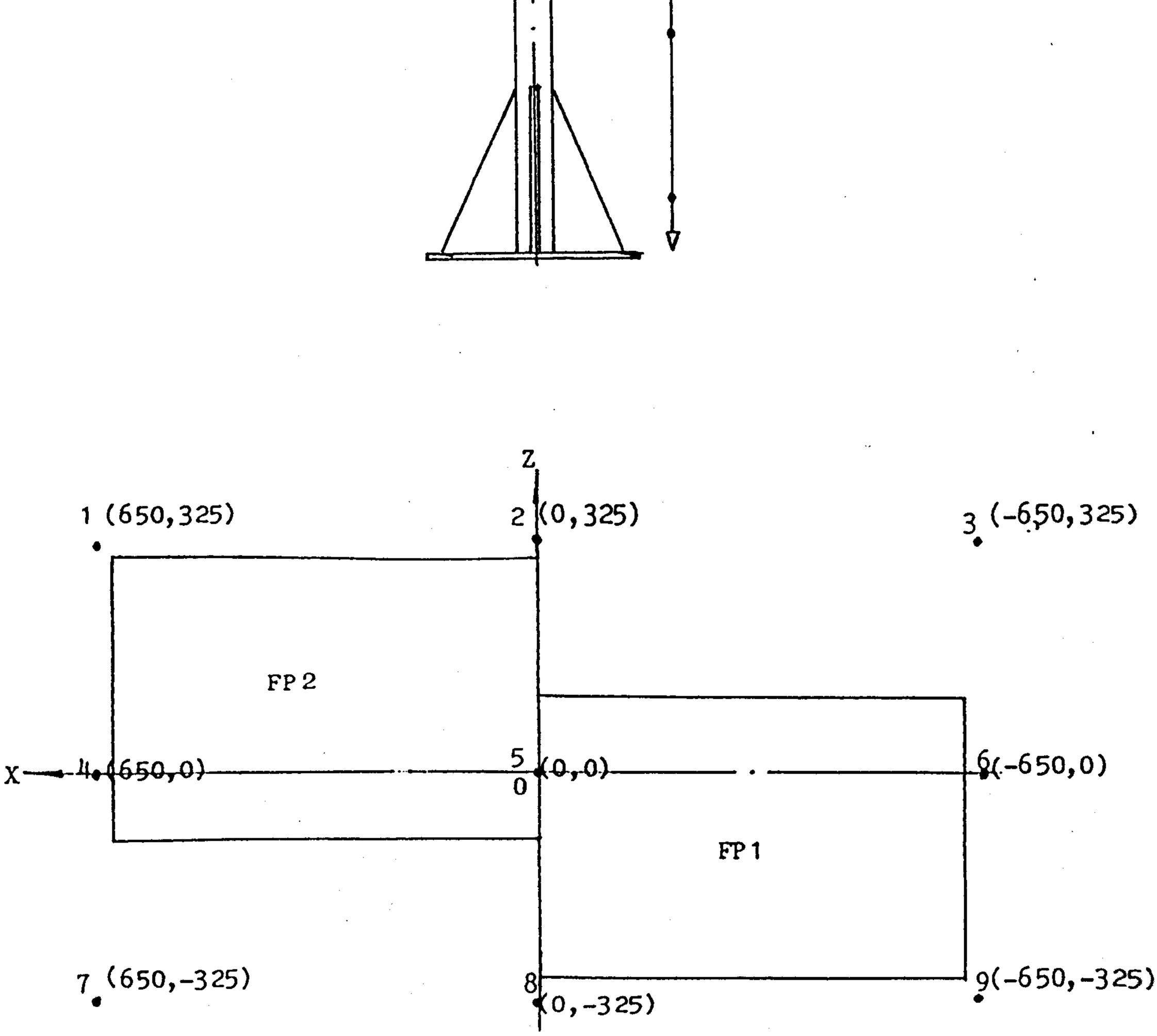

Fig. 4.14 positions of the plumb line round the forceplates.

§4.3.4 Calibration methods

The accuracy with which a physical quantity can be estimated depends not only on the quality of the measuring equipment used but also on the calibration procedure adopted. In calibrating a measuring system, a model is used which relates the physical quantity estimated to the output readings of the system by a number of parameters. The model can be very simple or extremely complicated. Selecting a calibration method is a difficult task and it is always a compromise amongst time, cost and accuracy. For example, when one camera is used and plane motion is analyzed, the vertical and horizontal scales may be sufficient. On the other hand, when more than one camera is used and 3-D motion is analyzed, a complex calibration method has to be adopted to achieve as accurate results as possible.

There are a number of different calibration approaches used in 3-D gait analysis. At one extreme, Woltring (1980) suggested a complex procedure which required considerable mathematical ability for implementation. At another end, Paul (1967) used a simple calibration for vertical and horizontal scale together with the parallax correction. The calibration method with intermediate complexity is typified by the Direct Linear Transformation (DLT) method proposed by Marzan and Karara (1975).

In order to select a suitable calibration procedure for the project described in this thesis, a comparison experiment was conducted using three different calibration methods: a 4-point, a 10-point and the (DLT) methods. The performances of the calibration methods were judged by comparing precisely measured marker positions with those obtained from the TV-computer system. In order to do this, markers fixed on strings at different levels were placed at nine locations in the field surrounding the forceplates, see Fig. 4.14. Thirty samples of data were recorded and the differences in the coordinates were calculated and averaged.

§4.3.4.1 The 4-point calibration method Implied in this method, the alignment of the camera pair must meet certain preconditions, that is, the three cameras must be aligned in the same horizontal plane and the optical axis of each

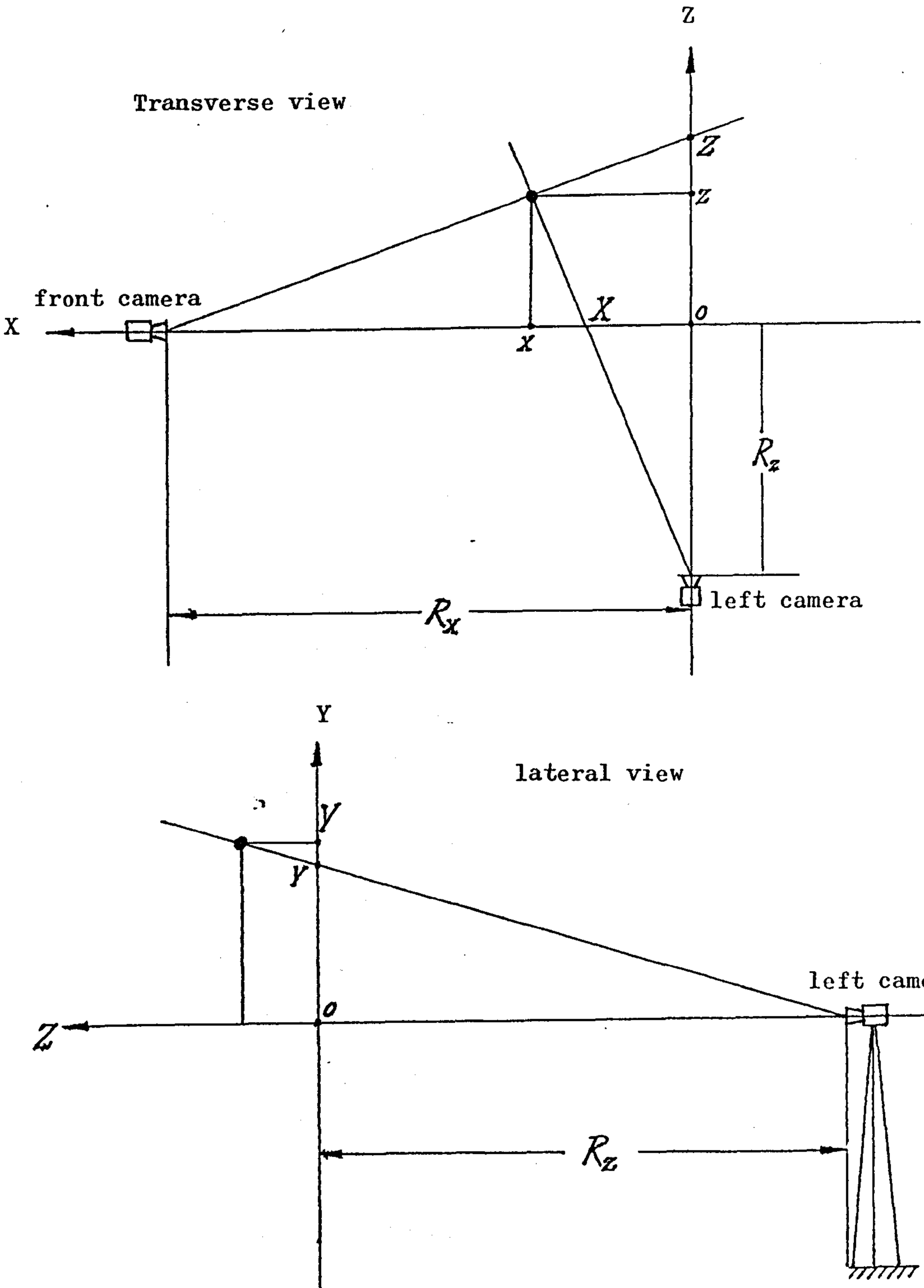

Fig. 4.15 Parallax Correction.

camera is parallel to the relevant axis of the ground frame of reference.

In calibrating the TV-computer system, four control points at the end of a cross, formed by the fourth line and the fifth column markers of the calibration board, were used to scale the object space. For the side cameras, we have

$$DX = \frac{LXs}{HCs(4)\text{-}HCs(3)}, \qquad DY = \frac{LYs}{VCs(4)\text{-}VCs(3)} \tag{4.22}$$

where $LXs=1.600m$, $LYs=1.000m$, HCs and VCs are TV readings of the control markers. This was done for every cameras. Then, referring to Fig. 4.15, The objective coordinates of any point are

$$\begin{cases} x = \dfrac{X(1\text{-}Z/R_z)}{1\text{-}XZ/R_z/R_x} \\ z = Z(1\text{-}x/R_x) \\ y = Y+[z(H\text{-}Y)/R_z] \end{cases} \tag{4.23}$$

where the apparent coordinates of the marker are

$$\begin{cases} X = [HCs\text{-}HCs(4)]\ DXs \\ Y = [VCs\text{-}\dot{V}\dot{C}s(4)\ \text{-}H/DYs]\ DYs \\ Z = [HCf\text{-}HCf(4)]\ DX_f \end{cases} \tag{4.24}$$

§4.3.4.2 The 10-point calibration method Considering that it is difficult to adjust the camera mechanically, this method attempts to partially compensate for the mal-alignment of the camera by modifying the magnification factors. From Equ. 4. it is possible to determine the constants in terms of least-square error. In practice, because the mal-alignment angle was very small, a linear regression was made by approximating the Equ. 4.21 as

$$MAG = c+dX \tag{4.25}$$

In calibrating the system, 10 markers forming the fourth row and fifth column of the calibration grid were used to estimate the constants c and d. Then the

coordinate of any marker can be found as

$$x' = X \quad MAG = cX + dX^2. \tag{4.26}$$

The validity of the regression was determined by the cross-correlation factor r defined as

$$r = \frac{xm}{L_{xx} L_{mm}} \tag{4.27}$$

where

$$\begin{cases} L_{xx} = \sum_i (X_i - X) \\ L_{mm} = \sum_i (MAG_i - MAG) \\ L_{xm} = \sum_i (X_i - X)(MAG_i - MAG) \end{cases} \tag{4.28}$$

When r was less than a certain value determined by the number of the variables X and the confidence level (say, 5 samples of X for each direction and 90% confidence in this work), no compensation was made for that particular camera and direction.

§4.3.4.3 The DLT method The theoretical detail of this method is described in Chapter 5. Basically, this method establishes a relationship between the 3-D coordinates of a marker and a pair of 2-D images of it by a collinear transformation without bothering about the internal parameters of the cameras.

In calibrating the system, markers on the strings at position 1, 3, 5, 7 and 9 were used to determine the DLT parameters, while the rest served for assessing the performance of the DLT method.

Table 4.4(a) Right/Front Camera Accuracy (Camera Set-1)

string no.	height of markers (mm)	residual = |measured-calculated| (mm)					
		4-point grid			10-point grid		
		X	Y	Z	X	Y	Z
1	95	6	12	3	2	11	1
2	96	3	1	7	3	1	5
3	98	11	4	7	6	5	5
4	95	9	5	6	4	5	6
5	96	3	2	7	3	3	7
6	98	11	7	6	6	8	6
7	95	12	7	11	7	6	9
8	96	6	4	11	6	5	9
9	98	11	7	12	6	8	10
1	469	7	12	4	3	12	2
2	465	2	1	4	2	1	3
3	466	11	4	3	6	4	2
4	469	9	8	3	4	8	3
5	465	3	1	4	3	1	4
6	466	10	8	3	6	8	3
7	469	7	10	6	2	10	4
8	465	3	1	7	3	1	5
9	469	9	8	9	4	8	7
1	791	8	15	1	4	13	3
2	790	3	3	0	3	1	1
3	789	12	4	1	8	7	1
4	791	10	11	2	5	8	2
5	790	4	3	1	4	0	1
6	789	13	7	1	8	10	1
7	791	13	11	3	7	9	1
8	790	2	0	3	2	3	1
9	789	13	7	7	8	10	5
co-ordinate average		8.1	6.5	4.9	4.6	6.1	4.0
overall average			6.5			4.9	

Table 4.4(b) *Left*/Front Camera Accuracy (Camera Set-1)

string no.	height of markers (mm)	residual = |measured-calculated| (mm)					
		4-point grid			10-point grid		
		X	Y	Z	X	Y	Z
1	95	10	1	4	4	7	5
2	96	1	4	7	1	1	9
3	98	6	7	7	0	2	8
4	95	11	1	6	5	4	6
5	96	0	4	7	0	1	7
6	98	4	9	6	1	4	6
7	95	11	2	10	7	6	12
8	96	2	3	10	2	1	12
9	98	4	7	12	1	3	13
1	469	10	4	4	5	4	6
2	465	1	4	4	1	3	5
3	466	7	8	4	2	8	5
4	469	9	1	3	4	1	3
5	465	0	4	4	0	3	4
6	466	5	11	3	0	10	3
7	469	11	0	6	7	1	8
8	465	1	4	7	1	3	8
9	469	6	10	8	0	9	10
1	791	11	10	0	6	9	2
2	790	2	19	1	2	0	2
3	789	9	25	1	3	5	3
4	791	10	12	2	4	5	2
5	790	1	18	1	1	0	1
6	789	6	24	1	1	6	1
7	791	11	12	2	7	5	4
8	790	2	17	3	2	1	5
9	789	5	23	6	0	7	8
co-ordinate average		5.8	9.0	4.8	2.5	4.0	6.1
overall average			6.5			5.4	

Table 4.5(a) Right/Front Camera Accuracy (Camera Set-2)

strin no.	height of markers (mm)	residual = |measured-calculated| (mm)								
		DLT method			4-point grid			10-point grid		
		X	Y	Z	X	Y	Z	X	Y	Z
1	95				5	0	1	5	9	2
2	98	2	1	2	2	11	1	2	2	1
3	96				3	17	5	3	7	4
4	95	0	8	1	4	5	1	4	4	1
5	98				2	10	1	2	1	1
6	96	2	3	6	1	16	2	1	7	2
7	95				7	2	2	7	6	3
8	98	0	4	3	1	10	4	1	2	3
9	96				4	14	16	5	10	15
1	790				8	3	5	8	5	5
2	789	4	3	5	1	2	5	1	0	4
3	791				2	6	11	2	3	11
4	790	3	2	1	7	7	8	7	2	7
5	798				1	4	7	1	1	7
6	791	1	2	0	2	9	7	2	6	7
7	790				9	4	6	9	6	6
8	789	1	2	1	1	0	8	1	2	7
9	791				3	8	7	3	6	6
1	1361				11	7	10	11	21	9
2	1361	1	3	5	1	10	13	2	18	13
3	1358				5	15	12	5	13	12
4	1361	2	5	6	10	7	8	10	20	8
5	1361				0	11	14	0	15	14
6	1358	5	5	0	3	17	11	3	9	12
7	1361				11	6	13	11	20	12
8	1361	10	4	2	3	6	15	3	18	14
9	1358				4	14	16	5	10	15
co-ordinate average		2.6	3.5	2.7	4.1	8.2	7.8	4.2	8.2	7.4
verall average		2.9			6.7			6.6		

Table 4.5(b) Left/Front Camera Accuracy (Camera Set-2)

strin no.	height of markers (mm)	residual = |measured-calculated| (mm)								
		DLT method			4-point grid			10-point grid		
		X	Y	Z	X	Y	Z	X	Y	Z
1	95				8	13	1	4	13	2
2	98	4	4	2	8	1	1	8	1	1
3	96				15	4	4	11	4	3
4	95	3	11	1	13	7	1	8	7	1
5	98				12	0	1	12	0	1
6	96	0	6	6	20	8	2	15	8	12
7	95				7	7	2	2	7	2
8	98	1	5	3	6	2	4	6	2	4
9	96				15	7	3	10	7	3
1	790				6	6	5	2	6	4
2	789	2	6	6	14	3	4	14	3	4
3	791				17	5	10	12	5	10
4	790	2	1	1	4	4	2	1	4	2
5	789				6	4	7	6	4	7
6	791	0	3	0	16	5	7	11	5	7
7	790				7	4	7	2	4	6
8	789	5	2	1	13	3	8	13	3	7
9	791				17	8	15	12	9	7
1	1361				13	7	9	8	7	8
2	1361	4	4	5	16	5	12	16	5	12
3	1358				15	0	12	11	0	11
4	1361	6	5	6	13	3	8	8	3	8
5	1361				15	3	14	15	3	14
6	1358	9	3	9	20	3	12	15	3	12
7	1361				16	6	14	11	6	13
8	1361	1	3	2	15	6	16	15	2	15
9	1358				16	8	16	11	7	16
co-ordinate average		3.1	4.4	3.5	12.7	4.7	7.3	9.6	4.7	7.1
overall average		3.7			8.2			7.1		

Table 4.6 Accuracy of the Camera Set-3
(DLT calibration method)

	string no.	height of markers (mm)	residual=|measured-calculated| (mm) X	Y	Z
Right/Front cameras	2	95	7	1	1
	4	96	2	5	1
	6	98	2	5	4
	8	95	1	5	0
	2	789	2	1	2
	4	790	0	3	1
	6	791	5	1	3
	8	789	4	0	2
	2	1361	6	4	0
	4	1361	0	4	2
	6	1358	3	2	1
	8	1361	7	1	1
	co-ordinate average		3.0	2.5	1.5
	overall average		2.3		
Left/Front cameras	2	95	3	2	0
	4	96	1	3	2
	6	98	2	5	5
	8	95	4	5	0
	2	789	1	0	2
	4	790	3	2	1
	6	791	1	1	5
	8	789	8	2	3
	2	1361	1	3	2
	4	1361	2	4	2
	6	1358	3	0	1
	8	1361	6	1	1
	co-ordinate average		2.9	2.3	2.0
	overall average		2.4		

The results of the comparison were listed in Table 4.4 to Table 4.6. For ease comparison, a collective table is presented in Table 4.7.

Comparing the 10-point grid with the 4-point grid method, it was found that there were no significant differences in the Z direction for lens set-1 nor for any other lens sets, although the residual of the X and Y directions reduced significantly in lens set-1 for the 10-point method. The gross basic resolution of lens set-2 may submerge the compensation effect of the 10-point method.

As far as the DLT method is concerned, the results proved it superiority in accuracy over other calibration methods used. An improvement of 50% accuracy was achieved by the DLT method. The calibration plumb strings are also easy to move around, can be accurately positioned and suffer less stress deformation than conventional calibration frame. The calibration procedure takes about 15 minutes to accomplish.

For the lens set-3 of the whole body system, the results showed a significant improvement in Y coordinates over lens set-2. This proved that the basic resolution plays a very important role in the accuracy of the TV-computer system.

The overall accuracy of the TV-computer system was assessed based on the data in Table 4.2 to Table 4.7. Noticing that the results presented above were obtained through averaging and only for static markers, the overall accuracy of the system may be represented by the sum of calibration error and frame-to-frame error, and results are show in Table 4.8.

§4.3.5 Accuracy of the cinematographic system

To define a marker centre on the film by an operator is believed to be a vulnerable source of error. In order to assess how accurately a marker centre could be defined, a marker with moderate contrast to the background on a film was sampled 20 times and a standard deviation of 0.18mm was found. Similarly, a standard deviation of 0.21mm was found for defining the intersection of the grid. Transforming these deviations to the laboratory coordinate system results in 0.86mm and 0.90mm deviations respectively. Since the marker position was measured relative

Table 4.7 Accuracy Comparision of Calibration Methods

calib. method		camera set-1 X (mm)	camera set-1 Y (mm)	camera set-1 Z (mm)	camera set-2 X (mm)	camera set-2 Y (mm)	camera set-2 Z (mm)	camera set-3 X (mm)	camera set-3 Y (mm)	camera set-3 Z (mm)
four-point		7.0	7.8	4.8	8.4	6.4	7.6			
	overall		6.5			7.4				
ten-point		3.6	5.1	5.0	6.9	6.4	7.2			
	overall		5.2			6.8				
DLT method					2.8	4.0	3.1	3.0	2.4	1.8
	overall					3.3			2.4	

Table 4.8 Overall Accuracies of Motion Recording Systems

calib. method		camera set-1 X (mm)	camera set-1 Y (mm)	camera set-1 Z (mm)	camera set-2 X (mm)	camera set-2 Y (mm)	camera set-2 Z (mm)	camera set-3 X (mm)	camera set-3 Y (mm)	camera set-3 Z (mm)
four-point		8.5	10.3	6.7	10.9	10.9	10.1			
	overall		8.4			10.3				
ten-point		5.1	7.6	6.5	9.4	10.9	9.7			
	overall		6.4			9.7				
DLT method					5.3	8.5	5.6	5.5	5.9	4.3
	overall					6.4			5.2	
Cinephotographic system						5.0				

to the intersection of the grid, the overall deviation of marker position is ±1.66mm, that is to say, an overall error of about ±5.0mm.

§4.3.6 Conclusion

Referring to Table 4.7, it may be concluded that:

(1) camera set-3 has better accuracy than camera set-2 in the *Y* coordinate when the DLT method is used;

(2) camera set-3 has similar accuracy to that of the cinematographic system when the DLT method is employed.

After considering the accuracy assessed and the amount of work involved, it has been decided to use the TV-computer system with the DLT calibration method to acquire kinematic data for the gait analysis presented in this thesis.

§4.4 Approaches of Biomechanical Gait Test

§4.4.1 Body marker system

Body markers used in the gait test were made from light weight wooden beads of 13mm diameters covered by small pieces of retro-reflective paper Scotchlite. These beads were affixed to sticks with different lengths which had wooden bases of 38mm diameters. In this way, the markers could be seen by both front and lateral side cameras, and additional to that, the relative distances between the markers were enlarged, leading to the reduction of the measurement error propagation.

Body marker system was designed according to the biomechanical model of the human body used and some practical considerations. For a 3-D gait analysis as presented in this thesis, at least 3 markers were stuck on to a body segment to determine the joint centre and to establish a local frame of reference. Furthermore, the positions on a segment at which the markers were stuck should satisfy following requirements:

(1) minimal movement between markers and underlying bones;

(2) maximal distances between markers;

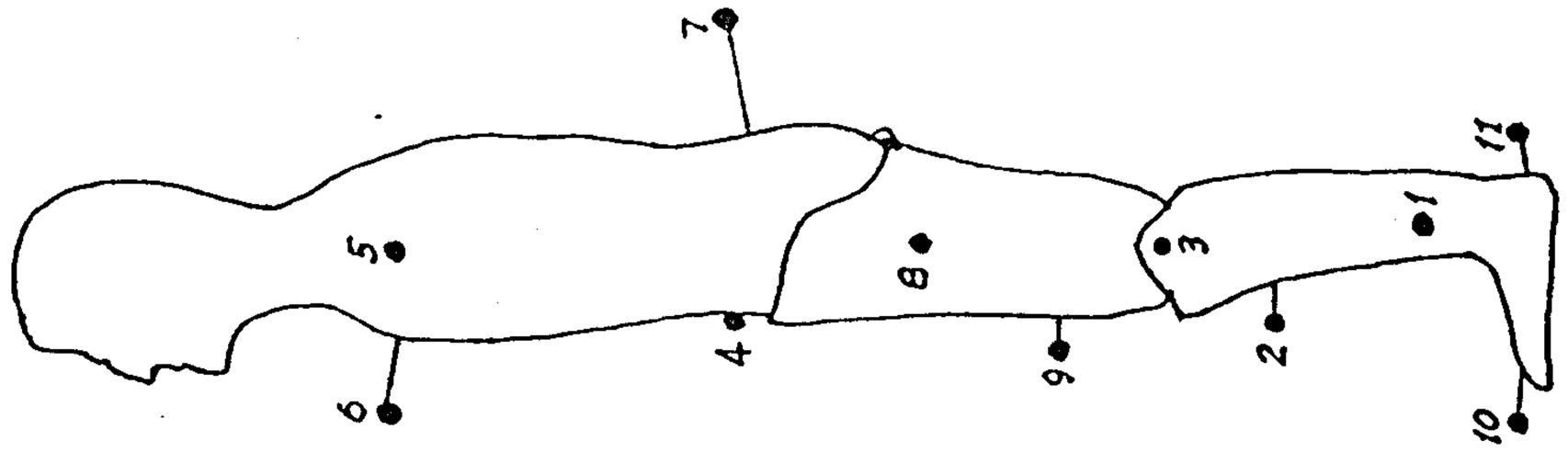

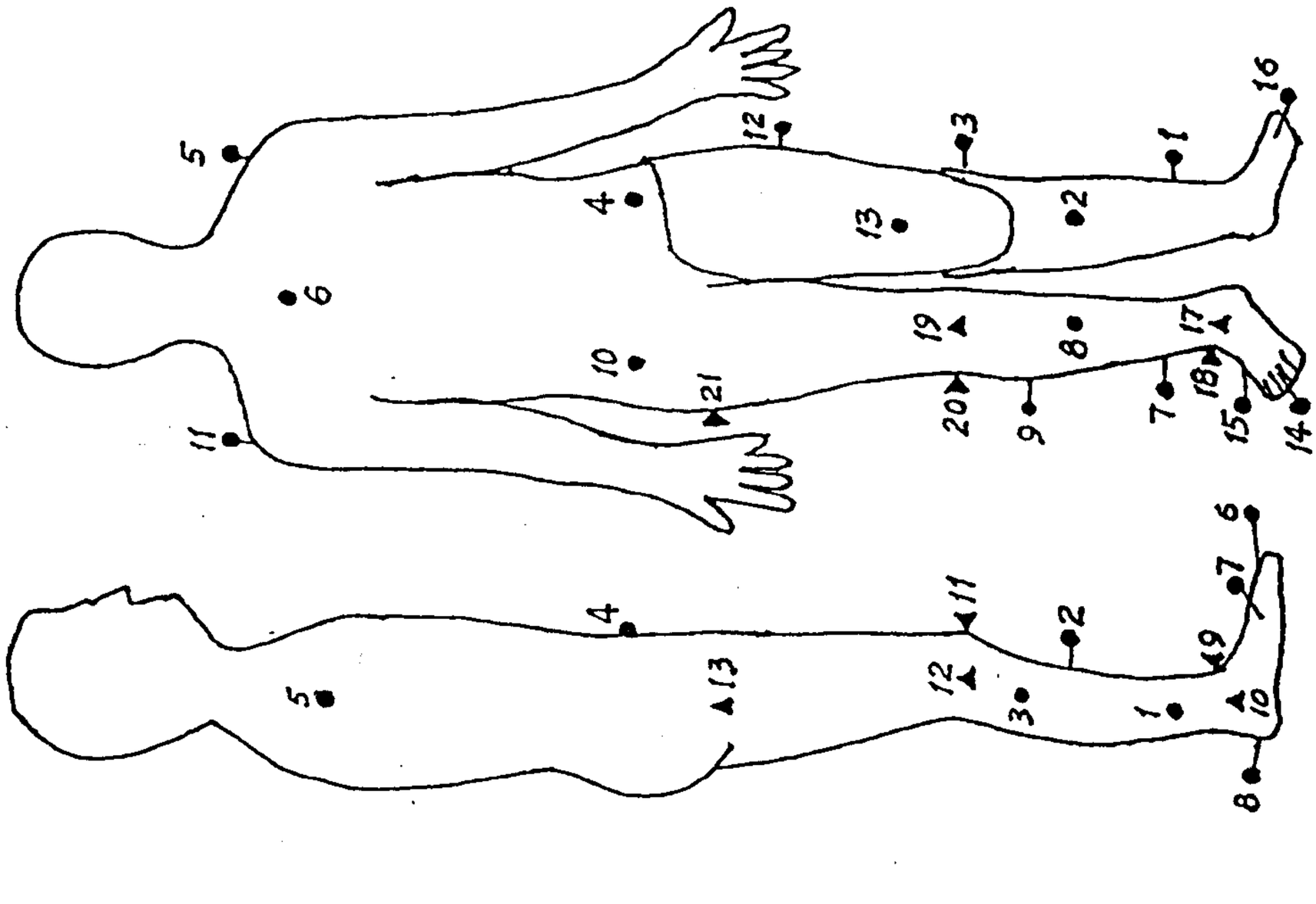

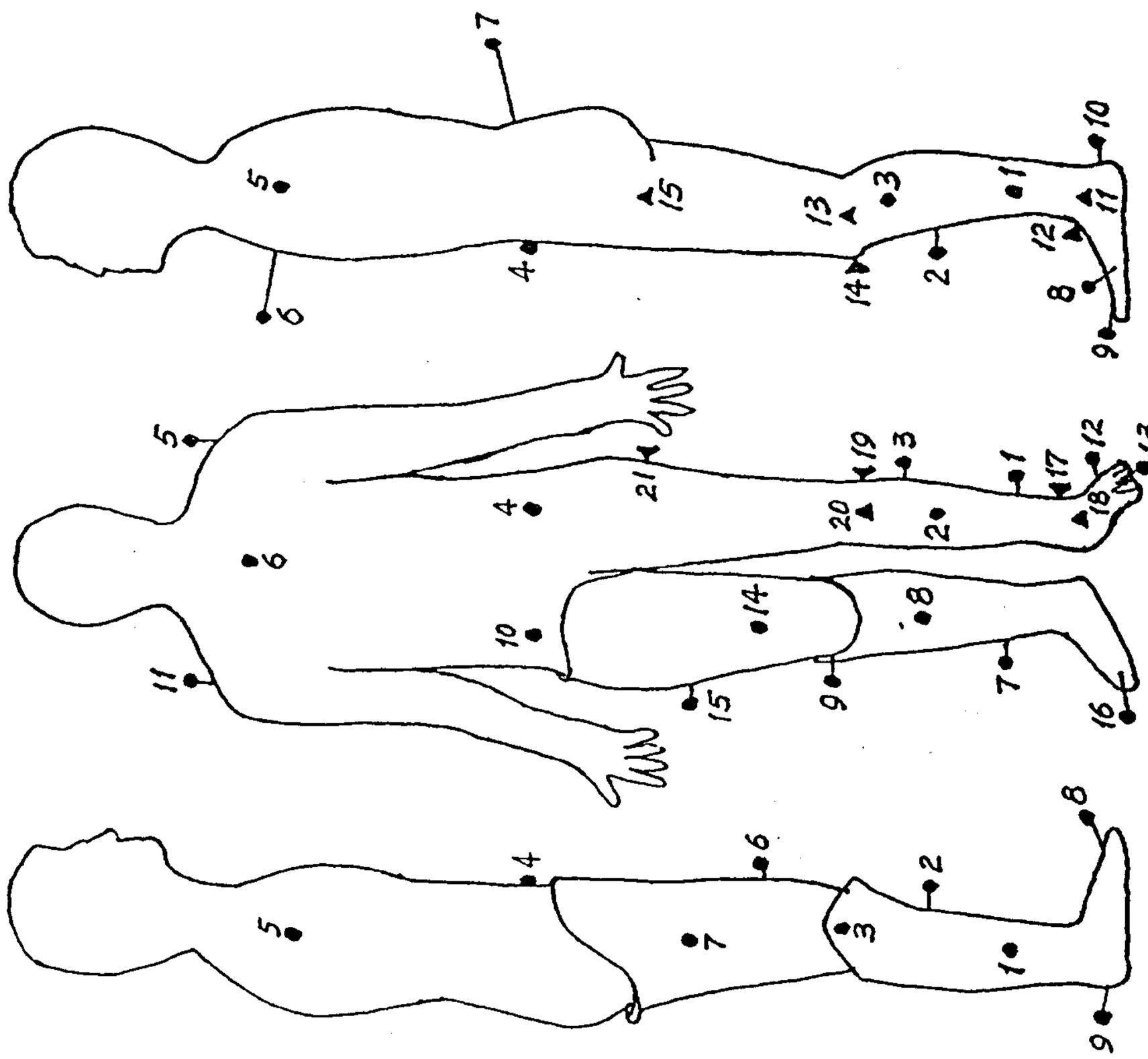

Fig. 4.16 Body marker system of the AK amputee and the labelling order in sorting program.

Table 4.9 Positions of the Body Markers

Class	Segments	Marker Locations	
	Upper torso	Left acromial process, Sternum, Right acromial process	
	Pelvis	Left anterior superior iliac spine, Sacral flat, Right anterior superior iliac spine	
		Prosthetic Side	Unaffected Side
Socket		Distal 1/3 on anterior wall Proximal 1/4 on lateral wall	
Shank		Distal 1/4 on lateral wall Proximal 1/3 on medio-anterior wall Lateral knee joint axle	5-10cms above lateral malleolus Proximal 1/3 on tibial flat 5-10cms below tibial plateau
Foot		Equivelant 5th metarsar base Mid-keel	5th metarsar base 2nd toetip Mid-calcaneus
Hip Joint		Lateral greater trochanter (frontal and lateral view)	
Knee joint		Lateral epicondyle of the femur,	Lower edge of the patella
Ankle joint		Lateral malleolus, midpoint between the medial and lateral malleoli (frontal view)	

(3) viewable at least by the front and either side cameras at any instant of time.

Fig. 4.16 shows a diagrammatic representation of a left and a right AK amputees with full marker system on, as well as the numbering system of the markers which indicates the order of labelling marker in sorting program. A total of 25 markers was used and their locations on the body segments were listed in Table 4.9.

There are two classes of body markers by their function: dynamic and static markers. The latter markers, as their names suggested, were used only during the static test to determine the positions of the anatomical joint centres and the anatomical

frame of reference of the segments. On the other hand, the dynamic markers were fixed to the body segments throughout the dynamic and static tests. These markers were used to form the marker frame of reference to which the joint centre and the anatomical frame of reference were related. How these various joint centres and frames of reference were established and related to each other are described in Chapter 5.

§4.4.2 Alignment change sequences (ACS)

Three alignment change sequences were designed for analyzing their effects on the amputees gait. They were

(1) the foot alignment change sequence (FACS): relative to the original position, the prosthetic foot was adjusted from 6° dorsiflexion to 6° plantar flexion in increments of 3°. If the ankle angle is denoted as Φ and plantar flexion direction is positive, the FACS can be written as

$$\Phi_{FACS} = \{ -6^\circ, -3^\circ, 0^\circ, 3^\circ, 6^\circ \} \tag{4.29}$$

(2) the socket alignment change sequence (SACS): Using the original inclination of the socket as a basis, the socket was sequentially extended by 6° and 3° and then flexed by 3° and 6°. If the socket A/P tilt angle is denoted as Ψ and flexion direction is positive, the SACS can be expressed as

$$\Psi_{SACS} = \{ -6^\circ, -3^\circ, 0^\circ, 3^\circ, 6^\circ \} \tag{4.30}$$

(3) the foot and socket alignment changes sequence (FSACS): relative to the original inclination of the foot and socket, the prosthetic foot was adjusted, by increment of 3°, from 6° plantar to 6° dorsi flexion coupled with the socket angular changes from extension to flexion by the same angle as that performed on the foot. Similarly, the FSACS can be mathematically expressed as

$$\Psi_{FSACS}+\Phi_{FSACS}=\Psi_{SACS}+(-\Phi_{FACS})\cdot\cdot \tag{4.31}$$

From now on, the ACS not only stands for the alignment change sequence, but also implies the specific order in which the alignment changes were made.

Only one ACS was tested in an amputee's single visit which usually consisted

PATIENT TEST RECORD

General Information

Name:
Height: 1. m
Weight: kg
Affected side: L/R

Date:
Phase delay:
Camera for phase delay: L/R
Amplifier: top/ bottom
Disk used: YL

Files Created During Test

Dynamic test 1:
Dynamic test 2:
Dynamic test 3:
Dynamic test 4:

Dynamic test 5:
Dynamic test 6:
Dynamic test 7:
Dynamic test 8:

Dynamic test 9:
Dynamic test 10:
Dynamic test 11:
Dynamic test 12:

Dynamic test 13:
Dynamic test 14:
Dynamic test 15:
Dynamic test 16:

Dynamic test 17:
Dynamic test 18:
Dynamic test 19:
Dynamic test 20:

TV field calibration:

Static calibration:

Comments on the test

NB:
NB:
NB:
NB:

NB:
NB:
NB:
NB:

NB:
NB:
NB:

NB:
NB:
NB:
NB:

NB:
NB:
NB:
NB:

NB:

NB:

Trunk measurement:

R. ASIS to Tail: 0. m
L. ASIS to Tail: 0. m
R. to L. ASIS: 0. m

Static Marker Measurement:

FTM1 to FTM3: 0.
FTM2 to FTM3: 0.

Fig.4.17(a) Form for amputee gait test.

of 20 successful test walks.

Two amputees wearing the Otto Bock prosthesis underwent three ACSs and altogether 60 successful test walks were taken and data recorded for each amputee. Another two amputees wearing the Endolite prosthesis underwent part of a the first two ACSs and a total of 32 test walks were taken and data recorded for each amputee

§4.4.3 Gait test protocol

In order to save experimental time, the prostheses worn by the amputees tested were measured a couple of days before the gait test. This involved the measurement of the mass properties and normal alignment of the prostheses, as described in §4.1.

On the day of test, the biomechanics laboratory was set ready for test at least one hour prior to the patient's arrival. Connections, switches and settings on the computer interface and amplifier boards were checked, a disk with sufficient space was mounted on the user disk driver, the TV and forceplate systems were turned on for warming up, and one or two trials on both the TV and forceplate systems were made and the results checked on the monitor to ensure that everything was right.

When the patient arrived, he was offerred a chair and had a rest. Meanwhile, the amputee was introduced to biomechanics laboratory, how gait test would be conducted and what he would be asked to do.

The actual gait test comprised three sessions which are described as follows.

§4.4.3.1 Dynamic test The dynamic markers were carefully positioned and stuck on to the patient wearing the normally aligned prosthesis. The patient was then permitted to walk around to get accustomed to the marker system.

The amputee was then directed to walk along the pathway towards the front camera at his own natural walking speed. An object was positioned above the front camera at the patient's eye level for the amputee to focus on when he was walking, so that he would not alter his step length in trying to strike the force platform. Before the

ANTHROPOMETRIC MEASUREMENT

General Information

Name: Date: / / 198

Height: 1. m Weight: kg

Amputation Level: AK / BK Affected Side: L / R

Anthropometric Measurement

1. Foot

Ankle Circ. Ca= mm Foot length Lf= mm

2. Shank

Shank Circ. Cs= mm Tibiale height Hti= mm

3. Thigh

Thigh Circ. Cth= mm Iliac Crest fat p= mm

4. Trunk

Chest Circ. Cch= mm

Trunk length Ltr= mm

Fig. 4 17(b) Form for anthropometric measurement of amputees.

test walk, several trials were required to determine the start point from where the amputee should strike both forceplates without changing his natural gait.

In every test walk, markers were checked to ensure that they were on the position and completely exposed to the cameras. Just before the left leg of the amputee contacted the forceplate No.1 the sampling switch was operated. Immediately after the right leg left the forceplate No.2 the sampling was terminated.

Usually four successful test walks were taken.

The alignment of the prosthesis was changed by a small amount by the prosthetist and the possible effects on the amputee were told to the patient for precautions. Then the procedure described above was repeated till all changes in a alignment change sequence were made.

§4.4.3.2 Static test The static markers were carefully positioned and stuck to the anatomical landmarks determined by palpation. The patient was then asked to stand at the origin of the ground frame of reference in a relaxed upright posture facing the front camera. Marker images on monitors of the TV system were checked to ensure every marker was picked up and a short sample of data were recorded. Then the marker distance and body measurements were taken according to the forms shown in Fig.4.17.

§4.4.3.3 Calibration of the TV field Three strings (a, b, c) were placed at nine locations around the forceplates (see Fig. 4.14), first time at position (1, 5, 9), second at position (7, 2, 6) and third at position (4, 8, 3). At each time, a short duration of samples of the markers on the string was recorded. Therefore, a total of 27 markers occupying a space of 1.3m×1.36m×0.65m were used to determine the factors of the DLT method.

§4.4.4 Preparing data for gait analysis on VAX

Standard procedures were used to prepare data for gait analysis on the Computer Centre's VAXs. The forceplate data were selected to include only those from a few frames before heel strike to a few frames after toe off. The TV data were

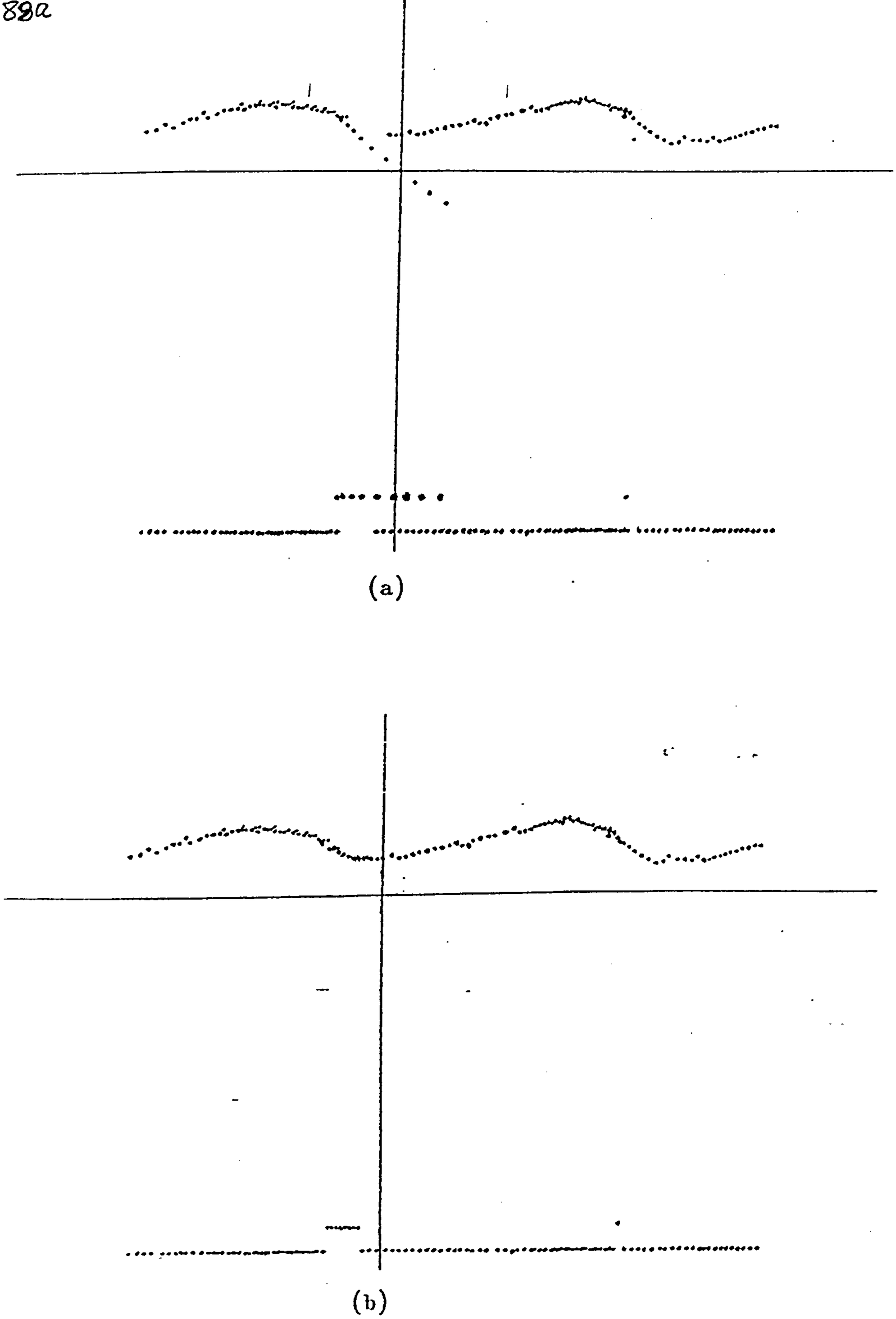

(a)

(b)

Fig. 4.18 Correction of the estimated marker positions.
(a) Before correction; (b) After correction.

averaged and sorted as described in §4.2.3.

In processing the TV raw data for present gait tests, this author encountered some difficulties in the sorting program. The trojectories of some markers in the front view intersected each other occasionally during swing phase, and the program failed to track the markers correctly. This problem was not evident until apparent errors appeared in the gait analysis results, wasting a lot of man power and computer time. So, a checking procedure was needed. Another difficulty was related to linear extrapolation. When a marker was missed from the data, the linear extrapolated estimations which the sorting program provided sometimes overshot from the trajectory of the marker, so that a correction was needed.

In order to overcome these difficulties, a new procedure was implemented by this author into PDP11 which read in sorted data, displayed marker trajectory one by one, identified the estimated marker positions and corrected marker positions, if necessary, by moving the cross cursor to where you like and striking the RETURN. Fig. 4.18 is such an example. For front camera, the horizontal and vertical components of a marker trajectory were displayed on separate field and against time, making the check and correction much easier. This program was written in FORTRAN 77. Although the new program increased the number of procedures for processing raw TV data, it saved re-work time and provided more confidence in the data.

CHAPTER 5

THEORETICAL ASPECT OF THE WORK

The theoretical aspect of the gait analysis presented in this thesis is described in this chapter.

First, an introduction is given in which the symbols and notations used in this chapter are explained and some data processing techniques adopted are presented. Then, a biomechanical model of the human body for this gait analysis is derived with its basic characteristics being detailed. Kinematic and kinetic analysis of the model during locomotion is presented and the kinematic and kinetic variables of the gait analysis defined.

This mechanical model was implemented into the Computer Centre's VAXs by a suit of program written in FORTRAN 77.

§5.1 Introduction

§5.1.1 Symbols, notations and their Meanings

In this chapter, various frames of reference and their relationships, segments and joints, forces and moments, and static and dynamic situations will be dealt with, so that a consistent system of symbols and notations is desirable for what is presented in this chapter to be simple and clear.

(A) Dynamic and Static Situations

Generally, any quantity measured in or derived from static test will be printed in CAPITAL, while quantity measured or derived from dynamic test is written in lower-case.

(B) Vectors

The position vector of any point in space is printed in **bold** face and has a form of

$$\begin{aligned} \boldsymbol{R}_{©\Delta} &= [\, X^{+}_{©\Delta},\, Y^{+}_{©\Delta},\, Z^{+}_{©\Delta}\,] \quad \text{(static situation)} \\ \boldsymbol{r}_{©\Delta} &= [\, x^{+}_{©\Delta},\, y^{+}_{©\Delta},\, z^{+}_{©\Delta}\,] \quad \text{(dynamic situation)} \end{aligned} \tag{5.1}$$

in which

$$\Delta = \begin{cases} A & \textit{the Ankle joint centre} \\ K & \textit{the knee joint centre} \\ H & \textit{the hip joint centre} \\ L & \textit{the L4 joint centre} \\ f & \textit{the CG of the foot} \\ s & \textit{the CG of the shank} \\ t & \textit{the CG of the thigh} \\ G & \textit{the Ground reactions} \end{cases} \tag{5.2}$$

$$© = \begin{cases} P & \textit{Prosthetic side} \\ U & \textit{Unaffected side} \end{cases} \tag{5.3}$$

$$+ = \begin{cases} G & \textit{Ground frame of reference} \\ M & \textit{Marker frame of reference} \\ P & \textit{Principal reference frame of inertia} \end{cases} \tag{5.4}$$

For example, $\boldsymbol{R}_{PK}$ means the static position vector of the prosthetic knee joint centre and $\boldsymbol{r}_{UG}$ the centre of pressure of the ground reactions at unaffected side.

The linear velocity and acceleration of a point are presented as

$$\boldsymbol{v}_{©\Delta} = \frac{d\boldsymbol{r}_{©\Delta}}{dt}, \qquad \boldsymbol{a}_{©\Delta} = \frac{d\boldsymbol{v}_{©\Delta}}{dt} \tag{5.5}$$

and the angular velocity and acceleration are written as

$$\omega_{©*} = \begin{bmatrix} \omega_x^{+} & \omega_y^{+} & \omega_z^{+} \end{bmatrix} \tag{5.6}$$

$$\varepsilon_{©*} = \begin{bmatrix} \varepsilon_x^{+} & \varepsilon_y^{+} & \varepsilon_z^{+} \end{bmatrix} \tag{5.7}$$

Unit vector of an axis of a frame of reference is written as

$$\boldsymbol{E}_i^{\copyright *} = \begin{bmatrix} D_{i1} & D_{i2} & D_{i3} \end{bmatrix}$$

$$\boldsymbol{e}_i^{\copyright *} = \begin{bmatrix} d_{i1} & d_{i2} & d_{i3} \end{bmatrix} \qquad (i = x, y, z) \tag{5.8}$$

where

$$* = \begin{cases} F & \textit{the Foot} \\ S & \textit{the Shank} \\ T & \textit{the Thigh} \\ P & \textit{the Pelvis} \\ U & \textit{the Upper tor} \end{cases} \tag{5.9}$$

Force and moment are all written in CAPITAL and have the form of

$$F_{\copyright\Delta} = [\, FX^{+}_{\copyright\Delta}, FY^{+}_{\copyright\Delta}, FZ^{+}_{\copyright\Delta} \,] \quad \text{(for force)}$$

$$M_{\copyright\Delta} = [\, MX^{+}_{\copyright\Delta}, MY^{+}_{\copyright\Delta}, MZ^{+}_{\copyright\Delta} \,] \quad \text{(for moment)} \tag{5.10}$$

for example, F_{PG} stands for ground reaction forces at the prosthetic side.

(C) Direction cosine

By nature, there are three different frames of reference used and their inter relationships are described by direction cosine matrix which will be written in form of

$$\left[DC@^{\copyright}_{*}\right]_{+-+} = \begin{bmatrix} d_{11} & d_{12} & d_{13} \\ d_{21} & d_{22} & d_{23} \\ d_{31} & d_{32} & d_{33} \end{bmatrix} = \begin{bmatrix} e_x^{\copyright\Delta} \\ e_y^{\copyright\Delta} \\ e_z^{\copyright\Delta} \end{bmatrix} \tag{5.11}$$

in which

$$@ = \begin{cases} S & \textit{Static situation} \\ D & \textit{Dynamic situation} \end{cases} \tag{5.12}$$

For example,$[DCS_F^{\,P}]_{P\text{-}G}$ stands for the direction cosine matrix of the principal axes of inertia with respect to the ground frame of reference for the prosthetic foot segment in static situation.

§5.1.2 Generation of 3-D spatial coordinates

(A) The DLT method

As mentioned in §4.3.4, the DLT method was used to calibrate the TV-computer system and generate 3D spatial coordinates of the markers. Here, only the basic DLT equations are given, and readers interested in the detail of the DLT technique are recommended to refer to Abdel-Aziz & Karara (1971).

Let

$$M_i = [x_i, y_i, z_i] = 3D\ control\ points \qquad (i=1,2,\ldots,N)$$
$$M1_i = [p1_i, q1_i] = 2D\ image\ of\ M_i\ in\ camera\text{-}1$$
$$M2_i = [p2_i, q2_i] = 2D\ image\ of\ M_i\ in\ camera\text{-}2 \tag{5.13}$$

where N is the number of control points. In this study, camera-1 can be referred to the front camera, camera-2 to one of the side camera and N=27.For a single control point, its true 3D spatial coordinates and image in a camera are related by a collinear equation

$$xA_1+yA_2+zA_3+A_4-xpA_9-ypA_{10}-zpA_{11} = p$$
$$xA_5+yA_6+zA_7+A_8-xqA_9-yqA_{10}-zqA_{11} = q \tag{5.14}$$

where

$$x=\begin{cases} x1 \\ x2 \end{cases} \quad y=\begin{cases} y1 \\ y2 \end{cases} \quad z=\begin{cases} z1 \\ z2 \end{cases} \qquad p=\begin{cases} p1 \\ p2 \end{cases} \quad q=\begin{cases} q1 \\ q2 \end{cases}$$

$$A_i = \begin{cases} A1_i \\ A2_i \end{cases} \qquad (i = 1,2,\ldots,11) \tag{5.15}$$

are depended on which camera is considered and A_i $(i=1,2,\ldots,11)$ are DLT parameters for a camera.Each control point has one pair of equation (5.14) and at least 6 control points (12 equations) are required to obtain the 11 DLT parameters for each camera. Now we have N control points, a resulting set of equations can be written as

$$\begin{bmatrix} x_1 & y_1 & z_1 & 1 & 0 & 0 & 0 & 0 & -x_1p_1 & -y_1p_1 & -z_1p_1 \\ 0 & 0 & 0 & 1 & x_1 & y_1 & z_1 & 1 & -x_1q_1 & -y_1q_1 & -z_1q_1 \end{bmatrix} \begin{bmatrix} A_1 \\ \vdots \\ A_{11} \end{bmatrix} = \begin{bmatrix} p_1 \\ q_1 \end{bmatrix}$$

$$\begin{bmatrix} x_2 & y_2 & z_2 & 1 & 0 & 0 & 0 & 0 & -x_2p_2 & -y_2p_2 & -z_2p_2 \\ 0 & 0 & 0 & 1 & x_2 & y_2 & z_2 & 1 & -x_2q_2 & -y_2q_2 & -z_2q_2 \end{bmatrix} \begin{bmatrix} A_1 \\ \vdots \\ A_{11} \end{bmatrix} = \begin{bmatrix} p_2 \\ q_2 \end{bmatrix}$$

$$\vdots \quad \vdots \quad \vdots \quad \vdots \quad \vdots \quad \vdots \quad \vdots \quad \vdots \quad \vdots \quad \vdots \quad \vdots \quad \vdots \quad \vdots$$

$$\begin{bmatrix} x_N & y_N & z_N & 1 & 0 & 0 & 0 & 0 & -x_Np_N & -y_Np_N & -z_Np_N \\ 0 & 0 & 0 & 0 & x_N & y_N & z_N & 1 & -x_Nq_N & -y_Nq_N & -z_Nq_N \end{bmatrix} \begin{bmatrix} A_1 \\ \vdots \\ A_{11} \end{bmatrix} = \begin{bmatrix} p_N \\ q_N \end{bmatrix} \qquad (5.16)$$

This is the equations for calibrating the TV-computer system in which the position of each control marker in ground frame of reference (x_i, y_i, z_i) and its image in a camera (p_i, q_i) are known and the DLT parameters $(A_1, A_2, \ldots, A_{11})$ are solved for.

After calibrating the system, the 2D-to-3D transformation of each marker in each frame can be made. In order to do this, the equation (5.14) be rewritten as

$$\begin{aligned} (pA_9-A_1)x+(pA_{10}-A_2)y+(pA_{11}-A_3)z &= A_4-p \\ (qA_9-A_5)x+(qA_{10}-A_6)y+(qA_{11}-A_7)z &= A_8-q \end{aligned} \qquad (5.17)$$

For each point, there are two pairs of equations (5.17), one for camera-1 and another for camera-2, that is

$$\begin{bmatrix} p_1A1_9-A1_1 & p_1A1_{10}-A1_2 & p_1A1_{11}-A1_3 \\ q_1A1_9-A1_5 & q_1A1_{10}-A1_6 & q_1A1_{11}-A1_7 \\ p_2A2_9-A2_1 & p_2A2_{10}-A2_2 & p_2A2_{11}-A2_3 \\ q_2A2_9-A2_5 & q_2A2_{10}-A2_6 & q_2A2_{11}-A2_7 \end{bmatrix} \begin{bmatrix} x \\ y \\ z \end{bmatrix} = \begin{bmatrix} A1_4-p_1 \\ A1_8-q_1 \\ A2_4-p_2 \\ A2_8-q_2 \end{bmatrix} \qquad (5.18)$$

where x, y, z are 3D coordinates of the marker to be generated.

The DLT method is implemented into the Computer Centre's VAXs. The source

program is supplied by Aziz & Karara, but some modifications in I/O format are made by this author to suit the TV-computer data.

(B) Markers only viewable to one camera

The DLT method is valid only if a marker is viewable to two cameras. In present body marker system, the tail and heel markers can not be seen by the front camera, thus only one pair of equations (5.17) is available which is not sufficient to generate 3D coordinates.

In order to overcome this difficulty, the property of a rigid body is employed: the distance between any two point in a rigid body is a constant. During the static test, the distance from each marker viewable to only one camera to two markers on the same segment with their positions known are measured, and the resulting set of equations can be written as

$$(pA_9-A_1)x+(pA_{10}-A_2)y+(pA_{11}-A_3)z = A_4-p$$

$$(qA_9-A_5)x+(qA_{10}-A_6)y+(qA_{11}-A_7)z = A_8-q$$

$$(x - x1)^2+ (y - y1)^2+ (z - z1)^2 = D1^2$$

$$(x- x2)^2+(y - y2)^2+ (z - z2)^2 = D2^2 \qquad (5.19)$$

It is noted that above equation is over-determined and non-linear, and a NAG library program E04GEF was used to solve the equations.

§5.1.3 Data smoothing and differentiation

The measuring system and data reduction process introduce random error into 3D spatial coordinates of a marker and the error will be amplified through differentiation for velocity and acceleration, affecting the accuracy of or even jeopardizing the validity of dynamic calculations. Therefore, a lot of algorithms have been proposed for smoothing and differentiating the error contaminated data. Plagenhoef (1968) adopted a Chebyshev least squares polynomial curve fitting technique to smooth the displacement data followed by a polynomial differentiation. Tooth (1976) used a 4th order butterworth digital filter reported by Andrews (1975)

and a Newtonian numerical differentiator described by Dorn & McCracken (1972). Zernicke *et al* suggested a cubic spline fitting followed by differentiating the fitted function.

Pezzack *et al* (1977) compared the analogue signal obtained from a accelerometer with the calculated acceleration using following techniques: 2nd order difference equations cited by Miller & Nelson (1973), Chebyshev polynomial fitting with differentiating, and 2 order butterworth digital filter followed by first order finite difference. They concluded that the acceleration obtained by butterworth filter with finite difference was most close to the measured one.

The smoothing and differentiation scheme used in this project was digital filter followed by finite difference. The filter is a fourth-order Butterworth low-pass digital filter developed by Andrews (1975):

$$y_k = \frac{1}{C_6}\,[\, C_1\,(x_k+4x_{k-1}+6x_{k-2}+4x_{k-3}+x_{k-4}) - (C_2y_{k-1}+C_3y_{k-2}+C_4y_{k-3}+C_5y_{k-4})\,] \qquad (5.20)$$

where C_i $(i = 1,2,\ldots,6)$ are functions of the 3dB cut-off frequency f_{cut} (in Hz) and the sampling interval T (s.) which the user could specify. In this study, f_{cut} =5Hz and T=0.02s. The time sequence of 3D spatial coordinates of each marker were passed through the filter twice, first along backward and second forward direction, so that the phase lag due to asymmetry of the filter was compensated for, but the cut-off frequency doubled to 10Hz at 6dB.

The numerical differentiator used in this project is one used by Tooth (1976):

$$f'(x) = \frac{1}{12T}\,[\, f(x_n-2T) - 8f(x_n-T) + 8f(x_n+T) - f(x_n+2T)\,] \qquad (5.21)$$

where x_n is the point under consideration.

§ 5.1.4 Time Normalization

In this project, usually three test walks were analyzed for each alignment

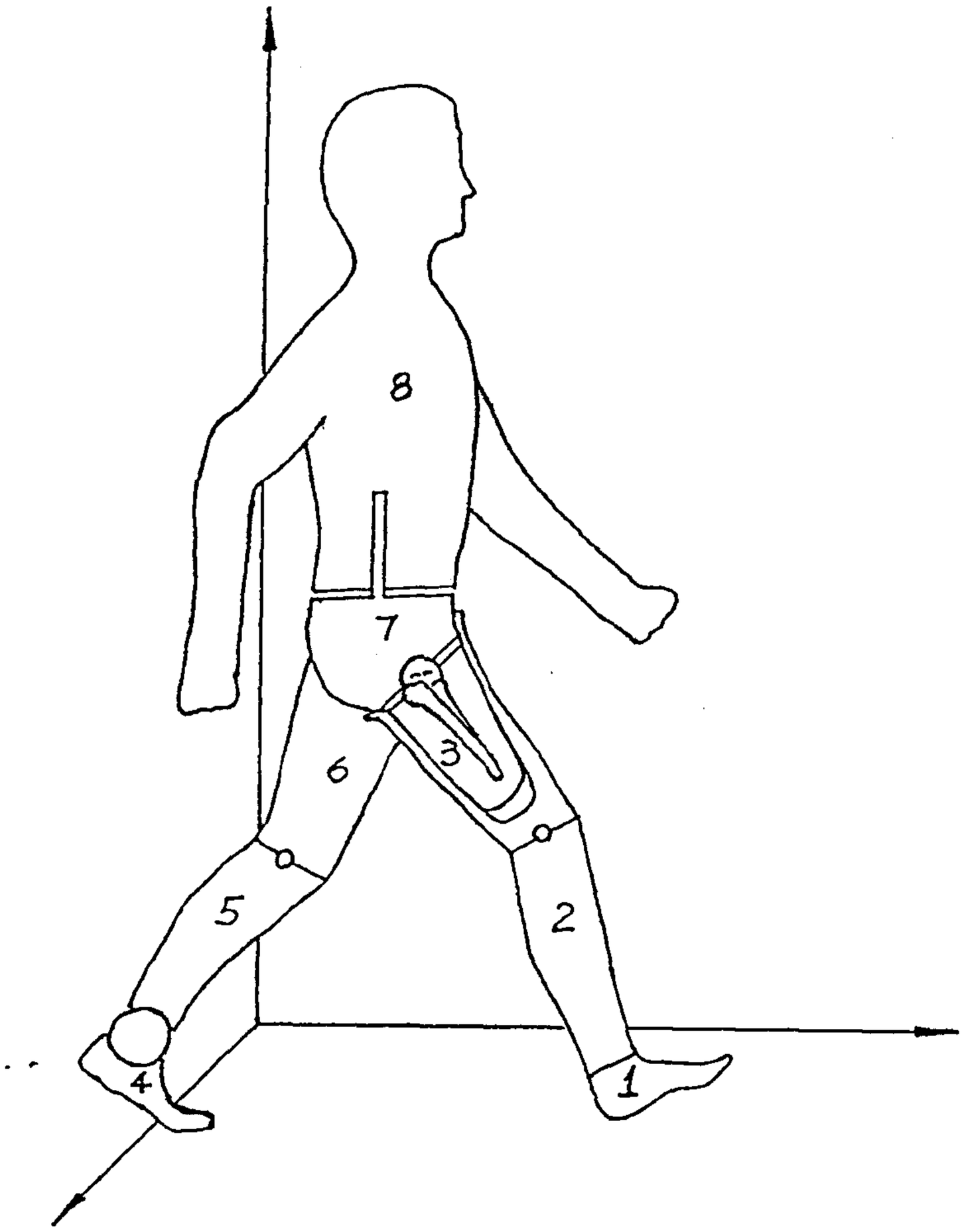

1. Prosthetic foot
2. Prosthetic shank
3. Prosthetic thigh
4. Unaffected foot
5. Unaffected shank
6. Unaffected thigh
7. the pelvis
8. the Upper torso

Fig. 5.1 The Mathematical Model of the AK amputee.

setting. Due to step-to-step variability, the test walks showed different periods for stance and swing phase timing, and as a result, it was not possible to average the resulting data by simple process of adding the signals without distorting the picture. Therefore a Fourier analysis technique was used to normalize the data. For a gait variable $\{X_i\}$ $(i=1,2,\ldots,N,N+1)$, it was first de-trended:

$$x'_1 = x_i - x_1 - \frac{x_{N+1} - x_1}{N}(i-1) \qquad (i = 1,2,\ldots,N,N+1) \tag{5.22}$$

then the amplitudes of its first n harmonics were determined as

$$A_j = \frac{2}{N}\sum_{i=1}^{N+1} x_i' \cos\frac{2j\pi(i-N)}{N}, \qquad B_j = \frac{2}{N}\sum_{i=1}^{N+1} x_i' \sin\frac{2j\pi(i-N)}{N}$$
$$(j = 0,1,2,\ldots,n) \tag{5.23}$$

Using these harmonics, a new data sequence of the variable with 100 samples was generated:

$$x_i = x_1 + \frac{x_{N+1}-x_1}{100}(i-1) + \frac{A_0}{2} + \sum_{j=1}^{j=n} A_j \cos\frac{2j\pi(i-100)}{100} + \sum_{j=1}^{j=n} B_j \sin\frac{2j\pi(i-100)}{100} \tag{5.24}$$

In this way, the three original signals were normalized into a common time base, the percentage of relevant duration (such as cycle time or stance phase), and their averages and standard deviations calculated.

§5.2 Biomechanical model of an above-knee amputee

A general consideration of the biomechanical model of the human body used in this thesis is given and the inertia properties of various segments are specified in detail.

§5.2.1 General consideration of the model

The biomechanical model of the human body adopted in this gait analysis is based on the mechanics of the rigid body and consists of eight segments connected by various types of joints, as shown in Fig. 5.1. The definitions of the anatomical segments are

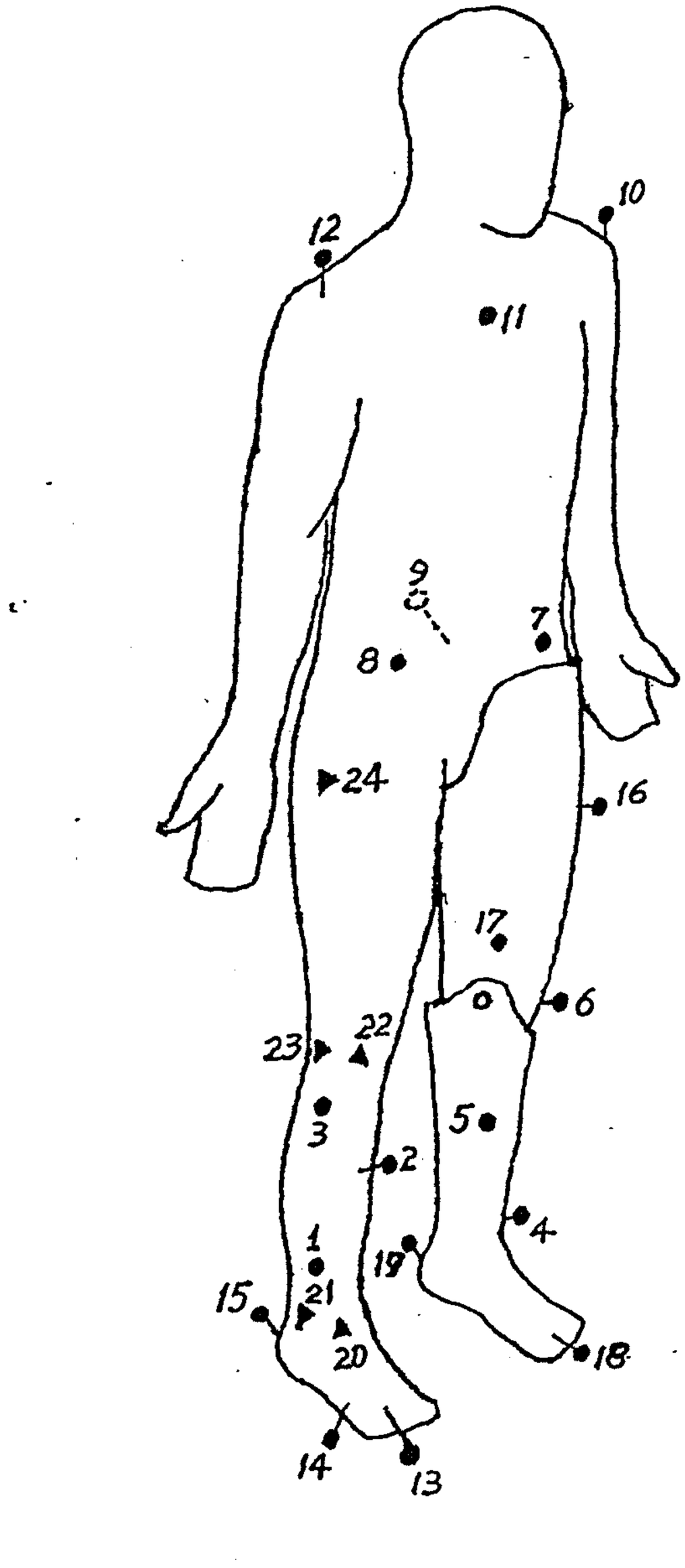

Fig. 5.2 Numbers assigned to the body markers.

(1) the foot: section through the upper talo-crural joint; (2) the shank: sections passing through the upper talo-crural joint and the knee joint;

(3) the thigh: section through the knee joint and inclined section conducted through the hip joint which leaves the femur intact; (4) the pelvis: a transverse section through the fourth lumbar vertebra and sections through the two hip joint;

(5) the upper torso: a transverse section through L4.

It was recognized that the upper limbs could prove to be a valuable parameter (Elftman, 1939), but including them into the model would make the gait test and analysis too complicated.

As far as the joints are concerned, the structure of various anatomical joints are very sophisticated and following assumptions are therefore made to simplify both the structure and the motion allowed:

(1) The L4 joint is a revolute and cylindrical joint which allows only relative transverse rotation between the upper torso and the pelvis.

(2) The hip joint is of ball-socket type and three dimensional rotation is permitted between the pelvis and the thigh.

(3) The knee joint is a single hinge joint capable of extending or flexing only.

(4) The ankle joint belongs to ball-socket type.

The features of the prosthetic joints depend on the prosthesis fitted to the amputee and they are described in §4.1.1.

The model is not completed until the inertia properties of each model segment are determined. The method to determined these properties are presented in early chapters and the evaluation of these properties will described in detail later in this section.

§5.2.2 Definitions of the lower-limb joint centres

The definitions of the prosthetic ankle and knee joint centres are defined in § 4.1

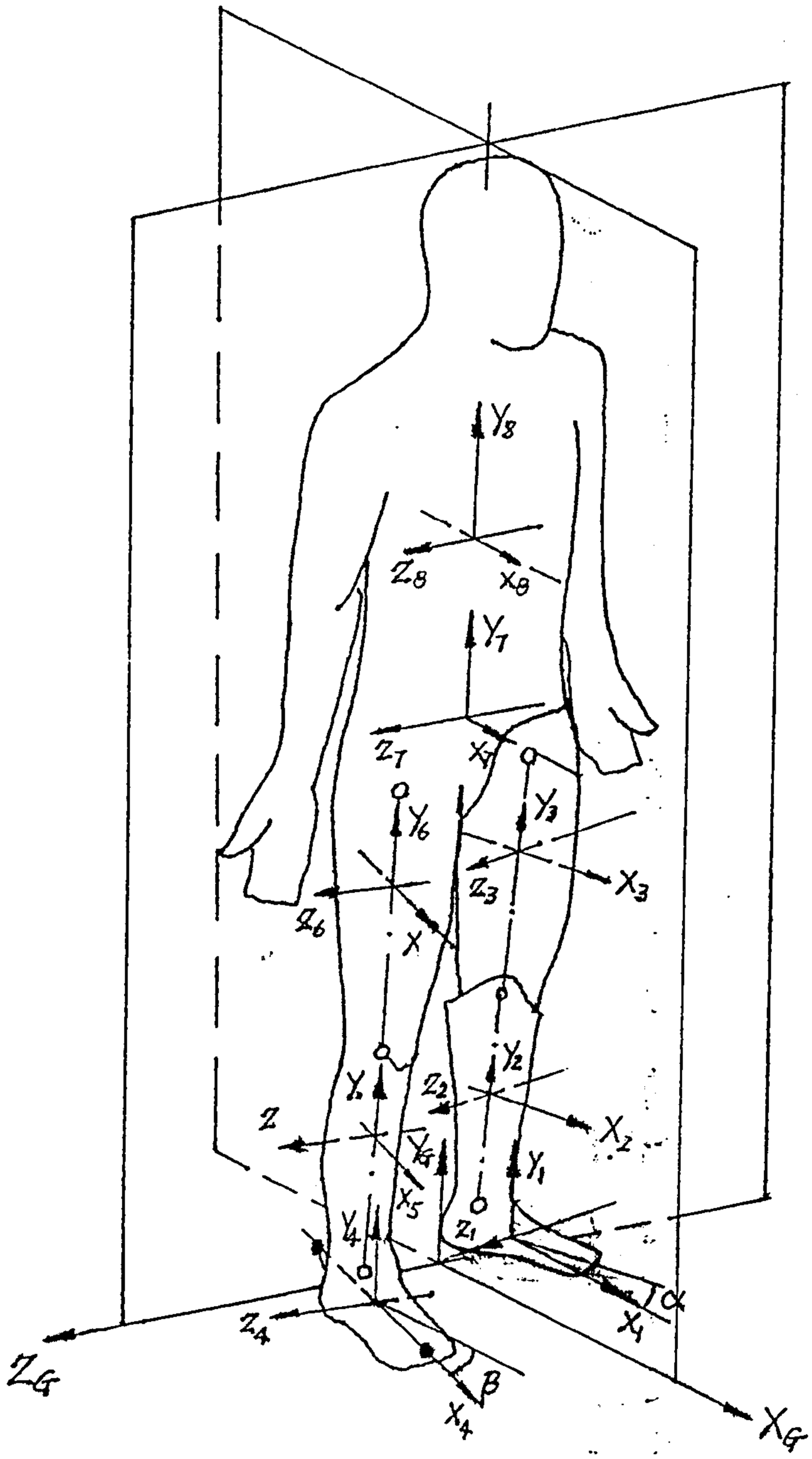

Fig. 5.4 The principal axes of inertia for each model segment.

in which the measurement of the alignment of a prosthesis is presented.

The anatomical ankle and knee joint centres of the model were identified through static markers stuck onto the anatomical landmarks as shown in Fig. 4.9. Therefore, the position of the joint centres with respect to the ground frame of reference are

$$\boldsymbol{R}_{UA} = \begin{bmatrix} X_{UA} & Y_{UA} & Z_{UA} \end{bmatrix} = \begin{bmatrix} X_{21} & Y_{21} & Z_{20} \end{bmatrix}$$

$$\boldsymbol{R}_{UK} = \begin{bmatrix} X_{UK} & Y_{UK} & Z_{UK} \end{bmatrix} = \begin{bmatrix} X_{23} & Y_{23} & Z_{22} \end{bmatrix} \tag{5.25}$$

To determine the hip joint centres, an anthropometric scaling technique coupled with direct measurement, used was adopted. The location of hip joint centre in the sagittal plane at the sound side was identified by the static marker on the greater trochanter, while the Z-coordinate of it was estimated to be 0.122·(width of the two ASISs) medial to the relevant ASIS (see Fig. 5.3), that is

$$\boldsymbol{R}_{UH} = \begin{bmatrix} X_{UH} & Y_{UH} & Z_{UH} \end{bmatrix} = \begin{bmatrix} X_{24} & Y_{24} & Z_{UH} \end{bmatrix} \tag{5.26}$$

where

$$Z_{UH} = Z_8 - 0.122 \cdot ILEG \cdot D_{78} \tag{5.27}$$

Similar relations are assumed to be exist for the HJC at the prosthetic side, that is

$$\boldsymbol{R}_{PH} = \begin{bmatrix} X_{PH} & Y_{PH} & Z_{PH} \end{bmatrix} = \begin{bmatrix} a_1 + X_7 & a_2 + Y_7 & a_3 + Z_7 \end{bmatrix} \tag{5.28}$$

in which

$$a_1 = X_{UH} - X_8, \quad a_2 = Y_{UH} - Y_8, \quad a_3 = 0.122 \cdot ILEG \cdot D_{78} \tag{5.29}$$

§5.2.3 Principal axes of inertia

Principal axes of inertia is one of inertia properties of a segment and defined as that in such a local frame of reference the matrix of moment of inertia is a diagonal one (see Harrison, 1978). For each lower limb in the model, its principal axes of inertia are specified and expressed as a direction cosine matrix, with respect to the ground frame of reference, as follows.

(A) The foot

For the prosthetic foot, its principal axes of inertia are assumed to be parallel to the frame of reference defined in §4.1.2.3. As the foot has a toe-out angle only, determined in §4.1.5, with respect to the ground frame of reference, its direction cosine matrix can be written as

$$[DCS_F^P]_{P\text{-}G} = \begin{bmatrix} cos\alpha & 0 & sin\alpha \\ 0 & 1 & 0 \\ -sin\alpha & 0 & cos\alpha \end{bmatrix} \tag{5.30}$$

where

$$ILEG = \begin{cases} 1 & left\ amputee \\ -1 & right\ amputee \end{cases} \tag{5.31}$$

$$\alpha = -\dot{T}OUT \cdot ILEG \tag{5.32}$$

For the anatomical foot, its principal axes of inertia are defined in a similar way as those for the prosthetic foot and identified in static test during which the amputee was asked to put his unaffected foot flat on the ground. Therefore the principal Y-axis of the foot is coincided with the ground system. Since the angle between the principal X-axis and the ground X-axis can be determined as

$$\beta = arc\ tg\left(\frac{Z_{15} - Z_{13}}{X_{13} - X_{15}}\right) \tag{5.33}$$

Therefore

$$[DCS_F^U]_{P\text{-}G} = \begin{bmatrix} cos\beta & 0 & sin\beta \\ 0 & 1 & 0 \\ -sin\beta & 0 & cos\beta \end{bmatrix} = \begin{bmatrix} E_x^{UF} \\ E_y^{UF} \\ E_z^{UF} \end{bmatrix} \tag{5.34}$$

(B) The Shank

The principal axes of inertia of the prosthetic shank is assumed to be parallel to the axes defined in §4.1.2.2 and their direction cosine can be derived as follows. Noticing that the principal Z-axis is parallel to the coronal plane and has a medial tilt angle θ determined in §4.1.4, the direct obtained

$$E_z^{PS} = \begin{bmatrix} 0 & cos(\theta\ ILEG) & -sin(\theta\ ILEG) \end{bmatrix} \tag{5.35}$$

Since the plane normal to E_Z^{PS} has an expression

$$E_Z^{PS}\,(R - R_{PH}) = 0 \tag{5.36}$$

and the line normal to above plane and passing through the AJC has an expression

$$R = R_{PA} + f E_Z^{PS} \tag{5.37}$$

the coordinate of the projection of the AJC (R') can be obtained by solving above two simultaneous equations to determine the constant f, that is

$$R' = R_{PA} + f E_Z^{PS} \tag{5.38}$$

where

$$f = E_Z^{PS} \cdot (R_{PK} - R_{PA}) \tag{5.39}$$

Now, the direction cosine of the principal Y-axis can be derived as

$$E_Y^{PS} = \frac{R_{PK} - R'}{|R_{PK} - R'|} \tag{5.40}$$

To complete the direction cosine matrix $[DCS_S^P]_{P\_G}$, the principal X-axis is constructed as

$$E_X^{PS} = E_Y^{PS} \times E_Z^{PS} \tag{5.41}$$

When the anatomical shank is considered in static test, its principal Y-axis is assumed to direct from the AJC to the KJC, so that we have

$$E_Y^{US} = \frac{R_{UK} - R_{UA}}{| R_{UK} - R_{UA} |} \tag{5.42}$$

Then, the Z_P-axis is constructed which is the cross-product of the X_G-axis and the Y_P-axis:

$$E_Z^{US} = E_X^{UA} \times E_Y^{US} \tag{5.43}$$

Finally

$$E_X^{US} = E_Y^{US} \times E_Z^{US} \tag{5.44}$$

(C) The thigh

For both the prosthetic and unaffected thigh segments, a similar procedure is used to determine their principal axes of inertia. First, the principal Y_P-axis is assumed to pass through the HJC and the KJC, and directs upward, that is,

$$E_Y^{©T} = \frac{R_{©H} - R_{©K}}{| R_{©H} - R_{©K} |} \tag{5.45}$$

Then the principal Z_P-axis is defined as the cross-product of the $E_Y^{©T}$ and the principal X_P-axis of the shank

$$E_Z^{©T} = E_X^{©S} \times E_Y^{©T} \tag{5.46}$$

Finally, the principal X_P-axis is determined

$$E_X^{©T} = E_Y^{©T} \times E_Z^{©T} \tag{5.47}$$

(D) The pelvis and the upper torso

As the amputee stands in a relaxed upright posture in the static test, the orientation of the principal axes of the pelvis and the upper torso are assumed to coincide with the ground frame of reference, that is

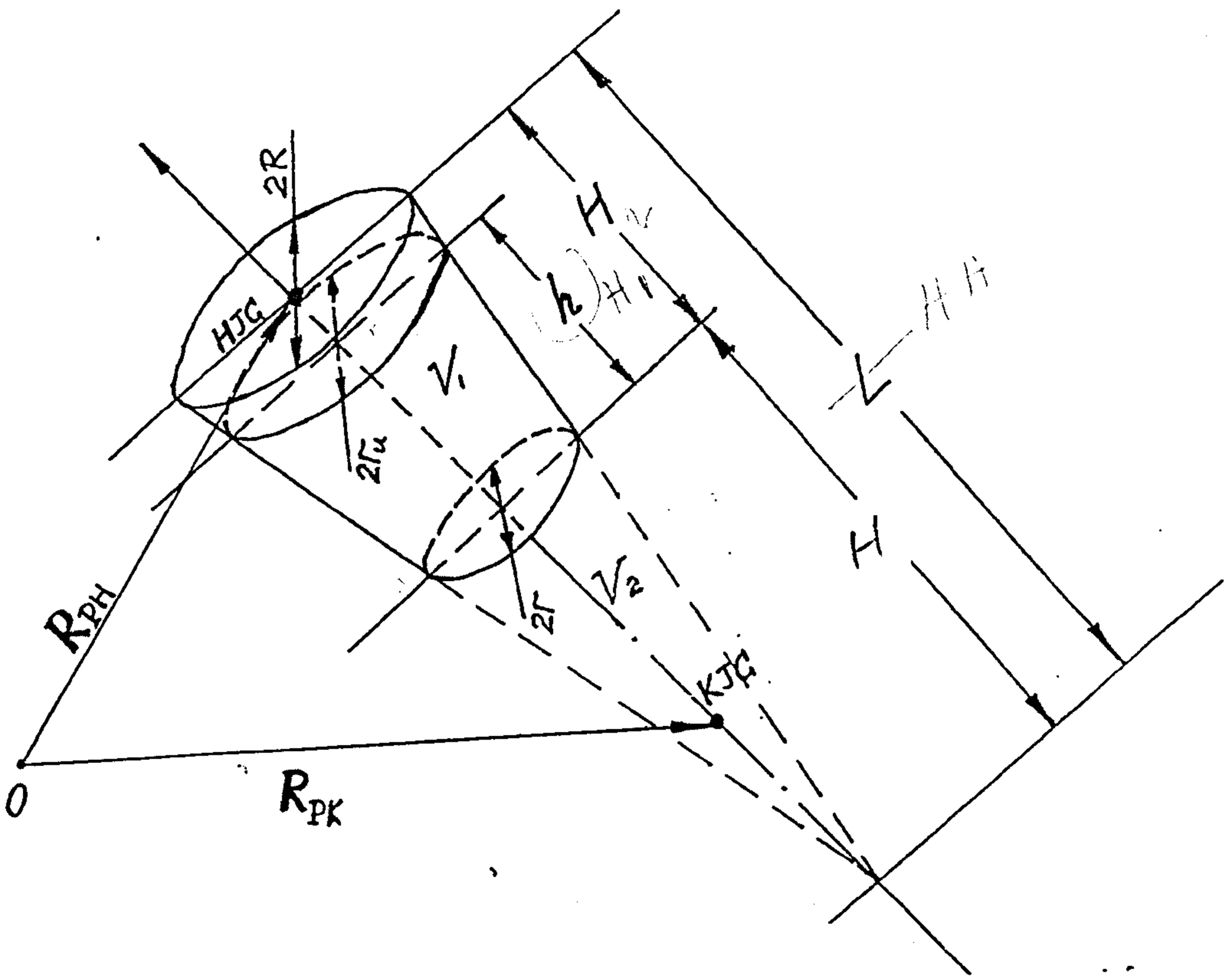

Fig. 5.5 Mathematical model of the AK stump for estimation of the inertia properties.

$$\left[DCS_U\right] = \left[DCS_P\right] = \begin{bmatrix} 1 & 0 & 0 \\ 0 & 1 & 0 \\ 0 & 0 & 1 \end{bmatrix} \tag{5.48}$$

§5.2.4 Inertia properties of the model segments

The moment of inertia of a segment about its longitudinal axis (Y-axis) was assumed to be negligible in this study, that is

$$I_{YY} = 0.0$$

(A) The prosthetic lower limbs

The inertia properties of the prosthesis are measured in §4.1.3. Since the moments of inertia measured is that about the KJC, they have to be transformed into that with respect to the CG of the segment. According to the parallel axes theorem, the moment of inertia of the prosthetic shank-foot segment about its principal axes is

$$I_{XX}^{PS} = I_{ZZ}^{PS} = I_{PS} - m_{PS} S_{PS}^2 \tag{5.49}$$

As the prosthetic thigh is concerned, what has been described in §4.1.3 is just for the socket, and the contribution of the stump is discussed here. In order to do this, the stump is modelled into a truncated circular cone V_1 with the bottom circle being the lower plane in Fig. 4.2 and the upper plane through the HJC, as shown in Fig. 5.5. If the position of the prosthetic HJC determined through static test (see §5.2.2) is R_{PH}, the diameter of the upper circle can be first specified:

$$R = \frac{u}{h} H + r \tag{5.50}$$

where

$$r_u = 0.5 \ |[RU] - [LU]|$$
$$r = 0.5 \ |[RL] - [LL]|$$
$$h = |[SU] - [SL]|$$
$$H = |R_{PH} - [SL]| \tag{5.51}$$

Then, from a mathematics handbook, the mass and the CG of the stump relative to the HJC be determined:

$$m_{ST} = \frac{\pi}{3}\rho H(R^2 + Rr + r^2)$$
$$S_{ST} = \frac{H(R^2 + 2Rr + 3r^2}{4(R^2 + Rr + r^2)} \tag{5.52}$$

in which $\rho = 1.069(kg/m^3)$ (Contini, 1972). Now the mass and the CG of the thigh (socket +stump) with respect to the HJC can be written as

$$m_{PT} = m_{ST} + m_{SO}$$
$$S_{PT} = C_{PT}/R_{PK} - R_{PH}/ = \frac{m_{ST}S_{ST} + m_{SO}(/R_{PK} - R_{PH}/ \cdot S_{SO})}{m_{PT}} \tag{5.53}$$

in which m_{SO} and S_{SO} are mass and the CG of the socket measured in §4.1.2. In order to use the handbook to determine the moment of inertia of the stump, an imaginary circular cone V_2 is added to V_1 to form a bigger cone V. According to parallel axis theorem, the moment of inertia of V about the HJC can be written as

$$[I_2 + (H + \frac{S}{4})^2 m_2] + [I_{ST} + S_{ST}^2 m_{ST}] = I + (\frac{L}{4})^2 m \tag{5.54}$$

Therefore

$$I_{ST} = [I + (\frac{L}{4})^2 m] - [I_2 + (H + \frac{S}{4})^2 m_2] - S_{ST}^2 m_{ST} \tag{5.55}$$

where

$$I = (\frac{\pi}{3}\rho R^2 L)\,[\frac{3}{80}(L^2+4R^2)$$

$$I_2 = (\frac{\pi}{3}\rho r^2 S)\,[\,\frac{3}{80}\,(S^2+4r^2)\,]$$

$$L = \frac{Rh}{r_u - r} \qquad (5.56)$$

Finally, the moment of inertia of the prosthetic thigh about its principal axes is obtained:

$$I_{XX}^{PT} = I_{ZZ}^{PT} = \left[I_{SO}+(|R_{PK}-R_{PH}| - S_{PT} - S_{SO})^2 m_{SO}\right]+\left[I_{ST}+(S_{PT} - S_{ST})^2 m_{ST}\right] \qquad (5.57)$$

(B) The anatomical lower limbs

Methods of estimation of the inertia properties of the anatomical lower limbs are presented in §2.3. With the anthropometric measurement results in Fig. 4.17(b) and the data in Table 2.1 & Table 2.2, we have

mass of the shank-foot segment

$$m_{US} = 0.111Cs+ 0.047Hti+ 0.074Ca+0.003+0.048Ca+0.027Lf \qquad (5.58)$$

mass of the thigh

$$m_{UT} = 0.074+ 0.123Cth+ 0.027\,(0.078p-0.27) \qquad (5.59)$$

the CG of the shank-foot segment from the KJC

$$l_{US} = C_2^{US} HGHT = 0.4673\ HGHT \qquad \textit{(HGHT: Height of the amputee)} \qquad (5.60)$$

the CG of the thigh from the HJC

$$l_{UT} = C_2^{UT}\ HGHT = 0.4169\ HGHT \qquad (5.61)$$

the moment of inertia of the shank-foot segment

$$I_{XX}^{US} = I_{ZZ}^{US} = m_{US}\,(C_3^{US} l_{US})^2 = m_{US}\,(0.3467\ l_{US})^2 \qquad (5.62)$$

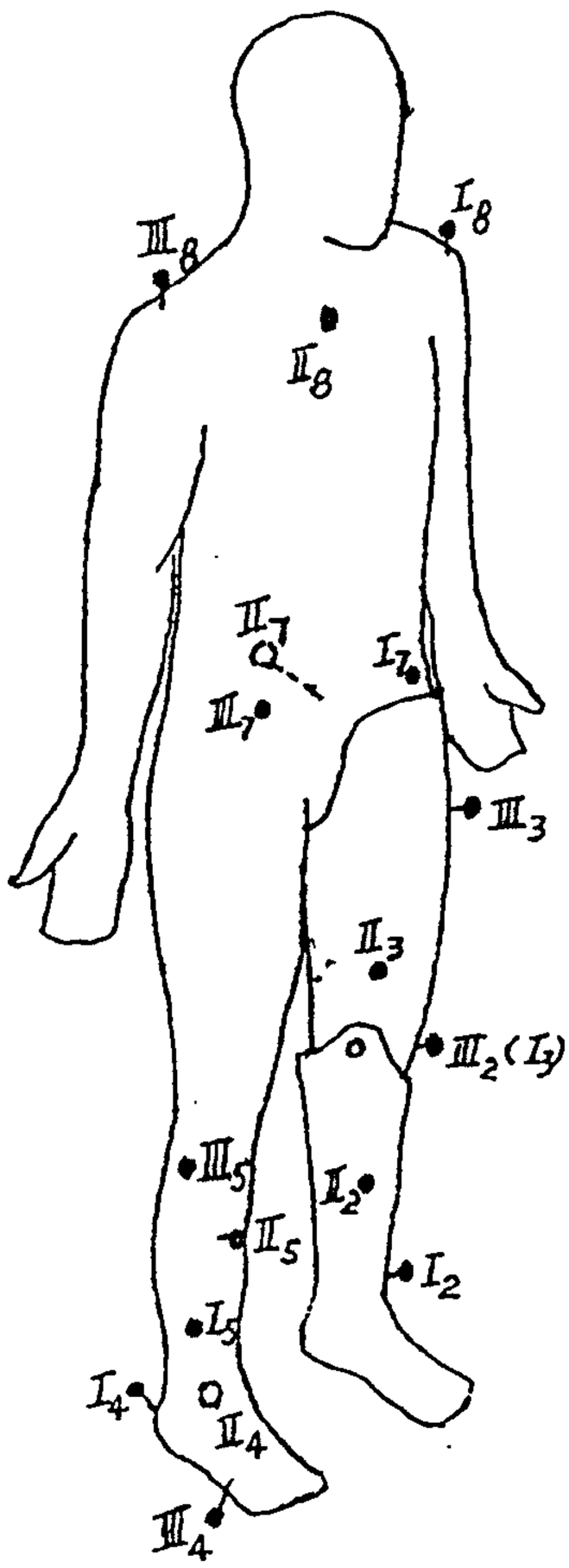

Fig. 5.6 Numberring system for marker frame of reference.

the moment of inertia of the thigh

$$I_{XX}^{UT}=I_{ZZ}^{UT}=m_{UT}(C_3^{UT}\,l_{UT})^2=m_{UT}(0.2912\,l_{UT})^2 \tag{5.63}$$

§5.3 Kinematic Analysis

Derivation of the position of the joint centres and the orientation of the model segments during locomotion is presented and the kinematic gait variables are defined.

§5.3.1 Marker frame of reference

Apart from the ground frame of reference and the principal axes of the segment, marker frame of reference at various segments are defined from the position of the body markers and served as a bridge between the first two frames of reference.

A standard procedure was adopted to establish the marker frame of reference. There are three markers on a body segment and they are numbered from I to III. The origin of the marker frame of reference is assigned to be on marker-I. The Y_m-axis is identified which directs from marker-I to marker-III, so that, its unit vector is

$$E_Y=\frac{R_{III}-R_I}{|R_{III}-R_I|}\,,\qquad e_Y=\frac{r_{III}-r_I}{|r_{III}-r_I|} \tag{5.64}$$

Then the X_m-axis is constructed as

$$E_X=E_Y\times\frac{R_{II}-R_I}{|R_{II}-R_I|}\qquad e_X=e_Y\times\frac{r_{II}-r_I}{|r_{II}-r_I|} \tag{5.65}$$

and finally

$$E_Z=E_X\times E_Y,\qquad e_Z=e_X\times e_Y \tag{5.66}$$

The numbering system of the markers for each body segment is shown in Fig. 5.6.

§5.3.2 Dynamic position of the Joint Centres

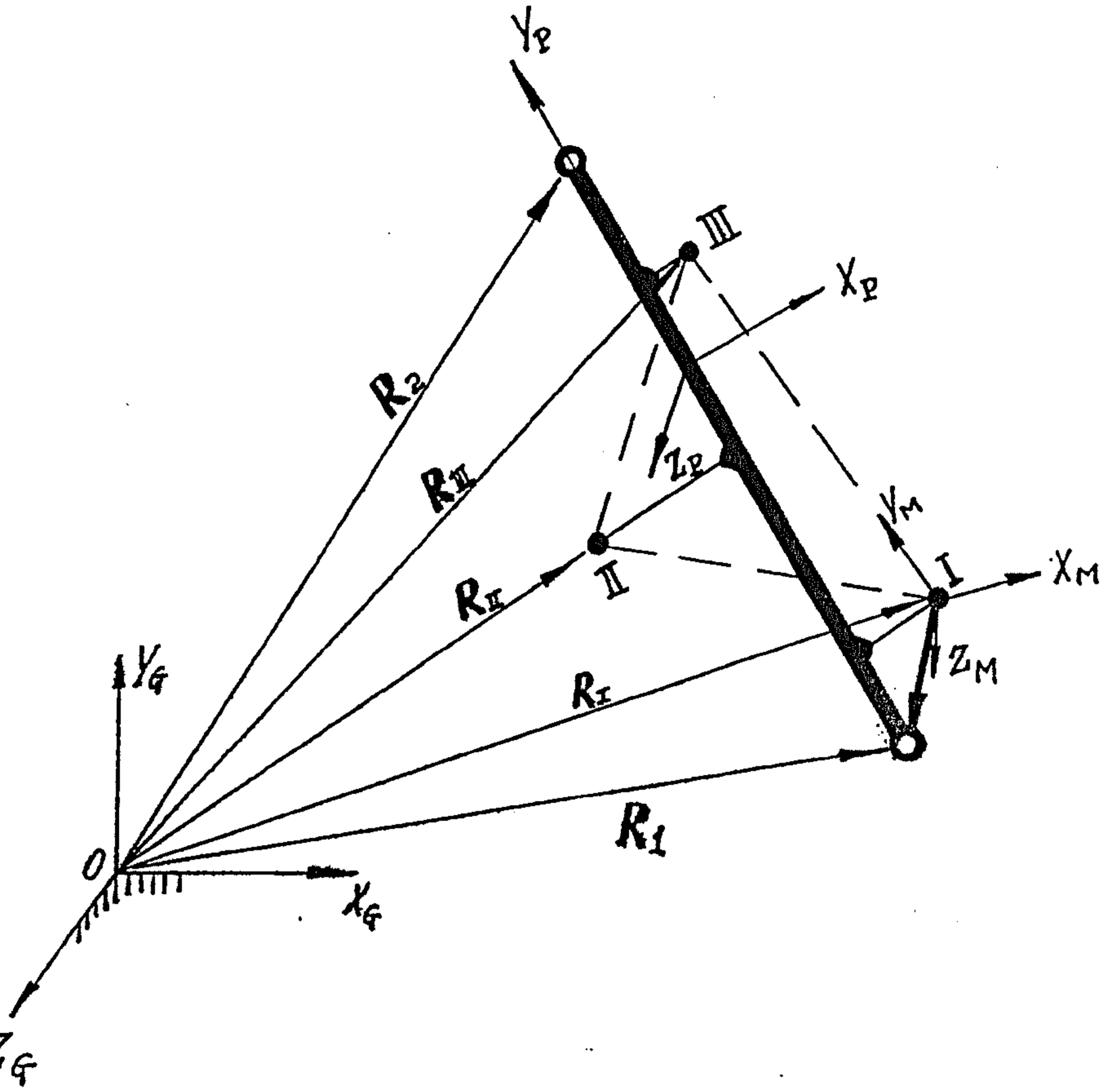

Fig. 5.7 Relationships among the ground frame of reference, marker frame of reference and principal axes of inertia. Determination of the dynamic position of the joint centres is also shown.

A standard procedure was used to determine the position of the joint centres during walking, as shown in Fig.6.7. First, the coordinates of the joint centres in static test are transformed into those with respect to the marker frame of reference of its adjacent segment, that is, the AJC and the KJC to the shank, the prosthetic HJC to the socket and the sound HJC to the pelvis. Mathematically, taking the unaffected ankle joint centre as an example, it follows that

$$\begin{bmatrix} X_{UA}^{M} \\ Y_{UA}^{M} \\ Z_{UA}^{M} \end{bmatrix} = \left[DCS_{A}^{U} \right]_{M-G} \begin{bmatrix} X_{UA}^{G} - X_{I}^{G} \\ Y_{UA}^{G} - Y_{I}^{G} \\ Z_{UA}^{G} - Z_{I}^{G} \end{bmatrix} \tag{5.67}$$

Since the position of the joint centre is constant with respect to the marker frame of reference, its dynamic position can be determined as

$$r_{UA} = \begin{bmatrix} x_{UA}^{G} \\ y_{UA}^{G} \\ z_{UA}^{G} \end{bmatrix} = \left[DCD_{A}^{U} \right]_{M-G}^{T} \begin{bmatrix} X_{UA}^{M} \\ Y_{UA}^{M} \\ Z_{UA}^{M} \end{bmatrix} + \begin{bmatrix} x_{I}^{G} \\ y_{I}^{G} \\ z_{I}^{G} \end{bmatrix} \tag{5.68}$$

or

$$r_{UA} = \begin{bmatrix} x_{UA}^{G} \\ y_{UA}^{G} \\ z_{UA}^{G} \end{bmatrix} = \left[DCD_{A}^{U} \right]_{G-M} \begin{bmatrix} X_{UA}^{M} \\ Y_{UA}^{M} \\ Z_{UA}^{M} \end{bmatrix} + \begin{bmatrix} x_{I}^{G} \\ y_{I}^{G} \\ z_{I}^{G} \end{bmatrix} \tag{5.69}$$

Having the joint centres defined during walking, the positions of the CG of each lower limbs are calculated

$$\begin{cases} r_{©s} = r_{©K} + C_{2}^{©S}(r_{©A} - r_{©K}) \\ r_{©t} = r_{©H} + C_{2}^{©T}(r_{©K} - r_{©H}) \end{cases} \tag{5.70}$$

§5.3.3 Dynamic orientation of the segments

Again, a standard procedure is followed to determine the orientation of the model segments during walking in terms of the orientation of the principal axes of the segment. Having the marker frame of reference and the principal axes of inertia of each model segment been identified with respect to the ground frame of reference, as described in §5.3.1 and §5.2.3, the relationship between the principal axes and the marker axes can be derived as

$$\left[DCS_{*}^{©}\right]_{P\text{-}G}^{T} = \left[DCS_{*}^{©}\right]_{M\text{-}G} \left[DCS_{*}^{©}\right]_{P\text{-}G}^{T} \tag{5.71}$$

or

$$\left[DCS_{*}^{©}\right]_{P\text{-}M} = \left[DCS_{*}^{©}\right]_{P\text{-}G} \left[DCS_{*}^{©}\right]_{M\text{-}G}^{T} \tag{5.72}$$

Since $[DCS^{©}]_{P\text{-}G}$ does not change during walking, the dynamic orientation of a segment can be found as

$$\left[DCD_{*}^{©}\right]_{P\text{-}G}^{T} = \left[DCD_{*}^{©}\right]_{M\text{-}G}^{T} \left[DCS_{*}^{©}\right]_{P\text{-}G}^{T} \tag{5.73}$$

that is,

$$\left[DCD_{*}^{©}\right]_{P\text{-}G} = \left[DCS_{*}^{©}\right]_{P\text{-}G} \left[DCD_{*}^{©}\right]_{M\text{-}G} \tag{5.74}$$

§ 5.3.4 Velocity and Acceleration

Linear velocity and acceleration of the joint centre of each model segment can be straight calculated by applying the differentiator (Equ. 5.21) to the displacement data. Mathematically,

$$v_{©\Delta} = \frac{dr_{©\Delta}}{dt}, \qquad a_{©\Delta} = \frac{dv_{©\Delta}}{dt} \tag{5.75}$$

It is followed that the linear velocity and acceleration of the CG of each lower limb be found

$$\begin{cases} v_{©s} = v_{©K} + C_2^{©S}(v_{©A} - v_{©K}) \\ a_{©s} = a_{©K} + C_2^{©S}(a_{©A} - a_{©K}) \end{cases} \tag{5.76}$$

$$\begin{cases} v_{©t} = v_{©H} + C_2^{©T}(v_{©K} - v_{©H}) \\ a_{©t} = a_{©H} + C_2^{©T}(a_{©K} - a_{©H}) \end{cases} \tag{5.77}$$

The angular velocity of a segment can be derived from the motion of its principal axes of inertia. According to Equ. 5.67, the position of any vector imbedded in a segment can be written as

$$\begin{bmatrix} x^P & y^P & z^P \end{bmatrix}^T = \begin{bmatrix} DCD \end{bmatrix}_{P\text{-}G} \begin{bmatrix} x^G & y^G & z^G \end{bmatrix}^T \tag{5.78}$$

or

$$\begin{bmatrix} x^G & y^G & z^G \end{bmatrix}^T = \begin{bmatrix} DCD \end{bmatrix}_{P\text{-}G}^T \begin{bmatrix} x^P & y^P & z^P \end{bmatrix}^T \tag{5.79}$$

Differentiating above equation leads to

$$\begin{bmatrix} v_x^G & v_y^G & v_z^G \end{bmatrix}^T = \frac{d}{dt}\begin{bmatrix} DCD \end{bmatrix}_{P\text{-}G}^T \quad \begin{bmatrix} x^P & y^P & z^P \end{bmatrix}^T$$

$$= \left(\frac{d}{dt}\begin{bmatrix} DCD \end{bmatrix}_{P\text{-}G}^T\right)\begin{bmatrix} DCD \end{bmatrix}_{P\text{-}G} \begin{bmatrix} x^G & y^G & z^G \end{bmatrix}^T \tag{5.80}$$

It can be proved that

$$\left(\frac{d}{dt}\left[DCD\right]_{P\text{-}G}^{T}\right)\left[DCD\right]_{P\text{-}G} = \begin{bmatrix} \dot{d}_{11} & \dot{d}_{21} & \dot{d}_{31} \\ \dot{d}_{12} & \dot{d}_{22} & \dot{d}_{32} \\ \dot{d}_{13} & \dot{d}_{23} & \dot{d}_{33} \end{bmatrix} \begin{bmatrix} d_{11} & d_{12} & d_{13} \\ d_{21} & d_{22} & d_{23} \\ d_{31} & d_{32} & d_{33} \end{bmatrix}$$

$$= \begin{bmatrix} 0 & -\omega_z & \omega_y \\ \omega_z & 0 & -\omega_x \\ -\omega_y & \omega_x & 0 \end{bmatrix} \tag{5.81}$$

where ω_i $(i=x, y, z)$ are angular velocity frame of reference. Explicitly, we have

$$\omega_X = \sum_{i=1}^{i=3} \dot{d}_{i2}\, d_{i3}\,, \qquad \omega_Y = \sum_{i=1}^{i=3} \dot{d}_{i3}\, d_{i1}\,, \qquad \omega_Z = \sum_{i=1}^{i=3} \dot{d}_{i1}\, d_{i2} \tag{5.82}$$

The angular acceleration of the segment with respect to the ground frame of reference is then obtained using the numerical differentiator in Equ. 5.21.

$$\varepsilon = \frac{d\omega}{dt} = \left[\frac{d\omega_X}{dt} \quad \frac{d\omega_Y}{dt} \quad \frac{d\omega_Z}{dt}\right] \tag{5.83}$$

§ 5.3.5 Kinematic Variables of Gait Analysis

The definitions of the kinematic variable used in this gait analysis are given as follows.

(A) Temporal-distance parameters

Since the arrangement of the two forceplates is such that each of them measures the ground reactions of only one leg for the whole stance phase, the first and last effective signals of the vertical component of the ground reactions indicate the heel strike and toe off events. For the FP1, if the first and last effective data occur at i_{LHS} *-th* and i_{LTO} *-th* sample, we have

$$left\ stance\ phase\ duration = 0.02\ (\ i_{LTO} - i_{LHS}\ )\qquad (s) \tag{5.84}$$

Similarly, for the FP2,

$$right\ stance\ phase\ duration = 0.02\ (\ i_{RTO} - i_{RHS}\ )\qquad (s) \tag{5.85}$$

In order to determine the cycle duration, the TV data has to be used since the second left heel strike is out of the platform of the FP1. Lanshamar (1987) presented an algorithm to estimated cycle duration from one landmark kinematic data:

$$V(j) = \frac{1}{n-1}\sum_{i=1}^{n-j} [\ x(i+j) - x(i)\ ]^2 \qquad (j = 1,2,\dots) \tag{5.86}$$

where $x(k)$ is the position data of the landmark, n the total number of samples, and $V(j)$ an object function to be minimized with respect to j. Trials of this method on the data of left heel marker failed to give reasonable results sometimes. Therefore, another algorithm is developed which searched for the first sample of the x-coordinate of the left heel marker that satisfying

$$x(i+7) - x(i) < 4\ (TV\ units) \qquad (i = i_{LTO}, i_{LTO+1}, \dots) \tag{5.87}$$

It is reckoned that this method is not very accurate due to error in TV-computer system, but it provides reasonable results without any failure. Therefore, we have

$$cycle\ duration = 0.02\ (\ i_{2LHS} - i_{LHS}\ )\qquad (s) \tag{5.88}$$

Once the temporal parameters be determined, the distance parameters are specified as follows:

$$\begin{aligned} left\ step\ length &= x_A(i_{RHS}\ ) \quad of\ the\ right\ AJC \\ &\quad - x_A(i_{LHS}\ ) \quad of\ the\ left\ AJC \\ right\ step\ length &= x_A(i_{2LHS}\ ) \quad of\ the\ left\ AJC \\ &\quad - x_A(i_{RHS}\ ) \quad of\ the\ right\ AJC \\ stride\ length &= left\ step\ length + right\ step\ length \end{aligned} \tag{5.89}$$

In calculating the mean walking speed, an averaging procedure is adopted.

First, the average speed of the left AJCs, KJCs, HJCs and the two acromial markers over a walking cycle are found by using the formula

$$V_j = \frac{x_j(i_{2LHS}) - x_j(i_{LHS})}{cycle\ duration} \tag{5.90}$$

and then the mean walking speed is found

$$V = \frac{1}{5}\sum_{j=1}^{5} V_j \tag{5.91}$$

(B) Trunk orientation angles

Trunk orientations in the A/P and M/L planes are represented by the orientations of the line connecting the two midpoints of the HJCs and the shoulder markers, that is,

$$\text{TOR EXT} = 57.3^\circ arc\ tg \left[\frac{(x_{PH} - y_{UH}) - (x_{10} + x_{12})}{(y_{10} + y_{12}) - (y_{PH} + y_{UH})}\right]$$

$$\text{TOR SWAY} = 57.3^\circ arc\ tg \left[\frac{(z_{10} + z_{12}) - (z_{PH} + z_{UH})}{(y_{10} + y_{12}) - (y_{PH} + y_{UH})}\right] \tag{5.92}$$

in which torso flexion and right sway are defined as positive. The transverse rotation of the trunk is approximated by the rotation of the line joining two shoulder markers, *ie*,

$$\text{TOR ROT} = 57.3^\circ\ arc\ tg\ \frac{x_{12} - x_{10}}{z_{12} - z_{10}} \tag{5.93}$$

and turning left is defined as positive.

(C) Thigh flexion/extension angle

Although the thigh can rotate about the hip joint in 3D, only the flexion/extension of the thigh is studied. It is defined as

$$\text{FEM FLEX} = 57.3^\circ \quad arc\ tg\ \frac{x_K - x_H}{y_H - y_K} \tag{5.94}$$

and flexion is positive.

(D) Knee joint flexion angle

Knee joint flexion angle is defined as the angle between the two principal *Y*-

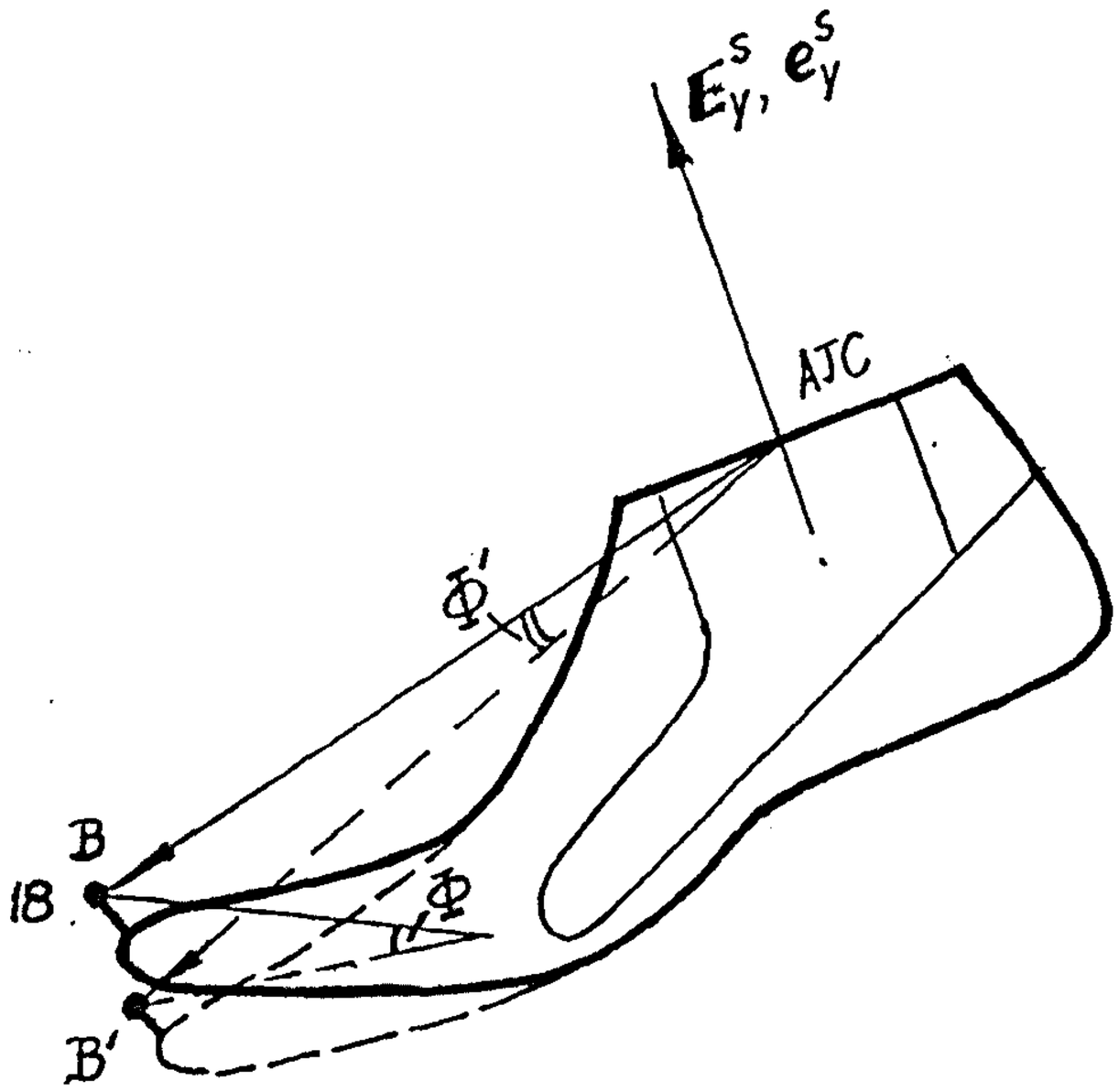

Fig. 5.8 Determination of the dorsi/plantar flexion of the prosthetic foot.

axes of the shank and the thigh, that is,

$$\text{KNEE FLE} = 57.3^\circ \arccos\left(e_y^S \cdot e_y^T\right) \tag{5.95}$$

(E) Ankle dorsi/plantar flexion angle

For the unaffected ankle joint, its rotation in A/P plane can be defined as the angle between the principal x-axis of the foot and the principal y-axis of the shank, *ie*,

$$\text{ANK DOR} = 57.3^\circ \left[\arccos\left(e_x^F \cdot e_y^S\right) - \arccos\frac{X_{UK}-X_{UA}}{|R_{UK}-R_{UA}|}\right] \tag{5.96}$$

In considering the prosthetic ankle joint, the angle between the shank y_P-axis and the line connecting the AJC and marker-18 is used

$$\Phi' = 57.3^\circ \left[\arccos\frac{E_Y^S \cdot (R_{18}-R_{PA})}{|R_{18}-R_{PA}|} - \arccos\frac{e_Y^S \cdot (r_{18}-r_{PA})}{|r_{18}-r_{PA}|}\right] \tag{5.97}$$

It is noted that Φ' represents different angles for different ankle-foot assemblies. For the Endolite system, it is the real dorsi/plantar angle of the Flexible ankle/foot assembly. For the SACH foot, however, it does not have a ankle joint and Φ' represents the bending angle of the fore foot, see Fig. 5.8. Since the distance from the marker-18 to the rotation centre of the fore-foot is about half of the distance from the marker-18 to the AJC, the real bending angle of the fore-foot can be approximated as

$$\text{ANK DOR} = 2\Phi' \tag{5.98}$$

§5.4 Kinetic Analysis

§5.4.1 The ground reactions

(A) Calibration of the Forceplate Data

As described in §4.2.1 , the digital data of the ground reaction from the

forceplates are in forms of the computer units which need to be calibrated and scaled into real mechanical values.

The scaling factors required depend on the setting of both the charge and buffer amplifiers. In this project, the charge amplifiers were set as

$$b = \begin{cases} 50\ mech.\ unit\ /\ volt. & for\ F_X, F_Z\ and\ M_Y \\ 200\ mech.\ unit\ /volt. & for\ F_Y, M_X\ and\ M_Z \end{cases}$$

and the buffer amplifiers were set

compoent	F_X	F_Y	F_Z	M_X	M_Y	M_Z
a	*1*	*1*	*2*	*1.25*	*2*	*1.25*

According to the results of latest calibration of the forceplate, the scaling factors are

	F_X	F_Y	F_Z	M_X	M_Y	M_Z
FP1	*-0.2843*	*-0.9923*	*0.1202*	*-0.2070*	*-0.0329*	*0.2068*
FP2	*0.2653*	*-1.0027*	*-0.1225*	*0.2070*	*-0.0329*	*-0.2117*

The unit for force scaling factor is (N/TV unit) and for moment scaling factor (N·m/TV unit). The function of the signs assigned to the scaling factors is to correct the positive directions of the resulting ground reactions acting on the body, so that they coincide with the ground frame of reference.Therefore, the forceplate data are calibrated as follows

$$Forces\ \mathbf{F'}_G\ (in\ Newtons) = scaling\ factor \cdot Forces\ \mathbf{F}_G\ (in\ 'PDP\ units')$$

$$Moment\ \mathbf{M'}_G\ (in\ N{\cdot}m\ ) = scaling\ factor \cdot Moment\ \mathbf{M'}_G\ (in\ 'PDP\ units')$$

These ground reactions are relative to the origin of the forceplate and need to be transformed into that with respect to the origin of the ground frame of reference. It is followed that

$$\mathbf{F}_G = \mathbf{F'}_G = \begin{bmatrix} FX_G & FY_G & FZ_G \end{bmatrix}$$

$$\mathbf{M}_G = \mathbf{M'}_G + \mathbf{R}_{FP} \times \mathbf{F'}_G = \begin{bmatrix} MX_G & MY_G & MZ_G \end{bmatrix} \qquad (5.99)$$

where

$$R_{FP} = \begin{cases} [-0.303 \quad -0.04 \quad -0.11] & \textit{for the FP1} \\ [\ 0.303 \quad -0.04 \quad 0.11] & \textit{for the FP2} \end{cases}$$

is the vector from the origin of the ground system to the origin of the forceplate.

(B) The centre of pressure (the CP)

The centre of pressure of the ground reactions is an effective point on the surface of the force platform where the resultant instantaneous force vector is applied. Noticing that at the CP the *MX* and *MZ* are vanishing, the CP can be determined with respect to the ground frame of reference as

$$y_G = 0, \quad y_G = \frac{-MZ_G}{FY_G}, \quad z_G = \frac{-MX_G}{FY_G} \tag{5.100}$$

The ground reactions acting at the CP are

$$F_{CP} = F_G, \quad M_{CP} = [0 \quad MY_{CP} \quad 0] \tag{5.101}$$

where

$$MY_{CP} = x_G \cdot FZ_G - z_G \cdot FX_G + MY_G \tag{5.102}$$

§ 5.4.2 Inter-Segmental Loads

Having the kinematic information of the model segments and the ground reactions been derived, the inter-segmental or the joint loads can be calculated as follows.

Referring to Fig. 5.9 in which a general model of a segment with all resultant forces and moments acting on the segment is shown. According to D'Alembert's principle, the equilibrium equation of the force for the system can be written as

$$F_1 + F_2 + F_i = 0 \tag{5.103}$$

where

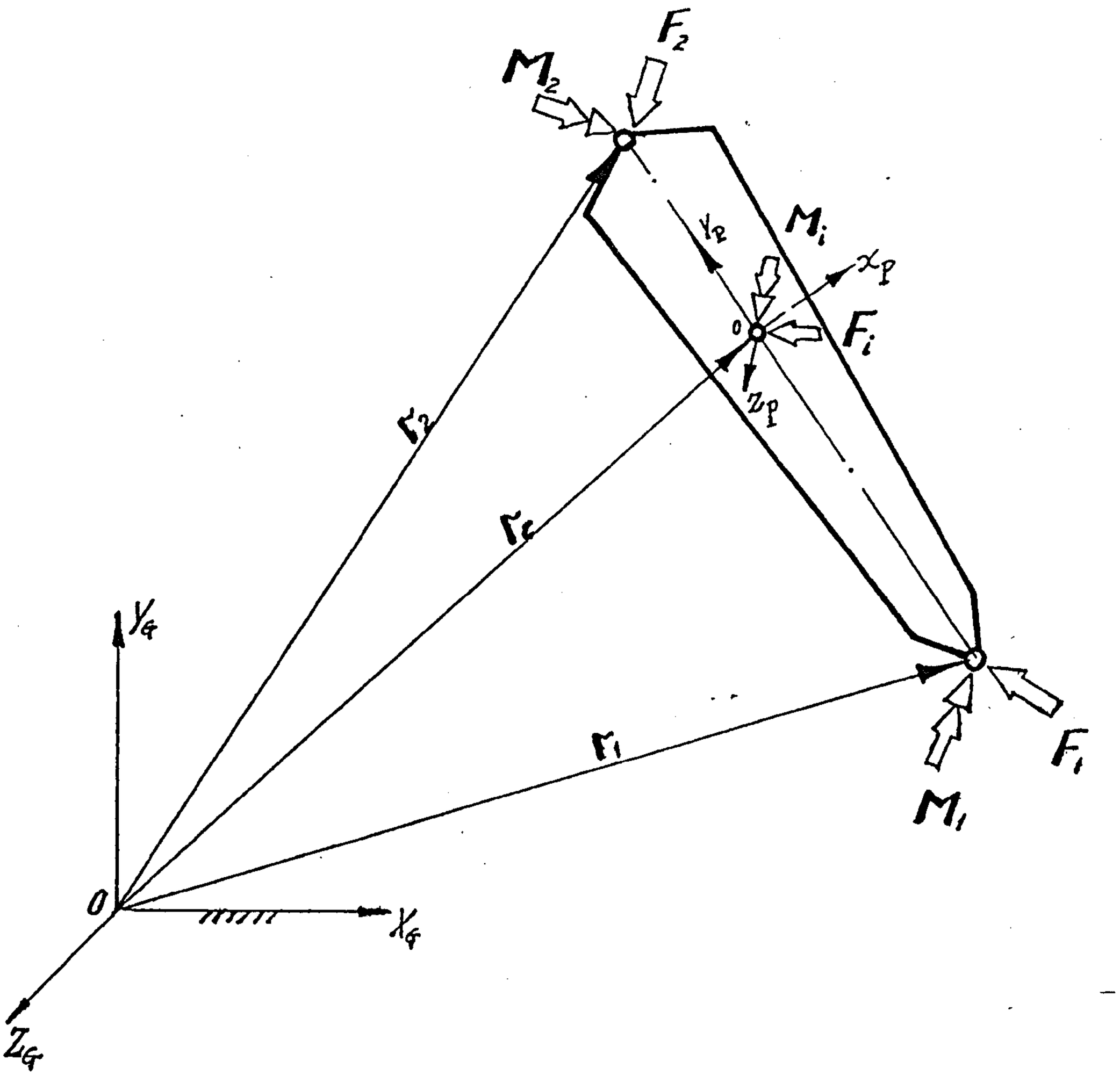

Fig. 5.9 An general segment with all resultant forces and moments applied to it.

F_1 = *resultant force acting at the distal joint . If the segment under consideration is the foot , F_1 denotes the ground reaction force acting at the centre of pressure.*

F_2 = *resultant force acting at the proximal joint and is resolved for.*

F_i = *resultant inertia force acting at the centre of gravity of the segment*

The resultant inertia force is determined by

$$F_i = - m (a_C + g) \tag{5.104}$$

in which a_C is acceleration of the CG and g=*[0 -0.9806 0]* is the gravity vector. Therefore the resultant force acting at the proximal joint can be found as

$$F_2 = - F_1 - F_i \tag{5.105}$$

Similarly, the D'Alembert's equation for the moment about the centre of gravity can be written as

$$M_1+M_2+M_i+(r_1-r_C) \times F_1+(r_2-r_C) \times F_2 = 0 \tag{5.106}$$

Therefore the resultant moment acting at the proximal joint is

$$M_2 = -M_1 -M_i - (r_1-r_C) \times F_1 -(r_2 -r_C) \times F_2 \tag{5.107}$$

in which

$$M_i = \left[DCD\right]^T_{P.G} \begin{bmatrix} I_{XX}\, \varepsilon_X^P - (I_{YY} - I_{ZZ})\, \omega_Y^P\, \omega_Z^P \\ I_{YY}\, \varepsilon_Y^P - (I_{ZZ} - I_{XX})\, \omega_Z^P\, \omega_Z^P \\ I_{ZZ}\, \varepsilon_Z^P - (I_{XX} - I_{YY})\, \omega_x^P\, \omega_Y^P \end{bmatrix} \tag{5.108}$$

The inter-segmental loads obtained above are with respect to the ground frame of reference. To refer them to the principal axes of inertia, the direction cosine matrix is used

$$F_2 = \begin{bmatrix} F_{2X}^P \\ F_{2Y}^P \\ F_{2Z}^P \end{bmatrix} = \left[DCD\right]_{P\text{-}G} \begin{bmatrix} F_{2X}^G \\ F_{2Y}^G \\ F_{2Z}^G \end{bmatrix}$$

$$M_2 = \begin{bmatrix} M_{2X}^P \\ M_{2Y}^P \\ M_{2Z}^P \end{bmatrix} = \left[DCD\right]_{P\text{-}G} \begin{bmatrix} M_{2X}^G \\ M_{2Y}^G \\ M_{2Z}^G \end{bmatrix}$$

These are the kinetic variables presented in next chapter.

Table 6.1 Subject Profiles

Subject Code	Sex	Age (years)	Mass (kg)	Height (m)	Prosthesis
NSAA	Male	38	69.2	1.67	(Normal Subject)
ALA	Male	56	78.6	1.78	Otto Bock
ALD	Male	52	78.0	1.71	Otto Bock
ALB	Male	62	88.4	1.80	Endolite
ARC	Male	53	72.0	1.73	Endolite

Explanation of the subject code:

1st code: A---Above knee amputee; NS---Normal subject.

2nd code: L---Left leg amputation; R---Right leg amputation.

3rd code: A, B, ... Subject identity code

4th code: A, B, ... Visit identification code.

CHAPTER 6

RESULTS AND DISCUSSION

This chapter, "Results and Discussion", is organized according to the gait analysis variables. For each gait variable studied, results obtained from a normal subject and four amputees with three different alignment change sequences are presented. Comparison was made between the normal subject and the amputees as a whole, and amongst different alignments in each alignment changes sequence for amputees. Because of the high interaction amongst the variables and the complexity of the problem, the discussion often involves more than one variable at a time

The normal individual was tested six times on the same day, and the results are presented in averaged form with plus and minus one standard deviation shown dotted. An overall variance of the data is presented and its definition is shown in Equ.2.3. Since symmetry between the left and right side exists for most biomechanical variables studied, data from one side only are presented.

The results from the amputees are shown in the form of the mean values of three test runs for each alignment setting, and their scatter will be discussed separately.

§ 6.1 Patient Profiles

A total of four above knee amputees participated in the work presented in this thesis and their general particulars are shown in Table 6.1. All the patients were in good health and their stumps were in good condition with full range of motion available at the hip joint. The two amputees wearing the Otto Bock system were fitted with quadrilateral suction sockets, uniaxial knee with extension bias and SACH foot, and are designated as "group-1" amputees. The "group-2" amputees wearing the

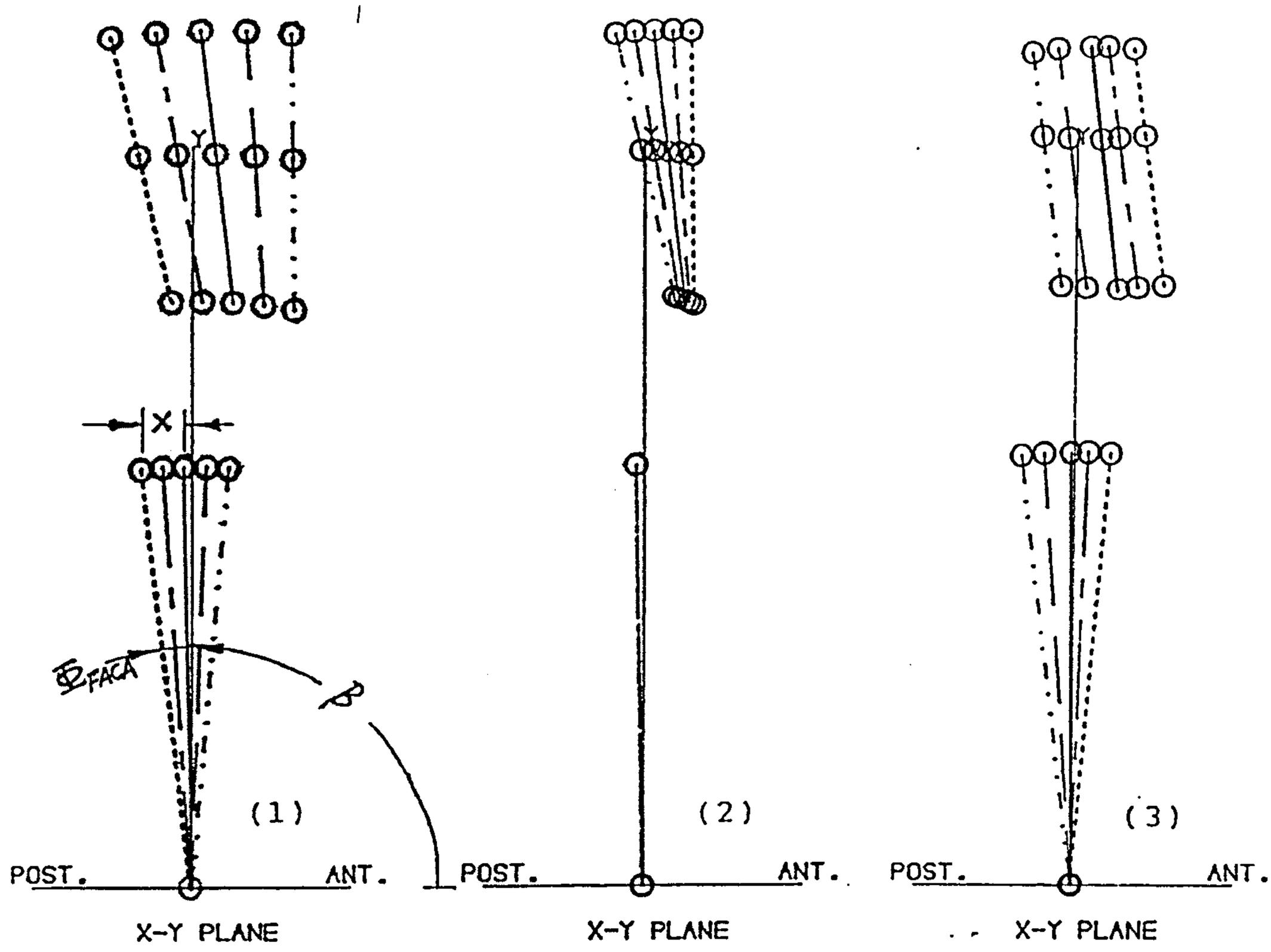

(FACS)	(SACS)	(FSACS)
Dorsi 6.0°	Extend 6.0°	Back 1.4cm
Dorsi 3.0°	Extend 3.0°	Back 0.7cm
Normal Ali.	Normal Ali.	Normal Ali.
Plant. 3.0°	Flexed 3.0°	Fore 0.5cm
Plant. 6.0°	Flexed 6.0°	Fore 1.0cm

Fig.6.1a The Alignment Change Sequences (ACS) with the AJC as a reference. (1) The Foot ACS (FACS); (2) The Socket ACS (SACS); (3) The Foot and Socket ACS (FSACS).

Endolite system had a metal socket with rigid pelvic band suspension, an Endolite Stabilize Knee with uniaxial knee joint and pneumatic swing phase control, and a flexible ankle-foot assembly (Multiflex foot) which allows three dimensional rotation of the ankle joint.

The basic information on the normal subject tested is also given in Table 6.1.

It is noted that the normal subject is much younger than the amputees. This difference in age is believed to have certain contribution to the gait difference between the normal subject and the amputees: younger people tends to walk faster. However, Murray *et al* reported that the temporal-distance parameters of gait and the angular displacement of the lower limbs did not vary systematically with age (from 20 to 55 years old) for normal men. Furthermore, comparing age with amputation, the latter certainly has much profound affects on gait. Therefore, despite the mismatch between the normal subject and the amputees,.the normal subject still can be used as a reference for assessing the pathology of the amputees' gait.

§ 6.2 Alignment Measurement Results

Table 6.2 shows the results of the alignment measurement on the prostheses tested. In addition to the alignment measurement results, the mean values and the standard deviations of the alignment parameters obtained by Zahedi *et al* (1984) are also shown in the table for comparison. It was found that all the parameters were within the range of three standard deviation s around the mean values except for the M/L tilt of the socket for patient ALA. High values for socket abduction are typical for patient ALA.

The three alignment change sequences (FACS, SACS, FSACS) employed during the experiments, as outlined in §4.4.2, are depicted in Fig.6.1(a). Since all alterations in alignment were restricted to the A/P plane, those parameters in the M/L and transverse planes remained unchanged and therefore are not included in the diagrams. The following discussion is also limited to the A/P plane.

Table 6.2 Alignment Measurement Results

(Normal alignment)

Subject Code	ALA	ALB	ARC	ALD	Mean (Zahedi *et al*,1986)
Socket:					
Forward set (cm)	1.6	-4.1	1.7	1.0	3.2 (±2.2)
Height (cm)	70.5	69.1	72.1	71.3	*
Set out (cm)	-0.2	-0.7	0.6	0.7	-0.4 (±1.4)
Flexion (°)	7.5	10.1	0.4	8.0	0.2 (±3.9)
Adduction (°)	-10.0	-2.3	0.2	-3.8	2.7 (±3.2)
Int. Rotation (°)	-0.5	0.0	-4.7	-4.1	*
Knee:					
Set Back (cm)	0.7	2.0	-1.0	0.8	0.4 (±1.3)
Height (cm)	40.8	44.0	40.6	40.7	*
Set out (cm)	0.1	0.1	-0.1	-0.1	0.0 (±1.1)
Medial tilt (°)	0.7	0.0	0.0	0.4	1.0 (±2.5)
Foot:					
Toe out (°)	-2.5	-7.3	4.1	-8.0	3.2 (±3.0)

NB: (1) *: No data available.

(2) Refer to Fig. 3.18 for sign convention.

The FACS changed all the alignment parameters: for the tilts by amounts equal to the angular changes of the foot and for the shifts by amounts determined by the following expression:

$$x = R\,[\sin(\Phi_{FACS}+\beta) - \sin(\beta)] \qquad (6.1)$$

where R is the distance from the AJC to the point under consideration , Φ_{FACS} change in foot angle (-6, -3, 0, 3, 6 degrees with plantar flexion positive) and β original inclination of the line connecting the AJC to the point. Due to the large height of the knee joint, even higher for the socket, considerable shifts occurred even with small angle changes at the foot. For patient ALA with 40.8 cm knee height and 70.5cm socket height, one degree of foot plantar flexion would result in 0.7cm backward shift of the knee joint centre and 1.2cm backward shift of the socket relative to the foot. However, it was noticed that the knee stability index (KSI), defined as the perpendicular distance from the KJC to the HJC-AJC line, was not influenced by the

FACS.

In the SACS, the adjustments were performed through the alignment mechanism above the knee joint centre, thus only the alignment parameters of the socket changed, that is, socket A/P tilt and A/P shift. The changes in socket tilt were merely the alignment changes performed, whereas the changes in socket shift can be calculated through Equ. 6.1 in which the AJC is replaced by the socket rotation centre (see §4.1.1) identified while measuring the alignment and Φ_{FACS} by Ψ_{SACS} (-6, -3, 0, 3, 6 degrees with flexion positive). Since the value of 'R' in Equ. 6.1 is about half of the value in the FACS, it is seen that the socket shifts in the SACS by about half of the amount in the FACS. It was noted that the KSI changed in the SACS, increasing with socket extension.

In the FSACS, adjustments made to the socket tilt in a flexion direction were coupled with adjustments made to the foot in a dorsiflexion direction and *vice versa*, that is,

$$\Psi_{FSACS}+\Phi_{FSACS}=\Psi_{SACS}+(-\Phi_{FACS}).$$

where

$$\Psi_{FSACS} = \Psi_{SACS} = (-6^\circ, -3^\circ, 0^\circ, 3^\circ, 6^\circ) \quad \text{(flexion positive)}$$

$$\Phi_{FSACS} = -\Phi_{FACS} = (6^\circ, 3^\circ, 0^\circ, -3^\circ, -6^\circ) \quad \text{(plantar flexion positive)}$$

The FSACS did not change the angular parameters of the prosthesis but altered the linear parameters. The amount of the KJC shift was equal to that in the FACS, while the socket shift was the combination of the FACS and the SACS. The KSI underwent the same changes as those in the SACS.

The above discussion is based on the definitions of the alignment parameters which are relative to the foot (see §4.1). If the socket is taken as a reference, quite a different picture emerges for alignment change sequences, see Fig. 6.1(b). It can now be seen that the FACS only altered the plantar/dorsi flexion of the foot, presenting a striking contrast to what was shown in Fig. 6.1(a). For the SACS, apart from the angular changes of the foot and shank, large shifts are exhibited in the AJC due to the

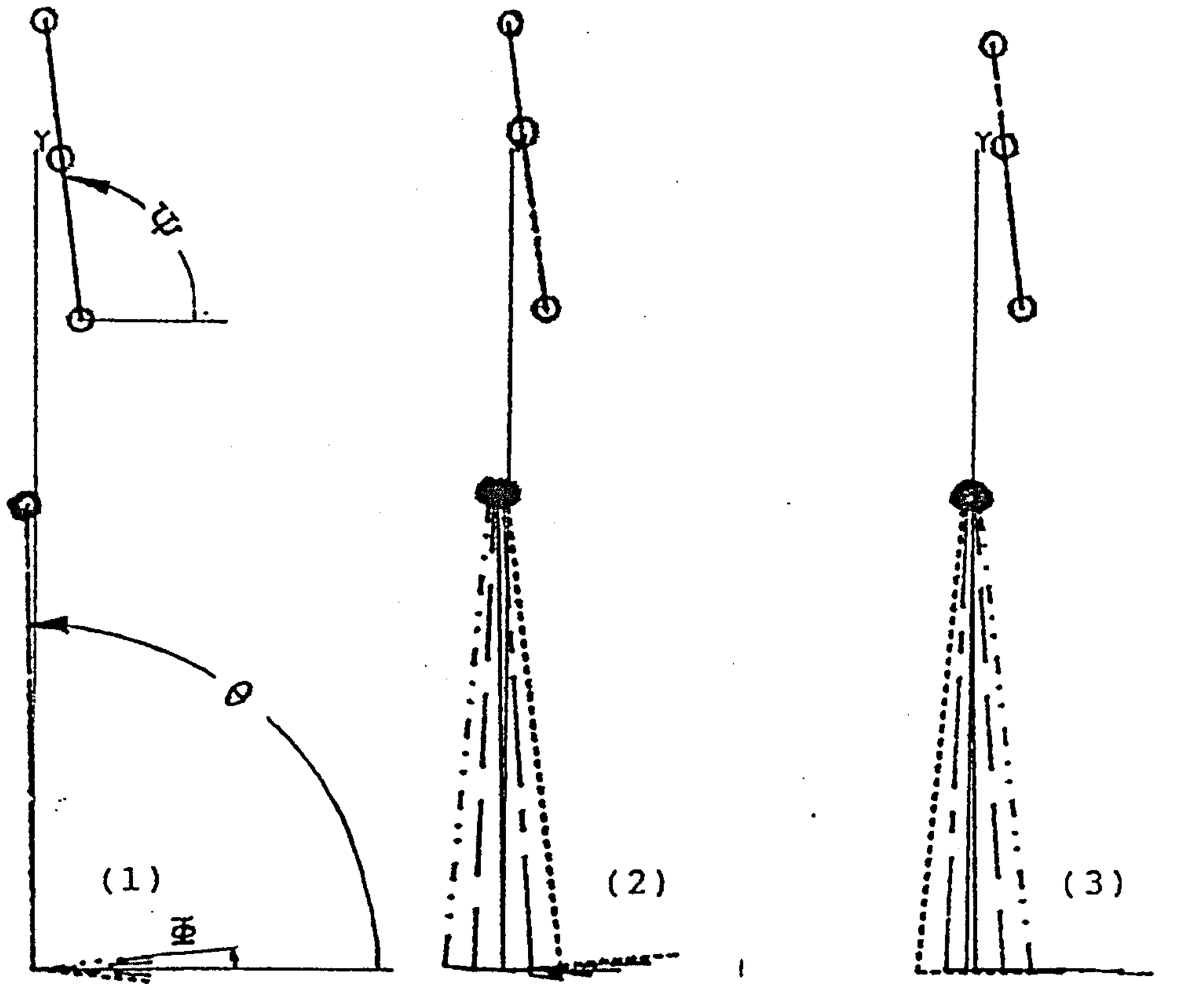

FACS	SACS	FSACS
Dorsi 6.0°	Extend 6.0°	Back 1.4cm
Dorsi 3.0°	Extend 3.0°	Back 0.7cm
Normal Ali.	Normal Ali.	Normal Ali.
Plant. 3.0°	Flexed 3.0°	Fore 0.5cm
Plant. 6.0°	Flexed 6.0°	Fore 1.0cm

Fig.6.1(b) The ACS with the socket as a reference.
(1) The FACS; (2) The SACS; (3) The FSACS.

length of the shank. In the FSACS, changes in the foot's orientation in the SACS are compensated by the FACS, leaving the foot orientation unchanged. However, large foot shifts are presented.

It would be interesting to visualize Fig. 6.1(b) as a composite picture of a prosthesis at walking. For each alignment setting of the three alignment changes sequences, a picture was assumed to be taken at an instant at which the prosthetic thigh reaches a constant angle relative to the ground. The pictures in the same alignment change sequence were superposed and the possible influence of the alignment changes could be assessed. Mathematically, the configuration of the prosthetic leg could be determined by the orientation angles of the foot, shank and thigh (socket) as shown in Fig. 6.1(b). If the configuration of the prosthesis at normal alignment be denoted by the subscript 'normal',that is,

$$\text{CNORM} = \{\Psi_{\text{NORMAL}},\ \theta_{\text{NORMAL}},\ \Phi_{\text{NORMAL}}\}$$

the configurations at the ACSs could be written as

$$\text{CFACS} = \{\Psi_{\text{NORMAL}},\ \theta_{\text{NORMAL}},\ \Phi_{\text{NORMAL}}-\Phi_{\text{FACS}}\} \qquad (6.2a)$$

$$\text{CSACS} = \{\Psi_{\text{NORMAL}},\ \theta_{\text{NORMAL}}-\Psi_{\text{SACS}},\ \Phi_{\text{NORMAL}}-\Psi_{\text{SACS}}\} \qquad (6.2b)$$

$$\text{CFSACS} = \{\Psi_{\text{NORMAL}},\ \theta_{\text{NORMAL}}-\Psi_{\text{FSACS}},\ \Phi_{\text{NORMAL}}\}$$

$$= \{\Psi_{\text{NORMAL}},\ \theta_{\text{NORMAL}}-\Psi_{\text{SACS}},\ \Phi_{\text{NORMAL}}\}. \qquad (6.2c)$$

where the "C" is included to denote "configuration".It can be seen clearly that the foot orientation angles are the same for the CFACS and the CSACS and that the shank orientations are the same for the CSACS and the CFSACS.

From the above discussion it is clear that the description of the alignment of a prosthesis differs depending on the reference considered. The question therefore arises as to which reference is the best. From the purely geometric point of view, any component of a prosthesis could serve equally well as a reference. The prosthetic foot, being convenient for locating the reference system, is used in this thesis for alignment measurement. However, when relating the prosthesis to the amputee, the socket seems to be the best choice since it is the socket that is directly connected to the

Table 6.3 Overall Temporal - Distance Parameters

(Normal ALignment)

	Speed (m/min)	Cycle Time (s)	Stride Length (m)	Step Length (% stride length)		Support Time (% cycle time)	
				Proth.	Sound	Proth.	Sound
Normal Subject	89.4 (0.004)	1.00 (0.02)	1.502 (0.033)	50 (3)		61 (1)	
A.K. Amputee	52.9 (0.098)	1.38 (0.07)	1.231 (0.082)	47 (4)	53 (5)	59 (3)	68 (4)
A.K Amputee*	60 (9.6)	1.38 (0.11)	1.36 (0.15)	46 (6)	54 (6)	60 (5)	68 (8)

NB: (1) Figures in bracket are ± one S.D.

(2) Refer to Fig. 2.21 for definition of the temporal-distance parameters.

(3) *: Data from Murray *et al* (1980).

patient. This argument will be developed further when the influence of the ACSs on the gait variables is discussed.

§ 6.3 Temporal-Distance Parameters

§ 6.3.1 Comparison between the normal subject and the amputees

Table 6.3 shows the averaged temporal-distance parameters for the subjects tested. Data for the amputees included only those with normally aligned prostheses. A total of 21 tests was averaged. The results were found to be consistent with those published in the literature, such as James & Oberg (1973) and Murray *et al* (1980).

Comparing the normal with the amputees, it was found that the amputees walked with significantly ($\rho \leq 1\%$) lower values in walking speed, cadence and stride length. It was also found that the step length and support time of the amputees were significantly less at the prosthetic side than at the sound side.

§ 6.3.2 Comparison among different alignments

Table 6.4 Temporal-distance Parameters for the FACS

Units: %

	Dsi 6	Dsi 3	Normal	Plt 3	Plt 6
Speed	100	100	100	97	98
	(3)	(5)	(3)	(2)	(4)
Cycle Duration	102	100	100	101	100
	(4)	(5)	(2)	(3)	(4)
Stride Length	101	100	100	97	97
	(4)	(2)	(2)	(3)	(4)
Step Length / Stride Length:					
Prosthetic	47	48	47	47	47
	(2)	(2)	(2)	(2)	(2)
Unaffected	53	52	53	53	53
	(2)	(2)	(2)	(2)	(2)
Support Time / Cycle Duration:					
Prosthetic	57	57	58	58	59
	(3)	(2)	(3)	(2)	(2)
Unaffected	66	63	66	66	68
	(2)	(3)	(3)	(3)	(3)

Table 6.5 Temporal-distance Parameters for the SACS
Units: %

	Ext. 3	Ext. 6	Normal	Flex 3	Flex 6
Speed *	93 (6)	96 (5)	100 (3)	99 (5)	95 (7)
Cycle Duration *	105 (5)	104 (3)	100 (2)	99 (3)	102 (2)
Stride Length	98 (5)	100 (3)	100 (2)	97 (2)	98 (5)
Step Length / Stride Length *					
Prosthetic	44 (1)	46 (4)	47 (2)	47 (2)	48 (2)
Unaffected	56 (2)	54 (4)	53 (2)	53 (2)	52 (2)
Support Time / Cycle Duration					
Prosthetic	56 (1)	58 (1)	58 (3)	55 (2)	57 (1)
Unaffected	68 (2)	65 (3)	66 (3)	67 (1)	67 (2)

Table 6.6 Temporal-distance Parameters for the FSACS
Units: %

	Back 2	Back 2	Normal	Fore 1	Fore 2
Speed *	91 (2)	90 (2)	100 (3)	97 (4)	102 (6)
Cycle Duration	109 (2)	114 (9)	100 (2)	100 (3)	100 (3)
Stride Length	97 (2)	97 (6)	100 (2)	98 (5)	99 (7)
Step Length / Stride Length *					
Prosthetic	43 (2)	45 (2)	47 (2)	48 (2)	52 (1)
Unaffected	57 (2)	55 (2)	53 (2)	52 (2)	48 (1)
Support Time / Cycle Duration:					
Prosthetic	58 (2)	58 (2)	58 (3)	56 (2)	55 (2)
Unaffected	69 (2)	66 (4)	66 (3)	68 (2)	70 (2)

In order to cancel any influences of the patient profiles on the results as much as possible, some parameters, to be discussed below, were expressed as a percentage of their values obtained with normal alignment. These were the walking speed, cadence and stride length.

The averaged temporal-distance parameters for the FACS are shown in Table 6.4. No significant changes ($\rho \leq 5\%$) were found. However, there was a tendency for the walking speed for the plantar flexed foot to be reduced, mostly due to shorter stride length.

Table 6.5 shows the results of the SACS in which parameters with a '*' were found significantly different ($\rho \leq 5\%$). The patient walked significantly slower when the alignment was changed, and the greater the changes in alignment, the more slowly they walked. The differences in walking speed were largely due to longer walking cycle durations and to a less extent due to shorter stride length. It was also found that the step length of the prosthesis increased and the step length of the sound leg decreased as the socket inclination was increased in a flexion direction.

The results for the FSACS are presented in Table 6.6. Due to both longer cycle duration and shorter stride length, the walking speed was significantly slower when the knee joint centre was shifted backwards than that for the normal alignment. The step length of the prosthesis for the alignment with the KJC backwards was also found to be shorter compared with that for the normal alignment.

Due to the fact that the measuring system used is not best suited for the recording of the temporal-distance parameters, no definite conclusion can be reached on the acquired data. Only the trends indicated above can be reasonably discussed.

§ 6.4 The Trunk Angular Movements

§ 6.4.1 The normal subject

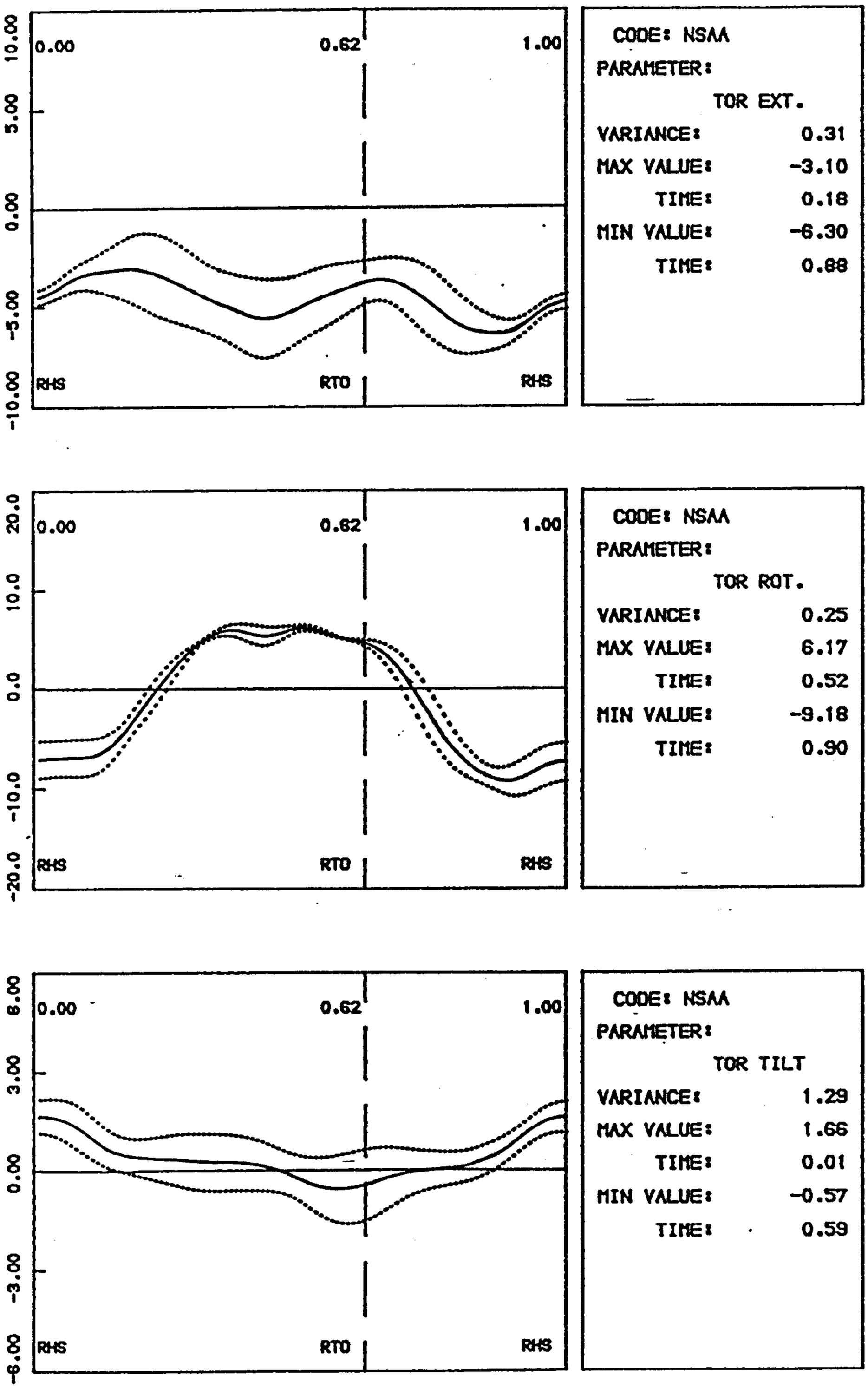

Fig.6.2 Angular displacements of the trunk of a normal subject test. All units are in degrees.

Fig. 6.2 shows the angular motions of the normal subject. It was observed that symmetry existed in the curves between the left and right steps. In the coronal plane (TRUNK M/L TILT), in which left--to-right tilt of the shoulder girdle relative to the pelvis was regarded positive, the torso tilted towards the standing leg during most of the stance phase, thus shifting the CG of the trunk towards the standing leg and assisting in the elevation of the hip of the swing leg. It was noted that the curve shows a complete oscillation during a walking cycle. The peak value of the variable is about 2 degrees. An overall variance (see Equ.2.3 for definition) of up to 129% was found, which may be partly due to the small magnitudes of the variable. In the transverse plane (TRUNK ROTATION.), in which a left-turn of the shoulder girdle was defined as positive, the shoulder girdle reached its maximum turning towards the leg which was at heel strike, then started to turn back at the toe-off of the contralateral leg. The girdle was at the neutral position at mid-stance, then continued to rotate towards the swinging contralateral leg and reached to another peak rotation value as the contralateral leg approached HS. It was noted that the curve displays a full oscillation during a walking cycle. The peak-to-peak value was about 13 degrees which was close to 10° obtained by Inman *et al* (1981). A variance of 25% was found which can hardly be regarded large for a biomechanical variable. The trunk movement in the saggital plane (TRUNK A/P TILT) performed two complete oscillations during a walking cycle about a base line of approximately 4 degrees flexion. During the early part of the stance phase the flexion angle decreased, then increased during the mid-stance phase and decreased again during late stance phase.

§ 6.4.2 The amputees with normal alignment

Table 6.7 shows the median and range of the trunk angular movements of the subjects tested. Data for the amputees included only those with normal alignment . Comparing the amputees with the normal subject, the ranges of the movements were found to be significantly different ($\rho \leq 1\%$), that is, movements in the A/P and M/L

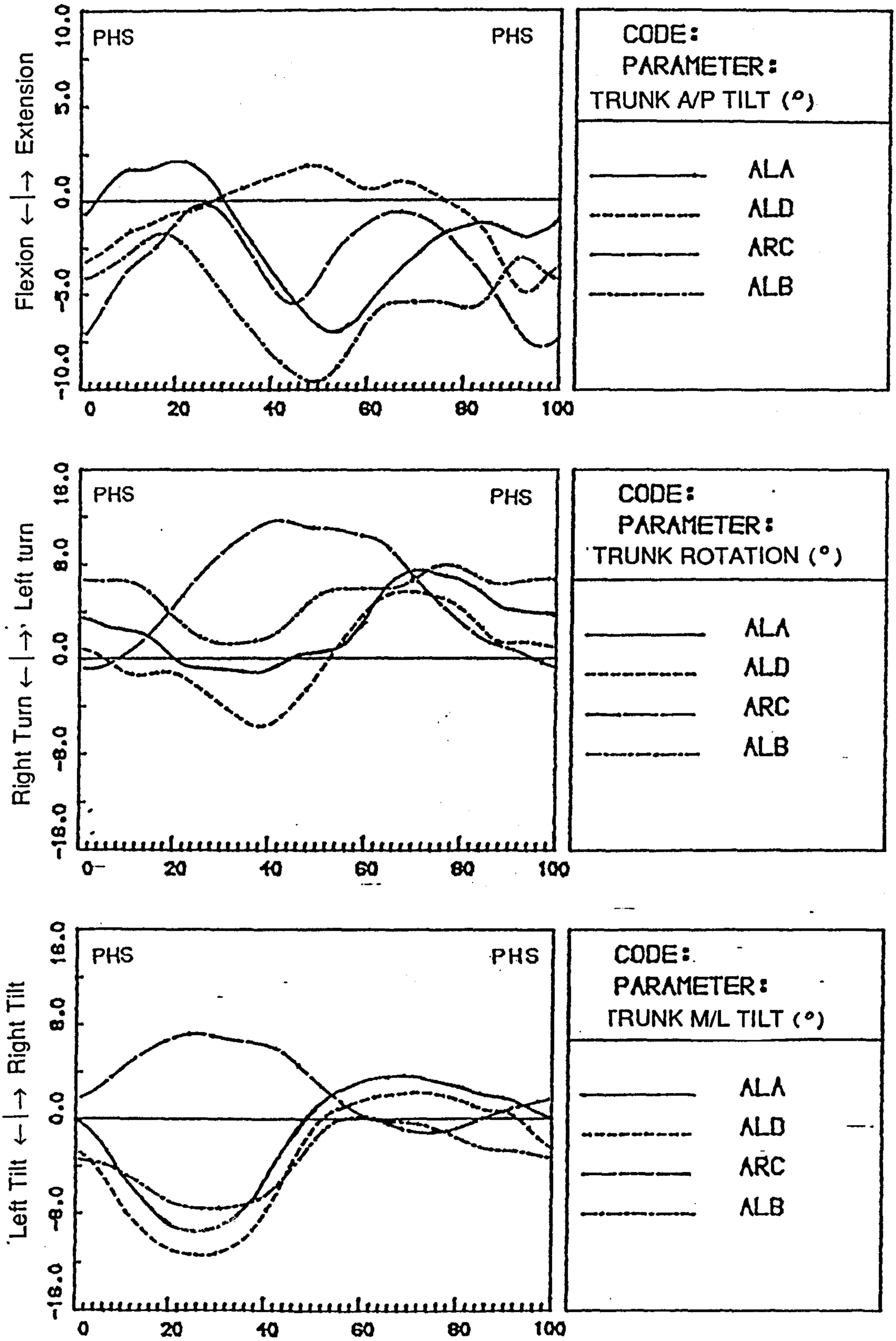

Fig.6.3 Angular displacements of the trunks of the above-knee amputees tested with normal alignments.

Table 6.7 Median and Range of the Trunk Angular Motion

Patient Code	Median M/L	Median Rot.	Median A/P	Ranges M/L	Ranges Rot.	Ranges A/P
NSA	0.5°	-2°	5°	2°	15°	3°
ALA	-3°	3°	-2°	13°	9°	9°
ALD	-5°	0°	-2°	14°	12°	7°
ALB	-4°	5°	-5°	8°	9°	7°
ARC	4°	5°	-4°	6°	13°	8°

planes were much larger for the amputees. These findings indicate that the amputees came across greater difficulties in maintaining M/L and A/P balance. It was also found that the median of the trunk medio-lateral tilts were biased towards the affected side, so that the trunk was more directly over the prosthesis during the stance phase and less hip function was needed for balance. It was also noted that the group-2 amputees (Endolite) displayed much smaller M/L tilt range than the group-1 amputees did and it perhaps is due to the hip and pelvic band worn by them.

Fig. 6.3 shows the patterns of the trunk angular displacements for the four amputees as tested with normal alignment prostheses. In the diagrams, the movements are presented from prosthetic heel strike to a successive prosthetic heel strike. In the coronal plane, the curves displays a consistent pattern: a complete oscillation during a walking cycle. It was noted that the amputees swayed to the prosthetic side considerably during the prosthetic stance phase. The transverse rotation of the shoulder girdle still shows a full oscillation during a walking cycle, but with more variations in the median and the range. The patterns of extension/flexion of the trunk are variable: three of the amputees displayed two full oscillation during a walking cycle, and one showed only one oscillation.

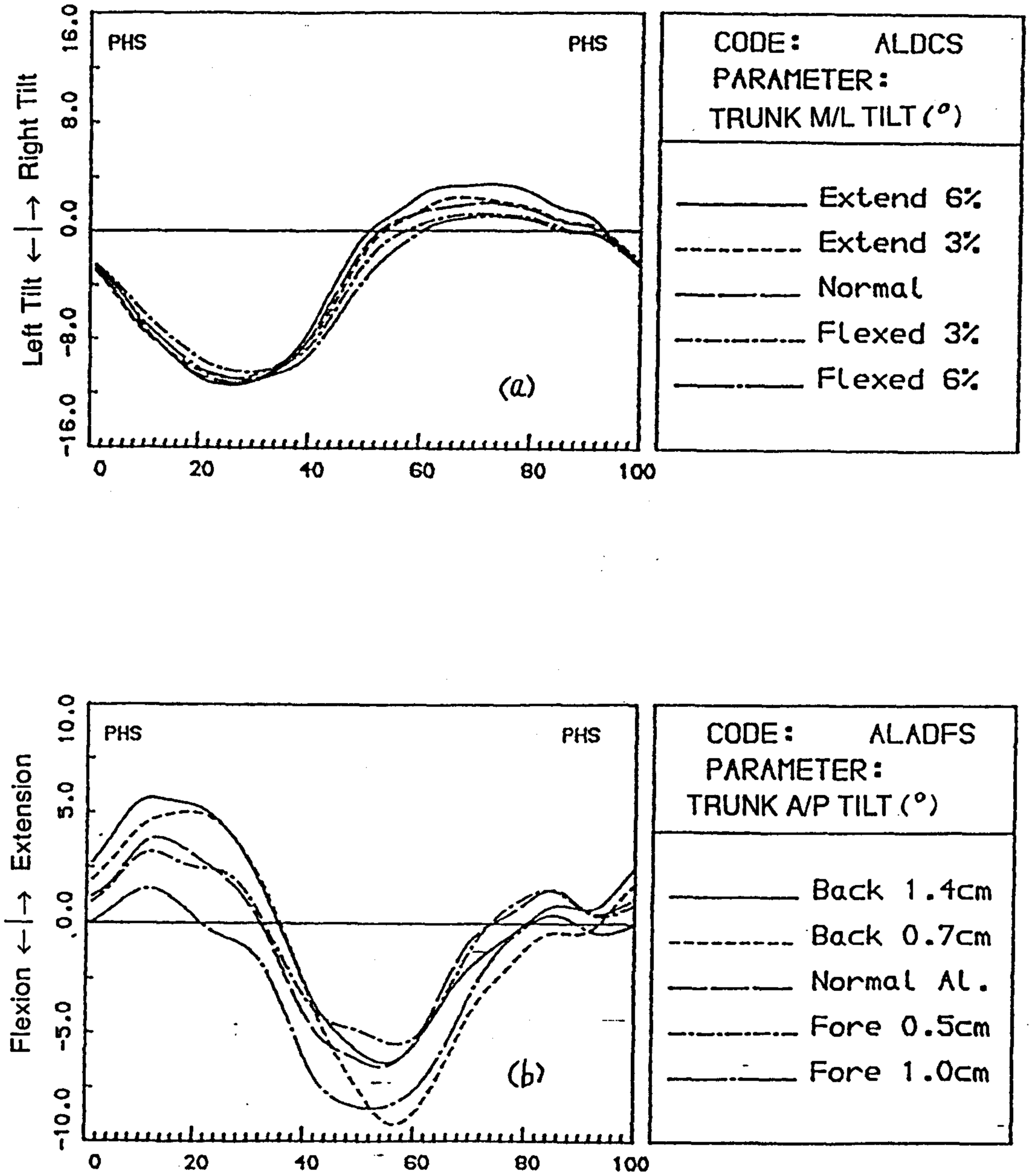

Fig.6.4 Typical trends of changes in the angular displacements of the trunk. (a) Effects of the SACS; (b) Effects of the FSACS.

§ 6.4.3 Influences of the ACSs

Generally, apparent differences were found in angular displacements of the trunk of the amputees between different steps and different alignments. However, the variations did not show any consistency in shape changes nor in parameter values, such as peak values.

Nevertheless, two trends were observed as discussed below.

In the SACS, it was observed that the lateral tilt of the trunk during prosthetic swing phase increased as the socket was changed towards an extension direction, as shown in Fig. 6.4(a). This finding was made in all the amputees tested, being most evident in those amputees wearing Otto Bock systems. The reason for this trend may lie in the fact that extending the socket, which was often originally flexed, would increase the effective length of the prosthesis, and as a result, the amputee would lean more over his supporting sound leg so as to ensure that the swinging prosthesis was clear of the ground.

In the FSACS, the trunk extension angles for amputee ALA decreased significantly during the first half or so of the prosthetic stance phase as the prosthetic knee was positioned progressively forwards, as demonstrated in Fig. 6.4(c). Another amputee who underwent the FSACS also showed this tendency but without statistical significance. As described in §6.2, the FSACS greatly changed the prosthetic knee stability. Decreasing the trunk extension angle has two effects, firstly it stretches the hip extensors to improve their function, and secondly it shifts the CG of the trunk forward in order to increase the moment lever of the trunk weight about the KJC, Both these effects increase the extension moment about the KJC, and thus prevent the prosthetic knee from collapsing

In summary, it might be stated that every amputee displayed his own pattern of the trunk angular movement and the alignment changes performed at the prosthetic foot or socket did not affect the trunk angular movement significantly whereas the alignment change in both the foot and socket had greater effects on the trunk angular movement. Since the patient was allowed to spend a few minute to get accustomed to

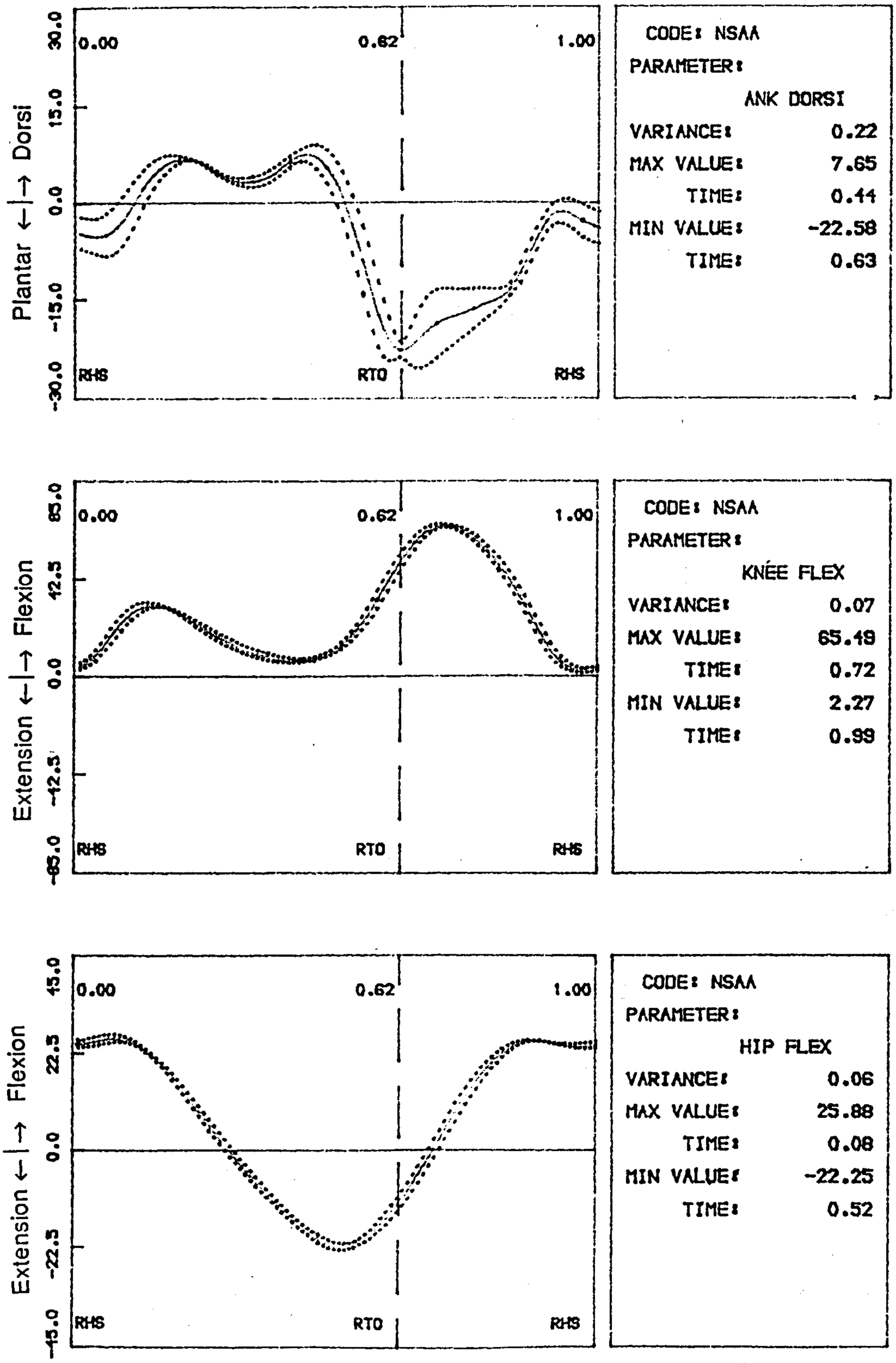

Fig.6.5 The sagittal angular displacements of the lower limb of the normal subject. All units are in degrees.

the changed alignment before actual test walk, it is therefore appears that it is difficult, if possible, to change an amputee's pattern of trunk angular movement through alignment changes to such an extent that it is the same as that of a normal subject.

§ 6.5 Angular Displacements of the Lower Limbs

§ 6.5.1 The normal subject

The saggital angular displacements of the lower limbs for the normal subject tested are shown in Fig. 6.5. The general shape of all curves is similar to that reported in the literature. The foot went into plantar flexion just after heel strike to about 5 degrees, then into dorsi flexion to about 8 degrees during the mid-stance phase and then into plantar flexion to 23 degrees at push off. The knee was flexed immediately after heel strike to about 30 degrees to absorb impact and flexed to 65 degrees at the beginning of the swing phase. The thigh was flexed about 26 degrees at heel strike and then extended about 22 degrees at late stance phase. The displacements of the thigh and the knee were highly consistent with about 7% overall variance (approximately 5 degrees). The ankle angles showed a relatively higher variability.It is thought that this variability is due to inaccuracy of the kinematic measuring system at ankle level.

§ 6.5.2 Comparison between the normal and the amputees

Fig. 6.6 shows patterns of angular displacements of the lower limbs for the amputees in the saggital plane for normal alignment. On the sound side, no great differences were found in the thigh and knee joint angles between the normal and the amputees. However, the patterns of the ankle dorsi/plantar flexion curves of the amputees wearing the Otto Bock prostheses differed from that of the normal in that the ankle was plantar flexed excessively during the stance phase. This action caused a

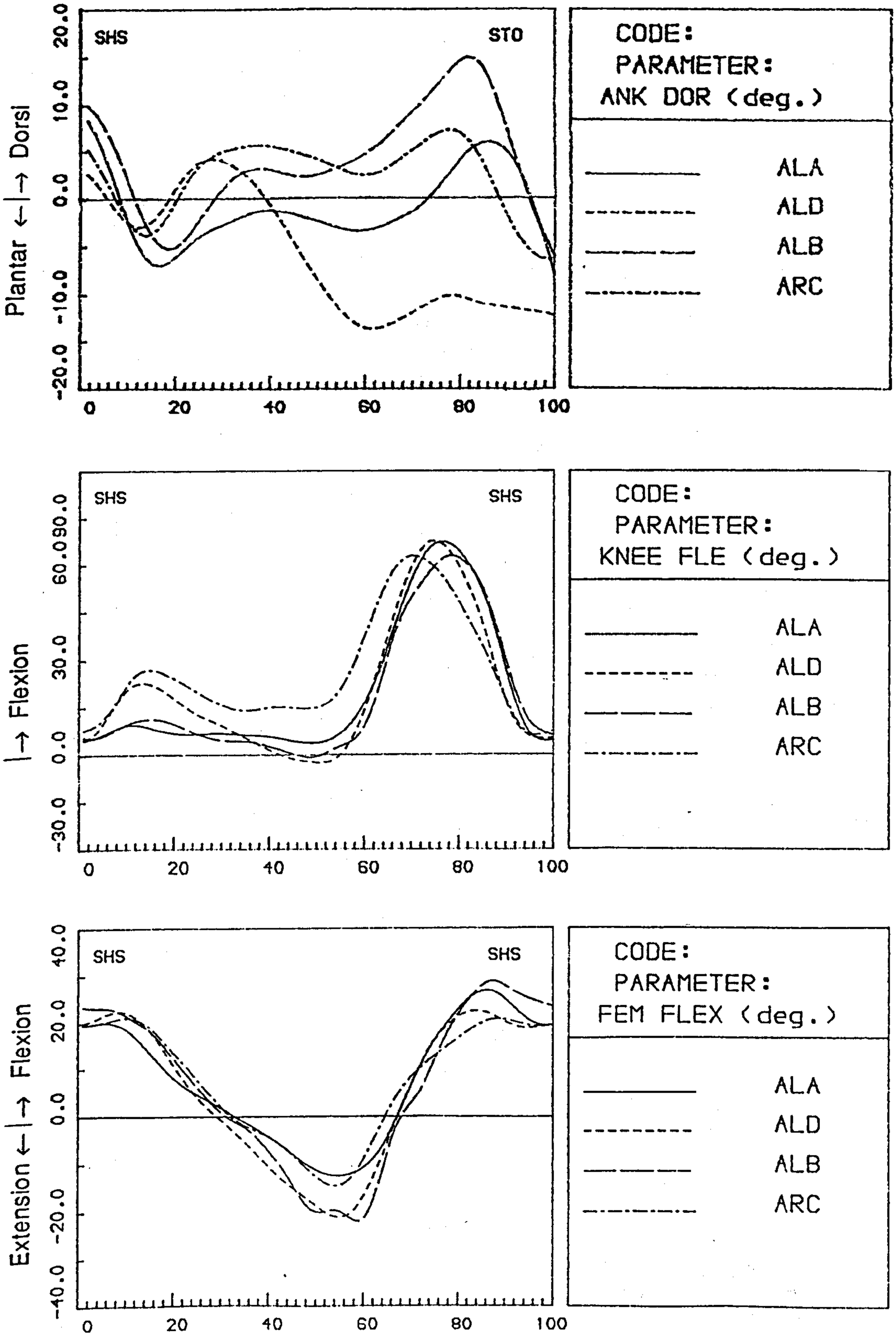

Fig.6.6a The sagittal angular displacements of the sound lower limb of the amputees. All units are in degrees.

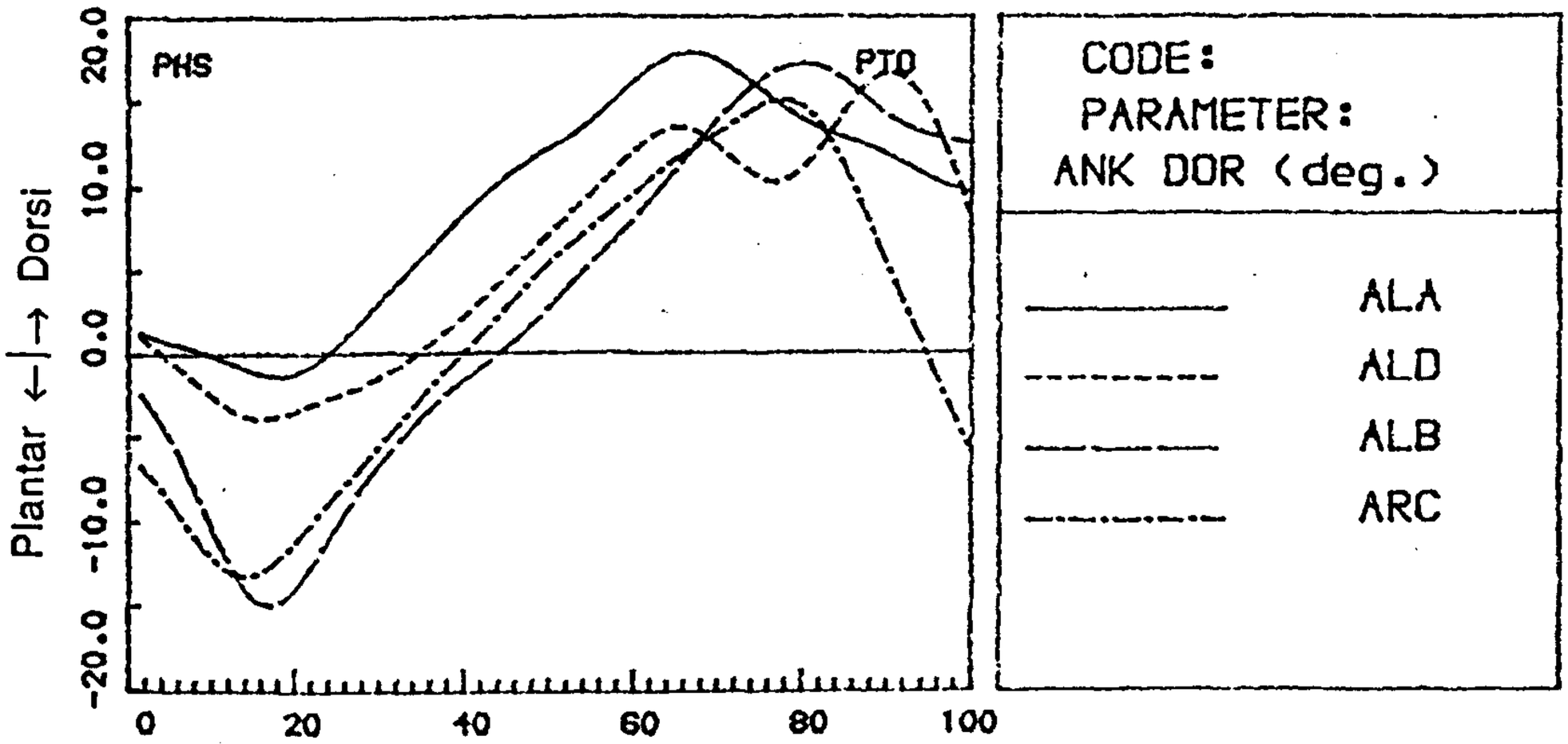

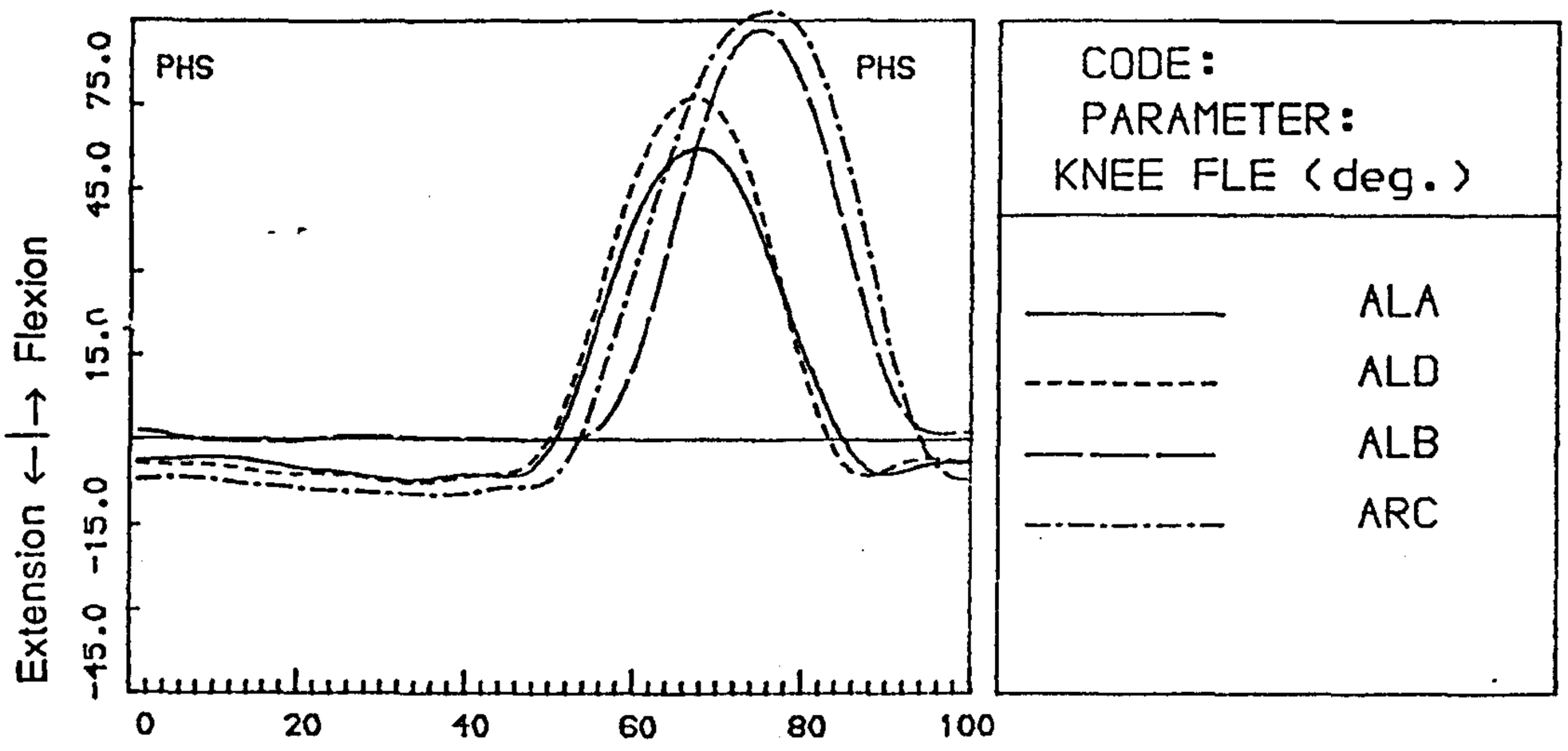

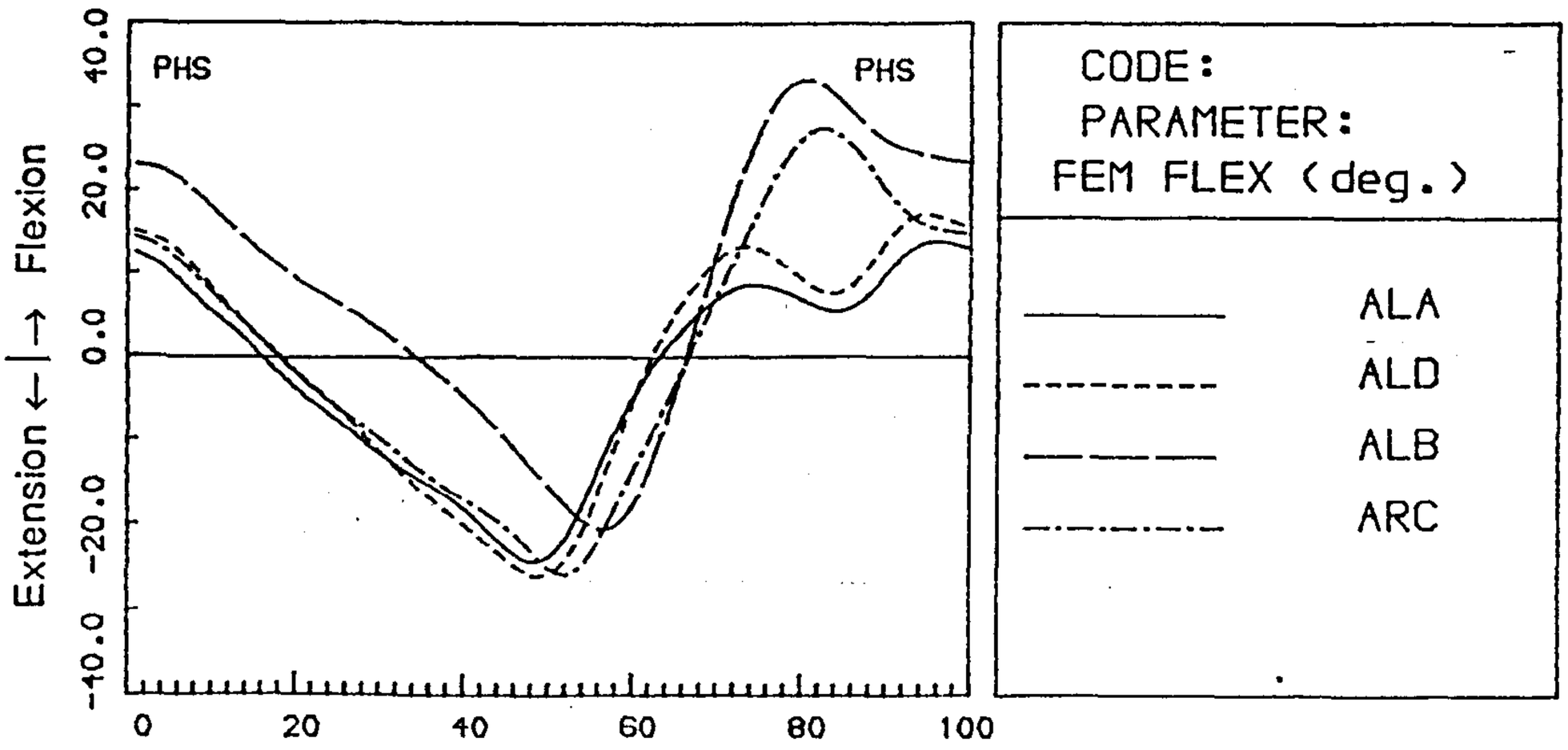

Fig.6.6b The sagittal angular displacements of the prosthetic lower limb of the amputees. All units are in degrees.

'vaulting' effect, ie, elevation of the body so that the swinging prosthesis could swing through without stubbing the toe. Group-2 amputees did not show this gait deviation. The reason behind this is not know but one explanation could be the shorter prostheses fitted to the group-2 amputees.

On the prosthetic side, large differences were exhibited between the normal and the amputees. In the case of the thigh flexion/extension angle, the general shape was similar to the normal's, but group-1 amputees showed differences in the patterns during swing. During this period, the patient held his prosthetic thigh in a constant or even reduced flexion angle in order to wait for the prosthetic shank and foot to swing forward, and the corresponding curves displayed a trough during that period. The prosthetic knee did not display any flexion at all during the prosthetic stance phase, and was fully extended and locked. The patterns of the prosthetic ankle dorsi/plantar flexion angles depended on the type of ankle-foot assembly fitted to the amputees. As described in §5.3.5, no movement occurred between the foot and the shank in the case of the SACH foot, and the curve represents bending of the fore foot, while for the Multiflex ankle-foot assembly, the curves represents true ankle angles. It was observed that the SACH foot displayed little, if any, plantar flexion during early stance phase due to heel compression, followed by about 15 degrees bending of the fore foot at about heel off. The Multiflex foot underwent approximately equal dorsi flexion and plantar flexion during the stance phase.

§ 6.5.3 Influences of the ACS

The ACS was not found to cause any significant and consistent changes in the saggital angular displacements of the sound lower limbs for the amputees tested. Effects of the ACS on the prosthetic lower limbs are presented as follows.

Fig. 6.7 shows the angular displacements of the prosthetic lower limbs for an amputee who underwent the FACS. Results from other amputees tested had similar changes in the patterns. It was found that the angular displacements of the thigh and

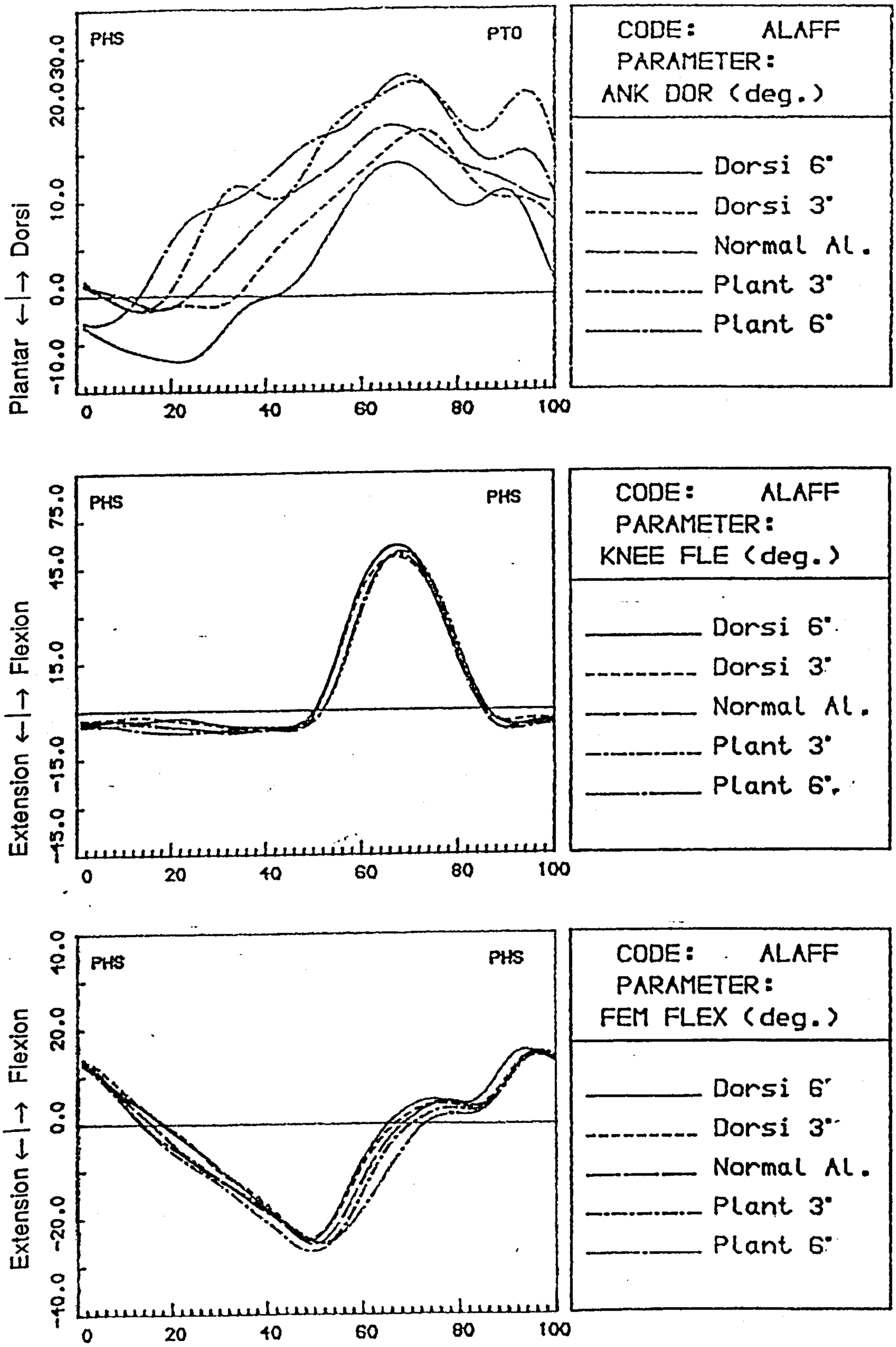

Fig.6.7 The sagittal angular displacement of the prosthetic lower limb for an amputee with the FACS. All units are in degrees.

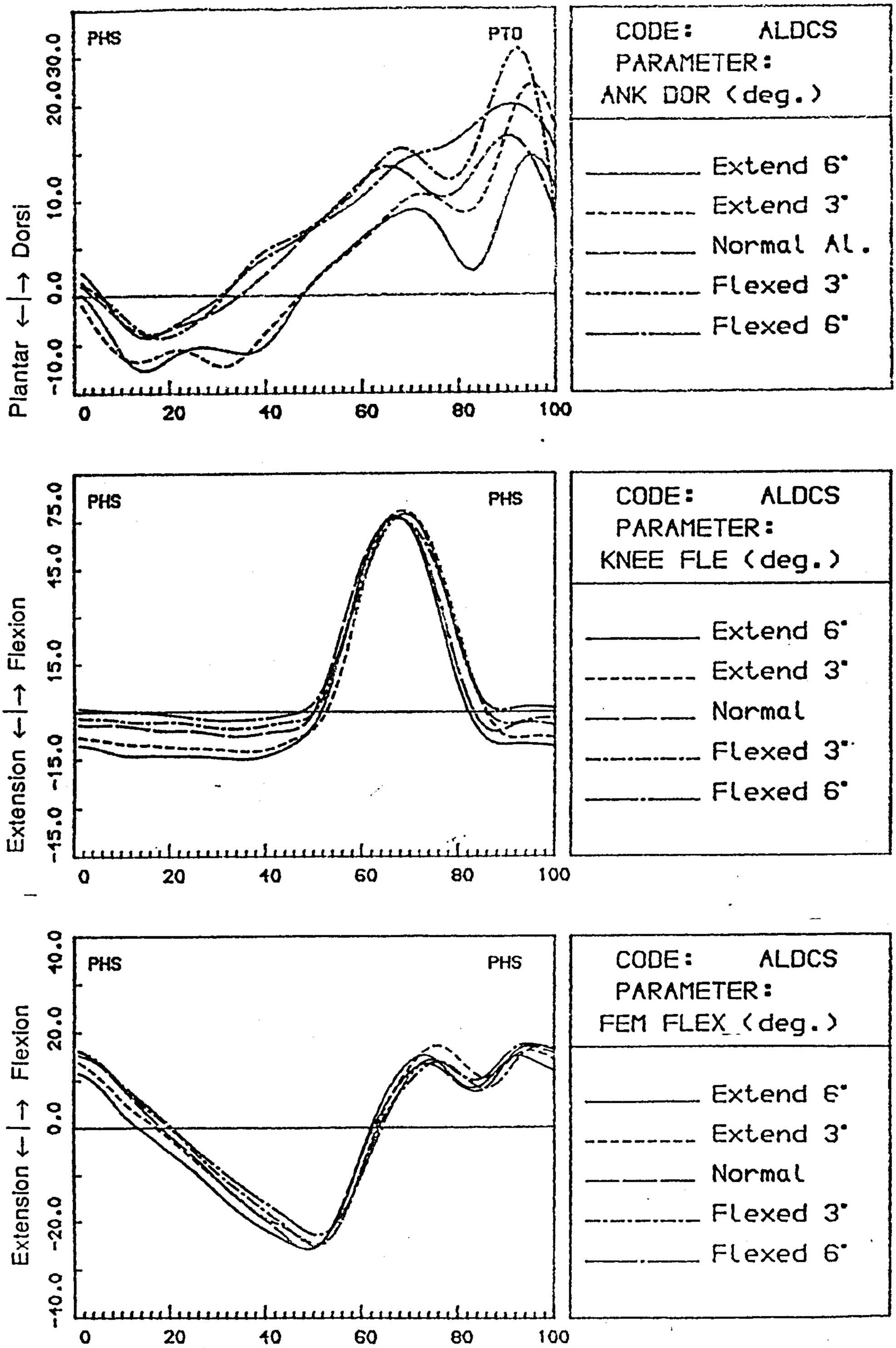

Fig.6.8 The sagittal angular displacement of the prosthetic lower limb for an amputee with the SACS. All units are in degrees.

the knee were not significantly affected by the FACS, whereas the ankle joint angles showed significant changes with the FACS, that is, the ankle curves shifted towards a dorsiflexion direction as the inclination of the foot was changed towards a plantar direction. This was as expected. As the orientations of the thigh and the shank did not change with the FACS, the plantarflexed foot had to dorsiflex more to allow the body to roll over the prosthesis in a similar way to that in the normal alignment.

Fig. 6.8 shows the angular displacements of the prosthetic lower limbs for a amputee who underwent the SACS. Results from other amputees had similar patterns. It was seen that the thigh angle curves tended to shift towards a flexion direction during stance phase as the socket inclination changed from an extension to flexion direction, increasing the inclination angles of the prosthetic shank and foot. For the knee joint, the extension angles during the stance phase moved towards flexion direction as the socket alignment was sequentially changed (ie with SACS) by increments of about 3 degrees, and the amount of shift suggested that the alignment changes were totally responsible for this shift as expected. The ankle angles showed a tendency to increase towards dorsi flexion with the SACS. As flexing the socket is equivalent to plantar flexing the foot ($\Phi_{FACS} = \Psi_{SACS}$), as far as the angular relation between the socket and the foot is concerned, similar explanations can be offered for the changes in the patterns of the ankle angles in the SACS as given in the FACS (previous paragraph).

For the FSACS, the angular displacements of the prosthetic lower limbs are shown in Fig. 6.9. It was observed that all variables tended to change as the knee joint centre was moved anteriorly (ie,with the FSACS). The thigh and the knee joint angles shifted towards a flexion direction with the FSACS by an increment of half the socket angular changes for the thigh, and by the same amount as the socket angular changes for the knee joint. The ankle angle curves shows dorsiflexion progressively later with the FSACS. As in the SACS, the differences in the knee joint angles were overwhelmingly a direct results of the FSACS; this is obviously a geometrical effect. From the differences in the pattern of the thigh angular displacement, it appeared that

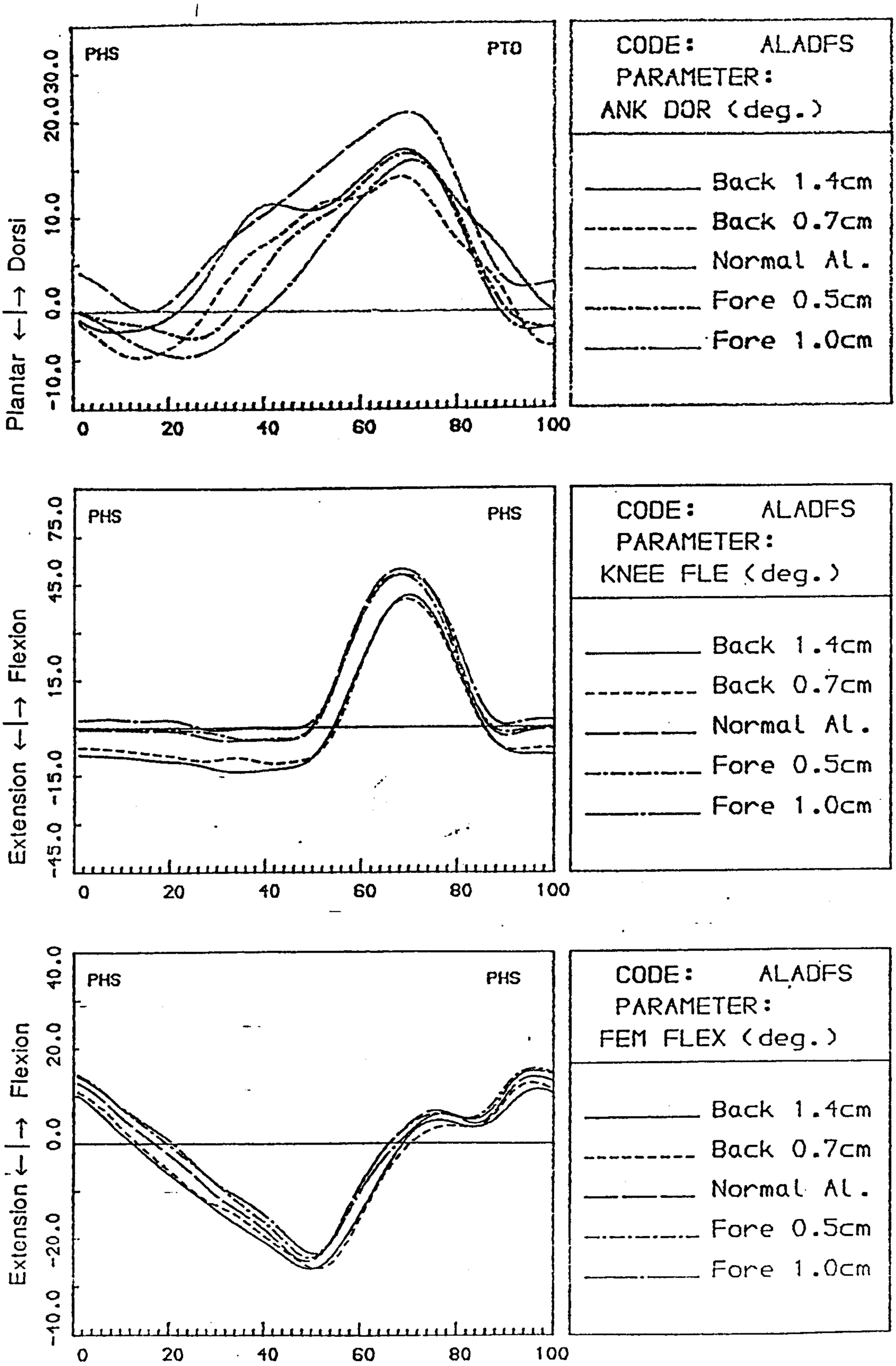

Fig.6.9 The sagittal angular displacement of the prosthetic lower limb for an amputee with the FSACS. All units are in degrees.

the patient tried to maintain a more or less similar orientation of the shank relative to the ground. As a result, the foot was more inclined to the ground with the FSACS and was dorsi flexed later with the FSACS.

It may be useful to express the saggital angular displacements of the lower limbs in terms of the absolute angles relative to the laboratory frame of reference. If the dynamic orientations of the prosthetic foot, shank and thigh at normal alignment are denoted as $\Phi(t)_{NORMAL}$, $\vartheta(t)_{NORMAL}$ and $\Psi(t)_{NORMAL}$ respectively, the dynamic configuration of the prosthetic lower limb at the normal alignment be written as

$$DNORM = \{\Psi(t)_{NORMAL}, \theta(t)_{NORMAL}, \Phi(t)_{NORMAL}\}.$$

Similarly, the dynamic configuration of the prosthetic lower limb in the FACS, designated as DFACS, can be expressed as

$$DFACS = \{\Psi(t)_{NORMAL}, \vartheta(t)_{NORMAL}, \Phi(t)_{NORMAL} - \Phi_{FACS}\}. \quad (6.3a)$$

Since the function $\Psi(t)$, the dynamic orientation angles of the thigh , has not been affected by the foot angular alignment changes as seen in Fig. 6.7, it is shown as $\Psi(t)_{NORMAL}$ in equation 6.3a. As the knee joint is fully extended throughout the stance phase (see Fig. 6.7) and the alignment changes did not alter the angular configuration of the shank and the socket relative to one another (see Fig. 6.1b), the function of the shank inclination with time $\theta(t)$ is denoted in the equation as ϑ_{NORMAL}. The function $\Phi(t)$, the variation of the foot orientation with time, is of course directly affected by the alignment changes at the foot Φ_{FACS}. Hence the term $[\Phi(t)_{NORMAL} - \Phi_{FACS}]$ is used to represent the $\Phi(t)$. It should be noted that the negative sign "—" in this term is included because the positive direction of the $\Phi(t)$ is counterclockwise while for the Φ_{FACS} it is clockwise, ie, plantar flexion.

For the SACS, as shown in Fig. 6.8, the range of variation of the thigh angle was about 6 degrees, ie, half of the range of the alignment adjustment, and the incremental changes of the thigh angle may be assumed to be uniform. The dynamic configuration of the prosthesis with the SACS can therefore be expressed as

$$DSACS = (\Psi(t)_{NORMAL}+0.5\Psi_{SACS}, \quad \vartheta(t)_{NORMAL}-0.5\Psi_{SACS},$$
$$\Phi(t)_{NORMAL}-0.5\Psi_{SACS}). \qquad (6.3b)$$

Since the thigh angle curves shifted towards a flexion direction (see Fig. 6.8) as the socket alignment was changed towards flexion, the $\Psi(t)$ term is shown in the equation as $\Psi(t)_{NORMAL}+0.5\Psi_{SACS}$. Since the inclination angle of the shank is reduced as the socket alignment is altered towards a flexion direction which is positive (see Fig. 6.1b) and the shift of the thigh angle towards a flexion direction with the SACS increases the inclination angle of the shank, the term for $\theta(t)$ is $\vartheta(t)_{NORMAL}-0.5\Psi_{SACS}$.

Similarly,

$$FSACS = \{\Psi(t)_{NORMAL}+0.5\Psi_{FSACS}, \quad \vartheta(t)_{NORMAL}-0.5\Psi_{FSACS},$$
$$\Phi(t)_{NORMAL}+0.5\Psi_{FSACS}\}$$
$$= \{\Psi(t)_{NORMAL}+0.5\Psi_{FSACS}, \quad \vartheta(t)_{NORMAL}-0.5\Psi_{SACS},$$
$$\Phi(t)_{NORMAL}+0.5\Psi_{SACS}\}. \qquad (6.3c)$$

Through Equ.6.3a-c, the dynamic configurations of the prosthetic leg with three ACSs during the prosthetic stance phase are determined and can be compared with each other and with the alignment configurations of the prosthesis (i.e. CFACS, CSACS & CFSACS in Equ.6.2a-c). It can be seen clearly that the orientations of the prosthetic thigh and shank in the DSACS and the DFSACS are the same, and that the foot orientation of the DFACS and DSACS changed in the same direction while that of the DFSACS was in the opposite direction. Comparison of the above equations with Equ. 6.2s would reveal that: (1) CFACS=DFACS; (2) through changes in thigh orientation made by the patient, the inclination of the shank and foot in the DSACS approached the dynamic configuration of the leg at normal alignment; (3) and also through changes the thigh orientation, the shank inclination was closer to that obtained with the normal alignment, but the foot orientation deviated.

Overall, it appeared that the amputees tested did not change their way of using the prostheses when adjustments to the foot inclination angle were made and the

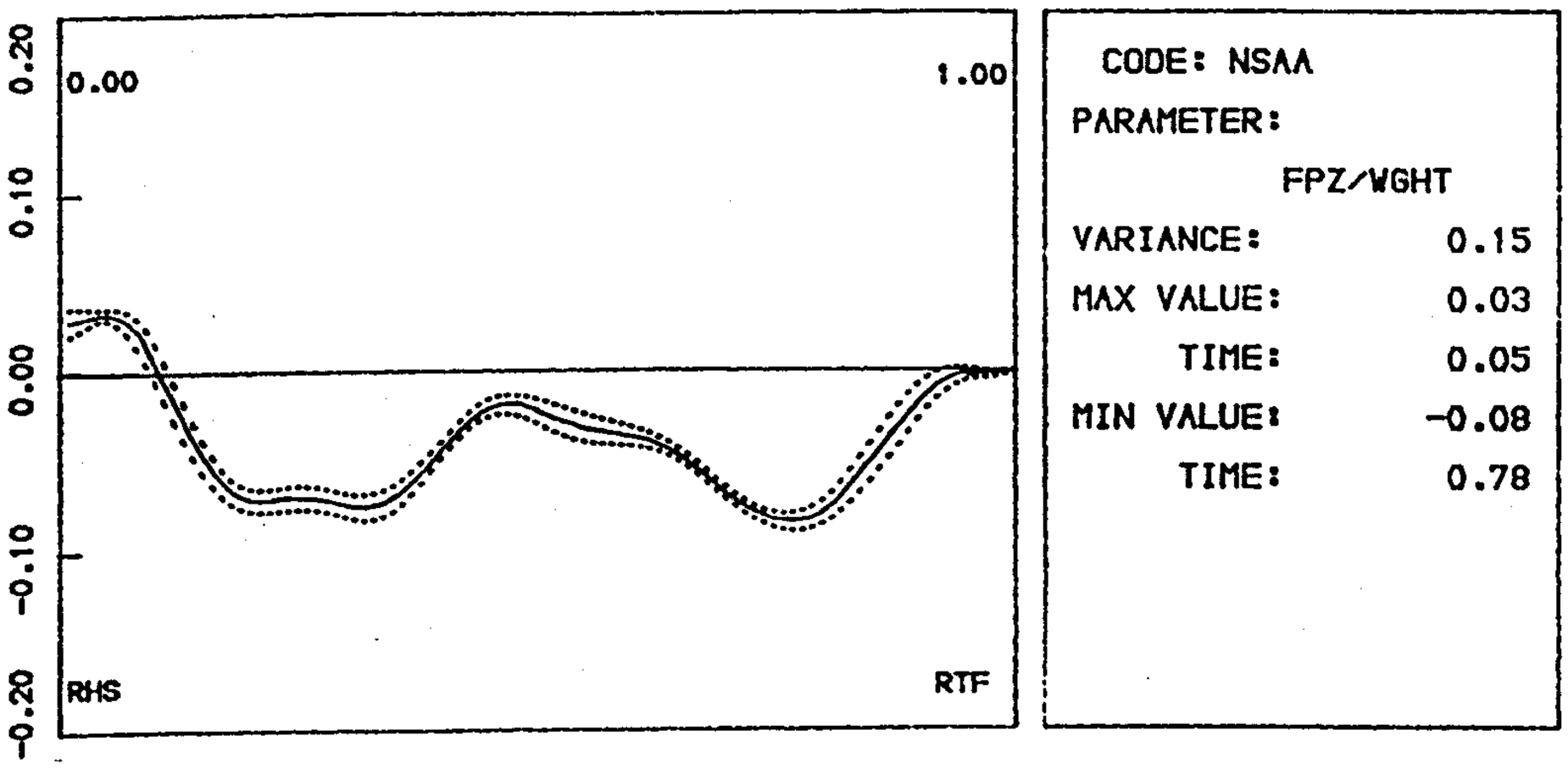

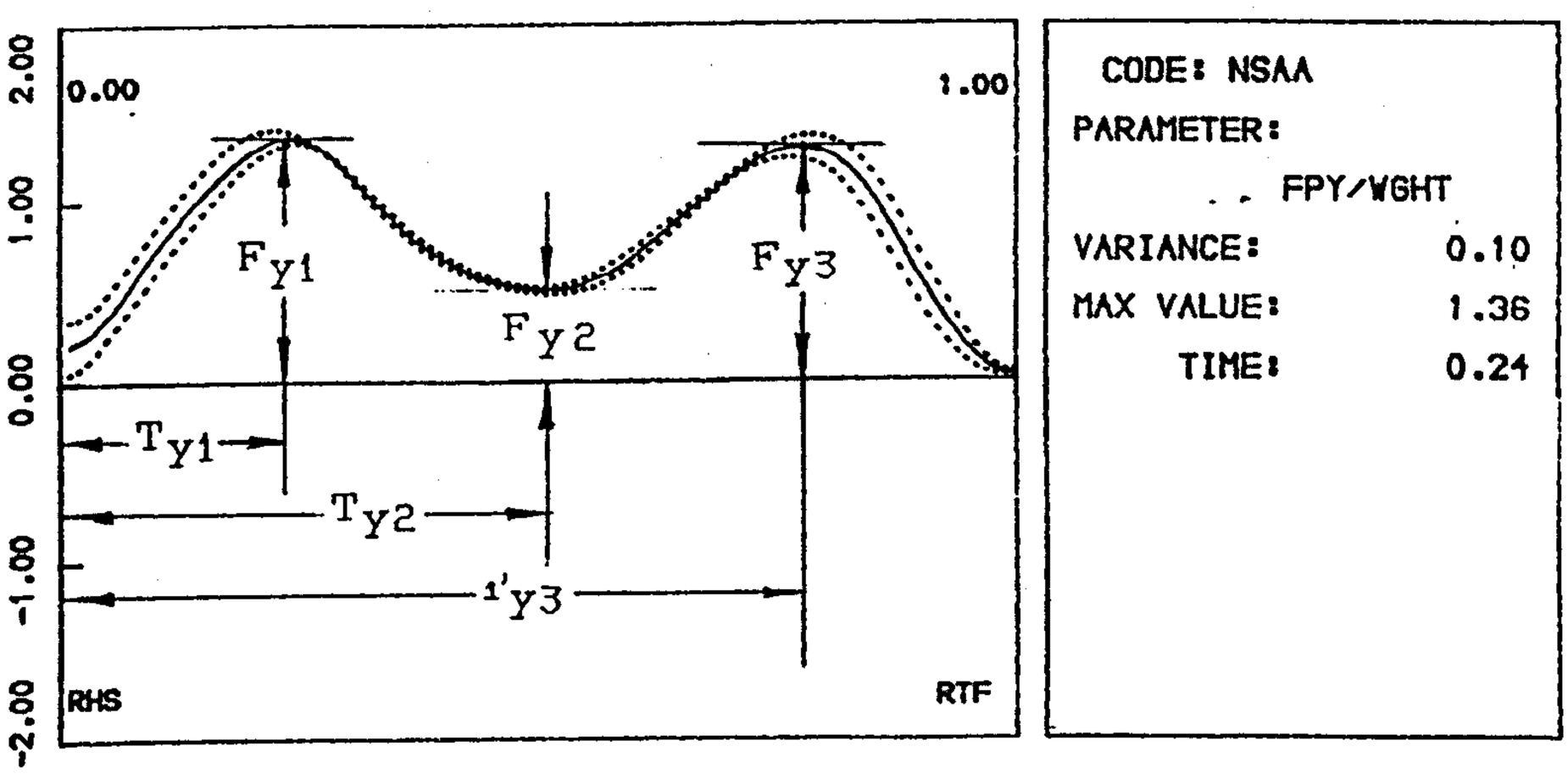

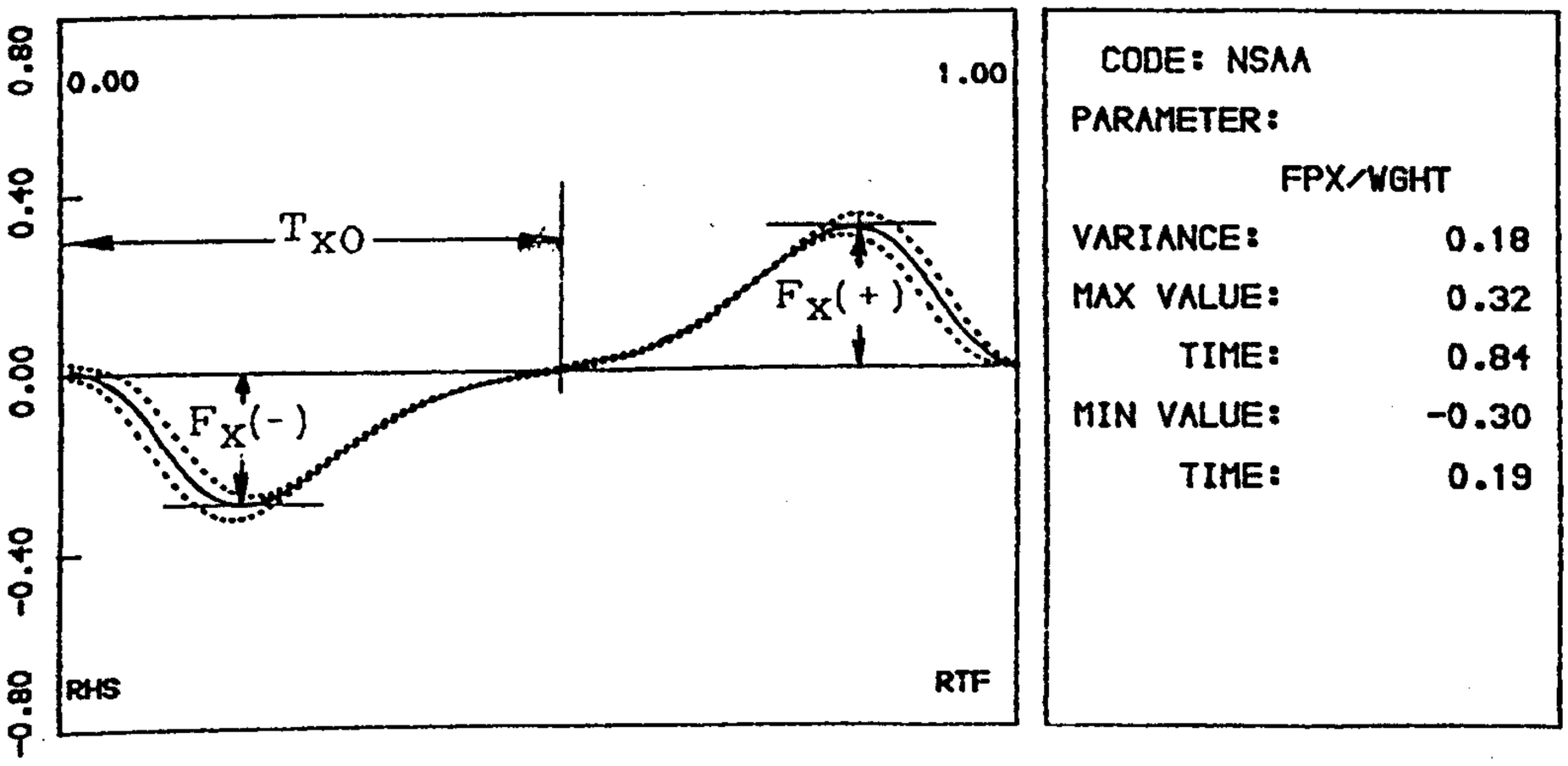

Fig. 6.10 Time-history of the ground reaction forces for the normal subject tested and definitions of the ground reaction parameters.

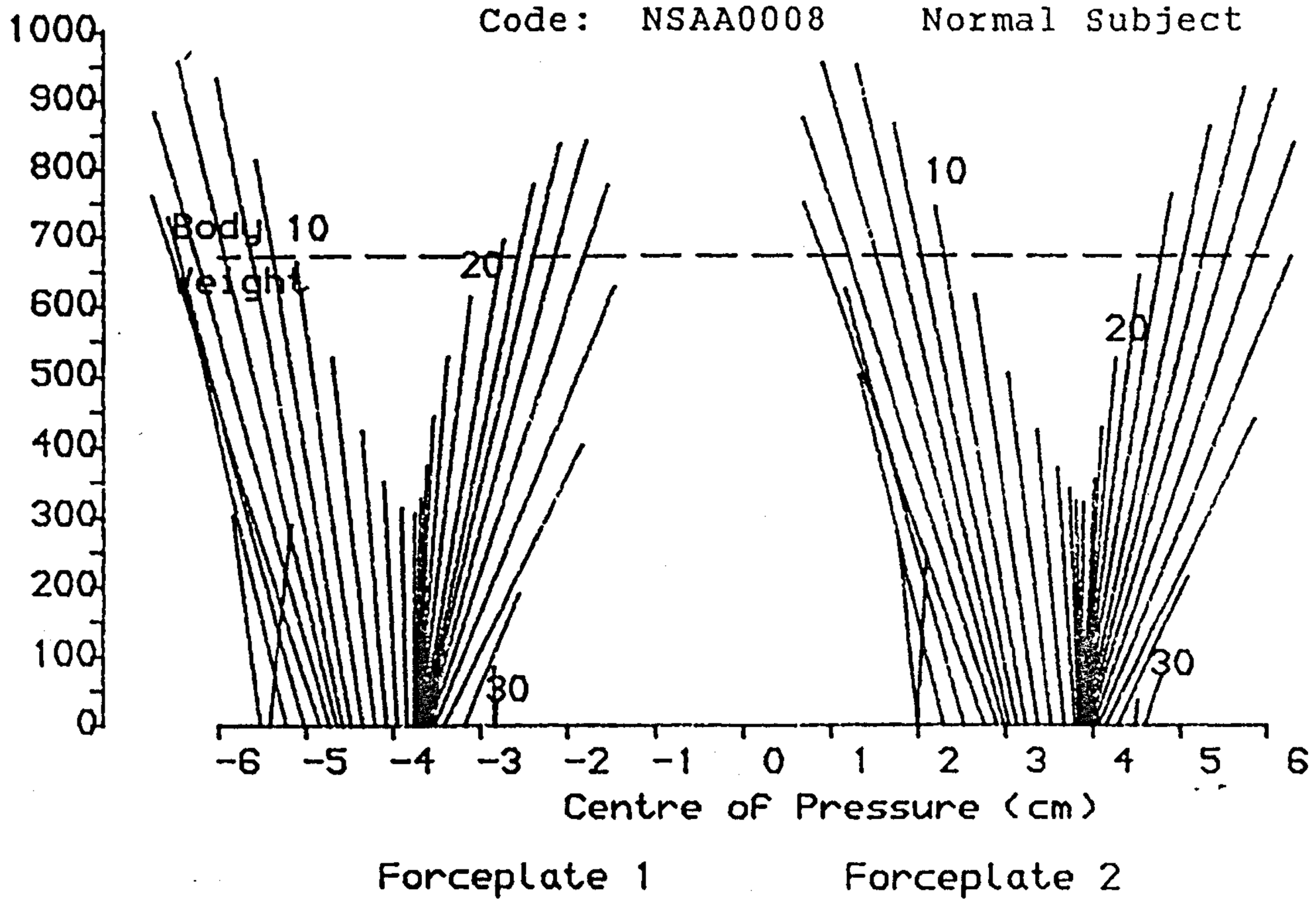

Fig. 6.11 A typical vector diagram or 'Butterfly' diagram of the ground reaction forces for the normal subject.

differences noted in the angular displacements of the prosthetic lower limb were mainly the direct effects of the alignment changes at the foot.With the SACS and FSACS, limited compensatory adjustments were made in coping with the alignment changes. The amputees evidently tried to maintain similar orientations of the prosthetic shank to those in normal alignment and the biomechanical implications of this argument will be discussed in later sections. This compensation action for alignment changes have not been reported in the literature on AK amputees and indeed, such a systematic approach to changing the prosthetic alignment and observing various gait parameters has not be attempted before by other investigators on AK amputees. Morimoto *et al* (1987) conducted a similar study on BK amputees and the results they obtained showed such compensatory action (see Fig.3.23).

§ 6.6 Ground Reaction Forces

§ 6.6.1 The normal subject

Fig.6.10 shows the average time-history of the ground reaction forces for the normal subject tested. The data were normalized to 100% stance phase in time and 100% body weight in forces. The shapes of the curves were consistent with those published in the literature, such as Cunningham (1950) (see Fig. 2.28), but the peak values presented here are relatively higher. The subject walked at a mean speed of 1.49m/s, which is faster than that reported in the literature (1.3m/s). Furthermore, the normal subject walked with larger oscillations than those of most subjects reported in the literature. This can be confirmed by higher knee flexion during early stance phase (see Fig.6.5). These two factors influence the peak values of the ground reaction forces. The overall variance of the data is 18%, 10% and 15% respectively for the fore-aft, vertical and lateral components of the ground reaction force, similar to the results obtained by Winter (1984).

In order to characterize the patterns of the ground reaction forces, some of the

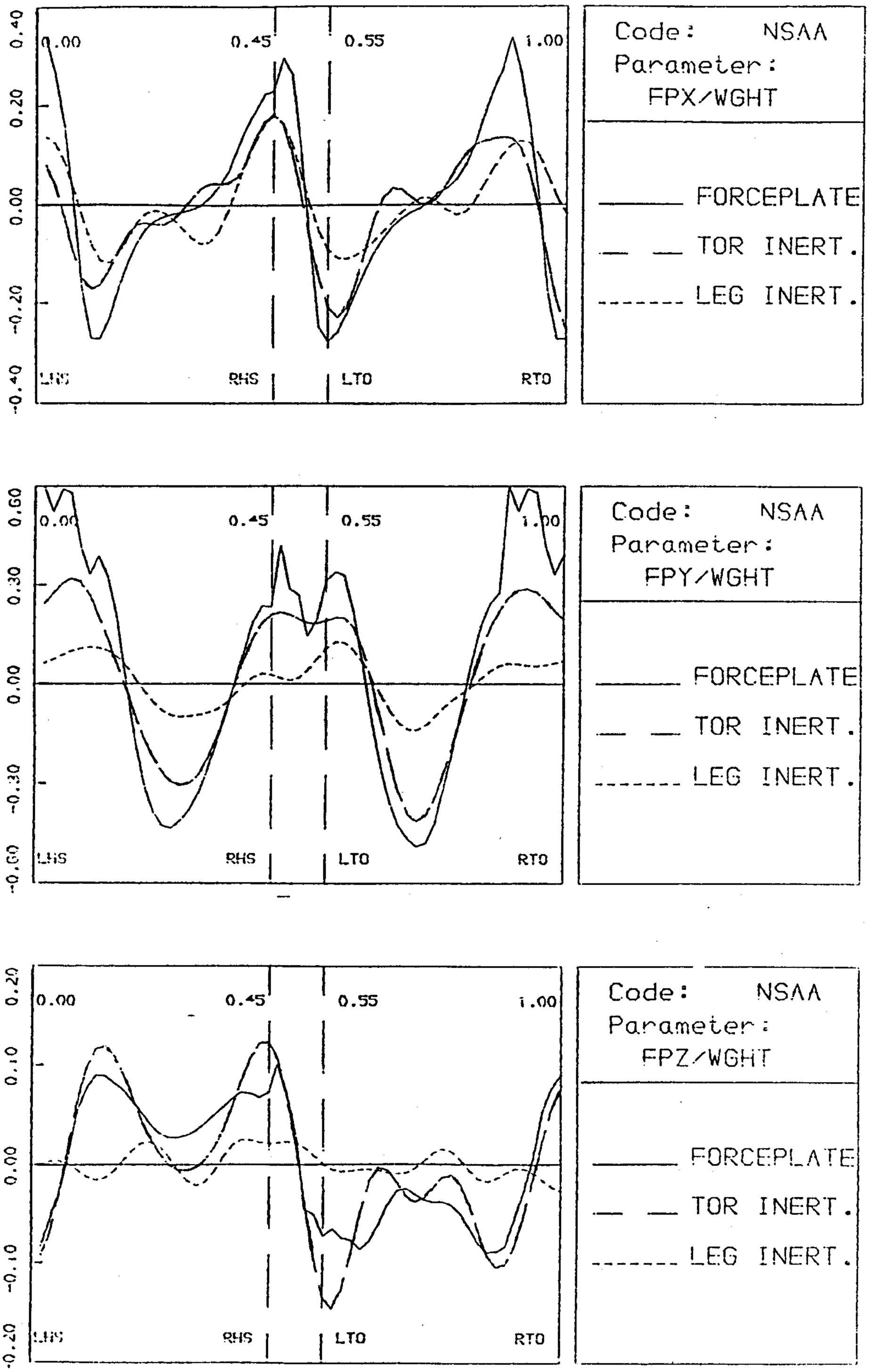

Fig. 6.12 Comparison between the total ground reaction forces and the inertia forces of the trunk & the lower limbs as a whole (normal subject).

parameters proposed by Andriacchi (1977) and Chao (1982) were determined and presented in Table 6.8. The definitions of the parameters are also presented in Fig. 6.10.

The progression of the centre of pressure (CP) indicates the manner in which the subject uses his foot during walking and can be studied through the vector diagram or the so-called 'butterfly' diagram of the ground reaction forces. Fig. 6.11 shows such a diagram in the saggital plane which is typical for the normal subject. Both the left and right sides are presented and they show a close similarity. During the first 47% (±4%) of the stance duration, the centre of pressure proceeds relatively fast to cover about 62% (±5%).of the CP displacement, and then progresses slowly within the metatarsal area before the foot finally leave the ground.

Interpretation of the ground reaction forces is very important for understanding the underlying biomechanics of walking, as these forces are the only interactions between the environment and the human body during walking. Furthermore, the ground reaction forces can be measured with high accuracy. On the other hand, it is difficult to explain every detail of the pattern of the ground reaction forces in terms of the movements of the body segments: the forces are an overall reflection of the summation of the mass-acceleration products of all body segments. With the combination of the motion tracking system and forceplates, body segmental movements and ground reaction forces can be recorded simultaneously, and the contributions of different body segments to the ground reaction forces can be assessed. Fig. 6.12 demonstrates such an analysis on the normal subject. The data obtained from the left and right forceplates were summed and the accelerations of the trunk and lower limbs as a whole were calculated. The vertical intercepts in the figure represents the variance from the body weight. It was found that the vertical inertial forces of the trunk followed the trace of the ground reaction forces well and contributed to about 66-70 percent of the ground reactions. Similarly, the lateral component of the inertial force of the trunk also follows the ground reaction pattern

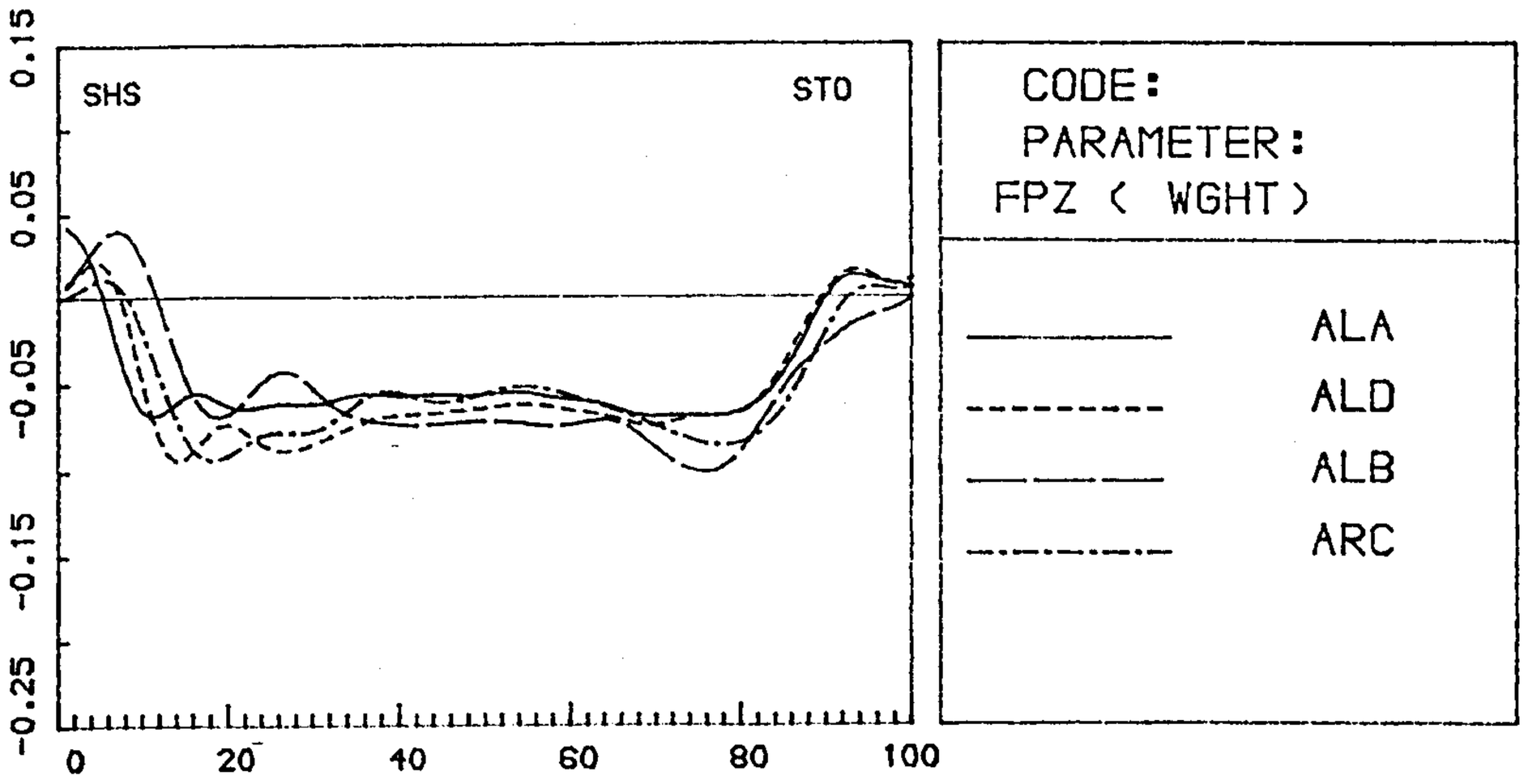

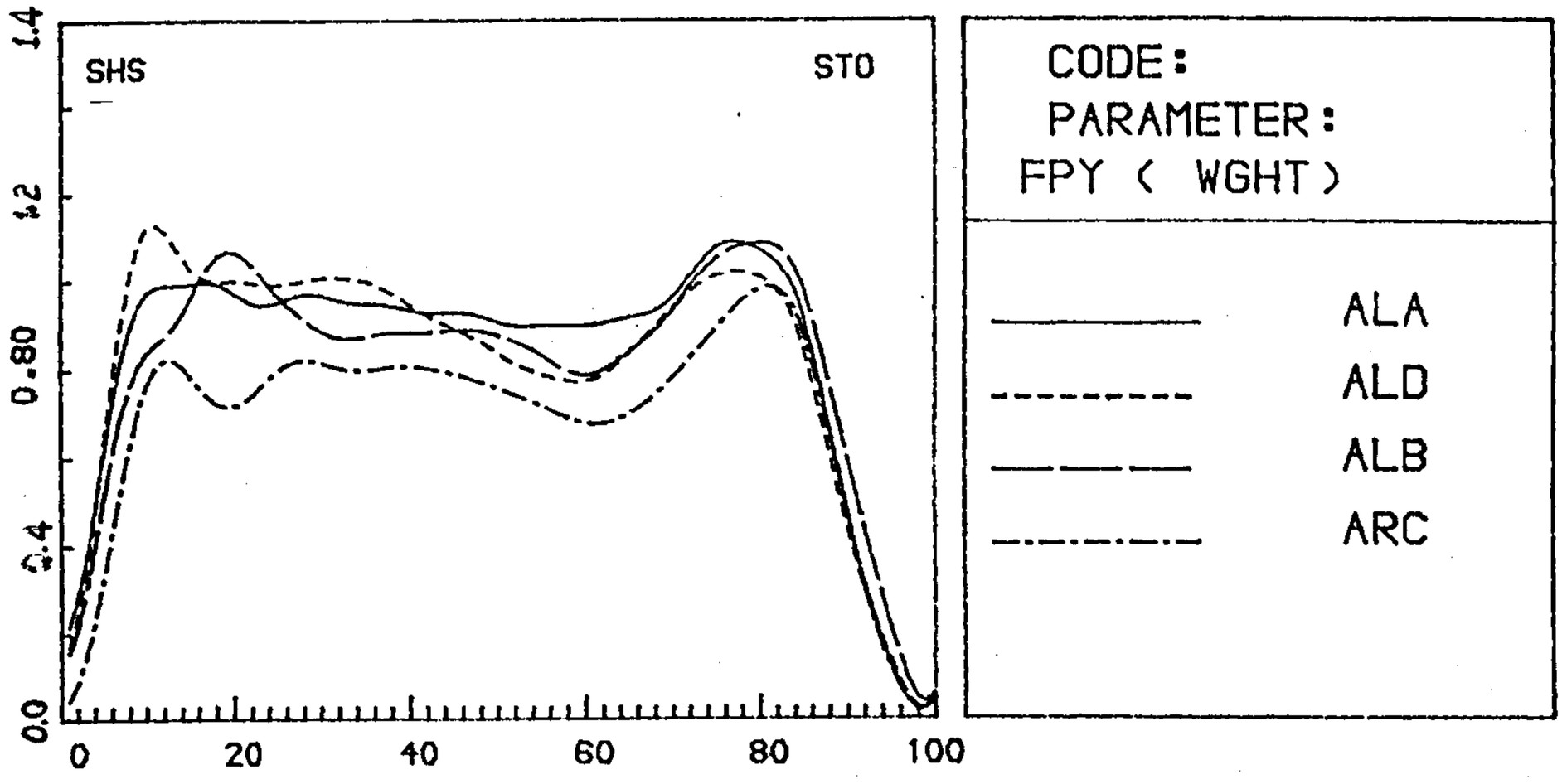

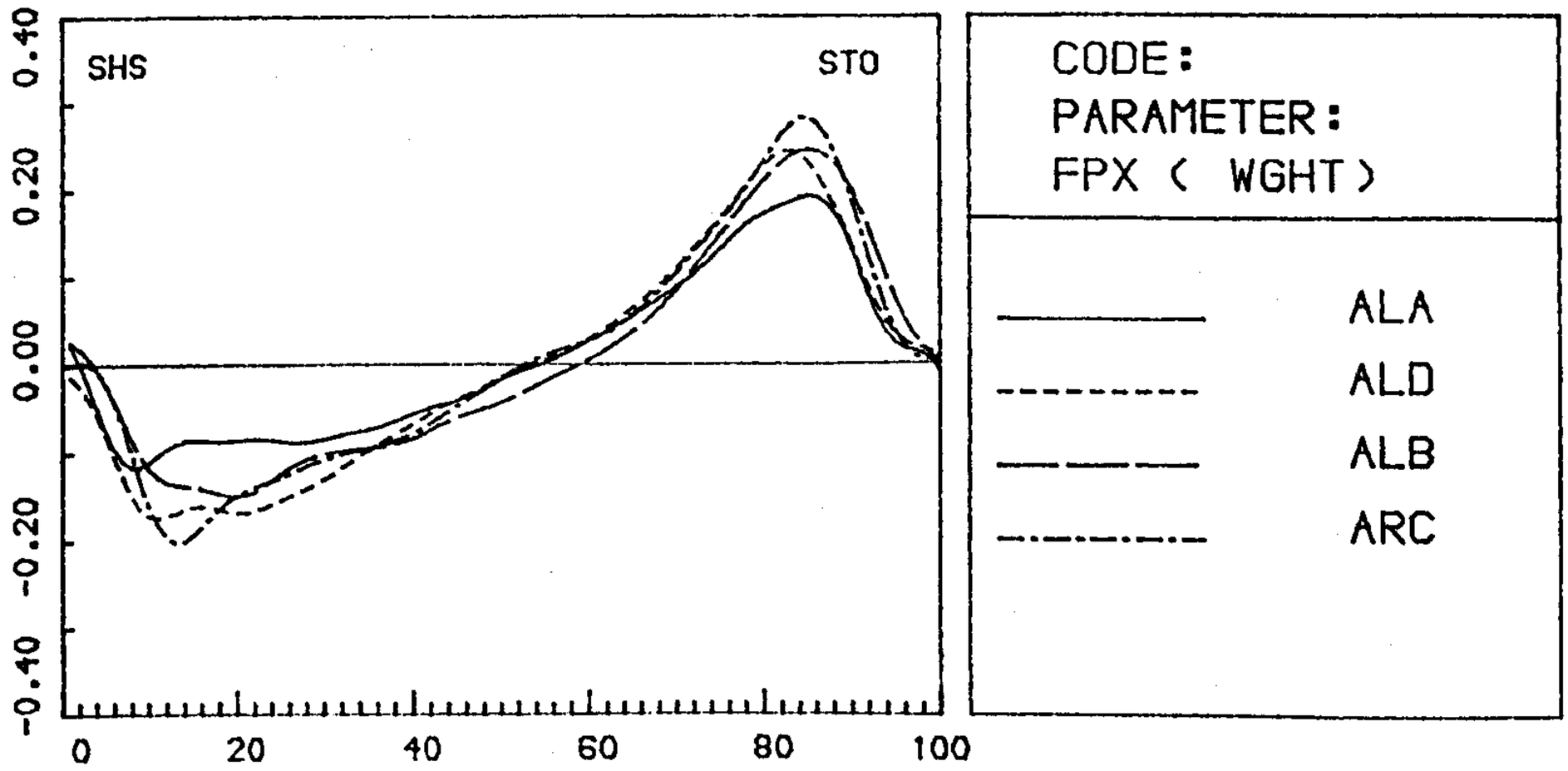

Fig.6.13a The patterns of the ground reaction forces for the amputees tested at normal alignment. All units are in the body weight.
(Unaffected Side)

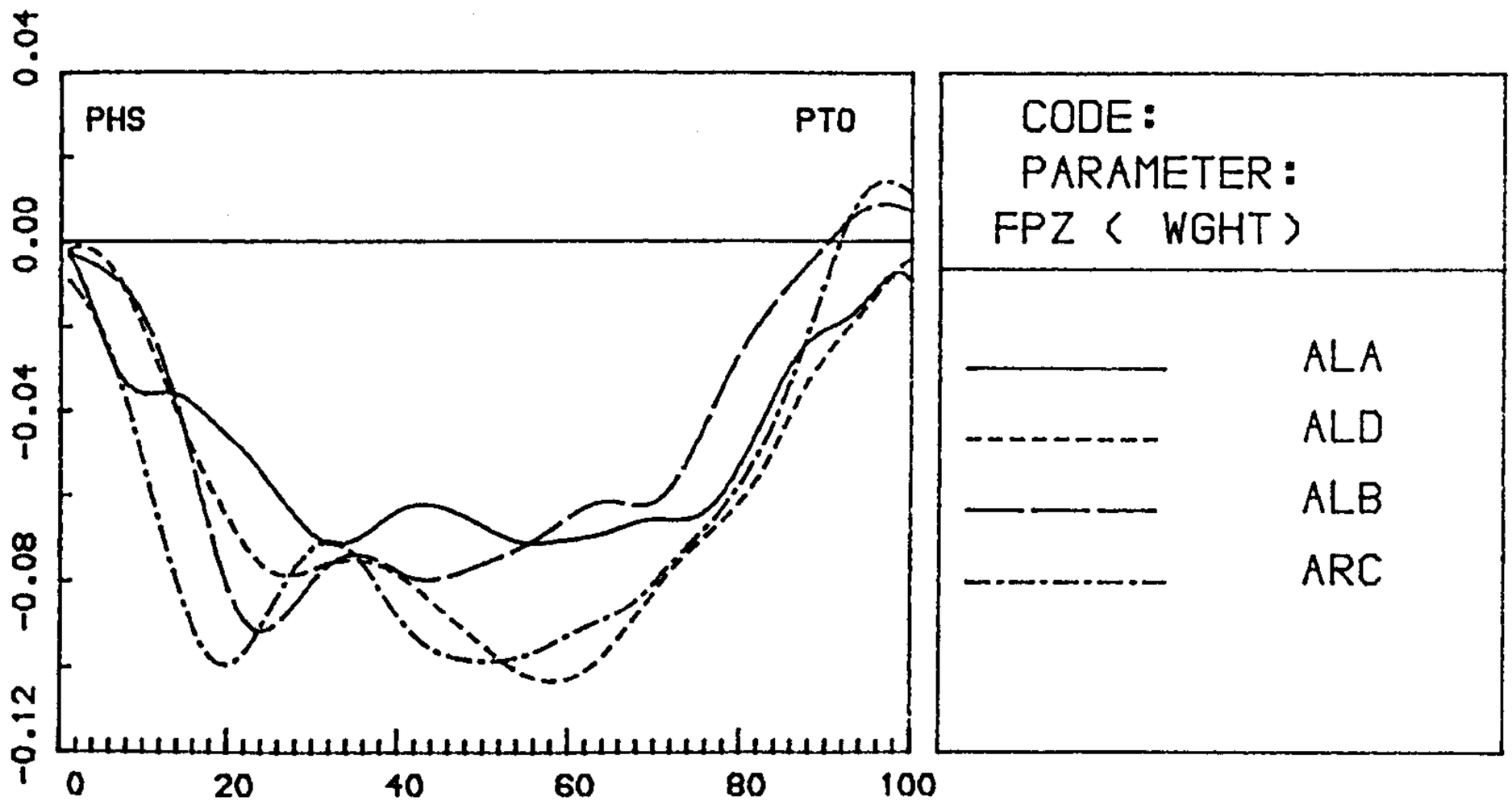

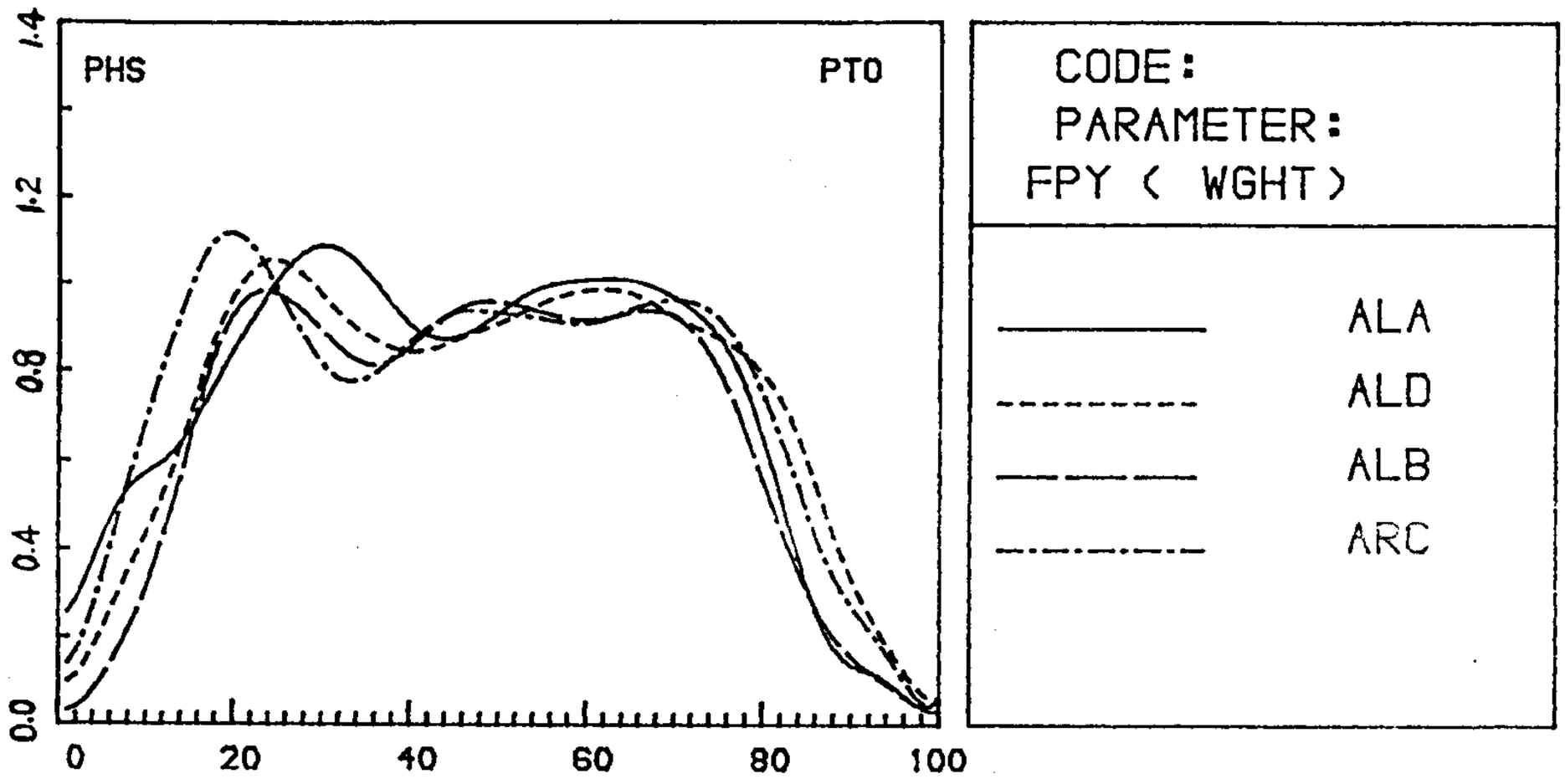

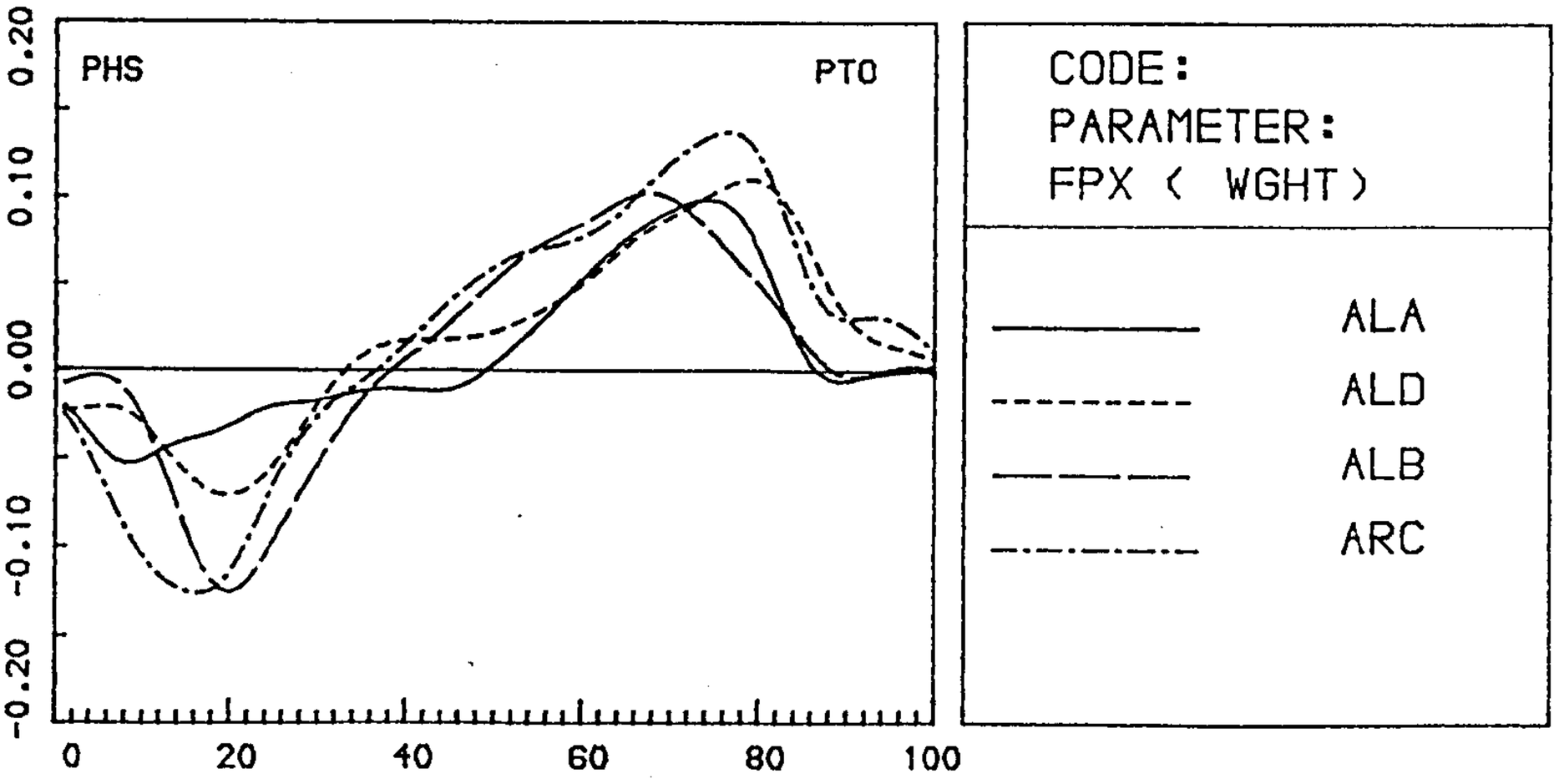

Fig.6.13b The patterns of the ground reaction forces for the amputees tested at normal alignment. All units are in the body weight.
(Prosthetic Side)

well. The inertial forces of the lower limbs for both the vertical and lateral components tended to have a similar pattern to that of the ground reactions and were considerably less than the values for the trunk. The fore-aft inertial force of the lower limbs was found to be of the same order as that of the inertial force of the trunk due to their higher acceleration, especially during the start and end of the swing phase.

§6.6.2 The Amputees with normal alignment

Fig. 6.13a and Fig.6.13b show the time-history of the ground reaction forces for the amputees tested with normal alignment. The basic pattern of the curves are similar to that obtained by Cunningham (see Fig.3.29). On the sound side (Fig. 6.13a), the patterns of the curves were similar to those for the normal subject, except for the vertical components which were no longer of the "two-peak-one-trough" type. An additional peak,which is more evident in the vector diagram (Fig. 6.14), appears during the mid-stance and is associated with the elevation of the CG of the body through 'vaulting'. This finding was evident in every walking test for the amputees tested. Since the amputees had lost knee and ankle control on the prosthetic side, they were compensating for the loss by the vaulting action in order to give sufficient clearance for the prostheses.

On the prosthetic side (Fig. 6.13b), differences were found in the vertical and fore-aft shear forces between the normal subjects and the amputees and between the two groups of the amputees. For the group-1 amputees who wore the Otto Bock prostheses, the vertical forces still show two peaks and a trough, being similar to that for the normal subject, but the second peak spreads broadly over late stance phase. During late stance phase, the amputees rolled over the ball of the SACH foot, with the prostheses fully extended, in a way similar to an inverted pendulum and the lack of active push-off of the prosthesis suppressed the second peak of the ground vertical force. The fore-aft shear forces of the group-1 amputees show a plateau during the mid-stance phase, suggesting an unsmooth transition from braking to push-off. This

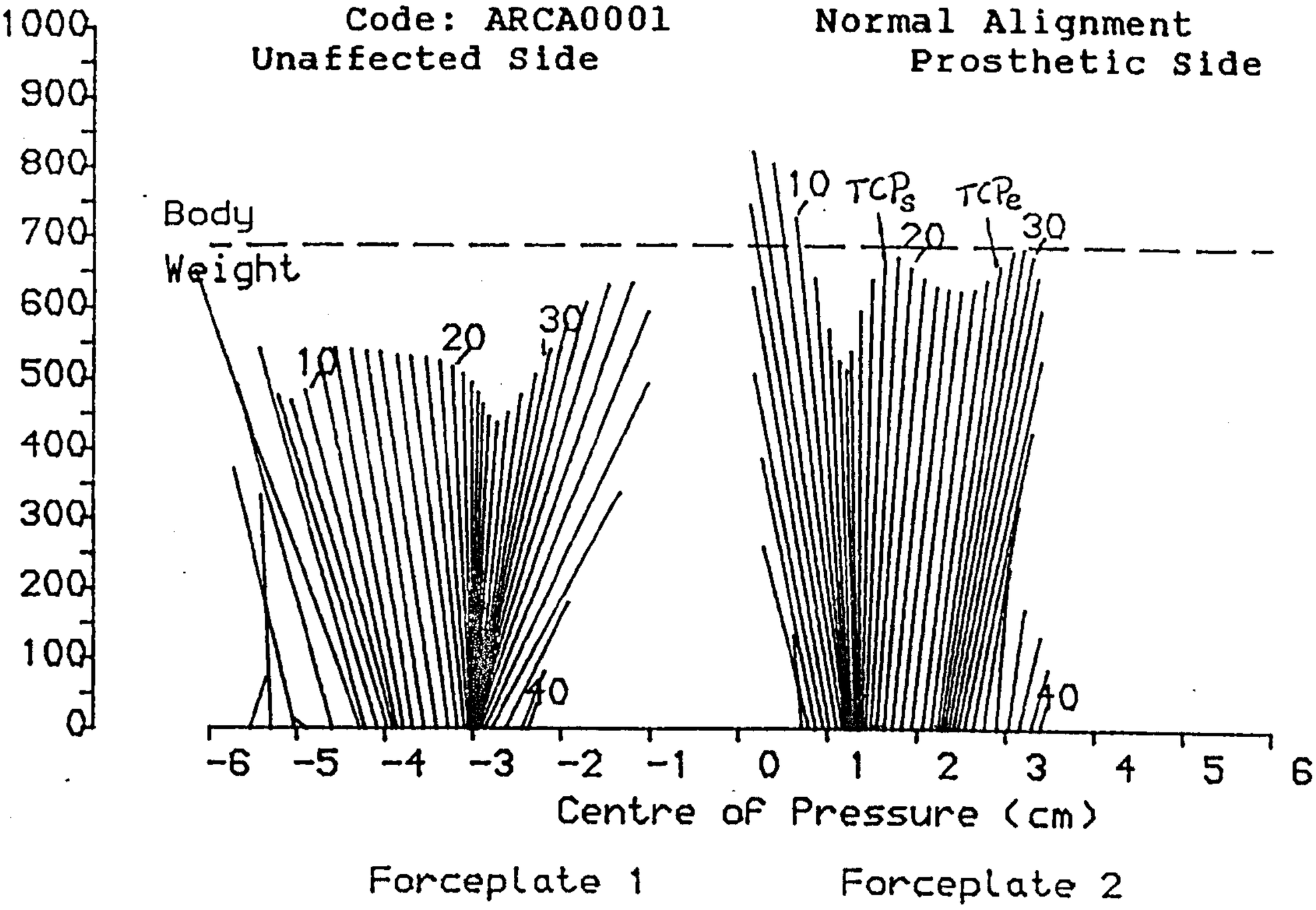

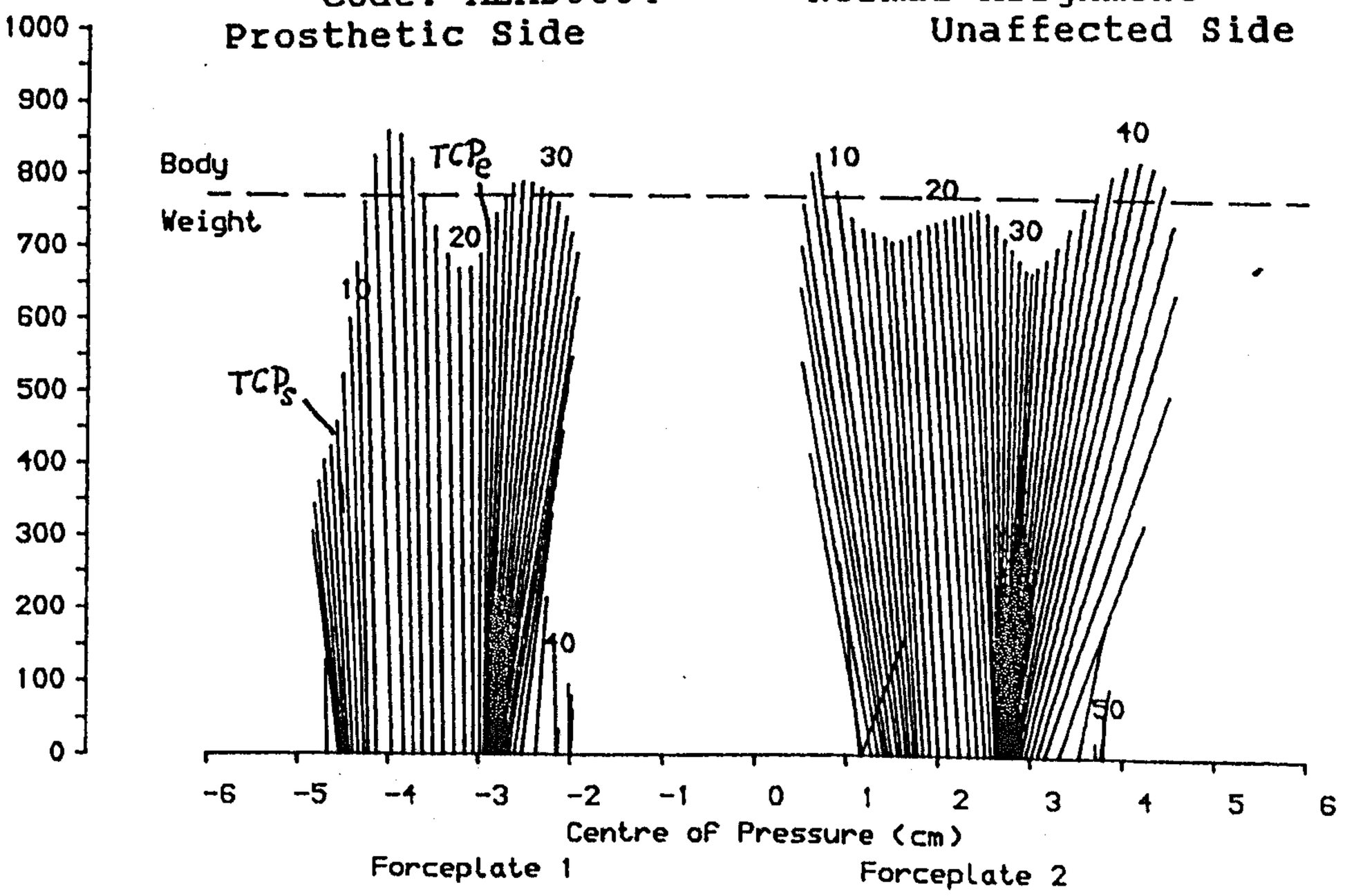

Fig.6.14 Typical vector diagrams of the ground reaction forces for the two groups of the amputees.

Table 6.8 Results of Parametric Analysis on the Ground reaction forces (Normal Alignment)

Subject Code	Group-1 Amputees ALA	ALD	Group-2 Amputees ARC	ALB	NSA
		prosthetic side			**left side**
$F_X(+)$	11.5	11.3	13.4	10.2	30.9
$F_X(-)$	4.6	6.9	12.4	12.5	31.2
T_{X0}	49.6	27.2	33.0	32.0	49.2
$I_X(+)$	2.32	2.17	3.4	2.35	12.8
$I_X(-)$	0.82	1.00	1.95	1.70	13.0
F_{Y1}	109.4	106.0	110.0	98.5	132.3
T_{Y1}	35.4	25.0	21.0	26.5	23.4
F_{Y2}	87.0	86.6	93.5	96.5	47.6
T_{Y2}	50.0	40.8	51.0	51.0	48.1
F_{Y3}	99.4	99.4	96.0	94.0	122.8
T_{Y3}	66.8	61.8	70.5	71.0	77.3
TCP_S	27.8	31.4	42.5	40.1	###
TCP_e	49.8	56.8	50.5	51.2	47.2
		Unaffected Side			**Right Side**
$F_X(+)$	18.8	23.3	27.3	26.1	32.0
$F_X(-)$	15.3	18.4	19.1	15.2	31.4
T_{X0}	51.0	48.0	51.0	57.0	50.7
$I_X(+)$	4.74	4.63	4.35	3.20	13.1
$I_X(-)$	4.10	4.81	4.11	4.01	12.7
F_{Y1}	109.2	111.2	88.0	108.0	135.4
T_{Y1}	16.4	12.8	13.5	20.5	24.1
F_{Y2}	95.4	104.0	80.5	91.0	48.3
T_{Y2}	38.2	34.0	29.5	40.5	49.2
F_{Y3}	107.4	101.4	95.0	110.0	125.0
T_{Y3}	78.4	80.0	85.0	83.0	75.3

NB: (1) $I_X(+)$ and $I_X(-)$ are the impulses of the push-off and braking forces respectively.
(2) Unit for peak force is (% body weight), for impulse (% body weight·s), for temporal parameter (% stance phase).
(3) All values are differences with the normal alignment data.
(4) Parameters underlined have statistical significance with confidence limit of 90%.
(5) "###" means no dwelling of the CP at the heel area.

plateau was also reported by Goh (1982) on patients wearing SACH feet. For the amputees wearing the Endolite systems, the fore-aft shear force was similar to that of the normal subject, but the vertical component exhibited a third peak at mid-stance phase. The exact reason for this additional peak is not known, but may be due to a sudden change in resistance as the foot/ankle progresses from plantar flexion to dorsiflexion which forced the amputee to accelerate upwards.

Table 6.8 shows the results of a parametric analysis of the ground reaction forces for the two groups of amputees with normal alignment. The definitions of the parameters are shown in Fig. 6.10. For the vertical forces which have three peaks, the parameters 'F_{Y2}' and 'T_{Y2}' designate the value and the occurrence time of the mid-peak. The impulses of the fore-aft shear forces are also presented in the table.

Comparing the amputees with the normal subject, all the peak values for the amputees are much lower than those of the normal subject. This is due to the significantly (ρ=1%) lower speed at which the amputees walked (52.9m/min for amputees and 89.4m/min for the normal subject). Considering the fore-aft shear forces, it was found that the push-off forces were much smaller on the prosthetic side than on the contralateral side, while the normal subject had the same values for both sides. This asymmetry was due to the absence of active plantar flexion of the prosthetic ankle joint. With the exception of the prosthetic side of the group-2 amputees, the peak braking forces F_X(-) of the amputees had much lower values than the peak push-off forces F_X(+), while these two forces were very close in value to each other for the normal subject. Furthermore, the time at which the braking force changed to the push-off forces, called "transition time", is significantly ($\rho \leq 5\%$) earlier at the prosthetic side, while it is almost at exactly mid-stance for the normal subject. As a result, the impulses of braking forces "I_X(-)" were much smaller than those of the push-off forces "I_X(+)" at the prosthetic side, and there were no significant ($\rho \leq 10\%$) differences between I_X(+) and I_X(-) at the contralateral side for the amputees and at the both sides for the normal subject. As far as the vertical force at the sound side is concerned, it reached its first peak significantly earlier than that of

the normal subject, indicating the amputees' eagerness to transfer the body weight from the prosthesis to the sound leg sooner.

Differences were also observed between the two groups of amputees which are probably a reflection of the types of feet and perhaps the knee mechanisms fitted to the prostheses. The prosthetic braking forces for group-1 amputees were significantly ($\rho \leq 5\%$) lower than the push-off forces, while for the group-2 amputees and the normal subject, they were of the same order. Thus much lower braking impulse was obtained in group-1 than in group-2 amputees.

Typical vector diagrams for the two groups of amputees were shown in Fig. 6.14. On the sound side, three peaks are clearly seen. On the prosthetic side, the diagram shows three peaks for group-2 amputees and two peaks for group-1 amputees. Attention was paid to the progression of the centre of pressure of the ground reaction forces. On the prosthetic side, the vector lines are grouped into two bunches: one at the heel and one at the ball of the foot with a transition period between the two. The start and the end instants of the transition period (TCP_s & TCP_e) were determined and their mean values were shown in Table 6.8. Unlike the normal subject whose CP rapidly moved to the toe area, the CP for the amputees progressed slowly within the heel region till about 30% stance phase for group-1 amputees and 41% for group-2 amputees, then it shifted through the arch of the foot to the ball area. The dwelling period of the CP in the heel region is due to the pivoting of the prosthetic limb about either the heel or the ankle joint before the keel of the foot comes into effect. On the contralateral side, the CP travelled in a similar way as that of the normal subject, although group-1 amputees demonstrated a slight "dwelling" of the CP progression at the heel area.

§ 6.6.3 Effects of the ACS

§ 6.6.3.1 Effects of the FACS The basic patterns of the ground reaction forces in the FACS were found to be similar to those for the normal alignment and

Table 6.9 Results of Parametric Analysis on the Ground reaction forces (The FACS)

	Group-1 Amputees					Group-2 Amputees				
	-6°	-3°	0°	3°	6°	-6°	-3°	0°	3°	6°
	(Dorsi ← | → Plantar)					(Dorsi ← | → Plantar)				
prosthetic Side										
$F_X(+)$	-0.4	0.6	0.0	-1.0	0.9	3.0	0.6	0.0	0.7	0.1
$F_X(-)$	1.9	-1.0	0.0	-0.4	-4.2	-0.4	0.8	0.0	1.6	0.6
T_{X0}	-7.4	-11.0	0.0	7.5	1.1	-2.1	0.7	0.0	0.7	-1.2
$I_X(+)$	0.6	0.9	0.0	-0.1	-1.6	0.5	0.3	0.0	0.2	-0.1
$I_X(-)$	0.2	-0.2	0.0	0.4	2.2	-0.0	0.1	0.0	0.2	-0.2
F_{Y1}	-12.6	-3.7	0.0	-4.5	-20.0	6.4	-4.3	0.0	-1.4	-7.8
T_{Y1}	2.9	6.0	0.0	1.0	-1.8	-2.0	1.3	0.0	-1.3	-3.8
F_{Y2}	-5.7	-0.5	0.0	0.0	-10.6	-3.3	-1.5	0.0	-0.8	-8.9
T_{Y2}	11.0	8.2	0.0	2.5	-4.4	-1.8	-2.0	0.0	-2.7	-13.3
F_{Y3}	-3.5	1.7	0.0	-1.2	-14.1	-0.4	-4.0	0.0	0.3	2.4
T_{Y3}	6.0	6.5	0.0	2.0	7.8	2.5	6.8	0.0	-0.5	-9.1
TCP_S	22	12	0	-6	###	10	8	0	-3	-12
TCP_e	22	14	0	-6	-23	8	7	0	-3	-14
Unaffected Side										
$F_X(+)$	-1.0	-0.5	0.0	-0.7	1.6	-0.6	-0.5	0.0	-1.2	-1.4
$F_X(-)$	3.9	3.7	0.0	0.1	0.5	2.2	3.1	0.0	1.4	2.4
T_{X0}	1	-2	0	-1	1	2	1	0	1	-2
$I_X(+)$	-0.7	-0.5	0.0	-0.5	0.4	-0.1	0.0	0.0	0.1	-0.2
$I_X(-)$	0.5	0.2	0.0	-0.2	-0.2	0.3	0.6	0.0	0.4	0.2
F_{Y1}	4.8	9.2	0.0	0.8	-3.2	17.0	21.0	0.0	3.3	9.0
T_{Y1}	-2.3	-2.0	0.0	-2.5	-0.8	-1.1	-1.5	0.0	-1.5	-1.1
F_{Y2}	0.8	-0.5	0.0	0.0	1.3	9.7	7.2	0.0	1.5	7.5
T_{Y2}	5.6	8.0	0.0	1.2	4.3	6.9	3.2	0.0	-3.2	6.5
F_{Y3}	-3.3	-2.2	0.0	-3.5	3.3	4.0	13.0	0.0	5.3	4.4
T_{Y3}	-1.1	2.2	0.0	-2.0	-2.0	0.2	-3.0	0.0	-2.7	0.0

NB: (1) $I_X(+)$ and $I_X(-)$ are the impulses of the push-off and braking forces respectively.
(2) Unit for peak force is (% body weight), for impulse (% body weight·s), for temporal parameter (% stance phase).
(3) All values are differences with the normal alignment data.
(4) Parameters underlined have statistical significance with confidence limit of 90%.
(5) "###" means no dwelling of the CP at the heel area

therefore only the results of the parametric analysis are presented. Table 6.9 shows the results of a parametric analysis of the ground reaction forces for the two groups of the amputees tested. In the table, the parameters which are underlined showed significant difference ($\rho \leq 10\%$) as the alignment of the prostheses was changed. All the parameters presented are the differences between the parameter values and the corresponding value at normal alignment.

The centre of pressure, as expected, left the heel area and entered the ball area sooner when the foot alignment was changed from the dorsi to plantar flexion. For group -1 amputees, the progression of the CP did not show a dwelling period or bunching up within the heel region when the foot was plantar flexed by 6 degrees. The amputee described the situation as walking with "totally no heel".

On the prosthetic side, there were no significant changes in the peak values of the fore-aft shear forces for group-2 amputees. However, significant changes were observed in both the braking forces and the transition time (T_{X0}) for group-1 amputees: the braking forces tended to increase and the transition time to advance in dorsi flexing the prosthetic foot. This finding is consistent with the results obtained by Mizrahi *et al* (1986) who reported a delay of the transition time (T_{X0}) as the prosthetic foot of the AK prosthesis was plantar flexed and the damping of the knee was increased. The above-mentioned trend of changes in the transition time suggests that, compared with the situation at normal alignment, the patient pivoted over the heel of the prosthetic foot for a longer period of time as the foot was dorsiflexed, and that the forward acceleration phase was extended. As a result, the amputees tended to roll over the prosthesis with higher speed at later stance phase. As far as the vertical forces are concerned, it is noted that the first peak and the trough were delayed when the alignment of the foot was changed from plantar to dorsi flexion (see T_{Y1} and T_{Y2}). As the prosthetic foot was dorsiflexed, the amputee dwelled on the heel for a longer period of time, which resulted in later weight acceptance, later foot-flat and later roll-over of the body.The roll-over is associated with the trough. It was also

Table 6.10 Results of Parametric Analysis on the Ground reaction forces (The SACS)

	Group-1 Amputees					Group-2 Amputees		
	-6°	-3°	0°	3°	6°	-4°	0°	4°
	(Extension ← | → Flexion)					(Extension ← | → Flexion)		
prosthetic Side								
$F_X(+)$	-1.2	-0.9	0.0	2.2	2.6	0.2	0.0	2.1
$F_X(-)$	1.6	1.7	0.0	-0.9	-1.5	7.5	0.0	-3.0
T_{X0}	-6.2	-2.2	0.0	-2.8	1.6	1.0	0.0	-3.3
$I_X(+)$	0.2	0.2	0.0	0.6	0.9	-0.1	0.0	0.2
$I_X(-)$	0.2	0.3	0.0	-0.2	-0.1	-0.7	0.0	0.4
F_{Y1}	2.0	-4.3	0.0	-6.2	-5.0	6.0	0.0	-0.7
T_{Y1}	-1.4	-0.2	0.0	0.0	-1.0	-3.0	0.0	3.0
F_{Y2}	1.2	1.9	0.0	3.4	3.2	-1.0	0.0	-1.2
T_{Y2}	4.8	2.2	0.0	3.6	1.8	-1.5	0.0	-14.0
F_{Y3}	4.1	2.1	0.0	-2.8	-1.4	-1.5	0.0	-0.3
T_{Y3}	-1.2	0.2	0.0	3.6	1.6	6.5	0.0	-0.2
TCP_S	11	5	0	-3	-7	8	0	-5
TCP_e	12	7	0	-1	-5	13	0	-2
Unaffected Side								
$F_X(+)$	-0.6	0.6	0.0	-1.5	-2.5	1.8	0.0	-4.3
$F_X(-)$	-1.0	-1.4	0.0	2.0	1.4	-0.8	0.0	4.6
T_{X0}	-2	1	0	1	1	1.	0	1
$I_X(+)$	0.1	0.2	0.0	-0.4	-0.5	0.5	0.0	-0.4
$I_X(-)$	-0.4	0.0	0.0	0.5	0.1	-0.3	0.0	0.6
F_{Y1}	-0.5	-5.2	0.0	2.2	-2.0	9.0	0.0	7.0
T_{Y1}	-0.2	-0.6	0.0	-0.6	-0.4	-2.5	0.0	0.5
F_{Y2}	2.0	2.3	0.0	2.4	3.0	-1.0	0.0	11.2
T_{Y2}	4.0	4.2	0.0	1.4	1.4	-0.5	0.0	-2.5
F_{Y3}	-3.4	-3.8	0.0	-1.2	-1.4	2.0	0.0	7.6
T_{Y3}	-2.2	-0.4	0.0	-0.4	-2.6	-1.0	0.0	-4.0

NB: (1) $I_X(+)$ and $I_X(-)$ are the impulses of the push-off and braking forces respectively.
(2) Unit for peak force is (% body weight), for impulse (% body weight·s), for temporal parameter (% stance phase).
(3) All values are differences with the normal alignment data.
(4) Parameters underlined have statistical significance with confidence limit of 90%.
(5) "###" means no dwelling of the CP at the heel area

noted that the lateral shear forces tended to increase with the FACS, indicating that the amputees encountered larger resistance in shifting their weight to the prostheses as the foot was progressively plantar flexed.

On the sound side, few parameters displayed significant and consistent changes for both group-1 and group-2 amputees. It is noted that the braking forces and the first peak of the vertical forces for group-1 amputees increased as the prosthetic foot was dorsiflexed. As discussed in the previous paragraph, the amputees tended to roll over the prostheses faster with the dorsiflexed foot at the late part of the prosthetic stance phase as the results of advancing of the forward acceleration phase. It was followed by the amputee's contacting the ground with his sound leg in such a way as to generate higher braking forces and vertical forces to attenuate the walking speed, as seen by the increase in the values of the parameter $F_X(-)$ and F_{Y1}.

§ 6.6.3.2 Effects of the SACS Although the socket alignment changes for the amputees tested did not affect the basic patterns of the ground reaction forces, differences were observed in the values of the the parameters at different alignments, as shown in Table 6.10.

The movement of the centre of pressure at the prosthetic side changed with the socket alignment changes. When the socket orientation angle was adjusted from extension to flexion direction, the transition period of the CP movement occurred earlier, see T_{X0} in Table 6.10. This finding was made on every amputees tested. As discussed in section 6.5.3, as the socket alignment was changed from extension to flexion direction, the amputees tried to compensate for this change by actually increasing the orientation angle of the prosthetic thigh $\Phi(t)$ (see Equ. 6.3b). However, this compensatory effect did not "fully compensate" for the alignment changes, resulting in the prosthetic foot being more plantar flexed relative to the ground. Therefore, the CP left the heel area and entered the ball area of the foot sooner with the SACS.

As far as the fore-aft shear forces are considered, two different trends were found. (1) On the prosthetic side, the forces shifted towards the positive direction, leading to a decrease of the braking force and an increase of the push-off force with the SACS. This trend of change may be caused by two factors: the orientation angles of the prosthetic thigh and the shank. As shown in Equ. 6.3b, the orientation angle of the prosthetic thigh was increased when the socket is changed from extension to flexion direction. As a result, the hip extensors were stretched, their function improved and a higher push-off force could be generated. Furthermore, the orientation angle of the prosthetic shank was decreased with the SACS, and as a result, a lower braking force at early stance phase and a higher push-off force at late stance phase were likely to be transmitted by the shank. (2) On the sound side, the braking force was increased and the push-off force was decreased with the SACS, exactly the opposite trend to the prosthetic side. The cause of this trend is not clear. It seems that the amputees re-arranged the share of propulsion that their two lower limbs had to generate in such a way that the overall propulsion was more or less constant.

Moreover, it was found that the transition time for the prosthetic fore-aft shear forces T_{X0} was delayed with the SACS. Since the trends of change in the orientation angle of the prosthetic foot $\Phi(t)$ are similar between the DFACS and the DSACS (see Equ. 6.3a and Equ. 6.3b), a similar explanation can be offered for the trend of change in T_{X0} with the SACS to that with the FACS.

For the vertical forces, only the last peak at the prosthetic side exhibited a change trend, that is, it decreased with the SACS.

§ 6.6.3.3 Effects of the FSACS The results of the parametric analysis on the ground reaction forces for the amputees undergoing the FSACS are shown in Table 6.11.

It was found that the transition period of the CP occurred progressively later

Table 6.11 Results of Parametric Analysis on the Ground reaction forces (The FSACS)

Variations of the KSI (mm)	-14	-7	-5	0	5	10
		Group-1 Amputees (KJC backward ← | → KJC forward)				
		prosthetic Side				
$F_X(+)$	-4.1	-2.2	-2.4	0.0	0.1	1.1
$F_X(-)$	2.6	2.2	2.8	0.0	-0.6	-1.8
T_{X0}	7.3	10.0	1.3	0.0	-7.3	-11.3
$I_X(+)$	- 1.1	-0.5	-0.4	0.0	0.3	0.6
$I_X(-)$	1.2	0.9	0.3	0.0	-0.2	-0.5
F_{Y1}	-3.3	-6.7	3.0	0.0	-2.3	-1.8
T_{Y1}	-6.7	-5.7	-4.3	0.0	1.5	1.7
F_{Y2}	3.0	4.3	-1.0	0.0	1.0	0.5
T_{Y2}	-7.3	-8.0	-4.3	0.0	3.8	4.0
F_{Y3}	2.0	3.0	1.7	0.0	2.0	1.5
T_{Y3}	-4.0	8.7	-5.0	0.0	4.2	4.7
TCP_S	-9	-5	-3	0	3	4
TCP_e	-11	-3	-2	0	4	6
		Unaffected Side				
$F_X(+)$	4.1	2.0	0.1	0.0	-2.0	-5.1
$F_X(-)$	-8.8	-7.6	-3.5	0.0	-0.2	2.2
T_{X0}	-1	1	0	0	0	1
$I_X(+)$	0.9	0.5	-0.1	0.0	-0.5	-0.8
$I_X(-)$	-1.1	-0.9	-1.0	0.0	-0.1	0.2
F_{Y1}	-15.3	-14.3	-11.0	0.0	-2.5	-2.5
T_{Y1}	1.7	2.0	5.3	0.0	-0.5	-1.2
F_{Y2}	8.3	3.0	0.3	0.0	4.3	1.5
T_{Y2}	4.3	2.7	-1.3	0.0	-2.7	-2.0
F_{Y3}	2.7	1.0	-4.0	0.0	0.0	-4.3
T_{Y3}	2.7	3.0	-5.3	0.0	-1.7	-4.2

NB: (1) $I_X(+)$ and $I_X(-)$ are the impulses of the push-off and braking forces respectively.
(2) Unit for peak force is (% body weight), for impulse (% body weight·s), for temporal parameter (% stance phase).
(3) All values are differences with the normal alignment data.
(4) Parameters underlined have statistical significance with confidence limit of 90%.
(5) "###" means no dwelling of the CP at the heel area

with the FSACS. As reported in 6.5.3, the amputees increased the orientation angle of the prosthetic thigh with respect to the ground as the prosthetic KJC was positioned anteriorly. Hence the orientation angle of the prosthetic foot was increased with the FSACS during stance phase (see Equ. 6.3b), that is, in an orientation which was more dorsiflexed than that at the previous alignment setting. As a result, the CP progression changed as observed.

On the prosthetic side, the braking force decreased, the push-off force increased and the transition time advanced significantly with the FSACS. For the vertical components, the two peak values and the trough, especially the trough, tended to occur later with the FSACS.

On the sound side, the fore-aft shear force shifted significantly towards the negative direction, that is, the push-off force decreased and the braking force increased. However, the transition time did not change with the FSACS. The vertical components showed that the first peak increased and time parameters tended to decrease or advance with the FSACS.

Further discussion on the effects of alignment changes on fore-aft shear and vertical forces is presented in the next section (§6.6.3.4)

§ 6.6.3.4 Comparison among the ACSs The purpose of this section is two fold. (1) As reported above, the ground reaction forces are affected significantly by alignment changes of the AK prosthesis and can therefore be used as an indicator for assessing the quality of alignment. Mizrahi *et al* (1986) and Zahedi (1988) demonstrated a procedure to reach optimal alignment by improving the smoothness of the fore-aft shear curve vs time. This procedure is still under investigation and needs verification through trials. Furthermore, without adequate knowledge of the correlation between the characteristics of the fore-aft shear and alignment parameters, this kind of procedure can not be efficient. In the project described in this thesis, certain alignment parameters of the prosthesis were systematically changed so that

Table 6.12 Trends of change in the Ground Reaction Parameters with the ASCs

Parameters	FACS	SACS	FSACS
	prosthetic Side		
$F_X(+)$	*	↑	↑
$F_X(-)$	*	↓	↓
T_{X0}	↑	↑	↓
$I_X(+)$	↓	↑	↑
$I_X(-)$	↑	↓	↓
F_{Y1}	∧	*	∧
T_{Y1}	↓	↑	↑
F_{Y2}	*	*	∧
T_{Y2}	↓	↓	↑
F_{Y3}	*	↓	*
T_{Y3}	∨	↓	↑
TCP_S	↓	↓	↑
TCP_e	↓	↓	↑
	Unaffected Side		
$F_X(+)$	*	↓	↓
$F_X(-)$	∨	↑	↑
T_{X0}	*	*	↓
$I_X(+)$	↑	↓	↓
$I_X(-)$	*	↑	↑
F_{Y1}	↓	*	↑
T_{Y1}	*	*	*
F_{Y2}	*	*	∨
T_{Y2}	*	*	∧
F_{Y3}	↑	*	↓
T_{Y3}	*	*	↓
Ψ	*	↑	↑
θ	*	↓	↓
Φ	↓	↓	↑

↑: increase with the ACS; ↓: decrease with the ACS; *: no significant changes;

∧: largest at normal alignment; ∨: smallest at normal alignment.

their effects on the ground reaction forces can be compared. In this way, it is possible to identify the effects of the alignment changes on the characteristics of the ground reaction forces. (2) In the discussion presented in §6.6.3, various explanations are offered which may result in the trends of change observed in the ground reaction forces. By comparing the effects of various alignment changes on the ground reaction forces, the suggested causes can be confirmed.

Table 6.12 shows the trends of the changes in the parameters of the ground reaction forces for the three ACSs together with the trends of the changes in the dynamic configurations of the prosthetic lower limbs.

As far as the peak values of the fore-aft force are concerned, the alignment changes which affect them mostly are not always apparent. One may think that the prosthetic push-off force could be increased by plantar flexing the prosthetic foot, but the results obtained in this study does not show the effect evidently. The prosthetic push-off force does not increase significantly with the FACS, nor does the orientation angle of the prosthetic foot relative to the ground $\Phi(t)$ appear to be a dominant factor to influence the peak values of the prosthetic fore-aft force: $\Phi(t)$ was decreased with the SACS and increased with the FSACS, but the trend of the change in the fore-aft force is the same with both the SACS and FSACS.

It is noted that the peak values of the fore-aft shear force changed in the same direction for the SACS and the FSACS, and that the orientation angles of the prosthetic thigh $\Psi(t)$ and the shank $\theta(t)$ were the same in the DSACS and DFSACS. This similarity in the trend of change suggest that $\Psi(t)$ and $\theta(t)$ affect the peak values of the fore-aft force most. As the thigh is flexed more, the hip extensors are able to function more efficiently and therefore produce higher push-off forces; but for the hip flexors, their efficiency is reduced and lower braking force is likely to be generated.The decrease in the dynamic orientation angle of the prosthetic shank has two effects: during early stance phase, the inclination angle of the shank will be decreased and as a result, less braking force is likely to be transmitted by the shank; at late stance phase, the inclination angle of the prosthetic shank increases and higher

push-off forces can be developed. It is noted that $\theta(t)$, although influenced by $\Psi(t)$, is dependent on the socket A/P tilt (see Equ. 6.2b and Equ. 6.2c). Furthermore, the compensatory changes in $\Psi(t)$ were observed in the SACS and FSACS, and the alignment adjustment performed to the socket was the same for the SACS and FSACS. It may therefore be deduced that the socket A/P tilt angle has a marked influence on the peak values of the fore-aft shear, that is, extending the socket increases the braking force and decreases the push-off, while flexing the socket improves push-off force but reduces the braking effect.

As far as the transition period of the CP is concerned, it is mostly influenced by the dynamic orientation angle of the prosthetic foot $\Phi(t)$ relative to the ground: as $\Phi(t)$ is increased, the foot is dorsiflexed more during early stance phase, the CP of the ground reaction forces dwells at the heel area for a longer period of time, and thus the transition period of the CP is delayed. This effect is evident in Table 6.12. It is interesting to note that the range of change in $\Phi(t)$ with the FACS is twice as much as those with the SACS and FSACS ($\pm 6^\circ$ for the FACS and $\pm 3^\circ$ for the SACS & FSACS), the range of change in the transition period of the CP with the FACS is also twice as much as those with the SACS and FSACS ($\pm 20\%$ for the FACS and $\pm 10\%$ for the SACS & FSACS). This finding confirms the argument above. It is noted that $\Phi(t)$ changed with all ACSs, suggesting that alignment adjustment performed at the prosthetic foot or the socket or both will change the transition period of the CP. However, a change in the dorsi/plantar flexion angle of the foot has a greater effect.

It is noted from Table 6.12 that the trends of the changes in the transition time of the fore-aft shear forces T_{X0} are opposite to those in the orientation angle of the prosthetic foot $\Phi(t)$ and from this, one can deduces that $\Phi(t)$ is the factor which affects T_{X0} mostly. However, the mechanism in which $\Phi(t)$ influences T_{X0} is not apparent. One may reason that as $\Phi(t)$ increases, the CP would dwell at the prosthetic heel, the braking force would be applied on the heel for a longer period of time, thus T_{X0} would be increased. This effect is contrary to what the results show. Therefore,

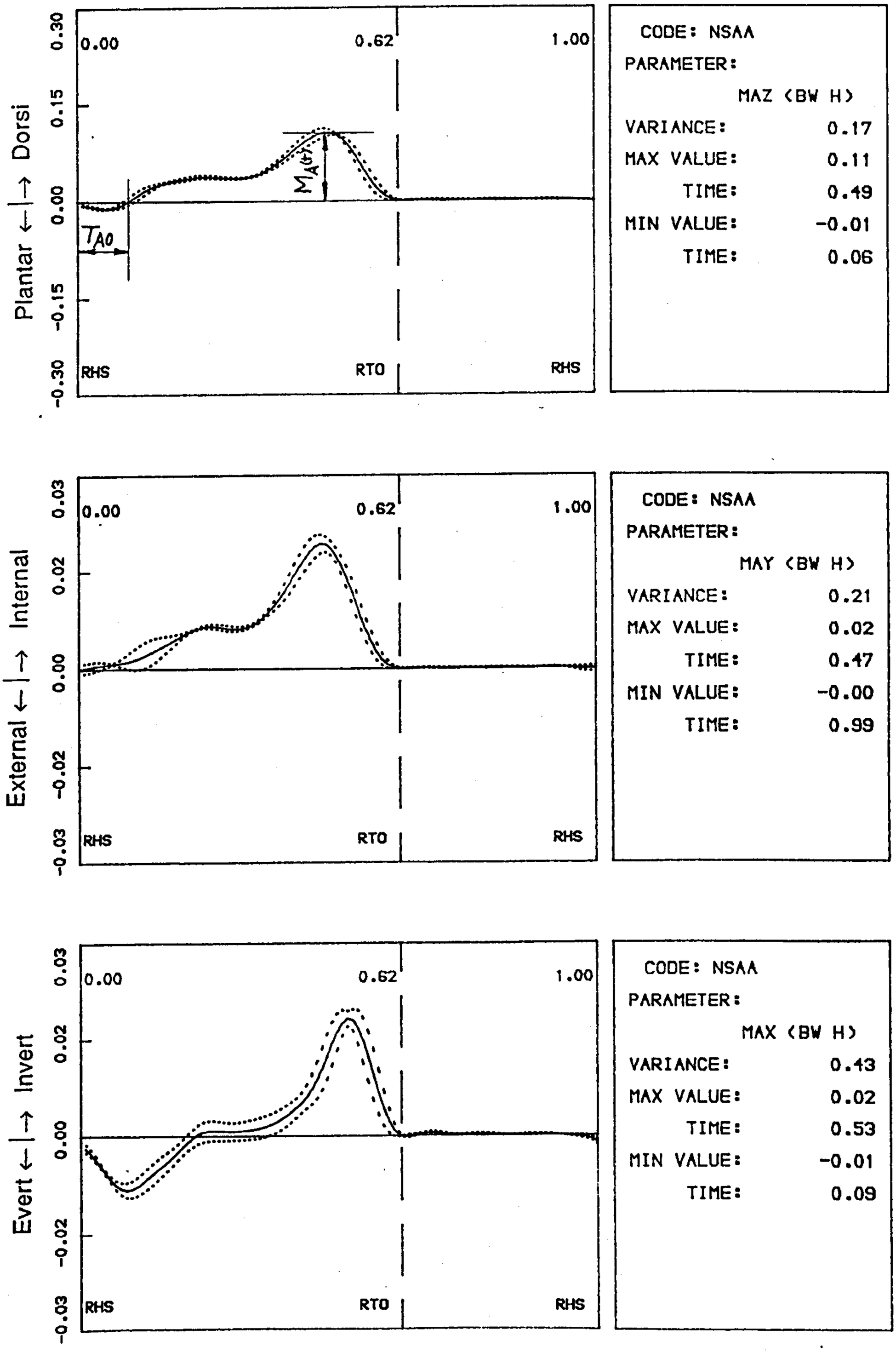

Fig.6.15 The ankle joint moments of the normal subject.

Table 6.13 Results of the Parametric Analysis On the Ankle Joint Moment

FACS	Group-1 Amputees 6°	3°	0°	-3°	-6°	Group-2 Amputees 6°	3°	0°	-3°	-6°
	(Plantar ← | → Dorsi)					(Plantar ← | → Dorsi)				
	prosthetic Side									
$M_A(+)$	1.25	0.14	6.8	0.14	0.12	-0.14	0.03	6.4	0.13	-0.86
$I_A(+)$	1.80	0.54	2.3	-0.22	-0.33	0.32	0.07	1.8	-0.40	-0.42
T_{A0}	-12	-6	24	7	9	-8	1	46	6	6
	Unaffected Side									
$M_A(+)$	-0.37	-1.26	9.1	-1.00	-0.73	-1.01	-0.18	9.7	-0.52	-0.92
$I_A(+)$	0.32	-0.34	4.9	-0.50	-0.17	-0.25	0.08	4.1	-0.02	-0.25
T_{A0}	2	3	12	4	5	-1	0	11	0	-1

SACS	Group-1 Amputees -6°	-3°	0°	3°	6°	Group-2 Amputees -4°	0°	4°
	(Extension ← | → Flexion)					(Extension ← | → Flexion)		
	prosthetic Side							
$M_A(+)$	-0.31	-0.07	6.8	0.16	0.06	-0.05	6.5	0.30
$I_A(+)$	-0.29	-0.59	2.3	0.20	0.58	-0.40	1.8	0.10
T_{A0}	6	10	24	-4	-4	9	46	-2
	Unaffected Side							
$M_A(+)$	-0.63	-0.75	9.1	-0.34	-0.42	-0.90	10.5	-0.18
$I_A(+)$	-0.25	-0.01	4.9	-0.18	-0.28	-0.10	4.35	-0.62
T_{A0}	5	3	12	-4	6	0	11	0

FSACS	Group-1 Amputees Displacement of the KSI (mm) -14	-7	-5	0	5	10
	(KJC backward ← | → KJC forward)					
	prosthetic Side					
$M_A(+)$	-0.07	-0.17	0.27	6.8	0.12	0.08
$I_A(+)$	0.50	0.53	0.37	2.33	-0.15	-0.23
T_{A0}	-1	2	-3	24	3	4
	Unaffected Side					
$M_A(+)$	0.23	0.03	-0.83	9.1	-0.42	-0.75
$I_A(+)$	0.93	0.60	-0.17	4.92	-0.05	-0.12
T_{A0}	5	11	-1	12	-1	-4

NB: (1) Values in normal alignment (0) are averaged data and those in changed alignments are differences from the normal values.
(2) Parameters underlined have statistical significance with confidence limit of 90%.
(3) Unit for maximum moment is (% body weight·height), for impulse is (% body weight·height·s), for transit time is % stance phase.

another explanation has to be found and a possible one may be as follows: as $\Phi(t)$ increases, the amputee pivots over the prosthetic heel for a longer period of time and moves forward at a considerable speed. As a result, the trunk of the amputee enters a forward acceleration phase earlier. This is reflected by the decrease in the values of T_{X0}. Since $\Phi(t)$ changes in all three ACSs, the alignment adjustment performed at the prosthetic foot or the socket or both will change the transition time of the fore-aft shear force.

To summaries, it was found that the ground reaction forces were significantly affected by alignment changes, especially the progression of the centre of pressure, the transition time and the peak values of the braking and push-off forces. Changes of alignment angles at the prosthetic foot (FACS) affected the progression of the CP and the transition time of the Fore-aft shear force, whereas changes of the angles at the socket (SACS) or the position of the prosthetic KJC (FSACS) affected, apart from the progression of the CP, both the temporal characteristics and the peak values of the fore-aft shear force.

§ 6.7 The Ankle Joint Moments

§ 6.7.1 The normal subject

Fig.6.15 shows the ankle joint moments for the normal subject tested. In the figure, the moments applied from below are presented about the three orthogonal axes of the shank segment:

MAX: moment about the fore-aft axis of the shank with its positive direction being the one tending to invert the foot;

MAY: moment about the longitude axis of the shank with its positive direction being the one tending to rotate the foot internally;

MAZ: moment about the medio-lateral axis of the shank with its positive direction being the one tending to dorsiflex the foot.

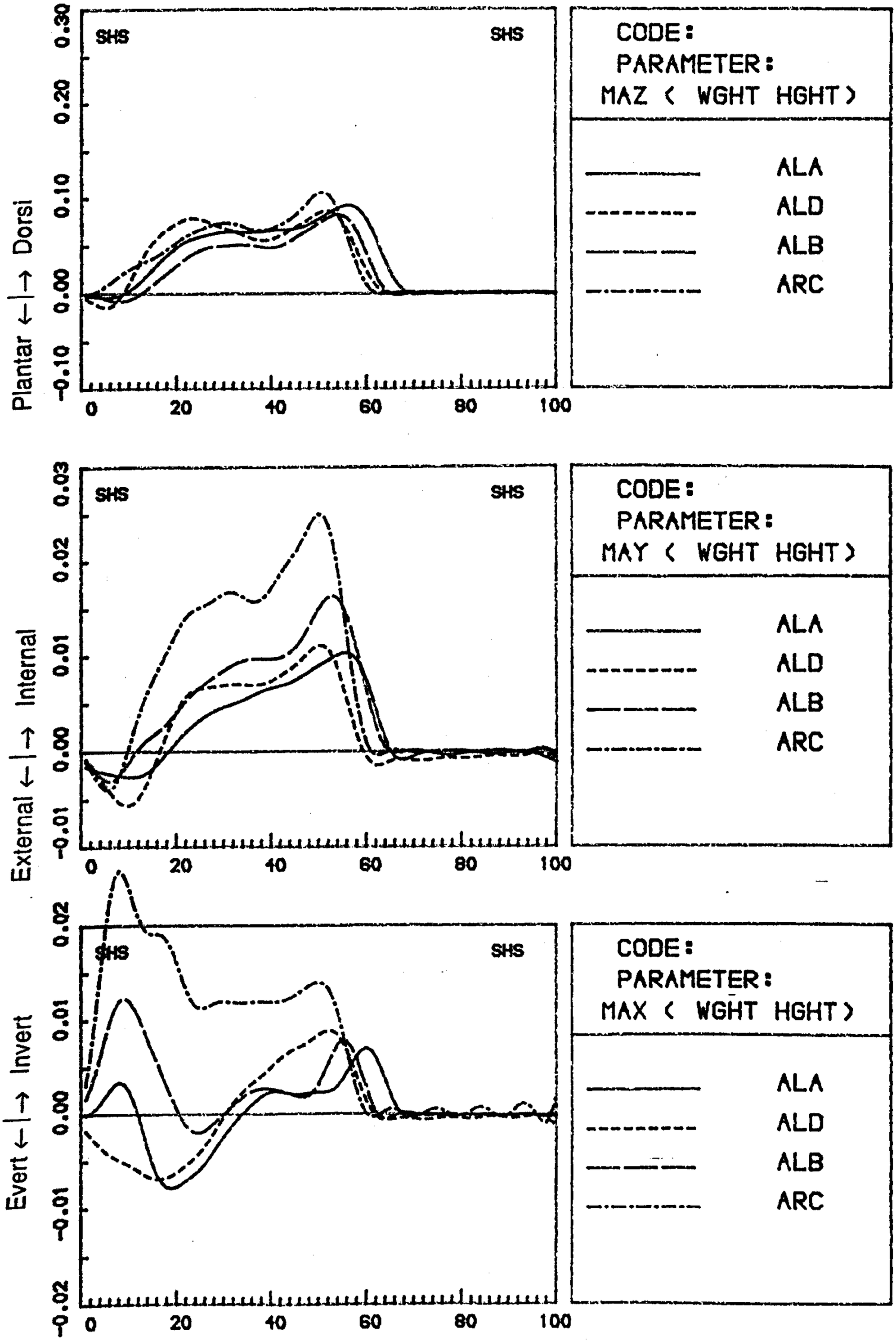

Fig.6.16a The averaged ankle joint moments for the amputees with normal alignment.
(Unaffected Side)

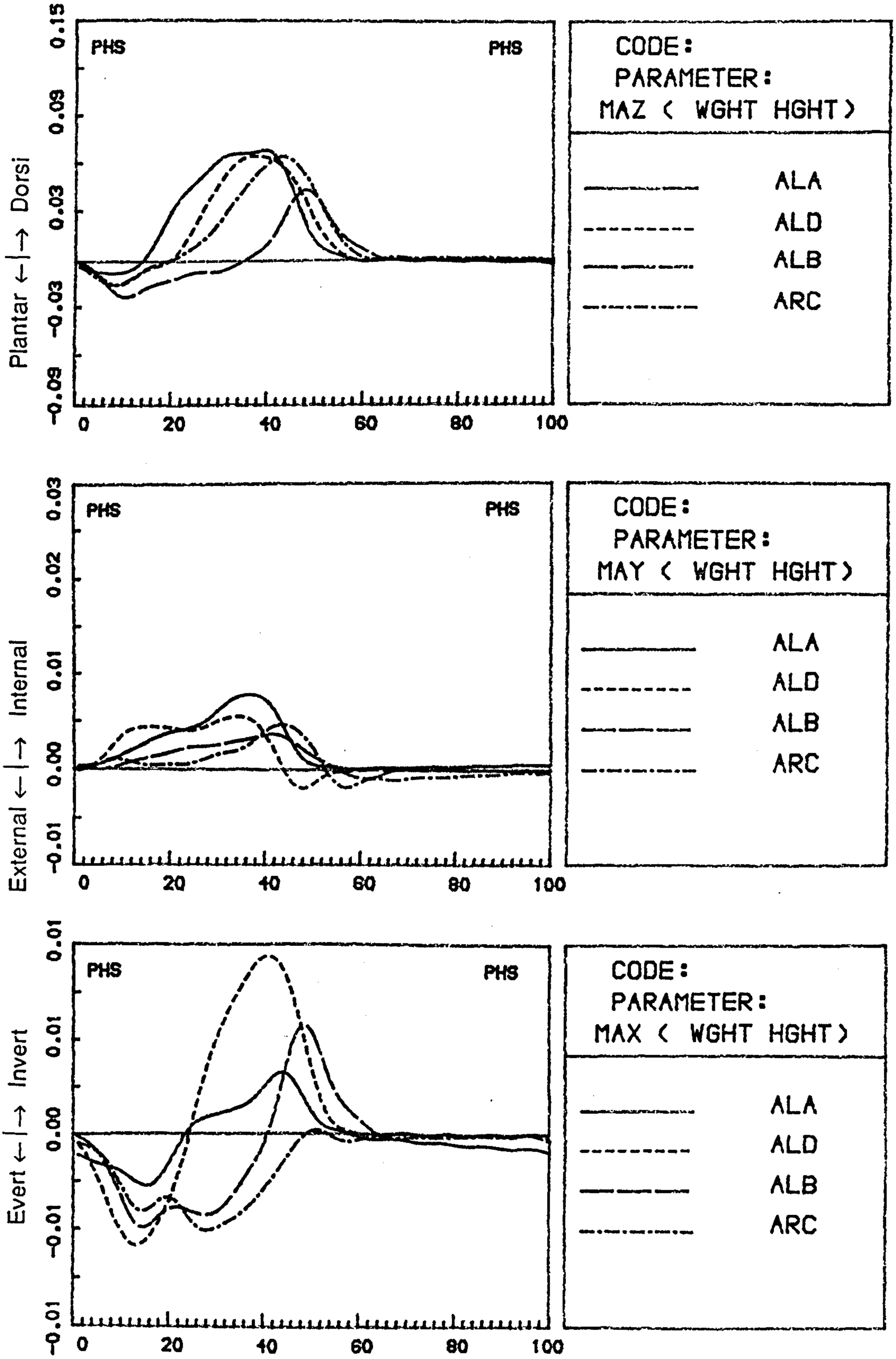

Fig.6.16b The averaged ankle joint moments for the amputees with normal alignment.
(Prosthetic Side)

The MAX is dominated by an eversion moment at early stance phase and an inversion moment at late stance phase. The MAY is overwhelmingly a internal rotation torque. The MAZ has a small plantarflexion moment for a short period of time (about 16% stance phase) just after heel strike, followed by a pronounced dorsiflexion moment that produces push-off action. Andriacchi and Strickland (1985) pointed out that the ankle joint moments for normal subjects were highly variable and could be classified into several patterns. The ankle joint moments obtained on the normal subject tested corresponded to their second, first and first patterns for the MAX, MAY and MAZ respectively.

Limited parameters of the extension moment were determined and their definitions are also in Fig. 6.15.

§ 6.7.2 The amputees with normal alignment

Fig. 6.16a and Fig.6.16b show the averaged curves of the ankle joint moments for the amputees tested with normal alignment. On the sound side (Fig. 6.16a), the ankle joint moment MAX is so variable among the subjects that each of them presents different patterns. The MAYs are generally of the same pattern, dominated by internal rotation torque but their magnitudes exhibit up to 100% differences. The MAZs showed the two-peak-one-trough type of patterns which can approximately be grouped into the pattern-2 of Andriacchi's classification.

On the prosthetic side (Fig. 6.16b), the MAXs also show a high variability as at the contralateral side. However, the group-2 amputees tended to have dominant eversion moment during the stance phase while the group-1 amputees display more or less equal eversion and inversion moments. The reason for the bias is probably due to variations in the alignment of the prosthesis and the position of the foot relative to the body during walking. The pattern of the MAYs is also variable, and the group-2 amputees tend to have lower internal rotation torque during the first two thirds of the stance phase. The pattern of the MAZs is more consistent, showing a plantar flexion moment during 21-25% of stance phase followed by a dorsiflexion moment.

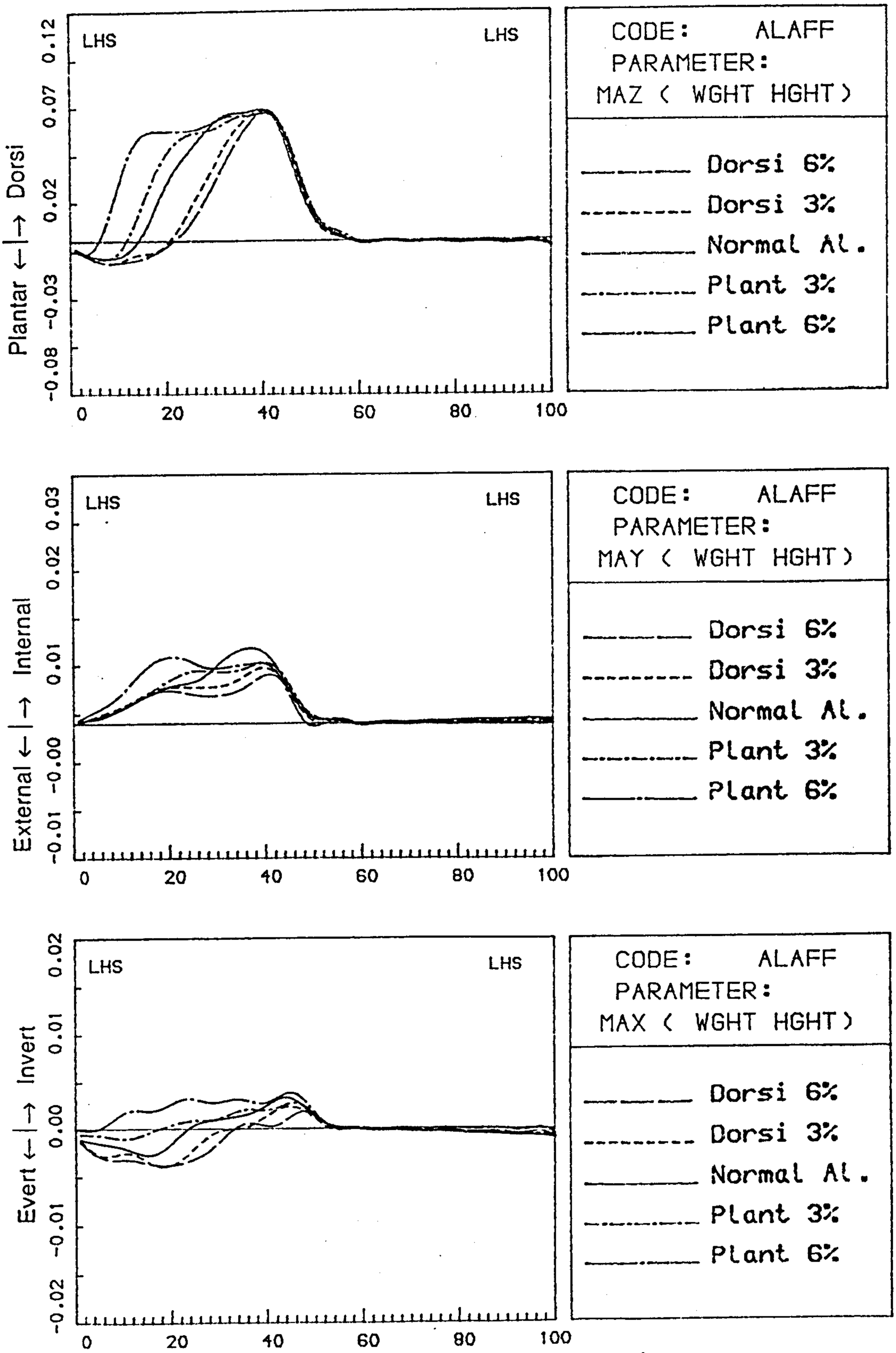

Fig.6.17 Typical changes in the patterns of the prosthetic ankle joint moments with the FACS.

However, the dorsiflexion moment for patient ALB occurred considerably later than that of the rest of the amputees. Compared with the normal subject, the plantar flexion moments lasted longer for the amputees (25% - 56% stance phase) than the normal subject (16% stance phase). This is due to the lack of adequate plantar flexion movement of the prosthetic ankle joint, resulting in the ground reaction forces being within the heel area for a longer period, and producing a plantar flexion moment at the AJC which lasts longer. The magnitudes of the dorsi/plantar flexion moment at the prosthetic ankle joint are much lower than those of the normal subject and of those on their sound side; a result of the absence of muscle power.

§ 6.7.3 Effects of the ACS

Having carefully examined the results for every amputee tested, the MAX and MAY of the sound side were found highly variable and no consistent change in pattern emerged. The basic characteristic patterns for each amputee remained similar to those displayed at normal alignment, indicating that the patients did not change their basic way of using their ankle joint. For the MAZ at the contralateral side, no significant changes in pattern were found with the ACS. However, some significant changes were observed in the parameters of the MAZ and these are discussed in the following sections.

The effects of the ACS on the prosthetic ankle joint moments are also presented in the following section.

§ 6.7.3.1 Effects of the FACS

Fig. 6.17 shows typical averaged prosthetic ankle joint moments for an amputee when the alignment of the foot was changed. The other amputees tested had similar changes in the patterns. The curves of the MAX shifted towards inversion moment direction significantly with the FACS, and in this example, they changed from being eversion dominant to inversion dominant. Since lateral shear ground force is increased with the FACS (see §6.6.3.1)

and the height of the AJC did not change during stance phase, the MAX, being partly the product of the M/L shear force and the height of the AJC, undergoes the observed change patterns. Another possible reason for this change in pattern is the fact that the centre of pressure of the ground reaction forces shifted medially relative to the sole of the prosthetic foot with the FACS. However, this could not be verified because the approach adopted in this work determined the CP with respect to the force platforms rather than the sole. The internal rotation moment displays a tendency to increase for all amputees tested. This may be mainly due to the advance of the transition period of the CP (see Table 6.9). As the transition period was advanced, the medial shear ground force tended to act at the toe area which was further anterior to the AJC, thus increasing the internal rotation torque that already existed. The MAZ shows significant changes with the FACS. With the FACS, the plantar flexion moment phase is decreased and the dorsiflexion moment phase is increased by about 35% stance phase, although their magnitudes are virtually unchanged. This advance of the transition time was mainly due to the advance of the transition period of the CP with the FACS, and this also resulted in significant changes in the joint moment impulses (see Table 6.9).

Comparing the two groups of amputees reveals that parameter T_{A0} undergoes less changes for group-2 amputees than for group-1 amputees (see Table 6.13). This difference may be caused by the different prosthetic feet fitted to the amputees. The Multiflex foot fitted to group-2 amputees seemed to be more flexible than SACH foot fitted to group-1 amputees.

On the sound side, the peak value of the extension moment for group-2 amputees and the impulse of the extension moment for group-1 amputees changed significantly with the FACS (see $M_A(+)$ and $I_A(+)$ in Table 6.13). It appeared that the values for both parameters were largest in normal alignment.

§ 6.7.3.2 Effects of the SACS Typical averaged prosthetic ankle joint

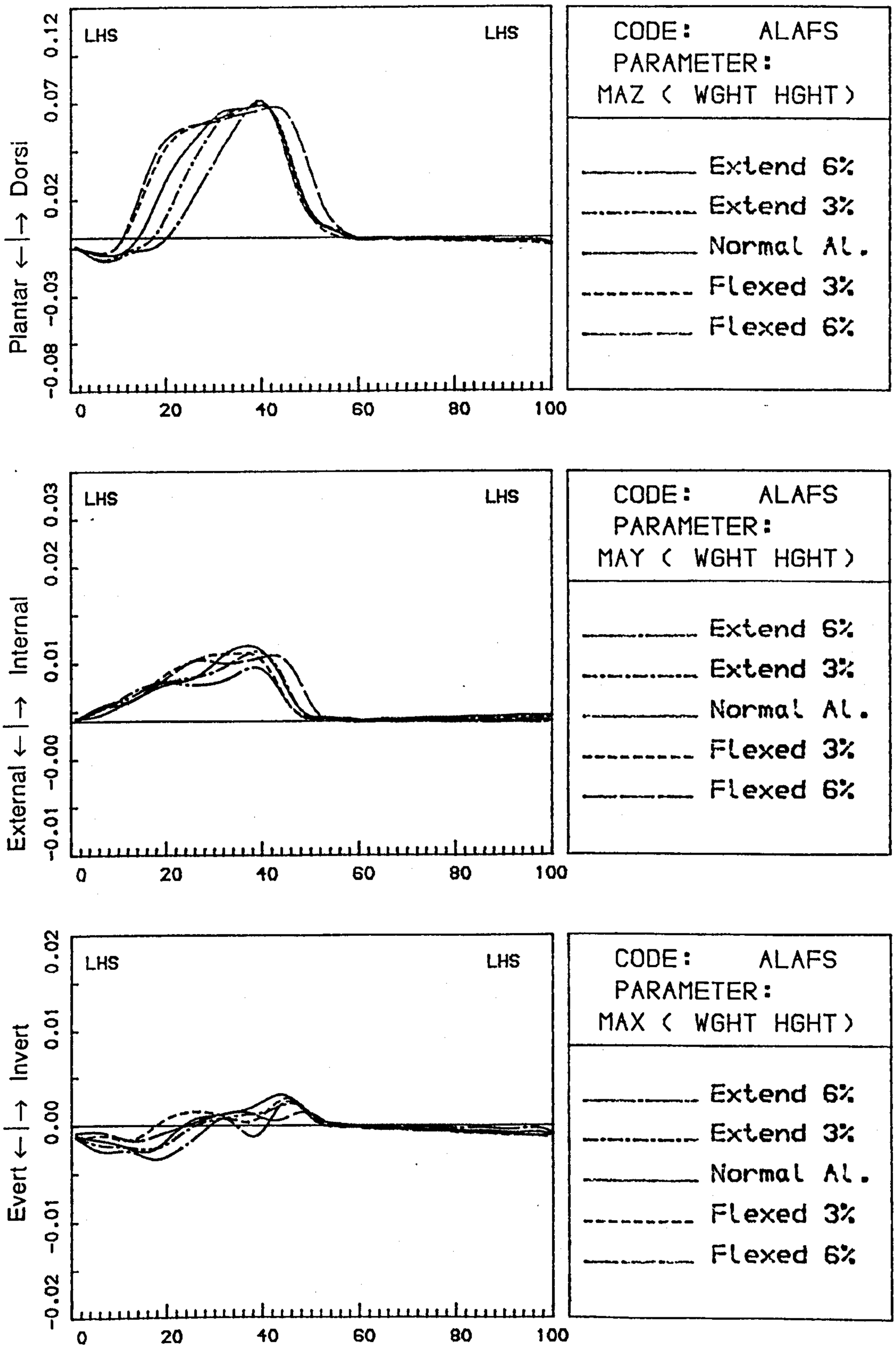

Fig.6.18 Typical changes in the patterns of the prosthetic ankle joint moments with the SACS.

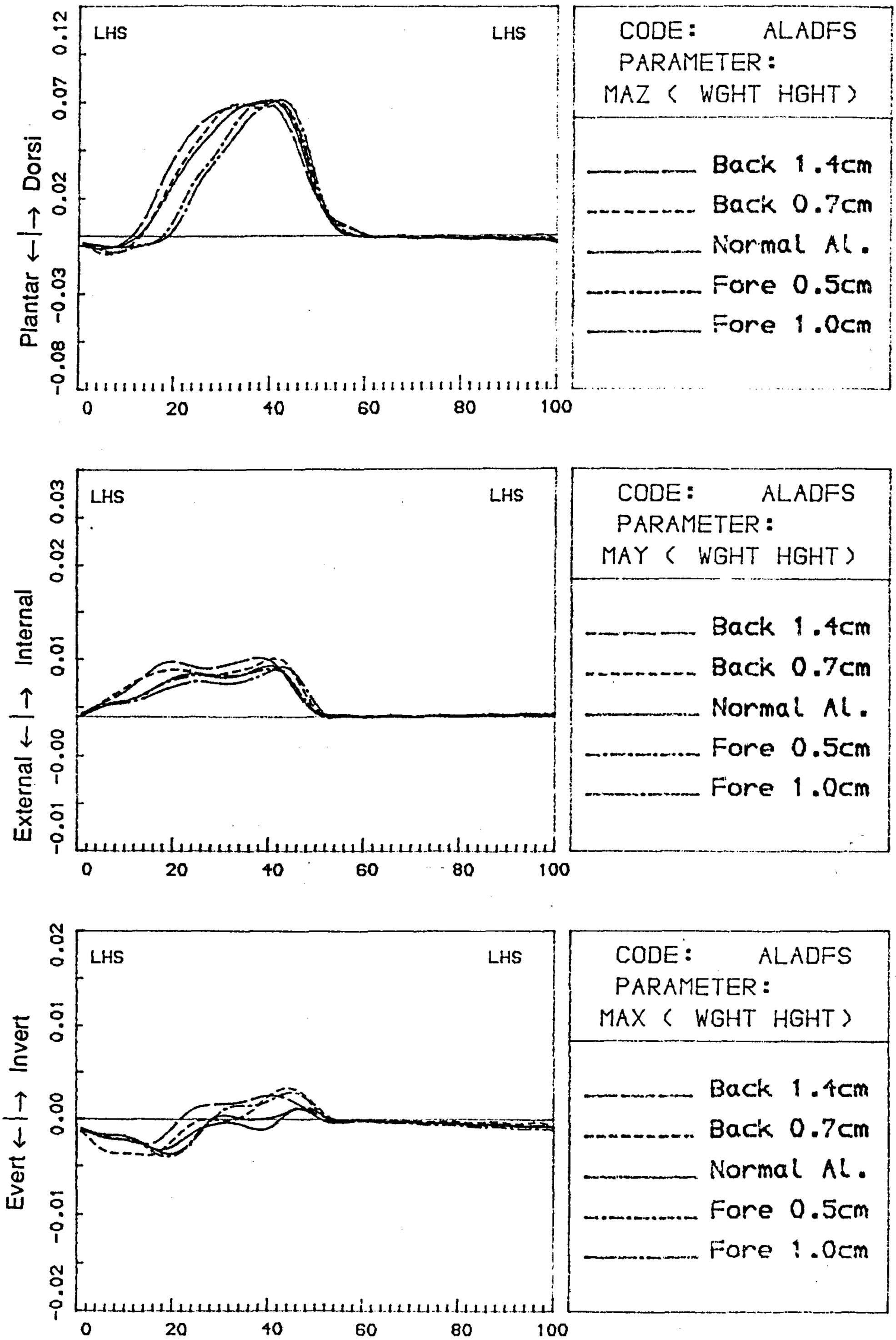

Fig.6.19 Typical changes in the patterns of the prosthetic ankle joint moments with the FSACS.

moments, as the socket alignment was changed, are shown in Fig. 6.18. The results from other amputees tested exhibited similar changes in the patterns. The MAX and MAY did not change significantly with the SACS. The magnitude of the MAZ did not change significantly with the SACS, but the transition time advanced with the SACS, greatly increasing the dorsiflexion moment impulse and decreasing the plantar flexion moment impulse, as shown in Table 6.13. The advance of the transition time of the MAZ can be traced back to the DSACS in which the inclination angles of the prosthetic foot decreased with the SACS (see Equ. 6.3a), resulting in the advance of the transition period of the CP that finally caused the observed effect

On the sound side, the peak value of the dorsiflexion moment decreased as the alignment of the socket was changed.

§ 6.7.3.3 Effects of the FSACS For all amputees tested, similar changes in the patterns of the prosthetic ankle joint moments were observed as the alignment of both the socket and the foot was changed. Fig. 6.19 shows typical patterns of the prosthetic ankle joint moments with the FSACS The MAX and the MAY showed a tendency to decrease with the FSACS. Although the magnitude of the dorsiflexion moment did not change significantly, its transition time was significantly advanced with the FSACS. As shown in Equ. 6.3c, the amputee increased his thigh orientation angle throughout the stance phase with the FSACS. The inclination of the prosthetic foot was increased relative to the ground , resulting in the delay of the transition time of the MAZ.

On the sound side, the dorsiflexion moment decreased and the transition time of the MAZ advanced significantly with the FSACS, resulting in a significant decrease in the impulse of the dorsiflexion moment. The causes of these changes are not clear, but the decrease trend of the push-off ground force with the FSACS is certainly one of the causes.

§ 6.7.3.4 Summary In summary, the alignment changes did not have

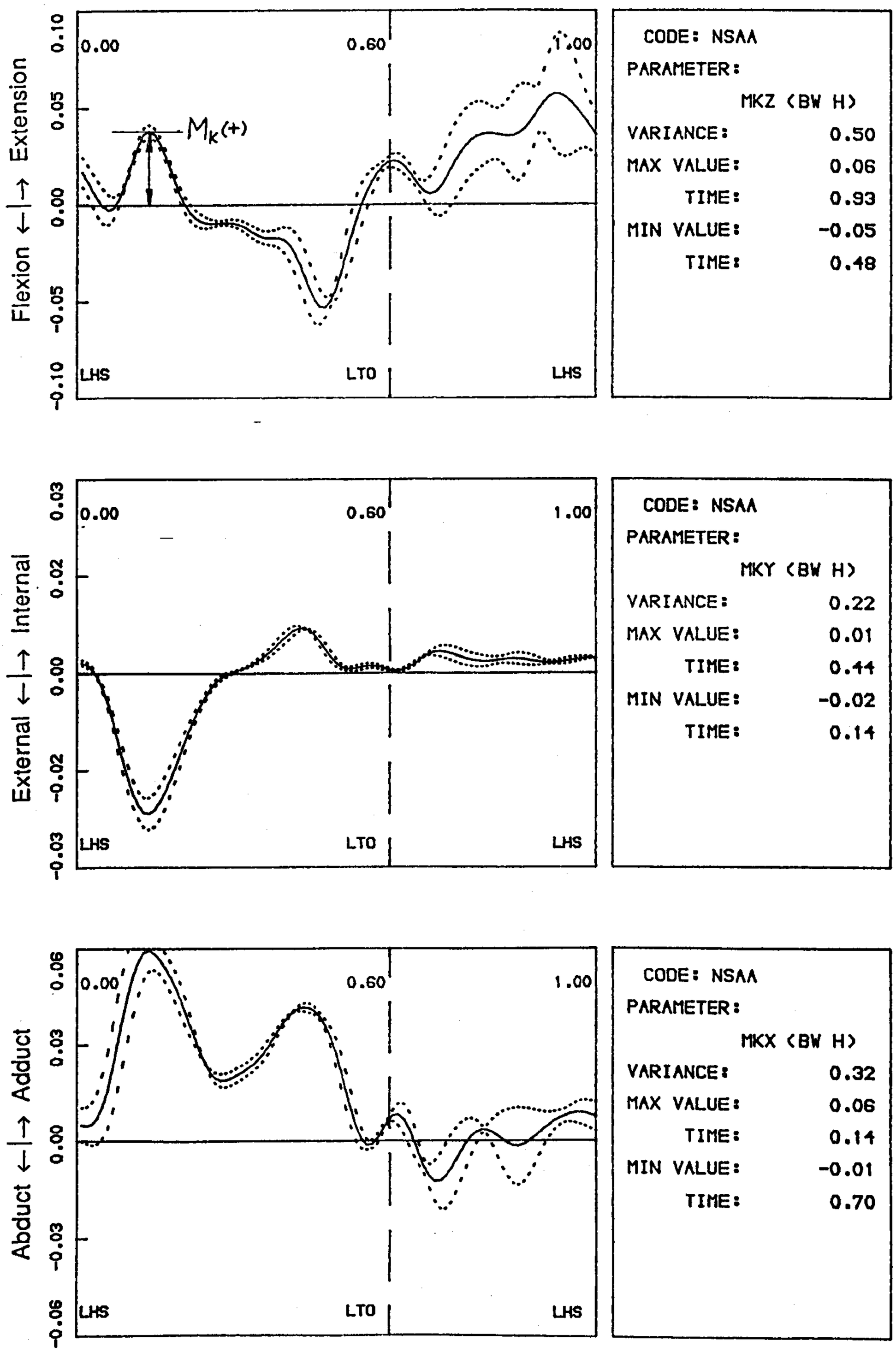

Fig.6.20 The averaged knee joint moments of the normal subject.

Table 6.14 Results of the Parametric Analysis On the Knee Joint Moment

FACS	Group-1 Amputees 6°	3°	0°	-3°	-6°	Group-2 Amputees 6°	3°	0°	-3°	-6°
	(Plantar ← | → Dorsi)					(Plantar ← | → Dorsi)				
	prosthetic Side									
M_K(+)	2.47	0.13	4.6	0.06	-0.33	0.36	0.50	3.2	0.13	-0.26
I_K(+)	1.66	0.43	1.7	-0.04	-0.04	0.21	0.25	1.3	-0.22	-0.39
	Unaffected side									
M_K(+)	-0.50	-0.88	3.6	-0.38	-1.13	-0.71	-0.48	4.1	-0.68	-1.17
I_K(+)	-0.02	-0.31	2.2	-0.34	-0.49	-0.16	0.13	2.1	-0.17	-0.50

SACS	Group-1 Amputees -6°	-3°	0°	3°	6°	Group-2 Amputees -4°	0°	4°
	(Extension ← | → Flexion)					(Extension ← | → Flexion)		
	prosthetic Side							
M_K(+)	0.36	0.52	4.6	-0.48	-1.14	0.55	3.2	-0.23
I_K(+)	0.26	0.20	1.7	-0.10	-0.20	0.15	1.25	-0.35
	Unaffected side							
M_K(+)	-0.82	-0.42	3.6	-0.48	-1.14	0.56	3.2	-0.23
I_K(+)	0.25	0.20	2.2	-0.48	-0.38	0.05	2.20	-0.60

FSACS	Group-1 Amputees Displacement of the KSI (mm) -14	-7	-5	0	5	10
	(KJC backward ← | → KJC forward)					
	Unaffected Side					
M_K(+)	2.17	1.27	0.97	4.6	-0.12	-0.92
I_K(+)	1.43	1.20	0.68	1.74	-0.17	-0.43
	Prosthetic side					
M_K(+)	1.07	0.60	-0.17	3.6	-0.30	-0.30
I_K(+)	0.83	0.60	-0.33	2.24	-0.17	-0.07

NB: (1) Values in normal alignment (0) are averaged data and those in changed alignments are differences from the normal values.
(2) Parameters underlined have statistical significance with confidence limit of 90%.
(3) Unit for maximum moment is (% body weight·height), for impulse is (% body weight·height·s), for transit time is % stance phase.

significant effects on the magnitude of the dorsiflexion moment about the prosthetic ankle joint; the magnitude is limited by the length of the foot. However, the transition time, at which the plantarflexion moment is reversed into dorsi-flexion moment is sensitive to alignment changes and is closely dependent on the orientation angle of the foot $\Phi(t)$.

§ 6.8 The Knee Joint Moments

§ 6.8.1 The normal subject

Fig. 6.20 shows the knee joint moments of the normal subject which applied to the KJC from below. In the diagram, the sign convention is: moment causing adduction of the shank is positive for the MKX; torque causing internal rotation of the shank is positive for the MKY; and moment causing extension of the shank is positive for the MKZ. The pattern of the moments is consistent with the data presented in the literature, such as Andriacchi & Strickland (1985) (see Fig.2 36). The MKX is dominated by an adduction moment. The MKY displays a substantial external rotation torque (about 2.5% body weight·height) during the first half of the stance phase, followed by a relatively lower internal rotation torque. The MKZ has an extension moment during the early stance phase which decreased to about zero just after HS. This decrease is due to the large flexion angle of the knee as presented in Fig.6.5. During late stance phase, the MKZ displays a high flexion moment as the subject pushed off. This pattern can be grouped into the pattern-2 according to Andriacchi & Strickland.

§ 6.8.2 The amputees with normal alignment

The knee joint moments for the amputees at normal alignment are shown in

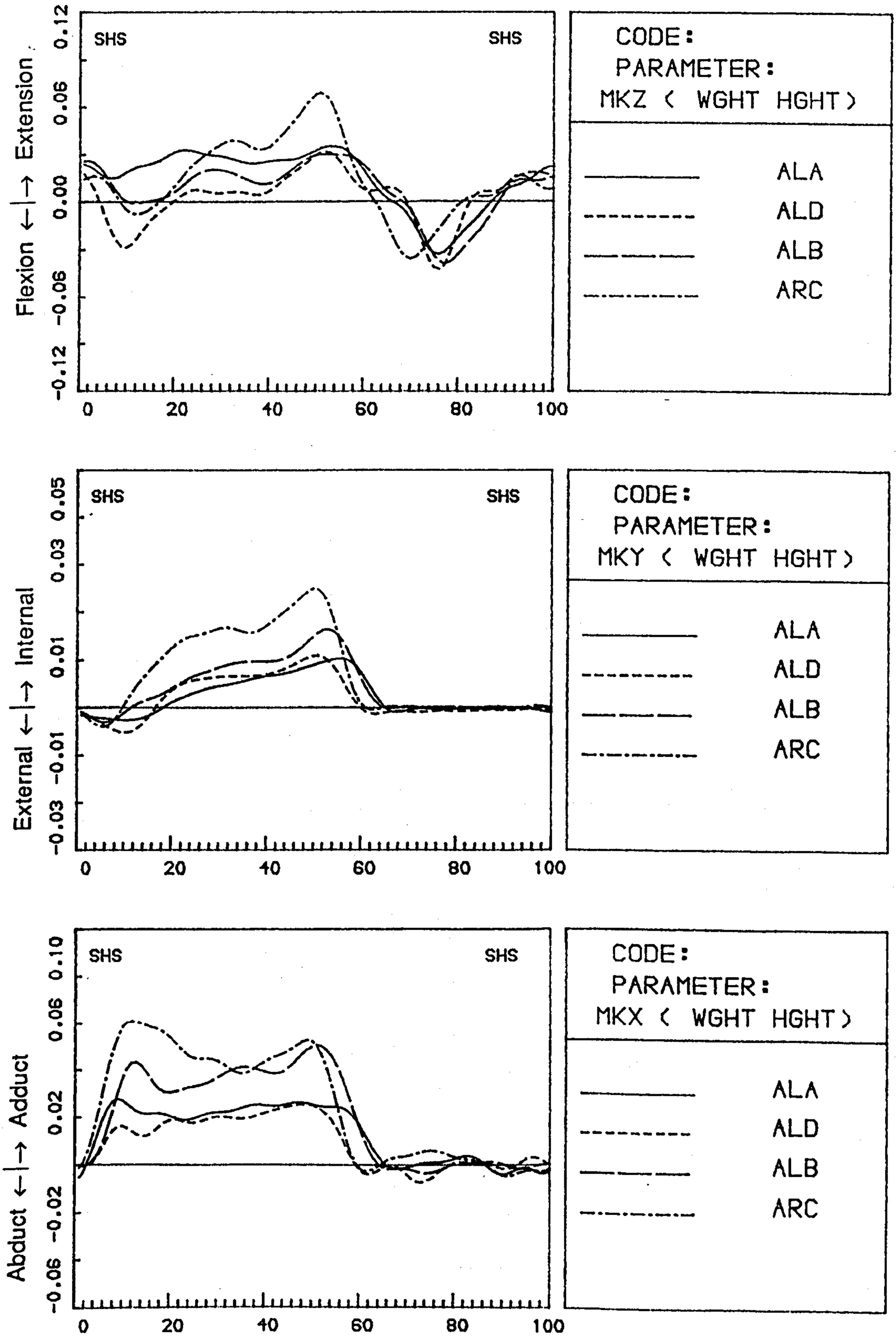

Fig.6.21a The averaged knee joint moments for the amputees with normal alignment. (Prosthetic Side)

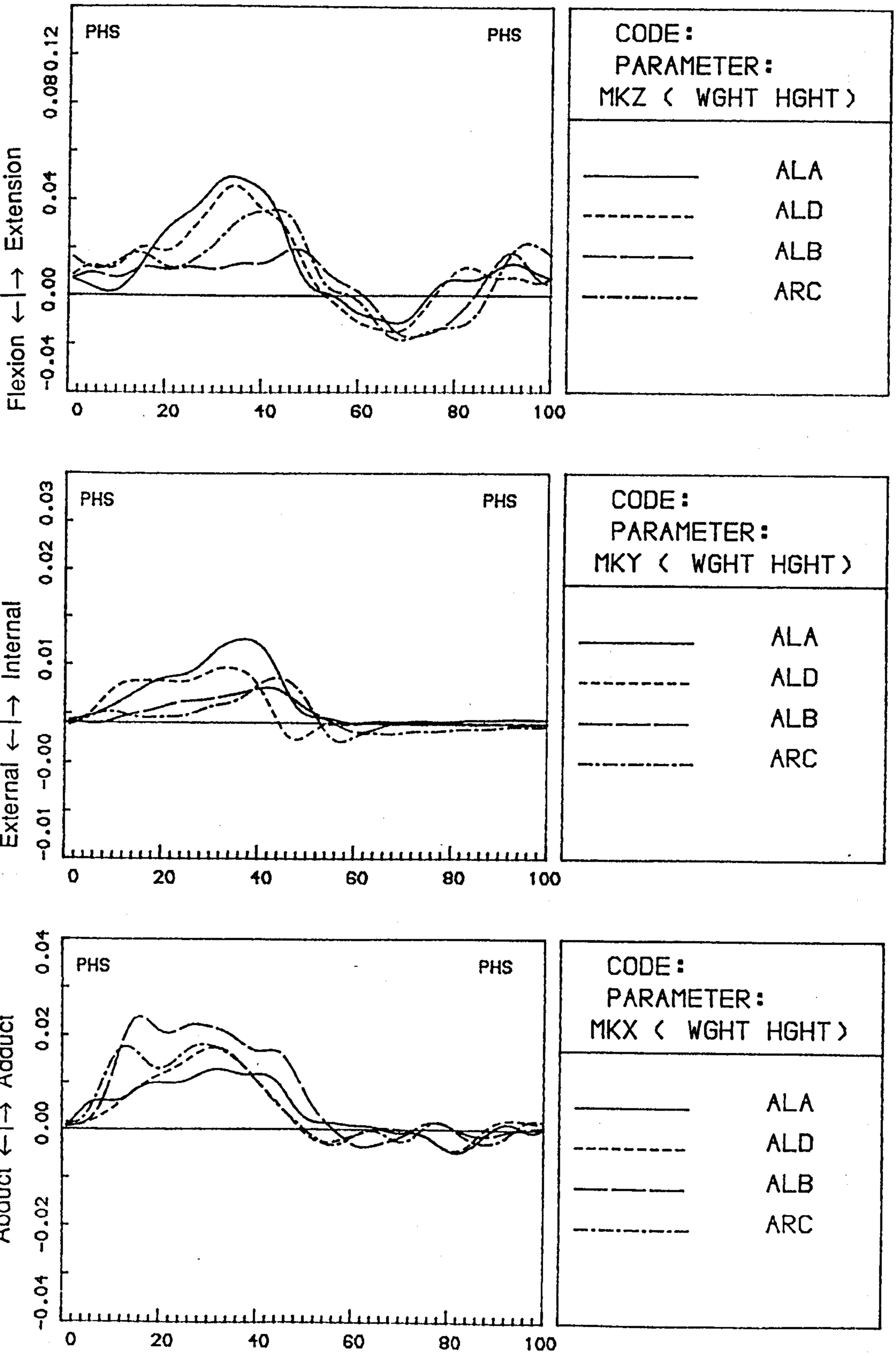

Fig.6.21b The averaged knee joint moments for the amputees with normal alignment.
(Prosthetic Side)

Fig. 6.21a-b. On the sound side (Fig. 6.21a), the MKX has a similar pattern to that of the normal subject with the adduction moment being dominant. The magnitudes of the MAX display a high variability amongst the amputees. It seemed that the group-2 amputees tended to have a higher adduction moment but the reason for this is not known. The MKY has a small external rotation torque at early stance phase, followed by a substantial internal rotation torque. The patterns of the MAZ are variable, covering Andriacchi's first and third patterns (refer to Fig.2.36). It is noted that the MKZ shows a peak at mid-stance which corresponds to the peak in the vertical ground force caused by vaulting.

On the prosthetic side, all three moments are basically positive, that is, dominated by an adduction moment, internal rotation torque and extension moment. However, the magnitude of the moments is quite variable amongst the amputees, especially for those of the MKZ. It appears that the extension moment of the group-1 amputees is higher than that of the group-2 amputees. The reason for this difference may due to the differences in the knee mechanisms fitted to the amputees. The group-2 amputees were fitted with Endolite stabilized knee which can sustain certain amount of flexion moment as the weight of the amputee was applied on it and thus less knee extension moment was needed to stabilize the knee. It is noticed that for the group-1 amputees the extension moment about the prosthetic knee joint is necessary for knee stability throughout the prosthetic single stance phase, since no locking mechanisms were put into effect during the gait tests.

§ 6.8.3 Effects of the ACS

The extension moment at the prosthetic knee joint MKZ indicates the stability of the knee joint during walking and deserves detailed discussion. If the moments due to the inertial and gravity forces of the prosthetic shank and foot are ignored during stance phase, the MKZ can be determined by following equation:

$$MKZ = [F_{GY}(X_G - X_K)] + [F_{GX}Y_K] \qquad (6.4)$$

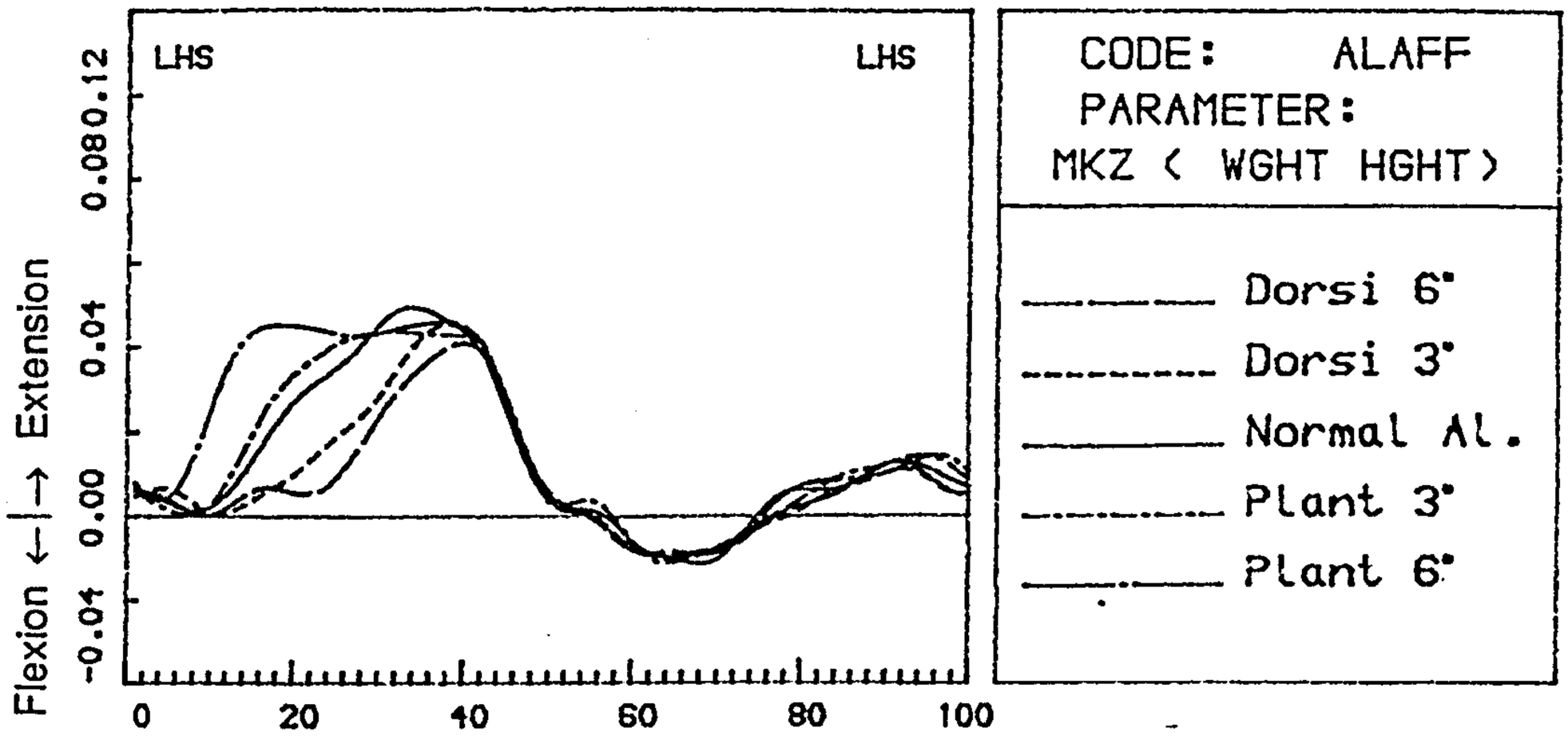

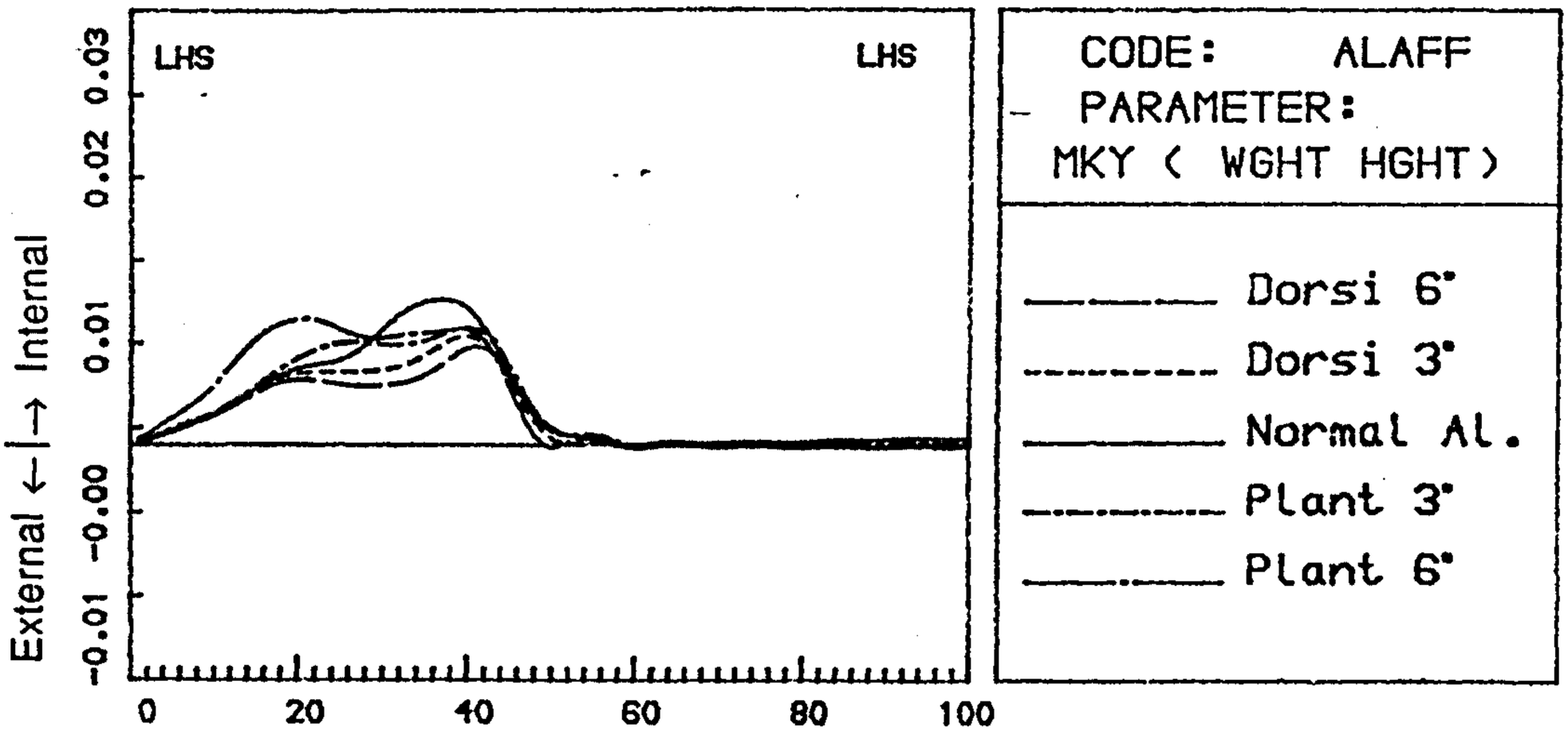

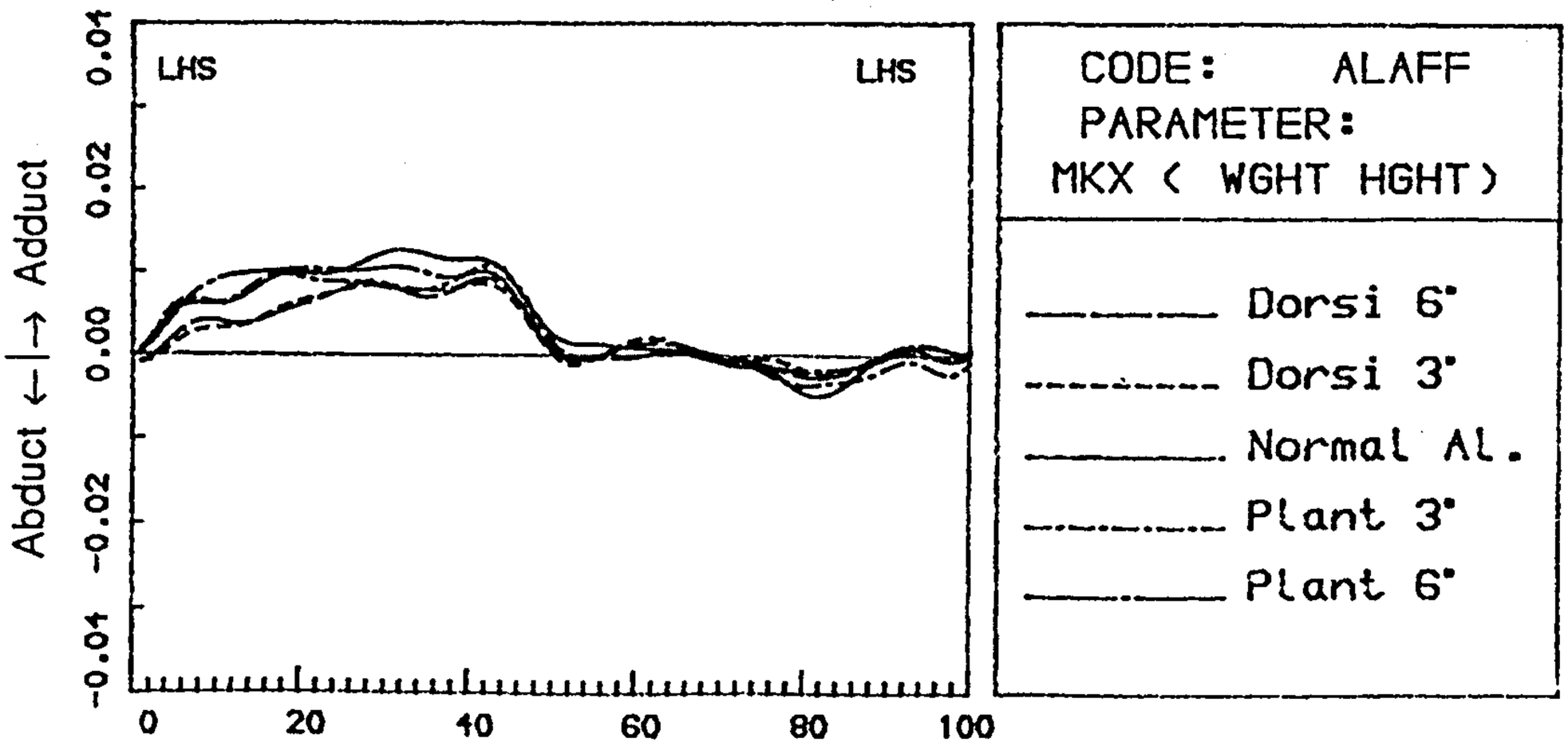

Fig.6.22 Typical changes in the patterns of the prosthetic knee joint moments with the FACS.

in which the terms F_{GX} and F_{GY} are the fore-aft and vertical components of the ground reaction forces respectively, X_G is the X-coordinate of the CP of the ground reaction forces, and X_K and Y_K are the coordinates of the KJC in the saggital plane. The term X_G is influenced by the time at which the transition period of the CP occurs: for a certain instant of stance phase, the advance in time of the transition period means that the CP is relatively more forward than it used to be. The term X_K is affected by the orientation angle of the shank, thus in turn by the alignment of the prosthesis. The terms F_{GY} and Y_K can be regarded as constants since they change only slightly during stance phase. The changes in the pattern of the MKZ with the ACSs will be discussed referring to Equ. 6.3.

§ 6.8.3.1 Effects of the FACS On the sound side, alignment changes in the prosthetic foot (the FACS) were found to have no apparent effects on the patterns of the contralateral knee joint moments. However, two amputees (ALA & ALB) displayed a decrease in the sound MKZ during the early stance phase but the reason for this trend was not known. The parametric analysis of the MAZ showed that only the peak values of the extension moment for group-1 amputees changed: it decreased significantly when the alignment was changed (see Table 6.14).

Much greater effects of the FACS were found on the prosthetic knee joint moments and Fig. 6.22 demonstrates the changes in the pattern for amputee ALA. Unless reported otherwise, the results from the other amputees had similar changes in the patterns. The shapes of the three knee joint moments during stance phase changed from triangle-like to square-like form with the FACS while the maximum magnitudes did not change significantly. It is noted that the time at which the extension moment reaches its full value is progressively advanced with the FACS, resulting in an increase in the impulse of the extension moment with the FACS (see Table 6.14). The changes in the pattern of the MKX may be caused by a decrease of the ground medial shear forces with the FACS. The changes in the pattern of the MKZ may be caused by the delay of the transition period of the CP with the FACS (see §6.6.3.1). With

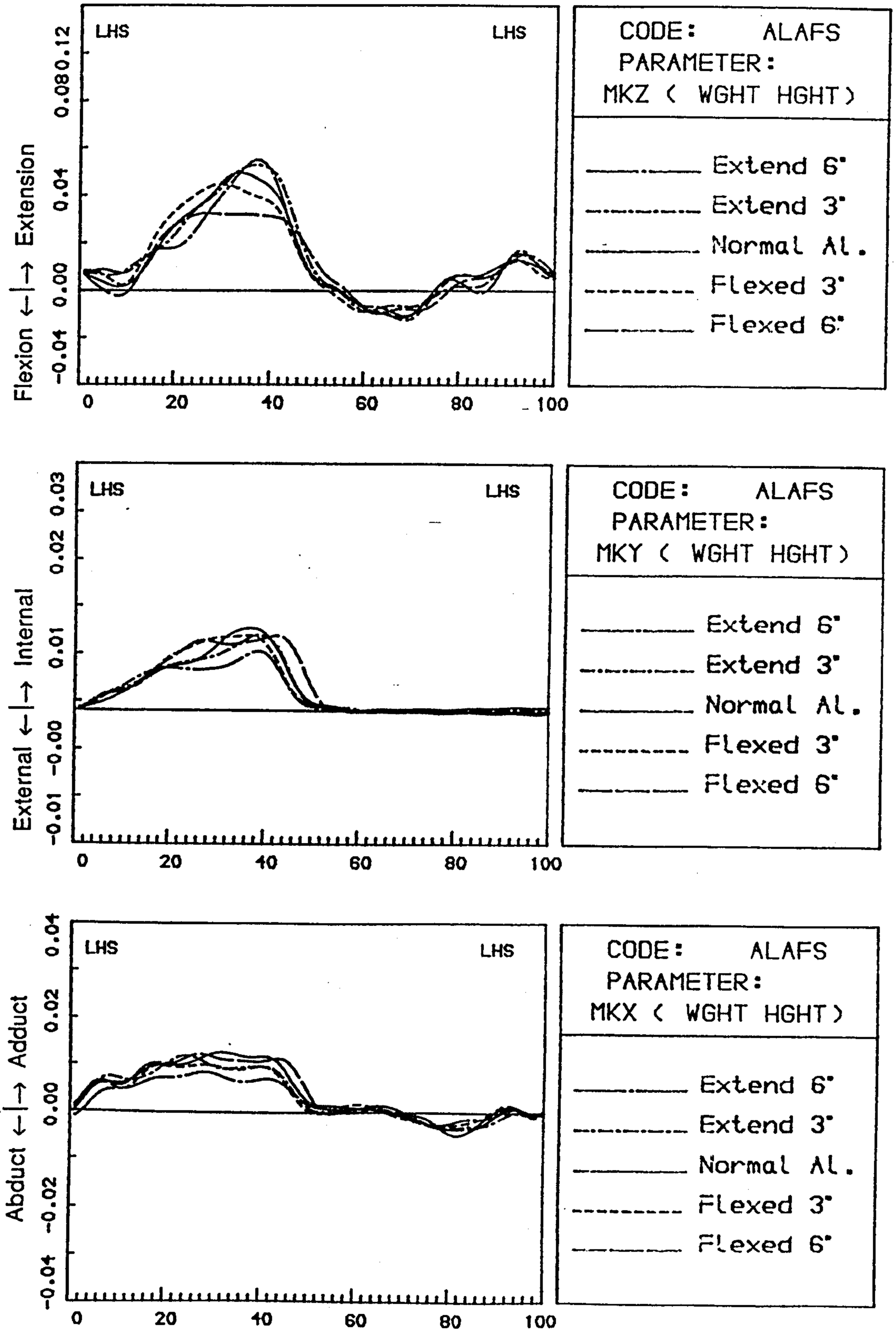

Fig.6.23 Typical changes in the patterns of the prosthetic knee joint moments with the SACS.

the FACS, the transition period of the CP advanced, that is, the X_G is increased, resulting in the increase of the first term of Equ. 6.3. Since the transition time of the F_{GX} is delayed with the FACS, the second term in Equ. 6.3 is decreased. From the fact that the MKZ is increased with the FACS, it can therefore be deduced that the first term in Equ. 6.4 dominates the pattern of the MKZ, and further that the transition period of the CP is a major factor in influencing the changes in the patterns of the MKZ.

It is noted that the extension moment in dorsiflexion alignment is very small during the very early period of the single stance phase, and this can be dangerous for the amputees.

Unlike what is shown in Fig. 6.22, the group-2 amputees did not exhibit consistent changes in the patterns of the MKX and the MKY, and the extent to which the extension moment decreased with the FACS was much smaller.

§ 6.8.3.2 Effects of the SACS The knee joint moments at the sound side did not present any consistent and significant changes in their patterns as the socket A/P tilt angle was changed (the SACS). However, the peak value and the impulse of the extension moment changed significantly with the SACS for group-1 amputees (see Table 6.14)

Fig. 6.23 shows the changes in the patterns of the prosthetic knee moments for amputee ALD with the SACS. Other amputees tested showed a similar change in pattern. No significant trends of change in the patterns of the MKX and MKY were observed with the SACS for all the amputees tested. The knee extension moment MKZ showed similar patterns at different alignments but the magnitudes decreased significantly with the SACS. With the SACS, X_G in Equ. 6.3 is increased due to the advance of the transition period of the CP (see Table 6.10), but X_K also increased as the result of the increase of the shank orientation angles (see Equ. 6.3b), thus the trend of the change in the first term of Equ. 6.3 can not be determined at the moment.

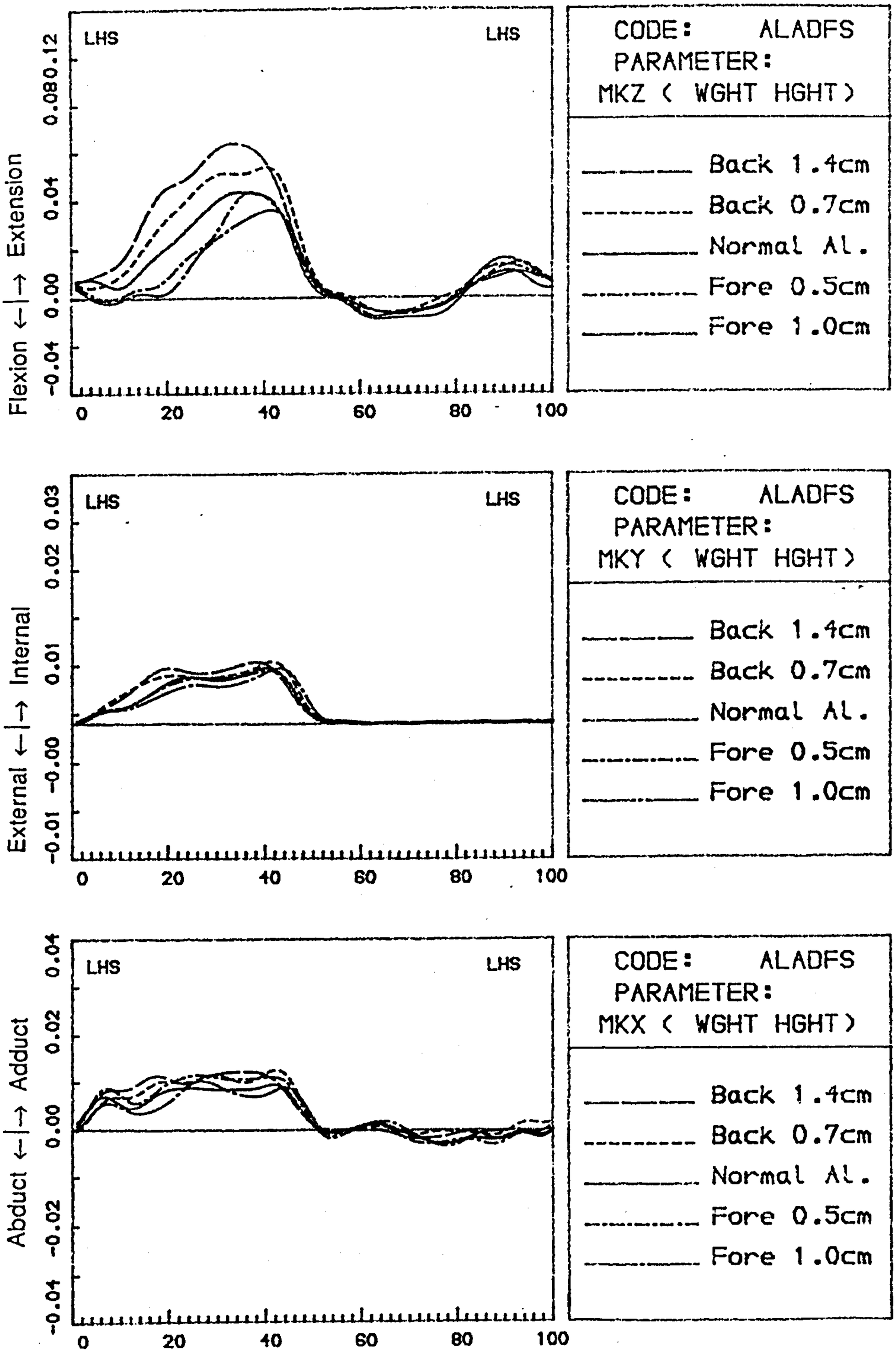

Fig.6.24 Typical changes in the patterns of the prosthetic knee joint moments with the FSACS.

The term F_{GX} increased with the SACS as a result of the advance of the transition time of the fore-aft ground force (see Table 6.10), suggesting that the trend of the second term in Equ. 6.4 is to increase the MKZ. However, the MKZ is actually found to decrease with the SACS, implying that X_K or the orientation angle of the shank is the controlling factor of the MKZ. It is noted that the knee stability index (KSI) is decreased with the SACS (see §6.2), being of the same trend of change as the $M_K(+)$.

§ 6.8.3.3 Effects of the FSACS No significant and consistent changes were observed in the patterns or the parameters of the sound knee joint moments for the amputees tested as the A/P tilt angle of both the socket and the foot was changed (the FSACS).

Fig. 6.24 shows the changes in the pattern of the prosthetic knee joint moments for amputee ALA with the FSACS. Another amputee showed a similar change. The MKX and the MKY did not change significantly in the patterns with the FSACS. The MKZ underwent significant and consistent changes, that is, it decreased with the FSACS. The results of the parametric analysis on the extension moment also show a trend of change (see. Table 6.14). With the FSACS, X_G in Equ. 6.4 is decreased as the result of delay of the transition period of the CP (see TCP_S and TCP_E in Table 6.11), and X_K is increased due to the increase in the shank orientation angle (see Equ. 6.3c), both tending to decrease the value of the first term in Equ. 6.4. The value of the term F_{XG} in Equ. 6.4 is increased as a result of the advance of the transition time of the fore-aft ground force (see T_{X0} in Table 6.11), tending to increase the extension moment. From the fact that the extension moment is decreased with the FSACS, it can be deduced that the first term in Equ. 6.4 is dominant.

It was noticed that the extension moment for the 'forward' alignment changes approached zero during early stance phase, indicating that the prosthetic knee joint was in a state of "critical stability".

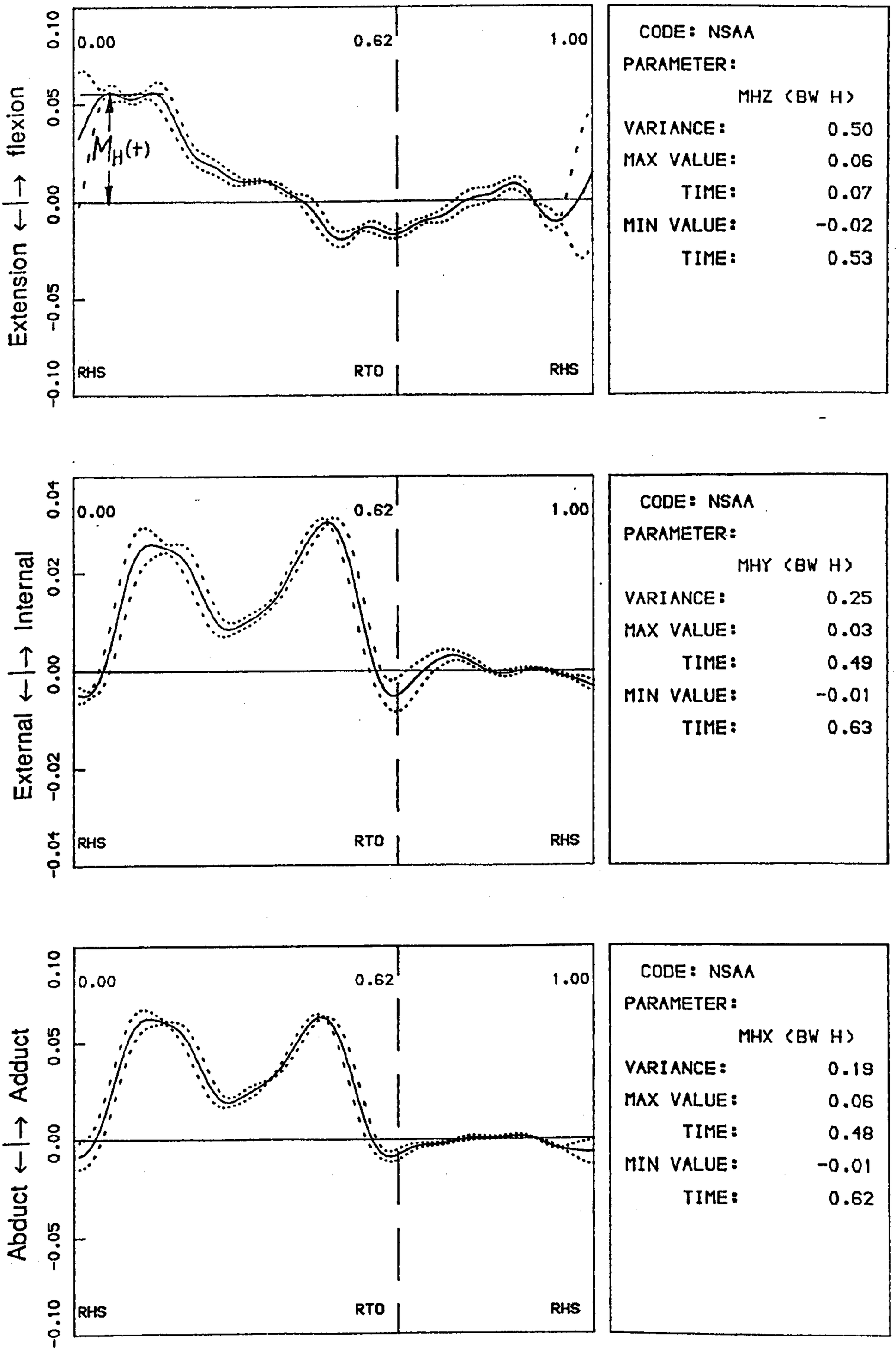

Fig.6.25 The averaged hip joint moments of the normal subject.

Table 6.15 Results of the Parametric Analysis On the Hip Joint Moment

FACS	Group-1 Amputees 6° (Plantar)	3°	0°	-3°	-6° (Dorsi)	Group-2 Amputees 6° (Plantar)	3°	0°	-3°	-6° (Dorsi)
	prosthetic side									
$M_H(+)$	2.78	-0.39	2.4	-0.32	0.32	0.14	1.00	2.4	0.97	1.94
$I_H(+)$	1.21	-0.26	0.6	-0.19	0.24	0.08	0.24	0.4	0.21	0.77
	unaffected side									
$M_H(+)$	-0.46	-0.41	4.1	0.98	0.02	-0.28	-0.07	6.8	0.93	0.44
$I_H(+)$	-0.16	-0.13	1.9	0.22	0.12	-0.43	0.52	2.6	0.22	-0.31

SACS	Group-1 Amputees -6° (Extension)	-3°	0°	3°	6° (Flexion)	Group-2 Amputees -4° (Extension)	0°	4° (Flexion)
	prosthetic side							
$M_H(+)$	-0.04	-0.32	2.4	0.04	0.16	0.20	2.2	0.00
$I_H(+)$	0.01	-0.12	0.6	0.08	0.10	0.20	0.34	0.09
	unaffected side							
$M_H(+)$	-0.02	-0.26	4.1	0.20	0.46	0.60	6.5	0.96
$I_H(+)$	-0.06	-0.14	1.9	0.02	0.06	0.30	3.15	0.05

FSACS	Group-1 Amputees Displacement of the KSI (mm) -14 (KJC backward)	-7	-5	0	5	10 (KJC forward)
	prosthetic side					
$M_H(+)$	-0.50	-0.27	-0.10	2.4	0.02	0.42
$I_H(+)$	0.21	0.03	0.07	0.64	0.12	0.27
	prosthetic side					
$M_H(+)$	-1.17	-0.39	0.20	4.1	0.17	0.43
$I_H(+)$	0.00	0.23	0.07	2.93	-0.03	0.13

NB: (1) Values in normal alignment (0) are averaged data and those in changed alignments are differences from the normal values.
(2) Parameters underlined have statistical significance with confidence limit of 90%.
(3) Unit for maximum moment is (% body weight·height), for impulse is (% body weight·height·s), for transit time is % stance phase.

§ 6.8.3.4 Summary In summary, the three alignment change sequences have significant effects on the extension/flexion moment about the prosthetic knee joint, in other words, on the stability of the prosthetic knee during stance phase. However, the manner in which they affect the MKZ is different: the changes in the A/P tilt angle of the prosthetic foot affects the time at which the extension moment reaches its peak value; the alignment changes in the socket A/P tilt angle affect the peak value of the extension moment; the alignment changes in both the foot and socket affect both aspects of the extension moment. It is noted that since the KSI changed with the SACS and FSACS in the same direction as the trend of change in the extension moment, the KSI can be a good indicator, as its name suggested.

§ 6.9 The Hip Joint Moments

§ 6.9.1 The normal subject

Fig. 6.25 shows the averaged hip joint moments of the normal subject. The patterns of the hip joint moments were found to be similar to those in the literature, such as Paul (1971) and Andriacchi & Strickland (1985) (refer to Fig.2.32 & Fig.2.36). The MHX is dominated by an adduction moment throughout the stance phase and is mainly caused by the medial shear ground force which displayed a similar pattern. During the single stance phase, the pelvis tended to dip to the swing side and a substantial abduction moment was generated by the hip abductors to limit the drop of the pelvis. The MHY has an overwhelming internal rotation moment and is caused by the external rotation of the trunk relative to the supporting leg. The MHZ displayed a flexion moment during the first two thirds of the stance phase with a maximum value of about 6% (body weight·height) at about foot flat, followed by an extension moment with a peak of 2% (body weight·height).

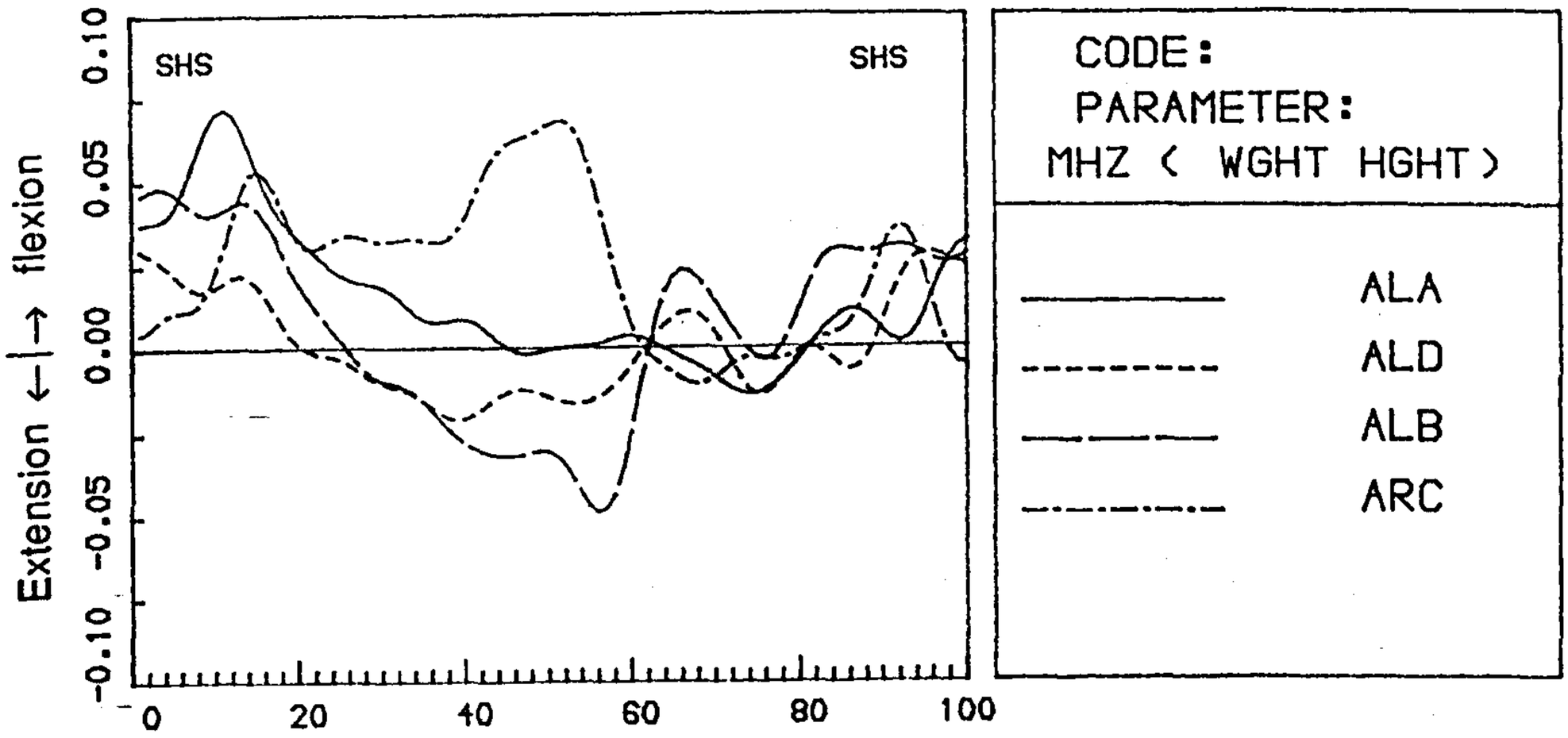

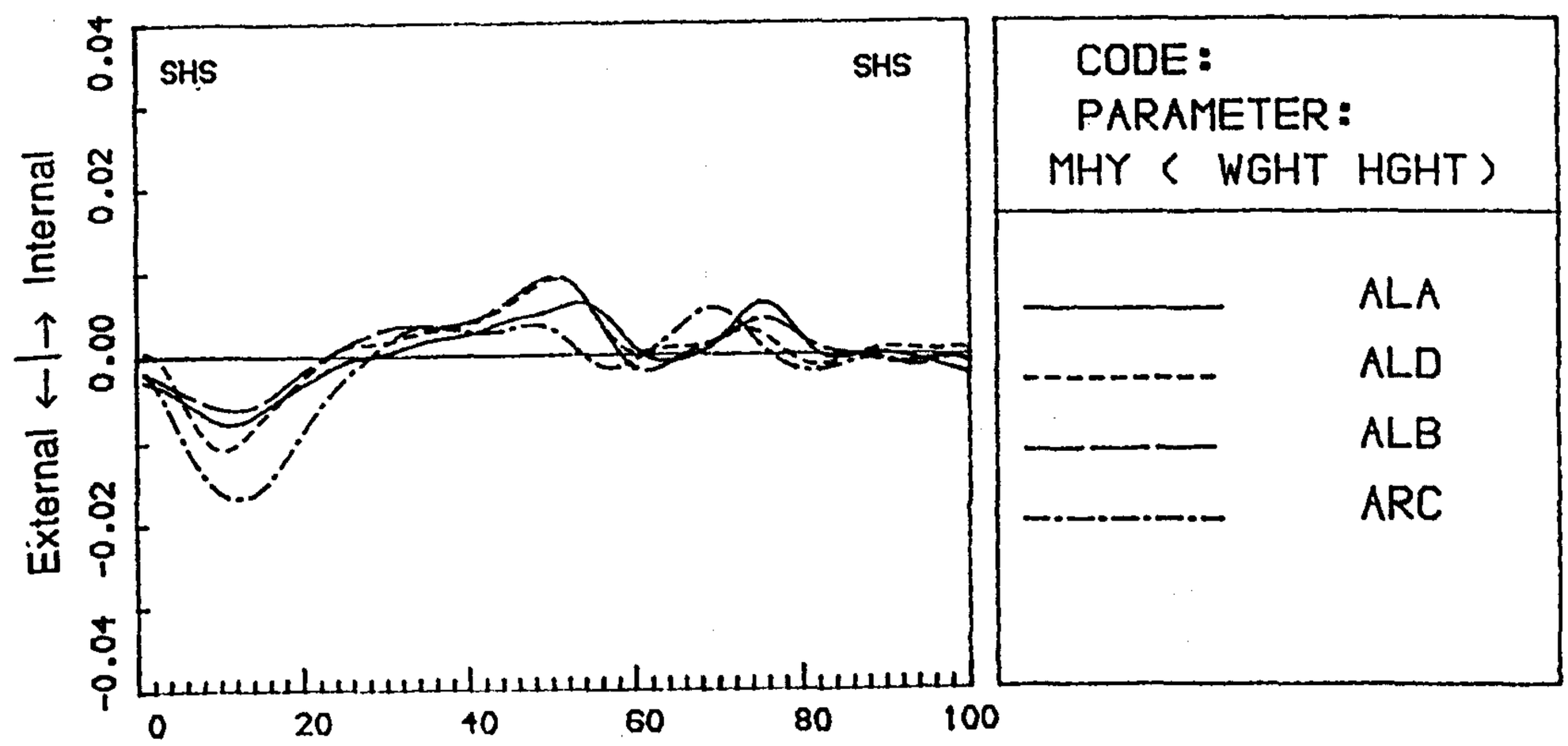

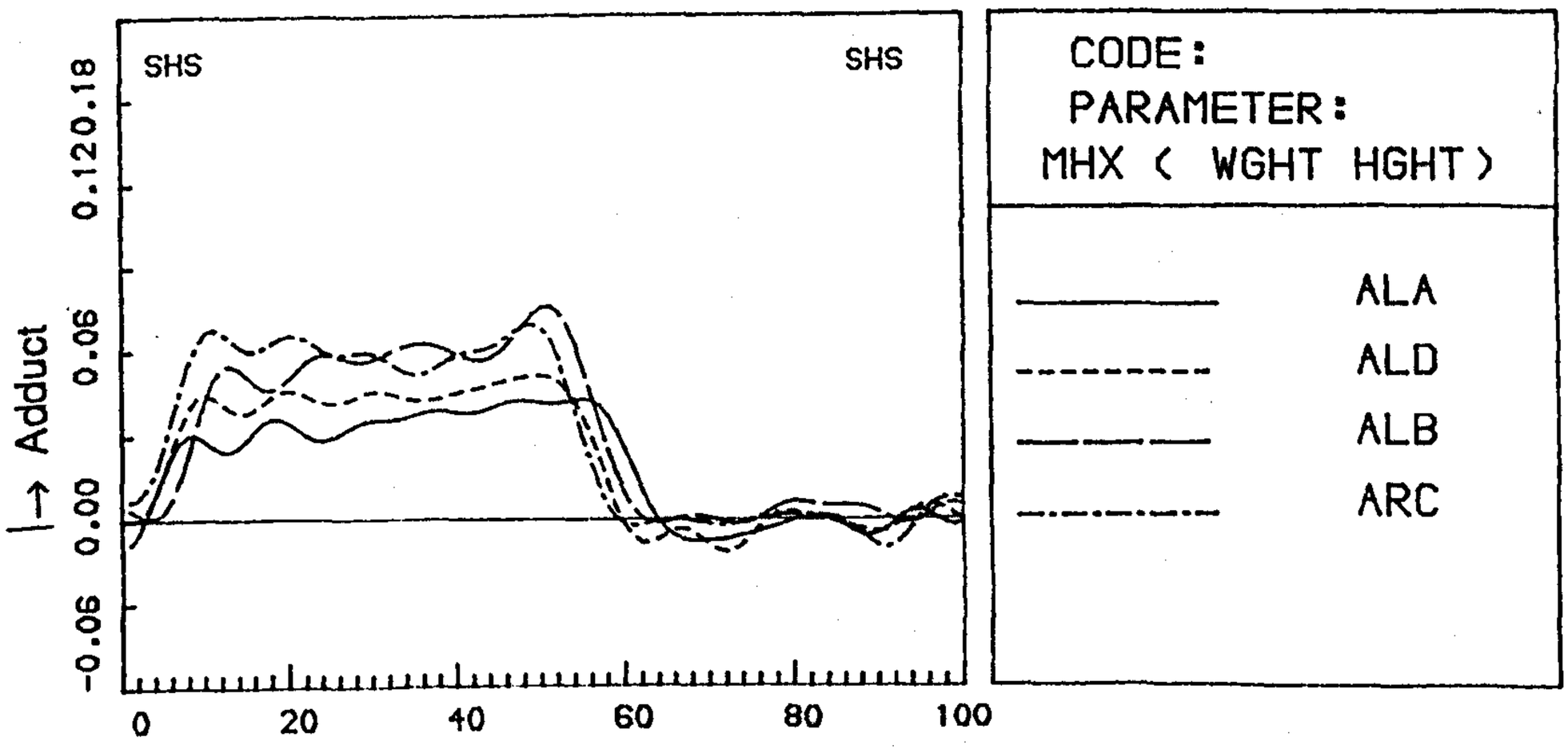

Fig.6.26a The averaged hip joint moments for the amputees with normal alignment.
(Unaffected Side)

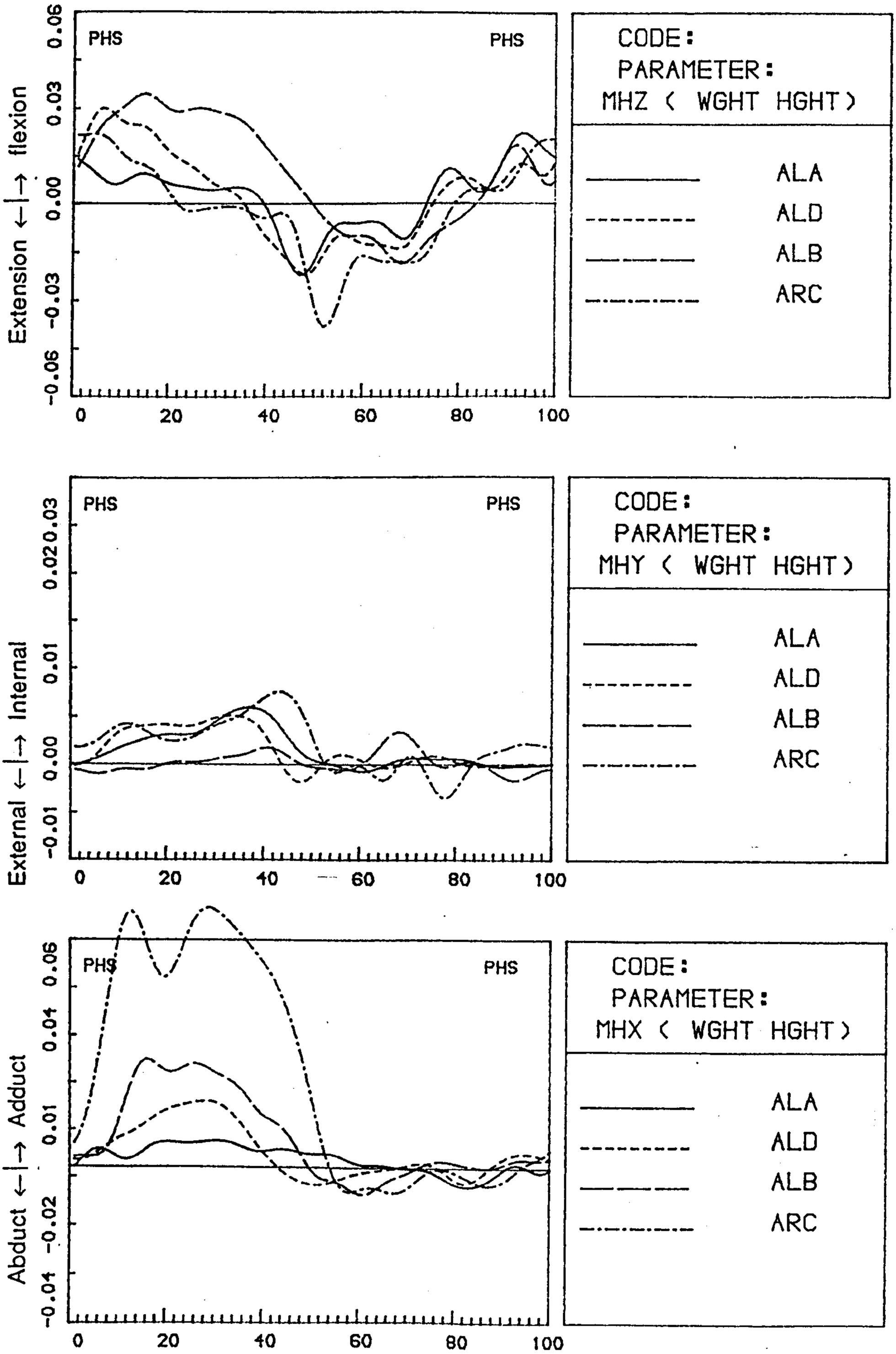

Fig.6.26b The averaged hip joint moments for the amputees with normal alignment.
(Prosthetic Side)

§ 6.9.2 The Amputees with normal alignment

The hip joint moments of the amputees tested with normal alignment are shown in Fig. 6.26a-b. The moments MHXs for both sides were mainly adduction moments during the stance phase, being similar to the normal subject, but their magnitudes were considerably different from one amputee to another. The group-2 amputees tended to have higher hip adduction moments. The shapes of the MHY were variable. On the sound side, the MHY kept to the basic pattern of external-internal rotation torque, similar to that of the normal subject; while on the prosthetic side, three amputees showed an dominant pattern of internal rotation torque while one amputee displayed a pattern of external-internal rotation torque. As far as the MHZ is concerned, variable patterns were displayed at the contralateral side: Two amputees showed a pattern of flexion-extension moment, similar to the normal subject, and two other amputees displayed a pattern of flexion moment being dominant. On the prosthetic side, all the amputees displayed a similar pattern, that is, flexion moment followed by extension moment. However, high variability in the magnitude of the MAZ is clearly displayed.

It should be noted that in calculating the hip joint moment presented in this thesis, the by-pass of the hip joint load due to the ischial bearing of the quadrilateral socket was not taken into account. It is considered that this study is mainly of comparative nature so that the ignorance of the by-pass effect does not affect the final result. Lawes (1982) investigated the forces acting on the ischial seat of the quadrilateral socket and found that about 50% to 60% vertical load by-passed the hip joint. Since the ischial seat is located posterior to the hip joint, this by-passed load resulted in the increase of the flexion moment and the decrease of the extension moment to about 20% to 50%.

§ 6.9.3 Effects of the ACS

Although the hip joint moments are extremely important for the understanding

154b

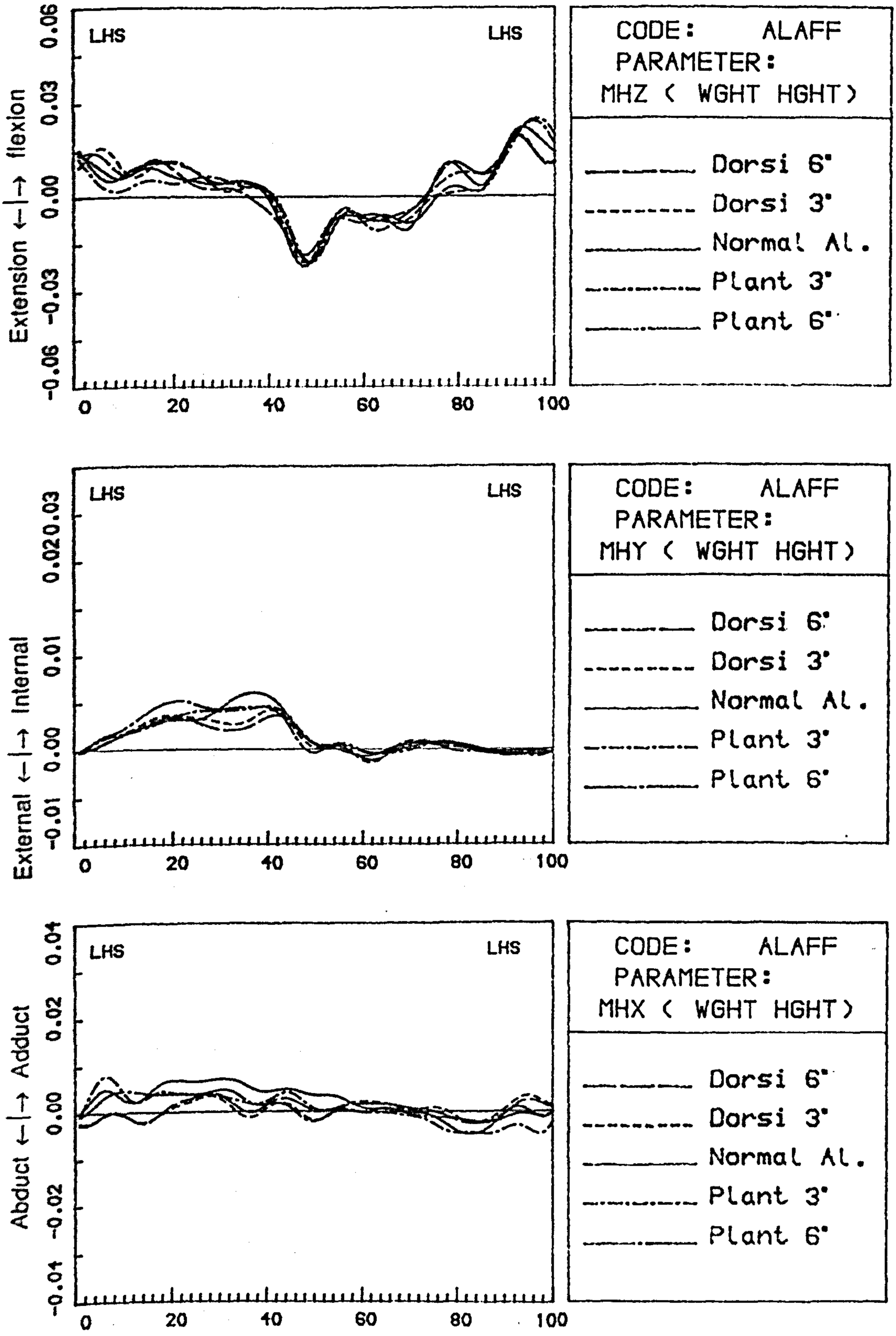

Fig.6.27b Typical changes in the patterns of the hip joint moments with the FSACS. (Prosthetic Side)

of the underlying mechanism of walking, especially at the prosthetic side, they are the only power source to manipulate the prosthesis and control the balance during various walking phases, they did not exhibit any significant and consistent changes in the patterns with the ACS for the amputees tested. Fig. 6.27 is an example.

However, some significant changes were observed in the results of the parametric analysis on the flexion moment, see Table 6.15. For group-2 amputees, the peak values of the prosthetic flexion moment $M_H(+)$ increased as the socket A/P tilt angle was changed (in the SACS). For the group-1 amputees, significant differences were also observed in the SACS, but no consistent trend of change was found. However, the $M_H(+)$ of the both prosthetic and sound sides increased as the prosthetic knee was progressively moved anterior to the HJC-AJC line (with the FSACS). This compensatory action is related to the stability of the prosthetic knee during walking. With the FSACS, the knee joint was moved anterior to the HJC-AJC line, and the prosthetic knee was less stable, as the KSI suggested. In overcoming this difficulty, the amputee increased his hip flexion moment, that is, increased the effort of his hip extensors. This compensatory action was first suggested by Radcliffe and has been considered in the guidelines for the aligning the AK prosthesis.

In an attempt to understand the underlying biomechanics of this compensatory action, or more generally, the means by which the amputee can control his prosthetic hip joint moment, the following equation, which is similar to Equ. 6.4, is used:

$$\begin{aligned} MHZ &= [F_{GY}(X_G - X_H)] + [F_{GX}Y_H] \\ &= MGY + MGX \end{aligned} \qquad (6.4)$$

where X_H and Y_H are the coordinates of the HJC in the sagittal plane. Fig. 6.28 shows an example of the change in the patterns of the two terms in the above equation with the FACS to assess the importance of the constituents of the terms. Since Y_H does not change significantly during the stance phase, the F_{GX} controls both the magnitude and the transition time of the second term MGX, as can be seen in the figure. For the first term MGY, it can be seen from the figure that its transition time is

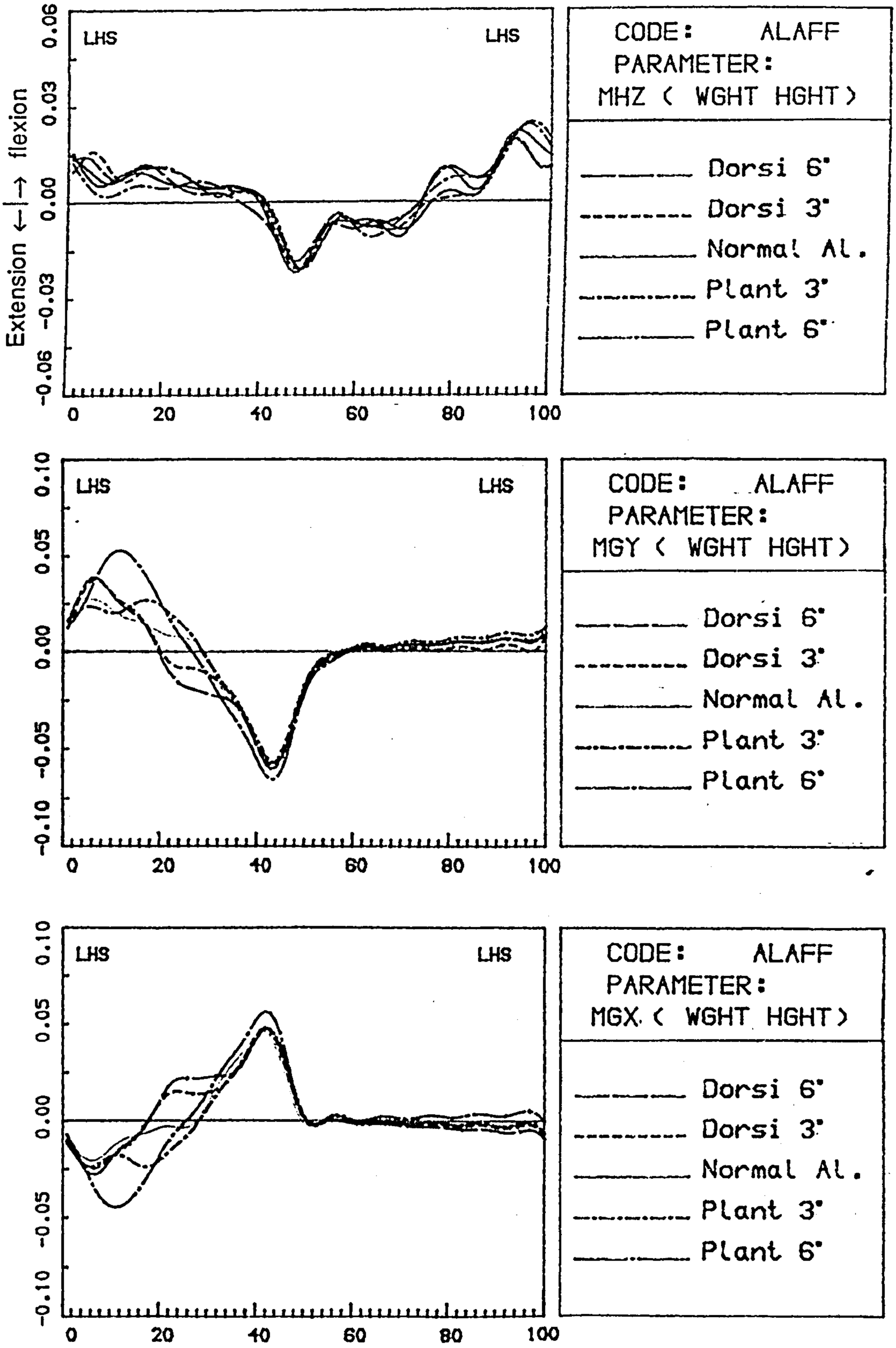

Fig.6.28 Typical changes in the patterns of the flexion moment at the prosthetic hip joint with the FACS in relation to Equ.6.4.

delayed due to the advance of the transition period of the CP with the FACS. As far as the general shapes of the MGY and MGX are concerned, they are out of phase with each other. However, the MHZ has a pattern similar to the MGY. Therefore, the amputee can control his prosthetic hip joint moment by changing F_{GX}, X_G and X_H according to the the changes in the motion and force conditions.

It is noted that no significant and consistent changes were observed in the hip joint moments for the amputees who underwent the FACS and SACS. In an attempt to understand the underlying biomechanics, one should recognize the possibility that, since the prosthetic hip joint moments are closely correlated to the pressure distribution in the stump-socket interface, it might be the amputees' objective to maintain similar hip joint moments or the stump-socket pressure distribution in different alignments by changing other gait variables. Another factor must be also taken into account as to the by-pass effect of the ischial bearing of the quadrilateral socket.

In summary, the maximum value of the hip joint moment was variable and did not change consistently with alignment changes. However, compensation was observed in the hip joint flexion/extension moment for gross alignment changes performed to both the socket and the foot (ie. when the knee was positioned forwards and thus the stability of the knee was reduced, the hip moment acted so that it was stabilizing the knee joint).

CHAPTER 7

CONCLUSIONS AND RECOMMENDATIONS

§ 7.1 Conclusions

The description of the alignment of an above knee prosthesis was found to be dependent on the reference system used. A reference system fixed on the prosthetic foot being is suitable for measuring the alignment, and the one on the socket is suitable for assessing and interpreting the effects of the alignment on the patients' gait.

Since the kinematic and kinetic data acquisition system used in this work is not ideal for recording the temporal-distance parameters of gait, no definite conclusion can be drawn from the acquired data . However, the observed trends in the results of the temporal distance parameters suggested that it is worthwhile to investigate these parameters further.

The angular displacements of the trunk were found to have a characteristic curve for each individual amputee tested and were not significantly affected by the alignment changes in only the socket or foot. Alignment changes to both the socket and the foot appeared to affect the trunk angular movement, but the extent of these effects was different from one amputee to another.

No significant changes were observed in the sagittal angular displacements of the sound lower limb when the alignment of the prosthesis was changed.

The relative angular displacements at the prosthetic knee and ankle joints during the prosthetic stance phase were found to be passively affected by the alignment changes. They are therefore not particularly useful in prosthetic gait analysis. However, the compensatory changes, made as a result of alignment changes, in the angular displacement of the prosthetic thigh affected the ankle angular

displacement pattern.

The angular displacement of the prosthetic thigh was found to be useful in prosthetic gait analysis: it represents the compensatory action the amputee adopted to cope with the alignment changes. It was found that an alignment change at the foot did not affect the angular movement of the prosthetic thigh, suggesting that the amputee did not change his way of using the prosthesis. It was noted, however, that as the alignment of the socket or of both the socket and the foot were changed, the amputee attempted, by altering the angular movement of his prosthetic thigh, to contact the ground with the prosthetic shank being at almost constant orientation angle relative to the ground.

The dynamic orientation angles of the prosthetic thigh, shank and foot relative to the ground were found to be very useful in interpreting the patterns of the kinetic variables (eg. joint moment and ground reaction forces) and their changes in the kinetic variables.

The ground reaction forces, especially the fore-aft shear force and the progression of the centre of pressure, were found to be very sensitive to the alignment changes. They can therefore be used for assessing the quality of the alignment of a prosthesis as long as a correlation between the alignment parameters and the characteristics of the ground reaction forces is established.

Although some significant effects of alignment changes on the ground reaction forces and the joint moments at the sound side were observed, no apparent or simple interpretation could be made on the underlying biomechanics.

Plantar/dorsi flexing the prosthetic foot had significant effects on the ground reaction forces and the joint moments at the prosthetic side. These were as follows: (1) shortening/extending the duration in which the CP is within the heel area; (2) shortening/extending the duration of the push-off force phase; (3) extending/shortening the duration of the dorsiflexion moment; (4) increase/decrease the duration of the full extension moment about the KJC, that is, increase/decrease the

knee stability.

Flexing/extending the socket had significant effects on the ground reaction forces and the joint moments at the prosthetic side. These were as follows: (1) shortening/extending the duration in which the CP is within the heel area; (2) shortening/extending the duration of the push-off force phase; (3) increase/decrease the maximum value of push-off force; (4) decrease/increase the maximum value of braking force; (5) extending/shortening the duration of the dorsiflexion moment; (6) decrease/increase the maximum value of extension moment about the KJC, that is, decrease/increase the knee stability.

Dorsi/plantar flexing the foot coupled with flexing/extending the socket had significant effects on the ground reaction forces and the joint moments at the prosthetic side. These were as follows: (1) extending/shortening the duration in which the CP is within the heel area; (2) extending/shortening the duration of the push-off force; (3) increase/decrease the maximum value of push-off force; (4) decrease/increase the maximum value of braking force; (5) shortening/extending the duration of the dorsiflexion moment; (6) decrease/increase both the peak value of extension moment and the duration of the full extension moment about the KJC, that is, decrease/increase the knee stability; (7) increase/decrease the maximum value of flexion moment about the hip joint.

§ 7.2 Recommendations to Further Work

The following are some ideas for future research on the alignment of the AK prosthesis.

(1) Continuing this investigation on more patients in order to establish a normative data base.

(2) Expanding this investigation to deal with alignment changes in the coronal plane.

(3) Development of a clinically-oriented gait analysis system for assisting the

prosthetist in the alignment process. Two systems are recommended: (a) a computer based and subject-wire-free system for recording and analyzing the temporal-distance parameters of human gait, especially the temporal parameters of stance phase: heel strike, foot flat, heel off, toe off. (b) a program package for analyzing and presenting the ground reaction forces. This program package should be able to analyze all aspects of the ground reaction forces, such as the centre of pressure, peak values and impulses of the forces, and even energy analysis (Rigas, 1987). The results should be presented to the prosthetists in a clear and easily-understood way. Since the ground reaction forces are very sensitive to the alignment and the result can be obtained almost instantly, it is believed that such a package will assist the prosthetist very efficiently.

(4) Computer simulation of the prosthetic gait in relation to the alignment. The simulation model should include all alignment parameters as variables, and any alignment parameter be able to be changes independently. Both the stance and swing phase should be considered in the model. Differences in the characteristics of various prosthetic components could also be considered in the model.

APPENDIX

COMPUTER PROGRAMS

The function of computer programs developed for performing the gait analysis of the model is described briefly in this appendix.

All the computer programs were written in the FORTRAN 77 and run consecutively under the control of a command program RUNAMPUD. Once the input data file "filename.MER" has been created, a single entry of command:

$@RUNAMPUD filename

will run all the programs.

A.1 Program "READAMPU"

This program is designed to validate the format of the data in the entry file "filename.MER". If any ill-formatted data is found, a location of the error is given. Several data files are created by this program and their contents are described as follows.

filename.TV1: format-validated TV data of the body markers;

filename.FM1: forceplate data;

filename.CA1: data for calculating the parameters of the DLT method for each TV camera.

filename.AL1: Alignment measurement results.

filename.AL2: Alignment measurement data for kinematic analysis.

A.2 Program "TVPHOTO"

This program reads in the data file "filename.CA1", calculates the parameters of the DLT method for each camera and outputs the parameters to the data file

"filename.CA3".

A.3 Program "OBJAMPU"

This program reads in the format-validated TV data file "filename.TV1" and the DLT parameters in "filename.CA3", transforms the 2-D image of the body markers into 3-D spatial coordinates with respect to the ground frame of reference and writes the resulting data into "filename.TV2".

A.4 Program "DYNAMPU1"

This program is designed to perform a kinematic analysis on the trunk and sound lower limb. The various joint centres and frames of reference are determined, and the velocity and acceleration of the joint centres and the element of the direction cosine matrices calculated. Following data files are created by this program:

filename.TV3: spatial coordinates of the body markers on the prosthesis.

filename.FM2: dynamic joint centres of the sound lower limb.

filename.PL1: angular displacement of the sound lower limb and the trunk.

filename.VL7: velocity and acceleration of the sound joint centres and the elements of the direction cosine matrices.

A.5 Program "DYNAMPU2"

This program has the same function as "DYNAMPU1" but performs on the prosthetic side. The contents of the data files created by this program are as follows:

filename.FM3: dynamic joint centres of the prosthetic lower limb.

filename.PL2: angular displacements of the prosthetic lower limb.

filename.VL8: velocity and acceleration of the prosthetic joint centres and the elements of the direction cosine matrices.

A.6 Program "PARASTIC"

This program calculated the temporal-distance parameters of gait and the results is write to a data file "filename.PAR".

A.7 Program "KINEAMPU"

Kinetic analysis of the AK amputee model is performed by this program. Linear acceleration of the centre of gravity and angular accelerations of various segments are calculated and the intersegmental loads (forces and moments) are determined. Following data files are created:

filename.PL3: intersegmental loads of the sound lower limb.

filename.PL4: intersegmental loads of the prosthetic lower limb.

A.8 Program "PLOTAMPU"

This program reads in all final results obtained by previous programs and outputs them into a single dada file "filename.RES". A plot file "filename.RCO" is also generated by this program.

Program Listings

Command file "RUNAMPUD.COM"

```
$ ASSIGN/USER_MODE 'P1'.MER FOR001
$ ASSIGN/USER_MODE 'P1'.TV1 FOR008
$ ASSIGN/USER_MODE 'P1'.AKH FOR003
$ ASSIGN/USER_MODE 'P1'.FM1 FOR007
$ ASSIGN/USER_MODE 'P1'.AL1 FOR002
$ ASSIGN/USER_MODE 'P1'.CA1 FOR004
$ ASSIGN/USER_MODE 'P1'.AL2 FOR010
$ ASSIGN/USER_MODE 'P1'.CH1 FOR012
$    RUN READAMPU
$ PURGE 'P1'.*


$ ASSIGN/USER_MODE 'P1'.CA1 FOR005
$ ASSIGN/USER_MODE 'P1'.CA2 FOR006
$ ASSIGN/USER_MODE 'P1'.CA3 FOR004
$     RUN TVPHOTO
$ DELETE 'P1'.CA1;*,'P1'.CA2;*


$ ASSIGN/USER_MODE 'P1'.TV1 FOR001
$ ASSIGN/USER_MODE 'P1'.CA3 FOR003
$ ASSIGN/USER_MODE 'P1'.TV2 FOR004
$ ASSIGN/USER_MODE 'P1'.CH2 FOR012
$    RUN OBJAMPU
$ PURGE 'P1'.*
$ DELETE 'P1'.CA3;*,'P1'.TV1;*


$ ASSIGN/USER_MODE 'P1'.TV2 FOR001
$ ASSIGN/USER_MODE 'P1'.TV3 FOR008
$ ASSIGN/USER_MODE 'P1'.FM2 FOR004
$ ASSIGN/USER_MODE 'P1'.PL1 FOR002
$ ASSIGN/USER_MODE 'P1'.CH3 FOR006
$ ASSIGN/USER_MODE 'P1'.VL7 FOR010
$    RUN DYNAMPU1
$ PURGE 'P1'.*
$ DELETE 'P1'.TV2;*


$ ASSIGN/USER_MODE 'P1'.TV3 FOR001
$ ASSIGN/USER_MODE 'P1'.AL2 FOR005
$ ASSIGN/USER_MODE 'P1'.FM1 FOR007
$ ASSIGN/USER_MODE 'P1'.HJC FOR002
$ ASSIGN/USER_MODE 'P1'.FM3 FOR004
$ ASSIGN/USER_MODE 'P1'.PL2 FOR008
$ ASSIGN/USER_MODE 'P1'.CH4 FOR006
$ ASSIGN/USER_MODE 'P1'.VL8 FOR010
$    RUN DYNAMPU2
$ PURGE 'P1'.*
```

```
$ DELETE 'P1'.TV3;*,'P1'.AL2;*


$ ASSIGN/USER_MODE 'P1'.CH3 FOR001
$ ASSIGN/USER_MODE 'P1'.CH4 FOR003
$ ASSIGN/USER_MODE 'P1'.FM1 FOR005
$ ASSIGN/USER_MODE 'P1'.PAR FOR004
$ ASSIGN/USER_MODE 'P1'.LEN FOR006
$     RUN PARASTIC
$ RENAME PFILE.RCO 'P1'.TRC
$ DELETE 'P1'.TRC;*
$ DELETE 'P1'.AKH;*,'P1'.CH*;*,'P1'.LEN;*


$ ASSIGN/USER_MODE 'P1'.FM1 FOR003
$ ASSIGN/USER_MODE 'P1'.FM2 FOR001
$ ASSIGN/USER_MODE 'P1'.FM3 FOR009
$ ASSIGN/USER_MODE 'P1'.PL3 FOR008
$ ASSIGN/USER_MODE 'P1'.PL4 FOR007
$ ASSIGN/USER_MODE 'P1'.CH5 FOR006
$ ASSIGN/USER_MODE 'P1'.VL7 FOR005
$ ASSIGN/USER_MODE 'P1'.VL8 FOR011
$    RUN KINEAMPU
$ PURGE 'P1'.*
$ DELETE 'P1'.VL*;*,'P1'.FM*;*,'P1'.CH*;*


$ RCO$FN=P1
$ ASSIGN/USER_MODE 'P1'.PL1 FOR003
$ ASSIGN/USER_MODE 'P1'.PL2 FOR009
$ ASSIGN/USER_MODE 'P1'.PL3 FOR001
$ ASSIGN/USER_MODE 'P1'.PL4 FOR005
$ ASSIGN/USER_MODE 'P1'.RES FOR007
$ ASSIGN/USER_MODE 'P1'.MAX FOR012
$          RUN PLOTAMPU
$ DELETE 'P1'.PL*;*
$ PURGE 'P1'.*
```

PROGRAM "READAMPU.FOR"

```
C*************************************************************************
C                                                                        *
C*  THIS PROGRAM READS IN FORCE PLATE DATA AND TELEVISION DATA, AND     *
C*  OUTPUT THE TELEVISION DATA IN THE FORMAT REQUIRED BY THE MARZAN-     *
C*  KARARA PROGRAM                                                      *
C                                                                        *
C*************************************************************************
C
      REAL MX,MY,MZ,MCX,MCY,MCZ,LX1,LZ1,LL,LY1,LX2,LY2,LZ2,
     1LXSF,LYSF,LZSF,MASS,IIFC,LX
      REAL DAL,DAR,DRL,DSJ,DSR,SD
      INTEGER FFPFLD,PHS,PTF,IFFC
      DIMENSION CAX(3),CAY(3),XX(200),YY(200)
      COMMON /FORCE/FX(256),FY(256),FZ(256),MX(256),MY(256),
     1MZ(256),FCX(256),FCY(256),FCZ(256),MCX(256),MCY(256),MCZ(256),
     1F(6,2),LX(3,2)
      COMMON /TVDATA/LIST(7),SSY(11),SFY(11),SSX(11),SFZ(11),IFC(256),
     1ILIST(5),IIFC(256),FFPFLD(25)
      DATA LX/-0.303,-0.04,-0.11,0.303,-0.04,0.11/
      REAL*8 XNAME,XLIMB
      COMMON /NAME/XNAME
C
C  *=*=*=*  BLOCK1-READS  *=*=*=*
C
      PRINT *,'          RATIONIZE RAW DATA'
      PRINT *,'BASIC INFORMATION'
      READ(1,301) XNAME,XLIMB
301   FORMAT(1X,8A,2X,8A)
      WRITE(3,301) XNAME,XLIMB
      WRITE(7,301) XNAME,XLIMB
C
C  READ THE CODE OF LEG INVOLVED
C
C                2: RIGHT LEG
C        (ILEG=
C                1: LEFT LEG
C
C
C
C                1: HJC DETERMINED BY ASIS MARKERS
C        IHJC=
C                0: HJC DETERMINED BY SOCKET MARKERS
C
C
C
C                0: HJC NON-COINCIDE WITH SOCKET AXIS
C        ISOK=
C                1: HJC COINCIDES EITH SOCKET AXIS
C
      READ(1,*) ILEG,ISOK
      READ(1,*) INERTIA,IHJC,FCUT
```

```
      WRITE(3,8511) ILEG
      WRITE(8,8511) ILEG,INERTIA,FCUT
8511  FORMAT(1X,2I3,6(2X,F10.4))
C
C ***READ ANTHROPOMETRIC PATIENT MEASUREMENTS ***
C
      READ(1,*) MASS,HEIGHT
      WEIGHT=MASS*9.81
      WRITE(7,7747) ILEG,INERTIA,FCUT,MASS,WEIGHT,HEIGHT
7747  FORMAT(1X,2I3,4(2X,F10.4))
      READ(1,*) CA,FL,CS,HTI,CTH,P,CCH
      WRITE(8,824) CA,FL,CS,HTI,CTH,P,CCH
824   FORMAT(2X,3(2X,F8.3))
C
C  READ THE DISTANCES AMONG PELVIS MARKERS AND FOOT MARKERS
C
      READ(1,*) DAR,DRL,DAL,F13,F23,F3
      WRITE(8,824) DAR,DRL,DAL,F13,F23,F3
C
      WRITE(10,7747) IHJC,ISOK
      CALL ALIGN(ILEG)
C
      READ(1,*) SM8,C2S8,PS8
      READ(1,*) TM8,C2T8,PT8
      WRITE(7,719) SM8,C2S8,PS8,TM8,C2T8,PT8
719   FORMAT(2X,6F10.5)
C
      READ(1,*)NOMCHK
      IF(NOMCHK.NE.99999) GO TO 520
C
C
C  *=*=*=*  BLOCK2-READS  *=*=*=*
C
C
C THIS PART OF THE PROGRAN READS IN THE CONTROL POINTS DATA
C
C
      PRINT *,'TV CALIBRATION DATA'
C
      CALL TVCALI(6,X01,X02,X03,Y01,Y02,Y03)
      WRITE(8,805) X01,X02,X03,Y01,Y02,Y03
805   FORMAT(1X,3(2X,F10.3))
      READ(1,*) NOMCHK
      IF (NOMCHK.NE.99999) GOTO 522
C
C
C  *=*=*=*  BLOCK3-READS  *=*=*=*
C  *=*=*=*=*=*=*=*=*=*=*=*=*=*=*=*
C
C
C  THIS PART OF THE PROGRAM READS IN THE STATIC DATA
C
C
C
      PRINT *,'READING STATIC DATA'
      WRITE(8,750)
750   FORMAT(1X,///)
      READ(1,*) KKST
      DO 103 K=1,KKST
```

```
      SSY2=0.0
      SSX2=0.0
      READ(1,*) NO
      DO 102 I=1,NO
      READ(1,*) FC,SSY1,SSX1,TLK
      IF (I.EQ.1) WRITE(12,709) SSX1,SSY1,TLK
      SSY2=SSY2+SSY1
      SSX2=SSX2+SSX1
102   CONTINUE
      SSY2=SSY2/NO
      SSX2=SSX2/NO
      WRITE(8,801) FC,SSX2,SSY2,TLK
103   CONTINUE
709   FORMAT(1X,6HSTATIC,3(2X,F10.3))
801   FORMAT(1X,4(2X,F10.2))
      READ(1,*)NOMCHK
      IF (NOMCHK.NE.99999) GO TO 523
C
C  FX1:FY1:FZ1:MX1:MY1:MZ1 ARE FORCES AND MOMENTS FROM FP1
C  FX2:FY2:FZ2:MX2:MY2:MZ2 ARE FORCES AND MOMENTS FROM FP2
C  FCX:FCY:FCZ:MCX:MCY:MCZ ARE FORCES AND MOMENTS RELATING
C  TO THE SYSTEM ORIGIN IE. AT CENTRAL INTERSECTION OF FP1 & FP2
C
C
      PRINT *,'FORCEPLATE DATA START'
      IIFP=1
      CALL FPINPUT(NF1,ITF1,IHS1,IIFP)
      IIFP=2
      CALL FPINPUT(NF2,ITF2,IHS2,IIFP)
C
      READ(1,*) NOMCHK
      IF (NOMCHK.NE.99999) GOTO 521
C
C
C  THE TV DATA IS NOW SCANNED AND THE LOAD BEARING
C  RANGE IS SELECTED
C
C  *=*=*=*  BLOCK5-READS  *=*=*=*
C  *=*=*=*=*=*=*=*=*=*=*=*=*=*=*
C
C
      LHJC=27
      IF(ILEG.EQ.2) LHJC=26
C     IF(IHJC.EQ.1) LHJC=26  !FOR ALBA0205.MER SOCKET MARKER MISSING
      PRINT *,'READING DYNAMIC DATA'
      NM=0
      READ(1,*) KKD                          ! NO. OF TOTAL DYNAMIC MARKER
49    WRITE(8,750)
      NM=NM+1
      READ(1,*)IFT
      IMARK=0
      DO 50 I=1,IFT
      READ(1,*) IIFC(I),VC,HC,TL
      IFC(I)=IFIX(IIFC(I))
C     IF (IFC(I).LT.(IHS1+FFPFLD(NM)).OR.IFC(I).GT.(ITF2+FFPFLD(NM)))
C     1GOTO 50
      IF (IFC(I).LT.IHS1-4.OR.IFC(I).GT.ITF2+4) GOTO 50
      IF (I.EQ.1)GOTO 51
      IF (IFC(I).NE.IFC(I-1)+1) GOTO 900
```

```
51      IMARK=1
        WRITE(8,803) IIFC(I),HC,VC,TL
        IF (I.EQ.30) WRITE(12,779) HC,VC,TL
        IF (NM.NE.LHJC) GO TO 50
        LL=IFIX(IIFC(I))
        YY(LL)=VC
        XX(LL)=HC
50      CONTINUE
        IF(IMARK.EQ.0) WRITE(6,611) IHS1,ITF2,NM
        IF (NM.LT.KKD) GOTO 49
C
        CALL LEFTHS(XX,IHS1,ITF2,NFN)
        WRITE(8,899) NFN
        TYPE *,'NFN= ',NFN
C
899     FORMAT(3X,I3)
611     FORMAT(1H0,'FIELD COUNTS OUTWITH RANGE',2I6,'FOR MARKER',I3)
803     FORMAT(1X,4(2X,F10.2))
779     FORMAT(1X,7HDYNAMIC,3(2X,F10.3))
C
        READ(1,*) NOMCHK
        IF (NOMCHK.NE.99999) GOTO 524
        GO TO 902
C
C
900     WRITE(6,901) NM,I
901     FORMAT(1H0, 'DYNAMIC DATA OF MARKER ',I2,'MISSING IN ',I1,'READS')
520     WRITE(6,625) NOMCHK
625     FORMAT(1H0,'*ERROR IN BLOCK1-READS*'//
        1'***CHECK NO = ',I7,1X,' ***')
        GO TO 902
521     WRITE(6,626)NOMCHK
626     FORMAT(1H0,'*ERROR IN BLOCK2-READS*'//
        1'***CHECK NO = ',I7,1X,' ***')
        GO TO 902
522     WRITE(6,627)NOMCHK
627     FORMAT(1H0,'*ERROR IN BLOCK3-READS*'//
        1'***CHECK NO = ',I7,IX,' ***')
        GO TO 902
523     WRITE(6,628)NOMCHK
628     FORMAT(1H0,'*ERROR IN BLOCK4-READS*'//
        1'***CHECK NO = ',I7,1X,' ***')
        GO TO 902
524     WRITE(6,629)NOMCHK
629     FORMAT  (1H0,'*ERROR IN BLOCK5-READS*'//
          1'***CHECK NO = ',I7,1X,' ***')
902       STOP
          END
C
C
C
C
      SUBROUTINE INPUT(ARRAY,NO,LOW)
      DIMENSION ARRAY(NO)
      READ(1,*)ARRAY
      IF(ARRAY(1).EQ.0)GOTO 500
      TEMP=ARRAY(1)
      DO 200 I=1,NO
200   ARRAY(I)=ARRAY(I)-TEMP
```

```
 500  IF(NO.LT.LOW)LOW=NO
      RETURN
      END
C
C
C
        SUBROUTINE FPINPUT(NF,ITF,IHS,IIFP)
        REAL MX,MY,MZ,MCX,MCY,MCZ,LX1,LZ1,LL,LY1,LX2,LY2,LZ2,
        1LXSF,LYSF,LZSF,MASS,IIFC,LX
        COMMON /FORCE/FX(256),FY(256),FZ(256),MX(256),MY(256)
        1,MZ(256),FCX(256),FCY(256),FCZ(256),MCX(256),MCY(256)
        2,MCZ(256),F(6,2),LX(3,2)
        DATA F/-0.2843,-0.9923,0.1202,-0.2070,-0.0329,0.2068
        1,0.2653,-1.0027,-0.1225,0.2070,-0.0329,-0.2117/
C
C
        READ(1,*)IS,NO
        LOW=NO
        CALL INPUT(FX,NO,LOW)
        READ(1,*)IS,NO
        CALL INPUT(FY,NO,LOW)
        READ(1,*)IS,NO
        CALL INPUT(FZ,NO,LOW)
        READ(1,*)IS,NO
        CALL INPUT(MX,NO,LOW)
        READ(1,*)IS,NO
        CALL INPUT(MY,NO,LOW)
        READ(1,*)IS,NO
        CALL INPUT(MZ,NO,LOW)
C
C
C  CALCULATE HEEL-STRIKE,TOE-OFF (HS1,TF1)
C
        I=1
 11     I=I+1
        IF(ABS(FY(1)-FY(I)).LT.8.0)GOTO 11
        HS=I
        I=LOW
 13     I=I-1
        IF (ABS(FY(LOW)-FY(I)).LT.8.0)GOTO 13
        TF=I
        NF=TF-HS+1
        ITF=TF+IS-1
        IHS=HS+IS-1
C
C CENTRE OF PRESSURE XO:YO:ZO
C
        WRITE(8,607) NF,ITF,IHS
        WRITE(7,607) NF,ITF,IHS
607     FORMAT(1X,3I6)
        YO=0.0
        DO 20 I=HS,TF
        FCX(I)=FX(I)*F(1,IIFP)
        FCY(I)=FY(I)*F(2,IIFP)
        FCZ(I)=FZ(I)*F(3,IIFP)
        MX(I)=MX(I)*F(4,IIFP)
        MY(I)=MY(I)*F(5,IIFP)
        MZ(I)=MZ(I)*F(6,IIFP)
        MCX(I)=MX(I)+LX(2,IIFP)*FCZ(I)-LX(3,IIFP)*FCY(I)
```

```
      MCY(I)=MY(I)+LX(3,IIFP)*FCX(I)-LX(1,IIFP)*FCZ(I)
      MCZ(I)=MZ(I)+LX(1,IIFP)*FCY(I)-LX(2,IIFP)*FCX(I)
      XO=MCZ(I)/FCY(I)
      ZO=-MCX(I)/FCY(I)
      MCY(I)=MCY(I)-ZO*FCX(I)+XO*FCZ(I)
      WRITE(7,608)
      WRITE(7,606)XO,YO,ZO
      WRITE(7,606)FCX(I),FCY(I),FCZ(I)
      WRITE(7,606)MCX(I),MCY(I),MCZ(I)
      WRITE(3,606) XO,YO,ZO
      WRITE(3,606) FCX(I),FCY(I),FCZ(I)
20    CONTINUE
606   FORMAT(1X,3(2X,F10.3))
608   FORMAT(1X,/)
C
      RETURN
      END
C
C
C
      SUBROUTINE TVCALI(ICAM,XO1,XO2,XO3,YO1,YO2,YO3)
      DIMENSION XO(27),YO(27),ZO(27)
      DATA XO,YO,ZO/3*-0.9,3*0.0,6*0.9,3*-0.9,6*0.0,3*0.9,3*-0.9
     1,0.098,0.789,1.554,0.096,0.791,1.553,0.095,0.790,1.549
     2,0.096,0.791,1.549,0.095,0.790,1.554,0.098,0.789,1.553
     3,0.095,0.790,1.553,0.098,0.789,1.549,0.096,0.791,1.554
     4,3*-0.4,3*0.0,3*0.4,3*-0.4,3*0.0,3*0.4,3*-0.4,3*0.0,3*0.4/
C
C  PLUMB 1 AT POSITION 1,4 AND 7
C  PLUMB 2 AT POSITION 2,5 AND 8
C  PLUMB 5 AT POSITION 3,6 AND 9
C
      ITV=2
      IF (ICAM.EQ.6) ITV=3
      WRITE(4,99) 1,11,ITV,1,27,0,0.001,0.001,0.001,0.001
99    FORMAT(1X,I1,///,2X,5I5,///,4(2X,F10.5),///)
C
      DO 10 I=1,27
      YO(I)=YO(I)-0.790
      WRITE(4,91) I,XO(I),YO(I),ZO(I)
10    CONTINUE
91    FORMAT(1X,I3,3(2X,F10.6))
C
      WRITE(4,999)
      CALL INPUTTV(1,XO1,YO1)
C     IF (ICAM.EQ.3) GOTO 601
C
C
      WRITE(4,999)
      CALL INPUTTV(2,XO2,YO2)
601   IF (ICAM.EQ.0) GOTO 603
C
C
      WRITE(4,999)
      CALL INPUTTV(3,XO3,YO3)
603   CONTINUE
C
999   FORMAT(1X,///)
      RETURN
```

```
      END
C
C
C
      SUBROUTINE INPUTTV(IJK,XXO,YYO)
      DIMENSION UX(27),VY(27)
      REAL X1,X2,VV,UU,XXO,YYO
      REAL II,IJ
C
      DO 9 K=1,3
      DO 10 I=1,9
      K1=(K-1)*9+I
      VV=0.0
      UU=0.0
      READ(1,*) N2
      AN=FLOAT(N2)
      DO 11 J=1,N2
      READ(1,*) II,X1,X2,IJ
      IF(J.EQ.1) WRITE(12,777) X2,X1,IJ
      IF(J.NE.1) GOTO 11
      VV=X1+VV
      UU=X2+UU
11    CONTINUE
      VY(K1)=VV
      UX(K1)=UU
C     VY(K1)=VV/AN
C     UX(K1)=UU/AN
10    CONTINUE
9     CONTINUE
C
      IF (IJK.EQ.1) GOTO 60
      YYO=VY(5)
      XXO=(UX(4)+UX(5)+UX(6))/3.0
      DO 20 I=1,27
      UU=UX(I)-XXO
      VV=VY(I)-YYO
      WRITE(4,50) UU,VV
20    CONTINUE
      GO TO 70
C
60    YYO=UX(5)
      XXO=(VY(4)+VY(5)+VY(6))/3.0
      DO 65 I=1,27
      UU=VY(I)-XXO
      VV=UX(I)-YYO
      WRITE(4,50) UU,VV
65    CONTINUE
C

50    FORMAT(2X,2(3X,F10.4))
777   FORMAT(1X,6HTVCALI,3(2X,F10.3))
70    RETURN
      END
C
C
C
      SUBROUTINE ALIGN(ILEG)
      DIMENSION XNAME(2),XLIMB(6),TOUT(6),XK(6),YK(6),ZK(6)
      DIMENSION THS(6),XT(6),YT(6),ZT(6),APTILT(6),ROTATE(6)
```

170a

```
      DIMENSION XI(6),YI(6),ZI(6),XH(6),YH(6),ZH(6)
      DIMENSION CG(6),DIST(6),X(6),Y(6),Z(6)
      DIMENSION PXL(6),PYL(6),PZL(6),CEN(3)
      REAL IH(6),MASS(6),KTILT(6),MLTILT(6),NOSC
        REAL*8 XNAME
        COMMON /NAME/XNAME
C
        I=1
C
        READ(1,*) ASOK,CEN     !SOCKET FLEXION IS POSITIVE!
        ASOK=ASOK*3.1415926/180.0
        READ(1,*) YAA,YAP,AL
        AFLEX=ATAN((YAA-YAP)/AL)
        READ(1,*) XAN,YAN,ZAN
        READ(1,*) XXU,ZZU,XXL,ZZL
        READ(1,*) XKR,YKR,ZKR,XKL,YKL,ZKL
        XXU=XAN-XXU
        XXL=XAN-XXL
        XKL=XAN-XKL
        XKR=XAN-XKR
        YKR=YKR-YAN
        YKL=YKL-YAN
        ZZU=ZZU-ZAN
        ZZL=ZZL-ZAN
        ZKR=ZKR-ZAN
        ZKL=ZKL-ZAN
        CEN(1)=XAN-CEN(1)
        CEN(2)=CEN(2)-YAN
        CEN(3)=CEN(3)-ZAN
C
        A=SQRT((XXU-XXL)**2+(ZZU-ZZL)**2)
        B=SQRT((XKR-XKL)**2+(ZKR-ZKL)**2)
        TOUT(1)=(XXL-XXU)*(XKR-XKL)+(ZZL-ZZU)*(ZKR-ZKL)
        TOUT(1)=3.1415926/2.0-ACOS(TOUT(1)/A/B)
        TTK=ATAN((XKR-XKL)/ABS(ZKR-ZKL))
C
        CALL AMULT(TTK,ZKR,XKR)
        CALL AMULT(TTK,ZKL,XKL)
        CALL AMULT(AFLEX,XKR,YKR)
        CALL AMULT(AFLEX,XKL,YKL)
        READ(1,*) XRT,YRT,ZRT
        XRT=XAN-XRT
        YRT=YRT-YAN-214.0
        ZRT=ZRT
        CALL AMULT(TTK,ZRT,XRT)
        CALL AMULT(AFLEX,XRT,YRT)
        CALL SOCKET(ASOK,CEN,XRT,YRT)
      READ(1,*) XLT,YLT,ZLT
        XLT=XAN-XLT
        YLT=YLT-YAN-214.0
        ZLT=ZLT-44.0
        CALL AMULT(TTK,ZLT,XLT)
        CALL AMULT(AFLEX,XLT,YLT)
        CALL SOCKET(ASOK,CEN,XLT,YLT)
      READ(1,*) XRL,YRL,ZRL
        XRL=XAN-XRL
        YRL=YRL-YAN-284.0
        ZRL=ZRL
        CALL AMULT(TTK,ZRL,XRL)
```

```
      CALL AMULT(AFLEX,XRL,YRL)
      CALL SOCKET(ASOK,CEN,XRL,YRL)
    READ(1,*) XLL,YLL,ZLL
      XLL=XAN-XLL
      YLL=YLL-YAN-284.0
      ZLL=ZLL-44.0
      CALL AMULT(TTK,ZLL,XLL)
      CALL AMULT(AFLEX,XLL,YLL)
      CALL SOCKET(ASOK,CEN,XLL,YLL)
C
      DO 12 J=1,5
      READ(1,*) X(J),Y(J),Z(J)
      IF(J.EQ.1.OR.J.EQ.4) Y(J)=Y(J)-285.0
      X(J)=XAN-X(J)
      Y(J)=Y(J)-YAN
      CALL AMULT(TTK,Z(J),X(J))
      CALL AMULT(AFLEX,X(J),Y(J))
      IF(J.GT.3) CALL SOCKET(ASOK,CEN,X(J),Y(J))
12    CONTINUE
C
C CHANGE RIGHT/2,LEFT/1 TO RIGHT/1,LEFT/-1
11    ILEG=ILEG*2-3
C
C PERFORM CALCULATIONS
      TOUT(I)=ILEG*TOUT(I)*57.3
      XK(I)=(XKL+XKR)/2.0*0.1
      YK(I)=(YKR+YKL)/2.0*0.1
      ZK(I)=(ZKR+ZKL)/2.0*0.1
      KTILT(I)=57.3*ATAN((YKR-YKL)/(ZKR-ZKL))*ILEG
      AFLEX=ATAN(XK(I)/YK(I))*57.3
      XT(I)=(XRT+XLT)/2.0*0.1
      YT(I)=(YRT+YLT)/2.0*0.1
      ZT(I)=(ZRT+ZLT)/2.0*0.1
      XL=(XRL+XLL)/2.0*0.1
      YL=(YRL+YLL)/2.0*0.1
      ZL=(ZRL+ZLL)/2.0*0.1
      PXL(I)=XL
      PYL(I)=YL
      PZL(I)=ZL
      APTILT(I)=-57.3*ATAN((XT(I)-XL)/(YT(I)-YL))
      MLTILT(I)=57.3*ATAN((ZT(I)-ZL)/(YT(I)-YL))*ILEG
      ROTATE(I)=ILEG*57.3*ATAN((XLT-XRT)/(ZRT-ZLT))
      PHI=-ATAN(XK(I)/YK(I))
C
C OUTPUT THE ALIGNMENT RESULTS INTO A TABLE
C
        XKR=(XKR+XKL)/2.0/1000.0
        YKR=YKR/1000.0
        ZKR=ZKR/1000.0
        YKL=YKL/1000.0
        ZKL=ZKL/1000.0
        XRT=XRT/1000.0
        YRT=YRT/1000.0
        ZRT=ZRT/1000.0
        XLT=XLT/1000.0
        YLT=YLT/1000.0
        ZLT=ZLT/1000.0
        XRL=XRL/1000.0
        YRL=YRL/1000.0
```

```
      ZRL=ZRL/1000.0
      XLL=XLL/1000.0
      YLL=YLL/1000.0
      ZLL=ZLL/1000.0
      WRITE(10,488) TOUT(1),XKR,YKR,ZKR,YKL,ZKL
      WRITE(10,488) XRT,YRT,ZRT,XLT,YLT,ZLT
      WRITE(10,488) XRL,YRL,ZRL,XLL,YLL,ZLL
      WRITE(10,488) XI(1),YI(1),ZI(1),XT(1),YT(1),ZT(1)
      WRITE(10,488) XL,YL,ZL,XK(1),YK(1),ZK(1)
      DO 44 J=1,5
44    WRITE(10,488) X(J),Y(J),Z(J)
488   FORMAT(3X,3(3X,F10.4))
C
      RETURN
      END
C
C
C
      SUBROUTINE AMULT(T,X,Y)
      XX=X*COS(T)+Y*SIN(T)
      YY=-X*SIN(T)+Y*COS(T)
      X=XX
      Y=YY
      RETURN
      END
C
C
      SUBROUTINE SOCKET(ASOK,CEN,X,Y)
      DIMENSION CEN(3)
      XX=X-CEN(1)
      YY=Y-CEN(2)
      CALL AMULT(-ASOK,XX,YY)
      X=XX+CEN(1)
      Y=YY+CEN(2)
      RETURN
      END
C
C
      SUBROUTINE LEFTHS(X,IHS1,ITF2,NFN)
      DIMENSION X(200),D(200)
C
      NF=ITF2-IHS1+9
      DO 10 J=ITF2,IHS1,-1
      AAA=ABS(X(J-8)-X(J))
      IF(AAA.GT.4.0) GOTO 20
10    CONTINUE
C
20    NFN=J-IHS1+1-6
      RETURN
      END
```

PROGRAM "TVPHOTO.FOR"

```
C
C      THIS PROGRAM WILL CALCULATE THE POSITION
C      OF POINTS IN SPACE ACCORDING TO THE METHOD
C      USED BY MARZAN AND KARARA BASED ON PREVIOUS
C     WORK OF ABDEL-AZIZ.
C      ************************************************************
C      THE INPUT SEQUENCE IS
C          CARD 1 NPROB (15) NUMBER OF TIMES ENTIRE PROGRAM
C          IS TO BE REPEATED
C
C      IP,NCAM,NREP,NNC,NPOINT
C      IP IS THE NUMBER OF UNKNWON PARAMETERS
C         (DLT AND LENS DISTORTION COEFFICIENTS)
C         CARRIED IN THE SOLUTION.
C      NCAM IS THE NUMBER OF CAMERAS(AT LEAST TWO)
C      NREP IS THE NUMBER OF TIMES THE FILM
C      COORDINATES ARE  FOR EACH KNOWN POINT.
C      NNC IS THE NUMBER OF KNOWN POINTS USED TO
C      ARRIVE AT THE SOLUTION.
C      NPOINT IS THE NUMBER OF UNKNOWN POINTS
C             WHICH WILL BE INPUT TO THE PROGRAM.
C
C
C      SX,XY,XZ,SEUKP(4F5.2)
C      THESE ARE THE STANDARD ERRORS OF THE OBJECTSPACE
C      COORDINATES OF THE KNOWN POINTS AND OF THE FILM
C      COORDINATES OF THE UNKNOWN POINTS.
C
C
C      NEXT SET OF CARDS(NCC IN NUMBER)NUM(I),(E(I,J),J=1,3)
C              NUM(I) IS THE NUMBER OF KNOWN POINT I
C              E8I,J) IS THE KNOWN OBJECT SPACE COORDINATE
C               FOR POINT I.J=1 FOR X,J=2 FOR Y,J=3 FOR Z.
C
C
C      NEXT SET OF CARDS(NNC*NREP IN NUMBER)XC,YC FORMAT18
C              XC AND YC ARE THE FILM COORDINATES FOT THE
C          FIRST CAMERA OF THE KNOWN POINTS,ALL REPEATED
C              DATA FOR ONE CAMERA MUST BE STACKED TOGETHER
C
C
C      NEXT SET(NNC*NREP IN NUMBER) XC,YC FORMAT 18
C              THE PREVIOUS SET IS REPEATED FOR THE SECOND CAMERA.
C
C
C      NEXT X8I,K9,Y(I,K),I=1,NPOINT,K=1
C           THESE ARE THE FILMCOORDINATES FOR EACH UNKNOWN
C           POINT FOR THE FIRST CAMERA.MAXIMUN 2300 POINTS
C
```

```
C      NEXT X(I,K),Y(I,K),I=1,NPOINT,K=2 FORMAT28
C           PREVIOUS SET REPEATED FOR CAMERA 2
C      ************************************************************
C
C
C
      IMPLICIT DOUBLE PRECISION (A-H,O-Z)
         DIMENSION Q(20),SO(20),A(4)
       COMMON/TRANS/D(4,20),XP(4),YP(4),W(20,20)
       COMMON/DATA/E(30,3),X(100,4),Y(100,4),NUM(30)
       COMMON/NUMBER/NNC,NCAM,NPOINT
C
        PRINT *,'          PARAMETERS OF TV CAMERAS'
        TOL=1.D-6
        READ(5,*)NPROB
        DO 500 IJK=1,NPROB
        READ(5,*) IP,NCAM,NREP,NNC,NPOINT
        READ(5,*)SX,SY,SZ,SEUKP
        DO 5 I=1,NNC
        READ (5,*)NUM(I),(E(I,J),J=1,3)
C
    5 CONTINUE
       SVV=0.0
       ICOUNT=0
       DF=NREP*(NREP-1)
       IF(NREP.EQ.1)DF=1.000
C
       DO 20 K=1,NCAM
        DO 22 I=1,NNC
        X(I,K)=0.0
        Y(I,K)=0.0
        VV=0.0
C
        DO 25 J=1,NREP
        READ(5,*) XC,YC
        ICOUNT=ICOUNT+1
        X(I,K)=X(I,K)+XC
        Y(I,K)=Y(I,K)+YC
        VV=VV+XC*XC+YC*YC
   25 CONTINUE
C
C**************************************************
C************************************************************
        VV=VV-(X(I,K)**2+Y(I,K)**2)/NREP
        SVV=SVV+DABS(VV)
        X(I,K)=X(I,K)/NREP
        Y(I,K)=Y(I,K)/NREP
   22 CONTINUE
   20 CONTINUE
C++++++++++++++++++++++++++++++++++++++++++++++++++++++++++++++
        SP=SVV/(2.000*DF*ICOUNT)
        SP=DSQRT(SP)
C
        WRITE(6,6876)
 6876 FORMAT('1')
          DO 26 K=1,NCAM
          WRITE(6,98)K
   98 FORMAT('0',5X,'FILMCOORDINATES,CAMERA',I3,//)
          DO 27 I=1,NNC
```

```
      WRITE (6,15) NUM(I),X(I,K),Y(I,K)
   15 FORMAT(12X,I4,4F12.4)
   27 CONTINUE
   26 CONTINUE
C
      WRITE(6,101)IP
  101 FORMAT('1',10X,'NUMBER OF UNKNOWN PARAMETERS=',I5)
      WRITE(6,102)SX,SY,SZ,SP,SEUKP
  102 FORMAT(' ',///,11X,'STANDARD ERRORS OF OBJECT SPACE COORDINATES',
     1//,15X,'SX=',F6.3,3X,'SY=',F6.3,3X,'SZ=',F6.3,//11X,
     2'STANDARD ERROR OF FILM COORDINATES OF KNOWN POINTS=',F10.5,//,
     311X,'STANDARD ERROR OF FILM COORDINATES OF THE FILM
     4 COORDINATES OF THE UNKNOWN POINTS=',F10.5,//)

C
      IPP1 =IP+1
      IPM1=IP-1
      IF(IP.LT.13)GO TO 29
      IPM2=IP-2
      IF(IP.EQ.14)GO TO 29
      IPM3=IP-3
       IPM4=IP-4
   29 CONTINUE
      WRITE(4,999) NCAM,IP,IPM1,IPM2,IPM3,IPM4
999   FORMAT(1X,6I6)
C+++++++++++++++++++++++++++++++++++++++++++++++++++++++++++++++
      DF=2.000*NNC-IP
      WRITE(6,104)DF
  104 FORMAT(' ',10X,'DEGREES OF FREEDOM=',F5.0,//)
C
      DO 30 L=1,NCAM
      XP(L)=0.0
C*=*=*
      YP(L)=0.0
      DO 31 LL=1,2
      VV=0.0
      DO 35 I=1,IP
      DO 35 J=1,IPP1
      W(I,J)=0.0
   35 CONTINUE
C
      DO 40 K=1,NNC
      IF(IP.EQ.11)GO TO 49
      XR=X(K,L)-XP(L)
      YR=Y(K,L)-YP(L)
      R1=XR**2
      R3=YR**2
      R2=R1+R3
      IF(IP.EQ.12)GO TO 49
      R4=R2*R2
      R6=R2*R4
      IF(IP.EQ.14)GO TO 49
      R7=2.000*R1+R2
      R8=2.000*R3+R2
      R9=2.000*XR*YR
C*=*=*

   49 CONTINUE
C
```

```
C
      DO 50 III=1,2
       DO 60 I=1,15
       Q(I)=0.0
60 CONTINUE
       AB=1.000
       A(L)=1.000
        IF(LL.EQ.1)GO TO 73
        DO 74 I=1,3
C
        A(L)=A(L)+D(L,I+8)*E(K,I)
74 CONTINUE
C
      GO TO (61,62),III
61 B1=(D(L,9)*X(K,L)-D(L,1))
       B2=(D(L,10)*X(K,L)-D(L,2))
       B3=(D(L,11)*X(K,L)-D(L,3))
       GO TO 63
62 B1=(D(L,9)*Y(K,L)-D(L,5))
       B2=(D(L,10)*Y(K,L)-D(L,6))
       B3=(D(L,11)*Y(K,L)-D(L,7))
63 CONTINUE
C
       AB=(A(L)*SP)**2+(B1*SX)**2+(B2*SY)**2+(B3*SZ)**2
       AB=DSQRT(AB)
73 CONTINUE
C
       GO TO (71,72),III
C
71 DO 70 I=1,3
       Q(I)=E(K,I)
       Q(I+8)=-1.000*E(K,I)*X(K,L)
70 CONTINUE
C
       Q(4)=10.000
       Q(IPP1)=X(K,L)
       IF(IP.EQ.11) GO TO 75
       IF(IP.EQ.12) GO TO 77
       IF(IP.EQ.14) GO TO 81
       Q(IPM4)=XR*R2*A(L)
       Q(IPM3)=XR*R4*A(L)
       Q(IPM2)=XR*R6*A(L)
       Q(IPM1)=R7*A(L)
       Q(IP)=R9*A(L)
        GO TO 75
81 CONTINUE
       Q(IPM2)=XR*R2*A(L)
       Q(IPM1)=XR*R4*A(L)
       Q(IP)=XR*R6*A(L)
       GO TO 75
77 Q(IP)=XR*R2*A(L)
       GO TO 75
72 DO 80 I=1,3
       Q(I+4)=E(K,I)
       Q(I+8)=-1.000*E(K,I)*Y(K,L)
80 CONTINUE
       Q(8)=10.000
       Q(IPP1)=Y(K,L)
       IF(IP.EQ.11) GO TO 75
```

```
                IF(IP.EQ.12) GO TO 78
                IF(IP.EQ.14) GO TO 82
                Q(IPM4)=YR*R2*A(L)
                Q(IPM3)=YR*R4*A(L)
                Q(IPM2)=YR*R6*A(L)
                Q(IPM1)=R9*A(L)
                Q(IP)=R8*A(L)
                GO TO 75
82 CONTINUE
                 Q(IPM2)=YR*R2*A(L)
                   Q(IPM1)=YR*R4*A(L)
                Q(IP)=YR*R6*A(L)
                GO TO 75
78 Q(IP)=YR*R2*A(L)
75 CONTINUE
C
                DO76 I=1,IPP1
              -  Q(I)=Q(I)/AB
76  CONTINUE
C
                VV=VV+Q(IPP1)*Q(IPP1)
C
                DO 90 I=1,IP
                DO 90 J=1,IPP1
                W(I,J)=W(I,J)+Q(I)*Q(J)
90 CONTINUE
C
                 DO 89 I=1,IPM1
                KL=I+1
                   DO 89 J=KL,IP
                 W(J,I)=W(I,J)
89 CONTINUE
50 CONTINUE
40 CONTINUE
                DO 91 I=1,IP
                Q(I)=W(I,IPP1)
91 CONTINUE
C
                CALL SWPMAT(W,1,IP,IPP1,KERR,TOL)
C
                DO 105 I=1,IP
                D(L,I)=W(I,IPP1)
                VV=VV-Q(I)*W(I,IPP1)
105 CONTINUE
C
     CALL XPYPC(L,LL)
C
                IF(LL.EQ.1) GO TO 31
C
                VV=DABS(VV/DF)
                STD=DSQRT(VV)
     WRITE(6,112) STD
112 FORMAT('D',10X,'STANDARD ERROR OF UNIT WEIGHT=',F10.4)
 31 CONTINUE
C
                WRITE(6,109) L
109 FORMAT(1HO,5X,'COMPUTED VALUES OF UNKNOWNS AND STANDARD
   1ERRORS, CAMERA',I3,//,16X,'DLT PARAMETERS',5X,'STANDARD
   2ERRORS',/)
```

```
C
              DO 110 I=1,IP
              DO 111 J=1,IP
              W(I,J)=W(I,J)*VV
C         WRITE(4,997) W(I,J)
  111 CONTINUE
C998     FORMAT(1X,D20.8)
              SD(I)=DSQRT(W(I,I))
  110 CONTINUE
C
              DO 120 I=1,11
              WRITE(6,300) D(L,I),SD(I)
         WRITE(4,997) D(L,I)
997      FORMAT(1X,D20.8)
  300 FORMAT(10X,2D20.8)
  120 CONTINUE
C
              IF (IP.EQ.11) GO TO 30
C
              WRITE(6,119)
  119 FORMAT('0',5X,'LENS DISTORTION COEFFICIENTS',2X,'STANDARD
     1ERRORS',/)
C
              DO 130 I=12,IP
              WRITE(6,300) D(L,I),SD(I)
  130 CONTINUE
   30 CONTINUE
              KNOWN=1
              CALL OBJECT(IPM4,IPM3,IPM2,IPM1,IP,SP,KNOWN)
C
               DO 23 K=1,NCAM
              DO 24 J=1,NPOINT
              READ(5,*)X(J,K),Y(J,K)
    24 CONTINUE
    23 CONTINUE
C
              WRITE (6,183)NPOINT
  183 FORMAT('I','THE NUMBER OF UNKNOWN POINTS IS',I5)
C
              KNOWN=0
              SP=SEUKP
              CALL OBJECT(IPM4,IPM3,IPM2,IPM1,IP,SP,KNOWN)
  500 CONTINUE
      STOP
      END
C
C*****************************************************************
C*****************************************************************
C**                                                             **
C**      END OF PROGRAM
C**      THE FOLLOWING PART CONTAINS
C**      THE SUBROUTINES USED IN THE
C**       MAIN PROGRAM
C**
C*****************************************************************
C*****************************************************************
      SUBROUTINE SWPMAT(A,IN,N,M,KERR,TOL)
      IMPLICIT DOUBLE PRECISION (A-H,O-Z)
             DIMENSION A(20,20)
```

```
C
            KERR=0
            DO 40 K=IN,N
            IF(DABS(A(K,K))-TOL)85,85,86
 86 X=1.000/A(K,K)
            DO 41 J=IN,M
 41 A(K,J)=A(K,J)*X
            A(K,K)=X
            DO 42 I=IN,N
            IF(I-K)50,42,50
 50 Y=A(I,K)
            A(I,K)=0.0
            DO 43 J=IN,M
 43 A(I,J)=A(I,J)-Y*A(K,J)
 42 CONTINUE
 40 CONTINUE
 99 RETURN
 85 KERR=K
            GO TO 99
            END
C
            SUBROUTINE XPYPC(L,LL)
C
    IMPLICIT DOUBLE PRECISION (A-H,O-Z)
            DIMENSION Q(5)
            COMMON/TRANS/D(4,20),XP(4),YP(4),W(20,20)
C
            DO 10 I=1,5
            Q(I)=0.0
 10 CONTINUE
C
            DO 30 I=1,3
            J=I+8
            K=I+4
            Q(1)=Q(1)+D(L,I)*D(L,J)
            Q(2)=Q(2)+D(L,K)*D(L,J)
            Q(3)=Q(3)+D(L,I)*D(L,I)
            Q(4)=Q(4)+D(L,K)*D(L,K)
            Q(5)=Q(5)+D(L,J)*D(L,J)
 30 CONTINUE
C
            XP(L)=Q(1)/Q(5)
            YP(L)=Q(2)/Q(5)
            CX=Q(3)/Q(5)-XP(L)*XP(L)
            CY=Q(4)/Q(5)-YP(L)*YP(L)
            CX=DSQRT(CX)
            CY=DSQRT(CY)
            C=(CX+CY)*0.500
C
            IF(LL.EQ.1) GO TO 40
            WRITE(6,100) L
100 FORMAT('0',10X,'INNER ORIENTATION,CAMERA',I3)
            WRITE(6,300)XP(L),YP(L),C
C       WRITE(4,996) XP(L),YP(L)
300 FORMAT(15X,'XP=',F10.4,5X,'YP=',F10.4,5X,'C=',F10.4)
 40 CONTINUE
C996    FORMAT(1X,2(2X,D20.8))
            RETURN
            END
```

```
C
                SUBROUTINE OBJECT(IPM4,IPM3,IPM2,IPM1,IP,SP,KNOWN)
C
      IMPLICIT DOUBLE PRECISION (A-H,O-Z)
       DIMENSION Q(10),T(20,20),XX(4),YY(4),R(20),F(20),AX(4),AY(4),A(4)
     1,XCC(3),SE(4),SSE(4),RES(500,3),SUMR(3),COOR(500,3),DMEAN(3)
              COMMON/TRANS/D(4,20),XP(4),YP(4),W(20,20)
              COMMON/DATA/E(30,3),X(100,4),Y(100,4),NUM(30)
              COMMON/NUMBER/NNC,NCAM,NPOINT
C
              TOL=1.D-6
C
              DO 1 I=1,3
              SUMR(I)=0.0
           DMEAN(I)=0.0
         1 CONTINUE
              SPOSR=0.0
              IF(KNOWN.EQ.0)GO TO 917
C
              WRITE (6,126) NCAM
       126  FORMAT('1',1X,'COMPUTATION FOR',I4,2X,'CAMERAS',//,1X,'POINT'
          1,16X,'GIVEN',27X,'COMPUTED',30X,'RESIDUAL',//,5X,3(9X,'X',9X,'Y',
          29X,'Z'),8X,'POS',//)
       917 CONTINUE
              DO 5 I=1,4
              SSE(I)=0.0
         5 CONTINUE
C
              DF=2*NCAM-3
C
C
C
      NPTS=NNC
      IF(KNOWN.EQ.0) NPTS=NPOINT
      DO 10 K=1,NPTS
C
C
       DO 15 L=1,NCAM
      AX(L)=1.000
      AY(L)=1.000
      IF(IP.EQ.11)GO TO 12
      XXX=X(K,L)-XP(L)
      YYY=Y(K,L)-YP(L)
      R1=XXX**2
      R3=YYY**2
      R2=R1+R3
      IF(IP.EQ.12)GO TO 14
      R4=R2*R2
      R6=R2*R4
       IF(IP.EQ.14)GO TO 17
      DK=D(L,IPM4)*R2+D(L,IPM3)*R4+D(L,IPM2)*R6
       R7=2.000*R1+R2
      R8=2.000*R3+R2
      R9=2.000*XXX*YYY
              XX(L)=X(K,L)-(XXX*DK+D(L,IPM1)*R7+D(L,IP)*R9)
      YY(L)=Y(K,L)-(YYY*DK+D(L,IPM1)*R9+D(L,IP)*R8)
      GO TO 15
   17 CONTINUE
      DK=D(L,IPM2)*R2+D(L,IPM1)*R4+D(L,IP)*R6
```

```
      GO TO 18
   14 CONTINUE
      DK=D(L,IP)*R2
   18 CONTINUE
      XX(L)=X(K,L)-XXX*DK
      YY(L)=Y(K,L)-YYY*DK
      GO TO 15
   12 CONTINUE
      XX(L)=X(K,L)
      YY(L)=Y(K,L)
   15 CONTINUE
C
C
      DO 20 M=1,2
      IF(M.EQ.1) GO TO 80
C
      DO 25 L=1,NCAM
      XXX=X(K,L)-XP(L)
      YYY=Y(K,L)-YP(L)
      A(L)=1.000
      DO 30 I=1,3
      A(L)=A(L)+D(L,I+8)*XCC(I)
   30 CONTINUE
C
      DO 35 II=1,2
      GG=0.0
      DO 40 I=1,11
      R(I)=0.0
      F(I)=0.0
   40 CONTINUE
C
      IF(II.EQ.2) GO TO 50
      DO 45 I=1,3
      J=I+8
      R(I)=XCC(I)
      R(J)=XCC(I)*X(K,L)
   45 CONTINUE
      R(4)=10.000
      GO TO 60
C
   50 CONTINUE
      DO 55 I=5,7
      J=I+4
      JJ=I-4
      R(I)=XCC(JJ)
      R(J)=XCC(JJ)*Y(K,L)
   55 CONTINUE
      R(8)=10.000
   60 CONTINUE
      AB=(A(L)*SP)**2
C
C
      DO 65 I=1,11
      DO 70 J=1,11
      F(I)=F(I)+R(J)*W(I,J)
   70 CONTINUE
      GG=GG+F(I)*R(I)
   65 CONTINUE
      IF(II.EQ.2) GO TO 75
```

```
      AX(L)=GG+AB
      AX(L)=DSQRT((AX(L)))
      GO TO 35
   75 AY(L)=GG+AB
      AY(L)=DSQRT((AY(L)))
   35 CONTINUE
   25 CONTINUE
   80 CONTINUE
      DO 85 I=1,3
      DO 85 J=1,4
      T(I,J)=0.0
   85 CONTINUE
      VV=0.0
C
      DO 90 L=1,NCAM
C
      DO 95 II=1,2
      GO TO (91,92),II
C
   91 DO 96 I=1,3
      J=I+8
      Q(I)=(D(L,J)*XX(L)-D(L,I))/AX(L)
   96 CONTINUE
      Q(4)=(D(L,4)*10.000-XX(L))/AX(L)
      GO TO 100
C
   92 DO 97 I=1,3
      J=I+8
      JJ=I+4
       Q(I)=(D(L,J)*YY(L)-D(L,JJ))/AY(L)
   97 CONTINUE
      Q(4)=(D(L,8)*10.000-YY(L))/AY(L)
  100 CONTINUE
C
C
      VV=VV+Q(4)**2
C
      DO 105 I=1,3
      DO 105 J=1,4
      T(I,J)=T(I,J)+Q(I)*Q(J)
  105 CONTINUE
   95 CONTINUE
   90 CONTINUE
C
      DO 110 I=1,3
      Q(I)=T(I,4)
  110 CONTINUE
C
C
      CALL SWPMAT(T,1,3,4,KERR,TOL)
C
C
      DO 115 I=1,3
      XCC(I)=T(I,4)
      VV=VV-Q(I)*T(I,4)
  115 CONTINUE
      IF(M.EQ.1) GO TO 20
      VV=DABS(VV/DF)
C
```

```
C
      SEUW=DSQRT(VV)
      SE(4)=0.0
C
      DO 120 I=1,3
      DO 125 J=1,3
      T(I,J)=VV*(T(I,J))
  125 CONTINUE
      SE(I)=T(I,I)
      SE(4)=SE(4)+SE(I)
  120 CONTINUE
   20 CONTINUE
C
C
      DO 130I=1,4
      SSE(I)=SSE(I)+SE(I)
      SE(I)=DSQRT(SE(I))
  130 CONTINUE
      IF(KNOWN.EQ.0) GO TO 300
C
C
      POS=0.0
      DO 210 I=1,3
      RES(K,I)=XCC(I)-E(K,I)
      DMEAN(I)=DMEAN(I)+DABS(RES(K,I))
      SSR=RES(K,I)**2
      SUMR(I)=SUMR(I)+SSR
      POS=POS+SSR
  210 CONTINUE
      POSR=DSQRT(POS)
      SPOSR=SPOSR+POS
      WRITE(6,200)NUM(K),(E(K,I),I=1,3),(XCC(I),I=1,3),
     1(RES(K,I),I=1,3),POSR
  200 FORMAT(' ',I6,10F10.3)
      IF(K.NE.NNC) GO TO 10
C
C
      DKI=K-I
      DO 209 I=1,3
      DMEAN(I)=DMEAN(I)/NNC
      SUMR(I)=DSQRT(SUMR(I)/DKI)
  209 CONTINUE
      SPOSR=DSQRT(SPOSR/DKI)
      WRITE(6,4123) (DMEAN(J),J=1,3)
 4123 FORMAT(34X,'MEAN ERROR:',3F12.3)
      WRITE(6,400)NNC,(SUMR(I),I=1,3),SPOSR
  400 FORMAT('0',14X,'AVERAGE MEAN SQUARE ERRORS FOR',I3,2X,'POINTS ARE'
     1,10X,4F9.4)
      GO TO 10
  300 CONTINUE
C
      DO 320 I=1,3
      COOR(K,I)=XCC(I)
  320 CONTINUE
      IF(K.NE.NPTS)GO TO 10
      WRITE(6,430)
  430 FORMAT(' ',/////////,14X,'TRANSFORMED POINTS',//,6X,'POINT',12X,
     1'X',11X,'Y',11X,'Z',//)
      DO 11 I=1,NPTS
```

```
      WRITE(6,325) (COOR(I,JJ),JJ=1,3)
  325 FORMAT((' ',14X,3(2X,F10.3)))
   11 CONTINUE
   10 CONTINUE
      RETURN
      END
```

Program "OBJAMPU.MAJ"

```
      IMPLICIT DOUBLE PRECISION (A-H,O-Z)
      DIMENSION Q(10),T(20,20),XX(4),YY(4),R(20),F(20),AX(4),AY(4),A(4)
     1,XCC(3),SE(4),SSE(4),RES(500,3),SUMR(3),XU(3,20,300),YV(3,20,300)
     2,FDIS(2,3),XYZ(300,3)
      COMMON/DATA2/ P(3)
      COMMON/TRANS/D(3,11),XP(4),YP(4),W(11,11),COOR(300,3),COR(300,3)
      COMMON/DATA/E(30,3),X(300,3),Y(300,3),NUM(30)
      COMMON/NUMBER/NNC,NCAM,DIS1,DIS2,NK1,KN1,KCAM
C
      PRINT *,'        CALCULATE OBJECT COORDINATES OF MARKERS'
C
C ================================================================
C *                                                              *
C *     READING IN THE THE TRANSFORMATION MATRIX OF THE CAMERAS  *
C *                                                              *
C ================================================================
C
      PRINT *,'READ CAMERA PARAMETERS'
      READ(3,*) NCAM,IP,IPM1,IPM2,IPM3,IPM4
      DO 2 L=1,NCAM
      READ(3,*) (D(L,I),I=1,11)
2     CONTINUE
      SP=0.001
C
      READ(1,*) ILEG,INERTIA,FCUT
      READ(1,*) CA,FL,CS,HTI,CTH,PP,CCH
      READ(1,*) DLA,DRA,DLR,F13,F23,F3
      READ(1,*) X01,X02,X03,Y01,Y02,Y03
C
      WRITE(4,996) ILEG,INERTIA,FCUT
      WRITE(4,999) CA,FL,CS,HTI,CTH,PP,CCH
      WRITE(4,999) DLA,DRA,DLR,F13,F23,F3
998   FORMAT(1X,I8)
996   FORMAT(1X,2I5,3X,F5.2)
999   FORMAT(1X,3(2X,F12.4))
C
C ================================================================
C *                                                              *
C *     READING IN THE STATIC DATA AND TRANSFORMING THEM INTO OBJECTIVE
C *     COORDINATES                                              *
C *                                                              *
C ================================================================
C
      PRINT *,'STATIC CALCULATION'
      DO 20 J=1,21
      READ(1,*) FC,Y(J,1),X(J,1),TI
20    CONTINUE
      IN=11
```

```
      IF(ILEG.EQ.2) IN=15
      DO 25 J=1,IN
      READ(1,*) FC,X(J,2),Y(J,2),TI
25    CONTINUE
      IN=13
      IF (ILEG.EQ.2) IN=9
      DO 30 J=1,IN
      READ(1,*) FC,X(J,3),Y(J,3),TI
30    CONTINUE
C
C
C   CENTRALIZING THE COORDINATES
C
      DO 52 I=1,30
      X(I,1)=X(I,1)-X01
      X(I,2)=X(I,2)-X02
      X(I,3)=X(I,3)-X03
      Y(I,1)=Y(I,1)-Y01
      Y(I,2)=Y(I,2)-Y02
      Y(I,3)=Y(I,3)-Y03
52    CONTINUE
C
      WRITE(12,796) X01,Y01,X02,Y02,X03,Y03
796   FORMAT(///,2X,6HSTATIC,//,11HX01,Y01,...,/
      1,2(2X,3(2X,F10.4)))
      WRITE(4,950)
950   FORMAT(1X,///)
C
C   LEFT SHANK MARKERS AND ASIS MARKER
C
      CALL OBJECT1(2,IPM4,IPM3,IPM2,IPM1,IP,SP,4)
      DO 460 J=1,4
460   WRITE(4,499) (COOR(J,I),I=1,3)
      DO 55 I=1,3
      COR(4,I)=COOR(4,I)
55    CONTINUE
C
C   RIGHT SHANK MARKERS AND ASIS MARKER
C
      DO 60 J=7,10
      X(J-6,1)=X(J,1)
      Y(J-6,1)=Y(J,1)
60    CONTINUE
      CALL OBJECT1(3,IPM4,IPM3,IPM2,IPM1,IP,SP,4)
      DO 461 J=1,4
461   WRITE(4,499) (COOR(J,I),I=1,3)
C
C   TAIL MARKER
C
      X(4,2)=X(7,2)
      Y(4,2)=Y(7,2)
      KN1=4
      NK1=4
      KCAM=2
      DIS1=DLA
      DIS2=DRA
      CALL OBJECT2
      WRITE(4,499) (P(I),I=1,3)
C
```

```
C     LEFT SHOULDER AND STERN MARKERS
C
          DO 80 I=1,2
          DO 80 J=5,6
          X(J-4,I)=X(J,I)
          Y(J-4,I)=Y(J,I)
80        CONTINUE
          CALL OBJECT1(2,IPM4,IPM3,IPM2,IPM1,IP,SP,2)
          DO 462 J=1,2
462       WRITE(4,499) (COOR(J,I),I=1,3)
C
C     RIGHT SHOULDER MARKER
C
          X(1,3)=X(5,3)
          Y(1,3)=Y(5,3)
          X(1,1)=X(11,1)
          Y(1,1)=Y(11,1)
          CALL OBJECT1(3,IPM4,IPM3,IPM2,IPM1,IP,SP,1)
          WRITE(4,499) (COOR(1,I),I=1,3)
C
C     LEFT FOOT OR SOCKET MARKERS
C
          DO 85 J=12,13
          X(J-11,1)=X(J,1)
          Y(J-11,1)=Y(J,1)
85        CONTINUE
          DO 86 J=8,9
          X(J-7,2)=X(J,2)
          Y(J-7,2)=Y(J,2)
86        CONTINUE
          CALL OBJECT1(2,IPM4,IPM3,IPM2,IPM1,IP,SP,2)
          DO 463 J=1,2
463       WRITE(4,499) (COOR(J,I),I=1,3)
C
          IF (ILEG.EQ.2) THEN
          KN1=1
          NK1=1
          KCAM=2
          X(1,2)=X(10,2)
          Y(1,2)=Y(10,2)
          DO 88 K=1,3
88        COR(1,K)=COOR(2,K)          !COOR(1,*) CORRESPONDING TO FR13
          DIS1=FL13                   !COR(1,*) CORRESPONDING TO FR23
          DIS2=FL23
          CALL OBJECT2
          WRITE(4,499) (P(I),I=1,3)
C
          ELSE
          X(1,1)=X(16,1)
          Y(1,1)=Y(16,1)
          X(1,2)=X(10,2)
          Y(1,2)=Y(10,2)
          CALL OBJECT1(2,IPM4,IPM3,IPM2,IPM1,IP,SP,1)
          WRITE(4,499) (COOR(1,I),I=1,3)
          END IF
C
C     RIGHT FOOT OR SOCKET MARKERS
C
          DO 90 J=14,15
```

```
      X(J-13,1)=X(J,1)
      Y(J-13,1)=Y(J,1)
90    CONTINUE
      DO 91 J=6,7
      X(J-5,3)=X(J,3)
      Y(J-5,3)=Y(J,3)
91    CONTINUE
      CALL OBJECT1(3,IPM4,IPM3,IPM2,IPM1,IP,SP,2)
      DO 464 J=1,2
464   WRITE(4,499) (COOR(J,I),I=1,3)
C
      IF(ILEG.EQ.1) THEN
      KN1=1
      NK1=1
      KCAM=3
      X(1,3)=X(8,3)
      Y(1,3)=Y(8,3)
      DO 92 K=1,3
92    COR(1,K)=COOR(2,K)            !COOR(1,*) CORRESPONDING TO FL23
      DIS1=FR23                     !COR(1,*) CORRESPONDING TO FL13
      DIS2=FR13
      CALL OBJECT2
      WRITE(4,499) (P(I),I=1,3)
C
      ELSE
      X(1,1)=X(16,1)
      Y(1,1)=Y(16,1)
      X(1,3)=X(8,3)
      Y(1,3)=Y(8,3)
      CALL OBJECT1(3,IPM4,IPM3,IPM2,IPM1,IP,SP,1)
      WRITE(4,499) (COOR(1,I),I=1,3)
      END IF
C
C     JOINT CENTERS OF THE UNAFFECTED LOWER LIMB
C
      IF (ILEG.EQ.1) THEN
      ICAM=3
      I1=9
      I2=13
      ELSE
      ICAM=2
      I1=11
      I2=15
      END IF
C
      DO 100 J=17,21
      X(J-16,1)=X(J,1)
      Y(J-16,1)=Y(J,1)
100   CONTINUE
      DO 101 J=I1,I2
      LK=J-I1+1
      X(LK,ICAM)=X(J,ICAM)
      Y(LK,ICAM)=Y(J,ICAM)
101   CONTINUE
      CALL OBJECT1(ICAM,IPM4,IPM3,IPM2,IPM1,IP,SP,5)
      DO 466 J=1,5
466   WRITE(4,499) (COOR(J,I),I=1,3)
C
C *=================================================================*
```

```
C *                                                                      *
C *     READ THE DYNAMIC DATA AND TRANSFORMING THEM TO OBJECTIVE  SPACE  *
C *                                                                      *
C *======================================================================*
C
      PRINT *,'READING DYNAMIC DATA'
      READ(1,*) NF1,ITF1,IHS1,NF2,ITF2,IHS2
      WRITE(4,998) NF1,ITF1,IHS1,NF2,ITF2,IHS2
      NF=ITF2-IHS1+1+8
      CX1=0.0
      CX2=0.0
      CX3=0.0
      CY1=0.0
      CY2=0.0
      CY3=0.0
C
      KKCAM=1
      DO 120 J=1,16
      DO 115 L=1,NF
      READ(1,*) FC,YYY,XXX,TI
      FC2=FC
      IF(L.EQ.1) FC1=FC-1.0
      IF(FC2.NE.FC1+1.0) GOTO 1234
      FC1=FC2
      XU(1,J,L)=XXX-X01
      YV(1,J,L)=YYY-Y01
115   CONTINUE
120   CONTINUE
C
      KKCAM=2
      I1=10
      IF(ILEG.EQ.1) I1=11
      DO 125 J=1,I1
      DO 125 L=1,NF
      READ(1,*) FC,XXX,YYY,TI
      FC2=FC
      IF(L.EQ.1) FC1=FC-1.0
      IF(FC2.NE.FC1+1.0) GOTO 1234
      FC1=FC2
      XU(2,J,L)=XXX-X02
      YV(2,J,L)=YYY-Y02
125   CONTINUE
C
      KKCAM=3
      I1=8
      IF(ILEG.EQ.2) I1=9
      DO 130 J=1,I1
      DO 130 L=1,NF
      READ(1,*) FC,XXX,YYY,TI
      FC2=FC
      IF(L.EQ.1) FC1=FC-1.0
      IF(FC2.NE.FC1+1.0) GOTO 1234
      FC1=FC2
      XU(3,J,L)=XXX-X03
      YV(3,J,L)=YYY-Y03
130   CONTINUE
C
      READ (1,*) NFN
C
```

```
      PRINT *,'COMPUTING DYNAMIC CO-ORDINATE'
C
C    LEFT SHANK MARKERS AND ASIS MARKER
C
      DO 150 J=1,4
      PRINT *,'  MARKER',J
      DO 145 I=1,2
      DO 145 L=1,NF
      X(L,I)=XU(I,J,L)
      Y(L,I)=YV(I,J,L)
145   CONTINUE
      WRITE(4,950)
      CALL OBJECT1(2,IPM4,IPM3,IPM2,IPM1,IP,SP,NF)
      CALL FILTERING(FCUT,NF,COOR)
150   CONTINUE
C
      DO 155 I=1,3
      DO 155 L=1,NF
      COR(L,I)=COOR(L,I)
155   CONTINUE
C
C    RIGHT SHANK MARKERS AND ASIS MARKER
C
      DO 170 J=7,10
      PRINT *,'  MARKER',J-2
      DO 165 L=1,NF
      X(L,1)=XU(1,J,L)
      Y(L,1)=YV(1,J,L)
      X(L,3)=XU(3,J-6,L)
      Y(L,3)=YV(3,J-6,L)
165   CONTINUE
      WRITE(4,950)
      CALL OBJECT1(3,IPM4,IPM3,IPM2,IPM1,IP,SP,NF)
      CALL FILTERING(FCUT,NF,COOR)
170   CONTINUE
C
C    TAIL MARKER
C
      WRITE(4,950)
      PRINT *,'  MARKER          9'
      KCAM=2
      DIS1=DLA
      DIS2=DRA
      DO 175 L=1,NF
      X(L,2)=XU(2,7,L)
      Y(L,2)=YV(2,7,L)
      NK1=L
      CALL OBJECT2
      DO 345 I=1,3
345   XYZ(L,I)=P(I)
175   CONTINUE
      CALL FILTERING(FCUT,NF,XYZ)
C
C    SHOULDER MARKERS
C
      DO 195 J=5,6
      K=J+5
      PRINT *,'  MARKER',K
```

```
      DO 190 L=1,NF
      DO 190 I=1,2
      X(L,I)=XU(I,J,L)
      Y(L,I)=YV(I,J,L)
190   CONTINUE
      WRITE(4,950)
      CALL OBJECT1(2,IPM4,IPM3,IPM2,IPM1,IP,SP,NF)
      CALL FILTERING(FCUT,NF,COOR)
195   CONTINUE
C
      DO 200 L=1,NF
      X(L,1)=XU(1,11,L)
      Y(L,1)=YV(1,11,L)
      X(L,3)=XU(3,5,L)
      Y(L,3)=YV(3,5,L)
200   CONTINUE
      WRITE(4,950)
      CALL OBJECT1(3,IPM4,IPM3,IPM2,IPM1,IP,SP,NF)
      CALL FILTERING(FCUT,NF,COOR)
      PRINT *,'  MARKER          12'
C
C    LEFT FOOT OR SOCKET MARKERS
C
      DO 215 J=8,9
      K=J+5
      PRINT *,'  MARKER',K
      DO 210 L=1,NF
      X(L,1)=XU(1,J+4,L)
      Y(L,1)=YV(1,J+4,L)
      X(L,2)=XU(2,J,L)
      Y(L,2)=YV(2,J,L)
210   CONTINUE
      WRITE(4,950)
      CALL OBJECT1(2,IPM4,IPM3,IPM2,IPM1,IP,SP,NF)
      CALL FILTERING(FCUT,NF,COOR)
      IF(J.EQ.9) GOTO 215
      DO 211 I=1,3
      DO 211 L=1,NF
      COR(L,I)=COOR(L,I)
211   CONTINUE
215   CONTINUE
C
      WRITE(4,950)
      PRINT *,'  MARKER          15'
C
      IF(ILEG.EQ.2) THEN
      DIS1=FL23                    !COOR(*,*) CORRESPONDING TO FR23
      DIS2=FL13                    !COR(*,*) CORRESPONDING TO FR13
      KCAM=2
      DO 220 L=1,NF
      X(L,2)=XU(2,10,L)
      Y(L,2)=YV(2,10,L)
      KN1=L
      NK1=L
      CALL OBJECT2
      DO 346 I=1,3
346   XYZ(L,I)=P(I)
220   CONTINUE
      CALL FILTERING(FCUT,NF,XYZ)
```

```
C
        ELSE
        DO 270 L=1,NF
        X(L,1)=XU(1,16,L)
        Y(L,1)=YV(1,16,L)
        X(L,2)=XU(2,10,L)
        Y(L,2)=YV(2,10,L)
270     CONTINUE
        CALL OBJECT1(2,IPM4,IPM3,IPM2,IPM1,IP,SP,NF)
        CALL FILTERING(FCUT,NF,COOR)
        END IF
C
C    RIGHT FOOT OR SOCKET MARKERS
C
        DO 250 J=6,7
        K=J+10
        PRINT *,'  MARKER',K
        DO 230 L=1,NF
        X(L,1)=XU(1,J+8,L)
        Y(L,1)=YV(1,J+8,L)
        X(L,3)=XU(3,J,L)
        Y(L,3)=YV(3,J,L)
230     CONTINUE
        WRITE(4,950)
        CALL OBJECT1(3,IPM4,IPM3,IPM2,IPM1,IP,SP,NF)
        CALL FILTERING(FCUT,NF,COOR)
        IF(J.EQ.7) GOTO 250
        DO 240 I=1,3
        DO 240 L=1,NF
        COR(L,I)=COOR(L,I)              !COR(*,*) CORRESPONDING TO FL23
240     CONTINUE
250     CONTINUE
C
        WRITE(4,950)
        PRINT *,'  MARKER          18'
C
        IF(ILEG.EQ.1) THEN
        DIS1=FL13                       !COOR(*,*) CORRESPONDING TO FR13
        DIS2=FL23                       !COR(*,*) CORRESPONDING TO FR23
        KCAM=3
        DO 260 L=1,NF
        X(L,3)=XU(3,8,L)
        Y(L,3)=YV(3,8,L)
        KN1=L
        NK1=L
        CALL OBJECT2
        DO 347 I=1,3
347     XYZ(L,I)=P(I)
260     CONTINUE
        CALL FILTERING(FCUT,NF,XYZ)
C
        ELSE
        DO 280 L=1,NF
        X(L,1)=XU(1,16,L)
        Y(L,1)=YV(1,16,L)
        X(L,3)=XU(3,8,L)
        Y(L,3)=YV(3,8,L)
280     CONTINUE
        CALL OBJECT1(3,IPM4,IPM3,IPM2,IPM1,IP,SP,NF)
```

```
      CALL FILTERING(FCUT,NF,COOR)
      END IF
C
C
      WRITE(4,457) NFN
457   FORMAT(1X,I5)
C
499   FORMAT(1X,3(5X,F10.7))
1324  STOP
1234  PRINT *,'DATA MISSING IN:',KKCAM,J,L
      GO TO 1324
      END
C
C
C
      SUBROUTINE FILTERING(FCUT,NF,XXX)
      DIMENSION RAW1(150),RAW2(150),RAW3(150),XYZ(150,3)
      DOUBLE PRECISION XXX(300,3)
C
      DO 5 I=1,3
      DO 5 J=1,NF
5     XYZ(J,I)=XXX(J,I)
      DO 10 J=1,NF
      RAW1(J)=XYZ(J,1)
      RAW2(J)=XYZ(J,2)
      RAW3(J)=XYZ(J,3)
10    CONTINUE
      CALL FILTER(RAW1,NF,FCUT,0.02)
      CALL FILTER(RAW2,NF,FCUT,0.02)
      CALL FILTER(RAW3,NF,FCUT,0.02)
      DO 20 J=1,NF
20    WRITE(4,499) RAW1(J),RAW2(J),RAW3(J)
499   FORMAT(1X,3(5X,F10.7))
      RETURN
      END
```

Program "OBJECT.SUB"

```
      SUBROUTINE LEFTHS(X,I,NF,NFN)
      DIMENSION X(3,20,300),Y(200)
C
      DO 10 J=1,NF-2
      Y(J)=0.0
      DO 5 II=1,NF-J
      Y(J)=Y(J)+ABS(X(2,I,II+J)-X(2,I,II))
5     CONTINUE
      Y(J)=Y(J)/FLOAT(NF-J-1)
10    CONTINUE
C
      XX=10.0**30
      DO 20 J=1,NF-2
      IF(XX.LE.Y(J)) GOTO 20
      XX=Y(J)
      NFN=J
20    CONTINUE
      RETURN
      END
C
C
C
C
C
      SUBROUTINE LSFUN2(M,N,XC,FVECC,FJACC,LJC)
      IMPLICIT DOUBLE PRECISION (A-H,O-Z)
      DIMENSION Q(8),XC(N),FVECC(M),FJACC(LJC,N)
      COMMON/TRANS/D(3,11),XP(4),YP(4),W(11,11),COOR(300,3),COR(300,3)
      COMMON/DATA/E(30,3),X(300,3),Y(300,3),NUM(30)
      COMMON/NUMBER/NNC,NCAM,DIS1,DIS2,NK1,KN1,KCAM
      INTEGER M,N,LJC
C
      DO 10 K1=1,3
      Q(K1)=X(NK1,KCAM)*D(KCAM,8+K1)-D(KCAM,K1)
      Q(K1+4)=Y(NK1,KCAM)*D(KCAM,8+K1)-D(KCAM,K1+4)
10    CONTINUE
      Q(4)=X(NK1,KCAM)-D(KCAM,4)
      Q(8)=Y(NK1,KCAM)-D(KCAM,8)
C
      FVECC(1)=Q(1)*XC(1)+Q(2)*XC(2)+Q(3)*XC(3)+Q(4)
      FVECC(2)=Q(5)*XC(1)+Q(6)*XC(2)+Q(7)*XC(3)+Q(8)
      XX=XC(1)-COOR(NK1,1)
      YY=XC(2)-COOR(NK1,2)
      ZZ=XC(3)-COOR(NK1,3)
      FVECC(3)=XX*XX+YY*YY+ZZ*ZZ-DIS1*DIS1

C
      DO 20 J=1,3
      FJACC(2,J)=Q(J+4)
```

```
20      FJACC(1,J)=Q(J)
        FJACC(3,1)=2.0*XX
        FJACC(3,2)=2.0*YY
        FJACC(3,3)=2.0*ZZ
C
        XX=XC(1)-COR(KN1,1)
        YY=XC(2)-COR(KN1,2)
        ZZ=XC(3)-COR(KN1,3)
        FVECC(4)=XX*XX+YY*YY+ZZ*ZZ-DIS2*DIS2
        FJACC(4,1)=2.0*XX
        FJACC(4,2)=2.0*YY
        FJACC(4,3)=2.0*ZZ
C
        RETURN
        END
C
C
C
        SUBROUTINE OBJECT2
        IMPLICIT DOUBLE PRECISION (A-H,O-Z)
        DIMENSION W(78)
        COMMON/DATA2/ P(3)
        COMMON/NUMBER/NNC,NCAM,DIS1,DIS2,NK1,KN1,KCAM
        INTEGER IW(1)
C
        P(1)=0.0
        P(2)=0.4
        P(3)=0.0
        LW=78
        IFAIL=1
C
        CALL E04GEF(4,3,P,FSUM,IW,1,W,78,IFAIL)
C
        P(2)=P(2)+0.790
C       WRITE(4,99) (P(I),I=1,3)
        WRITE(12,99) (P(I),I=1,3)
99      FORMAT(10X,3(2X,F10.4))
C
        RETURN
        END
C
C
C
C*************************************************************
      SUBROUTINE SWPMAT(A,IN,N,M,KERR,TOL)
      IMPLICIT DOUBLE PRECISION (A-H,O-Z)
            DIMENSION A(20,20)
C
            KERR=0
            DO 40 K=IN,N
            IF(DABS(A(K,K))-TOL)85,85,86
   86 X=1.000/A(K,K)
            DO 41 J=IN,M
   41 A(K,J)=A(K,J)*X
            A(K,K)=X
            DO 42 I=IN,N
            IF(I-K)50,42,50
   50 Y=A(I,K)
            A(I,K)=0.0
```

```
            DO 43 J=IN,M
   43 A(I,J)=A(I,J)-Y*A(K,J)
   42 CONTINUE
   40 CONTINUE
   99 RETURN
   85 KERR=K
            GO TO 99
            END
C
C
C
      SUBROUTINE XPYPC(L,LL)
      IMPLICIT DOUBLE PRECISION (A-H,O-Z)
      DIMENSION Q(5)
      COMMON/TRANS/D(3,11),XP(4),YP(4),W(11,11),COOR(300,3),COR(300,3)
C
           DO 10 I=1,5
           Q(I)=0.0
   10 CONTINUE
C
           DO 30 I=1,3
           J=I+8
           K=I+4
           Q(1)=Q(1)+D(L,I)*D(L,J)
           Q(2)=Q(2)+D(L,K)*D(L,J)
           Q(3)=Q(3)+D(L,I)*D(L,I)
           Q(4)=Q(4)+D(L,K)*D(L,K)
           Q(5)=Q(5)+D(L,J)*D(L,J)
   30 CONTINUE
C
           XP(L)=Q(1)/Q(5)
           YP(L)=Q(2)/Q(5)
           CX=Q(3)/Q(5)-XP(L)*XP(L)
           CY=Q(4)/Q(5)-YP(L)*YP(L)
           CX=DSQRT(CX)
           CY=DSQRT(CY)
           C=(CX+CY)*0.500
C
           IF(LL.EQ.1) GO TO 40
           WRITE(6,100) L
  100 FORMAT('0',10X,'INNER ORIENTATION,CAMERA',I3)
           WRITE(6,300)XP(L),YP(L),C
  300 FORMAT(15X,'XP=',F10.4,5X,'YP=',F10.4,5X,'C=',F10.4)
   40 CONTINUE
C
      RETURN
      END
C
C
C
C
      SUBROUTINE OBJECT1(ICAM,IPM4,IPM3,IPM2,IPM1,IP,SP,NPOINT)
C
      IMPLICIT DOUBLE PRECISION (A-H,O-Z)
      DIMENSION Q(10),T(20,20),XX(4),YY(4),R(20),F(20),AX(4)
      1,AY(4),A(4),XCC(3),SE(4),SSE(4),RES(500,3),SUMR(3)
      COMMON/TRANS/D(3,11),XP(4),YP(4),W(11,11),COOR(300,3),COR(300,3)
      COMMON/DATA/E(30,3),X(300,3),Y(300,3),NUM(30)
      COMMON/NUMBER/NNC,NCAM,DIS1,DIS2,NK1,KN1,KCAM
```

```
C
      IC1=1
      IC2=ICAM
      N=NPOINT
C
      IF(N.GT.4) GOTO 166
      DO 168 I=1,N
      WRITE(12,723) IC1,X(I,1),Y(I,1)
168   WRITE(12,723) IC2,X(I,IC2),Y(I,IC2)
      GO TO 167
166   WRITE(12,723) IC1,X(1,1),Y(1,1)
      WRITE(12,723) IC2,Y(1,IC2),Y(1,IC2)
167   TOL=1.D-6
      KNOWN=0
723   FORMAT(10X,I1,2(2X,F10.3))
C
            DO 1 I=1,3
            SUMR(I)=0.0
  1 CONTINUE
            SPOSR=0.0
            IF(KNOWN.EQ.0)GO TO 917
C
            WRITE (6,126) NCAM
126  FORMAT('1',1X,'COMPUTATION FOR',I4,2X,'CAMERAS',//,1X,'POINT'
     1,16X,'GIVEN',27X,'COMPUTED',30X,'RESIDUAL',//,5X,3(9X,'X',9X,'Y',
     29X,'Z'),8X,'POS',//)
917 CONTINUE
            DO 5 I=1,4
            SSE(I)=0.0
  5 CONTINUE
C
            DF=2*ICAM-3
C
C
C
      NPTS=NNC
      IF(KNOWN.EQ.0) NPTS=NPOINT
      DO 10 K=1,NPTS
C
C
       DO 15 L=1,ICAM,ICAM-1
      AX(L)=1.000
      AY(L)=1.000
      IF(IP.EQ.11)GO TO 12
      XXX=X(K,L)-XP(L)
      YYY=Y(K,L)-YP(L)
      R1=XXX**2
      R3=YYY**2
      R2=R1+R3
      IF(IP.EQ.12)GO TO 14
      R4=R2*R2
      R6=R2*R4
       IF(IP.EQ.14)GO TO 17
      DK=D(L,IPM4)*R2+D(L,IPM3)*R4+D(L,IPM2)*R6
       R7=2.000*R1+R2
      R8=2.000*R3+R2
      R9=2.000*XXX*YYY
            XX(L)=X(K,L)-(XXX*DK+D(L,IPM1)*R7+D(L,IP)*R9)
      YY(L)=Y(K,L)-(YYY*DK+D(L,IPM1)*R9+D(L,IP)*R8)
```

```
      GO TO 15
   17 CONTINUE
      DK=D(L,IPM2)*R2+D(L,IPM1)*R4+D(L,IP)*R6
      GO TO 18
   14 CONTINUE
      DK=D(L,IP)*R2
   18 CONTINUE
      XX(L)=X(K,L)-XXX*DK
      YY(L)=Y(K,L)-YYY*DK
      GO TO 15
   12 CONTINUE
      XX(L)=X(K,L)
      YY(L)=Y(K,L)
   15 CONTINUE
C
C
      DO 20 M=1,2
      IF(M.EQ.1) GO TO 80
C
      DO 25 L=1,ICAM,ICAM-1
      XXX=X(K,L)-XP(L)
      YYY=Y(K,L)-YP(L)
      A(L)=1.000
      DO 30 I=1,3
      A(L)=A(L)+D(L,I+8)*XCC(I)
   30 CONTINUE
C
      DO 35 II=1,2
      GG=0.0
      DO 40 I=1,11
      R(I)=0.0
      F(I)=0.0
   40 CONTINUE
C
      IF(II.EQ.2) GO TO 50
      DO 45 I=1,3
      J=I+8
      R(I)=XCC(I)
      R(J)=XCC(I)*X(K,L)
   45 CONTINUE
      R(4)=10.000
      GO TO 60
C
   50 CONTINUE
      DO 55 I=5,7
      J=I+4
      JJ=I-4
      R(I)=XCC(JJ)
      R(J)=XCC(JJ)*Y(K,L)
   55 CONTINUE
      R(8)=10.000
   60 CONTINUE
      AB=(A(L)*SP)**2
C
C
      DO 65 I=1,11
      DO 70 J=1,11
      F(I)=F(I)+R(J)*W(I,J)
   70 CONTINUE
```

```
      GG=GG+F(I)*R(I)
   65 CONTINUE
      IF(II.EQ.2) GO TO 75
      AX(L)=GG+AB
      AX(L)=DSQRT((AX(L)))
      GO TO 35
   75 AY(L)=GG+AB
      AY(L)=DSQRT((AY(L)))
   35 CONTINUE
   25 CONTINUE
   80 CONTINUE
      DO 85 I=1,3
      DO 85 J=1,4
      T(I,J)=0.0
   85 CONTINUE
      VV=0.0
C
      DO 90 L=1,ICAM,ICAM-1
C
      DO 95 II=1,2
      GO TO (91,92),II
C
   91 DO 96 I=1,3
      J=I+8
      Q(I)=(D(L,J)*XX(L)-D(L,I))/AX(L)
   96 CONTINUE
      Q(4)=(D(L,4)*10.000-XX(L))/AX(L)
      GO TO 100
C
   92 DO 97 I=1,3
      J=I+8
      JJ=I+4
       Q(I)=(D(L,J)*YY(L)-D(L,JJ))/AY(L)
   97 CONTINUE
      Q(4)=(D(L,8)*10.000-YY(L))/AY(L)
  100 CONTINUE
C
C
      VV=VV+Q(4)**2
C
      DO 105 I=1,3
      DO 105 J=1,4
      T(I,J)=T(I,J)+Q(I)*Q(J)
  105 CONTINUE
   95 CONTINUE
   90 CONTINUE
C
      DO 110 I=1,3
      Q(I)=T(I,4)
  110 CONTINUE
C
C
      CALL SWPMAT(T,1,3,4,KERR,TOL)
C
C
      DO 115 I=1,3
      XCC(I)=T(I,4)
      VV=VV-Q(I)*T(I,4)
  115 CONTINUE
```

```
      IF(M.EQ.1) GO TO 20
      VV=DABS(VV/DF)
C
C
      SEUW=DSQRT(VV)
      SE(4)=0.0
C
      DO 120 I=1,3
      DO 125 J=1,3
      T(I,J)=VV*(T(I,J))
  125 CONTINUE
      SE(I)=T(I,I)
      SE(4)=SE(4)+SE(I)
  120 CONTINUE
   20 CONTINUE
C
C
      DO 130I=1,4
      SSE(I)=SSE(I)+SE(I)
      SE(I)=DSQRT(SE(I))
  130 CONTINUE
      IF(KNOWN.EQ.0) GO TO 300
C
C
      POS=0.0
      DO 210 I=1,3
      RES(K,I)=XCC(I)-E(K,I)
      SSR=RES(K,I)**2
      SUMR(I)=SUMR(I)+SSR
      POS=POS+SSR
  210 CONTINUE
      POSR=DSQRT(POS)
      SPOSR=SPOSR+POS
      WRITE(6,200)NUM(K),(E(K,I),I=1,3),(XCC(I),I=1,3),
     1(RES(K,I),I=1,3),POSR
  200 FORMAT(' ',I6,10F10.3)
      IF(K.NE.NNC) GO TO 10
C
C
      DKI=K-I
      DO 209 I=1,3
      SUMR(I)=DSQRT(SUMR(I)/DKI)
  209 CONTINUE
      SPOSR=DSQRT(SPOSR/DKI)
      WRITE(6,400)NNC,(SUMR(I),I=1,3),SPOSR
  400 FORMAT('0',14X,'AVERAGE MEAN SQUARE ERRORS FOR',I3,2X,'POINTS ARE'
     1,10X,4F9.4)
      GO TO 10
  300 CONTINUE
C
      DO 320 I=1,3
      COOR(K,I)=XCC(I)
  320 CONTINUE
      IF(K.NE.NPTS)GO TO 10
      DO 11 I=1,NPTS
        COOR(I,2)=COOR(I,2)+0.790
        IF((NPTS.LT.5).OR.(I.LT.2)) WRITE(12,325) (COOR(I,JJ),JJ=1,3)
C       WRITE(4,325) (COOR(I,JJ),JJ=1,3)
  325 FORMAT(4X,3(2X,F10.5))
```

```
11 CONTINUE
10 CONTINUE
   RETURN
   END
```

Program "DYNAMPU1.MAJ"

```
C ********************************************************
C *                                                      *
C *   THIS PROGRAM DO KINEMATIC ANALYSIS ON THE          *
C *   UNAFFECTED LIMB AND TORSO.                         *
C *                                                      *
C ********************************************************
      COMMON /BLOCK1/SSX(30),SSY(30),SFZ(30)
      COMMON /BLOCK2/SX3(20,150),SY3(20,150),FZ3(20,150)
      COMMON /BLOCK3/AJC(3),KJC(3),SXL(3),HJC(3)
      COMMON NF
      DIMENSION RAW1(150),RAW3(150),RAW2(150),DTAD(150,3,3)
     2,T(3,3),TD(3,3),VLASTAT(3),VAD(3),HJC7(3),TT(3,3)
     3,VLKSTAT(3),EKD(3),VLA(3),VLK(3),VLAL(3),VLKL(3)
     4,TXL(3),FT(3,3),LIST(7),VH7C(3),VH8C(3),KANG(150)
     5,VH7(3),TP(3,3),HJC8(3),ASIS1(3),ASIS2(3),HANG(150)
     6,XP(3),YP(3),ZP(3),TAIL(3),TIB(3,3),ATZ(150),DAA(150)
     7,PTOG(3,3),SH7(3),SH8(3),SH7ST(3),SH8ST(3),FTT(3,3)
     8,APX(150),APY(150),APZ(150),ATX(150),ATY(150)
     9,DTHI(150,3,3),DSHA(150,3,3),AJCX(150),AJCY(150)
     1,AJCZ(150),KJCX(150),KJCY(150),KJCZ(150),CSZ(150)
     2,CPX(150),CPY(150),CPZ(150),CSX(150),CSY(150)
     3,CTOX(150),CTOY(150),CTOZ(150),HJCX(150),HJCY(150)
     4,TAS(3,3),TAST(3,3),TAMD(3,3),TAD(3,3),HJCZ(150)
     5,PELD(3,3),PELS(3,3),PELV(3,3)
      INTEGER CAM1
      REAL MASS,LL,LXSF,LYSF,LZSF,KJC,KA,KAA,KJCX,KJCY,KJCZ,KANG
C
C
C
      PRINT *,'          KINEMATIC ANALYSIS OF UNAFFECTED SIDE'
      READ(1,*) ILEG,INERTIA,FCUT
      READ(1,*) CA,FL,CS,HTI,CTH,P,CCH
      READ(1,*) DLA,DRA,DLR,F13,F23,F3
      WRITE(4,889) CA,FL,CS,HTI,CTH,P,CCH
889   FORMAT(1X,3(2X,F10.5))
890   FORMAT(1X,716)
      IILEG=1
      IF(ILEG.EQ.2) IILEG=-1
C
      IF(ILEG.EQ.2) THEN
      I1=1
      I2=2
      I3=3
      I4=4
      I5=5
      I6=6
      I7=7
      I8=8
      I9=9
      I13=13
```

```
      I14=14
      I15=15
      I16=16
      I17=17
      I18=18
      I19=19
      I20=20
      I21=21
      I22=22
      I23=23
C
      ELSE
      I1=4
      I2=5
      I3=6
      I4=1
      I5=2
      I6=3
      I7=8
      I8=7
      I9=9
      I13=17
      I14=16
      I15=18
      I16=14
      I17=13
      I18=15
      I19=20
      I20=19
      I21=22
      I22=21
      END IF
C
C
C *=================================================================*
C *                                                                 *
C *    THE INPUT ORDER OF THE STATIC MARKERS ARE: 1-3,7,4-6,8-23    *
C *                                                                 *
C *=================================================================*
C
1234  PRINT *,'READ STATIC DATA'
      DO 10 J=1,2
      DO 5 I=1,3
      K=I+(J-1)*3
      READ(1,*) SSX(K),SSY(K),SFZ(K)
5     CONTINUE
      READ(1,*) SSX(J+6),SSY(J+6),SFZ(J+6)
10    CONTINUE
      READ(1,*) SSX(9),SSY(9),SFZ(9)
C
      DO 12 J=10,23
      READ(1,*) SSX(J),SSY(J),SFZ(J)
12    CONTINUE
C
C
C ****************************************************************
C *                                                              *
C *    THE INPUT ORDER OF THE DYNAMIC MARKERS ARE: 1-3,7,4-6,8-18    *
C *                                                              *
```

```
C ***************************************************************************
C
      PRINT *,'READ DYNAMIC DATA'
      READ(1,*) NF1,ITF1,IHS1,NF2,ITF2,IHS2
      NF=ITF2-IHS1+1
      WRITE(6,890) NF1,ITF1,IHS1,NF2,ITF2,IHS2
      WRITE(4,890) NF,NF1,NF2
      WRITE(8,890) ILEG,INERTIA,NF1,ITF1,IHS1,NF2,ITF2,IHS2
      WRITE(2,890) NF1,ITF1,IHS1,NF2,ITF2,IHS2
      WRITE(10,890) NF1,ITF1,IHS1,NF2,ITF2,IHS2
C
      NF=ITF2-IHS1+1+8
C
      DO 20 J=1,2
      DO 15 I=1,3
      K=I+(J-1)*3
      DO 15 L=1,NF
      READ(1,*) SX3(K,L),SY3(K,L),FZ3(K,L)
15    CONTINUE
      DO 16 L=1,NF
      READ(1,*) SX3(J+6,L),SY3(J+6,L),FZ3(J+6,L)
16    CONTINUE
20    CONTINUE
C
      DO 23 I=9,18
      DO 23 L=1,NF
      READ(1,*) SX3(I,L),SY3(I,L),FZ3(I,L)
23    CONTINUE
      READ(1,*) NFN
C
C  OUTPUT THE STATIC MARKER DATA
C
      WRITE(8,885)
      DO 50 I=14,16
      WRITE(8,887) SSX(I),SSY(I),SFZ(I)
50    CONTINUE
      WRITE(8,887) SSX(116),SSY(116),SFZ(116)
      WRITE(8,887) SSX(117),SSY(117),SFZ(117)
      WRITE(8,887) SSX(118),SSY(118),SFZ(118)
C
C  OUTPUT ALIGNMENT DYNAMIC DATA
C
      DO 35 I=14,16
      WRITE(8,885)
      DO 35 J=1,NF
      WRITE(8,887) SX3(I,J),SY3(I,J),FZ3(I,J)
35    CONTINUE
C
      DO 36 K=1,3
      I=116
      IF(K.EQ.2) I=117
      IF(K.EQ.3) I=118
      WRITE(8,885)
      DO 36 L=1,NF
      WRITE(8,887) SX3(I,L),SY3(I,L),FZ3(I,L)
36    CONTINUE
885   FORMAT(1X,///)
887   FORMAT(1X,3(2X,F10.5))
C
```

```
C ***************************************************************************
C *                                                                         *
C *                        STATIC CALCULATION                               *
C *                                                                         *
C ***************************************************************************
C
      PRINT *,'STATIC CALCULATION'
C
C  DISTANCES BETWEEN MARKER 1 TO ANCKLE CENTRE AND TO KNEE CENTRE
C
      VLA(1)=SSX(I19)-SSX(I1)
      VLA(2)=SSY(I19)-SSY(I1)
      VLA(3)=SFZ(I20)-SFZ(I1)
      VLK(1)=SSX(I21)-SSX(I3)
      VLK(2)=SSY(I21)-SSY(I3)
      VLK(3)=SFZ(I22)-SFZ(I3)
C
C  SH7 AND SH8 ARE THE VECTOR FROM THE ASIS MARKER TO THE HJC
C
      SH7(1)=SSX(23)-SSX(I7)
      SH7(2)=SSY(23)-SSY(I7)
C     SH7(1)=-DLR*0.1829-0.001*P
C     SH7(2)=-DLR*0.3049
      SH7(3)=DLR*0.1219
      IF (ILEG.EQ.1) SH7(3)=-SH7(3)
C     SSY(23)=SSY(I7)+SH7(2)
C     SSX(23)=SSX(I19)+(SSY(23)-SSY(I19))*DKAX
C     SH7(1)=SSX(23)-SSX(I7)
      SFZ(23)=SFZ(I7)+SH7(3)
      SFZ(I21)=SFZ(I22)
      SFZ(I19)=SFZ(I20)
C
C  HIP JOINT CENTER
C
      SH8(1)=SH7(1)
      SH8(2)=SH7(2)
      SH8(3)=-SH7(3)
      HJC8(1)=SSX(I8)+SH8(1)
      HJC8(2)=SSY(I8)+SH8(2)
      HJC8(3)=SFZ(I8)+SH8(3)
C     HJC8(1)=SSX(23)
C     HJC8(2)=SSY(23)
C     HJC8(3)=SFZ(I8)+SH8(3)
C     SH8(1)=HJC8(1)-SSX(I8)
C     SH8(2)=HJC8(2)-SSY(I8)
      WRITE(8,885)
      WRITE(8,887) HJC8,SSX(I19),SSY(I19),SFZ(I19)
      1,SSX(I21),SSY(I21),SFZ(I21)
C
C  STATIC KNEE FLEXSION ANGLE
C
      SHFA=ATAN((SSX(I21)-SSX(23))/(SSY(23)-SSY(I21)))*57.3
      SKFA=ATAN((SSX(I19)-SSX(I21))/(SSY(I21)-SSY(I19)))*57.3
      SKFA=HFA-KFA
C
C  LENGTKAH OF THE THIGHT AND SHANK
C
      TL=SQRT((SSX(23)-SSX(I21))**2.0+(SSY(23)-SSY(I21))**2.0
      1+(SFZ(23)-SFZ(I21))**2.0)
```

```
      SL=SQRT((SSX(I21)-SSX(I19))**2.0+(SSY(I21)-SSY(I19))**2.0
      1+(SFZ(I21)-SFZ(I19))**2.0)
      WRITE(4,700) SL,TL,SSY(I19)
C
C  HEIGHT OF THE TORSO, PELVIS AND HIP JOINT
C
C       HTO=SSY(11)
C       HPE=(SSY(7)+SSY(8))/2.0
C       HHJ=SSY(I7)-SH7(2)
C
C   T IS THE TRANSPOSE MATRIX RELATING SHANK
C      AND THE GROUND SYSTEMS
C
      CALL TSTAT(T,I1,I2,I3)
        CALL ORTHO(0,I1,T)
        XP(1)=SSX(I14)-SSX(I19)
        XP(2)=0.0
        XP(3)=SFZ(I14)-SFZ(I19)
        CALL AMULT(T,XP,TXL)
C
C  VLA IS VECTOR FROM MARKER 1 TO AJC
C  VLK IS VECTOR FROM MARKER 1 TO KJC
C
      CALL AMULT(T,VLA,VLASTAT)
      CALL AMULT(T,VLK,VLKSTAT)
C
C  T IS THE TRANSPOSE MATRIX RELATING PELVIC AND THE GROUND SYSTEMS
C
        CALL TSTAT(T,7,8,9)
        CALL ORTHO(0,7,T)
        CALL AMULT(T,SH7,SH7ST)
        CALL AMULT(T,SH8,SH8ST)
        CALL TRANSP(T,TT)
C
C  STATIC EXTENSION ANGLE OF THE UPPER TORSO
C  STATIC EXTENSION ANGLE OF THE PELVIC
C
        AX=(SSX(7)+SSX(8))*0.5
        AY=(SSY(7)+SSY(8))*0.5
        XA=(SSX(12)+SSX(10))*0.5
        YA=(SSY(12)+SSY(10))*0.5
        UPPERS=ATAN((AX-XA)/(YA-AY))*57.3
        PELVIS=ATAN((AY-SSY(9))/(AX-SSX(9)))
C
C   FOOT ORIENTATION
C
        CALL TSTAT(T,I15,I13,I19)
        CALL ORTHO(0,I15,T)
        DO 60 J=1,3
        DO 60 K=1,3
        TP(J,K)=T(K,J)
        TAS(J,K)=0.0
60      CONTINUE
C
        A=SQRT((SSX(I14)-SSX(I19))**2+(SFZ(I14)-SFZ(I19))**2)
        TAS(1,1)=(SSX(I14)-SSX(I19))/A
        TAS(1,3)=(SFZ(I14)-SFZ(I19))/A
        TAS(2,2)=1.0
        TAS(3,1)=-TAS(1,3)
```

```
      TAS(3,3)=TAS(1,1)
      CALL MATMUL(TAS,TP,TAST)
      CALL ORTHO(0,0,TAST)
C
C  STATIC ANKLE ANGLE IN SAGGITAL PLANE
C
      DKX=SSX(I21)-SSX(I19)
      DKY=SSY(I21)-SSY(I19)
      DKZ=SFZ(I21)-SFZ(I19)
C     DAX=SSX(I14)-SSX(I19)
C     DAY=SSY(I14)-SSY(I19)
C     DAZ=SFZ(I14)-SFZ(I19)
      DAX=TAS(1,1)
      DAY=TAS(1,2)
      DAZ=TAS(1,3)
      ANSTAT=ACOS((DKX*DAX+DKY*DAY+DKZ*DAZ)
      1/SQRT(DKX*DKX+DKY*DKY+DKZ*DKZ)
      1/SQRT(DAX*DAX+DAY*DAY+DAZ*DAZ))
C     ANSTAT=90.0-ATAN(DKX/DKY)*57.3
C     IF(DKX.LT.0.0) ANSTAT=90.0+ATAN(DKX/DKY)*57.3
C
C
C ***************************************************************************
C *                                                                         *
C *                KINEMIC ANALYSIS ON DYNAMIC DATA                         *
C *                                                                         *
C ***************************************************************************
C
C
      WRITE(8,885)
666   FORMAT(1X,I3)
      PRINT *,'DYNAMIC ANALYSIS '
C
C     WRITE(6,666) NFN
C
C
    DO 101 I=1,NF
C
C
      WRITE(4,882)
      WRITE(2,882)
882   FORMAT(1X,//)
C
C
      CALL TMAT(I,T,I1,I2,I3)
        CALL ORTHO(I,I1,T)
C
      DO 110 J=1,3
 110  TD(J,J)=T(J,J)
      TD(1,2)=T(2,1)
      TD(1,3)=T(3,1)
      TD(2,1)=T(1,2)
      TD(2,3)=T(3,2)
      TD(3,1)=T(1,3)
      TD(3,2)=T(2,3)
C
      CALL AMULT(TD,TXL,SXL)
C
C  ANKLE
```

```
      CALL AMULT(TD,VLASTAT,VAD)
C
C KNEE
      CALL AMULT(TD,VLKSTAT,EKD)
C
      AJC(1)=VAD(1)+SX3(I1,I)
      AJC(2)=VAD(2)+SY3(I1,I)
      AJC(3)=VAD(3)+FZ3(I1,I)
      KJC(1)=EKD(1)+SX3(I3,I)
      KJC(2)=EKD(2)+SY3(I3,I)
      KJC(3)=EKD(3)+FZ3(I3,I)
        AJCX(I)=AJC(1)
        AJCY(I)=AJC(2)
        AJCZ(I)=AJC(3)
        KJCX(I)=KJC(1)
        KJCY(I)=KJC(2)
        KJCZ(I)=KJC(3)
C
     CALL FMAT(I,FT)
        CALL ORTHO(I,200,FT)
        DO 302 J=1,3
        DO 302 K=1,3
        DSHA(I,J,K)=FT(J,K)
302     CONTINUE
C
C
C
C
        CALL TMAT(I,T,7,8,9)
        CALL ORTHO(I,7,T)
        DO 301 J=1,3
301     TD(J,J)=T(J,J)
        TD(1,2)=T(2,1)
        TD(1,3)=T(3,1)
        TD(2,1)=T(1,2)
        TD(2,3)=T(3,2)
        TD(3,1)=T(1,3)
        TD(3,2)=T(2,3)
        CALL AMULT(TD,SH7ST,VH7C)
        CALL AMULT(TD,SH8ST,VH8C)
C       CALL MATMUL(PELS,T,PELD)
C
        HJC7(1)=SX3(I7,I)+VH7C(1)
        HJC7(2)=SY3(I7,I)+VH7C(2)
        HJC7(3)=FZ3(I7,I)+VH7C(3)
        HJC8(1)=SX3(I8,I)+VH8C(1)
        HJC8(2)=SY3(I8,I)+VH8C(2)
        HJC8(3)=FZ3(I8,I)+VH8C(3)
        HJCX(I)=HJC7(1)
        HJCY(I)=HJC7(2)
        HJCZ(I)=HJC7(3)
C
        WRITE(8,887) (HJC8(J),J=1,3)
C
C  TRUNK ANGULAR MOVEMENT
C
        VAD(1)=(SX3(10,I)+SX3(12,I))/2.0
        VAD(2)=(SY3(10,I)+SY3(12,I))/2.0
        VAD(3)=(FZ3(10,I)+FZ3(12,I))/2.0
```

```
      XA=(HJC7(1)+HJC8(1))*0.5
      YA=(HJC7(2)+HJC8(2))*0.5
      ZA=(HJC7(3)+HJC8(3))*0.5
      CTOX(I)=VAD(1)-XA
      CTOY(I)=VAD(2)-YA
      CTOZ(I)=VAD(3)-ZA
      CTOX(I)=VAD(1)-CTOX(I)*0.45
      CTOY(I)=VAD(2)-CTOY(I)*0.45
      CTOZ(I)=VAD(3)-CTOZ(I)*0.45
      WRITE(14,700) CTOX(I),CTOY(I),CTOZ(I)
C
      ATZ(I)=ATAN((XA-VAD(1))/(VAD(2)-YA))
      ATY(I)=ATAN((SX3(12,I)-SX3(10,I))/(FZ3(12,I)-FZ3(10,I)))
      ATX(I)=ATAN((VAD(3)-ZA)/(VAD(2)-YA))
      C1TOR=0.45
C
C  PELVIS ANGULAR MOTION
C
      APZ(I)=ATAN((YA-SY3(9,I))/(XA-SX3(9,I)))-PELVIS
      APY(I)=ATAN((SX3(8,I)-SX3(7,I))/(FZ3(8,I)-FZ3(7,I)))
      APX(I)=ATAN((SY3(7,I)-SY3(8,I))/(FZ3(8,I)-FZ3(7,I)))
C
C  THIGHT FRAME OF REFERENCE
C
      DO 227 II=1,3
      HJC(II)=HJC7(II)
227   CONTINUE
      CALL FMATT(I,FTT)
      CALL ORTHO(I,300,T)
      DO 305 J=1,3
      DO 305 K=1,3
305   DTHI(I,J,K)=FTT(J,K)
C
C  FEMUR ANGULAR MOTION
C
      A=0.0
      B=0.0
      KA=0.0
      DO 333 J=1,3
      AA=KJC(J)-AJC(J)
      BB=HJC(J)-KJC(J)
      KA=KA+AA*BB
      A=A+AA*AA
      B=B+BB*BB
333   CONTINUE
      A=SQRT(A)
      B=SQRT(B)
C     B=FTT(2,1)*FT(2,1)+FTT(2,2)*FT(2,2)+FTT(2,3)*FT(2,3)
C     KA=ACOS(B)*57.3
      KA=KA/A/B
      IF (ABS(KA).GT.1.0) KA=1.0
      KA=ACOS(KA)*57.3-SKFA
      HA=ATAN((KJC(1)-HJC(1))/(HJC(2)-KJC(2)))*57.3-SHFA
C     KA=ATAN((AJC(1)-KJC(1))/(KJC(2)-AJC(2)))*57.3
C     KA=HA-KA
C
      HAA=ATAN((KJC(3)-HJC(3))/(HJC(2)-KJC(2)))
      HAA=HAA*180.0/3.1415926
      IF(ILEG.EQ.1) HAA=-HAA
```

```
      KAA=ATAN((AJC(3)-KJC(3))/(KJC(2)-AJC(2)))
      KAA=KAA*180.0/3.1415926
      IF(ILEG.EQ.1) KAA=-KAA
C
C   FOOT ORIENTATION
C
      SX3(20,I)=AJC(1)
      SY3(20,I)=AJC(2)
      FZ3(20,I)=AJC(3)
      CALL TMAT(I,T,I15,I13,20)
      CALL MATMUL(TAST,T,TAD)
      DO 150 J=1,3
      DO 150 K=1,3
150   DTAD(I,J,K)=TAD(J,K)
C
      DKX=KJC(1)-AJC(1)
      DKY=KJC(2)-AJC(2)
      DKZ=KJC(3)-AJC(3)
      DAX=TAD(1,1)
      DAY=TAD(1,2)
      DAZ=TAD(1,3)
C     DAX=AJC(1)-SX3(I15,I)
C     DAY=AJC(1)-SY3(I15,I)
C     DAZ=AJC(1)-FZ3(I15,I)
      ADA=ACOS((DKX*DAX+DKY*DAY+DKZ*DAZ)
      1/SQRT(DKX*DKX+DKY*DKY+DKZ*DKZ)
      1/SQRT(DAX*DAX+DAY*DAY+DAZ*DAZ))
      ADA=90.0-ADA*57.3
      DAA(I)=ADA
C     ADA=(ANSTAT-ADA)*57.3          !PLANTAR NEGTIVE
      ASA=(AJC(3)-HJC(3))*100.0
      IF(ILEG.EQ.1) ASA=-ASA
C
      IF(I.LT.5.OR.I.GT.NF-4) GOTO 226
      WRITE(6,775) (AJC(J),J=1,3),(KJC(J),J=1,3)
      1,(HJC7(J),J=1,3)
775   FORMAT(1X,9(2X,F8.5))
      WRITE(6,700) SX3(I14,I),SY3(I14,I),FZ3(I14,I)
      WRITE(6,700) SX3(10,I),SY3(10,I),FZ3(10,I)
      WRITE(6,700) SX3(12,I),SY3(12,I),FZ3(12,I)
C
      WRITE(4,700)(HJC(J),J=1,3)
      WRITE(4,700)(KJC(J),J=1,3)
      WRITE(4,700)(AJC(J),J=1,3)
      WRITE(4,700) ((FT(J,K),J=1,3),K=1,3)
      WRITE(4,700) ((FTT(J,K),J=1,3),K=1,3)
      WRITE(4,700) ((TAD(J,K),J=1,3),K=1,3)
      WRITE(2,701) HA,KA,HAA,KAA
      WRITE(2,701) ADA,ASA
226   CONTINUE
701   FORMAT(4(3X,F12.6))
C
101   CONTINUE
C
C   SECOND HELL STRIKE
C
C     AAA=500.0
C     DO 676 I=1,NF
C676  DAA(I)=ABS(DAA(I)-DAA(5))
```

```
C       DO 677 I=NF-4,NF-20,-1
C       IF(AAA.LT.DAA(I)) GOTO 677
C       IAA=I
C       AAA=DAA(I)
C677    CONTINUE
C       NFN=IAA
        WRITE(2,262) 99999
262     FORMAT(3X,I8)
        NFN=NFN+4
        TYPE *, 'SECOND L.H.S.  ',NFN
        WRITE(6,666) NFN
        WRITE(2,666) NFN
C
C  VELOCITY AND ACCELERATIONS
C
        CALL DIFFER(HJCX,NF)
        CALL DIFFER(KJCX,NF)
        CALL DIFFER(AJCX,NF)
        CALL DIFFER(ATX,NF)
        CALL DIFFER(CTOX,NF)
        CALL DIFFER(HJCY,NF)
        CALL DIFFER(KJCY,NF)
        CALL DIFFER(AJCY,NF)
        CALL DIFFER(ATY,NF)
        CALL DIFFER(CTOY,NF)
        CALL DIFFER(HJCZ,NF)
        CALL DIFFER(KJCZ,NF)
        CALL DIFFER(AJCZ,NF)
        CALL DIFFER(ATZ,NF)
        CALL DIFFER(CTOZ,NF)
C
        DO 476 J=1,3
        DO 476 K=1,3
        DO 475 I=1,NF
475     RAW1(I)=DTHI(I,J,K)
C       CALL SMOOTH(RAW1,NF,NF,8,1)
        CALL DIFFER(RAW1,NF)
476     CONTINUE
C
        DO 478 J=1,3
        DO 478 K=1,3
        DO 477 I=1,NF
477     RAW1(I)=DSHA(I,J,K)
C       CALL SMOOTH(RAW1,NF,NF,8,1)
        CALL DIFFER(RAW1,NF)
478     CONTINUE
C
        DO 578 J=1,3
        DO 578 K=1,3
        DO 577 I=1,NF
577     RAW1(I)=DTAD(I,J,K)
C       CALL SMOOTH(RAW1,NF,NF,8,1)
        CALL DIFFER(RAW1,NF)
578     CONTINUE
C
C
C  OUTPUT OF THE PELVIC AND TORSO
C
        DO 113 I=5,NF-4
```

```
      APX(I)=APX(I)*57.3
      APY(I)=APY(I)*57.3
      APZ(I)=APZ(I)*57.3
      ATX(I)=ATX(I)*57.3
      ATY(I)=ATY(I)*57.3
      ATZ(I)=ATZ(I)*57.3
      WRITE(2,700) APX(I),APY(I),APZ(I)
      WRITE(2,700) ATX(I),ATY(I),ATZ(I)
113   CONTINUE
C
C   TOE IN/OUT ANGLE
C
      J1=1
      J2=NF1
      IF(ILEG.EQ.1) J1=NF-NF2-10
      IF(ILEG.EQ.1) J2=NF-10
      CALL MINIMUM(SX3,I15,J1,J2,ISOLE)
      FANG=ATAN((FZ3(I14,ISOLE)-AJCZ(ISOLE))
      1/(SX3(I14,ISOLE)-AJCX(ISOLE)))*57.3*IILEG
      WRITE(6,700) FANG,SX3(I14,ISOLE),FZ3(I14,ISOLE)
C
C
700   FORMAT(3(2X,F16.10))
995   FORMAT(I6,3(F16.10,2X))
999   FORMAT(6E20.11)
      STOP
      END
C
C
C
      SUBROUTINE ORTHO(I,J,T)
      DIMENSION T(3,3)
      A=T(1,1)*T(2,2)*T(3,3)+T(1,2)*T(2,3)*T(3,1)
      1+T(1,3)*T(3,2)*T(2,1)-T(1,3)*T(2,2)*T(3,1)
      2-T(2,3)*T(3,2)*T(1,1)-T(1,2)*T(2,1)*T(3,3)
      A=ABS(A-1.0)
      IF(A.LT.0.0001) RETURN
      IF(J.EQ.0) TYPE *, I,J
      IF(I.NE.0) TYPE *, I,J
      RETURN
      END
```

Program "DYNAMPU2.MAJ"

```
C ***************************************************************
C *                                                             *
C *   THIS PROGRAM READS IN TV DATA FROM .TV3 AND ANALYSE       *
C *                  KINEMATICALLY PROSTHETIC SIDE              *
C *                                                             *
C ***************************************************************
      INTEGER CAM1
      REAL MASS,LL,LXSF,LYSF,LZSF,KJC,KJCX,KJCY,KJCZ
      COMMON /BLOCK3/AJC(3),KJC(3),SXL(3),HJC(3)
      COMMON /BLOCK1/SSX(30),SSY(30),SFZ(30)
      COMMON /BLOCK2/SX3(20,150),SY3(20,150),FZ3(20,150)
      COMMON NF
      DIMENSION TMS1(3,3),TMS2(3,3),TSS(3,3),TKS(3,3),TAS(3,3)
     1,TSMS2(3,3),TKMS1(3,3),TAMS1(3,3),TMSS1(3,3),TMSS2(3,3)
     2,TMD1(3,3),TMD2(3,3),TMD1T(3,3),TMD2T(3,3),TKD(3,3),TAD(3,3)
     3,TMS2T(3,3),TMS1T(3,3),THS(3,3),THMS2(3,3)
     2,THD(3,3),VLASTAT(3),VAD(3),HJC7(3),VLH(3),VLHSTAT(3)
     3,VLKSTAT(3),EKD(3),VLA(3),VLK(3),VLAL(3),VLKL(3)
     4,TXL(3,1),FT(3,3),VH7C(3),VH7(3),TP(3,3),HJC8(3)
     5,XP(3),YP(3),ZP(3),TIB(3,3),PTOG(3,3),SH7(3),SH7ST(3),RKA(3)
     6,R1KK(3),RKAK(3),TSD(3,3),R1KD(3),RK4D(3),RK4(3),RK4K(3)
     1,RK1(3),TKDT(3,3),RKAD(3),XHJ(3),XHJJ(3)
     2,R1K(3),RAD(3),THST(3,3),TSTS(3,3),TMSS1T(3,3)
     4,KJCX(150),KJCY(150),KJCZ(150),AJCX(150),AJCY(150),AJCZ(150)
     5,DTHD(150,3,3),DTKD(150,3,3),DTAD(150,3,3),DTSD(150,3,3)
     6,RAW1(150),RAW2(150),RAW3(150),RAW4(150)
     7,HJCX(150),HJCY(150),HJCZ(150)
C
C
C  READ THE ALIGNMENT DATA
C
      PRINT *,'      KINEMATIC ANALYSIS ON PROSTHETIC SIDE'
      READ(5,*) IHJC,ISOK
      READ(5,*) TOUT,XKRL,YKR,ZKR,YKL,ZKL
     1,XRT,YRT,ZRT,XLT,YLT,ZLT
     2,XRL,YRL,ZRL,XLL,YLL,ZLL
     3,XI,YI,ZI,XT,YT,ZT,XL,YL,ZL,XK,YK,ZK
      DO 10 I=1,5
      READ(5,*) SSX(I),SSY(I),SFZ(I)
      SSX(I)=SSX(I)/1000.0
      SSY(I)=SSY(I)/1000.0
      SFZ(I)=SFZ(I)/1000.0
10    CONTINUE
C
      XI=XI/100.0
      YI=YI/100.0
      ZI=ZI/100.0
      XT=XT/100.0
      YT=YT/100.0
      ZT=ZT/100.0
```

```
      XL=XL/100.0
      YL=YL/100.0
      ZL=ZL/100.0
      XK=XK/100.0
      YK=YK/100.0
      ZK=ZK/100.0
      SL8=SQRT(XK*XK+YK*YK+ZK*ZK)
C==========ANKLE DORSI FLEXION=======
      ANSTAT=90.0-ACOS(XK/SQRT(XK**2+YK**2))*57.3
C
      READ(7,*)
      READ(7,*) AA
      READ(7,*) SM8,C2S8,PS8,SOM,C2T8,PT8
      READ(1,*) ILEG,INERTIA,NF1,ITF1,IHS1,NF2,ITF2,IHS2
      IILEG=1
      IF(ILEG.EQ.1) IILEG=-1
C
C ***************************************************************
C *                                                             *
C *     THE INPUT ORDER OF THE DYNAMIC MARKERS ARE: 1-6         *
C *                                                             *
C ***************************************************************
C
      PRINT *,'READ MARKER POSITION DATA'
      DO 5 I=6,11
5     READ(1,*) SSX(I),SSY(I),SFZ(I)
C
      CALL TSTAT(T,1,2,3)
      XP(1)=SSX(5)-SSX(3)
      XP(2)=SSY(5)-SSY(3)
      XP(3)=SFZ(5)-SFZ(3)
      CALL AMULT(T,XP,YP)
      CALL TSTAT(T,6,7,8)
      CALL TRANSP(T,TSTS)
      CALL AMULT(TSTS,YP,ZP)
      SSX(10)=ZP(1)+SSX(8)
      SSY(10)=ZP(2)+SSY(8)
      SFZ(10)=ZP(3)+SFZ(8)
C
      NF=ITF2-IHS1+1+8
      DO 20 J=1,6
      DO 15 L=1,NF
      READ(1,*) SX3(J,L),SY3(J,L),FZ3(J,L)
15    CONTINUE
20    CONTINUE
C
      READ(1,*) HJC7,AJC,KJC
C
C
C ***************************************************************
C *                                                             *
C *              STATIC CALCULATION                             *
C *                                                             *
C ***************************************************************
C
C
C
      PRINT *,'STATIC CALCULATION'
C
```

```
C
C          ALIGNMENT SYSTEM
C
C
C
C   TMS IS THE TRANSPOSE MATRIX RELATING MARKER
C      AND THE GROUND SYSTEMS
C
          CALL TSTAT(TMS1,1,2,3)
          CALL TSTAT(TMS2,3,4,5)
          CALL TRANSP(TMS1,TMS1T)
          CALL TRANSP(TMS2,TMS2T)
C
C  VLA IS THE VECTOR FROM MARKER 3 TO AJC
C  VLK IS THE VECTOR FROM MARKER 3 TO KJC
C
          VLA(1)=-SSX(1)
          VLA(2)=-SSY(1)
          VLA(3)=-SFZ(1)
          VLK(1)=XK-SSX(3)
          VLK(2)=YK-SSY(3)
          VLK(3)=ZK-SFZ(3)
          CALL AMULT(TMS1,VLA,VLASTAT)
          CALL AMULT(TMS1,VLK,VLKSTAT)
          PRINT *,'VLASTAT=',VLASTAT
          PRINT *,'VLKSTAT=',VLKSTAT
C
C  TSS IS THE TRANSPOSE MATRIX RELATING SOCKET AND THE GROUND SYSTEMS
C
          DLT=SQRT((XT-XL)**2+(YT-YL)**2+(ZT-ZL)**2)
          TSS(2,1)=(XT-XL)/DLT
          TSS(2,2)=(YT-YL)/DLT
          TSS(2,3)=(ZT-ZL)/DLT
          DLT=SQRT((XRT-XLT)**2+(YRT-YLT)**2+(ZRT-ZLT)**2)
          TSS(3,1)=(XRT-XLT)/DLT
          TSS(3,2)=(YRT-YLT)/DLT
          TSS(3,3)=(ZRT-ZLT)/DLT
          TSS(1,1)=TSS(2,2)*TSS(3,3)-TSS(2,3)*TSS(3,2)
          TSS(1,2)=TSS(2,3)*TSS(3,1)-TSS(2,1)*TSS(3,3)
          TSS(1,3)=TSS(2,1)*TSS(3,2)-TSS(2,2)*TSS(3,1)
          DLT=SQRT(TSS(1,1)**2+TSS(1,2)**2+TSS(1,3)**2)
          DO 30 I=1,3
          TSS(1,I)=TSS(1,I)/DLT
30        CONTINUE
          TSS(3,1)=TSS(1,2)*TSS(2,3)-TSS(1,3)*TSS(2,2)
          TSS(3,2)=TSS(1,3)*TSS(2,1)-TSS(1,1)*TSS(2,3)
          TSS(3,3)=TSS(1,1)*TSS(2,2)-TSS(1,2)*TSS(2,1)
          DLT=SQRT(TSS(3,1)**2+TSS(3,2)**2+TSS(3,3)**2)
          DO 71 I=1,3
          TSS(3,I)=TSS(3,I)/DLT
71        CONTINUE
C
C  TAS IS THE TRANSPOSE MATRIX RELATING ANKLE AND THE GROUND SYSTEMS
C
          TAS(1,1)=COS(TOUT)
          TAS(1,2)=0.0
          TAS(1,3)=-SIN(TOUT)
          TAS(2,1)=0.0
          TAS(2,2)=1.0
          TAS(2,3)=0.0
```

```
      TAS(3,1)=-TAS(1,3)
      TAS(3,2)=0.0
      TAS(3,3)=TAS(1,1)
C
C TKS IS THE TRANSPOSE MATRIX RELATING SHANK AND THE GROUND SYSTEMS
C
C       Suppose the plane on which KJC is and normal to TKS(3,*) has
C   the equation:
C              TKS(3,1)*(X-XK)+TKS(3,2)*(Y-YK)+TKS(3,3)*(Z-ZK)
C   and ankle joint axis can be represented as:
C              X=AJC(1)+TAS(3,1)*DLT
C              Y=AJC(2)+TAS(3,2)*DLT
C              Z=AJC(3)+TAS(3,3)*DLT
C   the point at which the ankle joint axis meets the plane can be
C   found by determine the DLT in above equations as
C       DLT=(XK*TKS(3,1)+YK*TKS(3,2)+ZK*TKS(3,3)) /
C           (TAS(3,1)*TKS(3,1)+TAS(3,2)*TKS(3,2)+TAS(3,3)*TKS(3,3))
C
      DLT=SQRT((YKR-YKL)*(YKR-YKL)+(ZKR-ZKL)*(ZKR-ZKL))
      TKS(3,1)=0.0
      TKS(3,2)=(YKR-YKL)/DLT
      TKS(3,3)=(ZKR-ZKL)/DLT
      DLT=(XK*TKS(3,1)+YK*TKS(3,2)+ZK*TKS(3,3))
      1/(TAS(3,1)*TKS(3,1)+TAS(3,2)*TKS(3,2)+TAS(3,3)*TKS(3,3))
      TKS(2,1)=XK-DLT*TAS(3,1)
      TKS(2,2)=YK-DLT*TAS(3,2)
      TKS(2,3)=ZK-DLT*TAS(3,3)
      DLT=SQRT(TKS(2,1)**2+TKS(2,2)**2+TKS(2,3)**2)
      TKS(2,1)=TKS(2,1)/DLT
      TKS(2,2)=TKS(2,2)/DLT
      TKS(2,3)=TKS(2,3)/DLT
      TKS(1,1)=TKS(2,2)*TKS(3,3)-TKS(2,3)*TKS(3,2)
      TKS(1,2)=TKS(2,3)*TKS(3,1)-TKS(2,1)*TKS(3,3)
      TKS(1,3)=TKS(2,1)*TKS(3,2)-TKS(2,2)*TKS(3,1)
      DLT=SQRT(TKS(1,1)**2+TKS(1,2)**2+TKS(1,3)**2)
      TKS(1,1)=TKS(1,1)/DLT
      TKS(1,2)=TKS(1,2)/DLT
      TKS(1,3)=TKS(1,3)/DLT
C
C
C  CALCULATE HJC IN ALIGNMENT SYSTEM
C
C
      CALL TSTAT(TMSS1,6,7,8)
      CALL TSTAT(TMSS2,8,9,10)
      CALL TRANSP(TMSS1,TMSS1T)
      CALL AMULT(TMSS1T,VLKSTAT,VLK)
      CALL AMULT(TMSS1T,VLASTAT,VLA)
      AJC(1)=SSX(6)+VLA(1)
      AJC(2)=SSY(6)+VLA(2)
      AJC(3)=SFZ(6)+VLA(3)
      KJC(1)=SSX(8)+VLK(1)
      KJC(2)=SSY(8)+VLK(2)
      KJC(3)=SFZ(8)+VLK(3)
C
C  ZP IS THE VECTOR FROM MARKER 5 TO HJC
C
      ZP(1)=HJC7(1)-SSX(10)
      ZP(2)=HJC7(2)-SSY(10)
```

```
      ZP(3)=HJC7(3)-SFZ(10)
C
      CALL AMULT(TMS2,ZP,VLHSTAT)
      CALL AMULT(TMS2T,VLHSTAT,XP)
      HJC8(1)=SSX(5)+XP(1)
      HJC8(2)=SSY(5)+XP(2)
      HJC8(3)=SFZ(5)+XP(3)
C
      IF(ISOK.EQ.0) GOTO 534
C
      AA=(HJC8(2)-YT)/TSS(2,2)
      HJC8(1)=AA*TSS(2,1)+XT
      HJC8(3)=AA*TSS(2,3)+ZT
      ZP(1)=HJC8(1)-SSX(5)
      ZP(2)=HJC8(2)-SSY(5)
      ZP(3)=HJC8(3)-SFZ(5)
      CALL AMULT(TMS2,ZP,VLHSTAT)
C
534   TL8=SQRT((HJC8(1)-XK)**2.0+(HJC8(2)-YK)**2.0
     1+(HJC8(3)-ZK)**2.0)
      PRINT *,'VLHSTAT=',VLHSTAT
C
C  STATIC HIP FLEXION ANGLE SHFA
C  STATIC KNEE FLEXION ANGLE SKFA
C
C     SHFA=ATAN((XK-HJC8(1))/(HJC8(2)-YK))*57.3
C     SKFA=SHFA-ATAN((-XK)/YK)*57.3
      DO 87 J=1,3
87    HJC7(J)=HJC8(J)*100.0
      WRITE(2,299) (HJC7(J),J=1,3)
299   FORMAT(2X,3F12.3)
C
C  THS IS THE TRANSFORMATION MATRIX RELATING THE THIGH AND GROUND SYSTEM
C
      DLT=SQRT((HJC8(1)-XK)**2+(HJC8(2)-YK)**2+(HJC8(3)-ZK)**2)
      THS(2,1)=(HJC8(1)-XK)/DLT
      THS(2,2)=(HJC8(2)-YK)/DLT
      THS(2,3)=(HJC8(3)-ZK)/DLT
      THS(1,1)=THS(2,2)*TKS(3,3)-THS(2,3)*TKS(3,2)
      THS(1,2)=THS(2,3)*TKS(3,1)-THS(2,1)*TKS(3,3)
      THS(1,3)=THS(2,1)*TKS(3,2)-THS(2,2)*TKS(3,1)
      DLT=SQRT(THS(1,1)**2+THS(1,2)**2+THS(1,3)**2)
      DO 31 I=1,3
31    THS(1,I)=THS(1,I)/DLT
      THS(3,1)=THS(1,2)*THS(2,3)-THS(1,3)*THS(2,2)
      THS(3,2)=THS(1,3)*THS(2,1)-THS(1,1)*THS(2,3)
      THS(3,3)=THS(1,1)*THS(2,2)-THS(1,2)*THS(2,1)
      DLT=SQRT(THS(3,1)**2+THS(3,2)**2+THS(3,3)**2)
      DO 33 I=1,3
33    THS(3,I)=THS(3,I)/DLT
C
C  TKMS1 IS THE TRANSFORMATION MATRIX OF SHANK AND MARKER SYSTEMS
C  TAMS1 IS THE TRANSFORMATION MATRIX OF ANKLE AND MARKER SYSTEMS
C  TSMS2 IS THE TRANSFORMATION MATRIX OF SOCKET AND MARKER SYSTEMS
C  THMS2 IS THE TRANSFORMATION MATRIX OF THIGH AND MARKER SYSTEM
C
      CALL MATMUL(TAS,TMS1T,TAMS1)
      CALL MATMUL(TKS,TMS1T,TKMS1)
      CALL MATMUL(THS,TMS2T,THMS2)
```

```
      CALL MATMUL(TSS,TMS2T,TSMS2)
C
C  MARKERS ON THE SOCKET WERE MISSING DURING DYNAMIC TEST.
C  SOCKET FRAME IS RELATED TO THE THIGH FRAME AS FOLLOWS
C
      CALL TRANSP(THS,THST)
      CALL MATMUL(TSS,THST,TSTS)
C
C
C     INERTIA PROTERTIES OF THE PROSTHETIC LIMB
C
C
C====== STUMP IS MODELED AS A FRUSTA OF CIRCULAR CONE =========
C
      DT=SQRT((XRT-XLT)**2+(ZRT-ZLT)**2
     1+(YRT-YLT)**2)/2000.0            !RADIUM OF UPPER SOCKET
      DL=SQRT((XRL-XLL)**2+(ZRL-ZLL)**2
     1+(YRL-YLL)**2)/2000.0            !RADIUM OF LOWER SOCKET
      H1=SQRT((XT-XL)**2+(YT-YL)**2    !DISTEANCE BETWEEN UPPER
     1+(ZT-ZL)**2)                     !AND LOWER SOCKET PLANES
      RT=DT+((DT-DL)/H1)*0.025  !RADIUM OF BIGGER BASE
      RL=DL-((DT-DL)/H1)*0.025  !RADIUM OF SMALLER BASE
      HH=RT*H1/(DT-DL)               !HEIGHT OF THE ORIGNAL CONE
      H=DL*H1/(DT-DL)                !HEIGHT OF THE CONE REMOVED
      H2=HH-H                        !HEIGHT OF THE FRUSTA
      V2=H2/3.0*3.1415926*(RT*RT+RL*RL+RT*RL)   !VOLUMN OF THE FRUSTA
C
      CG=H2*(RT*RT+2.0*RT*RL+3.0*RL*RL)/        !C.G OF THE FRUSTA TO
     1(RT*RT+RL*RL*RT*RL)/4.0                   !BIGGER BASE
C
      V=3.1416*RT*RT*HH/3.0          !VOLUMN OF THE ORIGINAL CONE
      V1=3.1416*RL*RL*H/3.0          !VOLUMN OF THE REMOVED CONE
      STUM2=V2*1.069*1000.0
      CI=(HH*HH+4.0*RT*RT)*3.0/80.0*V   !MOMENT OF ORIGINAL CONE
      CII=(H*H+4.0*RL*RL)*3.0/80.0*V1   !MOMENT OF REMOVED CONE
C
      C2I=(CI+(HH/4.0)**2*V)-              !MOMENT OF FRUSTA TO ITS
     1(CII+(H2+H/4.0)**2*V1)-CG*CG*V2     !  C.G
C
C ===== COMBINATION OF THE SOCKET AND THE STUMP ======
C
      SOKI=9.806*SOM*C2T8*PT8*PT8   !MOMENT OF SOCKET RELATIVE
     1/4.0/3.1416/3.1416/100.0      ! TO THE KNEE
C
      SOSI=SOKI-C2T8*C2T8*SOM    !MOMENT OF SOCKET TO ITS C.G
      LL=SQRT((XK-XT)**2+(YK-YT)**2+(ZK-ZT)**2)
C
      THHI=(C2I+(TL8-LL+CG)**2*V2)*1.069   !MOMENT OF THIGH
     1+SOSI+(TL8-C2T8)**2*SOM    ! RELATIVE TO HJC
C
      CGTH=(SOM*(TL8-C2T8)+STUM2   ! C.G OF THIGH RELATIVE TO
     1*(TL8-LL+CG))/(STUM2+SOM)   !   HJC
C
      SHKI=9.806*SM8*C2S8*PS8*PS8   !MOMENT OF SHANK RELATIVE
     1/4.0/3.1416/3.1416/100.0      ! TO THE KNEE
C
      THM=SOM+STUM2                  !MASS OF THIGH
C
C
```

```
      WRITE(4,441) SL8,SM8,C2S8,SHKI
      WRITE(4,441) TL8,THM,CGTH,THHI
441   FORMAT(2X,2F16.9)
C
C  STATIC ANKLE ANGLE
C
      A1=SSX(11)-AJC(1)
      A2=SSY(11)-AJC(2)
      A3=SFZ(11)-AJC(3)
      B1=KJC(1)-AJC(1)
      B2=KJC(2)-AJC(2)
      B3=KJC(3)-AJC(3)
      AA=SQRT(A1*A1+A2*A2+A3*A3)
      BB=SQRT(B1*B1+B2*B2+B3*B3)
      SAA=ACOS((A1*B1+A2*B2+A3*B3)/AA/BB)*57.3
C     SAA=SAA-ATAN(XK/YK)*57.3
C
C
C ************************************************************
C *                                                          *
C *            KINEMIC ANALYSIS ON DYNAMIC DATA              *
C *                                                          *
C ************************************************************
C
C
      WRITE(6,666) NF-8
666   FORMAT(1X,I3)
      PRINT *,'DYNAMIC CALCULATION'
      DO 101 I=1,NF
C
C ======= CALCULATE THE JOINT CENTRES ==========
C
      CALL TMAT(I,TMD1,1,2,3)
      CALL TMAT(I,TMD2,3,4,5)
      CALL TRANSP(TMD1,TMD1T)
      CALL TRANSP(TMD2,TMD2T)
C
      CALL AMULT(TMD1T,VLASTAT,VAD)
      CALL AMULT(TMD1T,VLKSTAT,EKD)
C
      DO 115 J=1,3
      AJC(J)=0.0
115   KJC(J)=0.0
      AJC(1)=VAD(1)+SX3(1,I)
      AJC(2)=VAD(2)+SY3(1,I)
      AJC(3)=VAD(3)+FZ3(1,I)
      AJCX(I)=AJC(1)
      AJCY(I)=AJC(2)
      AJCZ(I)=AJC(3)
      KJC(1)=EKD(1)+SX3(3,I)
      KJC(2)=EKD(2)+SY3(3,I)
      KJC(3)=EKD(3)+FZ3(3,I)
      KJCX(I)=KJC(1)
      KJCY(I)=KJC(2)
      KJCZ(I)=KJC(3)
      READ(1,*) (HJC7(J),J=1,3)
      IF (IHJC.EQ.1) GOTO 323
      CALL AMULT(TMD2T,VLHSTAT,VLH)
      HJC7(1)=SX3(5,I)+VLH(1)
```

```
      HJC7(2)=SY3(5,I)+VLH(2)
      HJC7(3)=FZ3(5,I)+VLH(3)
323   CONTINUE
      HJCX(I)=HJC7(1)
      HJCY(I)=HJC7(2)
      HJCZ(I)=HJC7(3)
C
C ======= THIGH FLEXION AND ABDUCTION =======
C
      AH=ATAN((KJC(1)-HJC7(1))/(HJC7(2)-KJC(2)))
      AH=AH*180.0/3.1415926
      HAA=ATAN((KJC(3)-HJC7(3))/(HJC7(2)-KJC(2)))
      HAA=HAA*180.0/3.1415926
      IF(ILEG.EQ.2) HAA=-HAA
C
      WRITE(8,797)
      WRITE(4,797)
797   FORMAT(1X,//)
C
C ==========TRANSFORMATION OF THE DIFFERENT SYSTEM ===============
C
C  TKD IS THE TRANSFORMATION RELATING KNEE AND GROUND SYSTEMS
C  THD IS THE TRANSFORMATION RELATING THIGH AND GROUND SYSTEM
C
      CALL MATMUL(TKMS1,TMD1,TKD)
      CALL MATMUL(TAMS1,TMD1,TAD)
      IF (IHJC.EQ.1) THEN
      DLT=SQRT((HJC7(1)-KJC(1))**2+(HJC7(2)-KJC(2))**2
      1+(HJC7(3)-KJC(3))**2)
      THD(2,1)=(HJC7(1)-KJC(1))/DLT
      THD(2,2)=(HJC7(2)-KJC(2))/DLT
      THD(2,3)=(HJC7(3)-KJC(3))/DLT
      THD(1,1)=THD(2,2)*TKD(3,3)-THD(2,3)*TKD(3,2)
      THD(1,2)=THD(2,3)*TKD(3,1)-THD(2,1)*TKD(3,3)
      THD(1,3)=THD(2,1)*TKD(3,2)-THD(2,2)*TKD(3,1)
      DLT=SQRT(THD(1,1)**2+THD(1,2)**2+THD(1,3)**2)
      DO 311 K=1,3
311   THD(1,K)=THD(1,K)/DLT
      THD(3,1)=THD(1,2)*THD(2,3)-THD(1,3)*THD(2,2)
      THD(3,2)=THD(1,3)*THD(2,1)-THD(1,1)*THD(2,3)
      THD(3,3)=THD(1,1)*THD(2,2)-THD(1,2)*THD(2,1)
      DLT=SQRT(THD(3,1)**2+THD(3,2)**2+THD(3,3)**2)
      DO 331 K=1,3
331   THD(3,K)=THD(3,K)/DLT
      CALL MATMUL(TSTS,THD,TSD)
      ELSE
      CALL MATMUL(TSMS2,TMD2,TSD)
      CALL MATMUL(THMS2,TMD2,THD)
      END IF
C
C
C     A=0.0
C     B=0.0
C     AB=0.0
C     DO 44 J=1,3
C     RK4D(J)=KJC(J)-AJC(J)
C     R1KD(J)=HJC7(J)-KJC(J)
C     A=A+RK4D(J)*RK4D(J)
C     B=B+R1KD(J)*R1KD(J)
```

```
C       AB=AB+RK4D(J)*RIKD(J)
C44     CONTINUE
C       A=SQRT(A)
C       B=SQRT(B)
C       AKAKD=ACOS(AB/A/B)*57.3
        AKAKD=ATAN((AJC(1)-KJC(1))/(KJC(2)-AJC(2)))*57.3
        AKAKD=AH-AKAKD
C
        ASOK=-ATAN(TSD(2,1)/TSD(2,2))*57.3
C
        AKA=ATAN((AJC(3)-KJC(3))/(KJC(2)-AJC(2)))
        AKA=AKA*180.0/3.1415926
        IF(ILEG.EQ.2) AKA=-AKA
C  ============== ANKLE ANGLES ==========
        A1=SX3(6,I)-AJC(1)
        A2=SY3(6,I)-AJC(2)
        A3=FZ3(6,I)-AJC(3)
        B1=KJC(1)-AJC(1)
        B2=KJC(2)-AJC(2)
        B3=KJC(3)-AJC(3)
        AA=SQRT(A1*A1+A2*A2+A3*A3)
        BB=SQRT(B1*B1+B2*B2+B3*B3)
        ADOR=SAA-ACOS((A1*B1+A2*B2+A3*B3)/AA/BB)*57.3
        ADOR=ADOR-ANSTAT
C  ============= LATERAL SWING =============
        AZA=(AJC(3)-HJC7(3))*100.0
        IF(ILEG.EQ.2) AZA=-AZA
C
C ======OUTPUT THE RESULTS FOR DYNAMIC ANALYSIS ==========
C
        IF(I.LT.5.OR.I.GT.NF-4) GOTO 7234
        WRITE(6,601) (AJC(J),J=1,3),(KJC(J),J=1,3),(HJC7(J),J=1,3)
601     FORMAT(1X,9(2X,F10.5))
        WRITE(6,700) SX3(6,I),SY3(6,I),FZ3(6,I)
        WRITE(4,700) (HJC7(K),K=1,3),(KJC(K),K=1,3),(AJC(J),J=1,3)
        WRITE(4,700) ((THD(J,K),J=1,3),K=1,3)
        WRITE(4,700) ((TKD(J,K),J=1,3),K=1,3)
        WRITE(4,700) ((TAD(J,K),J=1,3),K=1,3)
        WRITE(4,700) ((TSD(J,K),J=1,3),K=1,3)
        WRITE(8,710) AH,AKAKD,HAA,AKA
        WRITE(8,710) ADOR,AZA,ASOK,AZA
7234    CONTINUE
C
        DO 140 J=1,3
        DO 140 K=1,3
        DTHD(I,J,K)=THD(J,K)
        DTKD(I,J,K)=TKD(J,K)
        DTAD(I,J,K)=TAD(J,K)
140     CONTINUE
C
101     CONTINUE
C
        J1=1
        J2=NF1
        IF(ILEG.EQ.2) J1=NF-NF1-10
        IF(ILEG.EQ.2) J2=NF-10
        CALL MINIMUM(SX3,6,J1,J2,ISOLE)
        FANG=ATAN((FZ3(6,ISOLE)-AJCZ(ISOLE))/
        1(SX3(6,ISOLE)-AJCX(ISOLE)))*57.3*IILEG
```

196a

```
      WRITE(6,606) FANG,SX3(6,ISOLE),FZ3(6,ISOLE)
606   FORMAT(2X,3(2X,F8.3))
C
C     CALL SMOOTH(HJCX,NF,NF,8,1)
C     CALL SMOOTH(KJCX,NF,NF,8,1)
C     CALL SMOOTH(AJCX,NF,NF,8,1)
C     CALL SMOOTH(HJCY,NF,NF,8,1)
C     CALL SMOOTH(KJCY,NF,NF,8,1)
C     CALL SMOOTH(AJCY,NF,NF,8,1)
C     CALL SMOOTH(HJCZ,NF,NF,8,1)
C     CALL SMOOTH(KJCZ,NF,NF,8,1)
C     CALL SMOOTH(AJCZ,NF,NF,8,1)
      CALL DIFFER(HJCX,NF)
      CALL DIFFER(KJCX,NF)
      CALL DIFFER(AJCX,NF)
      CALL DIFFER(HJCY,NF)
      CALL DIFFER(KJCY,NF)
      CALL DIFFER(AJCY,NF)
      CALL DIFFER(HJCZ,NF)
      CALL DIFFER(KJCZ,NF)
      CALL DIFFER(AJCZ,NF)
C
      DO 155 J=1,3
      DO 155 K=1,3
      DO 150 I=1,NF
      RAW1(I)=DTHD(I,J,K)
150   CONTINUE
C     CALL SMOOTH(RAW1,NF,NF,8,1)
      CALL DIFFER(RAW1,NF)
155   CONTINUE
C
      DO 165 J=1,3
      DO 165 K=1,3
      DO 160 I=1,NF
      RAW2(I)=DTKD(I,J,K)
160   CONTINUE
      CALL DIFFER(RAW2,NF)
165   CONTINUE
C
      DO 175 J=1,3
      DO 175 K=1,3
      DO 170 I=1,NF
      RAW3(I)=DTAD(I,J,K)
170   CONTINUE
      CALL DIFFER(RAW3,NF)
175   CONTINUE
C
700   FORMAT(1X,3(2X,F12.8))
999   FORMAT(1X,3(2X,F12.8))
710   FORMAT(1X,4(2X,F12.8))
      STOP
      END
```

PROGRAM "DYNAMICS.SUB"

```
      SUBROUTINE MINIMUM(A,L,I1,I2,K)
      DIMENSION A(20,150)
      DO 10 I=I1+1,I2-1
      AA=A(L,I+1)-A(L,I-1)
      IF(AA.LE.0.005) GOTO 20
10    CONTINUE
20    K=I
      RETURN
      END
C
C
C
      SUBROUTINE XMULT(D,E,F)
C CALCULATES THE CROSS PRODUCT OF D WITH E
      REAL D,E,F
      DIMENSION D(3),E(3),F(3)
      F(1)=D(2)*E(3)-D(3)*E(2)
      F(2)=D(3)*E(1)-D(1)*E(3)
      F(3)=D(1)*E(2)-D(2)*E(1)
      RETURN
      END
CkB
C
C
C
C
C
      SUBROUTINE TMAT(I,T,N1,N2,N3)
      DIMENSION T(3,3)
      COMMON /BLOCK2/SX3(20,150),SY3(20,150),FZ3(20,150)
      INTEGER CAM1,N1,N2,N3
      M=N3
      L=N2
      K=N1
105   CONTINUE
      VKMX=SX3(M,I)-SX3(K,I)
      VKMY=SY3(M,I)-SY3(K,I)
      VKMZ=FZ3(M,I)-FZ3(K,I)
      VLKX=SX3(L,I)-SX3(K,I)
      VLKY=SY3(L,I)-SY3(K,I)
      VLKZ=FZ3(L,I)-FZ3(K,I)
C     S=-(VKMX*VLKX+VKMY*VLKY+VKMZ*VLKZ)
C     1/(VKMX*VKMX+VKMY*VKMY+VKMZ*VKMZ)
C    CL1=-VLKX-S*VKMX
C    CM1=-VLKY-S*VKMY
C    CN1=-VLKZ-S*VKMZ
      CL1=-VLKY*VKMZ+VLKZ*VKMY
      CM1=-VLKZ*VKMX+VLKX*VKMZ
      CN1=-VLKX*VKMY+VLKY*VKMX
```

```
      CL=CL1*CL1+CM1*CM1+CN1*CN1
      CL=SQRT(CL)
      T(1,1)=CL1/CL
      T(1,2)=CM1/CL
      T(1,3)=CN1/CL
      CL2=VKMX
      CM2=VKMY
      CN2=VKMZ
      CM=CL2*CL2+CM2*CM2+CN2*CN2
      CM=SQRT(CM)
      T(2,1)=CL2/CM
      T(2,2)=CM2/CM
      T(2,3)=CN2/CM
      CL3=T(1,2)*T(2,3)-T(1,3)*T(2,2)
      CM3=T(1,3)*T(2,1)-T(1,1)*T(2,3)
      CN3=T(1,1)*T(2,2)-T(1,2)*T(2,1)
        CN=CL3*CL3+CM3*CM3+CN3*CN3
        CN=SQRT(CN)
        T(3,1)=CL3/CN
        T(3,2)=CM3/CN
        T(3,3)=CN3/CN
        RETURN
      END
C
C
C
C
      SUBROUTINE AMULT(A,B,C)
C
C C(3*1)=A(3*3) X B(3*1)
C
        REAL A,B,C
      DIMENSION A(3,3),B(3),C(3)
      DO 100 I=1,3
      C(I)=0.0
      DO 100 J=1,3
  100 C(I)=C(I)+A(I,J)*B(J)
      RETURN
      END
C
C
C
C
        SUBROUTINE TSTAT(T,C1,C2,C3)
C
C THIS ROUTINE USES THE STATIC DATA
C
        DIMENSION T(3,3)
        COMMON /BLOCK1/SSX(30),SSY(30),SFZ(30)
        INTEGER CAM1,C1,C2,C3
      M=C3
      L=C2
      K=C1
  105 CONTINUE
      VKMX=SSX(M)-SSX(K)
      VKMY=SSY(M)-SSY(K)
      VKMZ=SFZ(M)-SFZ(K)
      VLKX=SSX(L)-SSX(K)
      VLKY=SSY(L)-SSY(K)
```

```
      VLKZ=SFZ(L)-SFZ(K)
        CL1=-VLKY*VKMZ+VLKZ*VKMY
        CM1=-VLKZ*VKMX+VLKX*VKMZ
        CN1=-VLKX*VKMY+VLKY*VKMX
        CL=CL1*CL1+CM1*CM1+CN1*CN1
      CL=SQRT(CL)
      T(1,1)=CL1/CL
      T(1,2)=CM1/CL
      T(1,3)=CN1/CL
      CL2=VKMX
      CM2=VKMY
      CN2=VKMZ
      CM=CL2*CL2+CM2*CM2+CN2*CN2
      CM=SQRT(CM)
      T(2,1)=CL2/CM
      T(2,2)=CM2/CM
      T(2,3)=CN2/CM
      CL3=T(1,2)*T(2,3)-T(1,3)*T(2,2)
      CM3=T(1,3)*T(2,1)-T(1,1)*T(2,3)
      CN3=T(1,1)*T(2,2)-T(1,2)*T(2,1)
        CN=CL3*CL3+CM3*CM3+CN3*CN3
        CN=SQRT(CN)
        T(3,1)=CL3/CN
        T(3,2)=CM3/CN
        T(3,3)=CN3/CN
      RETURN
      END
C
C
C
        SUBROUTINE FMAT(I,T)
        DIMENSION T(3,3)
        COMMON /BLOCK3/AJC(3),KJC(3),SXL(3),HJC(3)
        COMMON /BLOCK1/SSX(30),SSY(30),SFZ(30)
        COMMON /BLOCK2/SX3(20,150),SY3(20,150),FZ3(20,150)
        REAL KJC
      VKMX=KJC(1)-AJC(1)
      VKMY=KJC(2)-AJC(2)
      VKMZ=KJC(3)-AJC(3)
      VLKX=SXL(1)
      VLKY=SXL(2)
      VLKZ=SXL(3)
C      S=-(VKMX*VLKX+VKMY*VLKY+VKMZ*VLKZ)/
C     1 (VKMX*VKMX+VKMY*VKMY+VKMZ*VKMZ)
C      CL1=+VLKX+S*VKMX
C      CM1=+VLKY+S*VKMY
C      CN1=+VLKZ+S*VKMZ
        CL1=VLKY*VKMZ-VLKZ*VKMY
        CM1=VLKZ*VKMX-VLKX*VKMZ
        CN1=VLKX*VKMY-VLKY*VKMX
       CL=CL1*CL1+CM1*CM1+CN1*CN1
      CL=SQRT(CL)
      T(3,1)=CL1/CL
      T(3,2)=CM1/CL
      T(3,3)=CN1/CL
      CL2=VKMX
      CM2=VKMY
      CN2=VKMZ
      CM=CL2*CL2+CM2*CM2+CN2*CN2
```

```
      CM=SQRT (CM)
      T(2,1)=CL2/CM
      T(2,2)=CM2/CM
      T(2,3)=CN2/CM
      CL3=T(2,2)*T(3,3)-T(2,3)*T(3,2)
      CM3=T(2,3)*T(3,1)-T(2,1)*T(3,3)
      CN3=T(2,1)*T(3,2)-T(2,2)*T(3,1)
        CN=CL3*CL3+CM3*CM3+CN3*CN3
        CN=SQRT(CN)
        T(1,1)=CL3/CN
        T(1,2)=CM3/CN
        T(1,3)=CN3/CN
      RETURN
      END
C
C
C
        SUBROUTINE FMATT(I,T)
        DIMENSION T(3,3)
        COMMON /BLOCK3/AJC(3),KJC(3),SXL(3),HJC(3)
        COMMON /BLOCK1/SSX(30),SSY(30),SFZ(30)
        COMMON /BLOCK2/SX3(20,150),SY3(20,150),FZ3(20,150)
        REAL KJC
      VKMX=HJC(1)-KJC(1)
      VKMY=HJC(2)-KJC(2)
      VKMZ=HJC(3)-KJC(3)
      VLKX=SXL(1)
      VLKY=SXL(2)
      VLKZ=SXL(3)
C      S=-(VKMX*VLKX+VKMY*VLKY+VKMZ*VLKZ)/
C     1 (VKMX*VKMX+VKMY*VKMY+VKMZ*VKMZ)
C      CL1=+VLKX+S*VKMX
C      CM1=+VLKY+S*VKMY
C      CN1=+VLKZ+S*VKMZ
        CL1=VLKY*VKMZ-VLKZ*VKMY
        CM1=VLKZ*VKMX-VLKX*VKMZ
        CN1=VLKX*VKMY-VLKY*VKMX
       CL=CL1*CL1+CM1*CM1+CN1*CN1
      CL=SQRT(CL)
      T(3,1)=CL1/CL
      T(3,2)=CM1/CL
      T(3,3)=CN1/CL
      CL2=VKMX
      CM2=VKMY
      CN2=VKMZ
      CM=CL2*CL2+CM2*CM2+CN2*CN2
      CM=SQRT (CM)
      T(2,1)=CL2/CM
      T(2,2)=CM2/CM
      T(2,3)=CN2/CM
      CL3=T(2,2)*T(3,3)-T(2,3)*T(3,2)
      CM3=T(2,3)*T(3,1)-T(2,1)*T(3,3)
      CN3=T(2,1)*T(3,2)-T(2,2)*T(3,1)
        CN=CL3*CL3+CM3*CM3+CN3*CN3
        CN=SQRT(CN)
        T(1,1)=CL3/CN
        T(1,2)=CM3/CN
        T(1,3)=CN3/CN
        RETURN
```

```
      END
C
C
C
C
      SUBROUTINE SMOOTH(X,N1,N2,N3,N4)
      DIMENSION A(10),B(10),X(N1),Y(150)
      1,VL(150),AC(150),X1(150)
C
      OFFSET=X(N1)-X(1)
      PED=X(1)
      DO 1 I=1,N1
      V=FLOAT(I-1)/FLOAT(N1-1)
 1    X1(I)=X(I)-V*OFFSET-PED
      CALL FORFIT(X1,N1,A,B,N3,AZERO)
      CALL FORGEN(A,B,AZERO,N3,N1,Y,N2,VL,AC)
CC
C     NOW PUT IN TREND AND PEDISTAL
CC
      DO 2 I=1,N2
      V=FLOAT(I-1)/FLOAT(N2-1)
      Y(I)=Y(I)+V*OFFSET+PED
     VL(I)=VL(I)+OFFSET/FLOAT(N2-1)
 2    X(I)=Y(I)
C
     IF(N4.EQ.0) GOTO 899
     WRITE(10,777)
     DO 20 I=1,N2
20   WRITE(10,99) X(I),VL(I),AC(I)
99   FORMAT(2X,3(2X,F20.12))
777  FORMAT(5X,/)
899  RETURN
      END
C
C
C
C
      SUBROUTINE FORFIT(F,LIM,A,B,NHARMS,AZERO)
      DIMENSION V(100),SNN(100),CSS(100),U(100)
      DIMENSION A(NHARMS),B(NHARMS),SS(100),F(LIM)
C
      ZERO=0.0
      PI=3.14159265
      N=LIM/2
      NH=NHARMS
      FN=N
      M=N-1
      FLIM=(2.0*FN-1.0)/FN
CC
CC    BASIC SINE AND COSINES
CC
      V(1)=0.0
      V(2)=1.0
      CF=COS(PI/FN)
      SF=SIN(PI/FN)
      MP1=N+1
      DO 80 K=3,MP1
      V(K)=2.0*CF*V(K-1)-V(K-2)
      SNN(K-1)=SF*V(K)
```

```
            CSS(K-1)=CF*V(K)-V(K-1)
 80         CONTINUE
            CSS(1)=CF
            SNN(1)=SF
CC
C           COEFFICIENT LOOP
CC
            SSUM=0.0
            DO 82 I=1,LIM
 82         SSUM=F(I)+SSUM
            AZERO=SSUM/FN
            U(1)=0.0
            U(2)=F(LIM)
            DO 95 K=1,NH
            DO 85 I=3,LIM
            INDEX=LIM-I+2
 85         U(I)=U(I-1)*2.0*CSS(K)-U(I-2)+F(INDEX)
            A(K)=(CSS(K)*U(LIM)-U(LIM-1)+F(1))/FN
            B(K)=SNN(K)*U(LIM)/FN
 95         CONTINUE
            SUMS=0.0
            DO 101 I=1,LIM
 101        SUMS=SUMS+F(I)*F(I)
CC
C           CALCULATE ERROR SUM OF SQUARES
CC
 107        TEMP=FN*AZERO*AZERO/2.0
            SSO=TEMP
            DO 108 K=1,NH
 108        SS(K)=(A(K)**2+B(K)**2)*FN
            SS(NH)=(A(NH)*A(NH)*0.25)*FN
            RETURN
            END
C
C
C
      SUBROUTINE FORGEN(A,B,AZERO,NHARMS,N1,OUT,NOUT,VL,AC)
     DIMENSION A(10),B(10),OUT(NOUT),VL(150),AC(150)
C
      PI=3.14159265
      FN=FLOAT(NOUT-1)
      W=2.0*PI/FN
      WO=2.0*PI/(FLOAT(N1)-1.0)/0.02
      NH=NHARMS
C
      DO 200 KKK=1,NOUT
      FK=FLOAT(KKK-1)
      TI=0.0
      TVL=0.0
      TAC=0.0
      DO 125 K=1,NH+1
      J=K-1
      IF(J)123,122,123
122   TI=TI+AZERO/2.0
      GOTO 125
123   FJ=FLOAT(J)
      W1=W*FJ*FK
      SS=SIN(W1)
      CC=COS(W1)
```

```
      TVL=TVL-A(J)*SS*WO*FJ
      TVL=TVL+B(J)*CC*WO*FJ
      TAC=TAC-A(J)*CC*WO*WO*FJ*FJ
      TAC=TAC-B(J)*SS*WO*WO*FJ*FJ
      TI=TI+A(J)*CC
      TI=TI+B(J)*SS
125   CONTINUE
      OUT(KKK)=TI
      VL(KKK)=TVL
      AC(KKK)=TAC
200   CONTINUE
      RETURN
      END
C
C
C
      SUBROUTINE DIFFER(Q,NF)
      DIMENSION Q(150),VL(150),AC(150)
C
      CALL FILTER(Q,NF,10.0,0.02)
C     CALL SMOOTH53(NF,Q)
C
      DO 10 I=1,NF
      IF(I.LT.3.OR.I.GT.NF-2) GOTO 10
      VL(I)=50.0*(Q(I-2)-8.0*(Q(I-1)-Q(I+1))-Q(I+2))/12.0
C     AC(I)=50.0*50.0*(16.0*(Q(I-1)+Q(I+1))-(Q(I-2)+Q(I+2))
C     1-30.0*Q(I))/12.0
10    CONTINUE
C     CALL FILTER2(VL,NF,15.0,0.02)
C     CALL SMOOTH53(NF,VL)
      DO 20 I=3,NF-2
      IF(I.LT.5.OR.I.GT.NF-4) GOTO 20
      AC(I)=50.0*(VL(I-2)-8.0*(VL(I-1)-VL(I+1))-VL(I+2))/12.0
5     WRITE(10,99) Q(I),VL(I),AC(I)
20    CONTINUE
99    FORMAT(2X,3(2X,F16.10))
      RETURN
      END
C
C
C
      SUBROUTINE FILTER2(Q,N,FCUT,T)
      DIMENSION C(5,7),Q(150),W(150),WI(150)
      DATA C/0.2929,0.5858,0.2929,0.0,-0.1716
     1,0.2066,0.4132,0.2066,0.3695,-0.1959
     2,0.15505,0.3101,0.15505,0.6202,-0.2404
     3,0.1212,0.2424,0.1212,0.8030,-0.2878
     4,0.0884,0.1768,0.0884,1.0011,-0.3547
     5,0.06745,0.1349,0.06745,1.1430,-0.4128
     6,0.0495,0.0990,0.0495,1.2796,-0.4776/
C
      KF=IFIX(50.0/FCUT)-4
C
      W(1)=Q(1)
      W(2)=Q(2)
      DO 10 L=3,N
      W(L)=C(1,KF)*Q(L)+C(2,KF)*Q(L-1)+C(3,KF)*Q(L-2)
     1+C(4,KF)*W(L-1)+C(5,KF)*W(L-2)
10    CONTINUE
```

```
C
      DO 20 L=1,N
20    W1(L)=W(N-L+1)
      W(1)=W1(1)
      W(2)=W1(2)
      DO 30 L=3,N
      W(L)=C(1,KF)*W1(L)+C(2,KF)*W1(L-1)+C(3,KF)*W1(L-2)
     1+C(4,KF)*W(L-1)+C(5,KF)*W(L-2)
30    CONTINUE
C
      DO 40 L=1,N
40    Q(L)=W(N-L+1)
C
      RETURN
      END
C
C
C
      SUBROUTINE FILTER(Q,N,FCUT,T)
C
C NOTE: TREND AND PEDESTAL REMOVED BEFORE FILTER,
C       ADDED IN AFTER FILTERING PROCESS
C
      DIMENSION C(10),Q(150),AD(150),W1(150),W(150)
      NR=N+20.0
      TR=Q(N)-Q(1)
      IF(FCUT.GE.1.0/(2.0*T))GOTO 17
      XPI=3.1415265
      T1=SIN(XPI*FCUT*T)
      T2=COS(XPI*FCUT*T)
      TT=T1/T2
      A=COS(XPI/8.0)*TT
      B=SIN(XPI/8.0)*TT
      C(1)=2*(A+B)
      C(2)=2*(A+B)**2
      C(3)=2*((A**2+B**2)*(A+B))
      C(4)=(A**2+B**2)**2
      C(5)=1+C(1)+C(2)+C(3)+C(4)
      C(6)=-4+4*C(4)-2*C(1)+2*C(3)
      C(7)=6+6*C(4)-2*C(2)
      C(8)=-4+2*C(1)-2*C(3)+4*C(4)
      C(9)=1-C(1)+C(2)+C(4)-C(3)
      DO 30 K44=N,130
30    AD(K44)=0.0
      DO 2 L=1,N
      AD(L+4)=Q(L)-(L-1)*TR/(N-1)-Q(1)
2     CONTINUE
      DO 9 L=1,4
      AD(L)=0.0
      W(L)=0.0
9     CONTINUE
      N1=N+24
      DO 18 K=1,NR
      W(K+4)=(C(4)*(AD(K+4)+4*AD(K+3)+6*AD(K+2)+4*AD(K+1)
     1+AD(K))-(W(K+3)*C(6)+W(K+2)*C(7)+W(K+1)*C(8)+W(K)*
     1C(9)))/C(5)
18    CONTINUE
      DO 37 JKJ=1,NR
37    W(JKJ)=W(JKJ+4)
```

```
      DO 15 K=1,4
      K4=N1-K
      W1(K4+1)=0.0
      W(K4+1)=0.0
15    CONTINUE
      DO 16 K=1,NR
      K5=N1-K
      W1(K5-3)=(C(4)*(W(K5-3)+4*W(K5-2)+6*W(K5-1)
     1+4*W(K5)+W(K5+1))-(W1(K5-2)*C(6)+W1(K5-1)*C(7)
     2+W1(K5)*C(8)+W1(K5+1)*C(9)))/C(5)
16    CONTINUE
      DO 21 K=1,N
21    W1(K)=W1(K)+(K-1)*TR/(N-1)+Q(1)
      DO 17 K=1,N
      Q(K)=W1(K)
17    CONTINUE
      RETURN
      END

C
C
C
C
      SUBROUTINE MATMUL(D1,D2,D3)
      REAL D1,D2,D3
      DIMENSION D1(3,3),D2(3,3),D3(3,3)
      DO 30 I=1,3
      DO 20 J=1,3
      D3(I,J)=0.0
      DO 10 K=1,3
      D3(I,J)=D1(I,K)*D2(K,J)+D3(I,J)
10    CONTINUE
20    CONTINUE
30    CONTINUE
      RETURN
      END
C
C
C
      SUBROUTINE TRANSP(D1,D2)
      REAL D1,D2
      DIMENSION D1(3,3),D2(3,3)
      DO 10 I=1,3
10    D2(I,I)=D1(I,I)
      D2(1,2)=D1(2,1)
      D2(1,3)=D1(3,1)
      D2(2,1)=D1(1,2)
      D2(2,3)=D1(3,2)
      D2(3,1)=D1(1,3)
      D2(3,2)=D1(2,3)
      RETURN
      END
C
C
      SUBROUTINE SMOOTH53(N,Y)
      DIMENSION YP(150),Y(150)
      DO 10 I=1,N
10    YP(N-I+1)=Y(I)
      CALL SMOOTHH(N,YP)
```

```
      DO 20 I=1,N
20    Y(N-I+1)=YP(I)
      CALL SMOOTHH(N,Y)
      RETURN
      END
C
C
      SUBROUTINE SMOOTHH(N,Y)
      DIMENSION YP(500),Y(150),YY(500),YOF(150)
      DO 10 I=1,N
10    YP(I+49)=Y(I)
      DO 20 I=2,50
20    YP(51-I)=-Y(I)+2.0*Y(1)
      DO 30 I=1,49
30    YP(N+I+49)=-Y(N-I)+2.0*Y(N)
C
      NN=N+49*2
      YY(1)=(69.9*YP(1)+4.0*(YP(2)+YP(4))-6.0*YP(3)-YP(5))/70.0
      YY(2)=(2.0*(YP(1)+YP(5))+27.0*YP(2)+12.0*YP(3)-8.0*YP(4))/35.0
      NO2=NN-2
      DO 220 I=3,NO2
220   YY(I)=(12.0*(YP(I-1)+YP(I+1))-3.0*(YP(I-2)+YP(I+2))+17.0*YP(I))/35.0
      YY(N-1)=(2.0*(YP(N-4)+YP(N))-8.0*YP(N-3)+12.0*YP(N-2)
     1+27.0*YP(N-1))/35.0
      YY(N)=(4.0*(YP(N-3)+YP(N-1))-YP(N-4)-6.0*YP(N-2)+69.0*YP(N))/70.0
C
      DO 300 I=1,N
300   Y(I)=YY(I+49)
      RETURN
      END
```

PROGRAM "KINEAMPU.MAJ"

```
      REAL MCX,MCY,MCZ,MASS,MAX,MAY,MAZ,MKX,MKY,MKZ
     1,MHX,MHY,MHZ,MSX,MSY,MSZ,KA,KJC,MGH,MP,KAA,MH
     2,KF,KM,MC,KJCV7,KJCV8,MCC,ME
     3,MTX,MTY,MTW,MGX,MGY,MLW
      DIMENSION FT(3,3),XFC(3),XMC(3),MC(3),FC(3)
     1,SL(3),TL(3),F(3),S(3),T(3),AJC(3),SJC(3)
     2,KJC(3),HJC(3),XH(3),YH(3),ZH(3),FTH(3,3),FS(3,3)
     3,XS(3),FH(3),MH(3),MGH(3),P(3),MP(3),FTI(3,3)
     4,AF(3),AM(3),KF(3),KM(3),SF(3),SM(3),HF(3),HM(3)
     5,TSD(3,3),TKD(3,3),TAD(3,3),THD(3,3),FTT(3,3)
     6,CTH7(150,3),CTV7(150,3),CTA7(150,3),TAX7(150)
     7,CSH7(150,3),CSV7(150,3),CSA7(150,3),SAX7(150)
     8,DTH7(150,3,3),DTV7(150,3,3),TAY7(150),TAZ7(150)
     9,DSH7(150,3,3),DSV7(150,3,3),SAY7(150),SAZ7(150)
     6,CTH8(150,3),CTV8(150,3),CTA8(150,3),TAX8(150)
     7,CSH8(150,3),CSV8(150,3),CSA8(150,3),SAX8(150)
     8,DTH8(150,3,3),DTV8(150,3,3),TAY8(150),TAZ8(150)
     9,DSH8(150,3,3),DSV8(150,3,3),SAY8(150),SAZ8(150)
     8,TAAX7(150),TAAY7(150),TAAZ7(150),FE(3),FGRA(3)
     9,SAAX7(150),SAAY7(150),SAAZ7(150),FTIA(3)
     8,TAAX8(150),TAAY8(150),TAAZ8(150),CEN2(3)
     9,SAAX8(150),SAAY8(150),SAAZ8(150),CEN1(3)
     9,CTRD(150,3),CTRV(150,3),CTRA(150,3),XXO(3)
     1,AJCV7(150,3),KJCV7(150,3),HJCV7(150,3),XO(3)
     2,AJCV8(150,3),KJCV8(150,3),HJCV8(150,3)
     3,AJCD7(150,3),AJCA7(150,3),AJCD8(150,3),AJCA8(150,3)
     4,DTA7(150,3,3),DTA8(150,3,3),DSA7(150,3,3),DSA8(150,3,3)
     5,RAW1(150),RAW2(150),RAW3(150),RAW4(150),RAW5(150),ME(3)
     6,DFT7(150,3,3),DFV7(150,3,3),DFA7(150,3,3)
     6,DFT8(150,3,3),DFV8(150,3,3),DFA8(150,3,3)
     6,APD(150,3),APV(150,3),APA(150,3)
     6,ATD(150,3),ATV(150,3),ATA(150,3)
      COMMON /FORCE/FCC(3),MCC(3),THF(3),GRAV,FD(3)
      DATA FTI /1.0,3*0.0,1.0,3*0.0,1.0/
C
C
      PRINT *,'       KINETIC ANALYSIS'
      PRINT *,'READ IN KINEMATIC DATA'
C
      READ(3,1) XNAME,XLIMB
      READ(3,*) ILEG,INERTIA,FCUT,MASS,WEIGHT,HEIGHT
      READ(3,*) SM8,C2S8,PS8,TM8,C2T8,PT8
      READ(1,*) CA,FL,CS,HTI,CTH,PP,CCH
      READ(1,*) NF,NF1,NF2
      READ(1,*) SL7,TL7,ANY
      READ(9,*) SL8,SM8,C2S8,SHKI,TL8,TM8,CGTH,THHI
      READ(5,*) NF1,ITF1,IHS1,NF2,ITF2,IHS2
C
C  INERTIA PARAMETERS OF THE PROSTHETIC LIMB
C
```

```
      SL8=SL8+ANY
      SC2=C2S8/SL8
      SC3=SQRT(SHKI/SM8)/SL8
      TC2=C6TH/TL8
      TC3=SQRT(THHI/TM8)/TL8
C
      WRITE(8,1) XNAME,XLIMB
      WRITE(7,1) XNAME,XLIMB
1     FORMAT(1X,8A,2X,8A)
      WRITE(8,721) MASS,WEIGHT
      WRITE(7,721) MASS,WEIGHT
721   FORMAT(1X,2(2X,F10.5))
C
      IF(INERTIA.EQ.0) GOTO 12345
C
      DO 10 J=1,3
      DO 5 I=1,NF
      READ(5,*) X,VL,AC
      CTH7(I,J)=X
      HJCV7(I,J)=VL
      RAW1(I)=AC
5     CONTINUE
C
      DO 12 I=1,NF
      READ(5,*) X,VL,AC
      CSH7(I,J)=X
      KJCV7(I,J)=VL
      RAW2(I)=AC
12    CONTINUE
C
      DO 13 I=1,NF
      READ(5,*) X,VL,AC
      AJCD7(I,J)=X
      AJCV7(I,J)=VL
      RAW3(I)=AC
13    CONTINUE
C
      DO 14 I=1,NF
      READ(5,*) X,VL,AC
      APD(I,J)=X
      RAW4(I)=VL
      APA(I,J)=AC
14    CONTINUE
C
      DO 15 I=1,NF
      READ(5,*) X,VL,AC
      ATD(I,J)=X
      ATV(I,J)=VL
      RAW5(I)=AC
15    CONTINUE
C
      CALL FILTER(RAW1,NF,10.0,0.02)
      CALL FILTER(RAW2,NF,10.0,0.02)
      CALL FILTER(RAW3,NF,10.0,0.02)
      CALL FILTER(RAW4,NF,10.0,0.02)
      CALL FILTER(RAW5,NF,10.0,0.02)
C
      DO 18 I=1,NF
      CTA7(I,J)=RAW1(I)
```

```
            CSA7(I,J)=RAW2(I)
            AJCA7(I,J)=RAW3(I)
            APV(I,J)=RAW4(I)
            ATA(I,J)=RAW5(I)*0.6682*MASS
            CTH7(I,J)=CTH7(I,J)*0.5831+CSH7(I,J)*0.4169
            CTV7(I,J)=HJCV7(I,J)*0.5831+KJCV7(I,J)*0.4169
            CTA7(I,J)=CTA7(I,J)*0.5831+CSA7(I,J)*0.4169
            CSH7(I,J)=CSH7(I,J)*0.5327+AJCD7(I,J)*0.4673
            CSV7(I,J)=KJCV7(I,J)*0.5327+AJCV7(I,J)*0.4673
            CSA7(I,J)=CSA7(I,J)*0.5327+AJCA7(I,J)*0.4673
   18       CONTINUE
C
   10       CONTINUE
C
            DO 25 J=1,3
            DO 25 K=1,3
            DO 22 I=1,NF
            READ(5,*) X,VL,AC
            DTH7(I,J,K)=X
            DTV7(I,J,K)=VL
            RAW1(I)=AC
   22       CONTINUE
            CALL FILTER(RAW1,NF,FCUT,0.02)
            DO 21 I=1,NF
   21       DTA7(I,J,K)=RAW1(I)
   25       CONTINUE
C
            DO 30 J=1,3
            DO 30 K=1,3
            DO 27 I=1,NF
            READ(5,*) X,VL,AC
            DSH7(I,J,K)=X
            DSV7(I,J,K)=VL
            RAW1(I)=AC
   27       CONTINUE
            CALL FILTER(RAW1,NF,FCUT,0.02)
            DO 28 I=1,NF
   28       DSA7(I,J,K)=RAW1(I)
   30       CONTINUE
C
            DO 330 J=1,3
            DO 330 K=1,3
            DO 327 I=1,NF
            READ(5,*) X,VL,AC
            DFT7(I,J,K)=X
            DFV7(I,J,K)=VL
            RAW1(I)=AC
  327       CONTINUE
            CALL FILTER(RAW1,NF,FCUT,0.02)
            DO 328 I=1,NF
  328       DFA7(I,J,K)=RAW1(I)
  330       CONTINUE
C
C   RIGHT SIDE
C
            DO 35 J=1,3
            DO 33 I=1,NF
            READ(11,*) X,VL,AC
            CTH8(I,J)=X
```

```
            HJCV8(I,J)=VL
            RAW1(I)=AC
   33       CONTINUE
   C
            DO 42 I=1,NF
            READ(11,*) X,VL,AC
            CSH8(I,J)=X
            KJCV8(I,J)=VL
            RAW2(I)=AC
   42       CONTINUE
   C
            DO 34 I=1,NF
            READ(11,*) X,VL,AC
            AJCD8(I,J)=X
            AJCV8(I,J)=VL
            RAW3(I)=AC
   34       CONTINUE
   C
            CALL FILTER(RAW1,NF,10.0,0.02)
            CALL FILTER(RAW2,NF,10.0,0.02)
            CALL FILTER(RAW3,NF,10.0,0.02)
            DO 36 I=1,NF
            CTA8(I,J)=RAW1(I)
            CSA8(I,J)=RAW2(I)
            AJCA8(I,J)=RAW3(I)
            CTH8(I,J)=CTH8(I,J)*(1.0-TC2)+CSH8(I,J)*TC2
            CTV8(I,J)=HJCV8(I,J)*(1.0-TC2)+KJCV8(I,J)*TC2
            CTA8(I,J)=CTA8(I,J)*(1.0-TC2)+CSA8(I,J)*TC2
            CSH8(I,J)=CSH8(I,J)*(1.0-SC2)+AJCD8(I,J)*SC2
            CSV8(I,J)=KJCV8(I,J)*(1.0-SC2)+AJCV8(I,J)*SC2
            CSA8(I,J)=CSA8(I,J)*(1.0-SC2)+AJCA8(I,J)*SC2
   36       CONTINUE
   C
   35       CONTINUE
   C
   C
            DO 45 J=1,3
            DO 45 K=1,3
            DO 43 I=1,NF
            READ(11,*) X,VL,AC
            DTH8(I,J,K)=X
            DTV8(I,J,K)=VL
            RAW1(I)=AC
   43       CONTINUE
            CALL FILTER(RAW1,NF,FCUT,0.02)
            DO 442 I=1,NF
   442      DTA8(I,J,K)=RAW1(I)
   45       CONTINUE
   C
            DO 72 J=1,3
            DO 72 K=1,3
            DO 47 I=1,NF
            READ(11,*) X,VL,AC
            DSH8(I,J,K)=X
            DSV8(I,J,K)=VL
            RAW1(I)=AC
   47       CONTINUE
            CALL FILTER(RAW1,NF,FCUT,0.02)
            DO 722 I=1,NF
```

```
722     DSA8(I,J,K)=RAW1(I)
72      CONTINUE
C
        DO 372 J=1,3
        DO 372 K=1,3
        DO 347 I=1,NF
        READ(11,*) X,VL,AC
        DFT8(I,J,K)=X
        DFV8(I,J,K)=VL
        RAW1(I)=AC
347     CONTINUE
        CALL FILTER(RAW1,NF,FCUT,0.02)
        DO 3722 I=1,NF
3722    DFA8(I,J,K)=RAW1(I)
372     CONTINUE
C
C  CALCULATE THE ANGULAR VELOCITY
C
        PRINT *,'ANGULAR VELOCITY AND ACCELERATION'
        DO 60 I=1,NF
        TAX7(I)=0.0
        TAY7(I)=0.0
        TAZ7(I)=0.0
        SAX7(I)=0.0
        SAY7(I)=0.0
        SAZ7(I)=0.0
        TAX8(I)=0.0
        TAY8(I)=0.0
        TAZ8(I)=0.0
        SAX8(I)=0.0
        SAY8(I)=0.0
        SAZ8(I)=0.0
C
        TAAX7(I)=0.0
        TAAY7(I)=0.0
        TAAZ7(I)=0.0
        SAAX7(I)=0.0
        SAAY7(I)=0.0
        SAAZ7(I)=0.0
        TAAX8(I)=0.0
        TAAY8(I)=0.0
        TAAZ8(I)=0.0
        SAAX8(I)=0.0
        SAAY8(I)=0.0
        SAAZ8(I)=0.0
        DO 59 J=1,3
        TAX7(I)=DTV7(I,J,3)*DTH7(I,J,2)+TAX7(I)
        TAY7(I)=DTV7(I,J,1)*DTH7(I,J,3)+TAY7(I)
        TAZ7(I)=DTV7(I,J,2)*DTH7(I,J,1)+TAZ7(I)
        SAX7(I)=DSV7(I,J,3)*DSH7(I,J,2)+SAX7(I)
        SAY7(I)=DSV7(I,J,1)*DSH7(I,J,3)+SAY7(I)
        SAZ7(I)=DSV7(I,J,2)*DSH7(I,J,1)+SAZ7(I)
        TAX8(I)=DTV8(I,J,3)*DTH8(I,J,2)+TAX8(I)
        TAY8(I)=DTV8(I,J,1)*DTH8(I,J,3)+TAY8(I)
        TAZ8(I)=DTV8(I,J,2)*DTH8(I,J,1)+TAZ8(I)
        SAX8(I)=DSV8(I,J,3)*DSH8(I,J,2)+SAX8(I)
        SAY8(I)=DSV8(I,J,1)*DSH8(I,J,3)+SAY8(I)
        SAZ8(I)=DSV8(I,J,2)*DSH8(I,J,1)+SAZ8(I)
C
```

```
      TAAX7(I)=DTA7(I,J,3)*DTH7(I,J,2)+TAAX7(I)+DTV7(I,J,3)*DTV7(I,J,2)
      TAAY7(I)=DTA7(I,J,1)*DTH7(I,J,3)+TAAY7(I)+DTV7(I,J,1)*DTV7(I,J,3)
      TAAZ7(I)=DTA7(I,J,2)*DTH7(I,J,1)+TAAZ7(I)+DTV7(I,J,2)*DTV7(I,J,1)
      SAAX7(I)=DSA7(I,J,3)*DSH7(I,J,2)+SAAX7(I)+DSV7(I,J,3)*DSV7(I,J,2)
      SAAY7(I)=DSA7(I,J,1)*DSH7(I,J,3)+SAAY7(I)+DSV7(I,J,1)*DSV7(I,J,3)
      SAAZ7(I)=DSA7(I,J,2)*DSH7(I,J,1)+SAAZ7(I)+DSV7(I,J,2)*DSV7(I,J,1)
      TAAX8(I)=DTA8(I,J,3)*DTH8(I,J,2)+TAAX8(I)+DTV8(I,J,3)*DTV8(I,J,2)
      TAAY8(I)=DTA8(I,J,1)*DTH8(I,J,3)+TAAY8(I)+DTV8(I,J,1)*DTV8(I,J,3)
      TAAZ8(I)=DTA8(I,J,2)*DTH8(I,J,1)+TAAZ8(I)+DTV8(I,J,2)*DTV8(I,J,1)
      SAAX8(I)=DSA8(I,J,3)*DSH8(I,J,2)+SAAX8(I)+DSV8(I,J,3)*DSV8(I,J,2)
      SAAY8(I)=DSA8(I,J,1)*DSH8(I,J,3)+SAAY8(I)+DSV8(I,J,1)*DSV8(I,J,3)
      SAAZ8(I)=DSA8(I,J,2)*DSH8(I,J,1)+SAAZ8(I)+DSV8(I,J,2)*DSV8(I,J,1)
59    CONTINUE
C
60    CONTINUE
C
      CALL AMULT2(NF,DTH7,TAX7,TAY7,TAZ7)
      CALL AMULT2(NF,DSH7,SAX7,SAY7,SAZ7)
      CALL AMULT2(NF,DTH8,TAX8,TAY8,TAZ8)
      CALL AMULT2(NF,DSH8,SAX8,SAY8,SAZ8)
      CALL AMULT2(NF,DTH7,TAAX7,TAAY7,TAAZ7)
      CALL AMULT2(NF,DSH7,SAAX7,SAAY7,SAAZ7)
      CALL AMULT2(NF,DTH8,TAAX8,TAAY8,TAAZ8)
      CALL AMULT2(NF,DSH8,SAAX8,SAAY8,SAAZ8)
C
      CALL FILTER(TAAX7,NF,10.0,0.02)
      CALL FILTER(TAAY7,NF,10.0,0.02)
      CALL FILTER(TAAZ7,NF,10.0,0.02)
      CALL FILTER(SAAX7,NF,10.0,0.02)
      CALL FILTER(SAAY7,NF,10.0,0.02)
      CALL FILTER(SAAZ7,NF,10.0,0.02)
      CALL FILTER(TAAX8,NF,10.0,0.02)
      CALL FILTER(TAAY8,NF,10.0,0.02)
      CALL FILTER(TAAZ8,NF,10.0,0.02)
      CALL FILTER(SAAX8,NF,10.0,0.02)
      CALL FILTER(SAAY8,NF,10.0,0.02)
      CALL FILTER(SAAZ8,NF,10.0,0.02)
C
12345 CONTINUE
C
      ISTEP=1
      IF(ILEG.EQ.1) GOTO 1001
C
C
1002  PRINT *,'UNAFFECTED SIDE'
      READ(3,*) NF1,ITF1,IHS1
      WRITE(8,720) ISTEP,NF1,ITF1,IHS1
720   FORMAT(2X,I7)
      IF(ISTEP.EQ.2) LL=IABS(IHS2-IHS1)+1
C
      DO 100 I=1,NF
C
      DO 62 J=1,3
      XO(J)=0.0
      FCC(J)=0.0
      MCC(J)=0.0
      FE(J)=0.0
      ME(J)=0.0
      MP(J)=0.0
```

```
      CEN1(J)=0.0
      FTIA(J)=0.0
      MGH(J)=0.0
      XMC(J)=0.0
62    CONTINUE
C

      IF(ISTEP.EQ.1.AND.I.GT.NF1) GOTO 1011
      IF(ISTEP.EQ.2.AND.I.LT.LL) GOTO 1011
C
      READ(3,*) (XO(J),J=1,3)
      READ(3,*) (FCC(J),J=1,3)
      READ(3,*) (MCC(J),J=1,3)
C
1011  WRITE(8,603)
      WRITE(8,600) (XO(J),J=1,3)
      WRITE(8,600) (FCC(J),J=1,3)
      WRITE(8,600) (MCC(J),J=1,3)
      READ(1,*) (HJC(J),J=1,3)
      READ(1,*) (KJC(J),J=1,3)
      READ(1,*) (AJC(J),J=1,3)
      READ(1,*) ((FT(J,K),J=1,3),K=1,3)
      READ(1,*) ((FTT(J,K),J=1,3),K=1,3)
      READ(1,*) ((TAD(J,K),J=1,3),K=1,3)
C
      MGH(2)=FCC(3)*XO(1)-FCC(1)*XO(3)+MCC(2)
      PPELY=MGH(2)
      PPELX=(XO(3)-AJC(3))*FCC(1)
      PPELZ=-(XO(1)-AJC(1))*FCC(3)
      CALL AMULT(FT,MGH,ME)
      CALL AMULT(FT,FCC,AF)
      CALL MOMENT(XO,AJC,1.0,FCC,MGH)
      CALL AMULT(FT,MGH,AM)
C
      CALL MOMENT(XO,KJC,1.0,FCC,MGH)
      CALL AMULT(FT,MGH,KM)
      CALL AMULT(FT,FCC,KF)
      DO 818 J=1,3
      AM(J)=AM(J)+ME(J)
818   KM(J)=KM(J)+ME(J)
C
C     SM7=0.111*CS+0.047*HTI+0.074*CA-4.208
C     1+0.003*MASS+0.048*CA+0.027*FL-0.869
      SM7=0.0632*MASS
C
      IF(INERTIA.EQ.0) GOTO 12347
C
      CEN1(1)=-CSA7(I,1)*SM7
      CEN1(2)=-(9.806*+CSA7(I,2))*SM7
      CEN1(3)=-CSA7(I,3)*SM7
      CALL AMULT(FT,CEN1,FTIA)
      CALL MOMENT1(0.4673,0.3467,0.0,SL7,SM7,I,SAAX7,SAAY7,SAAZ7
      1,XMC,NF,SAX7,SAY7,SAZ7)
      CALL MOMENT(AJC,KJC,0.4673,CEN1,MGH)
      CALL AMULT(FT,MGH,MP)
12347 DO 201 J=1,3
      S(J)=-CEN1(J)
      KF(J)=KF(J)+FTIA(J)
201   KM(J)=KM(J)+MP(J)-XMC(J)
```

```
      S(2)=CSA7(I,2)*SM7
C
      CALL TRANSP(FT,FTH)
      CALL AMULT(FTH,KF,FC)
C
      PST7=0.0
      WSF7=0.0
      EST7=0.0
      DO 111 J=1,3
      PST7=PST7+SM7*CSV7(I,J)*CSA7(I,J)  ! Pt due to CG motion
      WSF7=WST7-FC(J)*KJCV7(I,J)         ! Pf done by joint forces
      EST7=EST7+0.5*SM7*CSV7(I,J)
     1*CSV7(I,J)                         ! Et of CG motion
111   CONTINUE
      PSR7=SM7*(0.3467*SL7)**2.0*(SAX7(I)
     1*SAAX7(I)+SAZ7(I)*SAAZ7(I))        ! Pr due to rotation
      PSG7=SM7*9.81*CSV7(I,2)            ! Pg due to gravity
      ESR7=0.5*SM7*(0.3467*SL7)**2.0*
     1(SAX7(I)**2.0+SAZ7(I)**2.0)        ! Er due to rotation
      ESP7=SM7*9.81*CSH7(I,2)            ! Eg due to gravity
      WSM7=(AM(1)-KM(1))*SAX7(I)+(AM(2)-KM(2))*SAY7(I)
     1+(AM(3)-KM(3))*SAZ7(I)             ! Pm done by joint moments
      ES7=EST7+ESR7+ESP7   !TOTAL ENERGY OF THE SHANK
      PS7=PST7+PSR7+PSG7   !TOTAL SHANK ENERGY CHANGE RATE
      WS7=WSF7+WSM7        !TOTAL JOINT LOAD POWER
C
C
      CALL AMULT(FTH,KM,MGH)
      CALL AMULT(FTT,FC,FE)
      CALL AMULT(FTT,MGH,ME)
C     TM7=0.074*MASS+0.123*CTH+0.027*PP*0.78-4.216
      TM7=0.1027*MASS
C
      CALL MOMENT(KJC,HJC,1.0,FC,MGH)
      CALL AMULT(FTT,MGH,HM)
      IF(INERTIA.EQ.0) GOTO 12348
C
      CEN1(1)=-CTA7(I,1)*TM7
      CEN1(2)=-(9.81+CTA7(I,2))*TM7
      CEN1(3)=-CTA7(I,3)*TM7
      CALL AMULT(FTT,CEN1,FTIA)
      CALL MOMENT1(0.4169,0.2912,0.0,TL7,TM7,I,TAAX7,TAAY7,TAAZ7
     1,XMC,MF,TAX7,TAY7,TAZ7)
      CALL MOMENT(KJC,HJC,0.4169,CEN1,MGH)
      CALL AMULT(FTT,MGH,MP)
12348 DO 202 J=1,3
      T(J)=ATA(I,J)
      F(J)=-CEN1(J)
      HF(J)=FTIA(J)+FE(J)
202   HM(J)=HM(J)+MP(J)+ME(J)-XMC(J)
      F(2)=CTA7(I,2)*TM7
C
      CALL TRANSP(FTT,FTH)
      CALL AMULT(FTH,HF,FC)
C
      PTT7=0.0
      WTF7=0.0
      ETT7=0.0
      DO 151 J=1,3
```

```
      PTT7=PTT7+TM7*CTV7(I,J)*CTA7(I,J)      ! Pt
      WTF7=WTF7-FC(J)*HJCV7(I,J)             ! Pf
      ETT7=ETT7+0.5*TM7*CTV7(I,J)*CTV7(I,J)  ! Et
151   CONTINUE
      PTR7=TM7*(0.2912*TL7)**2.0*(TAX7(I)
     1*TAAX7(I)+TAZ7(I)*TAAZ7(I))            ! Pr
      PTG7=TM7*9.81*CTV7(I,2)                ! Pg
      ETR7=0.5*TM7*(0.2912*TL7)**2.0
     1*(TAX7(I)**2.0+TAZ7(I)**2.0)           ! Er
      ETP7=9.806*TM7*CTH7(I,2)               ! Eg
      WTM7=(ME(1)-HM(1))*TAX7(I)+(ME(2)-HM(2))*TAY7(I)
     1+(ME(3)-HM(3))*TAZ7(I)                 ! Pr
      ET7=ETT7+ETR7+ETP7   !TOTAL THIGH ENERGY
      PT7=PTT7+PTR7        !TOTAL THIGH ENERGY CHANGE RATE
      WTF7=WTF7-WSF7       !JOINT FORCE POWER
      WT7=WTF7+WTM7        !TOTAL THIGH JOINT POWER
C
      EEST7=ES7+ET7    !TOTAL LEG ENERGY
      PPST7=PS7+PT7    !TOTAL LEG ENERGY CHANGE RATE
      WWST7=WS7+WT7    !TOTAL LEG JOINT POWER
C
C   POWER INTO TRUNK
C
      CALL AMULT(FTH,HM,ME)
      PTHIX=-ME(1)*TAX7(I)
      PTHIY=-ME(2)*TAY7(I)
      PTHIZ=-ME(3)*TAZ7(I)
C
C  DISCOMPOSITE OF THE HIP JOINT MOMENT
C
      MGX=FCC(1)*HJC(2)
      MGY=FCC(2)*(XO(1)-HJC(1))
      MLW=ME(3)-MGX-MGY
      MTX=ATA(I,1)*(ATD(I,2)-HJC(2))
      MTY=-ATA(I,2)*(ATD(I,1)-HJC(1))
      MTW=MASS*0.6682*9.806*(ATD(I,1)-HJC(1))
C
      WRITE(8,600) (S(J),J=1,3),(AM(J),J=1,3)
      WRITE(8,600) (F(J),J=1,3),(KM(J),J=1,3)
      WRITE(8,600) (T(J),J=1,3),(HM(J),J=1,3)
      WRITE(8,600) ES7,ET7,EEST7
      WRITE(8,600) PS7,PT7,PPST7
      WRITE(8,600) WS7,WT7,WWST7
      WRITE(8,600) PPELX,PPELY,PPELZ
      WRITE(8,600) PTHIX,PTHIY,PTHIZ
      WRITE(8,600) MTX,MTY,MTW
      WRITE(8,600) MGX,MGY,MLW
C
100   CONTINUE
C
      IF(ISTEP.EQ.2) GOTO 1005
      ISTEP=2
C
C
1001  PRINT *,'PROSTHETIC SIDE'
C

C
      READ(3,*) NF2,ITF2,IHS2
```

```
      WRITE(7,720) ISTEP,NF2,ITF2,IHS2
      IF(ISTEP.EQ.2) LL=IABS(IHS2-IHS1)+1
C
      DO 700 I=1,NF
C
      DO 762 J=1,3
      XO(J)=0.0
      FCC(J)=0.0
      MCC(J)=0.0
      FE(J)=0.0
      ME(J)=0.0
      MP(J)=0.0
      CEN1(J)=0.0
      FTIA(J)=0.0
      MGH(J)=0.0
      XMC(J)=0.0
762   CONTINUE
C
      IF(ISTEP.EQ.1.AND.I.GT.NF2) GOTO 1012
      IF(ISTEP.EQ.2.AND.I.LT.LL) GOTO 1012
C
      READ(3,*) (XO(J),J=1,3)
      READ(3,*) (FCC(J),J=1,3)
      READ(3,*) (MCC(J),J=1,3)
C
1012  WRITE(7,603)
      WRITE(7,600) (XO(J),J=1,3)
      WRITE(7,600) (FCC(J),J=1,3)
      WRITE(7,600) (MCC(J),J=1,3)
      READ(9,*) (HJC(J),J=1,3)
      READ(9,*) (KJC(J),J=1,3)
      READ(9,*) (AJC(J),J=1,3)
      READ(9,*) ((FTT(J,K),J=1,3),K=1,3)
      READ(9,*) ((FT(J,K),J=1,3),K=1,3)
      READ(9,*) ((TAD(J,K),J=1,3),K=1,3)
      READ(9,*) ((TSD(J,K),J=1,3),K=1,3)
C
      MGH(2)=FCC(3)*XO(1)-FCC(1)*XO(3)+MCC(2)
      PPELY=MGH(2)
      PPELX=(XO(3)-AJC(3))*FCC(1)
      PPELZ=-(XO(1)-AJC(1))*FCC(3)
      CALL AMULT(FT,MGH,ME)
      CALL AMULT(FT,FCC,AF)
      CALL MOMENT(XO,AJC,1.0,FCC,MGH)
      CALL AMULT(FT,MGH,AM)
C
      CALL MOMENT(XO,KJC,1.0,FCC,MGH)
      CALL AMULT(FT,MGH,KM)
      CALL AMULT(FT,FCC,KF)
      DO 828 J=1,3
      AM(J)=AM(J)+ME(J)
828   KM(J)=KM(J)+ME(J)
C
      IF(INERTIA.EQ.0) GOTO 12349
C
      CEN1(1)=-CSA8(I,1)*SM8
      CEN1(2)=-(9.806+CSA8(I,2))*SM8
      CEN1(3)=-CSA8(I,3)*SM8
      CALL AMULT(FT,CEN1,FTIA)
```

```
      CALL MOMENT1(SC2,SC3,0.0,SL8,SM8,I,SAAX8,SAAY8,SAAZ8
      1,XMC,NF,SAX8,SAY8,SAZ8)
      CALL MOMENT(AJC,KJC,SC2,CEN1,MGH)
      CALL AMULT(FT,MGH,MP)
12349 DO 203 J=1,3
      S(J)=-CEN1(J)
      KF(J)=KF(J)+FTIA(J)
203   KM(J)=KM(J)+MP(J)-XMC(J)
      S(2)=CSA8(I,2)*SM8
C
      CALL TRANSP(FT,FTH)
      CALL AMULT(FTH,KF,FC)
C
      PST8=0.0
      WSF8=0.0
      EST8=0.0
      DO 1111 J=1,3
      PST8=PST8+SM8*CSV8(I,J)*CSA8(I,J)
      WSF8=WSF8-FC(J)*KJCV8(I,J)
      EST8=EST8+0.5*SM8*CSV8(I,J)*CSV8(I,J)
1111  CONTINUE
      PSR8=SM8*(SC3*SL8)**2.0*(SAX8(I)*SAAX8(I)+SAZ8(I)*SAAZ8(I))
C     PSG8=SM8*9.81*CSV8(I,2)
      ESR8=0.5*SM8*(SC3*SL8)**2.0*(SAX8(I)**2.0+SAZ8(I)**2.0)
      ESP8=SM8*9.81*CSH8(I,2)
      WSM8=(AM(1)-KM(1))*SAX8(I)+(AM(2)-KM(2))*SAY8(I)
      1+(AM(3)-KM(3))*SAZ8(I)
      ES8=EST8+ESR8+ESP8
      PS8=PST8+PSR8
      WS8=WSF8+WSM8
C
C
      CALL AMULT(FTH,KM,MC)
      CALL AMULT(FTT,MC,ME)
      CALL AMULT(FTT,FC,FE)
C
      CALL MOMENT(KJC,HJC,1.0,FC,MGH)
      CALL AMULT(FTT,MGH,HM)
C
      IF(INERTIA.EQ.0) GOTO 1248
C
      CEN1(1)=-CTA8(I,1)*TM8
      CEN1(2)=-(9.806+CTA8(I,2))*TM8
      CEN1(3)=-CTA8(I,3)*TM8
      CALL AMULT(FTT,CEN1,FTIA)
      CALL MOMENT1(TC2,TC3,0.0,TL8,TM8,I,TAAX8,TAAY8,TAAZ8
      1,XMC,NF,TAX8,TAY8,TAZ8)
      CALL MOMENT(KJC,HJC,TC2,CEN1,MGH)
      CALL AMULT(FTT,MGH,MP)
1248  DO 204 J=1,3
      F(J)=-CEN1(J)
      HF(J)=FTIA(J)+FE(J)
204   HM(J)=HM(J)+MP(J)+ME(J)-XMC(J)
      F(2)=CTA8(I,2)*TM8
C
      CALL TRANSP(FTT,FTH)
      CALL AMULT(FTH,HF,FC)
C
      PTT8=0.0
```

```
      WTF8=0.0
      ETT8=0.0
      DO 1151 J=1,3
      PTT8=PTT8+TM8*CTV8(I,J)*CTA8(I,J)
      WTF8=WTF8-FC(J)*HJCV8(I,J)
      ETT8=ETT8+0.5*TM8*CTV8(I,J)*CTV8(I,J)
1151  CONTINUE
      PTR8=TM8*(TC3*TL8)**2.0*(TAX8(I)*TAAX8(I)+TAZ8(I)*TAAZ8(I))
C     PTG8=TM8*9.81*CTV8(I,2)
      ETR8=0.5*TM8*(TC3*TL8)**2.0*(TAX8(I)**2.0+TAZ8(I)**2.0)
      ETP8=TM8*9.81*CTH8(I,2)
      WTM8=(ME(1)-HM(1))*TAX8(I)+(ME(2)-HM(2))*TAY8(I)
     1+(ME(3)-HM(3))*TAZ8(I)
      ET8=ETT8+ETR8+ETP8
      PT8=PTT8+PTR8
      WTF8=WTF8-WSF8
      WT8=WTF8+WTM8
C
      EEST8=ES8+ET8
      PPST8=PS8+PT8
      WWST8=WS8+WT8
C
C   POWER INTO THE TRUNK
C
      CALL AMULT(FTH,HM,ME)
      PTHIX=-ME(1)*TAX8(I)
      PTHIY=-ME(2)*TAY8(I)
      PTHIZ=-ME(3)*TAZ8(I)
C
C  DISCOMPOSITE OF THE HIP JOINT MOMENT
C
      MGX=FCC(1)*HJC(2)
      MGY=FCC(2)*(XO(1)-HJC(1))
      MLW=ME(3)-MGX-MGY
      MTX=ATA(I,1)*(ATD(I,2)-HJC(2))
      MTY=-ATA(I,2)*(ATD(I,1)-HJC(1))
      MTW=MASS*0.6682*9.806*(ATD(I,1)-HJC(1))
C
      WRITE(7,600) (AF(J),J=1,3),(AM(J),J=1,3)
      WRITE(7,600) (KF(J),J=1,3),(KM(J),J=1,3)
      WRITE(7,600) (HF(J),J=1,3),(HM(J),J=1,3)
      WRITE(7,600) ES8,ET8,EEST8
      WRITE(7,600) PS8,PT8,PPST8
      WRITE(7,600) WS8,WT8,WWST8
      WRITE(7,600) PPELX,PPELY,PPELZ
      WRITE(7,600) PTHIX,PTHIY,PTHIZ
      WRITE(7,600) (S(J),J=1,3),(F(J),J=1,3)
      WRITE(7,600) MTX,MTY,MTW,MGX,MGY,MLW
C
700   CONTINUE
C
      IF(ISTEP.EQ.2) GOTO 1005
      ISTEP=ISTEP+1
      GO TO 1002
C
1005  CONTINUE
C
C
600   FORMAT(2X,3(F12.6,2X))
```

```
601   FORMAT(2X,2(F12.6,2X))
603     FORMAT(1X,//)
1200    WRITE(7,646) 99999
        WRITE(8,646) 99999
646     FORMAT(3X,I8)
        STOP
      END
```

PROGRAM "KINETICS.SUB"

```
      SUBROUTINE AMULT(A,B,C)
C
C     C(3*1)=A(3*3) X B(3*1)
C
        REAL A,B,C
      DIMENSION A(3,3),B(3),C(3)
      DO 100 I=1,3
      C(I)=0.0
      DO 100 J=1,3
  100 C(I)=C(I)+A(I,J)*B(J)
      RETURN
      END
C
C
C
C
        SUBROUTINE MOMENT(A,B,C2,F,XMC)
        DIMENSION A(3),XMC(3),B(3),F(3),C(3)
C
        XMC(1)=(A(2)-B(2))*F(3)-(A(3)-B(3))*F(2)
        XMC(2)=(A(3)-B(3))*F(1)-(A(1)-B(1))*F(3)
        XMC(3)=(A(1)-B(1))*F(2)-(A(2)-B(2))*F(1)
        DO 10 J=1,3
10      XMC(J)=XMC(J)*C2
        RETURN
        END
C
C
C
        SUBROUTINE MOMENT1(C2,C3,C4,SLL,SM,I,X,Y,Z,XM,N,WX,WY,WZ)
        REAL X,Y,Z,WX,WY,WZ,XM
        DIMENSION X(150),Y(150),Z(150),WX(150),WY(150),WZ(150),XM(3)
C
        SI=(C3*SLL)**2*SM
        SI=SI+SM*(C2*SLL)**2
        SIY=(C4*SLL)**2*SM
        XM(1)=X(I)*SI+(SI-SIY)*WY(I)*WZ(I)
        XM(2)=SIY*Y(I)
        XM(3)=Z(I)*SI+(SIY-SI)*WX(I)*WY(I)
        RETURN
        END
C
C
C
        SUBROUTINE TRANSP(T,TT)
        REAL T,TT
        DIMENSION T(3,3),TT(3,3)
C
        DO 10 J=1,3
```

```
      DO 10 K=1,3
      TT(J,K)=T(K,J)
10    CONTINUE
      RETURN
      END
C
C
C
      SUBROUTINE AMULT2(N,T,X,Y,Z)
      REAL X,Y,Z,T,XX,YY,TT
      DIMENSION X(150),Y(150),Z(150),T(150,3,3),XX(3),YY(3),TT(3,3)
C
      DO 30 I=1,N
      XX(1)=X(I)
      XX(2)=Y(I)
      XX(3)=Z(I)
      DO 10 J=1,3
      DO 10 K=1,3
10    TT(J,K)=T(I,J,K)
      DO 20 J=1,3
      YY(J)=0.0
      DO 20 K=1,3
      YY(J)=YY(J)+TT(J,K)*XX(K)
20    CONTINUE
      X(I)=YY(1)
      Y(I)=YY(2)
      Z(I)=YY(3)
30    CONTINUE
      RETURN
      END
```

PROGRAM "PLOTAMPU.MAJ"

```
      DIMENSION ASX1(150),ASY1(150),ASZ1(150),MAX1(150),MAY1(150),MAZ1(150)
     1,ATX1(150),ATY1(150),ATZ1(150),MKX1(150),MKY1(150),MKZ1(150)
     2,ATRX(150),ATRY(150),ATRZ(150),MHX1(150),MHY1(150),MHZ1(150)
     5,HA(150),KA(150),HAA(150),KAA(150),ES1(150),ET1(150),EEST1(150)
     6,FCX1(150),FCY1(150),FCZ1(150),ALX1(150),ALY1(150),ALZ1(150)
     1,FCX2(150),FCY2(150),FCZ2(150),FAX2(150),FAY2(150),FAZ2(150)
     7,ALX2(150),ALY2(150),ALZ2(150),MAX2(150),MAY2(150),MAZ2(150)
     8,MHX2(150),MHY2(150),MHZ2(150),ATX2(150),ATY2(150),ATZ2(150)
     9,ASX2(150),ASY2(150),ASZ2(150),PS1(150),PT1(150),PPST1(150)
     1,FHX2(150),FHY2(150),FHZ2(150),FKX2(150),FKY2(150),FKZ2(150)
     2,MKX2(150),MKY2(150),MKZ2(150),AH(150),AK(150),AAH(150),AAK(150)
     3,HTOD(150),HPED(150),HHJD(150),APX(150),APY(150),APZ(150)
     4,ATX(150),ATY(150),ATZ(150),WS1(150),WT1(150),WWST1(150)
     5,ES2(150),ET2(150),EEST2(150),PS2(150),PT2(150),PPST2(150)
     6,WS2(150),WT2(150),WWST2(150),ASW7(150),ASW8(150),VAUL7(150)
     7,VAUL8(150),ASOK(150),XO1(150),XO2(150),ZO1(150),ZO2(150)
     8,MHKZ1(150),MSPZ1(150),MKAZ1(150),MHKX1(150),MSPX1(150),MKAX1(150)
     8,MHKZ2(150),MSPZ2(150),MKAZ2(150),MHKX2(150),MSPX2(150),MKAX2(150)
     9,MHX(150),MHY(150),MHZ(150),AATX(150),AATY(150),AATZ(150)
     9,PX1(150),PY1(150),PZ1(150),PX2(150),PY2(150),PZ2(150)
     9,ABOX(150),ABOY(150),ABOZ(150),FCXX(150),FCYY(150),FCZZ(150)
     9,PHX1(150),PHY1(150),PHZ1(150),PHX2(150),PHY2(150),PHZ2(150)
     1,MTX1(150),MTY1(150),MTW1(150),MGX1(150),MGY1(150),MLW1(150)
     1,MTX2(150),MTY2(150),MTW2(150),MGX2(150),MGY2(150),MLW2(150)
      REAL MAX1,MAY1,MAZ1,MKX1,MKY1,MKZ1,MHX1,MHY1,MHZ1,ALX1,ALY1,ALZ1
     1,MHX2,MHY2,MHZ2,MASS,MKX2,MKY2,MKZ2,MAX2,MAY2,MAZ2
     2,KA,KAA,ALX2,ALY2,ALZ2,MHKZ1,MSPZ1,MKAZ1,MHKX1,MSPX1,MKAX1
     3,MHKZ2,MSPZ2,MKAZ2,MHKX2,MSPX2,MKAX2,MHX,MHY,MHZ
     4,MTX1,MTY1,MTW1,MGX1,MGY1,MLW1
     4,MTX2,MTY2,MTW2,MGX2,MGY2,MLW2
      INTEGER P1,P2
      CHARACTER*8 XNAME,XLIMB
      CHARACTER*9 PARA
      COMMON /CONS/A1,A2,FFF,IHS1,ITF1,IHS2,ITF2
C
C     READ IN VALUES FROM STAGE 4
C
        PRINT *,'        GRAPHIC OUTPUT OF THE RESULTS'
        PRINT *,'READ DATA'
        READ(5,1) XNAME
        READ(1,1) XNAME
1       FORMAT(1X,8A)
        READ(5,*) MASS,WEIGHT
        READ(1,*) MASS,WEIGHT
C
C
        READ(3,*) NF1,ITF1,IHS1,NF2,ITF2,IHS2
        NF=ITF2-IHS1+1
C
        READ(1,*) ISOUND,NFF,ITF,IHS
```

```
      READ(5,*) INVOLV,NFF,ITF,IHS
C
      DO 99 I=1,NF
      READ(1,*) XO1(I),AA,ZO1(I)          !CENTRE OF PRESSURE
      READ(1,*) FCX1(I),FCY1(I),FCZ1(I) !GROUND REACTIONS
      READ(1,*) ALX1(I),ALY1(I),ALZ1(I) !TEMPORAL DUMMY VARIABLE
      READ(1,*) ASX1(I),ASY1(I),ASZ1(I) !SHANK INERTIA
      READ(1,*) MAX1(I),MAY1(I),MAZ1(I) !ANKLE MOMENT
      READ(1,*) ATX1(I),ATY1(I),ATZ1(I) !THIGH INERTIA
      READ(1,*) MKX1(I),MKY1(I),MKZ1(I) !KNEE MOMENT
      READ(1,*) ATRX(I),ATRY(I),ATRZ(I) !TRUNK INERTIA
      READ(1,*) MHX1(I),MHY1(I),MHZ1(I) !HIP MOMENT
      READ(1,*) ES1(I),ET1(I),EEST1(I)
      READ(1,*) PS1(I),PT1(I),PPST1(I)
      READ(1,*) WS1(I),WT1(I),WWST1(I)
      READ(1,*) PX1(I),PY1(I),PZ1(I)     !PELVIC MOMENT POWER
      READ(1,*) PHX1(I),PHY1(I),PHZ1(I) !HIP MOMENT POWER
      READ(1,*) MTX1(I),MTY1(I),MTW1(I) !TORSO MOMENTS
      READ(1,*) MGX1(I),MGY1(I),MLW1(I) !HIP MOMENTS COMPONENTS
      MHKZ1(I)=MHZ1(I)+MKZ1(I)
      MKAZ1(I)=MKZ1(I)+MAZ1(I)
      MSPZ1(I)=MHKZ1(I)+MAZ1(I)
      MHKX1(I)=MHX1(I)+MKX1(I)
      MKAX1(I)=MKX1(I)+MAX1(I)
      MSPX1(I)=MHKX1(I)+MAX1(I)
   99 CONTINUE
      READ(1,*) ICHECK
      IF(ICHECK.NE.99999) PRINT *,'READ(1,*) ERROR'
C
C
C
      DO 300 I=1,NF
      READ(5,*) XO2(I),AA,ZO2(I)
      READ(5,*) FCX2(I),FCY2(I),FCZ2(I) !GROUND REACTIONS
      READ(5,*) ALX2(I),ALY2(I),ALZ2(I) !TEMPORAL DUMMY
      READ(5,*) FAX2(I),FAY2(I),FAZ2(I) !ANKLE FORCE
      READ(5,*) MAX2(I),MAY2(I),MAZ2(I) !ANKLE MOMENT
      READ(5,*) FKX2(I),FKY2(I),FKZ2(I) !KNEE FORCE
      READ(5,*) MKX2(I),MKY2(I),MKZ2(I) !KNEE MOMENT
      READ(5,*) FHX2(I),FHY2(I),FHZ2(I) !HIP FORCE
      READ(5,*) MHX2(I),MHY2(I),MHZ2(I) !HIP MOMENT
      READ(5,*) ES2(I),ET2(I),EEST2(I)
      READ(5,*) PS2(I),PT2(I),PPST2(I)
      READ(5,*) WS2(I),WT2(I),WWST2(I)
      READ(5,*) PX2(I),PY2(I),PZ2(I)     !PELVIC POWER
      READ(5,*) PHX2(I),PHY2(I),PHZ2(I) !HIP MOMENT POWER
      READ(5,*) ASX2(I),ASY2(I),ASZ2(I) !SHANK INERTIA
      READ(5,*) ATX2(I),ATY2(I),ATZ2(I) !THIGH INERTIA
      READ(5,*) MTX2(I),MTY2(I),MTW2(I) !TORSO MOMENTS
      READ(5,*) MGX2(I),MGY2(I),MLW2(I) !HIP MOMENTS COMPONENTS
      MHKZ2(I)=MHZ2(I)+MKZ2(I)
      MKAZ2(I)=MKZ2(I)+MAZ2(I)
      MSPZ2(I)=MHKZ2(I)+MAZ2(I)
      MHKX2(I)=MHX2(I)+MKX2(I)
      MKAX2(I)=MKX2(I)+MAX2(I)
      MSPX2(I)=MHKX2(I)+MAX2(I)
      MHX(I)=MHX1(I)+MHX2(I)
      MHY(I)=MHY1(I)+MHY2(I)  !TOTAL HIP MOMENT
      MHZ(I)=MHZ1(I)+MHZ2(I)
```

```
      FCXX(I)=FCX1(I)+FCX2(I)
      FCYY(I)=FCY1(I)+FCY2(I) !TOTAL GROUND REACTIONS
      FCZZ(I)=FCZ1(I)+FCZ2(I)
      ALX1(I)=ASX1(I)+ATX1(I)
      ALY1(I)=ASY1(I)+ATY1(I) !TOTAL LEG INERTIA
      ALZ1(I)=ASZ1(I)+ATZ1(I)
      ALX2(I)=ASX2(I)+ATX2(I)
      ALY2(I)=ASY2(I)+ATY2(I) !TOTAL LEG INERTIA
      ALZ2(I)=ASZ2(I)+ATZ2(I)
      ABOX(I)=MTX1(I)+MTY1(I)+MTW1(I)
      ABOX(I)=(MTX2(I)+MTY2(I)+MTW2(I)+ABOX(I))*0.5
      ABOY(I)=MHZ(I)
      ABOZ(I)=MHZ(I)-ABOX(I)
300   CONTINUE
      READ(5,*) ICHECK
      IF(ICHECK.NE.99999) PRINT *,'READ(5,*) ERROR'
C
      AKK=900.0
      BKK=900.0
      DO 302 I=1,NF
      READ(3,*) HA(I),KA(I),HAA(I),KAA(I)
      READ(3,*) VAUL7(I),ASW7(I)
      READ(9,*) AH(I),AK(I),AAH(I),AAK(I)
      READ(9,*) VAUL8(I),ASW8(I),ASOK(I)
      IF(AKK.GT.KA(I)) AKK=KA(I)
      IF(BKK.GT.AK(I)) BKK=AK(I)
302   CONTINUE
C
      READ(3,*) ICHECK
      IF(ICHECK.NE.99999) PRINT *,'READ(3,*) ERROR'
      READ(3,*) NFNF
      NFN=NFNF-4
C
      IF(ISOUND.EQ.2) THEN
      CALL IMPOSE(NF,NFN,FCXX,FCYY,FCZZ,FCX1,FCY1,FCZ1,FCX2,FCY2,FCZ2)
      CALL IMPOSE(NF,NFN,MHX,MHY,MHZ,MHX1,MHY1,MHZ1,MHX2,MHY2,MHZ2)
      ELSE
      CALL IMPOSE(NF,NFN,FCXX,FCYY,FCZZ,FCX2,FCY2,FCZ2,FCX1,FCY1,FCZ1)
      CALL IMPOSE(NF,NFN,MHX,MHY,MHZ,MHX2,MHY2,MHZ2,MHX1,MHY1,MHZ1)
      END IF
C
      IF(ISOUND.EQ.1) THEN
      IP11=1
      IP12=NF1
      IP1X=NF1
      IP21=NF-NF2+1
      IP2X=IP21
      IP22=NF
      IS1=1
      IS2=NFN
      IN1=NF-NFN+1
      IN2=NF
      ELSE
      IP11=NF-NF2+1
      IP12=NF
      IP1X=IP11
      IP21=1
      IP22=NF1
      IP2X=NF1
```

```
      IS1=NF-NFN+1
      IS2=NF
      IN1=1
      IN2=NFN
      END IF
C
      DO 323 I=1,NF
C     VAUL7(I)=VAUL7(I)-VAUL7(IP11)
      FCYY(I)=FCYY(I)-WEIGHT
C     WRITE(8,8888)
C     WRITE(8,8888) FCXX(I),FCYY(),FCZZ(I)
323   CONTINUE
C
      DO 303 I=1,NF
      READ(3,*) APX(I),APY(I),APZ(I)
      READ(3,*) ATX(I),ATY(I),ATZ(I)
303   CONTINUE
C  ====== DETREND =======
C     PXX=(APX(NFN)-APX(1))/FLOAT(NFN-1)
C     PYY=(APY(NFN)-APY(1))/FLOAT(NFN-1)
C     PZZ=(APZ(NFN)-APZ(1))/FLOAT(NFN-1)
C     AXX=(ATX(NFN)-ATX(1))/FLOAT(NFN-1)
C     AYY=(ATY(NFN)-ATY(1))/FLOAT(NFN-1)
C     AZZ=(ATZ(NFN)-ATZ(1))/FLOAT(NFN-1)
C     DO 543 I=1,NFN
C     APX(I)=APX(I)-PXX*FLOAT(I-1)
C     APY(I)=APY(I)-PYY*FLOAT(I-1)
C     APZ(I)=APZ(I)-PZZ*FLOAT(I-1)
C     ATX(I)=ATX(I)-AXX*FLOAT(I-1)
C     ATY(I)=ATY(I)-AYY*FLOAT(I-1)
C     ATZ(I)=ATZ(I)-AZZ*FLOAT(I-1)
C543  CONTINUE
C   ===== ANGULAR ACCELERATION =====
      CALL TORDIF(MASS,NFN,ATX,ATY,ATZ,AATX,AATY,AATZ)
C  ====== EXTEND NFN DATA TO NF ======
C     DO 544 I=NFN,NF
C     APX(I)=APX(I-NFN+1)
C     APY(I)=APY(I-NFN+1)
C     APZ(I)=APZ(I-NFN+1)
C     ATX(I)=ATX(I-NFN+1)
C     ATY(I)=ATY(I-NFN+1)
C     ATZ(I)=ATZ(I-NFN+1)
C     AATX(I)=AATX(I-NFN+1)
C     AATY(I)=AATY(I-NFN+1)
C     AATZ(I)=AATZ(I-NFN+1)
C544  CONTINUE
C
      IF(ISOUND.NE.1) GOTO 2
        DO 113 I=1,NF
        FCZ1(I)=-FCZ1(I)
        MAX1(I)=-MAX1(I)
        MAY1(I)=-MAY1(I)
        MKX1(I)=-MKX1(I)
        MKY1(I)=-MKY1(I)
        MHX1(I)=-MHX1(I)
        MHY1(I)=-MHY1(I)
        MHKX1(I)=-MHKX1(I)
        MKAX1(I)=-MKAX1(I)
        MSPX1(I)=-MSPX1(I)
```

```
113     CONTINUE
2       CONTINUE
C
C
        IF(INVOLV.NE.1) GOTO 1234
        DO 114 I=1,NF
        FCZ2(I)=-FCZ2(I)
        MAX2(I)=-MAX2(I)
        MAY2(I)=-MAY2(I)
        MKX2(I)=-MKX2(I)
        MKY2(I)=-MKY2(I)
        MHX2(I)=-MHX2(I)
        MHY2(I)=-MHY2(I)
        MHKX2(I)=-MHKX2(I)
        MKAX2(I)=-MKAX2(I)
        MSPX2(I)=-MSPX2(I)
114     CONTINUE
1234    CONTINUE
C
        AX=XO1(IP1X)
        AZ=ZO1(IP1X)
        DO 433 I=IP11,IP12
        XO1(I)=XO1(I)-AX
        ZO1(I)=ZO1(I)-AZ
433     CONTINUE
        AX=XO2(IP2X)
        AZ=ZO2(IP2X)
        DO 434 I=IP21,IP22
        XO2(I)=XO2(I)-AX
        ZO2(I)=ZO2(I)-AZ
434     CONTINUE
C
630     FORMAT(////,20X,'PATIENTS CODE:  ',8A)
631     FORMAT(5X,'         RIGHT ABOVE-KNEE AMPUTEE ',////)
632     FORMAT(5X,'         LEFT ABOVE-KNEE AMPUTEE ',////)
C
        PRINT *,'PRINT OUT THE RESULTS'
        ITEXT=0
        IF(ITEXT.EQ.0) GOTO 9011
        WRITE(7,630) XNAME
        IF(ISOUND.EQ.1) THEN
        WRITE(7,631)
        ELSE
        WRITE(7,632)
        END IF
C
9011    IF(ITEXT.EQ.1) WRITE(7,754) MASS,IHS1,ITF1,IHS2,ITF2
        IF(ITEXT.EQ.0) WRITE(7,7544) MASS,INVOLV,IHS1,ITF1,IHS2,ITF2,NFN
754     FORMAT(15X,'Mass=',F10.3,//,'Left HS=',I3,3X,'Left TF=',I3,6X
        1,'Right HS=',3X,'Right TF=',I3)
7544    FORMAT(2X,F10.3,6I5)
C
C
        IF(ITEXT.EQ.0) GOTO 9012
        WRITE(7,633)
633     FORMAT(//,10X,'UPPER TORSO AND PELVIS KINEMATIC DATA',////
        1,20X,'PELVIC ROTATION',30X,'TORSO ROTATION',15X,'TORSO HEIGHT'
        2,8X,'PELVIC HEIGHT',/,17X,'(Degrees)',36X,'(Degrees)',36X,
        3'(Meters)',//,4X,'I',6X,'APXD',11X,'APYD',11X,'APZD',11X
```

```
     4,'ATXD',11X,'ATYD',11X,'ATZD')
9012 DO 330 I=IN1,IN2
     IF(I.NE.IJI1.AND.IJI2.NE.I) THEN
     WRITE(7,634) I,ATX(I),ATY(I),ATZ(I),ATRX(I),ATRY(I),ATRZ(I)
     ELSE
     WRITE(7,6344)I,ATX(I),ATY(I),ATZ(I),ATRX(I),ATRY(I),ATRZ(I)
     END IF
330  CONTINUE
634  FORMAT(4X,I2,2X,8(F10.3,5X))
6344 FORMAT(4X,I2,'*',1X,8(F10.3,5X))
C
     DO 331 I=IN1,IN2
331  WRITE(7,634) I,FCXX(I),FCYY(I),FCZZ(I),ABOX(I),ABOY(I),ABOZ(I)

     IF(ITEXT.EQ.0) GOTO 9214
     WRITE(7,666)
666  FORMAT(1X,/////,30X,'DYNAMIC DATA OF THE PROSTHETIC SIDE',////)
9214 CONTINUE
C
C
C    ANGLE TABLES ARE OUTPUT HERE
C
       IF(ITEXT.EQ.0) GOTO 9003
     WRITE(7,35)
     WRITE(7,65)
35     FORMAT(9X,//,9X,'HIP & KNEE ADDUCTION & ABDUCTION ANGLES'
     1,10X,'GROUND REACTION FORCES')
65   FORMAT(1X,'I',6X,' HIP FLEX-EXT',4X,' KNEE FLEX',4X
     1,'HIP ABD-ADD',15X,'Fx              Fy              Fz')
C
9003 DO 305 I=IN1,IN2
C    AK(I)=AK(I)-BKK
     IF(IJI1.NE.I.AND.IJI2.NE.I) THEN
     WRITE(7,635) I,AH(I),AK(I),VAUL8(I),FCX2(I),FCY2(I),FCZ2(I)
     ELSE
     WRITE(7,6355) I,AH(I),AK(I),VAUL8(I),FCX2(I),FCY2(I),FCZ2(I)
     END IF
305  CONTINUE
635  FORMAT(1X,I2,8X,3(F8.3,7X),3X,3(F10.4,7X))
6355 FORMAT(1X,I2,'*',7X,3(F8.3,7X),3X,3(F10.4,7X))
C
     IF(ITEXT.EQ.0) GOTO 9015
     WRITE(7,601)
601  FORMAT(//,30X,'HIP FORCES AND MOMENTS IN FUNERAL SYSTEM')
     WRITE(7,602)
602  FORMAT(1X,' I',9X,'FHX',9X,'FHY',9X,'FHZ',
     119X,'MHX',7X,'MHY',7X,'MHZ',/)
9015 DO 603 I=IN1,IN2
     IF(IJI1.NE.I.AND.IJI2.NE.I) THEN
     WRITE(7,46) I,PX2(I),PY2(I),PZ2(I),MHX2(I),MHY2(I),MHZ2(I)
     ELSE
     WRITE(7,466) I,PX2(I),PY2(I),PZ2(I),MHX2(I),MHY2(I),MHZ2(I)
     END IF
603  CONTINUE
46   FORMAT(1X,I3,2X,3(F10.4,2X),10X,3(F10.4,2X))
466  FORMAT(1X,I3,'*',1X,3(F10.4,2X),10X,3(F10.4,2X))
C
     IF(ITEXT.EQ.0) GOTO 9016
     WRITE(7,605)
```

```
605     FORMAT(//,20X,'KNEE FORCES AND MOMENTS IN KNEE AXIS SYSTEM ')
        WRITE(7,620)
620     FORMAT(5X,'I',8XX,'FKX',9X,'FKY',9X,'FKZ',20X,
        1'MKX',8X,'MKY',8X,'MKZ',//)
9016    DO 604 I=IN1,IN2
        IF(IJI1.NE.I.AND.IJI2.NE.I) THEN
        WRITE(7,47) I,ALX2(I),ALY2(I),ALZ2(I),MKX2(I),MKY2(I),MKZ2(I)
        ELSE
        WRITE(7,477) I,ALX2(I),ALY2(I),ALZ2(I),MKX2(I),MKY2(I),MKZ2(I)
        END IF
604     CONTINUE
47      FORMAT(3X,I3,3(3X,F10.4),10X,3(3X,F10.4))
477     FORMAT(3X,I3,'*',3(3X,F10.4),10X,3(3X,F10.4))
C
        IF(ITEXT.EQ.0) GOTO 9017
        WRITE(7,619)
        WRITE(7,618)
619     FORMAT(//,10X,'ANKLE FORCES AND MOMENTS IN TIBIAL AXIS SYSTEM',/)
618     FORMAT(7X,'I',10X,'FAX',10X,'FAY',10X,'FAZ',
        120X,'MAX',10X,'MAY',10X,'MAZ',/)
9017    DO 42 I=IN1,IN2
        IF(IJI1.NE.I.AND.IJI2.NE.I) THEN
        WRITE(7,45) I,PHX2(I),PHY2(I),PHZ2(I),MAX2(I),MAY2(I),MAZ2(I)
        ELSE
        WRITE(7,455)I,PHX2(I),PHY2(I),PHZ2(I),MAX2(I),MAY2(I),MAZ2(I)
        END IF
42      CONTINUE
C
        IF(ITEXT.EQ.0) GOTO 9027
        WRITE(7,651)
        WRITE(7,652)
651     FORMAT(//,10X,'SUPPORT MOMENTS ',/)
652     FORMAT(7X,'I',10X,'MHKZ',10X,'MKAZ',10X,'MSPZ',
        120X,'MHKX',10X,'MKAX',10X,'MSPX',/)
9027    DO 427 I=IN1,IN2
        IF(IJI1.NE.I.AND.IJI2.NE.I) THEN
        WRITE(7,45)I,MHKZ2(I),MKAZ2(I),MSPZ2(I),MHKX2(I),MKAX2(I),MSPX2(I)
        ELSE
        WRITE(7,455)I,MHKZ2(I),MKAZ2(I),MSPZ2(I),MHKX2(I),MKAX2(I),MSPX2(I)
        END IF
427     CONTINUE
45      FORMAT(6X,I3,8X,3(F10.4,4X),8X,3(F10.4,4X))
455     FORMAT(6X,I3,'*',8X,3(F10.4,4X),8X,3(F10.4,4X))
C
        DO 7177 I=IN1,IN2
7177    WRITE(7,45) I,MTX2(I),MTY2(I),MTW2(I),MGX2(I),MGY2(I),MLW2(I)
C
        IF(ITEXT.EQ.0) GOTO 9019
        WRITE(7,711)
711     FORMAT(1X,//,10X,'ENERGY LEVEL, ENERGY CHANGE RATE AND POWER',/
        1,16X,'ENERGY LEVEL',30X,'ENERGY CHANGE RATE',30X,'POWER',/,2X
        2,'I',3(6X,'SHANK',8X,'THIGH',8X,'TOTAL',3X))
9019    DO 712 I=IN1,IN2
        IF(IJI1.NE.I.AND.IJI2.NE.I) THEN
        WRITE(7,713) I,ES2(I),ET2(I),EEST2(I),PS2(I),PT2(I),PPST2(I)
        1,WS2(I),WT2(I),WWST2(I)
        ELSE
        WRITE(7,7133) I,ES2(I),ET2(I),EEST2(I),PS2(I),PT2(I),PPST2(I)
        1,WS2(I),WT2(I),WWST2(I)
```

```
        END IF
712     CONTINUE
713     FORMAT(2X,I2,3X,3(3F12.1,3X))
7133    FORMAT(2X,I2,'*',2X,3(3F12.1,3X))
C
C
        IF(ITEXT.EQ.0) GOTO 9020
        WRITE(7,266)
266     FORMAT(/////,30X,'DYNAMIC DATA OF THE SOUND SIDE')
C
9020    CONTINUE
C
        IF(ITEXT.EQ.0) GOTO 9013
      WRITE(7,35)
      WRITE(7,65)
C
9013    DO 3005 I=IS1,IS2
C       KA(I)=KA(I)-AKK
        IF(IJI1.NE.I.AND.IJI2.NE.I) THEN
        WRITE(7,635) I,HA(I),KA(I),VAUL7(I),FCX1(I),FCY1(I),FCZ1(I)
        ELSE
        WRITE(7,6355) I,HA(I),KA(I),VAUL7(I),FCX1(I),FCY1(I),FCZ1(I)
        END IF
3005    CONTINUE
C
        IF(ITEXT.EQ.0) GOTO 9021
        WRITE(7,601)
        WRITE(7,602)
9021    DO 1603 I=IS1,IS2
        IF(IJI1.NE.I.AND.IJI2.NE.I) THEN
        WRITE(7,46) I,PX1(I),PY1(I),PZ1(I),MHX1(I),MHY1(I),MHZ1(I)
        ELSE
        WRITE(7,466) I,PX1(I),PY1(I),PZ1(I),MHX1(I),MHY1(I),MHZ1(I)
        END IF
1603    CONTINUE
C
        IF(ITEXT.EQ.0) GOTO 9022
        WRITE(7,605)
        WRITE(7,620)
9022    DO 1604 I=IS1,IS2
        IF(IJI1.NE.I.AND.IJI2.NE.I) THEN
        WRITE(7,47) I,ALX1(I),ALY1(I),ALZ1(I),MKX1(I),MKY1(I),MKZ1(I)
        ELSE
        WRITE(7,477) I,ALX1(I),ALY1(I),ALZ1(I),MKX1(I),MKY1(I),MKZ1(I)
        END IF
1604    CONTINUE
C
        IF(ITEXT.EQ.0) GOTO 9023
        WRITE(7,619)
        WRITE(7,618)
9023    DO 142 I=IS1,IS2
        IF(IJI1.NE.I.AND.IJI2.NE.I) THEN
        WRITE(7,45) I,PHX1(I),PHY1(I),PHZ1(I),MAX1(I),MAY1(I),MAZ1(I)
        ELSE
        WRITE(7,455)I,PHX1(I),PHY1(I),PHZ1(I),MAX1(I),MAY1(I),MAZ1(I)
        END IF
142     CONTINUE
C
        IF(ITEXT.EQ.0) GOTO 9028
```

```
      WRITE(7,651)
      WRITE(7,652)
9028  DO 428 I=IS1,IS2
      IF(IJI1.NE.I.AND.IJI2.NE.I) THEN
      WRITE(7,45)I,MHKZ1(I),MKAZ1(I),MSPZ1(I),MHKX1(I),MKAX1(I),MSPX1(I)
      ELSE
      WRITE(7,455)I,MHKZ1(I),MKAZ1(I),MSPZ1(I),MHKX1(I),MKAX1(I),MSPX1(I)
      END IF
428   CONTINUE
C
      DO 717 I=IS1,IS2
717   WRITE(7,45) I,MTX1(I),MTY1(I),MTW1(I),MGX1(I),MGY1(I),MLW1(I)
C
      IF(ITEXT.EQ.0) GOTO 9024
      WRITE(7,711)
9024  DO 714 I=IS1,IS2
      IF(IJI1.NE.I.AND.IJI2.NE.I) THEN
      WRITE(7,713) I,ES1(I),ET1(I),EEST1(I),PS1(I),PT1(I),PPST1(I)
      1,WS1(I),WT1(I),WWST1(I)
      ELSE
      WRITE(7,7133) I,ES1(I),ET1(I),EEST1(I),PS1(I),PT1(I),PPST1(I)
      1,WS1(I),WT1(I),WWST1(I)
      END IF
714   CONTINUE
C
C
C
      PRINT *,'WEIGHT-NORMALIZITION OF THE RESULTS'
      DO 110 I=1,NF
      FCXX(I)=FCXX(I)/WEIGHT
      FCYY(I)=FCYY(I)/WEIGHT
      FCZZ(I)=FCZZ(I)/WEIGHT
      ABOX(I)=ABOX(I)/WEIGHT
      ABOY(I)=ABOY(I)/WEIGHT
      ABOZ(I)=ABOZ(I)/WEIGHT
C
      MAX1(I)=MAX1(I)/WEIGHT
      MAY1(I)=MAY1(I)/WEIGHT
      MAZ1(I)=MAZ1(I)/WEIGHT
      ALX1(I)=ALX1(I)/WEIGHT
      ALY1(I)=ALY1(I)/WEIGHT
      ALZ1(I)=ALZ1(I)/WEIGHT
C
      ATRX(I)=ATRX(I)/WEIGHT
      ATRY(I)=ATRY(I)/WEIGHT
      ATRZ(I)=ATRZ(I)/WEIGHT
      MHX1(I)=MHX1(I)/WEIGHT
      MHY1(I)=MHY1(I)/WEIGHT
      MHZ1(I)=MHZ1(I)/WEIGHT
C
      ASX1(I)=ASX1(I)/WEIGHT
      ASY1(I)=ASY1(I)/WEIGHT
      ASZ1(I)=ASZ1(I)/WEIGHT
      ATX1(I)=ATX1(I)/WEIGHT
      ATY1(I)=ATY1(I)/WEIGHT
      ATZ1(I)=ATZ1(I)/WEIGHT
      MKX1(I)=MKX1(I)/WEIGHT
      MKY1(I)=MKY1(I)/WEIGHT
      MKZ1(I)=MKZ1(I)/WEIGHT
```

```
C
      MTX1(I)=MTX1(I)/WEIGHT
      MTY1(I)=MTY1(I)/WEIGHT
      MTW1(I)=MTW1(I)/WEIGHT
      MGX1(I)=MGX1(I)/WEIGHT
      MGY1(I)=MGY1(I)/WEIGHT
      MLW1(I)=MLW1(I)/WEIGHT
110   CONTINUE
C
C
      DO 111 I=1,NF
      FCX2(I)=FCX2(I)/WEIGHT
      FCY2(I)=FCY2(I)/WEIGHT
      FCZ2(I)=FCZ2(I)/WEIGHT
C
      MAX2(I)=MAX2(I)/WEIGHT
      MAY2(I)=MAY2(I)/WEIGHT
      MAZ2(I)=MAZ2(I)/WEIGHT
      FAX2(I)=FAX2(I)/WEIGHT
      FAY2(I)=FAY2(I)/WEIGHT
      FAZ2(I)=FAZ2(I)/WEIGHT
C
      FHX2(I)=FHX2(I)/WEIGHT
      FHY2(I)=FHY2(I)/WEIGHT
      FHZ2(I)=FHZ2(I)/WEIGHT
      MHX2(I)=MHX2(I)/WEIGHT
      MHY2(I)=MHY2(I)/WEIGHT
      MHZ2(I)=MHZ2(I)/WEIGHT
C
      FKX2(I)=FKX2(I)/WEIGHT
      FKY2(I)=FKY2(I)/WEIGHT
      FKZ2(I)=FKZ2(I)/WEIGHT
      MKX2(I)=MKX2(I)/WEIGHT
      MKY2(I)=MKY2(I)/WEIGHT
      MKZ2(I)=MKZ2(I)/WEIGHT
C
      ASX2(I)=ASX2(I)/WEIGHT
      ASY2(I)=ASY2(I)/WEIGHT
      ASZ2(I)=ASZ2(I)/WEIGHT
      ATX2(I)=ATX2(I)/WEIGHT
      ATY2(I)=ATY2(I)/WEIGHT
      ATZ2(I)=ATZ2(I)/WEIGHT
C
      MTX2(I)=MTX2(I)/WEIGHT
      MTY2(I)=MTY2(I)/WEIGHT
      MTW2(I)=MTW2(I)/WEIGHT
      MGX2(I)=MGX2(I)/WEIGHT
      MGY2(I)=MGY2(I)/WEIGHT
      MLW2(I)=MLW2(I)/WEIGHT
C
      MHX(I)=MHX(I)/WEIGHT
      MHY(I)=MHY(I)/WEIGHT
      MHZ(I)=MHZ(I)/WEIGHT
      ALX2(I)=ALX2(I)/WEIGHT
      ALY2(I)=ALY2(I)/WEIGHT
      ALZ2(I)=ALZ2(I)/WEIGHT
      MHKZ2(I)=MHKZ2(I)/WEIGHT
      MKAZ2(I)=MKAZ2(I)/WEIGHT
      MSPZ2(I)=MSPZ2(I)/WEIGHT
```

```
            MHKX2(I)=MHKX2(I)/WEIGHT
            MKAX2(I)=MKAX2(I)/WEIGHT
            MSPX2(I)=MSPX2(I)/WEIGHT
            MHKZ1(I)=MHKZ1(I)/WEIGHT
            MKAZ1(I)=MKAZ1(I)/WEIGHT
            MSPZ1(I)=MSPZ1(I)/WEIGHT
            MHKX1(I)=MHKX1(I)/WEIGHT
            MKAX1(I)=MKAX1(I)/WEIGHT
            MSPX1(I)=MSPX1(I)/WEIGHT
C
111         CONTINUE
C
C
            PRINT *,'PLOT THE RESULTS'
            HS1=FLOAT(IHS1)
            TF1=FLOAT(ITF1)
            HS2=FLOAT(IHS2)
            TF2=FLOAT(ITF2)
            BE2=0.0
            BE1=0.0
            FFF=TF2-HS1+1.0
            A1=(HS2-HS1+1.0)/FFF
            A2=(TF1-HS1+1.0)/FFF
            FFF=TF2-HS1+1.0
C
            IF(ISOUND.EQ.1) THEN
            P1=7
            P2=2
            ELSE
            P1=2
            P2=7
            END IF
C
C
            CALL RCO(14,'PFILE;')
            CALL UNITS(25.4)
            CALL DEVPAP(70.0,8.0,0)
            CALL SHIFT2(1.0,1.0)
C
C           CALL ZPLTT(20.0,20.0,1,1,0,0,0,NFN,0,'TORSO ANG*.',ATX,ATY
C           9,'X*.','Y*.',XNAME)
C           CALL ZPLTT(20.0,20.0,0,0,1,0,0,NFN,0,'TORSO ANG*.',ATZ,ATY
C           9,'Z*.','Y*.',XNAME)
C           CALL ZPLTT(20.0,20.0,0,0,1,1,1,NFN,2,'TORSO ANG*.',ATZ,ATX
C           9,'Z*.','X*.',XNAME)
C
C           CALL ZPLTT(20.0,20.0,0,0,0,0,0,NFN,0,'PEL A/P*.',APX,APY
C           9,'X*.','Y*.',XNAME)
C           CALL ZPLTT(20.0,20.0,0,0,1,0,0,NFN,0,'PEL ROT*.',APZ,APY
C           9,'Z*.','Y*.',XNAME)
C           CALL ZPLTT(20.0,20.0,0,0,1,0,1,NFN,2,'PEL M/L*.',APZ,APX
C           9,'Z*.','X*.',XNAME)
C
            CALL ZPLT(45.0,1,1,0,0,0,P1,NF,0,'ANK DOR.*.',VAUL7,1,0.0,4,XNAME)
            CALL ZPLT(45.0,0,0,0,0,0,P2,NF,0,'ANK DOR.*.',VAUL8,0,0.0,4,XNAME)
            CALL ZPLT(85.0,0,0,1,0,0,P1,NF,0,'KNEE FLEX.*.',KA,1,0.0,4,XNAME)
            CALL ZPLT(85.0,0,0,0,0,0,P2,NF,0,'KNEE FLEX.*.',AK,0,0.0,4,XNAME)
            CALL ZPLT(45.0,0,0,1,0,0,P1,NF,0,'FEM FLEX.*.',HA,1,0.0,4,XNAME)
            CALL ZPLT(45.0,0,0,0,1,1,P2,NF,2,'FEM FLEX.*.',AH,0,0.0,4,XNAME)
```

```
C
C       CALL ZPLT(40.0,1,1,0,0,0,P1,NF,0,' AATX*.',AATX,1,0.0,4,XNAME)
C       CALL ZPLT(80.0,0,0,1,0,0,P2,NF,0,' AATY*.',AATY,1,0.0,4,XNAME)
C       CALL ZPLT(40.0,0,0,1,1,1,P1,NF,2,' AATZ*.',AATZ,1,0.0,4,XNAME)
C
C       CALL ZPLT(20.0,1,1,0,0,0,P1,NF,0,'KNEE ADDU.*.',KAA,1,0.0,4,XNAME)
C       CALL ZPLT(20.0,0,0,0,0,0,P2,NF,0,'KNEE ADDU.*.',AAK,0,0.0,4,XNAME)
C       CALL ZPLT(20.0,0,0,1,0,0,P1,NF,0,'FEM ADDU.*.',HAA,1,0.0,4,XNAME)
C       CALL ZPLT(20.0,0,0,0,1,1,P2,NF,1,'FEM ADDU.*.',AAH,0,0.0,4,XNAME)
C
C       CALL ZPLT(20.0,1,1,0,0,0,P1,NF,0,'TOR. FLEX*.',ATX,1,0.0,4,XNAME)
C       CALL ZPLT(20.0,0,0,1,0,0,P1,NF,0,'TOR. SWING*.',ATZ,1,0.0,4,XNAME)
C       CALL ZPLT(20.0,0,0,1,1,1,P1,NF,2,'TOR. ROTATE*.',ATY,1,0.0,4,XNAME)
C
C       CALL ZPLT(20.0,1,1,0,0,0,P1,NF,0,'PEL. A/P*.',APX,1,0.0,4,XNAME)
C       CALL ZPLT(20.0,0,0,1,0,0,P1,NF,0,'PEL. M/L*.',APZ,1,0.0,4,XNAME)
C       CALL ZPLT(20.0,0,0,1,1,1,P1,NF,2,'PEL. ROT*.',APY,1,0.0,4,XNAME)
C
        CALL ZPLT(0.2,1,1,0,0,0,P1,NF,0,'FPZ/WGHT*.',FCZZ,1,BE1,4,XNAME)
        CALL ZPLT(0.2,0,0,0,0,0,4,NF,0,'FPZ/WGHT*.',ATRZ,0,BE2,4,XNAME)
C       CALL ZPLT(0.2,0,0,0,0,0,P1,NF,0,'FPZ/WGHT*.',ALZ1,0,BE2,4,XNAME)
C       CALL ZPLT(0.2,0,0,0,0,0,P2,NF,0,'FPZ/WGHT*.',ALZ2,0,BE2,4,XNAME)
C       CALL ZPLT(0.2,0,0,0,0,0,P2,NF,0,'FPZ/WGHT*.',FCZ2,0,BE2,4,XNAME)
C       CALL ZPLT(0.2,0,0,0,0,0,4,NF,0,'FPZ/WGHT*.',ABOZ,0,BE2,4,XNAME)
C
        CALL ZPLT(0.6,0,0,1,0,0,P1,NF,0,'FPY/WGHT*.',FCYY,1,BE1,4,XNAME)
        CALL ZPLT(0.6,0,0,0,0,0,4,NF,0,'FPZ/WGHT*.',ATRY,0,BE2,4,XNAME)
C       CALL ZPLT(0.6,0,0,0,0,0,P1,NF,0,'FPZ/WGHT*.',ALY1,0,BE2,4,XNAME)
C       CALL ZPLT(0.6,0,0,0,0,0,P2,NF,0,'FPZ/WGHT*.',ALY2,0,BE2,4,XNAME)
C       CALL ZPLT(0.6,0,0,0,0,0,4,NF,0,'FPY/WGHT*.',ABOY,0,BE2,4,XNAME)
C
        CALL ZPLT(0.4,0,0,1,0,0,P1,NF,0,'FPX/WGHT*.',FCXX,1,BE1,4,XNAME)
        CALL ZPLT(0.4,0,0,0,1,1,4,NF,2,'FPZ/WGHT*.',ATRX,0,BE2,4,XNAME)
C       CALL ZPLT(0.4,0,0,0,0,0,P1,NF,0,'FPZ/WGHT*.',ALX1,0,BE2,4,XNAME)
C       CALL ZPLT(0.4,0,0,0,0,0,P2,NF,0,'FPZ/WGHT*.',ALX2,0,BE2,4,XNAME)
C       CALL ZPLT(0.4,0,0,0,0,0,P2,NF,0,'FPX/WGHT*.',FCX2,0,BE2,4,XNAME)
C       CALL ZPLT(0.4,0,0,0,1,1,4,NF,2,'FPX/WGHT*.',ABOX,0,BE2,4,XNAME)
C
C       CALL ZPLT(0.8,0,0,0,0,0,P1,NF,0,'MPZ/WGHT*.',ALZ1,1,BE1,4,XNAME)
C       CALL ZPLT(0.8,0,0,0,0,0,P2,NF,0,'MPZ/WGHT*.',ALZ2,0,BE2,4,XNAME)
C       CALL ZPLT(0.06,0,0,1,0,0,P1,NF,0,'MPY/WGHT*.',ALY1,1,BE1,4,XNAME)
C       CALL ZPLT(0.06,0,0,0,0,0,P2,NF,0,'MPY/WGHT*.',ALY2,0,BE2,4,XNAME)
C       CALL ZPLT(0.2,0,0,1,0,0,P1,NF,0,'MPX/WGHT*.',ALX1,1,BE1,4,XNAME)
C       CALL ZPLT(0.2,0,0,0,0,1,P2,NF,2,'MPX/WGHT*.',ALX2,0,BE2,4,XNAME)
C
C
C       CALL ZPLT(0.2,1,1,0,0,0,P1,NF,0,'FHZ/WGHT*.',ATRZ,1,BE1,4,XNAME)
C       CALL ZPLT(0.2,0,0,0,0,0,P2,NF,0,'FHZ/WGHT*.',FHZ2,0,BE2,4,XNAME)
C       CALL ZPLT(2.0,0,0,1,0,0,P1,NF,0,'FHY/WGHT*.',ATRY,1,BE1,4,XNAME)
C       CALL ZPLT(2.0,0,0,0,0,0,P2,NF,0,'FHY/WGHT*.',FHY2,0,BE2,4,XNAME)
C       CALL ZPLT(0.5,0,0,1,0,0,P1,NF,0,'FHX/WGHT*.',ATRX,1,BE1,4,XNAME)
C       CALL ZPLT(0.5,0,0,0,1,1,P2,NF,2,'FHX/WGHT*.',FHX2,0,BE2,4,XNAME)
C
C       GO TO 11111
C
        CALL ZPLT(0.2,1,1,0,0,0,P1,NF,0,'MHZ/WGHT*.',MHZ1,1,BE1,4,XNAME)
        CALL ZPLT(0.2,0,0,0,0,0,P2,NF,0,'MHZ/WGHT*.',MHZ2,0,BE2,4,XNAME)
        CALL ZPLT(0.04,0,0,1,0,0,P1,NF,0,'MHY/WGHT*.',MHY1,1,BE1,4,XNAME)
        CALL ZPLT(0.04,0,0,0,0,0,P2,NF,0,'MHY/WGHT*.',MHY2,0,BE2,4,XNAME)
```

```
      CALL ZPLT(0.2,0,0,1,0,0,P1,NF,0,'MHX/WGHT*.',MHX1,1,BE1,4,XNAME)
      CALL ZPLT(0.2,0,0,0,1,1,P2,NF,2,'MHX/QGHT*.',MHX2,0,BE2,4,XNAME)
C
      CALL ZPLT(0.2,1,1,0,0,0,P1,NF,0,'MGX/WGHT*.',MGX1,1,BE1,4,XNAME)
      CALL ZPLT(0.2,0,0,0,0,0,P2,NF,0,'MGX/WGHT*.',MGX2,0,BE2,4,XNAME)
      CALL ZPLT(0.2,0,0,1,0,0,P1,NF,0,'MGY/WGHT*.',MGY1,1,BE1,4,XNAME)
      CALL ZPLT(0.2,0,0,0,0,0,P2,NF,0,'MGY/WGHT*.',MGY2,0,BE2,4,XNAME)
      CALL ZPLT(0.1,0,0,1,0,0,P1,NF,0,'MLW/WGHT*.',MLW1,1,BE1,4,XNAME)
      CALL ZPLT(0.1,0,0,0,1,1,P2,NF,2,'MLW/WGHT*.',MLW2,0,BE2,4,XNAME)
C
      CALL ZPLT(0.1,1,1,0,0,0,P1,NF,0,'MTX/WGHT*.',MTX1,1,BE1,4,XNAME)
      CALL ZPLT(0.1,0,0,0,0,0,P2,NF,0,'MTX/WGHT*.',MTX2,0,BE2,4,XNAME)
      CALL ZPLT(0.02,0,0,1,0,0,P1,NF,0,'MTY/WGHT*.',MTY1,1,BE1,4,XNAME)
      CALL ZPLT(0.02,0,0,0,0,0,P2,NF,0,'MTY/WGHT*.',MTY2,0,BE2,4,XNAME)
      CALL ZPLT(0.1,0,0,1,0,0,P1,NF,0,'MTW/WGHT*.',MTW1,1,BE1,4,XNAME)
      CALL ZPLT(0.1,0,0,0,1,1,P2,NF,2,'MTW/QGHT*.',MTW2,0,BE2,4,XNAME)
C
C
      CALL ZPLT(0.28,1,1,0,0,0,P1,NF,0,'MHZ/WGHT*.',MHZ,1,BE1,4,XNAME)
      CALL ZPLT(0.08,0,0,1,0,0,P1,NF,0,'MHT/WGHT*.',MHY,1,BE1,4,XNAME)
      CALL ZPLT(0.28,0,0,1,0,0,P1,NF,0,'MHI/WGHT*.',MHX,1,BE1,4,XNAME)
C
C     CALL ZPLT(0.28,1,1,0,0,0,P1,NF,0,'ZMH/WGHT*.',MHZ,1,BE1,4,XNAME)
C     CALL ZPLT(0.08,0,0,1,0,0,P1,NF,0,'YMH/WGHT*.',MHY,1,BE1,4,XNAME)
C     CALL ZPLT(0.28,0,0,1,0,0,P1,NF,0,'ZMH/WGHT*.',MHX,1,BE1,4,XNAME)
C
C
C     CALL ZPLT(0.4,1,1,0,0,0,P1,NF,0,'FKZ/WGHT*.',ATZ1,1,BE1,4,XNAME)
C     CALL ZPLT(0.4,0,0,0,0,0,P2,NF,0,'FKZ/WGHT*.',FKZ2,0,BE2,4,XNAME)
C     CALL ZPLT(2.0,0,0,1,0,0,P1,NF,0,'FKY/WGHT*.',ATY1,1,BE1,4,XNAME)
C     CALL ZPLT(2.0,0,0,0,0,0,P2,NF,0,'FKY/WGHT*.',FKY2,0,BE2,4,XNAME)
C     CALL ZPLT(0.4,0,0,1,0,0,P1,NF,0,'FKX/WGHT*.',ATX1,1,BE1,4,XNAME)
C     CALL ZPLT(0.4,0,0,0,1,1,P2,NF,2,'FKX/WGHT*.',FKX2,0,BE2,4,XNAME)
C
C     CALL ZPLT(0.2,1,1,0,0,0,P1,NF,0,'MKZ/WGHT*.',MKZ1,1,BE1,4,XNAME)
C     CALL ZPLT(0.2,0,0,0,0,0,P2,NF,0,'MKZ/WGHT*.',MKZ2,0,BE2,4,XNAME)
C     CALL ZPLT(0.04,0,0,1,0,0,P1,NF,0,'MKY/WGHT*.',MKY1,1,BE1,4,XNAME)
C     CALL ZPLT(0.04,0,0,0,0,0,P2,NF,0,'MKY/WGHT*.',MKY2,0,BE2,4,XNAME)
C     CALL ZPLT(0.2,0,0,1,0,0,P1,NF,0,'MKX/WGHT*.',MKX1,1,BE1,4,XNAME)
C     CALL ZPLT(0.2,0,0,0,1,1,P2,NF,2,'MKX/WGHT*.',MKX2,0,BE2,4,XNAME)
C
C
C     CALL ZPLT(0.4,1,1,0,0,0,P1,NF,0,'FAZ/WGHT*.',ASZ1,1,BE1,4,XNAME)
C     CALL ZPLT(0.4,0,0,0,0,0,P2,NF,0,'FAZ/WGHT*.',FAZ2,0,BE2,4,XNAME)
C     CALL ZPLT(2.0,0,0,1,0,0,P1,NF,0,'FAY/WGHT*.',ASY1,1,BE1,4,XNAME)
C     CALL ZPLT(2.0,0,0,0,0,0,P2,NF,0,'FAY/WGHT*.',FAY2,0,BE2,4,XNAME)
C     CALL ZPLT(0.4,0,0,1,0,0,P1,NF,0,'FAX/WGHT*.',ASX1,1,BE1,4,XNAME)
C     CALL ZPLT(0.4,0,0,0,1,1,P2,NF,2,'FAX/WGHT*.',FAX2,0,BE2,4,XNAME)
C
C     CALL ZPLT(0.4,1,1,0,0,0,P1,NF,0,'MAZ/WGHT*.',MAZ1,1,BE1,4,XNAME)
C     CALL ZPLT(0.4,0,0,0,0,0,P2,NF,0,'MAZ/WGHT*.',MAZ2,0,BE2,4,XNAME)
C     CALL ZPLT(0.04,0,0,1,0,0,P1,NF,0,'MAY/WGHT*.',MAY1,1,BE1,4,XNAME)
C     CALL ZPLT(0.04,0,0,0,0,0,P2,NF,0,'MAY/WGHT*.',MAY2,0,BE2,4,XNAME)
C     CALL ZPLT(0.04,0,0,1,0,0,P1,NF,0,'MAX/WGHT*.',MAX1,1,BE1,4,XNAME)
C     CALL ZPLT(0.04,0,0,0,1,1,P2,NF,2,'MAX/WGHT*.',MAX2,0,BE2,4,XNAME)
C
C
CC    CALL ZPLT1(50.0,1,1,0,0,0,P2,NF,0,'ENERGY*.',ES2,1,BE2,8,XNAME)
C     CALL ZPLT1(50.0,0,0,0,0,0,P2,NF,0,'ENERGY*.',ET2,0,BE2,8,XNAME)
```

```
C       CALL ZPLT1(50.0,0,0,0,1,0,P2,NF,0,'ENERGY*.',EEST2,0,BE2,8,XNAME)
C       CALL ZPLT1(200.0,0,0,0,0,0,0,P1,NF,0,'ENERGY*.',ES1,1,BE2,8,XNAME)
C       CALL ZPLT1(200.0,0,0,0,0,0,0,P1,NF,0,'ENERGY*.',ET1,0,BE2,8,XNAME)
C       CALL ZPLT1(200.0,0,0,0,0,0,0,P1,NF,0,'ENERGY*.',EEST1,0,BE2,8,XNAME)
C
C       CALL ZPLT(240.0,1,1,0,0,0,P2,NF,0,'EC RATE*.',PS2,1,BE2,4,XNAME)
C       CALL ZPLT(240.0,0,0,0,0,0,0,1,NF,0,'POWER*.',WS2,0,BE2,4,XNAME)
C       CALL ZPLT(240.0,0,0,1,0,0,P2,NF,0,'EC RATE*.',PT2,1,BE2,4,XNAME)
C       CALL ZPLT(240.0,0,0,0,0,0,0,1,NF,0,'POWER*.',WS2,0,BE2,8,XNAME)
C       CALL ZPLT(240.0,0,0,1,0,0,P2,NF,0,'EC RATE*.',PPST2,1,BE2,4,XNAME)
C       CALL ZPLT(240.0,0,0,0,1,1,1,NF,2,'POWER*.',WWST2,0,BE2,4,XNAME)
C
C       CALL ZPLT(240.0,1,1,0,0,0,P1,NF,0,'EC RATE*.',PS1,1,BE2,4,XNAME)
C       CALL ZPLT(240.0,0,0,0,0,0,0,1,NF,0,'POWER*.',WS1,0,BE2,4,XNAME)
C       CALL ZPLT(240.0,0,0,1,0,0,P1,NF,0,'EC RATE*.',PT1,1,BE2,4,XNAME)
C       CALL ZPLT(240.0,0,0,0,0,0,0,1,NF,0,'POWER*.',WS1,0,BE2,8,XNAME)
C       CALL ZPLT(240.0,0,0,1,0,0,P1,NF,0,'EC RATE*.',PPST1,1,BE2,4,XNAME)
C       CALL ZPLT(240.0,0,0,0,1,1,1,NF,2,'POWER*.',WWST1,0,BE2,4,XNAME)
C
C       CALL ZPLT(10.0,1,1,0,0,0,P1,NF,0,'AJCZ*.',ASW7,1,BE2,4,XNAME)
C       CALL ZPLT(10.0,0,0,0,0,0,0,P2,NF,0,'AJCZ*.',ASW8,0,BE2,4,XNAME)
C       CALL ZPLT(80.0,0,0,1,1,1,P1,NF,0,'VAULT*.',VAUL7,1,BE2,4,XNAME)
C       CALL ZPLT(80.0,0,0,1,1,1,P2,NF,0,'VAULT*.',VAUL8,1,BE2,4,XNAME)
C
        CALL DEVEND
        STOP
        END
C
C
C
        SUBROUTINE IMPOSE(NF,NFN,X,Y,Z,X1,Y1,Z1,X2,Y2,Z2)
        DIMENSION X(150),Y(150),Z(150),X1(150),Y1(150),Z1(150)
        1,X2(150),Y2(150),Z2(150)
        DO 10 I=1,NF-NFN+1
        X(I)=X(I)+X1(I+NFN-1)
        Y(I)=Y(I)+Y1(I+NFN-1)
        Z(I)=Z(I)+Z1(I+NFN-1)
        X(I+NFN-1)=X(I+NFN-1)+X2(I)
        Y(I+NFN-1)=Y(I+NFN-1)+Y2(I)
        Z(I+NFN-1)=Z(I+NFN-1)+Z2(I)
10      CONTINUE
        RETURN
        END
C
C
C
        SUBROUTINE TORDIF(MASS,NF,X,Y,Z,AX,AY,AZ)
        DIMENSION X(150),Y(150),Z(150),AX(150),AY(150),AZ(150)
        1,X1(200),Y1(200),Z1(200),Z2(200),Y2(200),X2(200)
        REAL MASS
C
        DO 10 I=1,8
        X1(I)=X(1)-X(10-I)
        Y1(I)=Y(1)-Y(10-I)
10      Z1(I)=Z(1)-Z(10-I)
        DO 20 I=1,NF
        X1(I+8)=X(I)
        Y1(I+8)=Y(I)
20      Z1(I+8)=Z(I)
```

```
      DO 30 I=NF-1,NF-8,-1
      K=NFN+8+(NF-I)
      X1(K)=X(NF)-X(I)
      Y1(K)=Y(NF)-Y(I)
30    Z1(K)=Z(NF)-Z(I)
C
      NFF=NF+16
      CALL FILTER(X1,NFF,5.0,0.02)
      CALL FILTER(Y1,NFF,5.0,0.02)
      CALL FILTER(Z1,NFF,5.0,0.02)
      DO 50 I=3,NFF-2
      X2(I)=50.0*(X1(I-2)-8.0*(X1(I-1)-X1(I+1))-X1(I+2))/12.0
      Y2(I)=50.0*(Y1(I-2)-8.0*(Y1(I-1)-Y1(I+1))-Y1(I+2))/12.0
      Z2(I)=50.0*(Z1(I-2)-8.0*(Z1(I-1)-Z1(I+1))-Z1(I+2))/12.0
50    CONTINUE
      DO 60 I=9,NFF-8
      AX(I-8)=50.0*(X2(I-2)-8.0*(X2(I-1)-X2(I+1))-X2(I+2))/12.0
      AY(I-8)=50.0*(Y2(I-2)-8.0*(Y2(I-1)-Y2(I+1))-Y2(I+2))/12.0
      AZ(I-8)=50.0*(Z2(I-2)-8.0*(Z2(I-1)-Z2(I+1))-Z2(I+2))/12.0
      AX(I-8)=AX(I-8)*3.1415926/180.0
      AY(I-8)=AY(I-8)*3.1415926/180.0
      AZ(I-8)=AZ(I-8)*3.1415926/180.0
60    CONTINUE
      CALL FILTER(AX,NF,5.0,0.02)
      CALL FILTER(AY,NF,5.0,0.02)
      CALL FILTER(AZ,NF,5.0,0.02)
C
      RETURN
      END
```

PROGRAM "PLOTRES.SUB"

```
      SUBROUTINE ZPLT(A,KPLOT,KSTRIP,KSTEP,KBACK,KSBA,IPEN,N,KTIME,NAME
     1,FM,IAXI,BEG,INT,XNAME)
      REAL*8 NAME
      DIMENSION FM(150),XI(150),YI(150),NAME(1)
      CHARACTER*(*) XNAME
      COMMON /CONS/A1,A2,FFF,IHS1,ITF1,IHS2,ITF2

C
      IF(KPLOT.EQ.0) GOTO 50
C
      CALL PICCLE
      CALL PENSEL(1,0.0,0)
      CALL MOVTO2(0.0,0.4)
      CALL CHAANG(90.0)
      CALL CHAHOL('NAME: *.')
      CALL CHASTR(XNAME)
      CALL MOVTO2(0.0,3.2)
      CALL CHAHOL('RIGHT SIDE*.')
      CALL MOVTO2(0.0,5.2)
      CALL CHAHOL('LEFT SIDE*.')
      CALL PENSEL(2,0.0,0)
      CALL MOVTO2(0.0,2.5)
      CALL LINTO2(0.0,3.1)
      CALL PENSEL(7,0.0,0)
      CALL BROKEN(3)
      CALL MOVTO2(0.0,4.7)
      CALL LINTO2(0.0,5.1)
      CALL CHAANG(0.0)
      CALL BROKEN(0)
C
      CALL SHIFT2(7.6,0.4)
C
C
50    IF(KSTEP.NE.0) CALL SHIFT2(-2.9,0.0)
C
      IF(IAXI.EQ.0) GOTO 100
C
      CALL PENSEL(1,0.0,0)
C     CALL DRAWBOX(-1.35,0.0,1.35,5.5)
      CALL DRAWBOX(-1.2,0.4,1.2,3.6)
      CALL DRAWBOX(-1.2,3.7,1.2,5.4)
      CALL MOVTO2(-0.9,3.7)
      CALL LINTO2(-0.9,5.4)
      CALL MOVTO2(-1.0,4.1)
      CALL CHAANG(90.0)
      CALL CHAHOL(NAME)
C
      CALL CHASIZ(0.07,0.07)
      CALL MOVTO2(-0.85,3.7)
      CALL LINTO2(-0.85,5.4)
```

```
      CALL MOVTO2(-0.65,3.7)
      CALL LINTO2(-0.65,5.4)
      CALL MOVTO2(-0.85,4.5)
      CALL LINTO2(1.2,4.5)
      CALL MOVTO2(1.2,4.95)
      CALL LINTO2(-0.85,4.95)
      CALL MOVTO2(-0.7,3.8)
      CALL CHAHOL('PARAMETER*.')
      CALL MOVTO2(-0.7,4.6)
      CALL CHAHOL('LEFT*.')
      CALL MOVTO2(-0.7,5.0)
      CALL CHAHOL('RIGHT*.')
      CALL MOVTO2(-0.47,3.8)
      CALL CHAHOL('MAX VALUE*.')
      CALL MOVTO2(-0.27,3.8)
      CALL CHAHOL('     TIME*.')
      CALL MOVTO2(-0.07,3.8)
      CALL CHAHOL('MIN VALUE*.')
      CALL MOVTO2(0.13,3.8)
      CALL CHAHOL('     TIME*.')
      CALL MOVTO2(0.33,3.8)
      CALL CHAHOL('IMPULSES*.')
      CALL MOVTO2(0.53,3.7)
      CALL CHAHOL(' POSIITIVE*.')
      CALL MOVTO2(0.73,3.8)
      CALL CHAHOL(' NEGATIVE*.')
C
      CALL CHASIZ(0.06,0.06)
      CALL AXIPOS(1,-1.2,0.4,2.4,1)
      CALL AXISCA(3,INT,A,-A,1)
      CALL AXIDRA(0,0,1)
      CALL AXIPOS(1,0.0,0.4,3.2,2)
      CALL AXISCA(3,1,0.0,1.0,2)
      CALL AXIDRA(0,0,2)
C
      CALL BROKEN(4)
      CALL GRAMOV(-A,A1)
      CALL GRALIN(A,A1)
      CALL GRAMOV(-A,A2)
      CALL GRALIN(A,A2)
C
      CALL BROKEN(0)
      CALL GRAMOV(-A*0.9,0.01)
      CALL CHAHOL('LHS*.')
      CALL GRAMOV(0.8*A,0.01)
      CALL CHAHOL('0.00*.')
      CALL GRAMOV(-A*0.9,A1-0.08)
      CALL CHAHOL('RHS*.')
      CALL GRAMOV(0.8*A,A1-0.08)
      CALL CHAFIX(A1,4,2)
      CALL GRAMOV(-A*0.9,A2+0.03)
      CALL CHAHOL('LTO*.')
      CALL GRAMOV(0.8*A,A2+0.03)
      CALL CHAFIX(A2,4,2)
      CALL GRAMOV(-A*0.9,0.92)
      CALL CHAHOL('RTO*.')
      CALL GRAMOV(0.8*A,0.92)
      CALL CHAFIX(1.0,4,2)
      CALL CHAANG(0.0)
```

```
C
      LU=2
      IF(A.GT.10.0) LU=1
      CALL CHAANG(180.0)
      CALL GRAMOV(0.7*A,-0.03)
      CALL CHAFIX(A,6,LU)
      CALL GRAMOV(-A*1.1,-0.03)
      CALL CHAFIX(-A,6,LU)
      DO 300 KK=2,INT
      Z=A-2.0*A*FLOAT(KK-1)/FLOAT(INT)
      ZZ=Z-0.2*A
      CALL GRAMOV(Z,0.0)
      CALL GRALIN(Z,0.02)
      CALL GRAMOV(ZZ,-0.03)
      CALL CHAFIX(Z,6,LU)
300   CONTINUE
      CALL CHAANG(0.0)
C
100   CONTINUE
C
      BP=0.0
      BN=0.0
      FMAX=-900.0
      FMIN=900.0
      CALL PENSEL(IPEN,0.0,0)
      IF(IPEN.EQ.7) CALL BROKEN(3)
      DO 103 IN=1,N
      IF(FMAX.LT.FM(IN)) THEN
      IMAX=IN
      FMAX=FM(IN)
      END IF
      IF(FMIN.GT.FM(IN)) THEN
      IMIN=IN
      FMIN=FM(IN)
      END IF
      IF(FM(IN).LT.0.0) THEN
      BN=BN+FM(IN)*0.02
      ELSE
      BP=BP+FM(IN)*0.02
      END IF
      XI(IN)=FLOAT(IN)/FFF+BEG
      YI(IN)=0.0
      IF (FM(IN).LE.A)GOTO 200
      FM(IN)=A
      PRINT *,'EXCESSIVE VALUE FOR Y',IN,FM(IN)
      GOTO 103
200   IF (FM(IN).GE.-A)GOTO 103
      FM(IN)=-A
      PRINT *,'EXCESSIVE VALUE FOR Y',IN,FM(IN)
103 CONTINUE
    NZ=N
    CALL GRAPOL(FM,XI,NZ)
      TMAX=FLOAT(IMAX)/FFF+BEG
      TMIN=FLOAT(IMIN)/FFF+BEG
C
      CALL BROKEN(0)
      CALL CHAANG(90.0)
      CALL CHASIZ(0.07,0.07)
      CALL PENSEL(1,0.0,0)
```

```
      AA=4.455
      IF(IPEN.EQ.2) AA=4.95
      CALL MOVTO2(-0.47,AA)
      CALL CHAFIX(FMAX,6,2)
      CALL MOVTO2(-0.27,AA)
      CALL CHAFIX(TMAX,6,2)
      CALL MOVTO2(-0.07,AA)
      CALL CHAFIX(FMIN,6,2)
      CALL MOVTO2(0.13,AA)
      CALL CHAFIX(TMIN,6,2)
      CALL MOVTO2(0.53,AA)
      CALL CHAFIX(BP,6,2)
      CALL MOVTO2(0.73,AA)
      CALL CHAFIX(BN,6,2)
      CALL CHAANG(0.0)
      CALL CHASIZ(0.1,0.1)
C
      IF(KSBA.EQ.0) GOTO 90
      IF(KTIME.EQ.1) CALL SHIFT2(2.9,0.0)
      IF(KTIME.EQ.2) CALL SHIFT2(5.8,0.0)
      CALL SHIFT2(-7.6,-0.4)
C
90    RETURN
      END
C
C
C
C
C
      SUBROUTINE ZPLT1(A,KPLOT,KSTRIP,KSTEP,KBACK,KSBA,IPEN,N
     1,KTIME,NAME,FM,IAXI,BEG,INT,XNAME)
      REAL*8 NAME
      DIMENSION FM(150),XI(150),YI(150),NAME(1)
      CHARACTER*(*) XNAME
      COMMON /CONS/A1,A2,FFF,IHS1,ITF1,IHS2,ITF2
C
      CALL SHIFT2(1.0,0.0)
C
      IF(KPLOT.NE.0) CALL PICCLE
C
      IF(KSTRIP.EQ.0) GOTO 50
      CALL PENSEL(1,0.0,0)
      CALL MOVTO2(0.0,6.2)
      CALL CHAHOL('NAME: *.')
C     CALL MOVTO2(0.6,6.2)
      CALL CHASTR(XNAME)
      CALL MOVTO2(3.1,6.2)
      CALL CHAHOL('RIGHT SIDE*.')
      CALL MOVTO2(6.1,6.2)
      CALL CHAHOL('LEFT SIDE*.')
      CALL PENSEL(2,0.0,0)
      CALL MOVTO2(2.0,6.2)
      CALL LINTO2(3.0,6.2)
      CALL PENSEL(7,0.0,0)
      CALL MOVTO2(5.0,6.2)
      CALL LINTO2(6.0,6.2)
C
C
50    IF(KSTRIP.NE.0) CALL SHIFT2(4.0,0.0)
```

```
      IF(KSTEP.NE.0) CALL SHIFT2(0.0,2.1)
C
      IF(IAXI.EQ.0) GOTO 100
      CALL CHASIZ(0.08,0.08)
      CALL PENSEL(1,0.0,0)
      CALL AXIPOS(1,0.2,0.2,2.8,1)
      CALL AXISCA(3,2,0.0,1.0,1)
      CALL AXIDRA(1,1,1)
      CALL AXIPOS(1,0.2,0.2,4.5,2)
      CALL AXISCA(3,INT,0.0,A,2)
      CALL AXIDRA(-1,-1,2)
      CALL MOVTO2(3.0,0.2)
      CALL LINTO2(3.0,4.7)
      CALL LINTO2(0.2,4.7)
C
      CALL BROKEN(0)
C
      CALL GRAMOV(0.01,A*1.01)
      CALL CHAHOL('LHS*.')
      CALL GRAMOV(A1,0.0)
      CALL GRALIN(A1,A)
      CALL GRAMOV(A1-0.05,A*1.01)
      CALL CHAHOL('RHS*.')
      CALL GRAMOV(A2,0.0)
      CALL GRALIN(A2,A)
      CALL GRAMOV(A2+0.05,A*1.01)
      CALL CHAHOL('LTO*.')
      CALL GRAMOV(0.9,A*1.01)
      CALL CHAHOL('RTO*.')
      CALL PENSEL(IPEN,0.0,0)
      CALL GRAMOV(0.4,A*1.1)
      CALL CHASIZ(0.1,0.1)
      CALL CHAHOL(NAME)
100   CONTINUE
C

    CALL PENSEL(IPEN,0.0,0)
    DO 103 IN=1,N
      XI(IN)=FLOAT(IN)/FFF+BEG
      YI(IN)=0.0
      IF (FM(IN).LE.A)GOTO 200
      FM(IN)=A
      PRINT *,'EXCESSIVE VALUE FOR Y',IN,FM(IN)
      GOTO 103
200   IF (FM(IN).GE.-A)GOTO 103
      FM(IN)=-A
      PRINT *,'EXCESSIVE VALUE FOR Y',IN,FM(IN)
103 CONTINUE
    NZ=N
    CALL GRAPOL(XI,FM,NZ)
C
      IF(KBACK.NE.0) CALL SHIFT2(-4.0,0,0)
      IF((KSBA.NE.0).AND.(KTIME.EQ.1)) CALL SHIFT2(0.0,-2.1)
      IF((KSBA.NE.0).AND.(KTIME.EQ.2)) CALL SHIFT2(0.0,-4.2)
C
      CALL SHIFT2(-1.0,0.0)
    RETURN
    END
C
```

```
C
      SUBROUTINE ZPLTT(B1,B2,KPLOT,KSTRIP,KSTEP,KBACK,KSBA,N,KTIME,NAME
     1,FM1,FM2,XX,YY,XNAME)
      REAL*8 NAME
      DIMENSION NL(5),FM1(150),FM2(150),XI(150),YI(150)
     1,NAME(1),XX(1),YY(1)
      CHARACTER*(*) XNAME
      COMMON /CONS/A1,A2,FFF,IHS1,ITF1,IHS2,ITF2
C
      CALL SHIFT2(0.8,-0.5)
      IF(KPLOT.NE.0) CALL PICCLE
C
      IF(KSTRIP.EQ.0) GOTO 50
      CALL PENSEL(1,0.0,0)
      CALL MOVTO2(0.0,6.2)
      CALL CHAHOL('NAME: *.')
      CALL CHASTR(XNAME)
      CALL MOVTO2(2.0,6.2)
      CALL CHAHOL('  Left HS*.')
      CALL MOVTO2(3.5,6.2)
      CALL CHAHOL('  Left TF*.')
      CALL MOVTO2(5.0,6.2)
      CALL CHAHOL('  Right HS*.')
      CALL MOVTO2(6.5,6.2)
      CALL CHAHOL('  Right TF*.')
      CALL MOVTO2(0.0,5.8)
      CALL PENSEL(2,0.0,0)
      CALL CHAHOL('  Angle-angle plot for torso (degrees)*.')
      CALL MOVTO2(0.0,2.9)
      CALL CHAHOL('  Lissajous Figure for pelvic (cm)*.')
      CALL PENSEL(5,0.0,0)
      CALL MOVTO2(2.0,6.25)
      CALL SYMBOL(1)
      CALL MOVTO2(3.5,6.25)
      CALL SYMBOL(5)
      CALL PENSEL(7,0.0,0)
      CALL MOVTO2(5.0,6.25)
      CALL SYMBOL(1)
      CALL MOVTO2(6.5,6.25)
      CALL SYMBOL(5)
C
50    IF(KSTRIP.NE.0) CALL SHIFT2(0.0,2.7)
      IF(KSTEP.NE.0) CALL SHIFT2(3.0,0.0)
C
      CALL PENSEL(1,0.0,0)
      CALL CHASIZ(0.06,0.06)
      CALL AXIPOS(1,0.2,1.6,2.0,1)
      CALL AXISCA(3,4,-B1,B1,1)
      CALL AXIDRA(1,1,1)
      CALL AXIPOS(1,1.2,0.6,2.0,2)
      CALL AXISCA(3,4,-B2,B2,2)
      CALL AXIDRA(-1,-1,2)
      CALL GRAMOV(B1*1.1,0.0)
      CALL CHAHOL(XX)
      CALL GRAMOV(0.0,B2*1.1)
      CALL CHAHOL(YY)
C
      CALL BROKEN(0)
C
```

```
      CALL PENSEL(2,0.0,0)
      DO 103 IN=1,N
      XI(IN)=0.0
      YI(IN)=0.0
      IF(FM1(IN).LE.B1) GOTO 200
      IF(FM2(IN).LE.B2) GOTO 200
      FM1(IN)=B1
      FM2(IN)=B2
      PRINT *,'EXCESSIVE VALUE FOR Y',IN,FM1(IN)
      GOTO 103
  200 IF(FM1(IN).GE.-B1) GOTO 103
      IF(FM2(IN).GE.-B2) GOTO 103
      FM1(IN)=-B1
      FM2(IN)=-B2
      PRINT *,'EXCESSIVE VALUE FOR Y',IN,FM1(IN)
  103 CONTINUE
      NZ=N
      CALL GRAPOL(FM1,FM2,NZ)
C
      CALL PENSEL(1,0.0,0)
      CALL CHASIZ(0.08,0.08)
      J=0
      K=0
      XMO=0.0
      YMO=0.0
      DO 123 I=1,NZ
      XMO=XMO+FM1(I)
      YMO=YMO+FM2(I)
      IF(FM1(I).GT.0) J=J+1
      IF(FM2(I).GT.0) K=K+1
  123 CONTINUE
      XMO=XMO/FLOAT(NZ)
      YMO=YMO/FLOAT(NZ)
      J1=NZ-J
      K1=NZ-K
      ITIME=J
      IF(K.LE.J) ITIME=K
      CALL GRAMOV(0.5*B1,-0.85*B2)
      CALL CHAHOL(XX)
      CALL CHAHOL('MEAN: *.')
      CALL GRAMOV(0.5*B1,-1.0*B2)
      CALL CHAFIX(XMO,5,2)
      CALL GRAMOV(-1.0*B1,0.9*B2)
      CALL CHAHOL(YY)
      CALL CHAHOL('MEAN: *.')
      CALL GRAMOV(-1.0*B1,0.75*B2)
      CALL CHAFIX(YMO,5,2)
      CALL GRAMOV(0.35*B1,0.9*B2)
      CALL CHAHOL(XX)
      CALL CHAHOL('(+): *.')
      CALL CHAINT(J,2)
      CALL GRAMOV(0.35*B1,0.75*B2)
      CALL CHAHOL(YY)
      CALL CHAHOL('(+): *.')
      CALL CHAINT(K,2)
      CALL GRAMOV(-1.0*B1,-0.85*B2)
      CALL CHAHOL(XX)
      CALL CHAHOL('(-): *.')
      CALL CHAINT(J1,2)
```

```
      CALL GRAMOV(-1.0*B1,-1.0*B2)
      CALL CHAHOL(YY)
      CALL CHAHOL('(-): *.')
      CALL CHAINT(K1,2)
C
      CALL PENSEL(5,0.0,0)
      CALL GRAMOV(FM1(1),FM2(1))
      CALL SYMBOL(1)
      I1=ITF1-IHS1+1
      CALL GRAMOV(FM1(I1),FM2(I1))
      CALL SYMBOL(5)
C
        CALL PENSEL(7,0.0,0)
        I1=IHS2-IHS1+1
        CALL GRAMOV(FM1(I1),FM2(I1))
        CALL SYMBOL(1)
        I1=ITF2-IHS1+1-N
        CALL GRAMOV(FM1(I1),FM2(I1))
        CALL SYMBOL(5)
C
        IF(KBACK.NE.0) CALL SHIFT2(0.0,-2.7)
        IF((KSBA.NE.0).AND.(KTIME.EQ.1)) CALL SHIFT2(-3.0,0.0)
        IF((KSBA.NE.0).AND.(KTIME.EQ.2)) CALL SHIFT2(-6.0,0.0)
C
        CALL SHIFT2(-0.8,0.5)
      RETURN
      END
C
C
C
      SUBROUTINE DRAWBOX(X0,Y0,X1,Y1)
      CALL MOVTO2(X0,Y0)
      CALL LINTO2(X1,Y0)
      CALL LINTO2(X1,Y1)
      CALL LINTO2(X0,Y1)
      CALL LINTO2(X0,Y0)
      RETURN
      END
```

BIBLIOGRAPHY

Abdel-Aziz Y. I. and Karara H. M. (1971) Direct Linear transformation from comparator coordinates into object space coordinates in close-range photogrammetry. *Proc. Symposium on Close-range Photogrammetry,* Urbana I11.

Aleshinsky S.U. (1986) An energy 'sources' and 'fraction' approach to the mechanical energy expenditure problem. *J. Biomechanics 19, 287-315.*

American Academy of Orthopaedic Surgeons (1960) *Orthopaedic Appliances Atlas, Vol. 2 - Artificial Limbs*. J. W. Edwards, Ann Arbor, Michigan.

American Academic of Orthopaedic Surgeons (1981) *Atlas on Limb Prosthetics: Surgical and Prosthetic Principles*. St. Louis, C. V. Mosby.

Andrews B. J., Nicol S. M., Thynne G. and Beale A. Q. (1981) The Strathclyde TV system for Human Motion Analysis. In: J. P. Paul *et al* (edt) *Computing in Medicine,* MscMillan Press, U.K.

Andrews B. J. (1975) Quantization effects in digital kinematic measurement and data processing systems. Internal report, Bioengineering Unit, University of Strathclyde, Glasgow, Scotland, U.K.

Andrews B. J., Cappozzo A. and Gazzani G. (1981) A quantitative method for assessment of different techniques used for locomotion analysis. In: *Computing in Medicine.* J. P. Paul *et al* (edt), Macmillan Press, U. K.

Andriacchi T. P., Ogle J. A. and Galante J. D. (1977) Walking speed as a basis for normal and abnormal gait measurements. *J. Biomechanics 10, 261-268.*

Andriacchi T. P. and Strickland A. B. (1985) Gait analysis as a tool to assess joint kinetics. In: N. Berm, A. E. Engin and K. M. Correia da Silva (edt) *Biomechanics of Normal and Pathological Articulating Joints*. Dordrecht, Netherland: Martinus Nijhoff.

Baumann W. (1974) New chronophotographic methods for three-dimentional Movement. In: *Biomechanics IV.*

Berme N., Purdie C. R. and Solomonidis S. E. (1978) Measurement of prosthetic alignment. *Prosth. Ortho. International 5, 73-76.*

Bernstein N. (1934) The technique of the study of movements. In: *The Co-ordination and Regulation of Movement,* Bernstein N., First English Edition, Pergamon Press, 1967.

Boccardi S., Chiesa G. and Pedotti A. (1977) New procedure for evaluation of normal and abnormal gait. *Amer. J. Phys. Med. 56, 163-182.*

Bontrager E. L. (1980) Footswitch redesign. In: *Annual Reports of Progress*, Feb. 1980 - Jan. 1981, Rancho Los Amigos Rehab. Eng. Centre, University of Southern California.

Braune W. and Fischer O. (1889) The centre of gravity of the human body as related to the equipment of the German infantryman. *Treat. Math-Phys. Class of the Royal Acad. of Science of Saxony 18, 409-492.*

Braune W. and Fischer O. (1894) *The Human Gait* . English translation by P. Maquet & R. Furlong, Springer - Verlag, London, 1987.

Bresler B. and Berry F. R. (1950) *Energy Characteristic of Normal and Prosthetic Ankle Joints*. Report Series 3, Issue 12, University of California, Berkeley, Proshtetic Devices Research Project.

Bresler B. and Frankel J. P. (1950) The forces and moments in the leg during level walking. *Trans. Amer. Soc. Mech. Eng. 72, 27-36.*

Bresler B. (1951) *Use of Energy Methods for Evaluation of Prostheses*. University of California, Berkeley.

Bresler B., Radcliffe C. W. and Berry F. R. (1957) *Energy and Power in the Legs of Above-Knee Amputees During Normal Level Walking*. Report Series 11, Issue 31, University of California, Berkeley.

Brull M.A. and Arcan M. (1974) A method and instrument for recording the pressure distribution between the foot and the ground. Paper presented at the World Congress of Prosthetics and Orthotics, Montreux, October 8 - 12.

Burgess E. W. and Matsen F. A. (1981) Determing amputation levels in peripheral vascular disease. *J. Born & Jnt. Surg. 63A, 1493-1497.*

Cappozzo A., Figura F., Leo T. and Macthetti M. (1976) Biomechanical evaluation of above knee prostheses. *Biomechanics V-A, 366-372.*

Cappozzo A. (1981) Analysis of the linear displacement of the head and trunk during walking at different speeds. *J. Biomechanics 14, 411-425.*

Cappozzo A. (1982) Head and trunk mechanics in level walking. PhD Thesis, University of Strathclyde, Glasgow, Scotland, U.K.

Cappozzo A. (1983) The forces and couples in the human trunk during level walking. *J. Biomechanics 16, 265-277.*

Cappozzo A. (1984) Gait analysis methodology. *Human Movement Science 3, 27-50.*

Cavagna G., Saibene F. and Margaria R. (1961) A three directional accelerometer for analysing body movements. *J. Appl. Phys. 16, 191-*

Cavagna G. A., Saibene F. R. nd Margaria R. (1963) Enternal work in walking. *J. Appl. Phys. 18, 1-9.*

Cavanagh P. R., Hennig E. M., Bunch R. P. and MacMillan N. M. (1983) A new device for the measurement of pressure distribution inside the shoe. *Biomechanics 4-B, 1089-1096.*

Chao E. Y. (1978) Experimental methods of joint kinematics. In: *CRC Handbook of Eng. in Med. & Biol. 1(B), 385-411.*

Chao E. Y., Rim K., Smidt G. L. and Johnson R. C. (1970) The application of 4×4 matrix method to the correction of the measurement of hip joint rotations. *J. Biomechanics 3, 459-471.*

Chao E. Y., Laughman R. K., Schneider E. and Stauffer R. N. (1983) Normative data of knee joint motion and ground reaction forces in adult level walking. *J. Biomechanics 16, 219-233.*

Chao E. Y. (1985) Gait analysis: a survey. In: *Gait Analysis: in Theory and Practice.* Lanshammar, H. (edt), Uppsala University.

Chandler R. F., Clauser C. E., McConville J. T., Reynolds H. M. and Young J. W. (1975) *Investigation of Inertia Properties of the Human Body.* Report No. DOT HS-801 430/AMRL-TR-74-137, Aerospace Medical Division, Research Laboratory, Wright-Patterson Air Force Base.

Chantinier K. D., Molen N. H. and Rozendal R. H. (1970) Step length, step frequency and temporal factorrs of the stride in human walking. In: N. H. Molen, *Problems on the Evaluation of Gait - with special reference to the comparison of normal subjects with below-knee amputees.*

Chodera J. D. and Lord M. (1978) Pedobarographic foot-pressure measurements and their applications. In: Kenedi R. M., Paul J. P. and Hughes J. (edt) *Disability - Proc. Seminar on Rehab. of the Disabled,* Bioengineering Unit, University of Strathclyde, Glasgow, U.K.

Contini R. (1972) Body segment parameters. Part II. *Artificial Limbs 16(1), 1-19.*

Committee on Prosthetics Research and Development (1971) *Cosmesis and Modular Limb Prostheses.* Report of a conference held in San Francisco, California, March 3-7, 1971, National Academy of Science, Washington, D. C.

Committee on Prosthetics Research and Development (1975) Draft Proposal for:

Standardization of Gait Analysis Parameters and Data Reduction Techniques - A Task Force Report. Distributed as minutes for limited distribution

Crowninshield R. D. and Brand R. A. (1978) Kinematics and kinetics of gait. In: *CRC Handbook of Engineering in Medicine and Biology 1(B), 413-425.*

Cunningham D. M. (1950) *Components of Floor Reactions During Walking*. Report Series 11, Issue 4, University of California , Berkeley, Prosthetic Devices Research Project.

Cunningham D. M. and Brown G. W. (1952) Two devices for measuring the forces on the human body during walking. *Proc. Soc. Exp. Stress Analysis 9(2).*

Davies E. J., Friz B. R. and Clippinger F. W. (1970) Amputees and their prostheses. *Artificial Limbs 14(2), 19-48.*

Day H. J. B. (1981) The assessment and description of amputee activity. *Prosthetics & Orthotics International 5, 23-29.*

Dempster W. T. (1955) *Space Requirements of the Seated Operator*. USAF, WADC, Technique Report 55-159, Wright-Patterson Air Force Base, Ohio.

Department of Health and Social Security (1973) *Lower Limb Modular Prostheses*. A Report on an International Conference on Specification , Ascot, England, 1972.

Department of Health and Social Security, Statistics and Research Division (1976 & 1978) *Amputation Statistics for England, Wales and N. Ireland.*

Draganich L. F., Andriacchi T. P., Strongwater A. M. and Galante J. O. (1980) Electronic measurement of instantaneous foot-floor contact patterns duirng gait. *J. Biomechanics 13, 875-880.*

Drillis R. J. (1958) Objective recording and biomechanics of pathological gait. *Ann. New York Acad. Sci. 74, 86-*

Drillis R. J. and Contini R. (1966) *Body Segment Parameters*. Technique Report No. 1166.03, New York University, School of Engineering and Science, Research Division.

Eberhart H. D. and Inman V. T. (1947) *Fundamental Studies of Human Locomotion and Other Information Relating to Design of Artificial Limbs*. University of California, Berkeley, Report to National Research Council, Committee on Artificial Limb.

Eberhart H. D., Inman V. T. and Bresler B. (1954) The principle elements in human locomotion. In: *Human Limbs and Their Substitute*. Klopsteg P. E., and Wilson P. D., *et al*.ed.

Elfman H. O. (1934) A kinematic study of the distribution of pressure in the human foot. *Anat. Record 59, 481-491.*

Elftman H. O. (1938) The measurement of the external force in walking. *Science 88, 152-*

Elftman H. O. (1939) Forces and energy changes in the leg duirng walking. *Amer. J . Phys. 125, 339-356.*

Elftman H. O. (1939) The function of arms in walking. *Human Biol. 2, 529-535.*

Elftman H. O. (1939) The force exerted by the ground in walking. *Arbeitsphysiolodie 10, 485-491.*

Fischer S. V. and Gullickson G. (1978) Energy cost of ambulation in health and disability: a literature review. *Arch. Phys. Med. & Rehabil. 59(3), 124-133.*

Fishman S., Berger N. and Watkins D. (1975) A survey of prosthetic practice: 1973-1974. *Orthotics and Prosthetics 29, 15-20.*

Frigo C. and Rodano R. (1982) Comparison between the reactive moments at the lower limb joints of normal and prosthetized subjects. In: *Control Aspect of Prosthetics and Orthotics*. Campbell, R. M. (edt), Pergamon Press, Oxford.

Foort J. (1979) Alignment of the above-knee prosthesis. *Prosthetics & Orthotics International 3, 137-139.*

Furnee E. H. (1967) Hybrid instrumentation in prosthetic research. *Proc. 7th Int. Conf. on Med. & Biol. Eng.*, Stockholm.

Gabel E. H., Johnston R. C. and Crowninshield R. D. (1979) A gait analyzer / trainer instrumentation system. *J. biomechanics 12, 543-549.*

Gage H. (1964) Accelerographic analysis of human gait. ASME paper No. 64-WA/HUF 8.

Garrison F. H. (1963) *An Introduction to the History of Medicine.* Philadelphia, W.B., Saunders Co.

Garton W. T. (1979) Measurement of metabolic energy expenditure in the disabled. In: *BRADU-Roehampton*, London, Report 1979, D.H.S.S.

Glattly H. W. (1964) A statistical study of 12,000 new amputees. *South. Med. J. 57, 1373-*

Godfrey C. M., Jousse A. T., Brett R. and Butler J. F. (1975) A comparison of some gait characteristics with six knee joints. *Orthotics and Prosthetics 29, 33-38.*

Goh J. C. H. (1982) Biomechanical evaluation of SACH and uniaxial feet . PhD Thesis, University of Strathclyde, Glasgow, Scotland, U. K.

Grieve D. W. and Gear R. J. (1966) The relationships between length of stride, step frequency, time of swing and speed of walking for children and adults. *Ergonomics 9, 329-399.*

Grieve D. W. (1968) Gait pattern and the speed of walking. *Biomed. Engng. 3, 119-*

Grieve D. W. (1969) A device called the Polgon for the measurement of the orientation of parts of the body relative to a fixed external axis. *J. Physiol. 201, 70-*

Grieve D. W., Miller D. I., Mitchelson D., Paul J. P. and Smith A. J. (1975) *Techniques for Analysis of Human Movement*. Lepus books, London.

Hamming R. W. (1977) *Digital Filters*. Prentice-Hall Signal Processing Series, Alan Oppenheim, Series Editor, Pentice-Hall, Inc., Englewood Cliffs, New Jersey.

Hannah R. E. (1984) Kinematic symmetry of the lower limbs. *Arch. Phys. Med. Rehabil. 65, 155-158.*

Hannah R. E., Morrison J. B. and Chapman A. E. (1984) Prosthetic alignment : effect of gait of persons with below-knee amputations. *Arch. Phys. Med. Rehabil. 65, 159-162.*

Hanavan E. P. (1964) Mathematical model of the human body. (AMRL-TR-64-102) Wright-Patterson Air Force Base, Ohio, U.S. A.

Harless E. (1860) The static moments of human limbs (in German). *Treat. Math-Phys. Class of the Royal Acad. of Sci. of Bavaria 8(1), 69-96 & 257-294.*

Harrison H. R. and Nettleton T. (1978) *Principles of Engineering Mechanics*. Edward Arnold Ltd., London.

Harry B., Skinner M. D., David J. and Effeney M. B. (1985) Gait analysis in amputees. *American J. Physical Med. 64, 82-89.*

Hatze H. (1980) A mathematical model for the computational determination of parameter values of anthropomorphic segments. *J. Biomechanics 13, 833-843.*

Hatze H. (1984) Quantitative analysis, synthesis and optimization of human motion. *Human Movement Science 3, 1-27.*

Inman V.T., Raltson H. J. and Radcliffe C. W. (1981) *Human Walking*. Williams and Wilkins, Baltimore, London.

International Society For Prosthetics & Orthotics (1978) Standards for lower-limb prostheses. Report of a conference 1977. Philadelphia: I.S.P.O.

Ishai G. and Bar A. (1983) Computer simulation for the prediction of stump loading in above-knee amputees. *Med. & Biol. Eng. & Comput. 21, 186-190.*

Ishai G. Bar A. and Susak Z. (1983) Effects of alignment variables on thigh axial torque during swing phase in AK amputee gait. *Prosthetics & Orthotics International 7, 41-47.*

Jacobs N. A., Skorecki J. and Charnley J. (1972) Analysis of the vertical component of force in normal and pathological gait. *J. Biomechanics 5, 11-34.*

James U. and Oberg K. (1973) Prosthetic gait patterns in unilateral AK amputees. *Scand. J. Rehab. Med. 5, 35-50.*

Jarrett M. O. (1976) Television-computer system for human locomotion analysis . PhD Thesis, University of Strathclyde, Glasgow, scotland, U.K.

Jarrett M. O. (1980) A clinical system for 3-dimentional gait analysis. Biological Engineering Society, 20th Anniversary International Conference, London.

Johnston R. C. and Smidt G. L. (1969) Measurement of hip joint motion during walking. *J. Bone & Surg. 51-A, 1083-1094.*

Johnson F., Watts W. G. and Evans D. F. (1981) Goniometer for continuous recording of knee angle. *Med. & Biol. Eng. & Comput. 19, 255-256.*

Jordan M. M. (1978) Direction cosine computational error. *NASA TR-R-304.*

Judge G. (1980) Survey of knee mechanisms for artificial legs. *BRADU 1977 to 1978, Revised 1980.*

Kay H. W. and Newman J. D. (1975) Relative incidence of new amputees - Statistical comparison of 6,000 new amputations. *Orthotics and Prosthetics 29, 3-*

Kinzel G. L., Hall A. S. and Hillberry B. M. (1972) Measurement of the total motion between two body segments. *J. Biomechanics 5, 93-105.*

Kistler A. G. (1977) *Information Bulletin for Electrical Measurements of Mechaical Values.* Trade Literature, Number 15.

Klopsteg P. E. and Wilson P. E. (1954) *Human Limbs And Their Substitutes.* Hafner Publishing Company, Reprinted 1968.

Kuhn G. G. (1956) Typische Fehler beim Oberschenkelkunstbeinball (Typical Faults in Above-knee Prostheses). Presisarbeit im Preisausschreibem des, Bundesministeriums fur Arbeit, Bonn.

Lamoreux L. W. (1971) Kinematic measurements in the study of human walking. *BPR Spring 1971, (10-15),*73-84.

Lanshammar H. (1982) On pratical evaluation of differentiation techniques for human gait analysis. *J. Biomechanics 15, 99-106.*

Lauru L. (1957) Physiological study of motion. *Advanced Management 22, 17-24.*

Lawes P. (1982) Alignment Kinetics in patient-prosthesis matching . PhD Thesis, University of Strathclyde, Glasgow, Scotland, U. K.

Lehneis H. R. (1985) Beyond the quadrilateral. *Clinical Prosthetics & Orthotics 9(4), 6-8.*

Lewallen R., Quanbury A.C., Ross K. and Letts R. M. (1985) A biomechanical study of normal and amputee gait. *Biomechanics IX-A, 587-592.*

Long I. A. (1985) Normal Shape - Normal Alignment (NSNA) above-knee prosthesis. *Clinical Prosthetics & Orthotics 9(4), 9-14.*

Lowe P. J. (1969) Knee mechanism performance in amputee activity. PhD Thesis, University of Strathclyde, Glasgow, Scotland, U.K.

Lyquist E. (1969) Recent variants of the PTB prosthesis (PTS, KBM & Air-Cushion Sockets). In: *Prosthetic and Orthotic Practice,* Murdoch G. edited.

Mansour J. M., Lesh M. D., Nowak M. D. and Simon S. R. (1982) A 3-D multi-segmental analysis of the energetics of normal and pathological human gait. *J. Biomechanics 15, 51-59.*

Marzan G. T. and Karara H. M. (1975) A computer program for direct linear transformation solution of the collinear condition and some applications of it. *Proc. Symposium on Close-Range Photogrammetric Systems.* Illinois: American Society of Photogrammetry.

Mayerson N. H. and Milano R. A. (1984) Goniometric measurement reliability in physical medicine. *Arch. Phys. Med. Rehabil. 65, 92-94.*

Mazrahi J., Susak Z., Seliktart T. and Najenson T. (1986) Alignment procedure for the optimal fitting of lower limb prostheses. *J. Biomed. Eng. 8, 229-234.*

McDonald I. (1961) Statistical studies of recorded enerfy expenditure of man. Part II, expenditure on walking related to weight, sex, age, height, speed and gradient. *Nutr. Abstr. Rev. 31, 739-762.*

Marsden J. P. and Montogomery S. R. (1972) An analysis of the dynamic characteristics of a force plate. *Measurement and Control 5, 102-106.*

Miller N. R., Shapiro R. and McLaughlin T. M. (1980) A technique for obtaining kinematic parameters of segments of biomechanical system from cinematographic data. *J. Biomechanics 13, 535-547.*

Mital M. A. and Pierce D. S. (1971) *Amputees and Their Prostheses.* Little and Brown Company, Boston.

Mitchelson D. A. (1975) Recording movement without photography. In: *Techniques for the Analysis of Human Movement.* The human movement series, Lepus Books.

Molen N. H. and Boon W. (1972) Measurement of momentary velocity in the study of human gait. *J. Biomechanics 5, 273-276.*

Molen N. H. (1973) *Problems on the Evaluation of the Gait with Special Reference to the Comparison of Normal Subjects with Below-Knee Amputees.*

Morris J. M. (1973) Accelerometry - A technique for the measurement of human body

movements. *J. Biomechanics 6, 729-736.*

Morinoto S., Aoyama T. and Tsuchiya K. (1987) Dynamic evaluation of prosthetic alignment using instrumented pylon and flexible electrogoniometer. *Proc. 9th International Symposium on ECHE.* Aug. 31-Sept. 5, Dubrovnik, Yugoslavia.

Movement Techniques Limited (1982) *CODA-3 Movement Monitoring Instrument.* Trade Literature. The Technique Centre, Epinal Way, Loughborough, LE11 0QE, England.

Morrison J. B. (1968) Bioengineering analysis of forces transmitted by the knee joint. *Biomedical Engng. 3, 164-170.*

Morrison J. B. (1970) The biomechanics of the knee joint in relation to normal walking. *J. Biomechanics 3, 51-61.*

Murdoch G. (1970) *Prosthetic And Orthotic Practice.* Based on a conference held in Dundee, June, 1969. E. Arnold, London.

Murray M. P., Drought A. B. and Kory R. C. (1964) Walking pattterns of normal men. *J. Born & Jnt. Surg. 46A, 335-360.*

Murray M. P., Kory R. C., Clarkson B. H. and Sepic S. B. (1966) Comparison of free and fast speed walking patterns of normal men. *Am. J. Phys. Med. 45, 8-24.*

Murray M. P., Sepic S. B., Gardner G. M. and Mollinger L. A. (1980) Gait patterns of above-knee amputees using constant friction knee components. *Bull. Pros. Res. 10-34, 35-45.*

Muybridge E. (1887) *The Human Figure in Motion.* New Edition 1955, Dover Publication, New York.

Nicol K. and Henning E. M. (1976) Time-dependent method for measuring force distribution using a flexible mat as a capacitor. *Biomechanics V-B, 433-440.*

Norman R., Sharratt M., Pezzack J. and Noble E. (1976) Re-examination of the mechanical efficiency of horizontal treadmill running. In: *Biomechanics V-B, 87-93.*

oberg K. (1981) *Quantitative Analysis of Gait Disorder.* Uppsala Universitet, Uppsala.

oberg K. (1985) Swedish attempts in using CAD/CAM principles for prosthetics and orthotics. *Clinical Prosthetics 9, 19-23.*

Opila K. A. (1985) Impulse characteristics and upper limb loadings of aided gait . PhD Thesis, University of Strathclyde, Glasgow, Scotland, U.K.

Oxfort Medical Systems Ltd. (1980) *VICON System Technical Summary.* Trade Literature.

Padgaonkar A. J., Krieger K.W. and King A. I. (1975) Measurement of angular acceleration of a rigid body using linear accelerometers. *J. Appl. Mech. 42, 552-556.*

Paul J. P. (1967) Forces transmitted by the joints in the human body. *Proc. Mech. Eng. 3,*

181-191.

Paul J. P. (1967) Forces at the human hip joint. PhD Thesis, University of Glasgow, Glasgow, Scotland, U.K.

Paul J. P. (1970) The effect of walking speed on the force actions transmitted at the hip and knee joints. *Proc. Royal Soc. Med. 63(2), 200-202.*

Paul J. P. (1971) Comparison of EMG signals from leg muscles with the corresponding force actions calculated from walkpath measurements. In: *Human Locomotion Engineering*. Proc. Conf. at University of Sussex, Inst. Mech. Engineers, London.

Paul J. P. and Nicol A. C. (1981) Usability of the SELSPOT system for biomechanical data acquisition. Report to the Scottish Home and Health Department (unpublished).

Pearson J. R., Holmgren, G., March, L. and oberg, K. (1973) Pressure in critical regions of below-knee patellar tendon bearing prosthesis. *Bull. Pros. Res., Spring, 52-76.*

Pederson H. E. (1968) The problem of the geriatric amputee. *Artificial Limbs 12, 1-3.*

Pezzack J. C., Norman R. W. and Winter D. A. (1977) An assessment of derivative determing techniques used for motion analysis. *J. Biomechanics 10, 377-382.*

Radcliffe C. W. (1955) Functional considerations in the fitting of above-knee prostheses. *Artificial Limbs 2,*

Radcliffe C. W. (1962) The biomechanics of below-knee prostheses in normal, level, bi-pedal walking. *Artificial Limbs 6, 16-24.*

Radcliffe C. W. (1969) Biomechanics of above-knee prostheses. In: *Prosthetic and Orthotic Practice,* G. Murdoch edited.

Ralston H. J. (1958) Energy-speed relation and optimal speed during level walking. *Int. Z. Angen. Physiol. einsch. Arbeitsphysiol. 17, 277-283.*

Ralston H. J. and Lukin L. (1969) Energy level of human body segments during level walking. *Ergonomics 12, 39-46.*

Robertson D. G. E. and Winter D. A. (1980) Mechanical energy generation, absorption and transfer amongst segments during walking. *J. Biomechanics 13, 845-854.*

Ryker N. J. and Bartholomew S. H. (1951) Determination of acceleration by use of accelerometers. Report Series 11, Issue 17, University of California, Berkeley, Prosthetic Devices Project.

Sabolich J. (1985) Contoured Adducted Trocanteric - Controlled Alignment Method (CAT-CAM): Introduction and basic principles. *Clinical Prosthetics & Orthotics 9(4), 15-26.*

Saleh M. (1985) Alignment and gait optimization in lower limb amputees. Paper presented in

the International Conf. and Advanced Course on Amputation Surgery and Lower Limb Prosthetics, 1st-5th July, Dundee, scotland, U.K.

Selcom A. B. (1975) *Trade Literature on the SELSPOT System*. Selective Electronic Company, P.O. Box 30, S-431 21, Molndal, Sweden.

Schneider E. and Chao E. Y. (1983) Fourier analysis of ground reaction forces in normals and patients with knee joint disease. *J. Biomechanics 16, 591-601.*

Seliktar R. and Mizrahi J. (1984) Control of alignment and socket fit of below-knee prosthesis with the aid of forceplates. *Proc. 2nd Int. Conf. on Rehab. Engng.* Ottawa, 265-267.

Sikhar N. B. (1982) *Rehabilitation Management of Amputees*. Williams and Wilkins, Baltimore, London.

Solomonidis S. E. (editor) (1975) *Modular Artificial Limbs*. First report on a continuing programme of clinical and laboratory evaluation, Below knee systems. Scottish Home & Health Department.

Solomonidis S. E. (editor) (1980) *Modular Artificial Limbs*. Second report on a continuing programme of clinical and laboratory evaluation, Above knee systems. Scottish Home & Health Department.

Saudan K. and Dierckx P. (1979) Calculation of derivatives and Fourier coefficients if human motion data while using spline functions. *J. Biomechanics 12, 21-26.*

Souden (1982) Standardization of gait kinematic data using a gait symmetry index and Fourier analysis. In: *Biomechanics: Principles and Applications*. R. Huiskes *et al* (edt), Martinus Nijhoff Publishers.

Staros A. (1963) Dynamic alignment of artificial legs with the adjustable coupling. *Artificial Limbs 7, 31-43.*

Staros A. (1979) Economics of modular prostheses. *Prosthetics & Orthotics Int. 3, 147-149.*

Stokes, V. P. (1984) A method for obtaining the 3D kinematics of the pelvis and thorax during locomotion. *Human Movement Science 3, 77-118.*

Symington, D. C. (1984) The goal of rehabilitation. *Arch. Phys. Med. Rehabil. 65, 427-430.*

Szulc, J. A. (1983) Development of the above knee telescopic limb prosthesis . PhD Thesis, University of Strathclyde, glasgow, Scotland, U. K.

Taylor, J. S. (1979) Above-knee prosthetic alignment. *Prosthetics and Orthotics International 3, 82-84.*

Thomas, A. (1944) Anatomical and physiological considerations in the alignment and fitting of amputation prostheses for the lower extremity. *J. Born & Joint Surgery* ***26-A****, 645-659.*

Towle, J. (1986) Increasing the precision of measurement of postures in free space . PhD Thesis, University of Nottingham, Nottingham, U. K.

Trnkoczy, A. and Bajd, T. (1975) A simple electrogoniometric system and its testing. *IEEE Trans. on Biomed. Engng.* ***BME-22****, 257-259.*

VICON: Oxfort Metrics Ltd, Manufacturer of VICON, Unit 8, 7 West Way, Botley, Oxfort, OX2 0JB, England.

Van de veen, P. G., Van der tempel, W. and De Vreiss, J. (1987) Bondgraph modelling and simulation of the dynamic behaviour of above-knee prostheses. *Prosthetics & Orthotics International* ***11****, 65-70.*

Veterans Administration Prosthetic Centre (1973) *Standards and Specifications for Prosthetic Foot/ankle Assemblies.* VAPC-L-7007-2, Veterans Administration Central Office, Washington, D. C. 20420.

Vitali M., Robinson K. P., Andrews B. G. and Harris E. E. (1978) *Amputation and Prostheses.* A. Bailliere Tindall Book, Pub. Cassel & Co. Ltd.

Wall J.C., Dhanenoran M. and Klenermal L. (1976) A method for measuring th temporal-distance factors of gait. *Biomed. Eng.* ***11****, 409-412.*

Wall J. C., Charteris J. and Hoare J. W. (1978) An automated on-line system for measuring the temporal patterns of foot.floor contact. *J. Med. Eng. & Tech.* ***4****, 187-190.*

Walt W. N., Van der And Wyndham C. H. (1973) An equation for prediction of energy expenditure of walking and running. *J. Appl. Physiol.* ***34****, 559-563.*

waters R. L., Berry J., Antonelli D. and Hislop H. (1976) Energy cost of walking of amputees: Influence of level of amputation. *J. Born & Jnt. Surg.* ***58(A)****, 42-46.*

Whittle, M.W. (1982) Calibration and performance of a 3-D television system for kinematic analysis. *J. Biomechanics* ***15****, 185-196.*

Williams, K. R. and Cavanagh, P. R. (1983) A model for the calculation of mechanical power during distance running. *J. Biomechanics* ***16****, 115-128.*

Wilson A. B. Jr (1970) Limb prosthetics - 1970. *Artificial Limbs* ***14****, 1-52.*

Winarski, D. J. and Pearson, J. R. (1984) Least-squares matrix correlations between stump stress and prosthesis loads for below-knee amputees. *ASME Trans.* ***109****, J. Biomech. Engng., 238-246.*

Winter D. A., Greenlaw R. K. and Hobson D. A. (1972) Television - computer analysis of

kinematics of human gait. *Comp. Biomed. Res. 5, 498-504.*

Winter D. A., Sidwall H. G. and Hobson D. A. (1974) Measurement and reduction of noise in kinematics of locomotion. *J. Biomechanics 9, 253-257.*

Winter, D. A. (1980) *Biomechanics of Human Movement.* John wiley, New York.

Winter, D. A. (1984) Kinematic and kinetic patterns in human gait: variability and compensating effects. *Human Movement Science 3, 51-76.*

Winter, D. A. and Sienko, S. E. (1988) Biomechanics of below-knee amputee gait. *J. biomechanics 21, 361-367.*

Woltring H. J. (1975) Single- and Dual-axis lateral photodetecors of rectangular shape. *IEEE Trans. Electronic Devices 22, 581-590.*

Woltring H. J. and Marsolais E. B. (1980) Optoelectric (Selspot) gait measurement in two and three dimensional space - a preliminary report. *BPR 10-34, 46-52.*

Wright, D. G., Desai, M. E. and Henderson, W. H. (1964) Action of the subtalar and ankle joint complex during the stance phase of walking. *J. Born & Jnt. Surg. 46-A, 361-382.*

Zahedi, M.S. (1985) Study of alignment of lower limb prostheses (PhD Thesis in preparation). University of Strathclyde, Glasgow, Scotland, U. K.

Zahedi, M. S., Spence, W. D. and Solomonidis, S. E. (1985) The influence of alignment on prosthetic gait. Paper presented in the International Conf. and Advanced Course on Amputation Surgery and Lower Limb Prosthetics, 1st-5th July, Dundee, scotland, U. K.

Zahedi, M. S., Spence, W. D., Solomonidis, S. E. and Paul, J. P. (1986) Alignment of lower-limb prostheses. *J. Rehab. Res. & Develop. 23, BPR10-44, 2-19.*

Zahedi, M. S., Spence, W. D., Solomonidis, S. E. and Paul, J. P. (1987) Repeatability of kinetic and kinematic measurements in gait studies of the lower limb amputee. *Prosthetics & Orthotics International 11, 55-64.*

Zarrugh M. Y. (1981) Power requirements and mechanical efficiency of treadmill walking. *J. Biomechanics 14, 157-165.*

Zarrugh M. Y., Todd F. N. and Ralston H. J. (1974) Optimization of energy expenditure during level walking. *Europ. J. Appl. Physiol. 33, 293-306.*

Zarrugh M. Y. and Radcliffe C. W. (1979) Computer generation of human gait kinematics. *J. Biomechanics 12, 99-110.*